Covalent modification and intrinsic disorder in the stability of the proneural protein Neurogenin 2

Gary Steven McDowell MSci, MA (Cantab)

Clare College

Department of Oncology
Faculty of Clinical Medicine
University of Cambridge

PhD

2011

DECLARATION

This dissertation is the result of my own work and includes nothing which is the outcome of work done in collaboration except where specifically indicated in the text. The data presented in this thesis will not be submitted for the purpose of any other degree or qualification at this or any other university. This thesis does not exceed 60,000 words in length.

Gary McDowell

July 2011

ACKNOWLEDGEMENTS

I would like to thank Anna Philpott, my supervisor, for the tremendous scientific and moral support she has given me throughout my PhD, and for everything she has taught me.

I am grateful to the Medical Research Council for the funding that has allowed me to undertake this study and to Clare College which has provided travel funding and support in my time here.

I would also like to thank members of the Philpott lab for teaching me new techniques and supporting me in my time here: Ryan Roark, Jon Vosper, Romana Kucerova, Fahad Ali, Ali Jones, and Xana Almeida.

I especially would like to thank Chris Hindley for all that he has taught me and for daily support and friendship he has given me in the lab since the day we both started here together and wish him all the best in the hope that one day we might work together again.

I would like to thank my collaborator Guy Lippens and his lab, particularly Isabelle Landrieu but also Isabelle Huvent and Xavier Hanoulle at the Université des Sciences et Technologies de Lille (USTL Lille 1). They supported me in my time in France, taught me new techniques and gave me a new perspective on my work.

Finally I would like to find my friends and family, who have supported me in the highs and lows of my PhD. They were the best of times; they were the worst of times; but I have no regrets. I would do it all over again.

Gary McDowell

July 2011

SUMMARY

Neurogenin 2 (Ngn2) is a basic Helix-Loop-Helix (bHLH) transcription factor regulating differentiation and cell cycle exit in the developing brain. By transcriptional upregulation of a cascade of other bHLH factors, neural progenitor cells exit the cell cycle and differentiate towards a neuronal fate. *Xenopus laevis* Ngn2 (xNgn2) is a short-lived protein, targeted for degradation by the 26S proteasome. I have investigated the stability of Ngn2 mediated by post-translational modifications and structural disorder.

Firstly I will describe work focused on ubiquitylation of xNgn2, targeting it for proteasomal degradation. xNgn2 is ubiquitylated on lysines, the recognized site of modification. I will discuss the role of lysines in ubiquitylation and stability of xNgn2.

In addition to canonical ubiquitylation on lysines, I describe ubiquitylation of xNgn2 on non-canonical sites, namely its amino-terminal amino group, and cysteine, serine and threonine residues. I show that the ubiquitylation of cysteines in particular exhibits cell cycle dependence and is also observed in mammalian cell lines, resulting in cell cycle-dependent regulation of stability.

I will then discuss whether phosphorylation, a regulator of xNgn2 activity, also affects xNgn2 stability. I will provide evidence of cell cycle-dependent phosphorylation of cyclin dependent kinase (cdk) consensus sites affecting the stability of xNgn2.

Finally I describe studies on the folding properties of Ngn2 to assess their role in protein stability. xNgn2 associates with DNA and its heterodimeric binding partner xE12 and may interact directly with the cyclin-dependent kinase inhibitor Xic1. I will discuss the role of these interaction partners in xNgn2 stability. xNeuroD, a downstream target of xNgn2, is a related bHLH transcription factor which is stable. Here I describe domain swapping experiments between these two proteins highlighting regions conferring instability on the chimeric protein. Finally I will provide nuclear magnetic resonance (NMR) data looking at the effect of phosphorylation on protein structure in mouse Ngn2 (mNgn2).

TABLE OF CONTENTS

Appendices

ABBREVIATIONS

AMP: adenosine monophosphate

APC/C: Anaphase Promoting Complex/Cyclosome

APF-1: ATP-dependent proteolysis factor 1

AR: androgen receptor

ash: achaete-scute homologue

ATP: adenosine triphosphate

bHLH: basic Helix-Loop-Helix

BMP: Bone Morphogenic Protein

°C: degrees centigrade

Cdc20: cell division cycle protein 20

Cdh1: Cdc20-homologue 1

Cdk: cyclin dependent kinase

Cdki: cyclin dependent kinase inhibitor

cDNA: complementary DNA

Cip: cdk interacting protein

CNS: central nervous system

CBP: CREB (cAmp Response Element Binding Protein)-Binding Protein

DMSO: dimethyl sulfoxide

DNA: Deoxyribonucleic Acid

DUB: Deubiquitylating enzyme

E2A: general class of gene products including E12 and E47

E12: E2A bHLH transcription factor

E47: E2A bHLH transcription factor

E1: Ub-activating enzyme

E2: Ub-conjugating enzyme

EDTA: Ethylenediaminetetraacetic acid

Emi1: early mitotic inhibitor 1

EMSA: Electrophoretic Mobility Shift Assay

ERAD: endoplasmic reticulum-associated degradation

FID: Free Induction Decay

GABAergic: emitting/secreting γ-aminobutyric acid

GFP: Green Fluorescent Protein

Gli: glioblastoma protein

GO: gene ontology

GSK3-β: glycogen synthase kinase 3 beta

HCV: Hepatitis C virus

HECT: homologous to E6-AP (E6-associated protein) carboxy terminus

Hes: Hairy enhancer of split

HIV: Human Immunodeficiency Virus

HPV: Human Papilloma Virus

HSQC: heteronuclear single quantum coherence

Id: Inhibitor of differentiation

ID: Intrinsic Disorder

IPTG: Isopropyl β-D-1-thiogalactopyranoside

ISH: *in situ* hybridisation

IVT: *in vitro* translation

IκB: nuclear factor of kappa light polypeptide gene enhancer in B-cells inhibitor

JAK-STAT: janus kinase-signal transducers

kDa: kiloDalton

Kip: Kinase inhibitory protein

MAPK: mitogen-activated protein kinase

Mash1: *Mus musculus* achaete-scute homologue 1

MBS: Modified Barth's Saline

Mdm2: murine double minute 2 protein

MEM: Minimum Essential Media

MG132: N-carbobenzoxyl–Leu–Leu–Leucinal

mins: minutes

MMR: Marc's modified Ringers

MoRE: molecular recognition element

mRNA: messenger Ribonucleic Acid

Myf5: Myogenic factor 5

MyoD: Myogenic Differentiation factor

NEM: N-ethyl maleimide

NeuroD: Neurogenic Differentiation factor

NICD: Notch intracellular domain

NMR: Nuclear Magnetic Resonance

NS5A: non-structured protein 5A

NT: N-terminus

Olig2: oligodendrocyte lineage 2 protein

PBS: Phosphate Buffered Saline

pI: Isoelectric point

PNS: peripheral nervous system

PTM: post-translational modification

qPCR: quantitative real-tome Polymerase Chain Reaction

Ras: rat sarcoma protein

RING: Really Interesting New Gene

SCF: Skp1-Cullin1-F-box

SDS-LB: sodium dodecyl sulfate loading buffer

SDS-PAGE: sodium dodecyl sulfate polyacrylamide gel electrophoresis

SEM: Standard Error of the Mean

Sic1: Substrate/Subunit Inhibitor of Cyclin-dependent protein kinase

Skp1/Skp2: S-phase kinase associated protein 1/2

SUMO: Small Ubl Modifier

TAT: tyrosine amino-transferase

TCR: T-Cell receptor

TMSP: Trimethylsilyl propanoic acid

Ub: ubiquitin

Ubc: Ub-conjugating enzyme

Ubl: Ub-like

UFD: Ub fusion degradation

UPS: Ub Proteasome System

Xash1: *Xenopus laevis* achaete-scute homologue 1

XB: extract buffer

Xebf3: *Xenopus laevis* early B-cell factor 3

Xic1: *Xenopus laevis* inhibitor of cyclin dependent kinases

xMyT1: *Xenopus laevis* Myelin Transcription factor
XPak3: *Xenopus laevis* p21-activated kinase 3
β-TRCP: beta-Transducin repeat containing protein

Neurogenin 2 proteins:

Ngn2: neurogenin 2
xNgn3: *Xenopus laevis* neurogenin 3
mNgn2: *Mus musculus* neurogenin 2
xNgn2: *Xenopus laevis* neurogenin 2

Ubiquitylation:

Ac2 prefix: N-terminus mutated to upregulate cotranslational N-terminal acetylation
Ac3 prefix: N-terminus mutated to downregulate N-terminal acetylation
Ac2xNgn2KO: all amino-based nucleophilic sites mutated or blocked
Ac2xNgn2CO: N-terminus targeted for acetylation, all cysteines mutated to alanines
Ac2xNgn2KOCO: all amino- and thiol-based nucleophilic sites mutated or blocked

C178AxNgn2: conserved cysteine 178 mutated to alanine
C(169,178)AxNgn2: conserved cysteines 169 and 178 mutated to alanine

KXXRxNgn2: lysine XX mutated to arginine
RXXKxNgn2KO: lysine XX reintroduced, all other lysines mutated to arginines
R(116,119)KxNgn2KO: bHLH lysines reintroduced to otherwise 'lysineless' protein
R(77,79,80)KxNgn2KO: KIKK lysines reintroduced to otherwise 'lysineless' protein

Ub-xNgn2: Ub fused linearly to N-terminus of xNgn2
Ub-9S-AxNgn2: Ub fused linearly to N-terminus, all SP serines mutated to alanines

xNgn2KO: 'lysineless' xNgn2; all lysines mutated to arginines
xNgn2CO: 'cysteineless' xNgn2; all cysteines mutated to alanines

Phosphorylation:

xS-A1: xNgn2 with most C-terminal SP serine, 184, mutated to alanine
xS-A2 – xS-A8: successive SP serines mutated to alanine from C-terminus, until;
xS-A9: xNgn2, SP serines 19, 29, 44, 47, 57, 164, 172, 181 and 184 mutated to alanine

2S-AxNgn2: GSK3-β consensus site SP serines (181, 184) mutated to alanine
7S-AxNgn2: all SP serines except GSK3-β site serines (181, 184) mutated to alanine

8S-AxNgn2SXX: all SP serines except serine XX mutated to alanine
9S-AxNgn2: all SP serines mutated to alanine – see xS-A9
9S-AxNgn2KO: all SP serines mutated to alanine and all lysines mutated to arginine
9S-AT149AxNgn2KO: see 9S-AxNgn2KO, also T149 mutated to alanine
9S-AT(118,149)AxNn2KO: see 9S-AxNgn2KO, also T118, T149 mutated to alanine
9S-AAc2xNgn2KO: see 9S-AxNgn2KO, also upregulated for N-terminal acetylation
9S-AT149AxNgn2: all SP and TP site serines/threonines mutated to alanine

CT-S-AxNgn2: all SP site serines in C-terminal domain mutated to alanine
CT-S-AT49AxNgn2: all C-terminal SP serines, and TP threonine, mutated to alanine
NT-S-AxNgn2: all SP site serines in N-terminal domain mutated to alanine
NT-S-AT49AxNgn2: all N-terminal SP serines, and TP threonine, mutated to alanine
T149AxNgn2: TP site mutated to alanine

Domain swap chimeras:

N-Ngn/BC-NeuroD:
N-terminal domain of xNgn2 fused to bHLH and C-terminal domains of xNeuroD
NB-Ngn/C-NeuroD:
N-terminal and bHLH domains of xNgn2 fused to C-terminal domain of xNeuroD
N-NeuroD/BC-Ngn:
N-terminal domain of xNeuroD fused to bHLH and C-terminal domains of xNgn2
NB-NeuroD/C-Ngn:
N-terminal and bHLH domains of xNeuroD fused to C-terminal domain of xNgn2

LIST OF FIGURES

LIST OF TABLES

CHAPTER 1

Introduction

bHLH Proteins

Basic Helix-Loop-Helix (bHLH) proteins are proteins of an ancient lineage (Rebeiz et al., 2005, Holland et al., 2000, Quan et al., 2004, Simionato et al., 2008) expressed in eukaryotes (Massari and Murre, 2000). They consist of a DNA-binding basic domain followed by two α-helices separated by a loop (Murre et al., 1994). Tissue-specific class II bHLH proteins bind as a heterodimer with the ubiquitously expressed class I bHLH E2A gene products, such as E12 or E47, to a consensus pseudo-palindromic E-box DNA motif, CANNTG (where N is any nucleic acid) (Ma et al., 1994, Ellenberger et al., 1994, see Appendix 1).

bHLH proteins function as transcription factors (Massari and Murre, 2000). Activation of transcription by bHLH proteins is involved in cell fate determination and differentiation. They have demonstrated roles in myogenesis (Yokoyama and Asahara, 2011), haematopoiesis and heart development (Jones, 2004), pancreatic development (Murtaugh and Melton, 2003) and sex determination (Bhandari et al., 2011). I have investigated bHLH transcription factors involved in brain development by controlling the process of neurogenesis (Philpott, 2010).

Neurogenesis

bHLH proteins are of immense importance in nervous development (Ik Tsen Heng and Tan, 2003, Kageyama and Nakanishi, 1997, Ross et al., 2003, Talikka et al., 2002) and tumorigenesis. Much work on *Drosophila* atonal proteins (homologous to neurogenins) or achaete-scute (relating to Xash/Mash in vertebrates) identifies functional roles that are conserved in vertebrates and, in particular, mammals (Farah et al., 2000, Garrell and Modolell, 1990, Hassan and Bellen, 2000, Hu et al., 2004, Korzh et al., 1998, Romani et al., 1989). bHLH proteins are heavily involved in the

development of both the central nervous system (CNS, chiefly the brain and spinal chord) and peripheral nervous system (PNS, nerves and ganglia largely outside the CNS) (Bertrand et al., 2002). bHLH transcription factors are involved in formation of cell subtypes in the cortex (Ross et al., 2003) and setting up the dorsal/ventral axis in the telencephalon (Fode et al., 2000).

There are two different groups of bHLH proneural proteins, the atonal homologues and the achaete-schute homologues of *Drosophila melanogaster* genes (Bertrand et al., 2002). Neurogenins are atonal related and achaete-scute homologues, or ash proteins, have species specific names e.g. Mash1 in mice and Xash1 in frogs. These two families carry out neurogenesis but with differing outcomes (Lo et al., 2002) producing neurons of different subtype identity (Parras et al., 2002). Neurogenins induce specification of glutamatergic and dopaminergic neurons whilst Mash1 expression leads to GABAergic neurons (Parras et al., 2002) and progenitors of olfactory neurons (Cau et al., 1997). The neurogenins inhibit proliferation and promote cell cycle exit (Ross et al., 2003) whereas Mash 1 expression can allow the cell cycle to continue (Kim et al., 2007). Ngn2 and Mash1 together specify cell subtype and number in neural development (Helms et al., 2005, Kim et al., 2007) and indeed Ngn2 itself can limit the activity of Mash1 (Helms et al., 2005). The bHLH proteins are intricately regulated throughout the brain in different regions and at different times to control cell subtype specification (Sugimori et al., 2007). In particular neurogenins and Mash1 dictate dorsal-ventral patterning of neurons in the forebrain (Fode et al., 2000) and promote neuronal cell fates whilst inhibiting gliogenesis in the cerebral cortex (Nieto et al., 2001, Tomita et al., 2000). Regulation of temporal expression in the CNS determines neuronal or glial cell fates (Qian et al., 2000) from radial glial cells (Gotz and Barde, 2005). A complicated network of bHLH protein expression controlling formation of neurons and glial cells in both time and space is becoming apparent (Sugimori et al., 2007).

Various signals control the expression of the bHLH proteins and induction of neurogenesis, such as morphogenic signals (Panchision and McKay, 2002) and transcriptional codes (Jessell, 2000, Shirasaki and Pfaff, 2002). In particular, in addition to inducing neuronal differentiation, proneural proteins activate

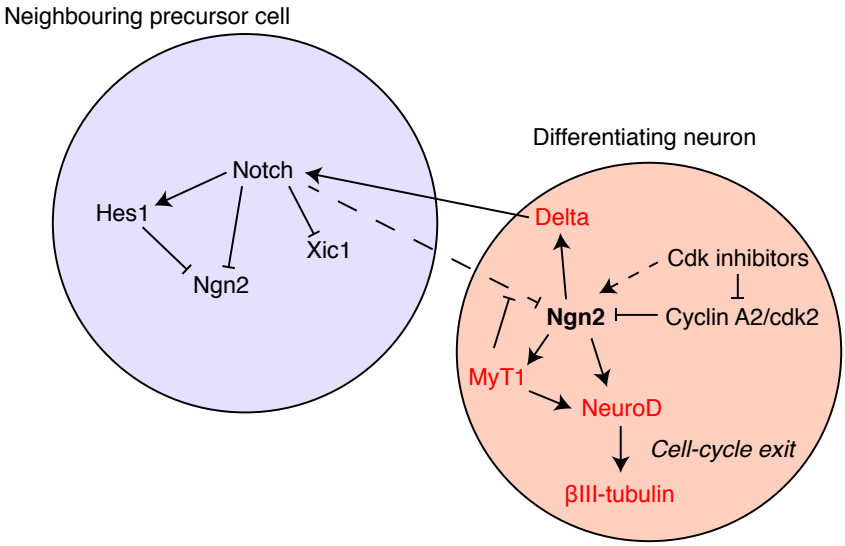

Figure 1.1: Pathways of Ngn2 action.

The various inhibitors and transcriptional targets of Ngn2 promote both neuronal differentiation and lateral inhibition of neighbouring precursor cells. Cyclin dependent kinase inhibitors (cdkis) relieve cyclin A2/cdk2 inhibition of Ngn2 allowing transcription of downstream targets such as NeuroD and MyT1 leading to neuronal differentiation. Cdkis also stabilise Ngn2 against proteasomal degradation. However the Notch ligand, Delta, is also transcribed, and binds to the Notch receptor of neighbouring cells. The Notch intracellular domain (NICD) forms part of a transcriptional complex producing proteins such as Hairy enhancer of split (Hes) 1 and Hes5. These transcriptional repressors prevent transcription of Ngn2 targets and the cell is held in a precursor state.

transcription of the Notch ligand, Delta (see Figure 1.1). Increasing levels of proneural proteins within a cell lead to increasing production of Delta, which induces Notch signalling in neighbouring cells. Activation of Notch, releasing the Notch intra-cellular domain (NICD) into the cytoplasm, leads to transcriptional activation of the Hairy enhancer of split (Hes) proteins Hes1 and Hes5. These proteins, also in the bHLH family, are repressors of transcription. Therefore Notch signalling leads to inhibition of the action of the proneural proteins in neighbouring cells and so leads to a network of lateral inhibition, where a differentiating neuronal cell maintains neighbouring cells in a precursor state (Chitnis and Kintner, 1996).

Many proteins interact with the bHLH pathway in neurogenesis. Glioblastoma (Gli) proteins affect neural plate development and are required for primary motor neuron, primary sensory neuron and primary interneuron production in *Xenopus*. These proteins are able to induce Ngn transcription and interact (albeit via an unknown mechanism) with the bHLH and Notch pathways (Nguyen et al., 2005). Transcriptional repressors can interact with bHLH proteins to regulate differentiation networks; for example the oligodendrocyte lineage 2 (Olig2) protein interacts with Ngn2 to affect motor neuron subtype specification (Novitch et al., 2001).

The role of the bHLH proteins in promoting neurogenesis whilst suppressing gliogenesis may also lead ultimately to control of cell fate in glial precursors. A role for the janus kinase-signal transducers (JAK-STAT) and mitogen-activated protein kinase (MAPK) pathways in differentiation of astrocytes has been identified (Rajan and McKay, 1998). A role for cytokines in promoting gliogenesis (Bonni et al., 1997) is linked to the action of proneural proteins indirectly. Neurogenesis precedes gliogenesis and neurons from the embryonic cortex (specified by proneural proteins as shown in (Ross et al., 2003)) secrete cytokines that promote differentiation of glial precursors into astrocytes (Barnabe-Heider et al., 2005).

Neurogenin

Neurogenin was identified in the mid-1990s from a cDNA library from rat dorsal root ganglia using consensus sequences from a particular protein fold family, the bHLH proteins (Ma et al., 1996). *Xenopus laevis* Ngn2 (xNgn2, also known as X-NGNR-1 (Nieber et al., 2009)) was found to induce neurogenesis, the process of neuron formation from neural precursors (see Figure 1.2). It activates the transcription of downstream targets such as the proneural bHLH protein xNeuroD (Ma et al., 1996) and the zinc-finger protein xMyT1 ((Bellefroid et al., 1996), see Figure 1.1). Not long after, it was found in mouse that 3 distinct neurogenins were present: Ngn1; Ngn2 and Ngn3, all with roles in determination of cell fate distinct from each other (Sommer et al., 1996) but acting upstream of NeuroD in determining the fate of progenitor cells as neural precursors. In *Xenopus laevis*, homologues to only Ngn2 and Ngn3 have been found but none for Ngn1.

Ngn2 acts as an activator of transcription for both itself and a cascade of other bHLH transcription factors (Mattar et al., 2004). The Ngn2/E12 heterodimer bound to DNA recruits transcriptional coactivators such as p300/CBP (Koyano-Nakagawa et al., 1999). The neuronal differentiation factor NeuroD, one of the transcriptional targets of the Ngn2/E12 complex, can itself go on to associate with the p300/CBP coactivator in activation of transcription of markers of neuronal formation such as neural β-tubulin; X-MyT1; Xebf3; or the kinase XPak3 which promotes cell cycle withdrawal (Seo et al., 2007, Souopgui et al., 2002).

xNgn2 is most closely related in sequence to mouse Ngn2 (mNgn2). mNgn2 is involved in formation of sensory neurons from the epibranchial placode (Fode et al., 1998). Both Ngn1 and Ngn2 are involved in neurogenesis in dorsal root ganglia (Ma et al., 1999). Ngn2 acts to determine the fate of progenitor cells as neuronal precursors and also to repress glial cell fates using separate mechanisms (Korzh and Strahle, 2002, Sun et al., 2001). Ngn2 also induces exit from the cell cycle (Guillemot, 2007), and if levels of Ngn2 become too high can mediate early cell death of neural precursors as a self-regulatory mechanism (Yeo and Gautier, 2005). Ngn2 demonstrates roles in reprogramming adult astroglial cells (Gross, 2000) in the

subventricular zone of the lateral ventricles (Rogelius et al., 2008) and the hippocampus (Ozen et al., 2007), and also a possible role in Alzheimer's treatment by producing dopaminergic neuronal precursors (Kele et al., 2006, Thompson et al., 2006). Cell motility is also affected by Ngn2, which can control the growth and migration of neurons (Heng et al., 2008).

The role of Ngn2 in neurogenesis in the developing embryo has led to research into other settings for inducing neuronal differentiation. Differentiation of neural stem cells can be induced by transfection of Ngn2 (Falk et al., 2002). Ngn2 can suppress glial cell fates in neural stem cells to increase the chance of success of introducing such cells into damaged regions of the spinal chord to repair damage (Hofstetter et al., 2005). Likewise roles for proneural genes are emerging, such as in the context of Notch signalling maintaining neural stem cells in a progenitor state (Imayoshi and Kageyama, 2011), which allow adult neurogenesis to take place.

In summary, Ngn2 acts to commit progenitor cells to a neuronal fate by exiting the cell cycle and directing subtype specification. It has further roles in other processes such as neuronal migration and neurite outgrowth (Hand 2005).

Ngn2 and the cell cycle

Neurogenesis appears to be under considerable regulatory control by the cell cycle (Ohnuma and Harris, 2003). Work on regulation of the cell cycle in *Xenopus laevis* (Vernon and Philpott, 2003a) and the *Xenopus* Cip/Kip family, including cyclin-dependent kinase inhibitor (cdki) Xic1 (Nguyen et al., 2006, Ohnuma et al., 1999, Su et al., 1995, Vernon et al., 2003, Vernon and Philpott, 2003b) in muscle and neuronal development found that Xic1 promotes neurogenesis. xNgn2 was stabilised against degradation by Xic1 but in a manner as yet unknown, although direct binding seems likely (Vernon et al., 2003). Likewise the cdki $p27^{Kip1}$ can stabilise mNgn2 (Nguyen et al., 2006).

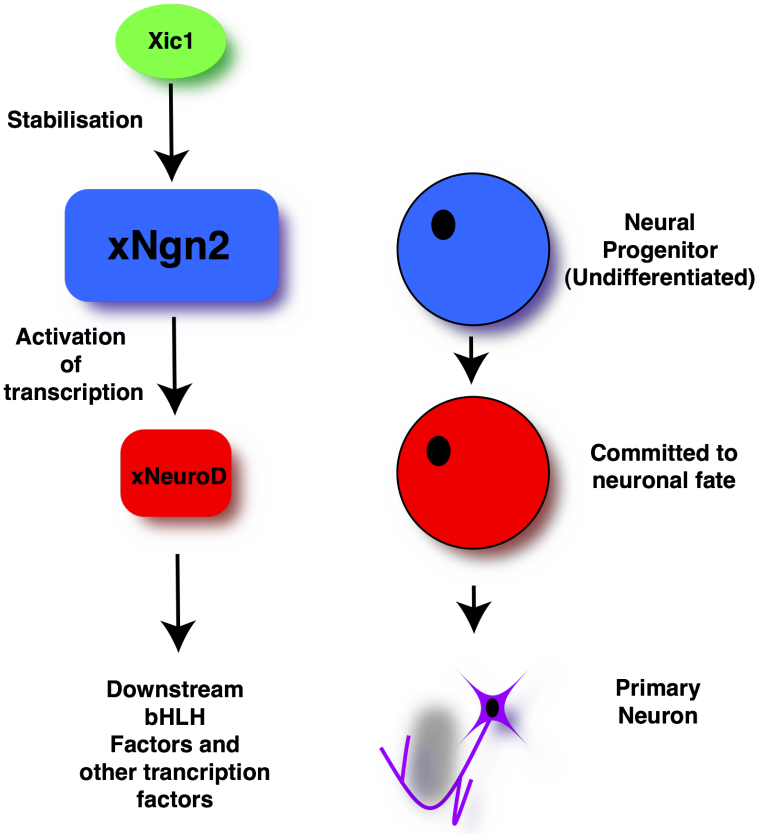

Figure 1.2: Schematic of Ngn2 action with respect to cell fate.

xNgn2, stabilised by Xic1, is expressed at the level of a neural progenitor cell. xNgn2 activates transcription of xNeuroD at which point the cell becomes committed to a neuronal cell fate. Further transcription of a cascade of bHLH factors and other factors results in primary neuron formation.

Ngn2, like Xic1, is controlled by lateral inhibition through Notch signalling (Chitnis and Kintner, 1996, Chitnis, 1999, Justice and Jan, 2002, Vernon et al., 2006). This results in differentiation of primary neurons in the neural crest surrounded by inhibited cells that may be directed to gliogenesis as has been shown in transient Notch expression experiments ((Morrison et al., 2000), see Figure 1.1).

Neurogenins and structural considerations

Whilst there is no published structural information for Ngn2, homologues such as MyoD and NeuroD bound to E47 as a heterodimer to DNA do have crystal structures available (Longo et al., 2008, Ma et al., 1994, Wendt et al., 1998, see Appendix 1). It is suggested that DNA binding is required for the protein to fold and also to heterodimerise through an unknown mechanism (Longo et al., 2008). However formation of the heterodimer before DNA-binding cannot be precluded. There is also an NMR structure of the bHLH Ngn1 homodimer bound to DNA (Aguado-Llera et al., 2010). No evidence exists for homodimers of Ngn2 binding DNA, whereas E2A homodimers can bind DNA, dependent on an intermolecular disulphide bond (Benezra, 1994). The Ngn1 homodimeric complex is described as "fuzzy" and remains highly dynamic even when bound to DNA (Aguado-Llera et al., 2010).

Ngn2 binds as a heterodimer with E2A gene products. E2A proteins are also ubiquitylated and degraded, in a Notch-dependent manner controlled by MAP kinase (Kho et al., 1997, Nie et al., 2003). Degradation of Inhibitor of differentiation (Id) proteins, which lack a basic domain and bind Ngn2 to inhibit its transcription factor activity, is also ubiquitin-dependent (Benezra et al., 1990, Berse et al., 2004). Mash is also degraded in a manner that is not only ubiquitin-dependent, but occurs in response to Notch signalling (Sriuranpong et al., 2002).

Ngn2 is phosphorylated upon association with E12 (Vosper et al., 2007). Mash also shows increased phosphorylation on heterodimerisation with E47 (Vinals et al., 2004). Phosphorylation of Ngn2 is also important in regulating its activity. Recent work has shown that phosphorylation on particular sites of Ngn2 is required for specification of motor neurons (Ma et al., 2008).

The Ubiquitin Proteasome System (UPS)

Proteins are produced through transcription and translation of genes in the cell, from information encoded in DNA through RNA to protein. Proteins are also broken down to terminate their function and recycle their amino acid components for the production of other proteins. But how does the degradation machinery recognize a protein that must be degraded? One method of signalling proteins for destruction is through attachment of a protein modifier, ubiquitin (Ub), itself a 7.6 kDa protein molecule. The process of ubiquitylation can target the substrate protein for degradation by a cellular structure, the 26S proteasome.

Discovery of ubiquitin

Protein degradation may seem a necessary requirement to remove a protein signal. Otherwise a protein produced would need to be swamped by a different protein to cancel its effects, and in turn this protein by another. This might lead to a frightening mass of protein before barely a few cell divisions in a developing embryo in a logical thought experiment, but in the early studies of protein metabolism this was not appreciated. The concept of protein catabolism had surprisingly controversial beginnings. A long established view that cellular proteins, once produced, are stable (Folin, 1905) was only challenged by work using isotopically labelled leucine fed to rats (Schoenheimer et al., 1939). Rather than passing straight through the rats, a large proportion of the label was incorporated into their tissue, suggesting that some form of protein turnover, replacing "endogenous" protein with labelled protein, was occurring. This led to Schoenheimer's proposal that protein levels were held in a dynamic state (Schoenheimer, 1942).

This rebellion from textbook-enshrined dogma was rebuffed by none other than Jacob Monod (Hogness et al., 1955), whose authority in the scientific establishment was so great as to suppress this concept until sufficient experimental evidence was produced to support Schoenheimer's theory. Protein catabolism became an accepted process in the metabolism of cellular proteins (Schimke and Doyle, 1970).

Cells contain a variety of proteolytic enzymes, such as the serine proteases, which can cleave polypeptide chains (Rawlings and Barrett, 1994). However observations on the ATP-dependence of the rapidly degraded tyrosine amino-transferase (TAT) protein (Hershko and Tomkins, 1971) suggested another component of degradation machinery was present in cells. Fractionation of a reticulocyte lysate system led to identification of a small protein, ATP-dependent proteolysis factor 1 (APF-1) (Ciechanover et al., 1978), later identified as the ubiquitous (throughout all eukaryotic cells) protein ubiquitin (Ub, (Wilkinson et al., 1980)). This Ub, covalently linked to proteins, was suggested to target proteins for degradation by a specific ATP-dependent protease (Hershko et al., 1980). This process of discovery (discussed in more detail in (Mayer, 2005)) carried on with identification of the particular ubiquitylation machinery that comprises the Ub proteasome system (UPS, reviewed in (Glickman and Ciechanover, 2002, Hershko and Ciechanover, 1998, Pickart, 2001b, Pickart, 2001a, Weissman, 2001)).

Roles of ubiquitylation

Ubiquitylation and modification by the related ubiquitin-like (Ubl) modifiers can have a variety of signalling effects on proteins (reviewed in (Kerscher et al., 2006)). These moieties are covalently linked to their substrates.

Ubiquitylation itself has roles in an array of cellular processes. DNA repair and histone modification (Pickart, 2002), receptor endocytosis (Hicke and Dunn, 2003), endocytic sorting (Katzmann et al., 2002) and inflammatory responses (Deng et al., 2000) can all be mediated by ubiquitylation.

However the role for which Ub was originally discovered is protein degradation (Ciechanover, 1994). This has proven to provide control in cell signalling (Haglund and Dikic, 2005) and to provide control in the cell cycle and differentiation (see below), for example in differentiation of mammalian stem and progenitor cells (Naujokat and Saric, 2007). Spatio-temporal regulation of ubiquitylation within the cell is organized to allow a dynamic signalling network (Grabbe et al., 2011). Therefore ubiquitylation of proteins can be controlled by the cell to allow a fluid

response to changing conditions.

Ubls such as the small Ub-like modifier, or SUMO (Johnson, 2004) are involved not in targeting for proteasomal degradation, but in localisation or activation of proteins. For example, SUMOylation induces localisation of proteins to nuclear pore complexes or promyelocytic leukemia (PML) nuclear bodies (Zhong et al., 2000). On the other hand, these Ubl modifiers can indirectly affect the stability of proteins against proteasomal degradation. Neddylation (modification by a Nedd8 Ubl modifier) of cullins is required for activation of Skp1-Cullin1-F-box (SCF, see below) complexes (Wu et al., 2005). Therefore activation of an enzyme complex, which ubiquitylates proteins to target for destruction itself, requires Ub-like modification.

Likewise the ubiquitylation machinery can be utilized to the detriment of a host cell by a virus, such as in HIV budding (Pornillos et al., 2002). Malfunctions in the ubiquitylation machinery also have implications in cancer, Parkinson's Disease and Alzheimer's (Kerscher et al., 2006).

The Ub-Proteasome System (UPS)

The process of ubiquitylation is illustrated in Figure 1.3. It begins with the adenylation of the C-terminus of Ub by the Ub-activating (E1) enzyme using energy from the hydrolysis of ATP (Hershko et al., 1981). This modification activates the Ub moiety energetically throughout the ubiquitylation cascade for eventual transfer to the substrate protein. Ub is then covalently fused via a thioester linkage to a cysteine residue in the E1 by attack of the cysteine at the C-terminus of Ub, releasing AMP (Ciechanover et al., 1981). The E1 cannot just take Ub straight to the substrate (though such a concept is possible such as in non-ribosomal polypeptide synthesis (Cane and Walsh, 1999)). Ub is shuttled onto a cysteine residue of another enzyme, the Ub-conjugating (E2) enzyme (Hershko et al., 1983), of which there are a larger number (~50) (Wu et al., 2003). This E2 can then pass on the Ub moiety in one of two ways, in concert with an Ub (E3) ligase (of which there are several hundred kinds described below). Specificity increases through the ubiquitylation cascade from a single Ub-specific E1, to a larger number of E2s and then to hundreds of E3s (Semple,

2003). The E2 binds to the E3 ligase which itself binds the substrate protein (Hershko et al., 1986). The E3 ligase confers specificity for the substrate protein on the ubiquitylation process (Hershko, 1988).

The E2 may pass Ub directly onto the substrate protein using the E3 ligase as a scaffold, such as with the SCF complexes (Jackson et al., 2000); or the E2 passes Ub to a cysteine residue of a HECT (Homologous to the E6-AP Carboxyl Terminus) E3 ligase, which then passes Ub to the substrate protein (Huibregtse et al., 1995). In either case, Ub is passed onto the substrate protein, canonically onto a lysine residue to form an isopeptide bond. The cycle can then be repeated to add further Ub moieties to the Ub already attached to the protein. E4 ligases also exist, which add a polyUb chain to a monoubiquitylated site: p300 can carry out this function on a site monoubiquitylated by Mdm2 on p53 (Grossman et al., 2003). Proteins with a K48-linked polyUb moiety containing at least 4 Ub subunits are targeted to the 26S proteasome (Thrower et al., 2000), a multimeric complex consisting of α and β barrels in the 20S complex, capped by "lids" of 19S proteasome complexes (Pickart and Cohen, 2004). Using energy from ATP hydrolysis, proteins are unfolded from an unfolding initiation site (Prakash et al., 2004) and fed through the narrow channel formed by the 26S proteasome, where the substrate is cleaved into small peptides.

E3 ligases

An E3 ligase is an enzyme that facilitates transfer of an Ub moiety from the ubiquitylation machinery onto the substrate protein. This allows selection of the substrate to be targeted by the ubiquitylation machinery. There are various types of E3 ligases with many different structures and yet similar functions (this may be explained in part by entropic gains in solvent exclusion, suggesting that E3s function similarly through an entropic payoff rather than through a similarly-structured interaction, which would function by an enthalpic contribution (Truong et al., 2011)).

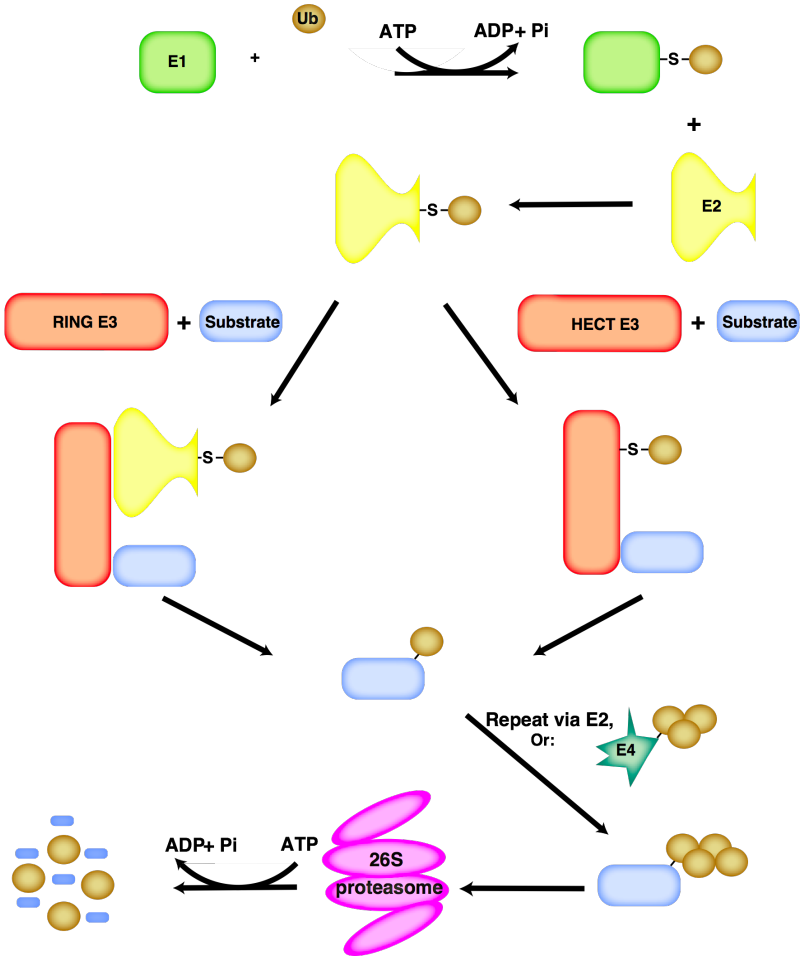

Figure 1.3: The Ubiquitin Proteasome System (UPS).

Ub is activated by an Ub-activating (E1) enzyme using energy from ATP hydrolysis and passed to an Ub-conjugating (E2) enzyme. Ub can then be passed to a substrate protein, specified by the particular E3 ligase that binds both the substrate and the E2. Many E3 ligases act as a scaffold to pass Ub from the E2 directly to the substrate protein whilst homologous to E6-AP carboxy-terminus (HECT) E3 ligases form a covalent bond with Ub themselves. The Ub moiety, covalently bound to the substrate protein, is then itself ubiquitylated by either successive rounds of ubiquitylation or by addition of a pre-assembled polyUb chain by the action of an E4 ligase. Once sufficiently ubiquitylated, the substrate is targeted to the 26S proteasome. The Ubs are cleaved from the protein by the action of de-ubiquitylating enzymes (DUBs) whilst the protein itself is, using energy from ATP hydrolysis and binding of ATP to the 26S proteasome, unfolded and cleaved into small peptides.

Really Interesting New Gene (RING) E3 ligases are the largest family of Ub ligases. They are assembled into a scaffold based on Cullin proteins and the most common are the S-phase kinase associated protein (Skp) 1-Cullin-F-box (SCF) complexes (Jackson et al., 2000). This multi-protein scaffold binds a particular F-box protein to generate the substrate specificity required of an E3 ligase (Petroski and Deshaies, 2005). SCF E3 ligases have a wide range of roles, not least in cell fate determination in a wide range of organisms mediated over a variety of tissue types (Hindley et al., 2011).

Homologous to E6-AP Carboxy-Terminus (HECT) E3 ligases share homologous C-terminal domains that are involved in ubiquitylation, whilst substrate specificity is achieved with a diverse range of N-termini. These ligases differ from all other E3 ligases in forming a covalent bond with the Ub moiety when picking it up from the E2 before passing it onto a substrate protein (Huibregtse et al., 1995). E6-AP itself is produced by human papilloma virus and is able to target p53 for degradation (Scheffner et al., 1993) thus promoting tumour formation in infected lesions.

The Anaphase Promoting Complex/Cyclosome (APC/C) is a multisubunit E3 Ub ligase (Sudakin et al., 1995, King et al., 1995). It is activated through the binding of Cell Division Cycle (Cdc) 20 in the metaphase-anaphase transition and Cdc20-homologue (Cdh) 1 in late mitosis-G1, releasing early mitotic inhibitor (Emi) 1 (Visintin et al., 1997). It remains active through to S phase. Cdh1 and Cdc20 are only active during late-M/G1/early-S and early-M phases of the cell cycle, respectively. Through this temporal control of the co-activators, the APC/C is able to control various checkpoints to prevent early or incorrect cell cycle progression (Manchado et al., 2010, Peters, 2006, van Leuken et al., 2008).

Mitotic cyclins are targeted as well as the complexes keeping sister chromatids together; the protein securin is cleaved by the APC/C allowing chromatid separation and the irreversible onset of anaphase (Zou et al., 1999). It also participates in targeting Skp2 (S-phase kinase-associated protein 2) degradation to prevent early S phase entry (Bashir et al., 2004).

The APC/C responds to DNA damage (Bassermann et al., 2008, Coster et al., 2007,

Townsend et al., 2009, Li and Zhang, 2009), and is implicated in tumorigenesis (Garcia-Higuera et al., 2008). Cell cycle-independent functions have also been established, particularly in the patterning and development of post-mitotic neurons (Manchado et al., 2010).

In addition, enzymes that can place pre-assembled polyUb chains onto ubiquitylated substrates have been discovered and are termed E4 ligases (Koegl et al., 1999). A good example is seen in the monoubiquitylation of p53 by Mdm2 (Lai et al., 2001), followed by addition of a K48-linked polyUb chain by E4 ligase activity of p300 (Grossman et al., 2003).

Modes of ubiquitylation

Ubiquitylation of a substrate protein is followed by ubiquitylation of the Ub itself on an internal lysine residue to build up a polyUb chain. The particular lysine ubiquitylated is regulated by the E2 (David et al., 2010) and various linkages of polyUb chains may confer various properties. For example, K48-linked chains target for proteasomal degradation (Thrower et al., 2000); but K11-linked chains can do so also (Song and Rape, 2011). Various other linked chains exist with various functions suggested (Pickart and Fushman, 2004). Many other possibilities of homologous, heterologous and branched Ub chains are possible and the functions of these are yet to be elucidated.

26 S proteasome

The structure of the 26S proteasome is complex and reviewed in (Coux et al., 1996). Basically the proteasome consists of a barrel-shaped core 20S particle flanked at either or both ends by a 19S regulatory particle (Schrader et al., 2009).

Proteins are targeted for the proteasome once a polyUb chain of at least 4 Ubs is covalently attached (Thrower et al., 2000). The 26S proteasome binds polyUb chains through the 19S lid component, which also contains an ATPase activity (Glickman et al., 1998). This regulatory particle unfolds proteins to allow them to feed through the

narrow channel at the centre of the 20S particle where proteolysis occurs (Braun et al., 1999). There is an interdependence between ubiquitylation sites and unfoldable regions of a protein to allow it to be unfolded (Prakash et al., 2004) and it may be that Ub itself can aid in this unfolding (Hagai and Levy, 2010).

At the lid of the proteasome, and indeed throughout all stages of the ubiquitylation process, de-ubiquitylating enzymes (DUBs (Wilkinson, 1997)) such as Rpn11 act to cleave Ub itself from the substrate (Verma et al., 2002). This adds reversibility to the polyubiquitylation pathway and prevents Ub itself from being cleaved by the proteasome. PolyUb chains are cleaved from the substrate at the surface of the proteasome to liberate free Ub. PolyUb chain 'trimming', releasing individual Ub units from a polyUb chain, assists proteasomal degradation and may facilitate loading of polyubiquitylated substrates at the proteasome (Zhang et al., 2011).

Ubiquitylation and the cell cycle

Ubiquitylation and proteasomal degradation of proteins is important in modulating the cell cycle and particularly in targeting cyclins for degradation (reviewed in (Hershko and Ciechanover, 1998)). The role of ubiquitylation in the cell cycle is demonstrated early on as even E2 enzymes can exhibit specific cell cycle roles. The E2 enzyme Ubc3/Cdc34 is particularly active in the G1 to S-phase transition (Mathias et al., 1996). E2-C is also involved in cell cycle regulation by ubiquitylation of cyclin B in concert with the APC/C (Hershko et al., 1994). Mitotic cyclin ubiquitylation can also be performed by Ubc11/Ubc4 (Yu et al., 1996).

Cyclin B is a mitotic cyclin which combines with the cyclin dependent kinase cdk1 to promote entry of the cell cycle into mitosis (Evans et al., 1983). Cyclin B degradation is mediated by the UPS (Hershko et al., 1991) in *Xenopus laevis* egg extracts (Glotzer et al., 1991) and by interaction with Hip2 (Bae et al., 2010). The degradation of cyclin B is regulated in a cell cycle-dependent manner by the reversible phosphorylation and hence activation of the APC/C (Lahav-Baratz et al., 1995). The degradation of cyclin B is absolutely required for processes allowing progression of the cell cycle past mitosis, such as reformation of the nuclear envelope and chromosome

decondensation (Murray, 1989).

G1-phase cyclins are also targeted for UPS-mediated degradation, but with a requirement for a priming phosphorylation, as observed for cyclin E (Won and Reed, 1996, Clurman et al., 1996) and cyclin D1(Diehl et al., 1997).

Canonical ubiquitylation

Canonical ubiquitylation sites are described as lysine residues in the definition of the UPS given above (Freiman and Tjian, 2003).

Unlike many post-translational modifications (PTMs) and even Ub-like modifiers such as SUMO, there is no known consensus site for identifying a ubiquitylation site (Peng et al., 2003). There are examples of protein ubiquitylation occurring on specified lysines, such as lysines 21 and 22 in IκBα (Baldi et al., 1996). Conversely there are proteins where ubiquitylation can occur on any lysine, for example c-Jun (Treier et al., 1994) and cyclin B (King et al., 1996).

From the canonical description of ubiquitylation (Freiman and Tjian, 2003), removal of all lysine residues in a protein should completely stabilise against Ub-mediated proteasomal degradation. Indeed there are examples of proteins that appear completely stabilised by removal of lysines, most commonly by mutation of lysines to arginines or even by chemical modification of lysines (Hershko et al., 1986). But many investigators observed that proteins were still being polyubiquitylated and that these polyUb chains could still target the substrate protein for proteasomal degradation. Where could this ubiquitylation be occurring?

N-terminal ubiquitylation

Lysine residues form a covalent linkage to Ub by formation of an isopeptide bond to the carboxy terminus of Ub, activated by the enzyme cascade in Figure 1.3, using the amino group. But all proteins contain another amino group. Polypeptides consist of a backbone created by peptide bond formation between amino acid residues. In a

linear chain there is therefore a free amino group (at the N-terminus) and a free carboxylate group (at the C-terminus). Theoretically, the N-terminus could be modified by Ub in the same way as lysines.

The xNgn2 homologue in myogenesis, MyoD, is also a short-lived protein (Thayer et al., 1989, Abu Hatoum et al., 1998) and is partially stabilised by mutation of all lysine residues to arginine residues (Breitschopf et al., 1998). Most lysines are in the N-terminal region of the protein and the stability is not affected by one individual lysine residue alone. Also no lysosomal degradation was observed for MyoD. Blocking of amino groups from ubiquitylation by reductive methylation, and of the N-terminal amino group of the peptide backbone specifically by carbamylation (Hershko et al., 1984), illustrated that not only did blocking the N-terminal amino group stabilise the protein, but that lysines were unable to be ubiquitylated. N-terminal ubiquitylation may be required as a 'priming' ubiquitylation (Breitschopf et al., 1998).

There are naturally occurring lysineless proteins where this non-canonical ubiquitylation (i.e. ubiquitylation on sites other than lysine amino groups) in fact must be essential for UPS-mediated degradation to occur, such as $p16^{INK4a}$ and HPV-58 E7 (Ben-Saadon et al., 2004).

Moreover, the Ub fusion degradation (UFD) pathway targets proteins for degradation where Ub is fused linearly via its C-terminus to the N-terminus of a protein (Johnson et al., 1995).

Here we differentiate ubiquitylation of the N-terminal amino group itself from ubiquitylation by the 'N-end rule' ((Wang et al., 2008), reviewed in (Varshavsky, 2011)). A destabilizing N-terminal residue in a protein can act as a degron to facilitate ubiquitylation and proteasomal degradation. However the Ub moiety in this case is fused to an internal lysine residue and not to the N-terminal amino group. Therefore the N-terminus acts as a signal but not as an acceptor for ubiquitylation.

The N-terminal residue of MyoD is not converted into a lysine (as occurs with conversion of some acidic residues to arginine to target for ubiquitylation (Ferber

and Ciechanover, 1987)). The effects of the N-end rule were also dismissed as N-end rule inhibitors had no effect on the stability of MyoD (Breitschopf et al., 1998). Fusion of a Myc-tag to the N-terminus did stabilise MyoD (Breitschopf et al., 1998) but there was no C-terminal fusion as a control.

This N-terminal ubiquitylation is apparent in a number of proteins (Breitschopf et al., 1998, Chen et al., 2004, Ciechanover and Ben-Saadon, 2004, Kuo et al., 2004, Mayer, 2005, Sadeh et al., 2008). Recent evidence has shown a role in cell cycle-regulating proteins such as cyclin G1 (Li et al., 2009). There are many ways in which the N-terminus can affect protein stability including N-terminal ubiquitylation, providing E3 ligase binding sites and N-terminal co-translational acetylation (Meinnel et al., 2005, Meinnel et al., 2006). N-terminal co-translational acetylation is suggested to occur in 75% of eukaryotic proteins (Polevoda and Sherman, 2003a) although investigation of N-terminal processing disputes this and places the figure at 30% (Meinnel et al., 2005). However studies had been made of protein degradation in N-terminally acetylated proteins (Polevoda and Sherman, 2002) and the process of N-terminal acetylation is well characterised, including N-terminal consensus sites for the regulation of acetylation (Bradshaw et al., 1998, Polevoda and Sherman, 2002, Polevoda and Sherman, 2003b, Polevoda and Sherman, 2003a, Utsumi et al., 2001). Acetylation is irreversible and so acetylation and ubiquitylation are mutually exclusive reactions. Therefore N-terminal mutations can be introduced to alter the N-terminal sequence and either up- or down-regulate co-translational acetylation.

How then to investigate N-terminal ubiquitylation? Deletion of a portion of the N-terminus - say the first 20 residues – might be used to demonstrate the importance of the N-terminus in targeting the substrate for polyubiquitylation. However this may not allow distinction of N-terminal ubiquitylation from ubiquitylation targeted by the N-End Rule (Varshavsky, 1997) - both may require a particular sequence at the N-terminus to target for ubiquitylation but the modification will occur at different sites in the two processes. The most obvious caveat is that there is always a free amino group at the N-terminus of a truncated protein. Therefore blocking the N-terminus more directly is necessary.

A common strategy is to add a bulky tag to the N-terminus of the protein (Trausch-Azar et al., 2010) under the rationale that such a group will physically block the normal N-terminal site from being ubiquitylated. In many cases this does seem to work, but there are many factors to consider under such an experimental design. Firstly, there is some debate as to what defines a "bulky" tag ((Trausch-Azar et al., 2010) and personal communication, Alan Schwartz). Is an HA tag sufficient? Or is a tag on the order of GFP required to block the site sufficiently? Secondly, once a tag is established as suitable and stabilises the protein when fused to the N-terminus, it is important to also check as a control that fusion of the same tag to the C-terminus does not also stabilise the protein and this is often not checked (Vosper et al., 2009). In the case of intrinsically disordered proteins it may well be the case that a tag, particularly a folded tag such as GFP, may stabilise the protein through blockage of unfolding initiation sites also required for proteasomal degradation (Prakash et al., 2004). This is indeed the case with the disordered protein Ngn2 (Supplementary data in (Vosper et al., 2009)). Work in our lab making fusion proteins with N- and C-terminal tags proved that use of bulky tags was an unreliable method for studying protein degradation at the N-terminus as tags at either end of the protein stabilised xNgn2, possibly due to steric or unfolding issues, rather than simply blocking N-terminal ubiquitylation (Vosper et al., 2009). N-terminal fusion of GFP stabilises xNgn2, but so does the C-terminal fusion, rendering discussion of N-terminal ubiquitylation unreliable using these results.

A third approach could be using chemical methods to block the N-terminus. This includes reductive methylation with sodium cyanoborohydride, guanidination with O-methylisourea or carbamylation (Breitschopf et al., 1998). Due to the similarity in functionality, blocking of all lysine residue side-chains will occur simultaneously with methylation. However guanidination is specific to lysine residues whilst carbamylation is specific to the N-terminal amino group only. I opted for a fourth method to specifically block the N-terminus alone. Particular amino acid residues at the N-terminus can up- or down-regulate the process of co-translational N-terminal acetylation (Bradshaw et al., 1998, Polevoda and Sherman, 2000, Polevoda and Sherman, 2003b, Polevoda and Sherman, 2003a) which is a mutually exclusive reaction to N-terminal ubiquitylation preventing further modification of the N-

terminus. The effect of N-terminal acetylation on protein stability can be checked by blocking acetylation using the Palmiter method (Palmiter, 1977).

Non-canonical ubiquitylation sites

By whatever means available, a wide range of substrates for N-terminal ubiquitylation have been identified (Ciechanover and Ben-Saadon, 2004). An additional site for ubiquitylation to the established lysines, the N-terminus still resembles them chemically. But it is possible to generalise the mechanism further. Lysines are able to form isopeptide bonds due to the presence of a nitrogen atom that can attack the thioester linkage between the Ub and E2 enzyme. In this manner the nitrogen is acting as a nucleophile, attracted to electropositive centres by virtue of its lone pair of electrons that can attack the thioester linkage at the electron-deficient carbonyl carbon, which acts therefore as an electrophile. There are however other examples of nucleophilic groups in proteins: I have already discussed the N-terminal amino group, but what about other nucleophiles aside from nitrogen? In fact there are several amino acid residues with the potential to attack electron-deficient carbonyl carbons as nucleophiles. Serines, threonines and tyrosines are all residues containing electron-rich oxygen atoms capable of forming hydroxyester bonds; and cysteine residues have the potential to act as nucleophiles using lone pairs of electrons on sulfur.

Two key questions must be asked with respect to non-canonical ubiquitylation: does it actually occur; and is it physiologically relevant?

Ub-thioester linkages

Non-canonical ubiquitylation is also beginning to appear in the literature, describing ubiquitylation on nucleophilic residues such as cysteine for peroxisomal degradation (Carvalho et al., 2007, Grou et al., 2008, Kragt et al., 2005, Leon and Subramani, 2007, Williams et al., 2007) and by viral E3 ligases (Cadwell and Coscoy, 2005, Cadwell and Coscoy, 2008).

That cysteine residues might undergo modification by ubiquitylation may seem at first counterintuitive - after all, thioester linkages (in a manner similar to disulphide bonds) can be broken under reducing conditions and the intracellular environment is often simply referred to as a "reducing" environment. However, as described above and in Figure 1.3, at each stage of the ubiquitylation process before loading Ub onto the substrate, the E1/2/3 enzymes are all able to carry Ub on a thioester linkage. Indeed it is this activated linkage that allows facile attack of the substrate nucleophile. The stability of these intermediates was recently discussed and found to be intrinsically highly stable (Song et al., 2009).

A role for cysteine ubiquitylation was first identified in the peroxisomal import factor Pxp5 to give a signalling role (Carvalho et al., 2007, Grou et al., 2008, Kragt et al., 2005, Leon and Subramani, 2007, Williams et al., 2007). Whilst signalling might be considered a transient process in which a weak thioester linkage to ubiquitylation might provide for a more dynamic system, it might seem unlikely that thioester linkages could be maintained long enough to allow development of a polyUb chain (canonically, a K48-linked Ub tetramer or longer) then targeting for degradation. The first evidence that this polyubiquitylation can occur, however, came from viral E3 ligase systems (Cadwell and Coscoy, 2005, Cadwell and Coscoy, 2008).

The caveat with this work is that viral systems may exhibit completely different behaviour to cellular systems in general. My work focuses on using the vertebrate system *Xenopus laevis* and the mammalian P19 embryonal carcinoma cell line.

Ub-ester linkages

My work in xNgn2 suggests a role for serines and threonines in ubiquitylation *in vitro* in *Xenopus laevis* extracts and P19 cell lines (McDowell et al., 2010). Evidence for this had previously been suggested in the apoptotic protein Bid (Tait et al., 2007) albeit with the caveat that structural properties such as folding stability could not be ruled out as targeting Bid for degradation.

The strongest evidence for Ub-ester linkages comes from research into the

endoplasmic reticulum-associated degradation (ERAD) pathway. Serines and threonines are sufficient for ubiquitylation of major histocompatibility complex I heavy chain by the viral E3 ligase mK3 targeting for ERAD (Wang et al., 2007). In this case lysines are also present in the cytoplasmic tail of the heavy chain.

However an absolute requirement for a serine residue in targeting a protein for ERAD was demonstrated in TCRα. The cytoplasmic tail of TCRα consists of the residues RLWSS and is not only ubiquitylated and degraded but replacement of serines with alanines reduces this ubiquitylation whilst mutation of serines to cysteines, threonines or lysines maintains ubiquitylation and degradation (Ishikura et al., 2010).

Whilst containing a similar nucleophilic hydroxyl group to serines and threonines, tyrosines consist of a phenolic group, which may be less reactive than the aliphatic serine and threonine residues. The presence of an aromatic ring in this residue may result in delocalisation of electron density around the aromatic system resulting in a less reactive lone pair of electrons on the hydroxyl group. No direct evidence for tyrosines as non-canonical sites of ubiquitylation has been demonstrated. Indeed, when replacing serines with tyrosines in the cytoplasmic tail of TCRα, no ubiquitylation was observed (Juan Bonifacino, personal communication) in contrast to replacing serines with threonines (Ishikura et al., 2010).

bHLH protein degradation

Transcription factors tend to be highly unstable proteins (examples in (Hershko and Ciechanover, 1998)) allowing highly dynamic protein levels, easily adjusted in response to intrinsic and extrinsic cell factors.

The role of the UPS in myogenesis has been extensively researched in the bHLH protein MyoD (Breitschopf et al., 1998) as discussed above. Myogenin, the downstream target of MyoD, is destabilized as a result of the action of Bone Morphogenic Protein (BMP) signalling through the Id proteins (Vinals et al., 2004). Id proteins, which contain the Helix-Loop-Helix motif but lack the basic domain and so prevent DNA binding, are themselves degraded by the proteasome (Bounpheng et al.,

1999).

However the role of the UPS in proneural protein regulation has only recently been investigated. The bHLH proneural protein and achaete-scute homologue, Mash1, is destabilized indirectly by BMP signalling (Shou et al., 1999). This is through UPS-mediated degradation (Vinals et al., 2004). Previous to work contained in this thesis, xNgn2 was found to be degraded by the UPS with a short half-life (Vosper et al., 2007). Interestingly the bHLH protein and downstream target of xNgn2, xNeuroD, is stable under the same conditions in *Xenopus laevis* egg extract (Vosper et al., 2007). However outside of unpublished data on the non-canonical ubiquitylation of xNgn2 in *Xenopus laevis* egg extract systems (Vosper, 2008), and a yeast two-hybrid screen suggesting possible E3 ligases for xNgn2 (Gabriel Markson and Anna Philpott, unpublished data), the mechanism of bHLH proneural protein degradation was largely unexplored. The differences in xNgn2 and xNeuroD stability illustrate different degradation behaviour within the same family of proteins. The UPS-mediated degradation of bHLH proteins cannot therefore be generalized and warrants further investigation.

Phosphorylation and Stability

Protein phosphorylation is a PTM that places a phosphate group upon a protein to act as a signal for a range of processes (Tarrant and Cole, 2009). The role of phosphorylation in the cell cycle is evident from the importance of kinases, enzymes that place phosphate moieties on proteins (Schafer, 1998). Phosphorylation has been implicated in targeting proteins for degradation (Thien and Langdon, 2001, Jimenez et al., 1999). Phosphorylation even affects the ubiquitylation process itself, for example by modulating the E2 activity of Cdc34 through allosteric effects on the catalytic site by phosphorylation in a particular region (Papaleo et al., 2011).

Transcription factor activity is tightly regulated and control can be achieved at the level of phosphorylation (Tootle and Rebay, 2005). The role of Xic1, a cdki, in stabilising xNgn2 led to interest in the phosphorylation of xNgn2 as a means of regulating stability (Vernon et al., 2003). Similarly $p27^{Kip1}$ stabilises mNgn2 in the

mouse cortex (Nguyen et al., 2006). xNgn2 has clearly been shown to be phosphorylated in a manner affecting its function (on Y241 in mNgn2, (Hand et al., 2005) and in motor neuron specification, (Ma et al., 2008)) and its stability (on T118 in xNgn2, (Vosper et al., 2007)). The phosphorylation state of the transcription factor Olig2 whilst bound to promoter regions of DNA regulates proliferation of neural progenitors (Sun et al., 2011) and the same may be the case for xNgn2.

There is a clear link between the signalling roles of phosphorylation and ubiquitylation for proteasomal degradation (Hunter, 2007). Targeting of substrates for degradation by the SCF complex (Skp-Cullin-F-box) requires phosphorylation of conditional 'phosphodegron' sites (Willems et al., 2004). This phosphorylation is required for the production of substrate-E3 ligase interactions (Mayer, 2005). Indeed phosphorylation, without ubiquitylation, can be sufficient to target proteins for proteasomal degradation (Machiya et al., 2010). Skp2 substrates require phosphorylation at an (S/T)P minimal motif (Bornstein et al., 2003). Also the GSK3-β consensus phosphorylation site in IκB targets for ubiquitylation and degradation (Winston et al., 1999) and likewise for β-TRCP-mediated degradation there are consensus SP phosphorylation sites in Sic1 that have been investigated (Nash et al., 2001).

The stability of many bHLH proteins such as MyoD is regulated by phosphorylation events (Kitzmann et al., 1999). In the case of MyoD degradation can be regulated by phosphorylation events on cdk consensus sites (Song et al., 1998).

Phosphorylation regulates transcriptional activation in another bHLH protein, Twist (Lu et al., 2011). However phosphorylation by MAPK also stabilises Twist against UPS-mediated degradation. Activation of the Ras signalling pathway results in elevated levels of Twist, leading to transition in breast cancer cells from epithelial to mesenchymal and promoting metastasis (Hong et al., 2011).

Ubiquitylation, even if assisted by phosphorylation, is not enough to target proteins for proteasomal degradation; an unfolding initiation site is also required (Prakash et al., 2004). This unfolding may be facilitated by structural disorder in proteins.

Intrinsic Disorder (ID)

What is ID?

Proteins carry out various roles in the cell as a function of their structure. Enzymes require specific active sites to carry out catalysis and structural proteins require particular conformations to achieve mechanical strength. However the problem of how a protein actually achieves its structure was posed in the protein folding paradox. How can a protein molecule, with all the possible conformations available to it through all possible angles of rotation around interatomic bonds, ever achieve a required structure? A random distribution gives the time taken to find a particular conformation as longer than the lifetime of the universe (Levinthal, 1969).

The solution lies in challenging the assumption that a protein arrives at a functional structure by random chance. The overall thermodynamic stability of the molecule as the sum of hydrophobic interactions, electrostatics and Van der Waal's forces is important. The formation of local interactions, such as hydrophobic interactions (Dyson et al., 2006) leading towards the final structure down a "folding funnel" energy landscape can contribute to allow a protein to find its structure in microseconds (reviewed in (Dill et al., 2008)).

However it has become apparent that many functional proteins are, in fact, not natively folded at all times in the cell (Dyson and Wright, 2006). Disorder in proteins arising from amino acid residue position variation leads to loss of electron density in X-ray crystallography (Bloomer et al., 1978). Highly dynamic protein regions are observable from nuclear magnetic resonance (NMR) experiments, such as the functional tail of histone H5 (Aviles et al., 1978) and even proteins that appear entirely disordered throughout their full length are common such as $p21^{Waf1/Cip1/Sdi1}$ (Kriwacki et al., 1996). Proteins that are natively unfolded and lacking regular structure are termed intrinsically disordered (ID) proteins (Dunker et al., 2001).

ID proteins show a lack of hydrophobicity (Gast et al., 1995) and extreme pI (isoelectric point) values at neutral pH due to a large net charge from a high

prevalence of charged residues (see Table 1 in (Weinreb et al., 1996)). In a comparison of ID protein databases, it was found that the amino acid residues W, F, Y, I, L, V, C and N, I, L and V were under-represented in ID proteins whilst A, G, P, R, Q, S, E and K were abundant (H, M, T and D showed no deviation from random prevalence either way) (Dunker et al., 2001). Length-dependent prediction of disorder (Peng et al., 2005) shows a propensity for G and D in short ID segments and K, E, and P in longer sections, while there was a reduction in I, V and L in short segments and G and N in the longer.

It has also been suggested that there is an increased rate of evolution in ID segments and proteins (Brown et al., 2002). Therefore it may be that in these regions there is a lack of function allowing unconstrained mutation; or perhaps the function of the protein is disorder itself and so a lack of evolutionary constraint on specific sequence allows a larger amount of variability. This also suggests that the behaviour of related proteins within families of similar folds may actually be quite different.

Roles of ID proteins

The investigation of ID proteins has advanced significantly in the last decade fuelled in part by the discovery that they are actually more common in eukaryotes than archaea or eubacteria, and by the large variety of cellular processes affected by unfolded proteins (Dunker et al., 2008a).

An investigation of the gene ontology (GO) terms associated with ID proteins highlights a significant number of proteins are involved in DNA-binding, transcription activation and acting as transcription factors (Ward et al., 2004). Predicting function of disordered proteins is difficult (Dunker et al., 2008b) due to the low sequence homology between possibly related proteins as a result of higher levels of mutation and lower sequence conservation in disordered regions of related proteins (Brown et al., 2002). Most function is assigned to ID proteins by individual study and in particular a role in cell cycle regulation has been highlighted by study of the ID proteins p21 and p27, which are cdk inhibitors (reviewed in (Galea et al., 2008)).

Many proteins appear to fold or have folding stabilised upon association with other binding factors ((Uversky et al., 2000, Sugase et al., 2007), reviewed in (Wright and Dyson, 2009)). Particular motifs for recognising and binding interacting partners, molecular recognition elements (MoREs), are proposed that become ordered upon binding (Oldfield et al., 2005). Furthermore, entire proteins may become folded upon binding, but may still be highly dynamic, forming "fuzzy complexes" (Tompa and Fuxreiter, 2008). Indeed, this is suggested to be the case for Ngn1, which overlaps in function with Ngn2 in neural development (Aguado-Llera et al., 2010).

Protein-protein and protein-nucleic acid binding interactions appear to be an important role for intrinsic disorder and thermodynamically this gives flexibility to signalling processes and assembly of complexes in the cell. The free energy of binding is counteracted by the free energy required to fold the structure and so overall there is a small free energy change. Whilst this allows only a low affinity of binding, there is therefore high specificity achieved by requiring the correct binding interactions and easy reversibility is obtained (Dunker et al., 2002). So small are the energy differences involved, perhaps it could allow minor changes to the structure of a protein, say by PTM, to alter the formation of multi-factor complexes dramatically. For example, this may allow tweaking of transcription dynamics to form slow or fast promoter complexes (Hager et al., 2009, Michel, 2009), particularly as ID proteins exhibit less transcriptional noise than structured proteins and so appear to be regulated at the point of destruction (Gsponer et al., 2008).

ID protein stability and phosphorylation

The presence of disordered regions in proteins allows access to sites for PTM, such as ubiquitylation and phosphorylation (Gsponer et al., 2008). Regulation of PTMs and blocking them by interaction with cofactors can regulate protein stability (Dunker et al., 2001, Grimmler et al., 2007, Kriwacki et al., 1996, Wu et al., 2007).

The mRNAs of ID proteins and the proteins themselves are unstable, and the level of formation of protein product is lower when compared with structured proteins (Gsponer et al., 2008). Proteases may be able to break down ID proteins but a

comparison of the literature suggests that this is not always the case. The activity of proteases can be prevented by their sequestration; by regulation of protease activity by the cell; or by preventing protease association with the protein by lacking targeting residues, or blocking off sites sterically. Protease sites could also be blocked by association with cofactors (all reviewed in (Dunker et al., 2002)). Ubiquitylation sites often contain charged residues and fewer hydrophobic residues. It is suggested that this could facilitate contact with an E2 (Cai et al., 2011). As mentioned above, ID proteins are more charged and less hydrophobic than more structured proteins (Dunker et al., 2001). Indeed association of a disordered region with another cofactor can prevent ubiquitylation such as in the case of β-catenin, which has PEST sequences targeting for ubiquitylation towards UPS-mediated degradation. However, on association with E-cadherin, this ubiquitylation is sterically blocked (Huber et al., 2001). It is suggested that a way of differentiating ID proteins and linker regions from misfolded proteins is the lack of hydrophobic residues exposed thus suggesting a way of allowing disorder to fulfil a function without being degraded (Dyson and Wright, 2005b).

There is a large correlation between amino acid composition of ID proteins and phosphorylation sites suggesting phosphorylation is promoted in disordered regions (Iakoucheva et al., 2004). Further, ID proteins are targeted by twice as many kinases as structured proteins (Gsponer et al., 2008). Many of those kinases whose substrates are mainly unstructured proteins also tend to be regulated in a cell cycle-dependent manner (Gsponer et al., 2008). This phosphorylation can regulate protein stability, as observed for p27 (Chu et al., 2007).

ID proteins may be particularly susceptible to proteasomal degradation by providing easily unfolded regions of a protein. An unfolding initiation site is required for proteasomal degradation (Prakash et al., 2004). In fact proteins with unstructured regions can be degraded by the UPS without PTM if they associate with ubiquitylated proteins (Prakash et al., 2009). Ub-independent proteasomal degradation is arguably demonstrated in a growing number of proteins (Jariel-Encontre et al., 2008) such as in virus-induced tumours (Hwang et al., 2011).

NMR studies of ID proteins

NMR spectroscopy allows us to investigate materials with atomic resolution. The technique relies on the properties of certain 'spin-active' nuclei when placed in a magnetic field. The basic principle is to perturb the equilibrium of spin-states of these nuclei by irradiating the molecule sample with a broad band of radio frequencies and to measure a free induction decay (FID) as the spins collapse back to equilibrium by a process called relaxation. Return to equilibrium is associated with a specific frequency for each nucleus or spin. In a macroscopic description, this can be viewed as a decrease of the signal in the xy plane whilst the net magnetisation increases back along the z-axis parallel to the static magnetic field. To translate the time domain into a frequency domain the FID is Fourier transformed.

The frequency of each individual nucleus is expressed as chemical shift in parts per million of the static field relative to a reference molecule within the sample so that measurements can be compared independently of the field of the spectrometer (e.g. 600 MHz or 900 MHz). The resonance of each individual nucleus is affected by the environment of the atom and therefore by the amino acid residue sequence, spatially close residues in a 3D structure or even the conformation of the residue itself (for example in an α-helix or β-sheet).

Protein NMR can be carried out using various spin-active nuclei. ^{1}H or proton NMR is possible for all proteins as the ^{1}H isotope has 100% natural abundance. ^{13}C and ^{15}N isotopes are spin active but have a low natural abundance and so proteins must be artificially enriched in these nuclei.

Studying large folded proteins is difficult using NMR because their nuclei are associated with a fast relaxation time due to the dynamic properties of these large objects. Large proteins do not reorient themselves rapidly enough in the magnetic field (corresponding to a large correlation time τ_C), creating local fluctuation of the magnetic field and faster relaxation. As a consequence, the resonances are broadened sometimes even beyond detection. ID proteins have in contrast fast molecular dynamics that allow a good averaging of the magnetic field during the data

acquisition. They have longer relaxation times compared to folded proteins of the same size, and narrow resonances that allow good detection and resolution (Cavanagh et al., 2006).

NMR can be carried out in proteins in one dimension by investigating a single species of spin-active isotope (e.g. ^{1}H only) or by combining the spectra by heteronuclear single quantum coherence (HSQC) of two isotopes (e.g. 2D ^{1}H-^{15}N HSQC) or even three (3D ^{1}H-^{15}N-^{13}C HSQC) (Bhavesh et al., 2001). 1D proton NMR of proteins is of limited use due to the number of nuclei present that will result in a spectrum of severely overlapped signals. Use of multiple dimensions will thus spread these signals in addition to giving information on several nuclei. The 2D ^{1}H-^{15}N HSQC acts as a "fingerprint" of the protein as it will give a point for each amino acid residue (except proline, which lacks a proton and so is not seen by 2D ^{1}H-^{15}N HSQC). In a HNCACB experiment, the additional ^{13}C dimension will allow identification of the amino acid residue associated with each ^{1}H-^{15}N correlation in the HSQC (CA and CB of residue i) and also connect it to its preceding residue in the sequence (CA and CB of residue i-1).

NMR can thus be used to study ID proteins (Dyson and Wright, 2005a, Dyson and Wright, 2004). Although these proteins do not have a 3D structure, they can have local transient secondary structures and preferred topologies that will influence their function, for example their interaction with other protein partners or their aggregation propensity. The transient secondary structure could be associated with a molecular recognition element (MoRE), but this is not always the case (Marsh et al., 2010).

NMR is a technique that will allow the characterisation of these very dynamic features. Specific examples of ID proteins studied by NMR include CREB, to investigate "fly-casting" using disordered regions to find binding partners and stabilise folding intermediates (Sugase et al., 2007). Studies have also identified natively unfolded domains in non-structured protein 5A (NS5A) from hepatitis C virus (HCV) (Hanoulle et al., 2009) and NMR has been used towards an investigation of the Tau protein associated with Alzheimer's disease (Verdegem, 2009).

Xenopus laevis

To study proneural protein structure and how this relates to function it is important to use a system where biochemical analysis can be easily translated into investigations of functionality.

Xenopus laevis have had a large contribution to research in developmental biology and other areas (Callery, 2006). *Xenopus laevis* represents a model organism that is very easy to work with: producing large volumes of large (therefore easily microinjected) eggs useful for both *in vivo* studies and *in vitro* assays.

Xenopus eggs and embryos can also be manipulated to make cytoplasmic extract systems (Murray, 1991) that can carry out various cellular processes such as ubiquitylation and phosphorylation.

Ubiquitylation processes are highly conserved in eukaryotes – Ub itself is conserved from yeast to humans – and so *Xenopus laevis* can be used to investigate ubiquitylation processes relevant to other organisms. Much work has been carried out on ubiquitylation processes in *Xenopus laevis* such as investigation of β-catenin stability (Salic et al., 2000) and investigation of the anaphase-promoting complex (APC) (Kimata et al., 2008, Yamano et al., 2004).

The uses of *Xenopus* in biophysical and protein structural methods are also being explored, for example allowing in-cell NMR of proteins (Selenko et al., 2008) and investigation of brain tissue using mass spectrometry (Serrano et al., 2010).

Xenopus embryos are easily manipulated and can be used to investigate the role of protein produced from microinjected mRNA, for example using *in situ* hybridisation to look for particular cell types. *Xenopus laevis* embryos have an added advantage in that the bilateral symmetry of the embryo is fixed at the first cleavage after fertilisation. Cells do not mix between the left and right sides. Therefore microinjection of mRNA into one of these two cells allows a comparison between the injected and uninjected sides of the embryo (Sive et al., 2000).

As a vertebrate organism *Xenopus laevis* allows study of developmental processes relevant to humans and has great promise for work in the future (Beck and Slack, 2001).

Aims

Controlling the level of a transcription factor in the cell is crucial to mediating its function. The transcription factor xNgn2 plays an important role in neurogenesis by determining cell fate and causing cell cycle exit.

Work in this dissertation investigates the regulation of stability of bHLH proteins and in particular the *Xenopus laevis* transcription factor Ngn2. The role of PTMs (such as ubiquitylation and phosphorylation), protein folding and intrinsic disorder are explored. The techniques used to carry out this work are described in detail in Chapter 2.

Chapter 3 details the role of ubiquitylation on lysine residues in regulating the stability of xNgn2. I aim to present detailed evidence of ubiquitylation of xNgn2 on lysine residues that affects xNgn2 stability. The relationship between stability and activity will be investigated *in vitro* and *in vivo* using *Xenopus laevis* extracts and embryo microinjection.

Chapter 4 then describes the role of other potential sites of ubiquitylation, such as the N-terminus, and nucleophilic residues such as cysteines, serines and threonines, on regulating xNgn2 stability. I aim to investigate the possible physiological relevance of non-canonical ubiquitylation in both *Xenopus* extract systems and the P19 embryonal carcinoma cell line. Chapters 4 and 5 will highlight the importance of ubiquitylation on various sites in xNgn2, which occurs in a cell cycle-dependent manner and is also observed in cell lines.

Chapter 5 introduces protein phosphorylation on cdk consensus sites and the role that this has in relation to xNgn2 stability *in vitro* and activity *in vivo*. I aim to show

the relationship between phosphorylation, ubiquitylation, and the role of xNgn2 at the promoter of downstream transcriptional targets.

Chapter 6 investigates the role of protein folding in stability, through experiments looking at binding of cofactors to xNgn2, to assess how stability of the active complex of xNgn2 is regulated. Using chimeric proteins of xNgn2 and xNeuroD, I will attempt to identify whether bHLH proteins contain regions which affect stability and possibly regulate degradation.

Finally, Chapter 7 will describe work carried out in collaboration with Guy Lippens and Isabelle Landrieu at the Université de Sciences et Technologies Lille, using NMR to study intrinsically disordered regions of mouse Ngn2. I will then provide evidence for phosphorylation of mNgn2 by cyclin dependent kinases and how this affects the structure of the intrinsically disordered protein.

CHAPTER 2

Materials & Methods

Plasmids

Plasmids used were pCS2 vectors containing the gene of interest, which had been kindly prepared for the lab previously by Ian Horan, Catherine Wilson, Helen Wise, Jonathan Vosper, Ali Jones or were prepared by myself as described in the text.

In Vitro Transcription/Translation

In vitro transcription and translation of radiolabelled proteins was carried out using the Promega SP6 (or in the case of MyoD KO, T7) TNT® Master Mix Kit. Aliquots of the reticulocyte lysate were defrosted from -80 °C by hand and to this 1/10 ^{35}S-methionine (Perkin Elmer) and 1/10 250 ng μl^{-1} plasmid solution (in H_2O) were added. IVTs were then incubated at 30 °C for 2 hours. IVTs were stored at -20 °C.

In Vitro Fertilisation & Embryo Handling (Sive et al., 2000)

Female wild type *Xenopus laevis* had been previously primed a week before required by injection of Pregnant Mare Serum Gonadotropin (PMSG) and ovulation induced the day before required using Human Chorionic Gonadotropin (HCG). Eggs were laid in Egg-Laying Solution (ELS: 110 mM NaCl; 2 mM KCl; 0.5 mM Na_2HPO_4; 15 mM Tris-base; 2 mM $NaHCO_3$; 1 mM $MgSO_4.7H_2O$; pH to 7.6 with glacial acetic acid) and were harvested and washed thoroughly with 1 x Modified Barth's Saline (MBS; from 10 x stock: 88 mM NaCl; 1 mM KCl; 0.7 mM $CaCl_2$; 1 mM $MgSO_4$; 5 mM HEPES pH 7.8; 2.5 mM $NaHCO_3$). Eggs were placed in Petri dishes and excess buffer carefully removed. A small section of wild type testis was then mashed in 200 μl of 0.1 x MBS for each Petri dish of eggs and spread over the eggs to fertilise *in vitro*. After 10 minutes the eggs were flushed with 0.1 x MBS. Eggs were then separated into further dishes to reduce crowding and incubated at 14 °C overnight. The dishes were drained of buffer

and 2 % cysteine solution (pH 7.7-7.9 using 10 M NaOH) was added for 5 minutes. Embryos were washed thoroughly in 0.1 x MBS, dead embryos were removed into 100% ethanol and embryos were incubated at either room temperature (~20 °C) or 14 °C until they had passed Stage 15 (Nieuwkoop and Faber, 1994).

Interphase Extracts (Murray, 1991)

Eggs from wild type *Xenopus laevis* were harvested and washed thoroughly with 1 x MBS. Abnormal/dead eggs were removed. 2 % cysteine solution (pH 7.7-7.9 using 10 M NaOH) was added for 10 minutes. Eggs were washed thoroughly with 2 x MMR (200 mM NaCl; 4 mM KCl; 2 mM $MgCl_2$; 4 mM $CaCl_2$; 0.2 mM EDTA; 10 mM HEPES pH 7.8 with NaOH), then activated in 2 x MMR supplemented with 0.5 μg ml^{-1} A23187 calcium ionophore (Sigma). Once activation was observed through contraction of pigment in the animal hemisphere, eggs were washed again in 2 x MMR then washed in chilled XB (extract buffer: 100 mM KCl; 1 mM $MgCl_2$; 0.1 mM $CaCl_2$; 50 mM sucrose; 10 mM HEPES (pH 7.7 using 10 M KOH) in H_2O). Eggs were pipetted into microcentrifuge tubes in a minimal amount of buffer using a plastic pipette and 2 μl 10 mg ml^{-1} Cytochalasin B. Tubes were spun 1 krpm for 1 minute at 4 °C and excess buffer was removed using a chilled glass pipette. Tubes were then spun at 13.2 krpm for 5 minutes at 4 °C and the cytoplasmic layer (sandwiched between the lipid layer and pelleted pigment) was removed into a new tube and the process repeated until a straw-coloured cytoplasmic extract was obtained.

When freezing extract for storage at -80 °C, extract was supplemented with 2 % v/v glycerol, then frozen as 16.5 μl beads in liquid nitrogen and stored at -80 °C. Previously frozen extracts are used in Figures: 3.10, 4.5 , 4.8, 6.6, 6.11 and 6.15.

High-Speed Interphase Extracts

Interphase egg extract was spun further at 55 krpm at 4 °C for 40 minutes and then used as described for degradation assays below.

Mitotic Extracts (Murray, 1991)

Eggs from wild type *Xenopus laevis* were prepared and used to make extract as described for interphase extracts above. However before use in assays, the cytoplasmic layer was supplemented with 5 μg of recombinant Cyclin B Δ90 (previously purified by Jonathan Vosper) per 100 μl extract. Extracts were incubated for 20 minutes at room temperature (~20 °C).

Neurula Extracts

Neurula stage embryos (Nieuwkoop and Faber, 1994) were prepared as described above and washed in 2 x MMR then washed in chilled XB (extract buffer: 100 mM KCl; 1 mM $MgCl_2$; 0.1 mM $CaCl_2$; 50 mM sucrose; 10 mM HEPES (pH 7.7 using 10 M KOH) in H_2O). Embryos were pipetted into 2 ml microcentrifuge tubes in minimal amount of buffer using a plastic pipette and 2 μl 10 mg ml^{-1} Cytochalasin B. Tubes were spun 0.8 krpm for 1 minute at 4 °C and excess buffer was removed using a chilled glass pipette. Tubes were then spun at 13.2 krpm for 5 minutes at 4 °C and the cytoplasmic layer (sandwiched between the lipid layer and pelleted pigment) was removed into a new tube and the process repeated until a grey-coloured cytoplasmic extract was obtained. Extracts could be frozen as described above and previously frozen neurula extracts were used in Figures: 3.8, 3.9 and 4.15.

Degradation Assays ((Murray, 1989) , see Figure 2.1)

Interphase, mitotic or neurula extracts (fresh or frozen), prepared as described above, were supplemented with: 10 μg ml^{-1} LPC (stock consists of 10 mg ml^{-1} leupeptin, 10 mg ml^{-1} pepstatin, 10 mg ml^{-1} chymostatin); 20 μg ml^{-1} cycloheximide; 1.5 mg ml^{-1} Ub from bovine erythrocytes (Sigma); 1/20 of ER (Energy Regeneration mix: 20 μl of 100 mM EGTA; 20 μl of 1 M $MgCl_2$; 150 μl 1 M phosphocreatine (Sigma); 200 μl of 100 mM adenosine 5'triphosphate (GE Healthcare)). 36 μl of supplemented extract was combined with 8 μl of IVT radiolabelled protein and incubated at 21 °C. At various time points, including t = 0 minutes, 5 μl of the degradation sample was

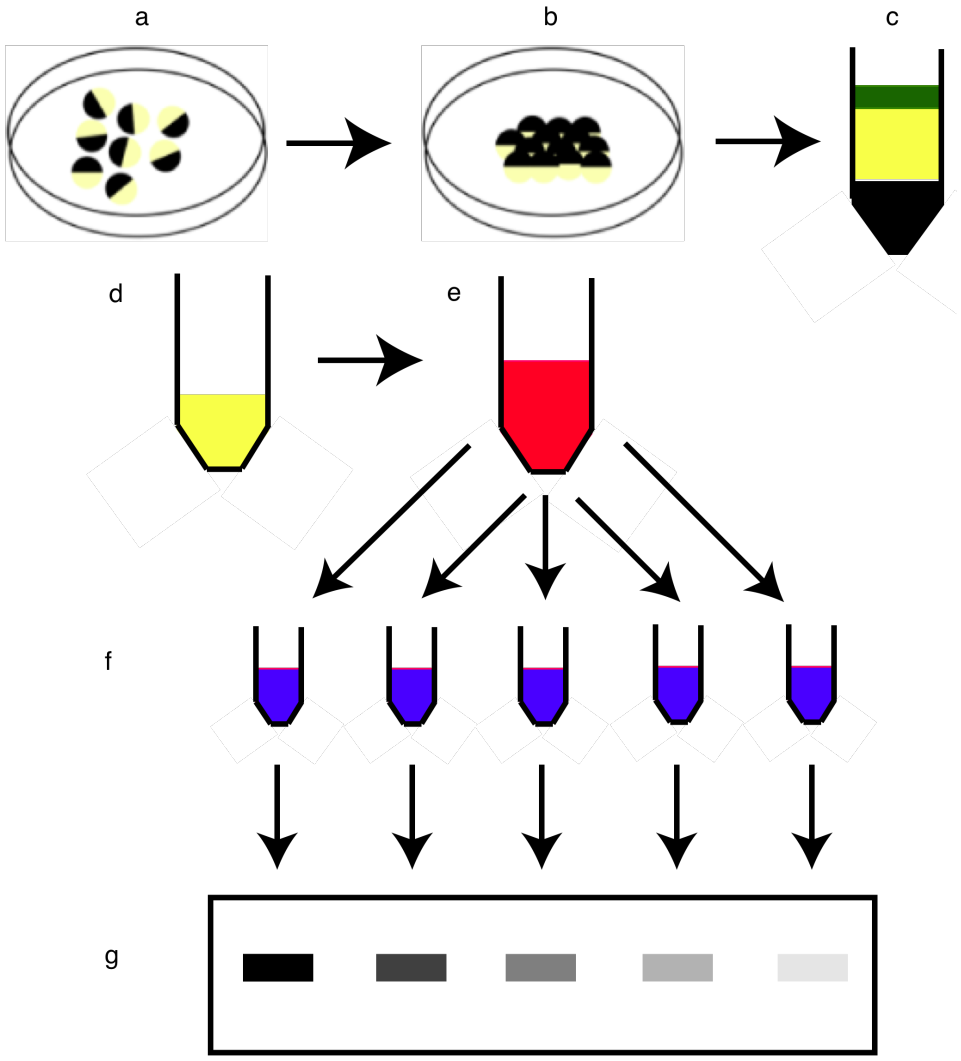

Figure 2.1: Degradation assays.

For interphase extracts, a) *Xenopus laevis* eggs are harvested and treated with calcium ionophore to mimic fertilization, resulting in b) the animal hemispheres (pigmented) being presented dorsally and contracting. c) Eggs are packed into Eppendorf tubes and spun at high speed to separate out layers of lipids (shown in green), cytoplasm (yellow) and pigment (black). d) The cytoplasmic layer is removed, supplemented with ATP and Ub and e) IVT radiolabelled protein is added. The sample is incubated at 21 °C and at particular timepoints f) aliquots of the degradation reaction are removed into quenching sodium dodecyl sulfate loading buffer (SDS-LB) which are then g) separated on a gel by sodium dodecyl sulfate polyacrylamide gel electrophoresis (SDS-PAGE).

removed and added to 15μl of SDS gel-loading buffer supplemented with β-mercaptoethanol then run out by SDS-PAGE. Gels were dried and placed with a phosphoscreen (Molecular Dynamics) and levels of protein sample quantified by phosphoimaging (FLA-5000 Fluoro Image Analyzer (Fujifilm) with Image Reader software; quantification with Image Gauge Software (Fuji Film Science lab)). Protein half-lives were determined by using first-order kinetic analysis (see below). Qualitative analysis was carried out by autoradiography. Degradation assays were carried out in triplicate in fresh extract unless otherwise stated.

ATP-depletion Degradation Assays

8 μl of *in vitro* translated ^{35}S-methione-labelled protein was combined with 40 μl of high speed interphase-activated egg extract, cleared of ribosomes by spinning at 107,400 x *g* for 40 min, supplemented with 200 μg/ml cycloheximide, 10 μg/ml leupeptin, pepstatin, and chymostatin, 1.5 mg/ml Ub, and 2 μl of Energy Regeneration mix (20 μl of 100 mM EGTA; 20 μl of 1 M $MgCl_2$; 150 μl of 1 M phosphocreatine (Sigma); 200 μl of 100 mM adenosine 5'-triphosphate (GE Healthcare)) or 0.8 μl of 1600 units/ml hexokinase with 0.8 μl of 1 M glucose. Samples were used as in a normal degradation assay, described above.

Acetylation-blocking Degradation Assays (Palmiter, 1977)

240 μl of SP6 TNT Master Mix was defrosted and 120 μl taken for acetyl-blocking whilst the other 120 μl was taken for controls. To each 120 μl set, 10.08 μl of citrate synthase from porcine heart was added (Sigma; 59.3 μl of suspension spun in ultracentrifuge at 50,000 x g for 5 minutes. Supernatant removed and citrate synthase resuspended in 500 μl H_2O). 6.9 μl of reticulocyte lysate was added to the control set, whereas 6.9 μl of oxaloacetic acid (500 μl of 500 mM stock added to 12 ml H_2O and 10 M KOH added til pH 7.5) was added to the acetyl-block set. Both sets were then incubated at 25 °C for 7 minutes. 3.24 μl of reticulocyte lysate (for the control set) or of 50 mM De-sulfo CoA lithium salt solution was added and treated reticulocyte lysates aliquoted into 23.37 μl samples. To these, 2 μl ^{35}S-methionine and 2 μl 250 ng μl^{-1} plasmid solution were added and incubated at 30 °C for 2 hours.

IVTs were passed through Zeba Microspin columns before being used as described for degradation assays above.

Alkylating Agent Degradation Assays: NEM

24 μl IVT radio-labelled proteins were prepared as described above and either 1.2 μl H_2O (for control) or 1.2 μl 100 mM NEM (N-ethylmaleimide) added. Samples were then incubated at 20 °C for 40 minutes and passed through Zeba MicroSpin columns before being used as described for degradation assays above.

Ubiquitylation Assays (see Figure 2.2)

Ubiquitylation assays were performed using either fresh neurula extract or frozen interphase extract (prepared as described above) as described in the results. Extract was supplemented with (if not already in the case of frozen extract): 10 μg ml^{-1} LPC (stock consists of 10 mg ml^{-1} leupeptin, 10 mg ml^{-1} pepstatin, 10 mg ml^{-1} chymostatin); 20 μg ml^{-1} cycloheximide; 1.5 mg ml^{-1} Ub from bovine erythrocytes (Sigma); 1/20 of ER (Energy Regeneration mix: 20 μl of 100 mM EGTA; 20 μl of 1 M $MgCl_2$; 150 μl 1 M phosphocreatine (Sigma); 200 μl of 100 mM adenosine 5'triphosphate (GE Healthcare)); 20 μM MG132 (N-carbobenzoxyl–Leu–Leu–Leucinal, Calbiochem). To the control set 3 μl 25 mg ml^{-1} regular bovine erythrocyte Ub (Sigma) was added for every 20 μl of extract; to the experimental sample the same concentration of his-tagged Ub was added.

20 μl aliquots of these supplemented extracts were taken and 5 μl IVT radio-labelled protein added to 2 samples (i.e. 5 μl to 2 control samples and 5 μl to 2 his-tagged samples). For the his-tagged and control sets, one of the two aliquots was labelled "reducing" and the other "non-reducing". All samples were heated at 20 °C for 90 minutes.

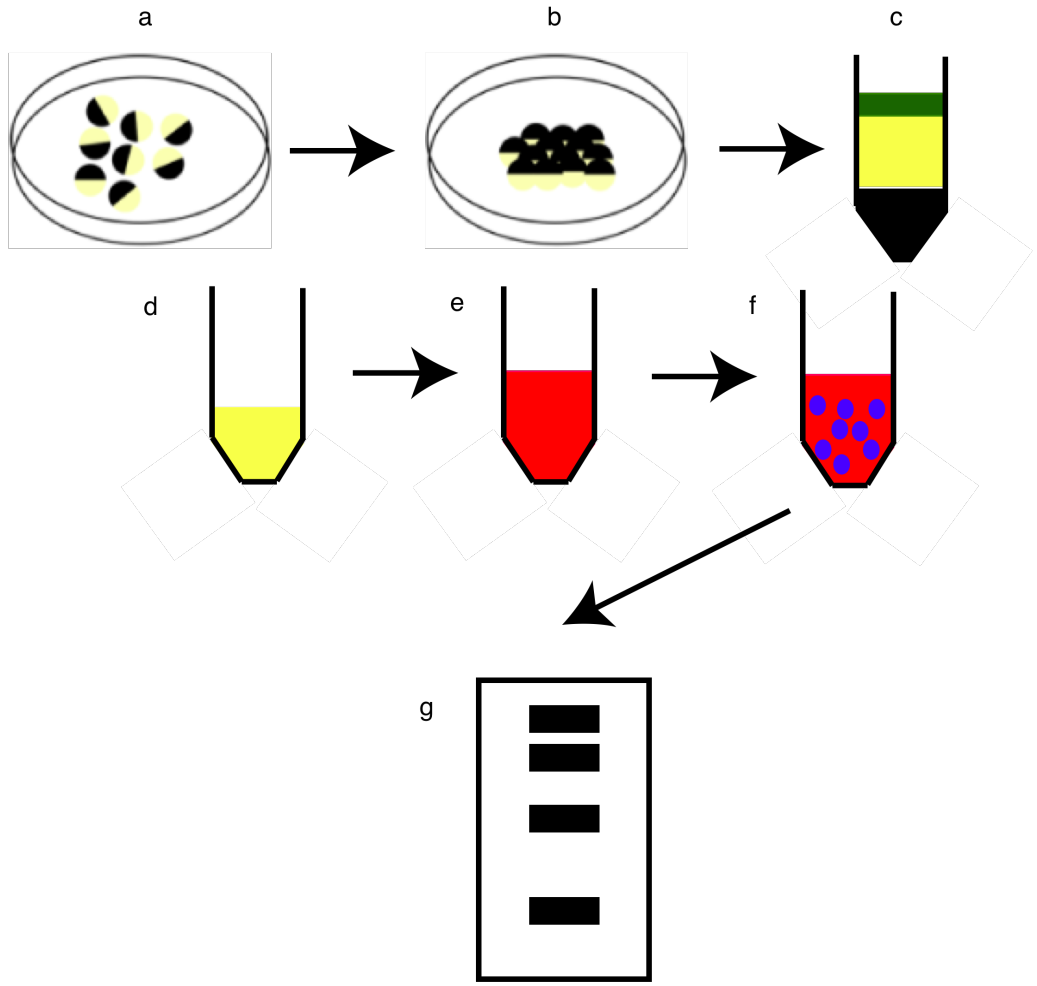

Figure 2.2: Ubiquitylation assays.

For interphase extracts, a) *Xenopus laevis* eggs are harvested and treated with calcium ionophore to mimic fertilization, resulting in b) the animal hemispheres (pigmented) being presented dorsally and contracting. c) Eggs are packed into Eppendorf tubes and spun at high speed to separate out layers of lipids (shown in green), cytoplasm (yellow) and pigment (black). d) The cytoplasmic layer is removed, supplemented with ATP, MG132 and Ub (either untagged or his-tagged) and e) IVT radiolabelled protein is added. The sample is incubated at 20 °C for 90 minutes and f) nickel chelating beads are added and incubated for a further 75 minutes with rolling. Samples are then treated with eluting sodium dodecyl sulfate loading buffer (SDS-LB) and are g) separated on a gel by sodium dodecyl sulfate polyacrylamide gel electrophoresis (SDS-PAGE).

Vosper buffer was prepared containing: 8.5 M urea; 0.1 M Tris pH 7.4; 20 mM imidazole; 6 mM NaCl; 1 % Nonidet P40 (v/v) (Sigma). A sample of this buffer was supplemented with 10 μg ml^{-1} LPC and 250 μl added to each sample at the end of the 90 minute incubation (or variable time of incubation if undertaking a ubiquitylation timecourse). 30 μl Ni-NTA agarose bead slurry from Qiagen was added to each sample and all samples rotated for 75 minutes at 14 rpm at room temperature (~20 °C).

All samples were then spun down at 0.8 rcf for 30 seconds, most of the supernatant removed and discarded and 400 μl Vosper buffer (supplemented with LPC) added. Samples were mixed by gentle inversion, spun down and the process repeated to give a total of 3 washes in Vosper buffer supplemented with LPC and one wash in Vosper buffer alone. After the final wash all supernatant was removed to leave 15 μl of bead slurry. To the reducing samples, 15 μl reducing 2 x SDS PAGE buffer (1000 μl 2 x SDS PAGE buffer pH 10 + 100 μl β-mercaptoethanol + 100 mM imidazole) was added. To the non-reducing samples, 15 μl non-reducing 2 x SDS PAGE buffer (1000 μl 2 x SDS PAGE buffer + 100 μl H_2O + 100 mM imidazole) was added. All samples were gently mixed and rocked at room temperature (~20 °C) for 20 minutes. Reducing samples were boiled at 98 °C for 5 minutes whilst non-reducing samples were incubated on ice for 5 minutes. Samples were stored at -20 °C until run out using SDS-PAGE and analysed by autoradiography.

Electrophoretic Mobility Shift Assay (EMSA)

DNA-binding activity of xNgn2 proteins was assayed by EMSA using ^{32}P-labelled DNA probe comprising the E1 E-box domain of the NeuroD promoter (Huang et al 2000). The probe incorporated the forward primer 5'-GGACCGGGAAGAC**CATATG**GCGCATGCCGGG-3' and the reverse primer 3'-CCTGGCCTTCTG**GTATAC**CGCGTACGGCCC-5', with the E-box domain emboldened. 10 μM of the complementary oligonucleotides were annealed in annealing buffer (100 mM NaCl, 10 mM Tris-HCl) at 95 ° C and gradually cooled at room temperature (~20 °C). 5' overhangs in the resulting DNA were filled in using Klenow fragment from

DNA polymerase (NEB). Probe-labelling reactions were prepared in a 20 μl reaction with 5 pmol dsDNA, 2mM each of dGTP, dATP, dTTP, 10 pmol ^{32}P-dCTP and 0.5 μl Klenow fragment. The mixture was incubated at room temperature (~20 °C) for 20 minutes, supplemented with 2 mM non-radiolabelled dCTP and incubated for a further 10 minutes. The reaction was diluted to 50 μl in STE buffer (100 mM NaCl, 10 mM Tris, 1 mM EDTA) and the Klenow heat-inactivated at 65 °C for 10 minutes. The reaction was passed through an Amersham ProbeQuant G-50 microcolumn by centrifugation at 3 krpm for 1 minute. ^{32}P-labelled E1 probe was diluted 1:2 in binding buffer (20 mM Tris-HCl pH 7.4, 2 mM $MgCl_2$, 50 mM KCl, 1 mM EDTA, 10 % glycerol, 1 mM DTT).

Non-radiolabelled IVT proteins were prepared (see above) and proteins (e.g. xNgn2 and E12) combined 1:1 by volume in *Xenopus* extract supplemented with 20 μM MG132 or XB buffer for 20 minutes at room temperature (~20 °C). Probe-binding was carried out using 4 μl IVT protein incubated in XB or extract; 0.2 mg ml^{-1} poly(dI-dC) and 1 μl E1 probe in a final volume of 10 μl. Samples were incubated for 20 minutes at room temperature (~20 °C). Samples were run out on 5 % non-denaturing PAGE in 0.25 x TBE (Tris/Borate/EDTA) buffer. Gels were visualised by autoradiography.

mRNA Synthesis

15 μg template DNA was linearised using *NotI* restriction enzyme (NEB). Reactions were cleaned with addition of 150 μg μl^{-1} proteinase K (Roche) and 0.5 % SDS and incubation at 50 °C for 1 hour, followed by phenol/chloroform extraction. DNA was precipitated overnight at -20 °C with 2.5 volumes of absolute ethanol and 0.25 volumes 7.5 M ammonium acetate. Precipitated samples were spun down at 13.2 krpm 4 °C for at least 45 minutes, washed with 70 % ethanol and spun again and dried. Pellets were resuspended in 10 μl H_2O (ultra-pure).

1 μg linearised DNA was used in a transcription reaction with transcription buffer, ribonucleotide mix and enzyme mix (all reagents supplied by Ambion) incubated at

37 °C for 2 hours. Samples were DNase (Ambion) treated for 15 minutes at 37 °C before addition of ammonium acetate stop solution (Ambion) and nuclease free water. RNA was phenol/chloroform extracted and precipitated in an equal volume of ice-cold isopropanol. Reactions were spun down at 13.2 krpm 4 °C for at least 45 minutes, washed with 70 % ethanol and spun again and resuspended in 100 μl RNase free water. RNA was precipitated overnight at -20 °C with 2.5 volumes of absolute ethanol and 0.25 volumes 7.5 M ammonium acetate. Precipitated samples were spun down at 13.2 krpm 4 °C for at least 45 minutes, washed with 70 % ethanol and spun again and dried. Pellets were resuspended in 10 μl H_2O (ultra-pure). Concentration was determined using the Nanodrop ND-1000 spectrophotometer and RNA was stored at – 80 °C in 0.5 μg μl^{-1} aliquots.

***Xenopus laevis* Embryo Microinjection** (see Figure 2.3)

Xenopus laevis eggs were collected, washed 3 times in MBS and fertilized *in vitro*. Fertilised embryos were treated with 2 % (w/v) L-cysteine solution (pH 7.8) to remove the jelly coat. Embryos were transferred to agarose dishes containing 0.1 x MBS with 4 % Ficoll solution and 50 μg ml^{-1} gentamycin. Embryos were injected using a Harvard Apparatus Medical Systems Picoinjector. 10 nl RNA solution (concentrations are specified in the text) was injected at the one cell stage in embryos destined for quantitative PCR experiments and in one of two cells at the two-cell stage in embryos used for in situ hybridization. Embryos were cultured at 14 °C.

***In situ* Hybridization (ISH)**

RNA Probes for ISH were prepared by first linearising template DNA with *NotI* and ethanol precipitation as described for mRNA synthesis. Transcription reactions were carried out using 1 μg linearised DNA with Digoxigenin labelling mix (Roche) and T7 (USB) RNA polymerase at 37 °C for 2 hours. The reaction was treated with DNaseI, stopped by addition of 0.4 μM EDTA and precipitated overnight in 0.5 M LiCl and 2.5 volumes of chilled absolute ethanol. RNA was spun down at 13.2 krpm 4 °C for at least 45 minutes, washed with 70 % ethanol and spun again. The dried pellet was resuspended in 50 μl hybridisation buffer (50 % formamide, 5 x SSC, 1 x Denhart's

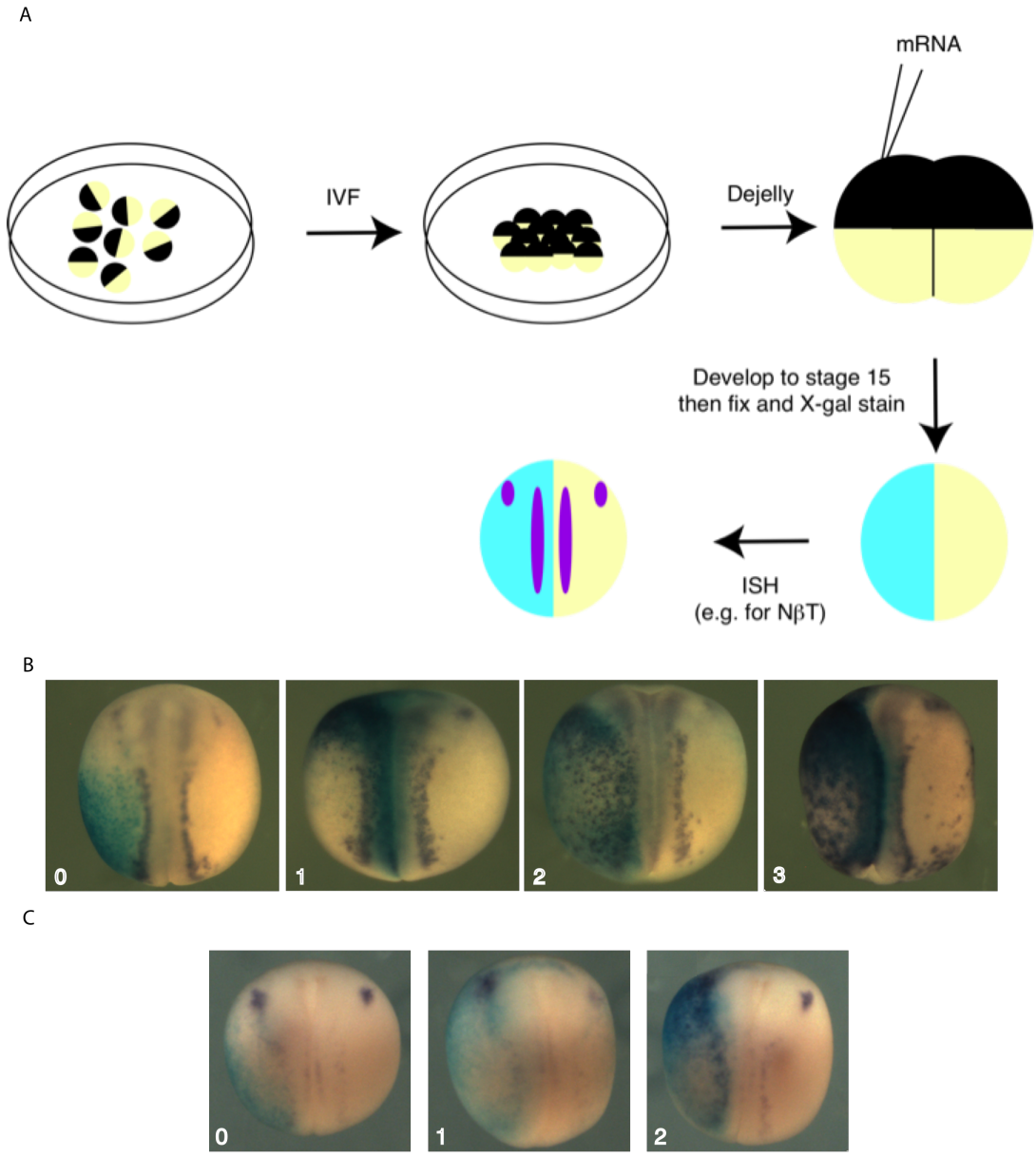

Figure 2.3: *Xenopus laevis* embryo microinjection.

A) Eggs are fertilized *in vitro* and injected in one cell at the two-cell stage (for ISH) with the mRNA of interest and mRNA for β-galactosidase. Embryos are cultured, fixed and stained using X-gal to highlight the injected side of the embryo before *in situ* hybridisation (ISH) is carried out probing for a marker of interest, for example neural β-tubulin. B) Representative embryos used for scoring ISH embryos for ectopic neurogenesis at the level of neural β-tubulin induction. C) Representative embryos used for scoring ISH embryos for ectopic neurogenesis at the level of NeuroD induction.

solution (0.02 % Dicoll, 0.02 % polyvinylpyrrolidine, 0.02 % BSA fraction V), 1 mM EDTA, 0.1 % Tween, 0.1 % CHAPS, 100 μg ml^{-1} heparin, 1 mg ml^{-1} torula RNA).

Embryos destined for ISH were coinjected with 500 pg β-galactosidase (β-gal) mRNA as well as the mRNA of interest. Embryos were first fixed in MEMFA (100 mM MOPS, 2 mM EGTA, 1 mM $MgSO_4$, 10 % formaldehyde) for 1 hour at room temperature (~20 °C) then washed with PBS. Embryos were then incubated in PBS supplemented with 2 mM $MgCl_2$ for 15 minutes at room temperature (~20 °C). Embryos were stained by incubation with X-Gal mixer (5.35 mM $K_3Fe(CN)_6$, 5.35 mM $K_4Fe(CN)_6.3H_2O$, 1.2 mM $MgCl_2$, 0.01 % sodium deoxycholate, 0.02 % Igepal in PBS) supplemented with 1 mg ml^{-1} X-Gal at 37 °C until stained. Embryos were dehydrated in methanol at -20 °C overnight.

ISH was carried out using a BioLane HTI *in situ* robot (Holle and Hunter) following programmes outlined in Tables 2.1 and 2.2 below.

Table 2.1 *In situ* hybridisation Day 1 programme

Solutions	Number of cycles	Duration (minutes)	Temperature (°C)
75 % methanol	1	10	22
50 % methanol	1	5	22
25 % methanol	1	5	22
PBS + 0.1 % Tween	4	5	22
0.5 μg μl^{-1} proteinase K in PBST	1	5	22
0.1 M triethanolamine	1	5	22
0.5 % (v/v) acetic anhydride in 0.1 M TEA	1	10	22
PBS + 0.1 % Tween	2	5	22
4 % formaldehyde in PBS + 0.1 % Tween	1	20	22
PBS + 0.1 % Tween	6	5	22

Table 2.2 *In situ* hybridisation Day 2 programme

Solutions	Number of cycles	Duration (minutes)	Temperature (°C)
2 x SSC (0.3 M NaCl, 30 mM sodium citrate)	1	5	60
2 x SSC	3	20	60
2 x SSC	1	10	60
0.2 x SSC	2	20	60
MAB (0.1 M maleic acid, 0.15 M NaCl, pH 7.5)	2	5	22
Blocking buffer (2 % blocking reagent (Roche) in MAB, 20 % heat inactivated lamb serum)	1	60	22
1:5000 Anti-Digoxigenin ALP antibody in blocking buffer	1	240	22
MAB	3	5	22
MAB	4	150	4

On Day 1 embryos are rehydrated and washed and permeabilised with proteinase K. Negatively charged proteins are neutralized by acetic anhydride buffered by triethanolamine. Embryos are re-fixed in formaldehyde and washed. Embryos were then incubated for 2 hours at 60 °C in hybridisation buffer and incubated overnight at 60 °C with rocking in hybridisation buffer supplemented with 2 ng μl^{-1} of the appropriate digoxigenin-labelled ISH probe.

On Day 2 embryos were washed to remove excess probe and incubated with blocking buffer before incubation with alkaline phosphatase-conjugated anti-digoxigenin antibody (Roche). Embryos were washed twice in NTMT buffer (100 mM Tris pH 9.5, 100 mM NaCl, 50 mM $MgCl_2$, 0.1 % Tween) for 10 minutes at room temperature (~20 °C) with rocking. Embryos were treated with BM Purple alkaline phosphatase substrate (Roche) supplemented with 2 mM levamisole at room temperature (~20 °C) with rocking until purple staining of all probe-interacting antibodies was observed. Staining was stopped by addition of methanol for 30 minutes at room

temperature (~20 °C) and embryos were fixed in MEMFA. Bleaching was carried out in a solution of 3 % H_2O_2, 5 % formamide, 1 x SSC in a light box at room temperature (~20 °C) until bleaching was complete. Embryos were photographed using a Leica MZ FLIII dissection microscope equipped with a Hamamatsu camera and then stored in MEMFA. Images were processed using Openlab software and minimal editing to arrange embryo orientation in Adobe Photoshop. Scoring of ISH embryos was carried out by comparison to the representative embryo scales depicted in Figure 2.3.

Molecular Cloning

Subcloning by PCR, restriction digest and ligation was carried out by standard procedures as described in Molecular Cloning (Sambrook et al., 1989).

Quantitative Reverse Transcriptase PCR (qRT-PCR) Assays

Embryos microinjected with mRNA in one cell at the one-cell stage were harvested at Stage 15 (Nieuwkoop and Faber, 1994) and lysed in 350 μl Buffer RLT supplemented with 1 % (v/v) β-mercaptoethanol (Qiagen RNeasy Mini Kit). Lysates were spun for 1 minute 13.2krpm 4 °C and the supernatant collected and mixed with 350 μl 70 % ethanol. RNA was purified using the Qiagen RNeasy Mini kit into 50 μl RNase-free H_2O. RNA was treated with 1 μl DNase I Turbo and 5 μl DNase I digestion buffer (Qiagen) for 1 hour at 37 °C. Digestion was terminated by addition of DNase inactivation solution and the sample spun for 2 minutes at 13.2 krpm. The supernatant was collected and RNA concentration determined by the Nanodrop ND-1000 spectrophotometer.

RNA samples were then used for cDNA synthesis by combining 0.5 μg μl^{-1} oligo dT primer, 10 mM dNTP mix and 2 μg RNA in a total volume of 13 μl in RNase-free H_2O. RNA was denatured by heating to 65 °C for 5 minutes followed by rapid chilling on ice for 1 minute. The reaction mixtures were supplemented with 4 μl 5 x First-strand buffer, 1 μl RNase OUT RNase inhibitor, 1 μl 0.1 M DTT and 1 μl Superscript III. Reactions were incubated for 30 minutes at 50 °C and the enzyme was heat-

inactivated at 70 °C for 15 minutes before cooling on ice. RNA was eliminated with 1 μl RNase H for 20 minutes at 37 °C. 1 μl cDNA sample was diluted to 5 μl in H_2O and added to 15 μl 1.5 x SybrGreen supplemented with 0.5 μl of each primer required for qPCR (provided by Fahad Ali). Samples were then read by Rotorgene.

***Mus musculus* P19 Embryonal Carcinoma Cell culture** (Rudnicki and McBurney, 1987)

P19 embryonal carcinoma cells were maintained in cell culture at 37 °C in α-modified Minimum Essential Medium (Invitrogen) supplemented with 7.5 % Bovine Calf Serum (Invitrogen); 2.5 % Foetal Bovine Serum (Invitrogen); 100mM Glutamax (Invitrogen) and 100 units penicillin with 100 μg streptomycin (Invitrogen). Cells were split every 2 days using trypsin (Invitrogen).

***Mus musculus* P19 Degradation Assays**

P19 embryonal carcinoma cells were plated onto polylysine-coated plates at a concentration of 400,000 cells per well and incubated in α-MEM (Minimum Essential Media) 37 °C. Media was removed after 24 hours and replaced with antibiotic-free α-MEM and incubated for 2 hours at 37 °C. 5 μg DNA with 250 μl OPTIMEM (Invitrogen) per well was incubated with 15 μl lipofectamine (Invitrogen) and 250 μl OPTIMEM per well for 20 minutes and 500 μl added to each well of P19 cells in 2 ml medium. Cells were transfected overnight at 37 °C. Where mentioned in the text, cells were treated with 20 μM MG132 (N-carbobenzoxyl–Leu–Leu–Leucinal, Calbiochem) or an equal volume of DMSO as a control. At the start of the assay, 100 μg ml^{-1} cycloheximide was added to each well and at each timepoint media was removed from the well, cells washed in warmed 1 x PBS, 50 μl lysis buffer (50 mM Tris pH 7.5; 150 mM NaCl; 1 % IgePal (Sigma); protease inhibitors (Sigma); 1 μM pepstatin) added and cells scraped, placed on ice, then stored -20 °C. Cells were sonicated in a sonicating water bath and centrifuged 13.2 krpm 4 °C 10 minutes. The supernatant was removed and protein levels quantified by BCA Protein Assay (Pierce). 20 μg protein was added to SDS gel-loading buffer supplemented with β-

mercaptoethanol then run out by SDS-PAGE and transferred to nitrocellulose membrane by Western Blot (BIORAD) at 100 V for 1 hour. Membranes were blocked in 5 % (w/v) skimmed milk in PBST (1 x PBS; 0.1 % Tween) at room temperature (~20 °C) for 1 hour. Primary antibody incubations in 2 % milk PBST were performed at 4 °C overnight. Secondary antibody incubations were performed in 2 % milk PBST at room temperature (~20 °C) for 1 hour. Immunodetection was performed using ECL Plus Western Blotting Reagent (GE Healthcare). Proteins were quantified using ImageJ (http://rsbweb.nih.gov/ij/) (Abramoff et al., 2004) software.

Mus musculus P19 IP-re-IP

P19 embryonal carcinoma cells were plated onto polylysine-coated plates at a concentration of 400,000 cells per well and incubated in α-MEM 37 °C. Media was removed after 24 hours and replaced with antibiotic-free α-MEM and incubated for 2 hours at 37 °C. 5 μg DNA with 250 μl OPTIMEM (Invitrogen) per well was incubated with 15 μl lipofectamine (Invitrogen) and 250 μl OPTIMEM per well for 20 minutes and 500 μl added to each well of P19 cells in 2 ml medium. Cells were transfected overnight at 37 °C. After 24 hours, cells were treated with 20 μM MG132 (N-carbobenzoxyl–Leu–Leu–Leucinal, Calbiochem). Media was removed from the well, cells washed in warmed 1 x PBS, 50 μl lysis buffer (50 mM Tris pH 7.5; 150 mM NaCl; 1 % IgePal (Sigma); protease inhibitors (Sigma); 1 μM pepstatin) added and cells scraped, placed on ice, then stored -20 °C. Cells were sonicated in a sonicating water bath and centrifuged 13.2 krpm 4 °C 10 minutes. The supernatant was removed and protein levels quantified by BCA Protein Assay (Pierce). 1.2 mg protein was pulled down with α-HA (Roche) or α-FLAG (Sigma) antibody and rolled at 4 °C overnight. Sepharose beads (G sepharose for HA immunoprecipitation, A sepharose for FLAG (GE Healthcare)) were added and samples rolled at 4 °C overnight for 2-4 hours. Proteins were eluted using 0.1 M glycine pH 2.4 at room temperature (~20 °C) for 10 minutes. SDS LB was added to 1/5 of the sample and frozen. 2/5 of the sample were treated with 1 % SDS at 70 °C for 20 minutes and the remaining 2/5 were kept on ice for 20 minutes. Both samples were divided into FLAG IP and HA IP samples and the IP procedure described above repeated. Proteins were eluted in SDS LB and

separated by SDS-PAGE. Primary antibody incubations in 2 % milk PBST were performed at 4 °C overnight. Secondary antibody incubations were performed in 2 % milk PBST at room temperature (~20 °C) for 1 hour. Immunodetection was performed using ECL Plus Western Blotting Reagent (GE Healthcare). Proteins were quantified using ImageJ (http://rsbweb.nih.gov/ij/) (Abramoff et al., 2004) software.

Protein NMR

Protein purification using GST-tagged mNgn2 or His-tagged mNgn2 was carried out as discussed in Chapter 7. Proteins were expressed in BL21 cells transformed with ampicillin resistant plasmids and grown in M9-based semi-rich medium (M9 medium (50 mM Na_2HPO_4, 15 mM KH_2PO_4, 8.5 mM NaCl) supplemented with MEM, 1mM $MgSO_4$, 100 μM CaCl2, 1 g l^{-1} ^{15}N-NH_4Cl, 2 g l^{-1} $^{13}C_6$-D-glucose (when ^{13}C labelling required, otherwise 4 g l^{-1} unlabelled glucose (Sigma) used), 0.7 g l^{-1} Isogro ^{13}C, ^{15}N powder growth medium (Sigma), 100 μg ml^{-1} ampicillin) at 37 °C to an OD_{600} of 0.6. Protein expression was induced with 0.4 mM IPTG at 20 °C overnight. Harvested cells were lysed using lysozyme and sonication. GST-tagged proteins were purified on a glutathione-bead containing column (Amersham) using an AKTA FPLC purifier (GE Healthcare). GST-tagged proteins were eluted by cleavage of the GST tag from the protein using PreScission Protease (GE Healthcare) overnight at 4 °C and elution in 1 x PBS + 2 mM EDTA.

mNgn2 was phosphorylated using CyclinA3/Cdk2 protein (supplied by Lippens lab) in 5 mM ATP, 12.5 mM MgCl2, 50 mM HEPES pH 8.0, 55 mM NaCl, 5 mM DTT, at 30 °C before passing through a Zeba spin column.

For NMR, protein samples were placed into buffer containing 50 mM Tris 25 mM NaCl 2.5 mM EDTA 2 mM DTT using Zeba Spin columns. 0.625 % (v/v) trimethylsilyl propanoic acid and 5 % (v/v) D_2O were added. NMR measurements were performed at 293 K on a Bruker Avance 600 MHz spectrometer using TMSP as a reference.

Calculating Half-Lives

Half-lives were calculated according to first-order rate kinetics:

If we define [*N*] as the amount of neurogenin (xNgn2) present in the sample, we can describe the rate of neurogenin degradation *in vitro*, assuming first order kinetics, as:

$$\frac{d[N]}{dt} = -K[N]$$

Where a *decrease* in neurogenin level is described by virtue of the negative rate law.
Rearranging:

$$\frac{d[N]}{[N]} = -Kdt$$

Integrating:

$$\ln[N] = -Kt + c$$

Where *c* is a constant of integration.
When t = 0 (i.e. at the initial point of addition of radio-labelled xNgn2 to extract):

$$\ln[N_0] = c$$

Where N_0 is the initial concentration of xNgn2 in the sample at time = 0.
Substituting this back into the integrated rate equation above gives:

$$\ln[N] = -Kt + \ln[N_0]$$

Rearranging:

$$\ln\left(\frac{N}{N_0}\right) = -Kt$$

We define the half-life as the time, $t_{1/2,}$ taken for the level of xNgn2 to fall to half of its initial value, i.e.:

$$[N] = \frac{1}{2}[N_0]$$

Therefore:

$$\ln\left(\frac{1}{2}\right) = -Kt_{\frac{1}{2}}$$

$$\ln(2) = Kt_{\frac{1}{2}}$$

$$t_{\frac{1}{2}} = \frac{\ln(2)}{K}$$

Therefore plotting ln[N] against t should give a straight-line plot of gradient K from which we are able to calculate half-life values.

Error Analysis

Half-lives were calculated relative to the wild type xNgn2 control and averaged over all experiments. The *standard deviation of the mean* was found using:

$$SDM = \sqrt{\frac{1}{N}\sum_{i=1}^{N}(x_i - \bar{x})^2}$$

From this, the *standard error of the mean* was calculated:

$$SEM = \frac{SDM}{\sqrt{n}}$$

Where *n* is the number of samples used to calculate the average (typically *n* = 3).

CHAPTER 3

Canonical Ubiquitylation of xNgn2

INTRODUCTION

xNgn2 undergoes Ub-mediated proteolysis (Vosper et al., 2007) and I am seeking to establish how xNgn2 activity and stability may be regulated and linked to control cell cycle progression and proliferation. The canonical description of ubiquitylation given in the literature describes transfer of Ub from a thiol linkage on the E2 Ub-conjugating enzyme to an internal lysine residue on the substrate protein (Freiman and Tjian, 2003), forming an isopeptide linkage.

MyoD, the myogenic homologue of xNgn2, is ubiquitylated particularly on lysine 133. Mutation of lysine 133 to arginine both stabilises the protein and raises its activity (Batonnet et al., 2004). Much work has been carried out on the degradation of MyoD (Abu Hatoum et al., 1998, Breitschopf et al., 1998, Thayer et al., 1989), other myogenic bHLH proteins such as Myf5 (Lindon et al., 2000) and their heterodimeric binding partners, the E2A proteins (Kho et al., 1997). However, relatively little has been established about the degradation of proneural proteins outside of Mash1 (Vinals et al., 2004).

Neurogenin contains 8 lysine residues: K5, K70, K77, K79 and K80 in the N-terminal (NT) region; K85 in the basic region; K116 in the loop and K119 on the NT cap of the 2nd helix of the bHLH motif. The role of the Ub proteasome system (UPS) in xNgn2 degradation has been shown (Vosper et al., 2007) and highlighted in relation to PTMs and stabilising factors of xNgn2 (Hand et al., 2005, Nguyen et al., 2006, Vernon and Philpott, 2003b). My aims in this chapter are to establish the role that conserved lysines, especially within structured regions of xNgn2 protein, may have in Ub-mediated proteolysis of xNgn2, and the effect that this may have on xNgn2 activity. I will be using *Xenopus laevis* extract systems as a convenient method for assaying xNgn2 degradation as it contains all components of the proteasomal degradation

machinery. To assay activity *Xenopus laevis* embryo mRNA microinjection will also be used followed by *in situ* hybridisation (ISH) of neuronal markers to assess whether particular xNgn2 lysine mutants affect the ability of xNgn2 to drive ectopic neurogenesis.

RESULTS

bHLH proteins undergo lysine-dependent degradation by the UPS in *Xenopus laevis*

To test for an appropriate assay system to investigate xNgn2 UPS-mediated degradation, *Xenopus laevis* interphase activated egg extract was supplemented with *in vitro* translated (IVT) ^{35}S-methionine radiolabelled xNgn2 protein in the presence or absence (using DMSO alone) of the proteasome inhibitor MG132 and incubated at 21°C. Aliquots of the degradation reaction were removed at increasing timepoints into quenching SDS loading buffer (SDS-LB) and separated by 15 % SDS-PAGE (see Figure 2.1). Half-lives for the rates of degradation were then calculated from three repeat experiments using first-order rate kinetics (Figure 3.1).

The half-life of xNgn2 in extract is short, at 22.9 +/- 1.0 mins (Figure 3.1, C). However upon addition of MG132, the half-life is extended beyond the length of the timecourse (60 mins). Therefore xNgn2 protein is stabilised *in vitro* in the presence of the proteasome inhibitor MG132. As xNgn2 stability is dependent upon the activity of the 26S proteasome in *Xenopus laevis* extract systems, these systems are suitable for assaying the rate of xNgn2 degradation by the UPS.

xNgn3 is a neurogenin protein involved in neurogenesis in the hippocampus (Salama-Cohen et al., 2006) and in pancreatic development (Gradwohl et al., 2000) as well as cell differentiation in the lining of the gut (Jenny et al., 2002). Sequence alignment of xNgn2 and xNgn3 by ClustalW2 alignment (Chenna et al., 2003) highlights the large degree of sequence similarity between the two proteins, particularly within the bHLH region (Figure 3.2, A). I wished to assay the stability of xNgn3 in extract systems to compare the degradation of related neurogenin proteins.

A

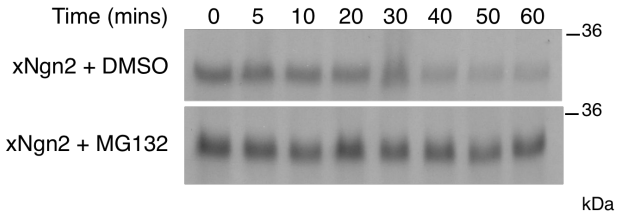

B

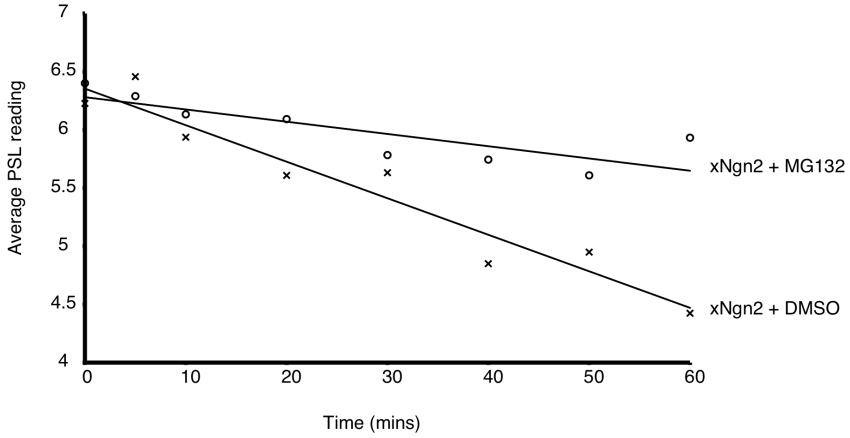

C

Sample	Half-life (mins)
xNgn2 + DMSO	22.9 +/- 1.0
xNgn2 + MG132	> 60

Figure 3.1: xNgn2 degradation in *Xenopus laevis* interphase activated egg extract is inhibited by the proteasome inhibitor MG132.

Xenopus laevis interphase activated egg extracts were supplemented with ^{35}S-labelled xNgn2 in the presence or absence of the proteasome inhibitor MG132. Samples were taken at the timepoints indicated and subjected to 15 % SDS-PAGE. Gels were analysed by autoradiography (A) and quantitative phosphorimaging analysis (B). (C) Half-lives in the presence or absence of MG132 were calculated using first-order rate kinetics, and errors calculated using the Standard Error of the Mean (SEM).

To find the stability of xNgn3 *in vitro*, *Xenopus laevis* interphase activated egg extract was supplemented with IVT ^{35}S-methionine radiolabelled xNgn3 protein and incubated at 21°C. Aliquots of the degradation reaction were removed at increasing timepoints into quenching SDS-LB and separated by 15 % SDS-PAGE. Half-lives were then calculated from three repeat experiments using first-order rate kinetics (Figure 3.2).

xNgn3 protein is slightly larger than xNgn2 (Figure 3.2, A, B) and has a shorter half-life than that typically exhibited by xNgn2 (12.9 +/- 1.0 mins (Figure 3.2, D) and 22.9 +/- 1.0 mins (Figure 3.1, C), respectively). Therefore both neurogenins identified in *Xenopus* are unstable in *Xenopus* extract.

Neurogenins regulate neurogenesis and other bHLH proteins regulate different cell specification pathways such as MyoD, the Ngn2 homologue in myogenesis (Walsh and Perlman, 1997). The stability of MyoD has been extensively studied in the work of the Ciechanover group and others (Abu Hatoum et al., 1998, Breitschopf et al., 1998, Thayer et al., 1989) with particular reference to the *Mus musculus* protein, mMyoD.

To compare stability of the similarly structured xMyoD and xNgn2, *Xenopus laevis* interphase activated egg extract was supplemented with IVT ^{35}S-methionine radiolabelled xNgn2 or xMyoD protein and incubated at 21°C. Aliquots of the degradation reaction were removed at increasing timepoints into quenching SDS-LB and separated by 15 % SDS-PAGE. Half-lives were then calculated from three repeat experiments using first-order rate kinetics (Figure 3.4, A).

xMyoD is unstable with a half-life of 33.7 +/- 1.5 mins. xNgn2 has a half-life here of 24.5 +/- 3.4 mins (Figure 3.4, A). Therefore the similarly structured proteins show similar rates of degradation in interphase extract.

Lysine residues are the canonical sites of ubiquitylation in a protein targeted for UPS-mediated degradation (Mayer, 2005). Ubiquitylation can therefore be blocked by site-directed mutagenesis of lysines to arginines. This semi-conservative mutation maintains the alkyl chain and basic charge within the protein but removes the

A

```
xNgn2   MVLLKCEYRDEEEDLTSASPCSVTSSFRSPATQTCSSD------DEQLLSPTSPGQHQGE 54
xNgn3   -MSPKSDCPQIERRSETELYYQISDNEVSPLSPPCTPGSPISPAESQECTPADGYPHPRE 59
         :  *.:  : *.   :    .::..  ** : .*:..      :.*  :*:.   *  *

xNgn2   ENSPRCRRSRGRAQGKSGETVLKIKKTRRVKANNRERNRMHNLNSALDSLREVLPSLPED 114
xNgn3   TDRKKQRVKRMRSKVKSDGVVVKQRRNRRVKANDRERNRMHNLNSALDALRSILPTFPDD 119
         :  : * .* *:: **. .*:* ::.******:**************:**.:**::*:*

xNgn2   AKLTKIETLRFAYNYIWALSETLRLGDPVHRSASTPAAAILVQDSSSS------QSPSWS 168
xNgn3   AKLTKIETLRFAHNYIWALSETLRMADQSLLSSGQQHLLDSLKKFPKSCLMMELSSPSSC 179
        ************:**********:.*    *:.      ::. ..*      .*** .

xNgn2   CSSSPSSSCCS-FSPASPASSTSDSIESWQPSELHLNPFMSASSAFI 214
xNgn3   ASSSEWDSLYSPLSQGSSLSPTGSMDELMPQSHPYLRHSTSLAVEFL 226
        .***  .*  * :* .*. *.*..  *    *. :*.   * :  *:
```

B

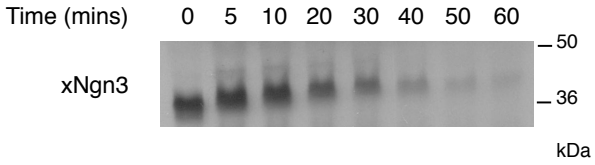

C

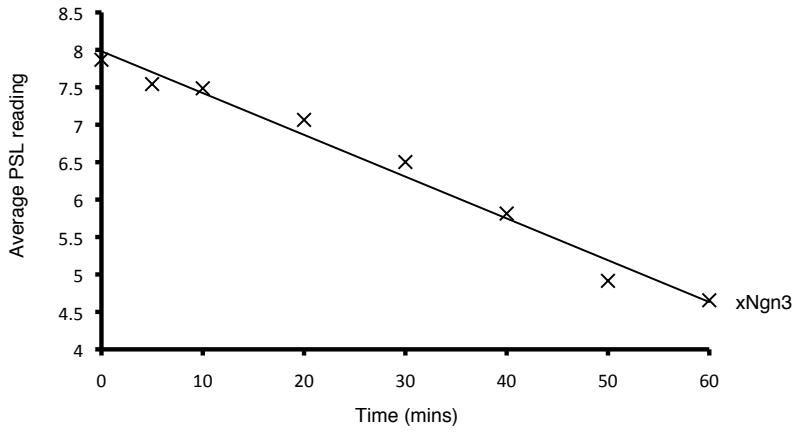

D

Sample	Half-life (mins)
xNgn3	12.9 +/- 1.0

Figure 3.2: xNgn3 is degraded in *Xenopus laevis* interphase activated egg extract.
(A) ClustalW2 analysis was carried out to align xNgn2 and xNgn3 sequences. Exact matches are denoted by * and decreasingly similar properties by : and . with no symbol present for no similarity. – highlights a gap in the sequence alignment. The disordered N-terminal domain is bordered in blue; the bHLH domain in red; and the disordered C-terminal domain in green. (B,C) *Xenopus laevis* interphase activated egg extracts were supplemented with ^{35}S-labelled xNgn3. Samples were taken at the timepoints indicated and subjected to 15 % SDS-PAGE. Gels were analysed by autoradiography (B) and quantitative phosphorimaging analysis (C). (D) The half-life for protein degradation was calculated using first-order rate kinetics, and errors calculated using the Standard Error of the Mean (SEM).

nucleophilic amine substituent. Therefore structure and electrostatics are preserved whilst reactivity is lost.

'Lysineless' mMyoD, with all lysines mutated to arginines, shows increased stability compared to wild type mMyoD (Breitschopf et al., 1998). Figure 3.3 shows the positions of lysine residues in xNgn2. Jonathan Vosper and Ian Horan carried out site-directed mutagenesis of lysines to arginines in xNgn2 generating the 'lysineless' mutant, xNgn2KO.

To compare xNgn2 and xNgn2KO stability, *Xenopus laevis* interphase activated egg extract was supplemented with IVT ^{35}S-methionine radiolabelled xNgn2 or xNgn2KO protein and incubated at 21°C. Aliquots of the degradation reaction were removed at increasing timepoints into quenching SDS-LB and separated by 15 % SDS-PAGE. Half-lives were then calculated from three repeat experiments using first-order rate kinetics (Figure 3.4, B).

xNgn2KO has a half-life of 47.8 +/- 7.9 mins, resulting in an average fold stabilisation of 1.95 +/- 0.23 compared to xNgn2, which has a half-life of 24.5 +/- 3.4 mins (Figure 3.4, B). This is consistent with results of Jonathan Vosper (Vosper et al., 2007). Therefore mutation of all lysines to arginines can stabilise xNgn2 in extract.

All mMyoD lysines have been mutated to arginines to form mMyoDKO but this mutagenesis has not been undertaken with xMyoD. To compare the stability of mMyoDKO with xNgn2, *Xenopus laevis* interphase activated egg extract was supplemented with IVT ^{35}S-methionine radiolabelled xNgn2 or mMyoDKO protein and incubated at 21°C. Aliquots of the degradation reaction were removed at increasing timepoints into quenching SDS-LB and separated by 15 % SDS-PAGE. Half-lives were then calculated from three repeat experiments using first-order rate kinetics (Figure 3.4, C).

The half-life of mMyoDKO is greater than the length of the timecourse (120 mins). xNgn2 has a half-life of 24.5 +/- 3.4 mins (Figure 3.4,C). Therefore mMyoDKO is

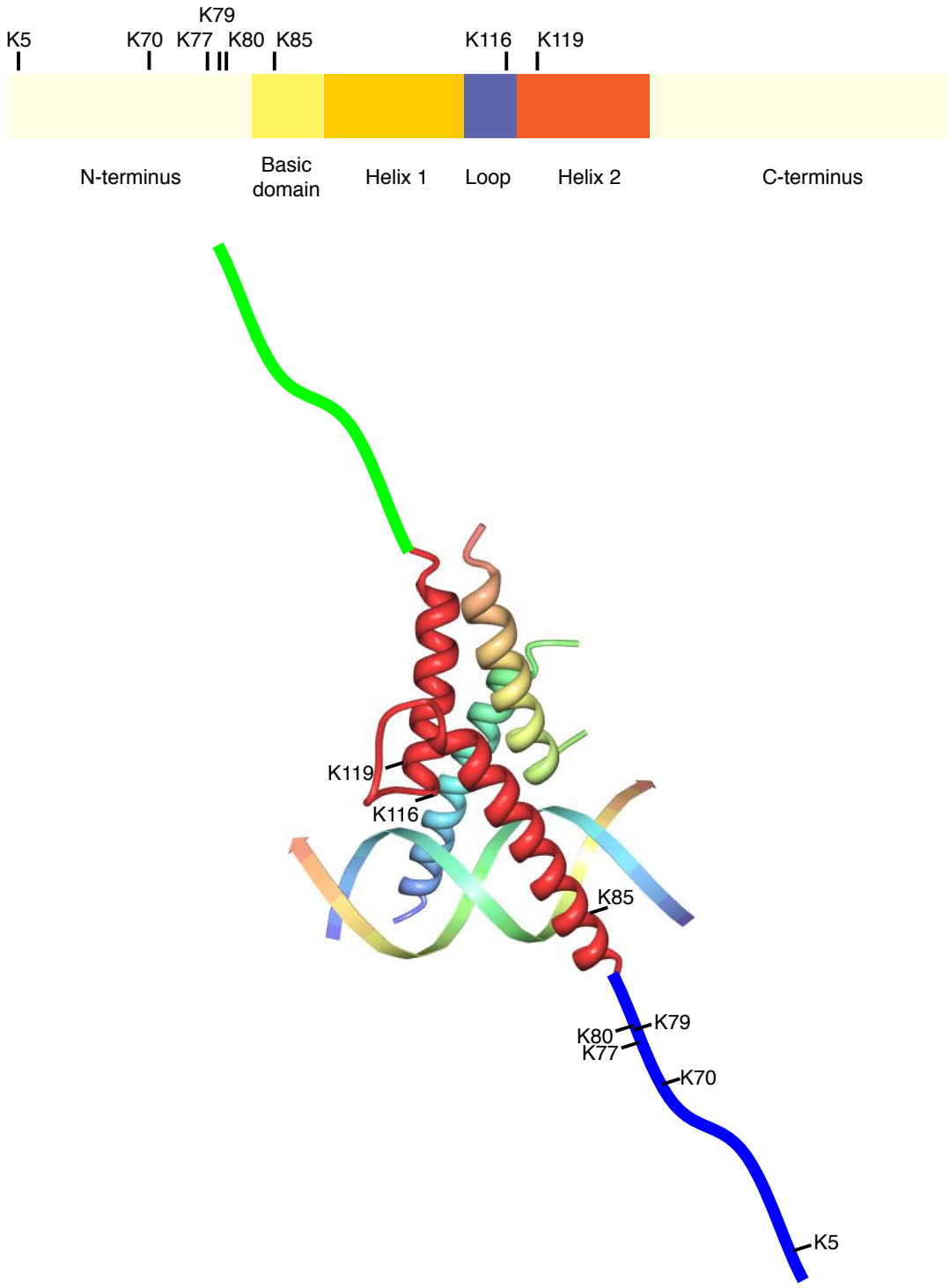

Figure 3.3: Positions of lysine residues in xNgn2.

Schematic of lysine positions and lysines modelled onto a structure of a proneural bHLH heterodimer complexed to DNA. The disordered N-terminal domain is bordered in blue; the bHLH domain in red; and the disordered C-terminal domain in green.

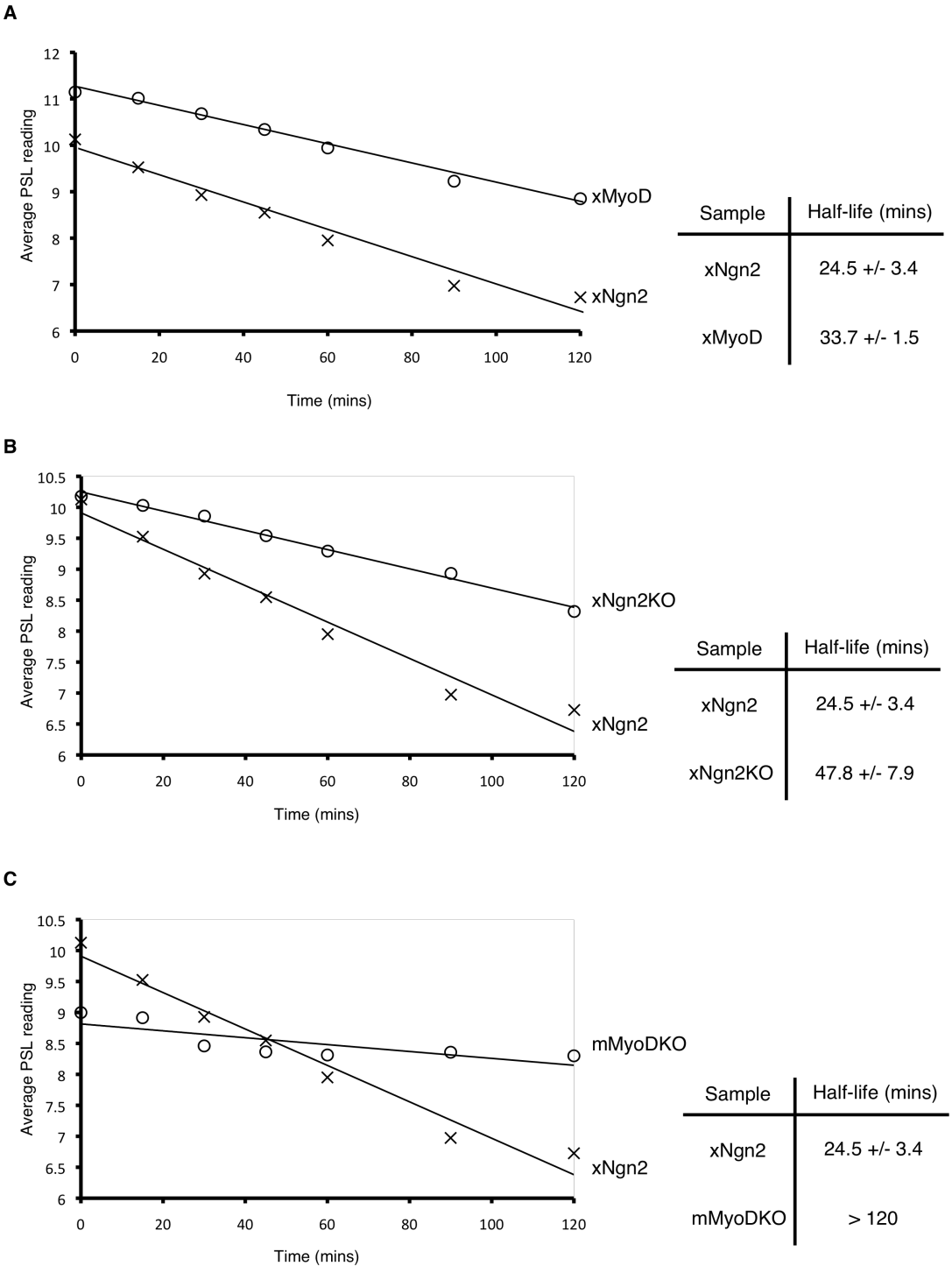

Figure 3.4: MyoD is degraded in *Xenopus laevis* interphase activated egg extract.

Xenopus laevis interphase activated egg extracts were supplemented with ^{35}S-radiolabelled xNgn2 or (A) xMyoD, (B) xNgn2KO or (C) mMyoDKO. Samples were taken at the timepoints indicated and subjected to 15 % SDS-PAGE. Gels were analysed by quantitative phosphorimaging analysis. The half-life for protein degradation was calculated using first-order rate kinetics, and errors calculated using the Standard Error of the Mean (SEM).

much more stable than xNgn2. Mutation of canonical ubiquitylation sites stabilises bHLH proteins.

No individual lysine alone targets xNgn2 for Ub-mediated proteolysis

Mutating all lysines to arginines stabilises xNgn2 and mMyoD. Like xNgn2, most lysines in mMyoD are in the N-terminal region of the protein and no single lysine is responsible for mMyoD instability (Breitschopf et al., 1998). I investigated whether any individual lysine is required to target xNgn2 for proteasomal degradation. Site-directed mutagenesis was carried out by Kate Wilson of individual lysines to arginines, generating mutants K5RxNgn2, K70RxNgn2, K77RxNgn2, K79TRxNgn2, K80RxNgn2, K85RxNgn2, K116RxNgn2 and K119RxNgn2 (see Figure 3.3 for a schematic of lysine positions).

To compare the stability of individual lysine mutants of xNgn2, *Xenopus laevis* interphase activated egg extract was supplemented with IVT ^{35}S-methionine radiolabelled xNgn2, xNgn2KO or individual lysine mutant protein and incubated at 21°C. Aliquots of the degradation reaction were removed at increasing timepoints into quenching SDS-LB and separated by 15 % SDS-PAGE. Half-lives were then calculated using first-order rate kinetics. The average ratio of protein stability with respect to wild type was also calculated. Experiments were carried out once by Kate Wilson and twice by myself to generate a triplicate data set (Figure 3.5).

Mutation of all lysines in xNgn2 to generate xNgn2KO results in a 1.56 +/- 0.14 fold stabilisation over wild type (Figure 3.5, A). No individual lysine mutation results in a change in half-life compared to wild type (Figure 3.5, B). No individual lysine to arginine mutant of xNgn2 stabilises xNgn2 protein. Therefore no individual lysine on its own targets xNgn2 for efficient Ub-mediated proteasomal degradation.

Conserved lysines play a role in Ub-mediated proteolysis of xNgn2

As no single lysine is essential for xNgn2 targeting to the proteasome, related bHLH proteins were compared to identify clusters of conserved lysines which may be

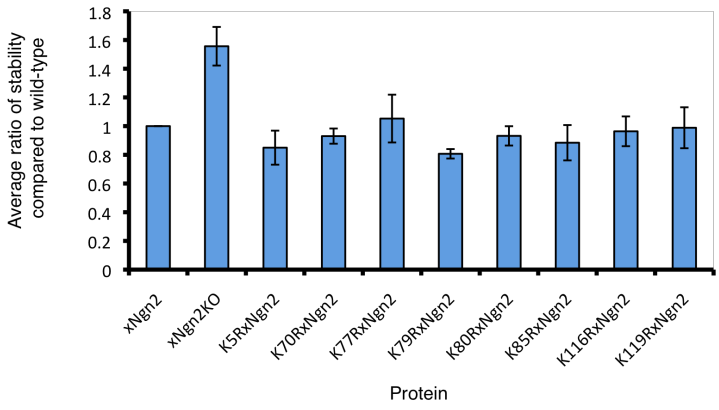

Sample	Half-life (mins)
xNgn2	30.0 +/- 3.5
xNgn2KO	46.0 +/- 4.2
K5RxNgn2	24.7 +/- 0.3
K70RxNgn2	28.0 +/- 4.0
K77RxNgn2	31.7 +/- 6.8
K79RxNgn2	24.0 +/- 2.1
K80RxNgn2	27.5 +/- 1.6
K85RxNgn2	25.7 +/- 0.3
K116RxNgn2	29.0 +/- 5.1
K119RxNgn2	30.0 +/- 6.7

Figure 3.5: No individual lysine mutant alone stabilises xNgn2 against proteasomal degradation.

Xenopus laevis interphase activated egg extracts were supplemented with ^{35}S-labelled xNgn2, xNgn2KO or individual lysine to arginine mutants as indicated. Samples were taken at 0, 15, 30, 45, 60, 90 and 120 mins and subjected to 15 % SDS-PAGE. Gels were analysed by quantitative phosphorimaging analysis. The half-life for protein degradation was calculated using first-order rate kinetics. Each half-life within an experiment was normalised to xNgn2 within the experiment and the ratios of stability compared to xNgn2 averaged over the 3 experiments. Errors were calculated using the Standard Error of the Mean (SEM). One of the 3 data sets used above was generated by Kate Wilson.

specifically required to target xNgn2 for degradation. ClustalW2 analysis (Chenna et al., 2003) was performed comparing sequences of *Xenopus laevis* neurogenins 2 and 3 (a neurogenin 1 homologue has not been identified in *X. laevis*); *Mus musculus* neurogenins 1, 2 and 3; *Homo sapiens* neurogenins 1, 2 and 3; and NeuroD sequences from *Xenopus laevis*, *Mus musculus* and *Homo sapiens* (Figure 3.6).

The most conserved lysines (as marked by * in Figure 3.6) are K85, K116 and K119 in the xNgn2 bHLH domain. K85 is in the basic domain, K116 in the loop and K119 on the N-terminus of helix 2 in the motif. These lysines are conserved in the only predicted structured region of the protein (Bertrand et al., 2002). Preceding the bHLH domain are lysines 77, 79 and 80. Lysines 79 and 80 are conserved across all Ngn2 sequences and K80 in particular is conserved across a majority of the bHLH proteins in this analysis. Similarly in all NeuroD proteins examined, there is a KKKK motif, indicating a conserved grouping of lysines N-terminal to the basic domain. Therefore this motif may be a conserved 'degron' providing a site to signal xNgn2 for proteasomal degradation.

Lysines 77, 79 and 80 form part of a bipartite basic motif (Dingwall and Laskey, 1991) reminiscent of a similar sequence in the androgen receptor (AR), a transcription factor regulated by steroid hormones (Heemers and Tindall, 2007). When the KLKK motif of AR is mutated to ALAA, localization of the receptor to the nucleus is reduced (Cutress et al., 2008). This motif is conserved in proneural bHLH proteins (Figure 3.6). Nuclear localisation is not important in the cell-free interphase extract system but nuclei are present in neurula extract.

Lysineless xNgn2 (xNgn2KO) was mutated by Alison Jones to reintroduce lysines residues. R79KxNgn2KO contains lysine 79 only; the double mutant R(79,80)KxNgn2KO contains both lysines 79 and 80; and the restored motif in R(77,79,80)KxNgn2KO contains lysines 77, 79 and 80. This series of mutants gradually reintroduces the lysines of the KIKK motif. If this motif is a destabilising signal in the protein then stability of the lysineless xNgn2 protein may decrease significantly as lysines are reintroduced into this motif.

Figure 3.6: bHLH proneural protein sequence alignment.

ClustalW2 analysis was carried out to align neurogenin and NeuroD sequences from *Xenopus laevis* (x), *Mus musculus* (m) and *Homo sapiens* (h). Exact matches are denoted by * and decreasingly similar properties by : and . with no symbol present for no similarity. – highlights a gap in the sequence alignment. The disordered N-terminal domain is bordered in blue; the bHLH domain in red; and the disordered C-terminal domain in green.

Figure 3.6: bHLH proneural protein sequence alignment, continued.

ClustalW2 analysis was carried out to align neurogenin and NeuroD sequences from *Xenopus laevis* (x), *Mus musculus* (m) and *Homo sapiens* (h). Exact matches are denoted by * and decreasingly similar properties by : and . with no symbol present for no similarity. – highlights a gap in the sequence alignment. The disordered C-terminal domain is bordered in green.

To investigate their stability, ^{35}S-radiolabelled IVT proteins of these xNgn2 mutants were added to *Xenopus laevis* interphase activated egg extract (Figure 3.7, A) and *Xenopus laevis* neurula embryo extract (Figure 3.7, B) and incubated at 21°C. Aliquots of the degradation reaction were removed at increasing timepoints into quenching SDS-LB and separated by 15 % SDS-PAGE. Half-lives were then calculated from three repeat experiments for interphase and two repeat experiments for neurula using first-order rate kinetics (Figure 3.7, C). Neurula embryo extract was used as it represents the developmental stage in which xNgn2 is normally expressed. It also has a much higher DNA concentration compared to egg extracts as eggs have a diploid genome within one cell whereas each neurula-stage embryo contains at least 6000 cells with diploid genomes within the same volume as an egg. Therefore association of xNgn2 with DNA may be possible to observe effects of DNA on xNgn2 stability.

K77RxNgn2, K79RxNgn2 and K80RxNgn2 are individual lysine 'knock-out' mutants of wild type xNgn2 with only one lysine mutated to arginine in the protein. xNgn2 has a half-life in interphase of 30.3 +/- 2.2 mins and K77RxNgn2, K79RxNgn2 and K80RxNgn2 have half-lives of 29.0 +/- 4.1 mins, 31.6 +/- 4.4 mins and 31.7 +/- 1.2 mins respectively (Figure 3.7, C). As in Figure 3.5, mutating the individual lysines to arginines in interphase does not affect the half-life of xNgn2. These lysines individually are not essential to target xNgn2 for proteasomal degradation.

Mutating arginines back to lysines in the lysineless protein gives the corresponding lysine 'knock-in' mutants of lysines 77, 79 and 80. xNgn2KO has a half-life in interphase of 49.8 +/- 0.8 mins and R79KxNgn2KO, R(79,80)KxNgn2KO and R(77,79,80)KxNgn2KO have half-lives of 35.4 +/- 2.6 mins, 28.1 +/- 1.0 mins and 28.7 +/- 1.1 mins respectively (Figure 3.7, C). Reintroducing lysines to the lysineless protein, by mutating arginines back to lysines at positions 77, 79 and 80, decreases the half-life of xNgn2KO to the approximate level of xNgn2 in interphase extract (Figure 3.7, A and C). The half-life of R79KxNgn2KO is significantly longer than xNgn2 but much less stable than xNgn2KO and the subsequent reintroduction of one more lysine renders the otherwise lysineless protein unstable.

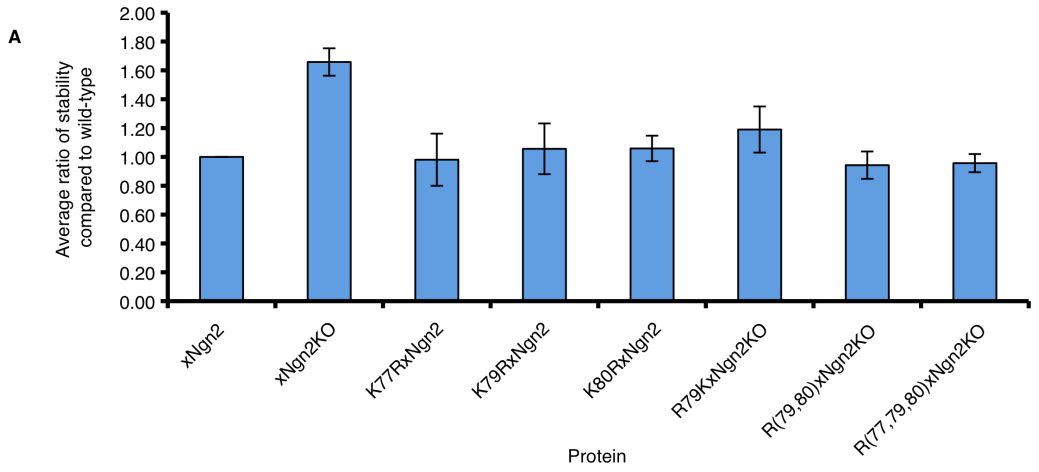

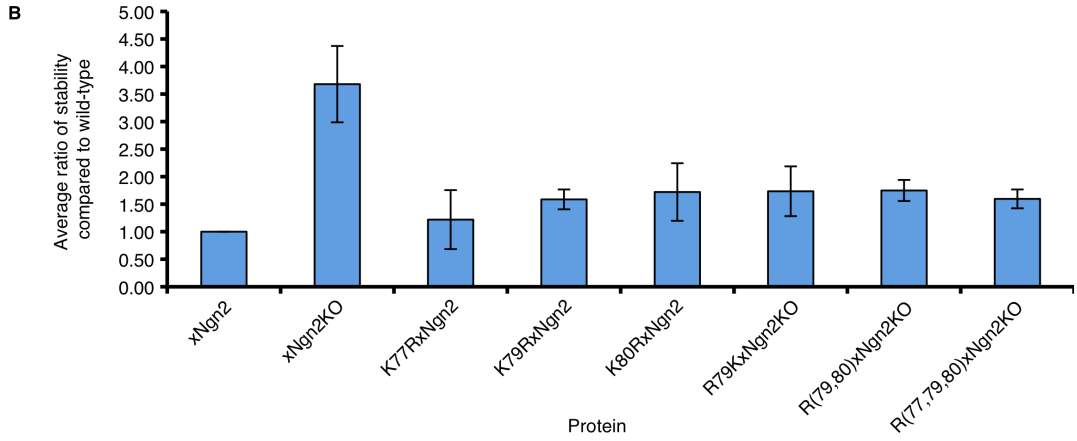

C

Interphase		Neurula	
Sample	Half-life (mins)	Sample	Half-life (mins)
xNgn2	30.3 +/- 2.2	xNgn2	29.3 +/- 2.5
xNgn2KO	49.8 +/- 0.8	xNgn2KO	106 +/- 11
K77RxNgn2	29.0 +/- 4.1	K77RxNgn2	34.4 +/- 12.7
K79RxNgn2	31.6 +/- 4.4	K79RxNgn2	46.1 +/- 1.4
K80RxNgn2	31.7 +/- 1.2	K80RxNgn2	49.2 +/- 11
R79KxNgn2KO	35.4 +/- 2.6	R79KxNgn2KO	49.8 +/- 9.0
R(79,80)KxNgn2KO	28.1 +/- 1.0	R(79,80)KxNgn2KO	50.8 +/- 1.3
R(77,79,80)KxNgn2KO	28.7 +/- 1.1	R(77,79,90)KxNgn2KO	46.4 +/- 1.1

Figure 3.7: Conserved KIKK lysines affect stability of xNgn2.

Xenopus laevis (A) interphase activated egg or (B) neurula embryo extracts were supplemented with ^{35}S-labelled xNgn2, xNgn2KO, xNgn2 mutations of lysine to arginines or xNgn2KO mutations of arginines back to lysines as indicated. Samples were taken at 0, 15, 30, 45, 60, 75, 90 and 120 mins and subjected to 15 % SDS-PAGE. The half-life for protein degradation was calculated using first-order rate kinetics (C). Each half-life within an experiment was normalised to xNgn2 within the experiment and the ratios of stability compared to xNgn2 averaged. Errors were calculated using the Standard Error of the Mean (SEM). Experiments in interphase were carried out in triplicate; experiments in neurula were carried out in duplicate.

These experiments were also carried out in neurula extract. In neurula the half-life of xNgn2 is 29.3 +/- 2.5 mins compared to xNgn2KO at 106 +/- 11 mins (Figure 3.7, B and C). Therefore xNgn2KO appears stabilised to a greater extent in neurula than in interphase, where it has a half-life of 49.8 +/- 0.8 mins (Figure 3.7, C).

Firstly the individual mutations of lysine to arginine in xNgn2 were compared in neurula extract. K77RxNgn2 in neurula has a half-life of 34.3 +/- 12.7 mins, similar to xNgn2 whereas K79RxNgn2 and K80RxNgn2 exhibit half-lives of 46.1 +/- 1.4 mins and 49.2 +/- 11 mins respectively which are significantly longer than xNgn2. Therefore mutation of lysines 79 and 80 alone has a stabilising effect on xNgn2 in neurula.

The mutants of lysineless xNgn2, reintroducing lysines to the KIKK motif, were also compared. R79KxNgn2KO, R(79,80)KxNgn2KO and R(77,79,80)KxNgn2KO have half-lives of 49.8 +/- 9.0 mins, 50.8 +/- 1.3 mins and 46.4 +/- 1.1 mins respectively. These are significantly shorter than the half-life of xNgn2KO at 106 +/- 11 mins, but significantly longer than the half-life for xNgn2 at 29.3 +/- 2.5 mins (Figure 3.7, C). This suggests that any lysine is sufficient for ubiquitylation targeting xNgn2 for proteasomal degradation, but degradation does not reach the same level of efficiency as when all lysines are present.

In both extracts, the presence of any lysines at all is destabilizing. In neurula embryo extract, there appears to be a small yet significant stabilisation relative to wild type xNgn2 on removal of lysines 79 and 80 – but not 77 – and the individual lysine knock-ins of the KIKK motif in an otherwise lysineless background are destabilised relative to xNgn2KO, but not entirely to the level of xNgn2. These lysines are ubiquitylated in neurula extract but cannot completely destabilise the otherwise lysineless xNgn2. It is possible that xNgn2 may be able to bind to DNA in these extracts, which is present at much higher levels than in interphase extract. Binding cofactors such as DNA may stabilise the folded structure of xNgn2 and protect certain sites from ubiquitylation.

Lysine 85, in the basic domain, and lysines 116 and 119 in the Helix-Loop-Helix domain are also conserved lysine residues (Figure 3.6). The single knock-out of K85

in wild type (K85RxNgn2) and knock-in of K85 into the otherwise lysineless protein (R85KxNgn2KO) were used to investigate the role of this lysine in the basic domain, which binds DNA at the E-box consensus sequence of target gene promoters (Bertrand et al., 2002). The role of lysine ubiquitylation in the Helix-Loop-Helix domain was assessed by using lysine to arginine mutants, K116RxNgn2 and K119RxNgn2, as well as mutants reintroducing HLH lysines to lysineless xNgn2, R116KxNgn2KO, R119KxNgn2KO and the double mutant, R(116,119)KxNgn2KO, restoring HLH lysines in an otherwise lysine-less background. Lysines 116 and 119 are predicted to have direct contact with the DNA bound by the active xNgn2/xE12 heterodimer (Bertrand et al., 2002).

To assess stability of these lysine mutants degradation assays in both *Xenopus laevis* fresh interphase activated egg (Figure 3.8, A) and previously frozen neurula embryo (Figure 3.8, B) extracts were carried out. Aliquots of the degradation reaction were removed at increasing timepoints into quenching SDS-LB and separated by 15 % SDS-PAGE. Half-lives were then calculated from three repeat experiments using first-order rate kinetics (Figure 3.8, C).

In interphase, xNgn2 has a half-life of 30.3 +/- 2.2 mins, K85RxNgn2 has a half-life of 29.2 +/- 0.5 mins and R85KxNgn2KO exhibits a half-life of 31.6 +/- 1.4 mins. However xNgn2KO is degraded more slowly than these proteins with a half-life of 49.8 +/- 0.8 mins (Figure 3.8, C). In interphase, lysine 85 shows no effect on xNgn2 stability (Figure 3.8, A). Mutation of this lysine to arginine in xNgn2 does not stabilise the protein suggesting it is not required for xNgn2 proteasomal degradation. When lysine 85 is the only lysine reintroduced into xNgn2KO, it is sufficient to allow UPS-mediated degradation as the stability returns to wild type levels once more.

In another interphase experiment, xNgn2 is again less stable than xNgn2KO (with a half-life of 25.8 +/- 5.3 mins compared to 43.4 +/- 2.3 mins (Figure 3.8,C)). The half-lives of the HLH lysine mutants R116KxNgn2KO, R119KxNgn2KO and R(116,119)KxNgn2KO (32.8 +/- 3.2 mins, 37.3 +/- 3.0 mins and 33.0 +/- 5.2 mins respectively) lie between the values of the wild type or lysineless proteins (Figure 3.8, C). The presence of either lysine in xNgn2KO results in a protein intermediate in

A

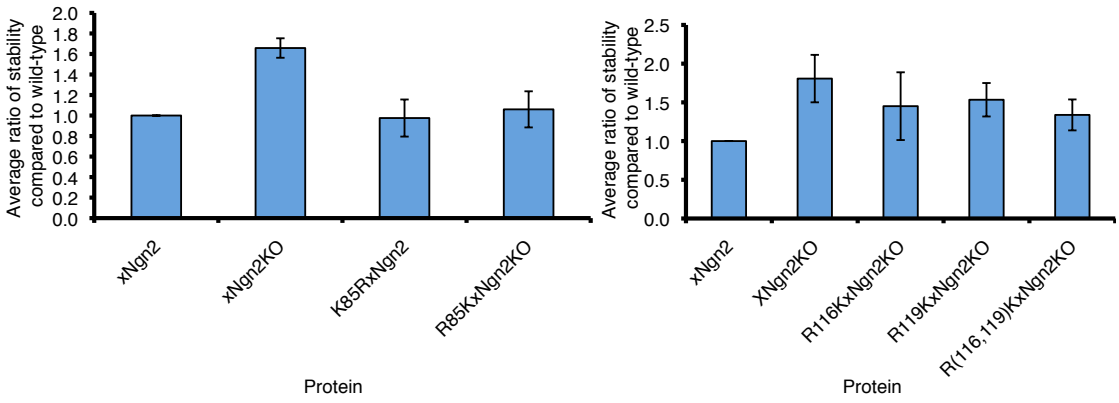

B

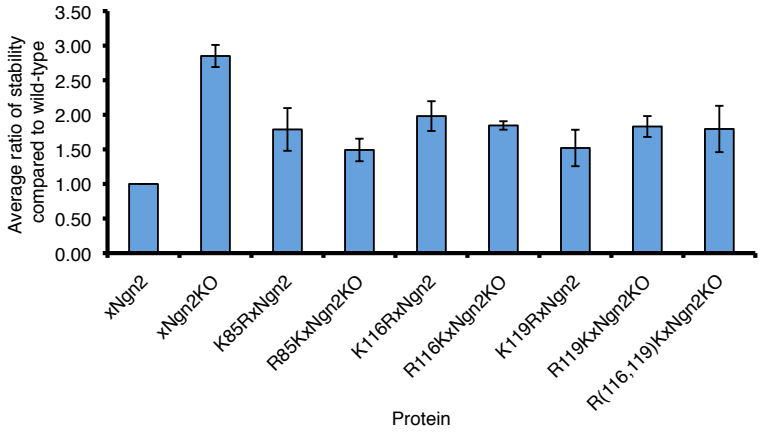

C

Interphase

Sample	Half-life (mins)
xNgn2	30.3 +/- 2.2
xNgn2KO	49.8 +/- 0.8
K85RxNgn2	29.2 +/- 0.5
R85KxNgn2KO	31.6 +/- 1.4

Sample	Half-life (mins)
xNgn2	25.8 +/- 5.3
xNgn2KO	43.4 +/- 2.3
R116KxNgn2KO	32.8 +/- 3.2
R119KxNgn2KO	37.3 +/- 3.0
R(116,119)KxNgn2KO	33.0 +/- 5.2

Neurula

Sample	Half-life (mins)
xNgn2	26.0 +/- 3.2
xNgn2KO	73.0 +/- 5.4
K85RxNgn2	45.4 +/- 7.0
R85KxNgn2KO	39.1 +/- 7.0
K116RxNgn2	51.3 +/- 8.7
R116KxNgn2KO	47.6 +/- 4.8
K119RxNgn2	37.9 +/- 3.7
R119KxNgn2KO	48.2 +/- 8.6
R(116,119)KxNgn2KO	44.9 +/- 6.4

Figure 3.8: bHLH lysines affect stability of xNgn2.

Xenopus laevis (A) interphase activated egg or (B) neurula embryo extracts were supplemented with ^{35}S-labelled xNgn2, xNgn2KO, xNgn2 mutations of lysine to arginines or xNgn2KO mutations of arginines back to lysines as indicated. Samples were taken at 0, 15, 30, 45, 60, 75, 90 and 120 mins and subjected to 15 % SDS-PAGE. The half-life for protein degradation was calculated using first-order rate kinetics (C). Each half-life within an experiment was normalised to xNgn2 within the experiment and the ratios of stability compared to xNgn2 averaged (A), (B). Errors were calculated using the Standard Error of the Mean (SEM).

stability between xNgn2 and xNgn2KO (Figure 3.8, A). This is in contrast to the lysine mutants R85KxNgn2 (Figure 3.8, A), and R79KxNgn2KO, R(79,80)KxNgn2KO, or R(77,79,80)KxNgn2KO (Figure 3.7), which all demonstrate half-lives for degradation identical to wild type xNgn2 (Figure 3.7, C and 3.8, C) in interphase extract.

In neurula, the average half-life of xNgn2 was 26.0 +/-3.2 mins, whereas the single lysine to arginine mutants of xNgn2 for lysines 85, 116 and 119 exhibited half-lives for degradation of 45.4 +/- 7.0 mins, 51.3 +/- 8.7 mins, and 37.9 +/- 3.7 mins respectively (Figure 3.8, B and C). The results of the degradation assays in neurula extract suggest that lysines in the putative structured region of xNgn2 play an important role in regulating stability. Arginine to lysine mutations of lysines 85, 116 and 119 significantly stabilise xNgn2. These particular lysine residues contact DNA in the active complex (Bertrand et al., 2002) and this is still possible upon mutation to arginines as the positive charge is preserved. However the functional nucleophilic group has been lost upon mutation of a lysine to arginine and so ubiquitylation at these sites can no longer occur. It would appear that the lysines in this structured region of xNgn2 capable of contacting DNA are able to target xNgn2 for UPS-mediated degradation on their own.

xNgn2KO has a half-life of 73.0 +/- 5.4 mins in neurula extract compared to the half-life of xNgn2 of 26.0 +/- 3.2 mins (Figure 3.8, C). The half-lives of proteins with bHLH lysines reintroduced into xNgn2KO, R85KxNgn2KO (39.1 +/- 7.0 mins), R116KxNgn2KO (47.6 +/- 4.8 mins), R119KxNgn2KO (48.2 +/- 8.6 mins) and R(116,119)KxNgn2KO (44.9 +/- 6.4 mins), lie between these values. Mutating arginines back to lysines therefore destabilises xNgn2KO in a neurula context, but does not result in a protein as unstable as wild type xNgn2 (Figures 3.8, B and 3.9).

The degradation assays in neurula extract were also carried out in duplicate using fresh neurula extract for mutants of lysines 116 and 119, to compare with extract that had been prepared previously and frozen with the addition of glycerol at -80 °C (Figure 3.9). R116KxNgn2KO appears to destabilise xNgn2KO to a greater extent than R119KxNgn2KO. Therefore there is not a significant difference between the results in fresh and previously frozen neurula extract, but the fresh extract results do

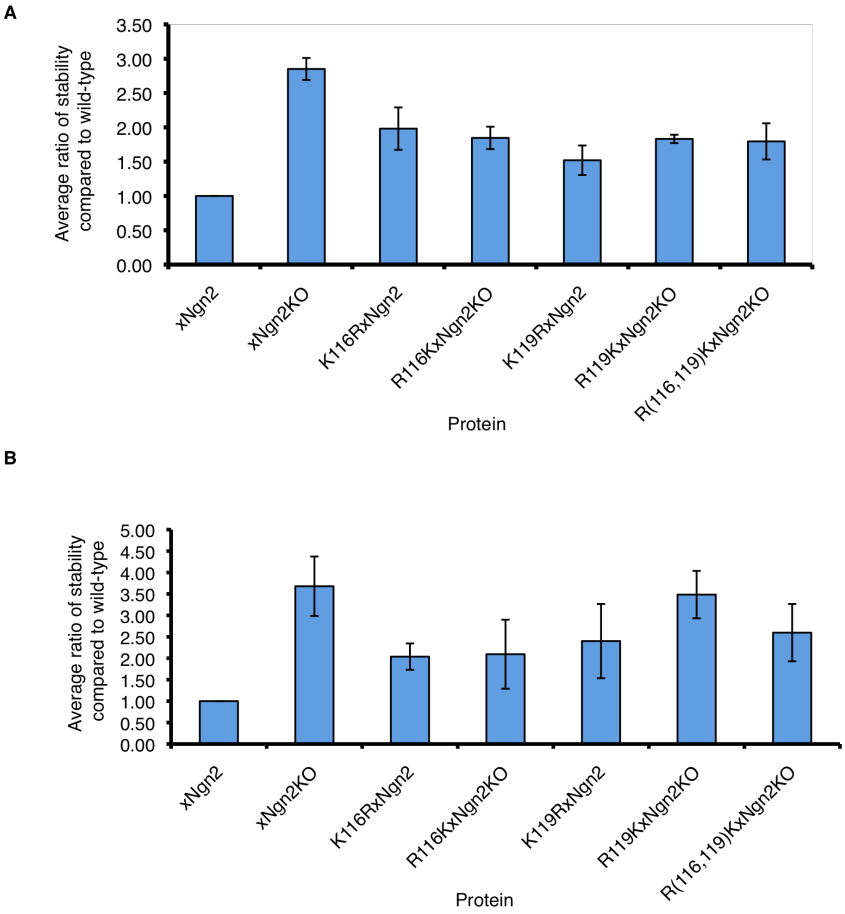

Figure 3.9: bHLH lysines affect stability of xNgn2 in neurula.

Xenopus laevis neurula embryo extracts, either A) previously frozen or (B) fresh, were supplemented with ^{35}S-labelled xNgn2, xNgn2KO, xNgn2 mutations of lysine to arginines or xNgn2KO mutations of arginines back to lysines as indicated. Samples were taken at 0, 15, 30, 45, 60, 75, 90 and 120 mins and subjected to 15 % SDS-PAGE. Each half-life within an experiment was normalised to xNgn2 within the experiment and the ratios of stability compared to xNgn2 averaged. Errors were calculated using the Standard Error of the Mean (SEM). The frozen extract experiments were a triplicate data set. The fresh extract experiments were a duplicate data set.

hint at a possible subtle difference between the ability of K116 and K119 to target xNgn2 for degradation (Figure 3.9, B). This would suggest K116 is a preferential site for modification by ubiquitylation compared to K119. However this apparent difference is not significant using the Standard Error of the Mean (SEM).

HLH lysines are not sufficient for xNgn2 DNA-binding

Lysines 116 and 119 are positioned to contact DNA in the E-box bound by the xNgn2/xE12 heterodimer. To see whether mutation of these residues could affect DNA-binding capability, analysis of DNA-binding by mutant xNgn2 proteins was carried out using electrophoretic mobility shift assay (EMSA). Non-radiolabelled IVT xNgn2 proteins were incubated in extract buffer (XB), with or without IVT xE12, and in *Xenopus laevis* interphase activated egg extract or mitotic interphase activated egg extract. Incubations were carried out in the presence of ^{32}P-labelled DNA probe containing the E-box consensus site of xNgn2 (Figure 3.10). xNgn2 and xNgn2KO were tested as well as R116KxNgn2KO and R119KxNgn2KO, the lysineless xNgn2 forms with only lysines 116 or 119 reintroduced. 9S-AxNgn2 was also used as a control; this is a form of xNgn2 where all serine-proline (SP) sites are mutated to alanine-proline (AP) and has been investigated as a form of xNgn2 with no consensus cyclin-dependent kinase (cdk) phosphorylation sites (Hindley, 2011). It was added to this EMSA as it binds to DNA probe in EMSA and binds with greater avidity to DNA in mitotic extract than xNgn2 (Hindley, 2011).

EMSA suggests that xNgn2KO has reduced binding to DNA compared to xNgn2, and that reintroduction of either lysine 116 or lysine 119 cannot rescue this reduced binding in either interphase or mitotic extract (Figure 3.10). This result is preliminary as it has only been carried out once but if correct, it would suggest that lysines are required for binding to DNA and lysines 116 or 119 alone are not sufficient to mediate this binding.

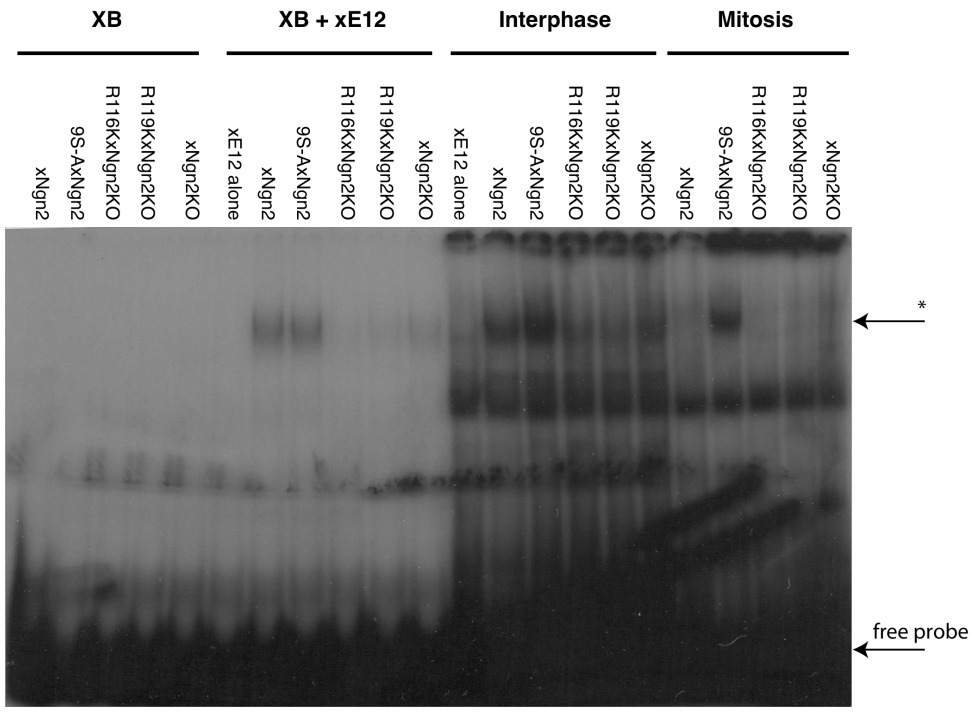

Figure 3.10: bHLH lysines do not restore DNA-binding in Electrophoretic Mobility Shift Assay (EMSA).

IVT xNgn2, xNgn2KO, xNgn2KO mutations of arginines back to lysines as indicated and 9S-AxNgn2, which contains no serine-proline motifs but only alanine-proline, were incubated in extract buffer (XB) or *Xenopus laevis* activated interphase or mitotic extracts, with ^{32}P-labelled E-box DNA probe. Samples were separated by SDS-PAGE and analysed by autoradiography. '*' denotes position of heterodimer bound to DNA probe. n = 1.

xNgn2KO is less active *in vivo* than xNgn2 but is not a dominant negative repressor

xNgn2 is stabilised when all lysines are mutated to arginines to form xNgn2KO (Figure 3.4) but these mutations reduce binding to DNA in EMSA (Figure 3.10). These results suggest that the protein may be more stable but binds to promoter regions less tightly. Hence, it is hard to predict its effect on xNgn2 activity *in vivo*. To test this, xNgn2 or xNgn2KO mRNA was injected into *Xenopus laevis* embryos (with GFP as an injection control) to assess *in vivo* activity by *in situ* hybridization (ISH). mRNA was injected into stage 2 *Xenopus laevis* embryos, which were allowed to develop and were fixed at stage 15 (Nieuwkoop and Faber, 1994). Ectopic neurogenesis was assessed using levels of neural β-tubulin expression revealed by ISH and comparing this expression in the injected side of the embryo to the uninjected side (Figure 3.11, scale of neurogenesis defined in Figure 2.3).

Compared to the control GFP injection, injection of xNgn2 leads to extensive ectopic neurogenesis as assessed by levels of neural β-tubulin expression (Figure 3.11). xNgn2KO mRNA microinjection also results in ectopic neurogenesis, but it shows a reduced activity compared to xNgn2. Therefore increased stability, by loss of canonical ubiquitylation sites, does not translate directly into increased activity. This may be because lysine mutation reduces the ability of xNgn2 to bind DNA.

Inhibitor of differentiation (Id) proteins prevent transcription factor activity of bHLH heterodimeric complexes (Sun and Baltimore, 1991). They bind E2A proteins but lack basic domains and so are unable to bind DNA. It is possible that xNgn2KO may be able to act as a dominant negative repressor of xNgn2 neurogenic activity by preventing DNA binding by the heterodimer in an analogous fashion. To check whether this is the case, xNgn2 and xNgn2KO mRNA were coinjected into *Xenopus laevis* embryos in the ratios of 20 pg xNgn2 : 40 pg xNgn2KO and 50 pg xNgn2 : 75 pg xNgn2KO. mRNA was injected into stage 2 *Xenopus laevis* embryos, which were allowed to develop and were fixed at stage 15 (Nieuwkoop and Faber, 1994). Ectopic neurogenesis was assessed using levels of neural β-tubulin expression revealed by

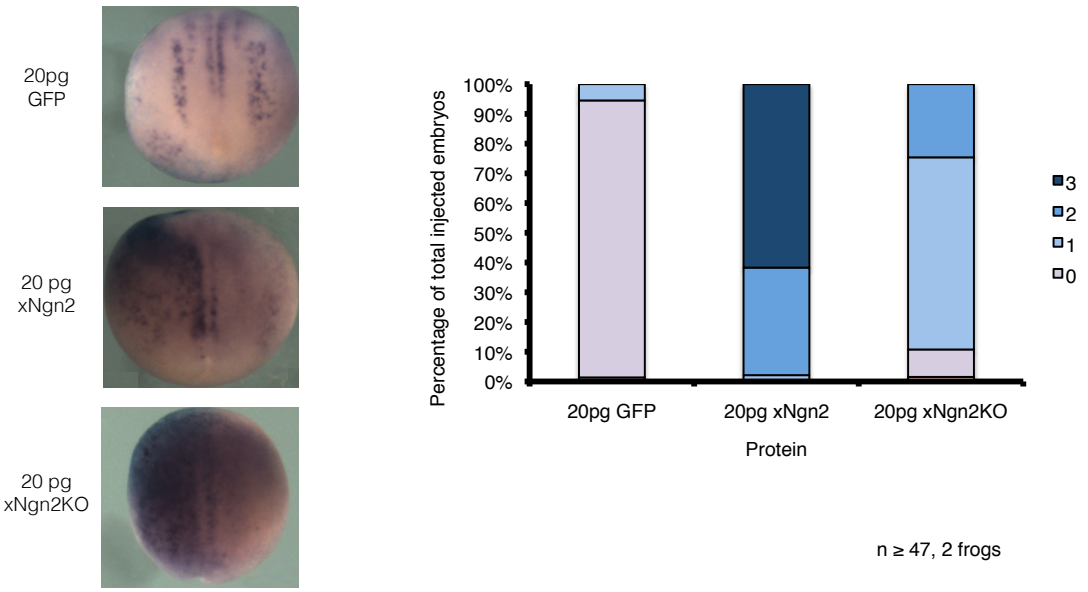

Figure 3.11: xNgn2KO has reduced activity *in vivo* compared to xNgn2 with respect to neural β-tubulin induction.

20 pg GFP, xNgn2 or xNgn2KO mRNA were coinjected with 500 pg β-galactosidase mRNA into 1 cell of Stage 2 embryos and allowed to develop to stage 15. Embryos were then fixed and *in situ* hybridization (ISH) performed for neural β-tubulin. Embryos were scored according to the extent of neurogenesis depicted (as defined in Figure 2.3). n ≥ 47 from 2 frogs.

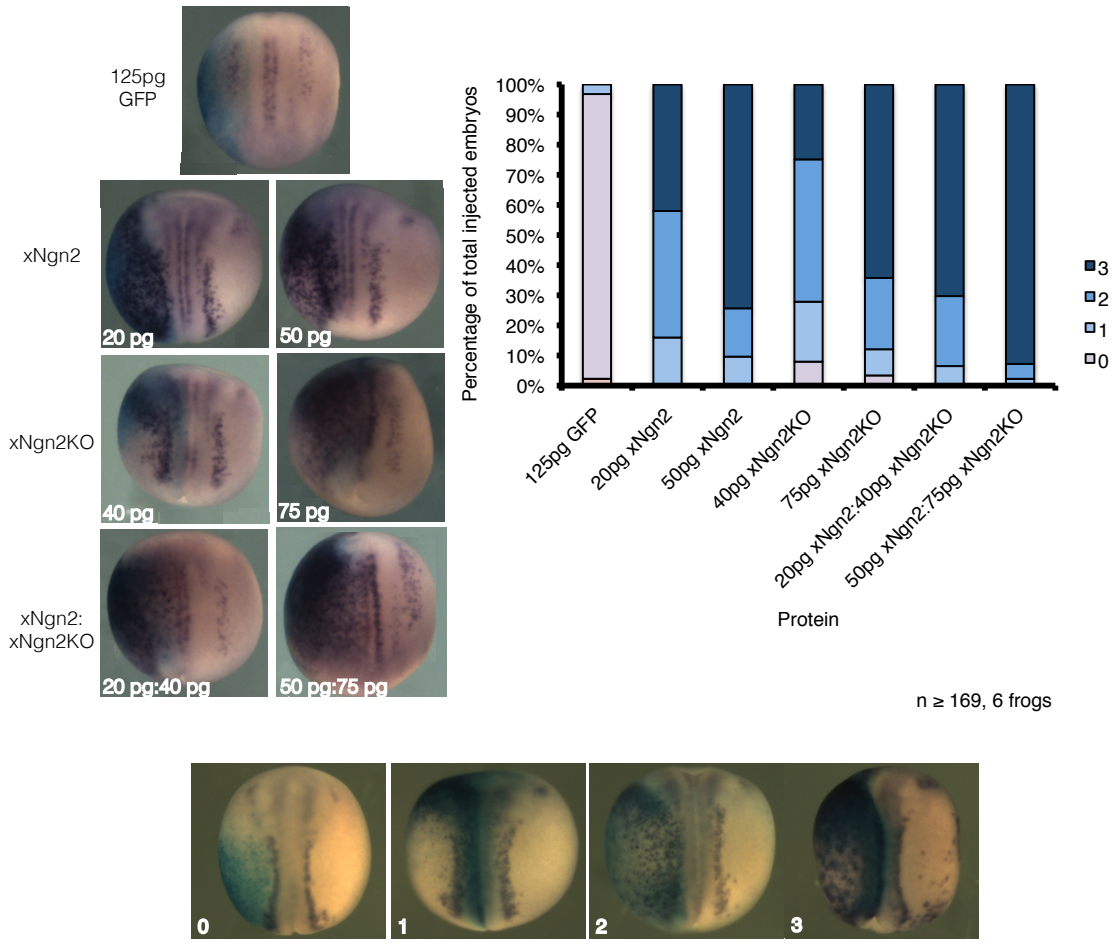

Figure 3.12: xNgn2KO does not act as a dominant negative inhibitor of neurogenesis.
GFP, xNgn2 or xNgn2KO mRNA were coinjected with 500 pg β-galactosidase mRNA into 1 cell of Stage 2 embryos at the levels indicated and allowed to develop to stage 15. Embryos were then fixed and *in situ* hybridization (ISH) performed for neural β-tubulin. Embryos were scored according to the extent of neurogenesis depicted. n ≥ 169 from 6 frogs.

ISH and comparing this expression in the injected side of the embryo to the uninjected side (Figure 3.12).

xNgn2KO induces less ectopic neurogenesis than xNgn2 (as in Figure 3.11) but this is less obvious when higher concentrations of xNgn2KO are injected (see Figure 3.11, 75 pg). Co-injection of xNgn2 and xNgn2KO together induce greater neurogenesis than xNgn2 alone (Figure 3.12). Therefore the xNgn2KO mutant is not acting as a dominant negative inhibitor of neurogenesis.

Mutation of lysines of xNgn2 reduces its ability to induce ectopic neurogenesis as assayed by neural β-tubulin expression (Figure 3.11) but to see if any effects are observed on a direct target of xNgn2, xNeuroD expression was investigated. 20 pg of xNgn2 or xNgn2KO were injected into stage 2 *Xenopus laevis* embryos and fixed at stage 15 (Nieuwkoop and Faber, 1994). ISH for xNeuroD was performed and the extent of ectopic xNeuroD expression scored (Figure 3.13, scoring scale defined in Figure 2.3).

xNgn2KO induces less xNeuroD expression than xNgn2 (Figure 3.13). Therefore xNgn2KO acts as a less active form of xNgn2 from the very earliest points at which xNgn2 exerts its activity.

DISCUSSION

The aim of the experiments presented in this chapter was firstly to establish the role of proteasomal degradation in xNgn2 instability and secondly to determine whether specific residues were responsible for directing Ub-mediated proteolysis. In particular I investigated the lysine residues of xNgn2, which are characterised in the literature as canonical sites of substrate protein ubiquitylation targeting for UPS-mediated degradation.

Xenopus laevis extract systems provide a convenient assay system for analysis of proteasomal degradation of proteins. xNgn2 (Figure 3.1), xNgn3 (Figure 3.2) and xMyoD (Figure 3.4, A) are degraded in *Xenopus laevis* extract and in a proteasome-

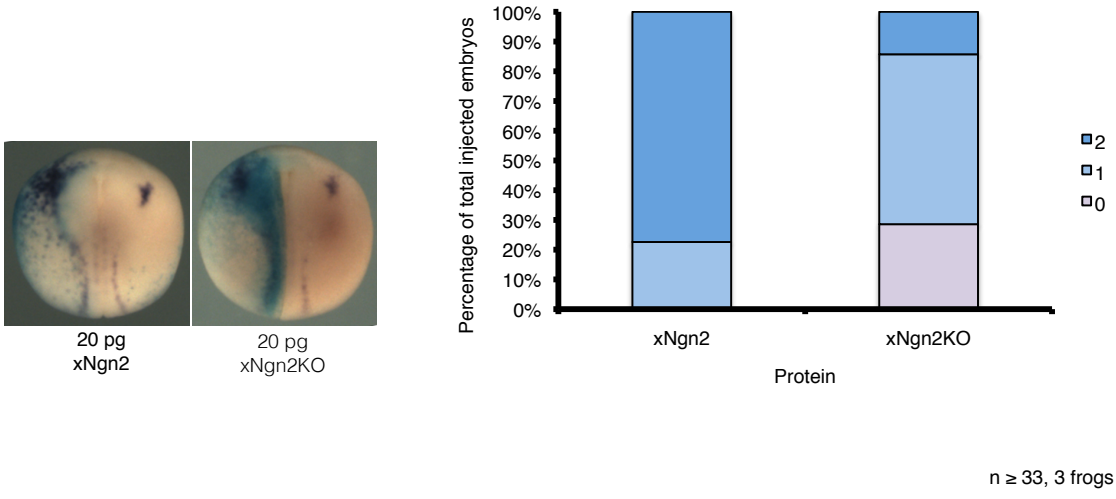

Figure 3.13: xNgn2KO induces lower levels of xNeuroD than xNgn2.

20 pg xNgn2 or xNgn2KO mRNA were coinjected with 500 pg β-galactosidase mRNA into 1 cell of Stage 2 embryos (Nieuwkoop and Faber, 1994) and allowed to develop to stage 15. Embryos were then fixed and *in situ* hybridization (ISH) performed for xNeuroD. Embryos were scored according to the extent of xNeuroD expression depicted (as defined in Figure 2.3). n ≥ 33 from 3 frogs.

dependent manner (Figure 3.1). These results demonstrate that the use of radiolabelled IVT proteins in extract systems allows a quick assay to investigate stability, with robust reproducible results, and that bHLH proteins can be rapidly degraded in extract.

Canonical ubiquitylation is regarded as a transfer of Ub from a thiol linkage on the E2 Ub-conjugating enzyme to an internal lysine residue on the substrate protein, forming an isopeptide linkage (Mayer, 2005). In some proteins there are specific lysines that target for Ub-mediated proteolysis (Baldi et al., 1996) whilst in other proteins several or any lysines are used for ubiquitylation (King et al., 1996). xNgn2 contains 8 lysine residues (Figure 3.3).

Figure 3.5 shows that mutation of any single lysine has no appreciable effect on the rate of xNgn2 degradation. Therefore no individual lysine residue is essential for Ub-mediated targeting of xNgn2 for UPS-mediated degradation. However mutation of all 8 lysines simultaneously results in marked stabilisation of xNgn2 indicating redundancy in sites of ubiquitylation.

Possibly there is non-selective ubiquitylation of any lysine residue in the protein, which can then target for proteasomal degradation as has been described for cyclin B degradation by APC/CCdc20 (King et al., 1996). It is possible that ubiquitylation usually occurs on a particular lysine residue, but once that lysine is mutated the ubiquitylation process can be easily switched to another lysine residue. It may also be the case that modification of more than one lysine is important in regulating stability. This was the rationale behind adding back individual lysines in a lysineless background as discussed below.

When all the lysines are mutated to arginines in xNgn2KO we see an increase in the half-life of the protein and so we can postulate that mutating all the lysines stabilises xNgn2. However, this increased half-life is still only around 40 minutes (approximately double that of the wild type protein) and so xNgn2KO is still an unstable protein. Work by Jonathan Vosper suggested a role for other non-canonical sites of ubiquitylation and this is work discussed both in the next chapter and

(Vosper, 2008, Vosper et al., 2009). The degradation assays for single lysine to arginine mutants of xNgn2 (Figure 3.5) were carried out in *Xenopus laevis* interphase activated egg extract. Later experiments with single lysine to arginine xNgn2 mutants in neurula embryo extract hint at a difference in stabilisation in this extract system and so a systematic analysis of all xNgn2 lysine to arginine mutants in neurula embryo extracts would be desirable.

Lysines in xNgn2 conserved amongst related bHLH proteins – namely 77, 79 and 80 (the KIKK motif) and the bHLH lysines 85, 116 and 119 – were assessed for their role in xNgn2 stability in interphase and neurula extract degradation assays (Figures 3.7, 3.8 and 3.9). The lysine 77, 79, 80 'KIKK' motif, and K85, destabilise xNgn2KO to the level of xNgn2. However, in both interphase and neurula extracts, lysines 116 and 119 alone are not sufficient to target for destruction at the same rate as the wild type protein. Restoration of lysines in the 'KIKK' motif does target xNgn2 for efficient degradation whereas K116 and K119 do not.

The 'KIKK' lysines are not implicated in DNA binding. Lysine 85, in the basic domain, is directly implicated in DNA binding, whilst lysines 116 and 119 are proposed to contact DNA in the E-box (Bertrand et al., 2002). This might explain the difference in stability in neurula extract, which has a higher DNA content than egg extract. Binding of xNgn2 to DNA may preclude ubiquitylation of lysines 85, 116 and 119 thus stabilising xNgn2 (Figure 3.9). However lysines 116 and 119 destabilise xNgn2KO less than reintroduction of other lysine residues (Figure 3.8) and this may be due to their location in the HLH domain, the only putative structured region in the largely unstructured bHLH proteins (McEwan et al., 1996). Whilst xNgn2 is most likely an intrinsically disordered, natively unfolded protein (Aguado-Llera et al., 2010), the HLH lysines may still be unavailable for ubiquitylation by being present in a region that tends towards lower disorder. The lysine-rich N-terminus is predicted to be highly disordered and so may provide more available sites for canonical ubiquitylation. However my results suggest that degradation of xNgn2 can still be mediated by the HLH lysines and most likely by polyubiquitylation. This might not have been expected of lysine residues in the only region of the protein that forms a structured motif, but is perhaps unsurprising in such a highly disordered protein.

In Figure 3.10, EMSA shows that whilst wild type xNgn2 can bind DNA in the presence of xE12 in interphase, the 9S-AxNgn2 phosphomutant can bind in both interphase and mitosis. However the lysineless xNgn2KO is reduced in its ability to bind DNA, and reintroducing lysines 116 or 119 to xNgn2KO does not increase binding in interphase and mitotic extract. This result could suggest that each lysine on its own is not sufficient to support binding so perhaps investigation of R(116,119)KxNgn2KO – the double knock-in of the HLH lysines – would show whether both are required. However efficient DNA binding may require the action of K85, or all 3 lysines in the bHLH domain, or even others besides.

The EMSA result also seems to contradict Figure 5 of (Vosper et al., 2009), where xNgn2KO and indeed all mutant forms of xNgn2 appear to bind to DNA in the presence of xE12 in EMSA with similar affinities. However in those particular experiments, no *Xenopus laevis* extract incubation was used, only IVT protein and radiolabelled DNA probe in extract buffer (XB buffer) with large volumes of IVT protein (Christopher Hindley, personal communication). Therefore under those conditions it may be that binding is still possible, whereas the conditions I have used are different. For example, it is possible that lysines are already ubiquitylated when extract is used and therefore unable to bind DNA. The appearance of binding in the absence of extract, but no binding with incubation in extract, could suggest extract-dependent PTM – for example, ubiquitylation or phosphorylation – which impairs binding. In theory, xNgn2KO should still bind DNA as all lysines have been replaced with arginines, which whilst lacking the nucleophilic amine group required for ubiquitylation still maintain the positive charge that would be required for a strong DNA-binding interaction.

Finally it should be noted that this EMSA result is preliminary as it has been carried out only once and so whilst being indicative of the binding affinity of the HLH lysine mutant proteins, should not be taken as a conclusive result.

As discussed, work by Christopher Hindley in EMSA has shown that xNgn2KO can still potentially bind to an E-box oligonucleotide (Vosper et al., 2009). Therefore it might be assumed that the lysineless protein is active *in vivo*. However, work carried out by

Helen Wise in mRNA microinjections of Xenopus laevis embryos has suggested that xNgn2KO is significantly impaired in its ability to induce primary neurons as compared to the wild type protein (Helen Wise, unpublished data). My own injections of xNgn2KO would suggest that xNgn2KO is less active than xNgn2 but not inactive (Figures 3.11, 3.12, 3.13). However I am typically injecting higher amounts of xNgn2KO mRNA (≥ 20 pg) than Helen Wise (10 pg), which result in greater activity of xNgn2KO. Nevertheless, xNgn2KO shows comparatively less activity than wild type xNgn2. It is possible that lysine residues, aside from acting as sites of ubiquitylation targeting for proteasomal degradation, are also acting at the level of transcription factor activity in xNgn2 in a structural manner not related to protein stability. Otherwise we would hypothesise that a more stable form of xNgn2 would also be more active. xNgn2KO is less active than xNgn2 at inducing neural β-tubulin expression (Figure 3.11) and at inducing its downstream target xNeuroD (Figure 3.13) therefore xNgn2KO is less active as a transcription factor. xNgn2KO does not appear to act as a dominant negative repressor of xNgn2 activity by sequestering xE12 without binding DNA, as xNgn2 can still promote ectopic neurogenesis even in the presence of xNgn2KO (Figure 3.12).

My data indicate that ubiquitylation can occur on most or all lysines to target xNgn2 for destruction. Firstly, although reintroduction of ubiquitylation sites seems the most likely cause of instability, other factors such as effects on the structure of the protein cannot be ruled out. Mass spectrometry could be used to definitively identify ubiquitylation at these sites. Also, it is thus far not clear whether these are consensus sites for ubiquitylation or whether the ubiquitylation machinery is so promiscuous that any lysine is suitable for targeting for degradation. Certainly mutating individual lysines to arginines showed no individual lysine is essential to target xNgn2 for degradation (Figure 3.5).

xNgn2KO is still unstable, with a half-life of only 47.8 +/- 7.9 mins (Figure 3.4, B) and work by Jonathan Vosper established that ubiquitylation of xNgn2 still occurs even when all lysines are mutated (Vosper et al., 2009). Therefore the next step was to investigate where else ubiquitylation targeting xNgn2 for degradation was occurring.

CHAPTER 4

Non-Canonical Ubiquitylation of xNgn2

INTRODUCTION

The ubiquitylation of proteins canonically takes place on internal lysine residues. However for an increasing number of proteins, ubiquitylation on other sites has been demonstrated. Modification of the N-terminus by polyubiquitylation to target for proteasomal degradation has been described and even proteins with all lysines mutated to arginines are ubiquitylated and degraded (Ben-Saadon et al., 2004, Breitschopf et al., 1998). Where ubiquitylation is still required for proteasomal degradation, N-terminal ubiquitylation can be invoked. There are also naturally occurring lysineless proteins where N-terminal ubiquitylation has been suggested (Ben-Saadon et al., 2004). Ubiquitylation on the N-terminal amine group is chemically identical to lysine ubiquitylation (Figure 4.1, A).

In fact, Aaron Ciechanover makes the point himself that many proteins are wrongly assumed to be ubiquitylated only on lysines. The evidence for lysine ubiquitylation is often indirect evidence based on mutational analyses. Chromatographic techniques or mass spectroscopy are suggested to be the only methods of directly identifying ubiquitylation sites (Chapter 2 in (Mayer, 2005)).

xNgn2 protein stability increases when lysine residues, the canonical sites of ubiquitylation, are no longer available. However xNgn2KO, the form of xNgn2 with all lysines mutated to arginines, is still an unstable protein. Moreover ubiquitylation of xNgn2 could still be observed by Jonathan Vosper (Vosper et al., 2009) and I have demonstrated that no particular lysine residue shows particular prominence as a regulator of xNgn2 stability, as is often observed in proteins demonstrating N-terminal ubiquitylation.

The N-terminal amine is not the only nucleophilic group besides lysine amines in proteins. There is a growing body of evidence for ubiquitylation on other nucleophilic residues such as thiol-containing cysteines (Figure 4.1, B) (Cadwell and Coscoy, 2005, Cadwell and Coscoy, 2008, Carvalho et al., 2007, Grou et al., 2008, Kragt et al., 2005, Leon and Subramani, 2007, Williams et al., 2007) and hydroxyl-containing residues such as serines, threonines and potentially tyrosines (Figure 4.1, C) (Ishikura et al., 2010, Tait et al., 2007, Vosper et al., 2009, Wang et al., 2007).

This chapter examines the role of non-canonical sites of ubiquitylation in xNgn2 stability firstly in *Xenopus laevis* extract but then also in the P19 *Mus musculus* embryonal carcinoma cell line (McBurney and Rogers, 1982), to verify that the phenomena examined are not merely an artefact of *Xenopus laevis in vitro* systems. P19 cells can differentiate into neurons (McBurney et al., 1982) and into both neurons and glial cells on treatment with retinoic acid (Jones-Villeneuve et al., 1982). Various genes associated with neurogenesis, including NeuroD, have been identified in differentiated P19 cells (Teramoto et al., 2005).

In this chapter I aim to determine if the N-terminus of xNgn2 is ubiquitylated in a manner that can be blocked by another protein modification, co-translational N-terminal acetylation. From this I investigate whether xNgn2 is ubiquitylated on non-canonical sites, whether such modification has physiological relevance, and whether non-canonical ubiquitylation can be verified in the mouse embryonal carcinoma P19 cell line.

RESULTS

xNgn2 N-terminal ubiquitylation is blocked by co-translational acetylation

Acetylation and ubiquitylation on specific residues are mutually exclusive reactions in the cell (Polevoda and Sherman, 2000, Polevoda and Sherman, 2002) (Figure 4.2). To assess whether N-terminal ubiquitylation in xNgn2 is possible, a series of N-terminal cotranslational acetylation mutants was constructed.

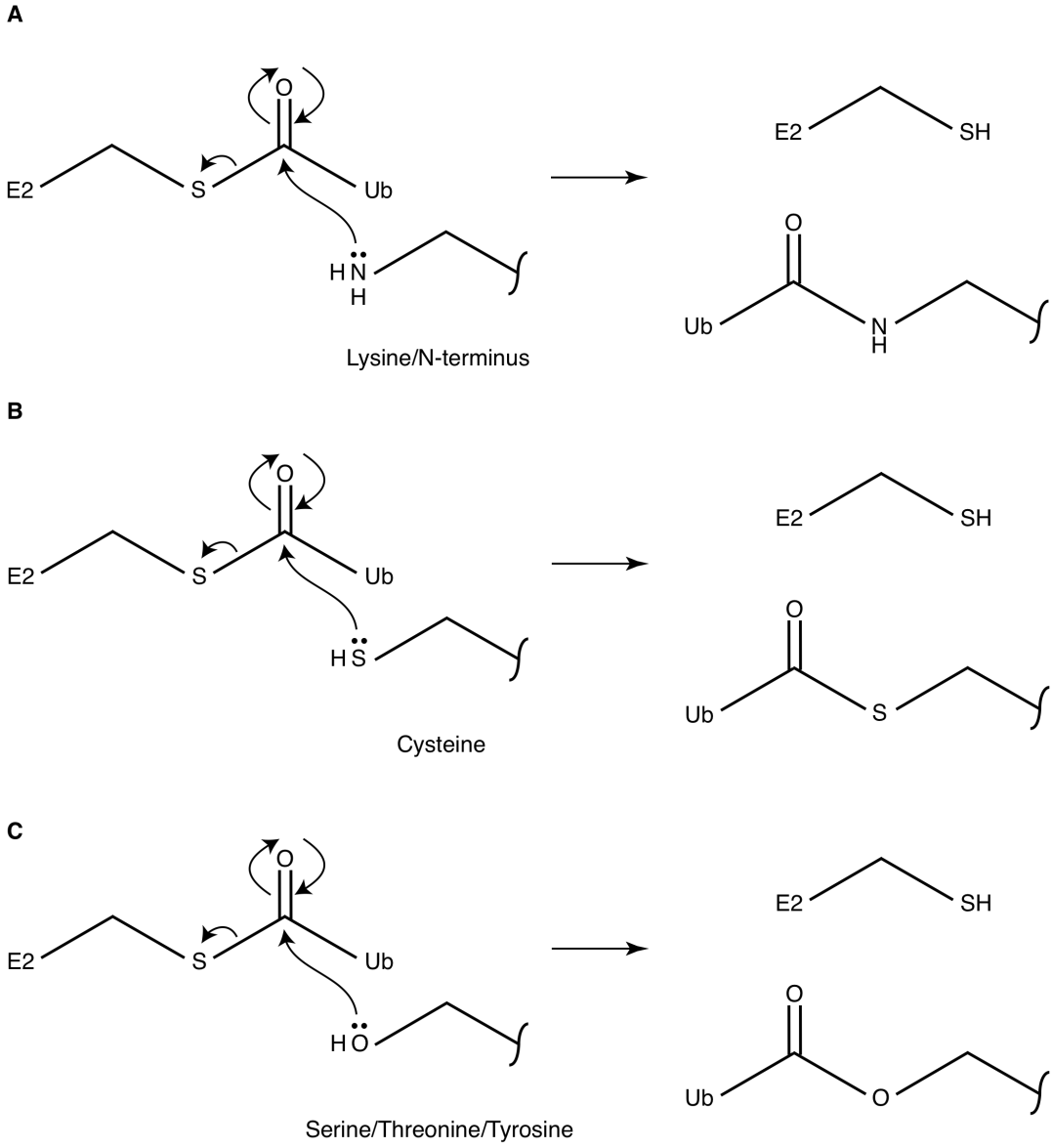

Figure 4.1: Nucleophilic sites of ubiquitylation.

Proteins contain many nucleophilic sites capable of attacking an E2-Ub thioester linkage and becoming ubiquitylated. The best-described sites are (A) the amine-containing internal lysine residues and the free amine of the N-terminus of the polypeptide backbone. However (B) cysteine thiols and (C) hydroxyls on serines, threonines and tyrosines could also potentially be ubiquitylated by an identical mechanism.

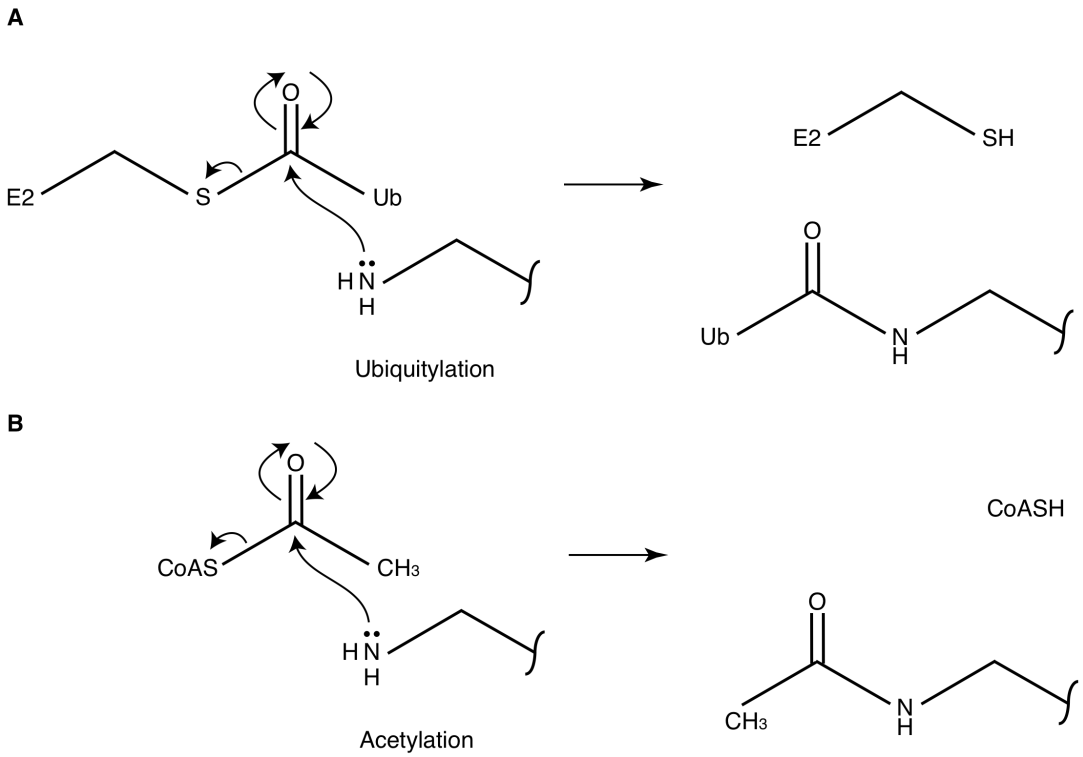

Figure 4.2: N-terminal acetylation and ubiquitylation are mutually exclusive reactions.
The N-terminal amine group of polypeptides can potentially either be (A) ubiquitylated or (B) acetylated.

N-terminal consensus sequences can target a protein for co-translational acetylation with high probability (Polevoda and Sherman, 2003b, Polevoda and Sherman, 2003a) and so constructs were designed by Jonathan Vosper and Ian Horan to both potentiate and inhibit co-translational acetylation; Ac1xNgn2 (mutation of N-terminal sequence from MVLL to MSES); Ac2xNgn2 (mutation of MVLL to MAES) and Ac3xNgn2 (mutation of MVLL to MPLL). Ac1xNgn2 and Ac2xNgn2 are both predicted to be acetylated whilst co-translational acetylation should be blocked in Ac3xNgn2. The effect of the Ac3 mutation cannot necessarily be predicted. The presence of a proline at the N-terminus of β-galactosidase stabilises the protein (Bachmair et al., 1986) whereas addition of a non-cleavable Ub moiety to the N-terminus is destabilizing (Johnson et al., 1992).

Work on the stability of acetylation mutants has been carried out previously, showing that blocking the N-terminus by co-translational acetylation stabilises xNgn2 and that an acetylated form of xNgn2 with all lysines mutated to arginines shows an even greater increase in stability (Vosper et al., 2009). To investigate whether co-translational acetylation is being regulated as predicted in the acetylation constructs, I blocked protein acetylation during *in vitro* translation and performed degradation assays using *Xenopus laevis* interphase activated egg extracts.

Acetylation was blocked according to the method of Palmiter (Palmiter, 1977). Addition of citrate synthase and oxaloacetate depletes the acetyl CoA within the reticulocyte lysate and metabolises it to citrate. Therefore there is no available Acetyl CoA for protein acetylation. This treated reticulocyte lysate was then used for *in vitro* translation followed by degradation assays.

Acetylation blocking experiments were carried out using lysineless forms of xNgn2. In xNgn2KO all lysines are mutated to arginines, thereby removing the possibility of ubiquitylation on lysines. In Ac2xNgn2KO, the N-terminus of the lysineless protein has been mutated to the co-translational acetylation consensus sequence; and in Ac3xNgn2KO, the N-terminus of the lysineless protein has been mutated to a sequence associated with repression of co-translational acetylation. Radiolabelled proteins were translated *in vitro* in reticulocyte lysate depleted of Acetyl CoA

(Palmiter, 1977) and added to *Xenopus laevis* interphase activated egg extracts. Aliquots of the degradation reaction were removed at increasing timepoints into quenching SDS-LB and separated by 15 % SDS-PAGE. Half-lives for the rates of degradation were then calculated using first-order rate kinetics (Figure 4.3).

xNgn2KO has a half-life of 60.9 +/- 15.7 mins in acetylation blocking conditions and a half-life of 67.8 +/- 19.2 mins without acetylation blocking. Ac3xNgn2KO has half-lives of 53.7 +/- 11.4 mins and 41.2 +/- 6.6 mins in the same respective conditions. Therefore these proteins show similar half-lives to one another and no stabilisation when cotranslational acetylation is blocked.

Ac2xNgn2KO is more stable than xNgn2KO or Ac3xNgn2KO in the control experiment (91.4 +/- 10.1 mins compared to 67.8 +/- 19.2 mins and 41.2 +/- 6.6 mins respectively) but when acetylation is blocked, Ac2xNgn2KO, xNgn2KO and Ac3xNgn2KO all have similar half-lives (42.5 +/- 5.9 mins, 60.9 +/- 15.7 mins and 53.7 +/- 11.4 mins respectively, Figure 4.3, B). Hence blocking acetylation destabilises Ac2xNgn2KO to the level of xNgn2KO, which has a wild type N-terminal sequence.

It is predicted that the wild type and Ac3 N-termini of xNgn2 are not normally co-translationally acetylated, but the Ac2 protein is (Vosper et al., 2009). Under conditions allowing protein acetylation, Ac2xNgn2KO is acetylated, blocking ubiquitylation, conferring stability on the protein. xNgn2KO and Ac3xNgn2KO are not acetylated and therefore can be N-terminally ubiquitylated and degraded. When co-translation acetylation is blocked, Ac2xNgn2KO can be N-terminally ubiquitylated again, leading to decreasing stability. The Ac2 mutants are therefore correctly targeted for N-terminal acetylation and the N-terminus of xNgn2KO acts as a site targeting for proteasomal degradation.

A

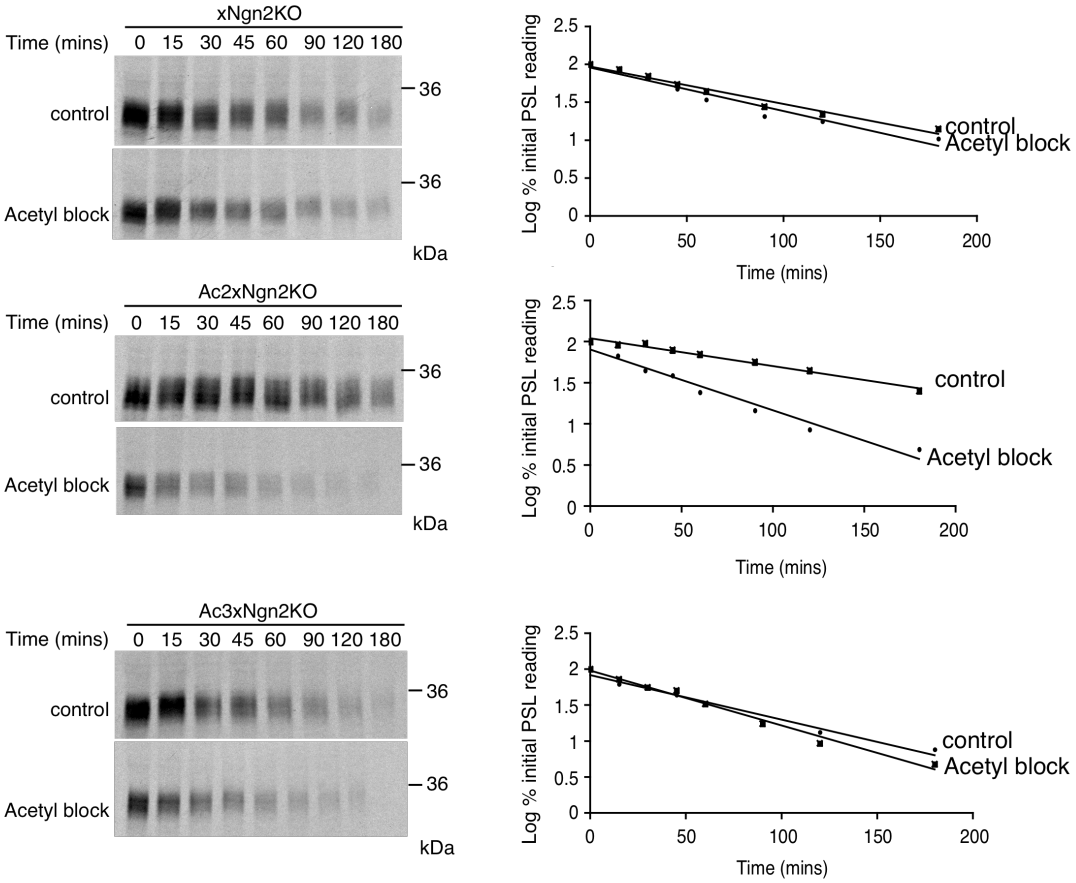

B

Construct	Half life (mins) (acetyl block)	Half life (mins) (control)
xNgn2KO	60.9 +/- 15.7	67.8 +/- 19.2
Ac2xNgn2KO	42.5 +/- 5.9	91.4 +/- 10.1
Ac3xNgn2KO	53.7 +/- 11.4	41.2 +/- 6.6

Figure 4.3: xNgn2 N-terminal ubiquitylation and acetylation are mutually exclusive.
Xenopus laevis interphase activated egg extracts were supplemented with ^{35}S-labelled xNgn2KO, Ac2xNgn2KO or Ac3xNgn2KO in the presence or absence of citrate synthase and oxaloacetate, which depletes the reticulocyte lysate of acetyl CoA. Samples were taken at the timepoints indicated and subjected to 15 % SDS-PAGE. Gels were analysed by autoradiography and quantitative phosphorimaging analysis, plotting readings at each timepoint as a log of the reading as a percentage of the reading at 0 mins (A). (B) Half-lives in the presence or absence of acetylation-blocking conditions were calculated using first-order rate kinetics, and errors calculated using the Standard Error of the Mean (SEM).

xNgn2 and Ac2xNgn2KO degradation are ATP-dependent

N-terminal acetylation can stabilise xNgn2 against proteasomal degradation but Ac2xNgn2KO – with all canonical sites of ubiquitylation blocked – is still degraded with a half-life of 91.4 +/- 10.1 mins (Figure 4.3, B). To determine if Ac2xNgn2KO is still degraded by the proteasome, I investigated the ATP-dependence of xNgn2 stability. Degradation by the 26S proteasome is ATP-dependent, requiring energy to activate the Ub moiety and then to unfold the protein at the 26S proteasome (Glickman and Ciechanover, 2002). *Xenopus laevis* extract systems can be depleted of ATP to assess whether IVT radiolabelled proteins added to the extract are still degraded in a proteasome-independent manner. ^{35}S-radiolabelled IVT xNgn2 or Ac2xNgn2KO were added to high-speed *Xenopus laevis* interphase activated egg extract cleared of ribosomes by spinning at 107,400 x g for 40 mins and treated with either ER (energy regeneration mix) or 0.8 μmoles glucose and 1.3 units hexokinase to deplete the extract of ATP. Aliquots of the degradation reaction were removed at increasing timepoints into quenching SDS-LB and separated by 15 % SDS-PAGE. Half-lives for the rates of degradation were then calculated using first-order rate kinetics (Figure 4.4).

xNgn2 has a half-life of 30.6 +/- 2.1 mins in the presence of ATP but is stabilised to 175.5 +/- 2.2 mins in the absence of ATP (Figure 4.4, C). Ac2xNgn2KO is substantially more stable in ATP-containing extract compared with wild type xNgn2 with a half-life of 130.7 +/- 38.3 mins, roughly 4-fold higher than xNgn2 (Figure 4.4, C). However in an ATP-depleted environment Ac2xNgn2KO half-life increases beyond the range of the timecourse (> 240 mins).

Degradation of both xNgn2 and Ac2xNgn2KO is ATP-dependent. This has already been demonstrated for xNgn2 using the proteasome inhibitor MG132 (Figure 3.1). Ac2xNgn2KO lacks all canonical lysine ubiquitylation sites as well as the N-terminal amino group. Therefore Ac2xNgn2KO must be targeted for proteasomal degradation using other factors. One possible route is by ubiquitylation on non-canonical sites.

A

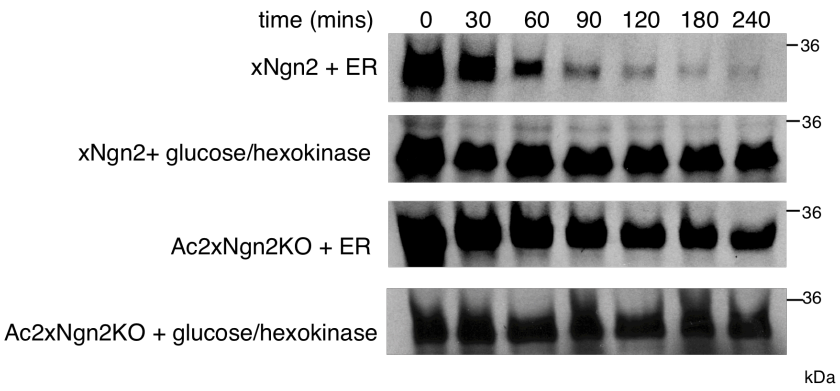

B

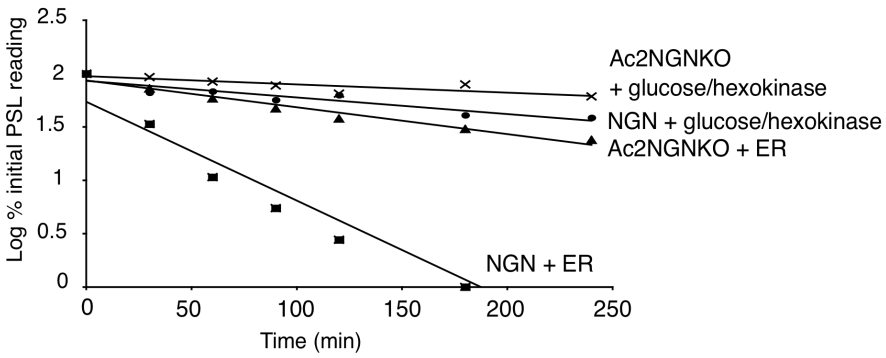

C

Protein	Half-life (mins)
xNgn2+ ER	30.6 +/- 2.1
xNgn2 + glucose/hexokinase	175.5 +/- 2.2
Ac2xNgn2KO + ER	130.7 +/- 38.3
Ac2xNgn2KO + glucose/hexokinase	> 240

Figure 4.4: ATP-depletion stabilises xNgn2 and Ac2xNgn2KO.

High-speed *Xenopus laevis* interphase activated egg extracts were supplemented with ^{35}S-labelled xNgn2 or Ac2xNgn2KO in the presence of either energy regeneration (ER) mix or 1.3 units hexokinase with 0.8 μmoles glucose, to deplete the extract of ATP. Samples were taken at the timepoints indicated and subjected to 15 % SDS-PAGE. Gels were analysed by autoradiography (A) and quantitative phosphorimaging analysis, plotting readings at each timepoint as a log of the reading as a percentage of the reading at 0 mins (B). (C) Half-lives in the presence or absence of acetylation-blocking conditions were calculated using first-order rate kinetics, and errors calculated using the Standard Error of the Mean (SEM).

Labile ubiquitylation linkages in xNgn2 are also present in mMyoD

xNgn2 is polyubiquitylated in *Xenopus* extract (Vosper et al., 2007). An example of a ubiquitylation assay (see Figure 2.2) of xNgn2 in *Xenopus laevis* extract is shown in Figure 4.5A. ^{35}S-radiolabelled IVT xNgn2 was added to *Xenopus laevis* interphase activated egg extract supplemented with MG132 (to prevent proteasomal degradation) and either His_6-Ub (Sigma) or untagged Ub (Sigma). This reaction was incubated at 20 °C for 90 mins. Samples were then incubated with denaturing Vosper buffer (containing 8.5 M urea) and nickel-chelating agarose beads (Ni-NTA, Invitrogen) to purify his-tagged protein. In samples using his-tagged Ub this therefore pulls down ubiquitylated proteins, resulting in the polyubiquitylation ladder on 12 % SDS-PAGE (Figure 4.5, A). This depicts xNgn2 being modified progressively by multiple Ub moieties. In samples with untagged Ub, anything appearing on the autoradiograph will be due to non-specific binding of proteins to the beads. Therefore this acts as a control for background, non-specific protein pulldown in an experiment.

Before separation by SDS-PAGE, the samples are eluted in a high pH reducing (R) SDS-LB, or in a non-reducing (N) SDS-LB. In Figure 4.5, A, lanes 1 and 2 both show a ladder of ubiquitylated forms of xNgn2. Lane 1, the reducing (R) lane, shows an higher mobility band (highlighted by an arrow). This band runs at the level of unmodified xNgn2. Such a band may appear if unmodified xNgn2 binds to the beads non-specifically; or if a ubiquitylated form of xNgn2 loses its polyUb chain after being pulled down by the nickel beads. The difference between lanes 1 and 2 is that the sample in lane 1 has been subjected to reducing conditions at high pH, which can rupture labile linkages such as ester and thioester links. Such links can be made between cysteines, serines or threonines to the C-terminus of ubiquitin in an analogous fashion to the lysine-Ub isopeptide bond. Therefore in lane 1, such links may have been broken to liberate the unmodified xNgn2 protein after pulldown, whilst in lane 2 the more gentle treatment of the sample maintains these labile linkages.

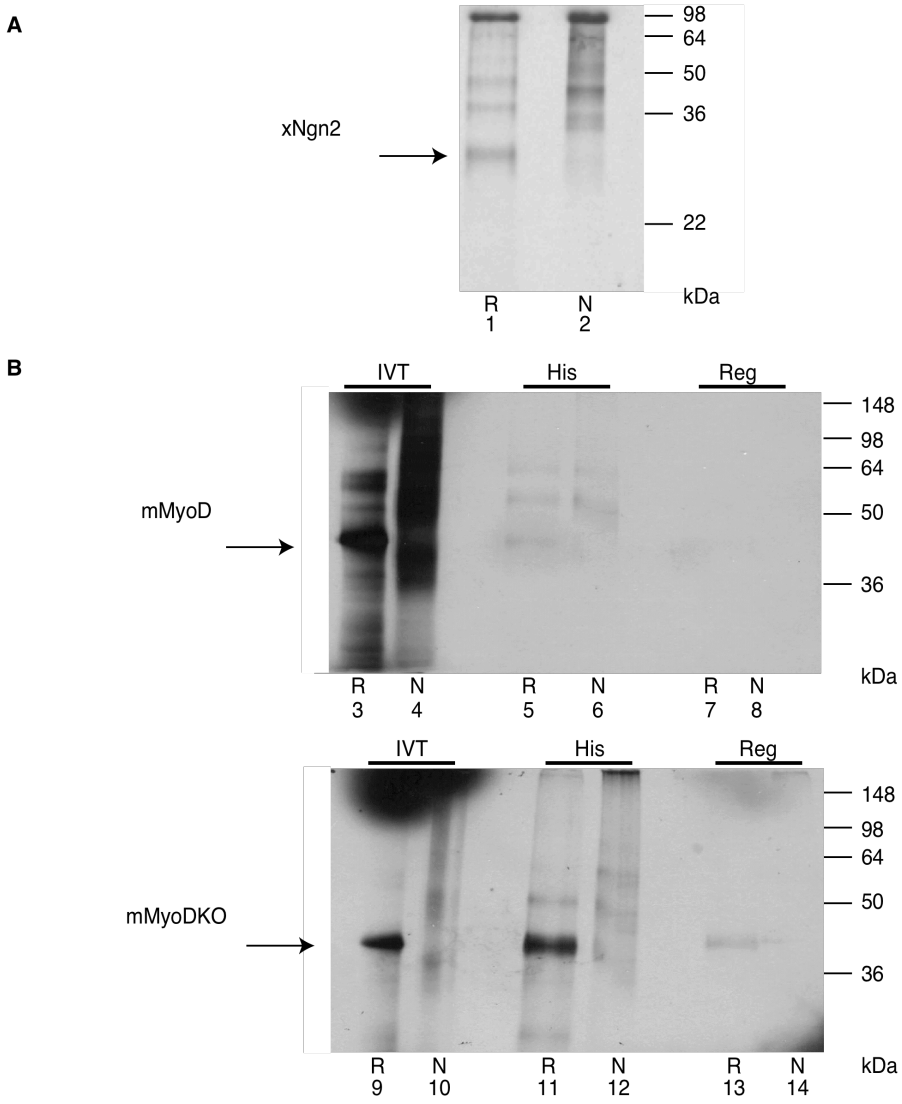

Figure 4.5: Reducing agent dependence of xNgn2, mMyoD and mMyoDKO ubiquitylation.
Xenopus laevis interphase activated egg extracts were supplemented with ^{35}S-radiolabelled xNgn2 (A), mMyoD or mMyoDKO (B) in the presence of MG132 and either His_6-ubiquitin (His) or untagged ubiquitin as a control for background binding (Reg). Samples were isolated in either high pH 10 % β-mercaptoethanol reducing loading buffer (R) or non-reducing loading buffer (N). Sample of *in vitro* translated (IVT) radiolabelled protein were run out with samples on 12 % SDS-PAGE. Lanes are numbered 1-14 as described in text. Arrows highlight the position of bands representing unmodified protein.

The reducing agent dependence of xNgn2 and xNgn2KO was demonstrated by Jonathan Vosper (Vosper et al., 2009). To investigate whether other proteins undergo reducing agent-dependent ubiquitylation, a ubiquitylation assay was carried out with the related bHLH proteins mMyoD and mMyoDKO (Figure 4.5, B).

Unmodified mMyoD is released under reducing conditions (Figure 4.5, B, comparing lanes 3 and 5, highlighted by arrow). This band does not appear under non-reducing conditions (Figure 4.5, B, comparing lanes 5 and 6). This indicates ubiquitylation of mMyoD via labile linkages to non-canonical sites.

This effect is present also in mMyoDKO, but to a much more obvious extent (Figure 4.5, B, lane 11 compared to lanes 9 and 12 and highlighted by arrow), even accounting for a low level of background binding of protein (Figure 4.5, B, lane 13). Therefore non-canonical ubiquitylation also occurs in the lysineless form mMyoDKO where the only non-labile linkage site remaining is the N-terminal amino group.

Non-canonical ubiquitylation is evident in both xNgn2 (Figure 4.5, A, (Vosper et al., 2009)) and mMyoD (Figure 4.5, B) and their lysineless forms. I wished to investigate which particular non-canonical sites may be targeting for proteasomal degradation in xNgn2.

Cysteines are ubiquitylation sites in xNgn2

xNgn2 and mMyoD can be ubiquitylated in the absence of canonical ubiquitylation sites. Other nucleophilic residues, such as cysteines, could form labile thioester bonds with the C-terminus of Ub (Figure 4.1, B). Some examples of cysteine ubiquitylation have been described in peroxisomal degradation and in viral systems (Cadwell and Coscoy, 2005, Cadwell and Coscoy, 2008, Carvalho et al., 2007, Grou et al., 2008, Kragt et al., 2005, Leon and Subramani, 2007, Williams et al., 2007). Suggestions of ubiquitylation on serine and threonine have also been made (Ishikura et al., 2010, Tait et al., 2007, Wang et al., 2007). However ubiquitylation simultaneously on canonical and non-canonical sites has not been demonstrated to

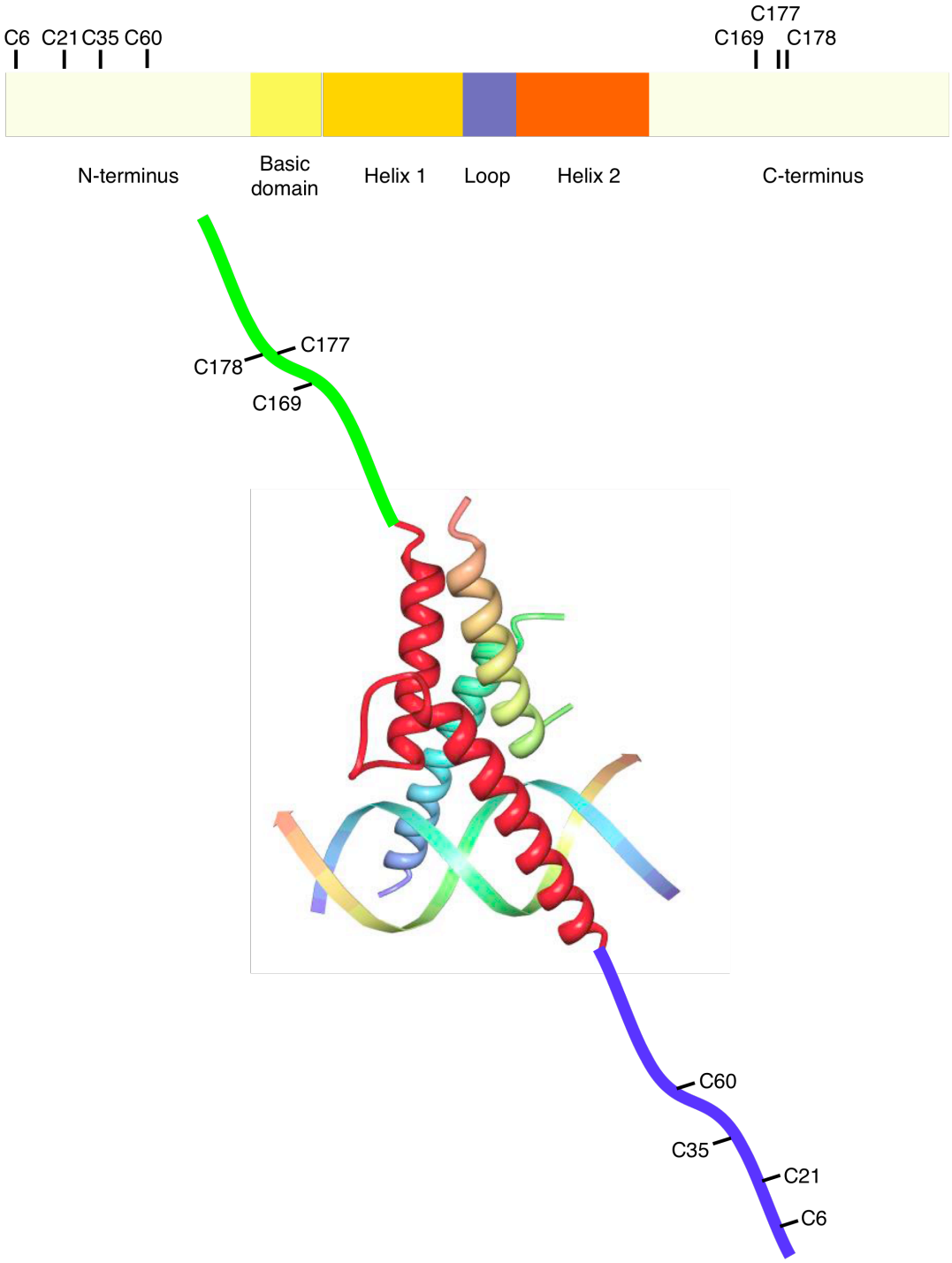

Figure 4.6: Cysteine residues in xNgn2.

Schematic of cysteine positions and cysteines modelled onto a structure of a proneural bHLH heterodimer complexed to DNA. The disordered N-terminal domain is bordered in blue; the bHLH domain in red; and the disordered C-terminal domain in green.

target proteins for proteasomal degradation. xNgn2 has 7 cysteine residues (Figure 4.6).

A mutant of xNgn2 with cysteines mutated to alanines was created by site-directed mutagenesis to produce xNgn2CO, to investigate any effect of loss of cysteines from xNgn2 on stability. ^{35}S-radiolabelled IVT xNgn2 or xNgn2 mutants lacking canonical or non-canonical putative ubiquitylation sites were added to *Xenopus laevis* interphase activated egg extract and incubated at 21 °C. Aliquots of the degradation reaction were removed at increasing timepoints into quenching SDS-LB and separated by 15 % SDS-PAGE. Half-lives for the rates of degradation were then calculated using first-order rate kinetics (Figure 4.7).

xNgn2CO exhibits a half-life of 33.3 +/- 2.1 mins compared to the stability of xNgn2 (21.5 +/- 0.2 mins). However the stabilisation is much less than the stabilisation provided by blocking off internal lysines (xNgn2KO, 60.2 +/- 1.4 mins), the N-terminus (Ac2xNgn2, 52.4 +/- 6.3 mins), or all canonical sites (Ac2xNgn2KO, 138 +/- 20 mins) from ubiquitylation. xNgn2CO is significantly more stable than xNgn2 but much less stable than xNgn2KO or Ac2xNgn2. This indicates cysteines do target for UPS-mediated degradation but not as efficiently as canonical ubiquitylation sites.

To confirm that all these mutants are being degraded by Ub-mediated proteolysis, ubiquitylation assays were carried out in *Xenopus laevis* interphase activated egg extract. ^{35}S-radiolabelled IVT xNgn2, Ac2xNgn2KO, Ac2xNgn2CO or Ac2xNgn2KOCO were added to *Xenopus laevis* interphase activated egg extract supplemented with MG132 to prevent proteasomal degradation, and either His_6-Ub (Sigma) or untagged Ub (Sigma). An IVT reaction using empty pCS2+ vector (as a control) was also included. This reaction was incubated at 20 °C for 90 mins. Samples were then incubated with denaturing Vosper buffer (containing 8.5 M urea) and nickel-chelating agarose beads (Ni-NTA, Invitrogen) to purify his-tagged protein. Samples were eluted in a high pH reducing (R) SDS-LB, or in a non-reducing (N) SDS-LB and run out on 12 % SDS-PAGE (Figure 4.8, A).

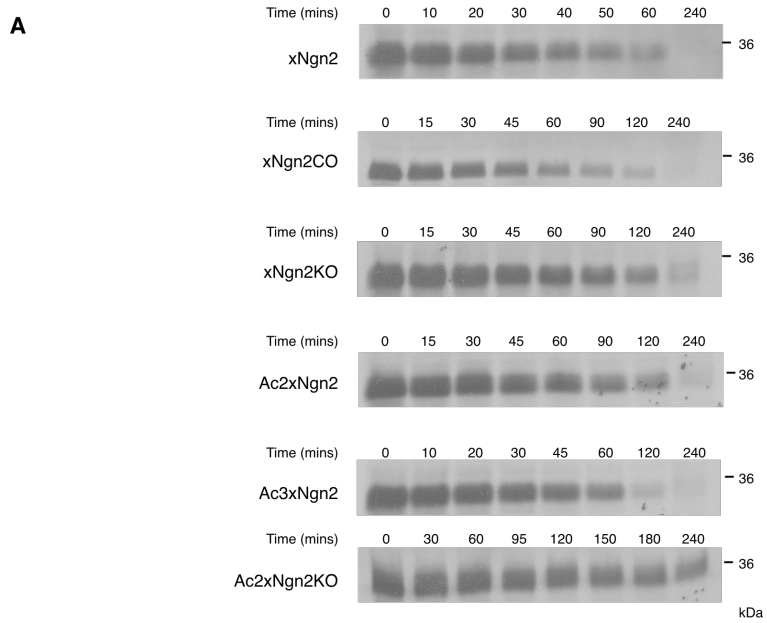

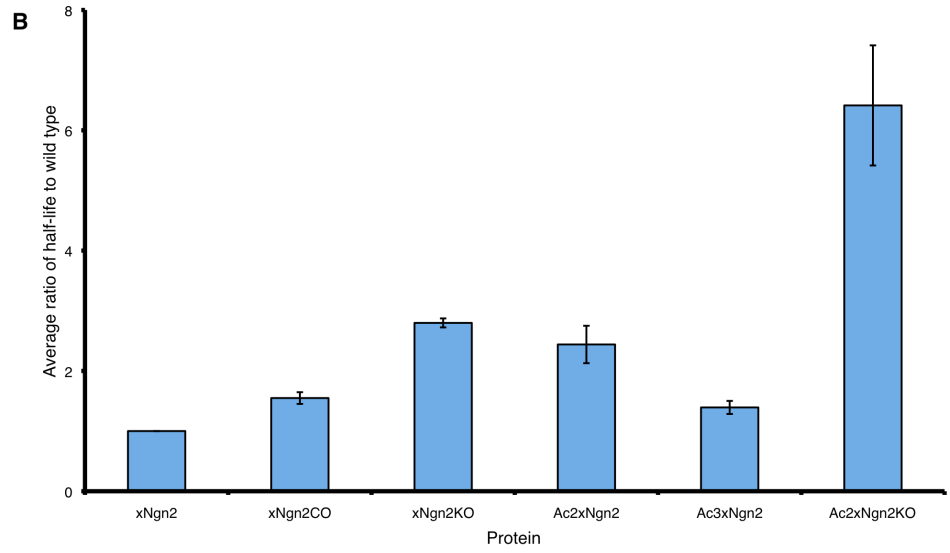

C

Sample	Half-life (mins)
xNgn2	21.5 +/- 0.2
xNgn2CO	33.3 +/- 2.1
xNgn2KO	60.2 +/- 1.4
Ac2xNgn2	52.4 +/- 6.3
Ac3xNgn2	29.9 +/- 2.1
Ac2xNgn2KO	138 +/- 20

Figure 4.7: Comparison of stability of canonical and non-canonical xNgn2 ubiquitylation site mutants in *Xenopus* interphase egg extract.

Xenopus interphase extracts were supplemented with ^{35}S-labelled xNgn2, xNgn2CO, xNgn2KO, Ac2xNgn2, Ac3xNgn2 or Ac2xNgn2KO. Samples were taken at the timepoints indicated and subjected to 15 % SDS-PAGE. Gels were analysed by autoradiography (A). (B) Half-lives were normalised to xNgn2 stability in each experiment and the average ratio of stability of each protein with respect to wild type plotted. (C) Half-lives were calculated using first-order rate kinetics, and errors calculated using the Standard Error of the Mean (SEM).

In Figure 4.8, A, all xNgn2 proteins are ubiquitylated. For xNgn2 (Figure 4.8, A, lanes 5 and 6), Ac2xNgn2KO (Figure 4.8, A, lanes 9 and 10), Ac2xNgn2CO (Figure 4.8, A, lanes 13 and 14) and Ac2xNgn2KOCO (Figure 4.8, A, lanes 17 and 18) there are polyubiquitylation ladders that show a dependence on high pH and reducing conditions, displaying a band at the mass of unmodified protein under reducing (R) conditions (Figure 4.8, A, lanes 5, 9, 13 and 17).

The labile linkages that are broken to release unmodified protein are produced even in wild type xNgn2 (Figure 4.8, A, lane 5), where canonical sites of ubiquitylation are present. In Ac2xNgn2CO (Figure 4.8, A, lane 13) whilst there is some unmodified protein liberated under reducing conditions, there are still lysines present in the protein that can be ubiquitylated. Comparing xNgn2 (lanes 5 and 6) with Ac2xNgn2CO (lanes 13 and 14) it is clear that mutation of cysteines to alanines leads to formation of clearer, tighter bands on the gel. Ac2xNgn2KO demonstrates the most dramatic collapse of the polyubiquitylation ladder (lane 10) to an unmodified band (lane 9) as only non-canonical, non-amine nucleophiles remain in the protein. When cysteines are mutated as well as the N-terminus and the lysines, in Ac2xNgn2KOCO, ubiquitylation still persists (lanes 17 and 18). Therefore ester linkages through hydroxyl-containing amino acid residues, for example serine and threonine, are also formed in the ubiquitylation assay and broken in reducing conditions.

There is a single band apparent in the untagged Ub gel under reducing (R) conditions (Figure 4.8, A lanes 7 and 11 particularly, also lanes 15 and 19). This suggests insufficient washing of the nickel beads resulting in a high level of background binding especially for xNgn2 and Ac2xNgn2KO.

To assess whether ubiquitylation on reducing-agent/high pH/high temperature dependent sites is specific to bHLH proteins, ubiquitylation assays were carried out with the important anaphase promoting complex/cyclosome (APC/C) substrate Mes1 (Kimata et al., 2008, Yamano et al., 2004) and its lysineless mutant Mes1KO (Figure 4.8, B). ^{35}S-radiolabelled IVT Mes1 or Mes1KO were added to *Xenopus laevis* interphase activated egg extract supplemented with MG132 to prevent proteasomal degradation, and either His_6-Ub (Sigma) or untagged Ub (Sigma). This reaction was

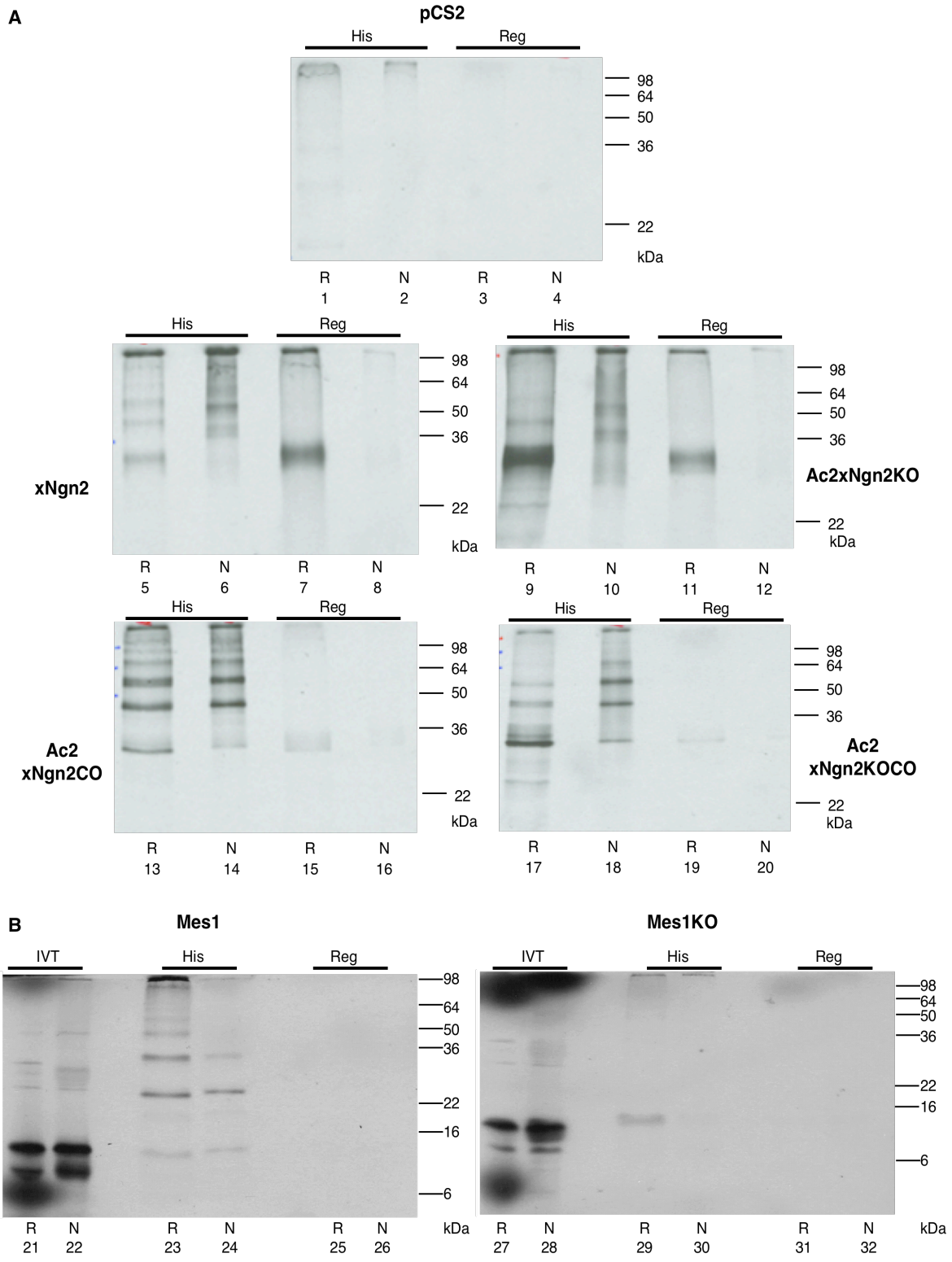

Figure 4.8: Ubiquitylation assays highlighting cysteine ubiquitylation in *Xenopus* extract.
Xenopus laevis interphase extracts were supplemented with (A) ^{35}S-radiolabelled xNgn2, Ac2xNgn2KO, Ac2xNgn2CO, Ac2xNgn2KOCO or pCS2+ and (B) the yeast protein Mes1 or its lysineless form Mes1KO. Either His_6-Ub (His) or untagged Ub (Reg) were added. Samples were isolated in either reducing SDS-LB (R) or non-reducing SDS-LB (N) and run on 12 % SDS-PAGE.

incubated at 20 °C for 90 mins. Samples were then incubated with denaturing Vosper buffer (containing 8.5 M urea) and nickel-chelating agarose beads (Ni-NTA, Invitrogen) to purify his-tagged protein. Samples were eluted in a high pH reducing (R) SDS-LB, or in a non-reducing (N) SDS-LB and run out on 12 % SDS-PAGE (Figure 4.8, B).

Mes1 is polyubiquitylated as demonstrated by the polyubiquitylation ladder produced in reducing (R) and non-reducing (N) conditions (Figure 4.8, B, lanes 23 and 24). However neither sample exhibits a strong band running at the level of the IVT proteins in lanes 21 and 22. Therefore there is not a reducing agent dependence in Mes1 ubiquitylation. In Mes1KO, the reducing conditions produce a band running at the level of the unmodified IVT protein (lane 29 compared to lanes 27 and 28). There is no evidence of a polyubiquitylation ladder in lanes 29 and 30. Therefore Mes1KO is not highly ubiquitylated but the appearance of an unmodified protein band liberated in reducing conditions suggests that, in the absence of lysines, some ubiquitylation is possible on non-canonical sites, using labile linkages.

The behaviour of Mes1 ubiquitylation is very different to xNgn2 and xMyoD. Therefore non-canonical ubiquitylation is specific to the particular proteins present in *Xenopus* extract and not the extract itself. As this ubiquitylation occurs on xNgn2 I wished to investigate particular non-canonical sites of ubiquitylation further.

There are 2 cysteine residues conserved in the sequence of *Homo sapiens*, *Mus musculus* and *Xenopus laevis* Ngn2 proteins, cysteines 169 and 178, highlighted in the ClustalW2 analysis in Figure 4.9. To assess whether these conserved cysteines may be important ubiquitylation sites, Christopher Hindley performed site-directed mutagenesis to create mutants of cysteine residues in xNgn2 to alanine, creating C178AxNgn2 and C(169,178)AxNgn2, which were then assessed by degradation assay. ^{35}S-radiolabelled IVT xNgn2 or xNgn2 cysteine mutants were added to *Xenopus laevis* interphase activated egg extract and incubated at 21 °C. Aliquots of the degradation reaction were removed at increasing timepoints into SDS-LB and separated by 15 % SDS-PAGE. Half-lives for the rates of degradation were then calculated using first-order rate kinetics (Figure 4.10).

Figure 4.9: Alignment highlighting conserved cysteines in xNgn2.

Cysteines 169 and 178 are conserved cysteines in Ngn2 across species, shown in boxes above. ClustalW2 analysis was carried out to align neurogenin and NeuroD sequences from *Xenopus laevis* (x), *Mus musculus* (m) and *Homo sapiens* (h). Exact matches are denoted by * and decreasingly similar properties by : and . with no symbol present for no similarity. – highlights a gap in the sequence alignment. The disordered C-terminal domain is bordered in green.

A

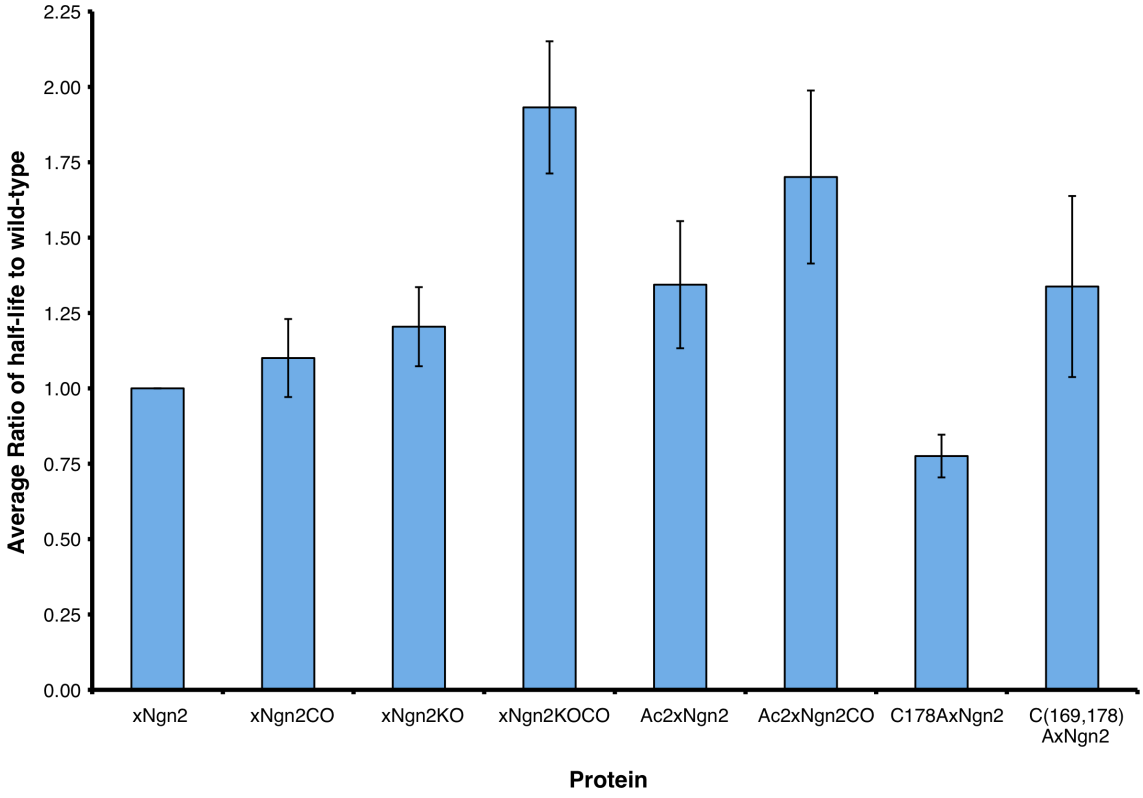

B

Sample	Half-life (mins)
xNgn2	30.5 +/- 2.5
xNgn2CO	33.0 +/- 2.0
xNgn2KO	36.3 +/- 2.9
xNgn2KOCO	64.2 +/- 10.2
Ac2xNgn2	43.3 +/- 3.5
Ac2xNgn2CO	50.8 +/- 6.1
C178AxNgn2	23.3 +/- 0.9
C(169,178)AxNgn2	39.5 +/- 6.7

Figure 4.10: The role of conserved cysteines in stability in *Xenopus* interphase egg extract. *Xenopus laevis* interphase extracts were supplemented with ^{35}S-labelled xNgn2, xNgn2 C178AxNgn2 or C(169,178)AxNgn2 and incubated at 21 °C. Samples were taken at 0, 15, 30, 60, 90, 120, 180 mins and subjected to 15 % SDS-PAGE. (A) Half-lives were normalised to xNgn2 stability in each experiment and the average ratio of stability of each protein with respect to wild type plotted. (B) Half-lives were calculated using first-order rate kinetics, and errors calculated using the Standard Error of the Mean (SEM).

The half-life for the single cysteine to alanine mutant, C178AxNgn2, is 23.3 +/- 0.9 mins compared to the average wild type value of 30.5 +/- 2.5 mins. Loss of both conserved cysteine residues, in C(169,178)AxNgn2, results in a half-life for degradation of 39.5 +/- 6.7 mins.

The value for wild type is larger than usually observed, most likely due to the use of frozen egg extract, and so I conclude that loss of C178 does not increase xNgn2 half-life. However loss of both cysteines can inhibit xNgn2 proteasomal degradation.

To investigate the effect on stability of inhibiting cysteine ubiquitylation by methods other than mutation, alkylation experiments on xNgn2 cysteine mutants were carried out using N-ethyl maleimide (NEM), which selectively reacts with cysteines to block their nucleophilic potential. As this alkylation also inhibits the action of Ub-activating (E1), Ub-conjugating (E2) and de-ubiquitylating (DUB) enzymes, IVT proteins were purified away from NEM after treatment. ^{35}S-radiolabelled IVT xNgn2, xNgn2CO, Ac2xNgn2KO or Ac2xNgn2KOCO, treated with NEM (or with buffer alone as a control) were added to *Xenopus laevis* interphase activated egg extract and incubated at 21 °C. Aliquots of the degradation reaction were removed at increasing timepoints into SDS-LB and separated by 15 % SDS-PAGE. Half-lives for the rates of degradation were then calculated using first-order rate kinetics (Figure 4.11).

The half-life of xNgn2 treated with buffer alone is 37.5 +/- 2.7 mins and with NEM treatment is 32.3 +/- 4.2 mins. This suggests that NEM has no effect in the wild type protein and therefore that modifying cysteines has no effect on the rate of degradation.

xNgn2CO has a half-life of 57 +/- 12.4 mins in buffer alone which increases to 86.7 +/- 26.9 mins in NEM. As cysteines are modified by NEM no effect would be expected on NEM treatment. xNgn2CO is not significantly stabilised by NEM treatment. The same applies to Ac2xNgn2KOCO which has half-lives of 131 +/- 73 mins and 125 +/- 46 mins with and without NEM treatment respectively.

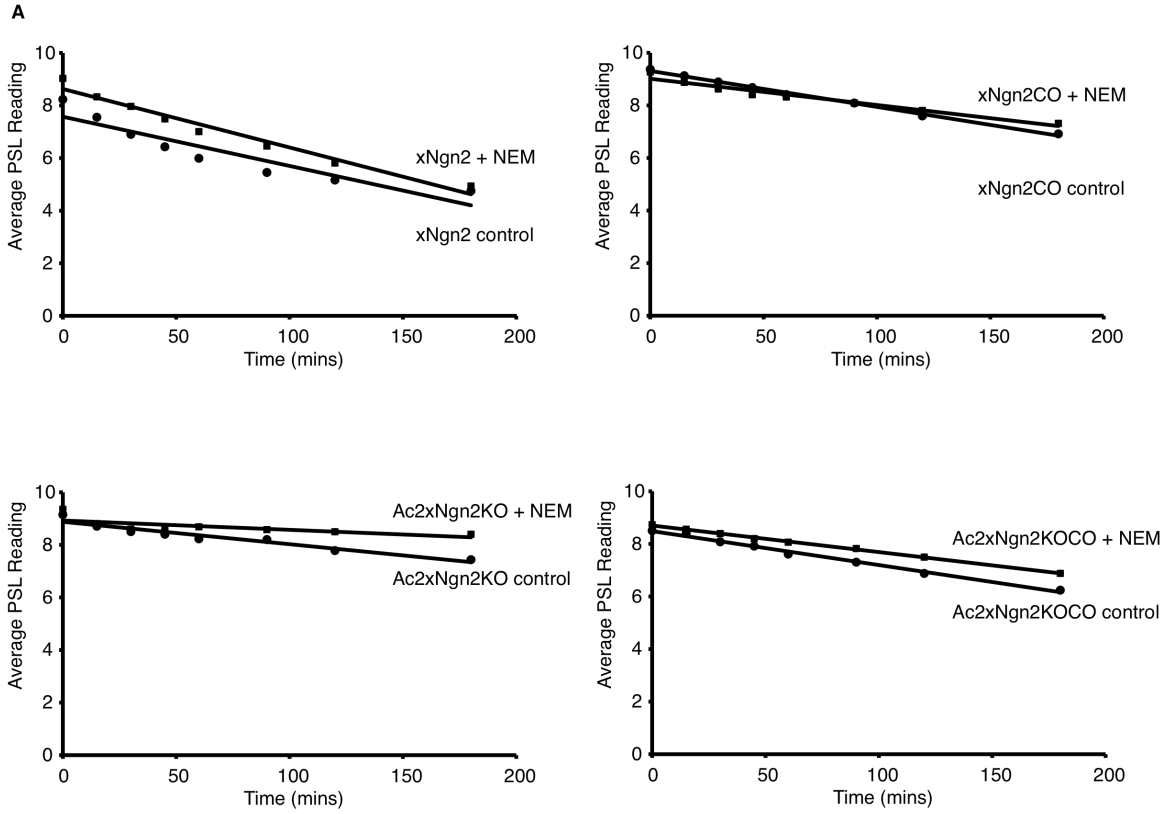

B

Sample	Control Half-life (mins)	NEM Half-life (mins)
xNgn2	37.5 +/- 2.7	32.3 +/- 4.2
xNgn2CO	57.0 +/- 12.4	89.7 +/- 26.9
Ac2xNgn2KO	124 +/- 22	> 180
Ac2xNgn2KOCO	131 +/- 73	125 +/- 46

Figure 4.11: NEM treatment modifies cysteines to affect stability.

Xenopus laevis interphase activated egg extracts were supplemented with ^{35}S-labelled xNgn2, xNgn2CO, Ac2xNgn2KO and Ac2xNgn2KOCO IVT proteins which had been pre-treated with N-ethyl maleimide (NEM), and incubated at 21 °C. Samples were taken at 0, 15, 30, 60, 90, 120, 180 mins and subjected to 15 % SDS-PAGE. (A) Gels were analysed by quantitative phosphorimaging analysis and levels of protein plotted against time. (B) Half-lives in the presence or absence of NEM were calculated using first-order rate kinetics, and errors calculated using the Standard Error of the Mean (SEM).

Ac2xNgn2KO stability is affected by NEM treatment, which increases the protein half-life from 124 +/- 22 mins to a half-life greater than the length of the timecourse (294 mins, but this cannot be stated with confidence as it exceeds the length of the timecourse).

Thus, cysteines do not appear to target wild type xNgn2 for degradation in interphase but are sufficient to target for proteasomal degradation in the absence of canonical and amino-based sites of ubiquitylation.

IVT radiolabelled proteins were purified by small-scale purification columns to isolate the proteins from NEM before being added to extract and this may have affected the half-lives, as they differ from expected levels in extract as shown in preceding figures.

Cysteine residues regulate stability in a cell cycle-dependent manner

Cysteine residues demonstrate a role in xNgn2 Ub-mediated proteolysis in *Xenopus laevis* interphase extract. To examine whether this was the case in other developmental settings, other extracts were employed to investigate the possible role of cysteines in regulating xNgn2 stability.

Xenopus laevis mitotic activated egg extract is made using interphase extract treated with non-degradable cyclin B protein, which forces the extract into a mitosis-like state, and effects on degradation rate can be compared to the rate seen in interphase extracts. To test the role of cysteines in regulating xNgn2 stability, ^{35}S-radiolabelled IVT xNgn2, xNgn2CO, xNgn2KO or Ac2xNgn2KO were added to *Xenopus laevis* mitotic activated egg extract and incubated at 21 °C. Aliquots of the degradation reaction were quenched at increasing timepoints in SDS-LB and separated by 15 % SDS-PAGE. Protein half-lives were then calculated using first-order rate kinetics (Figure 4.12).

xNgn2 is degraded in mitotic extract more quickly (with a half-life of 15.8 +/- 2.1 mins, Figure 4.12, C) than in interphase extract (with a half-life of 22.9 +/- 1.0 mins, Figure 3.1, C). However in mitotic extract xNgn2CO and xNgn2KO have similar half-

A

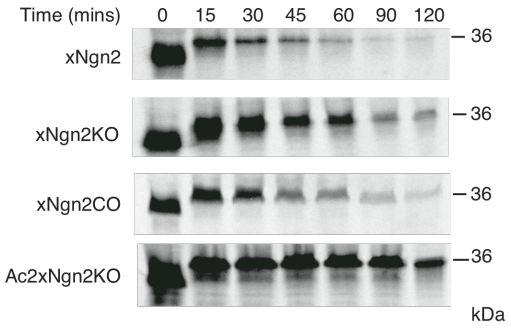

B

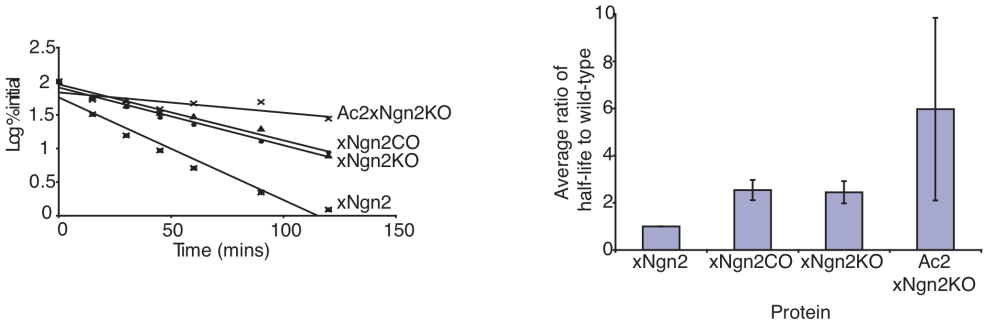

C

Construct	Half-life (mins)
xNgn2	15.8 +/- 2.1
xNgn2KO	35.6 +/- 2.7
xNgn2CO	38.3 +/- 5.4
Ac2xNgn2KO	82.0 +/- 47.8

Figure 4.12: Mutation of cysteines is sufficient to stabilise xNgn2 in *Xenopus* mitotic egg extract.

Xenopus laevis mitotic activated egg extracts were supplemented with ^{35}S-labelled xNgn2, xNgn2CO, xNgn2KO or Ac2xNgn2KO IVT proteins and incubated at 21 °C. Samples were taken at the timepoints indicated and subjected to 15 % SDS-PAGE. Gels were analysed by autoradiography (A) and quantitative phosphorimaging analysis (B) and average ratios of half-lives normalised to wild type stability in each experiment calculated. (C) Half-lives were calculated using first-order rate kinetics and errors calculated using the Standard Error of the Mean (SEM). n = 4

lives, of 35.6 +/- 2.7 mins and 38.3 +/- 5.4 mins respectively (Figure 4.12, C) giving similar average ratios of stabilisation (Figure 4.12, C). Therefore cysteines and lysines are similarly important for targeting xNgn2 for degradation in mitosis.

Cysteine residues affect Ub-mediated proteolysis of xNgn2 in a cell-cycle dependent manner. I went on to investigate Ub-mediated proteolysis of xNgn2 in neurula embryo extracts, made at the developmental stage at which xNgn2 is usually expressed.

To test the role of cysteines in regulating xNgn2 stability in neurula stage extract, ^{35}S-radiolabelled IVT xNgn2, xNgn2CO, xNgn2KO, Ac2xNgn2, Ac3xNgn2 or Ac2xNgn2KO were added to *Xenopus laevis* neurula embryo extract and incubated at 21 °C. Aliquots of the degradation reaction were removed at increasing timepoints into SDS-LB and separated by 15 % SDS-PAGE. Half-lives for the rates of degradation were then calculated using first-order rate kinetics (Figure 4.13).

xNgn2CO has an average half-life of 125 +/- 62 mins in neurula extract (Figure 4.13, C) where xNgn2KO has a half-life of 107 +/- 29 mins and Ac2xNgn2 has a half-life of 89.4 +/- 17.2 mins. Mutation of cysteines, lysines or the N-terminus has a similar effect on protein stability.

To take this analysis further ^{35}S-radiolabelled xNgn2, Ac2xNgn2KO or Ac2xNgn2KOCO were added to *Xenopus laevis* neurula embryo extract and subjected to degradation assay (Figure 4.14). This was to investigate whether non-canonical ubiquitylation could direct proteolysis in the absence of canonical ubiquitylation sites in neurula extracts.

In this experiment, xNgn2 demonstrated an average half-life for degradation of 42.8 +/- 2.4 mins, and Ac2xNgn2KO a half-life of 112 +/- 7 mins. The half-life for degradation of Ac2xNgn2KOCO, however, was extended beyond the length of the degradation assay timecourse of 240 mins. Therefore I can conclude that ubiquitylation on cysteines can direct proteolysis in the absence of canonical ubiquitylation, in neurula stage extracts.

A

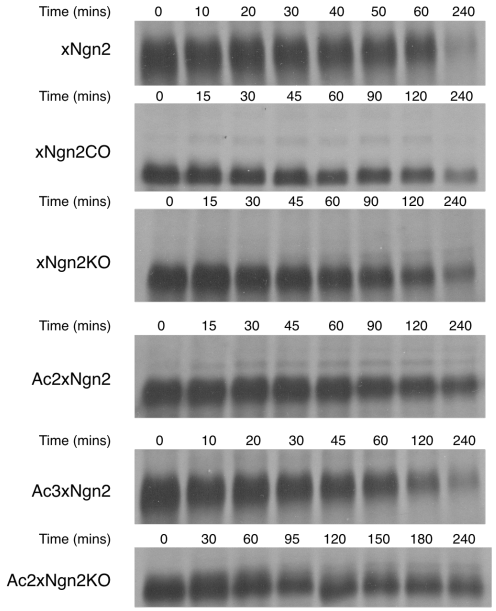

B

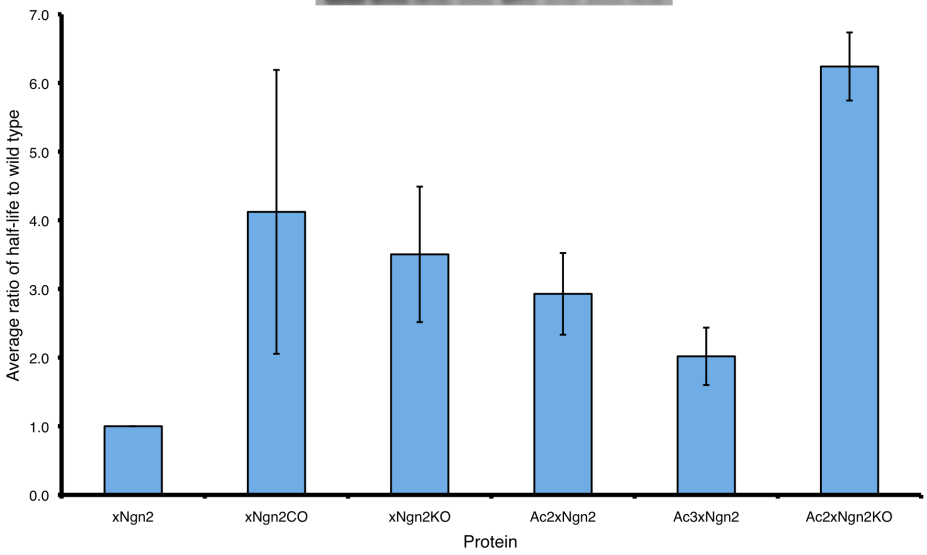

C

Sample	Half-life (mins)
xNgn2	30.6 +/- 0.3
xNgn2CO	125 +/- 62
xNgn2KO	107 +/- 29
Ac2xNgn2	89.4 +/- 17.2
Ac3xNgn2	61.6 +/- 12.1
Ac2xNgn2KO	191 +/- 13

Figure 4.13: xNgn2 cysteine mutants affect stability in *Xenopus* neurula embryo extract.
Xenopus laevis neurula extracts were supplemented with ^{35}S-labelled xNgn2, xNgn2CO, xNgn2KO, Ac2xNgn2, Ac3xNgn2 or Ac2xNgn2KO IVT proteins. Samples were taken at the timepoints indicated and subjected to 15 % SDS-PAGE. Gels were analysed by autoradiography (A) and average ratios of half-lives normalised to wild type stability in each experiment calculated (B). (C) Half-lives were calculated using first-order rate kinetics and errors calculated using the Standard Error of the Mean (SEM). This experiment is based on a duplicate data set.

A

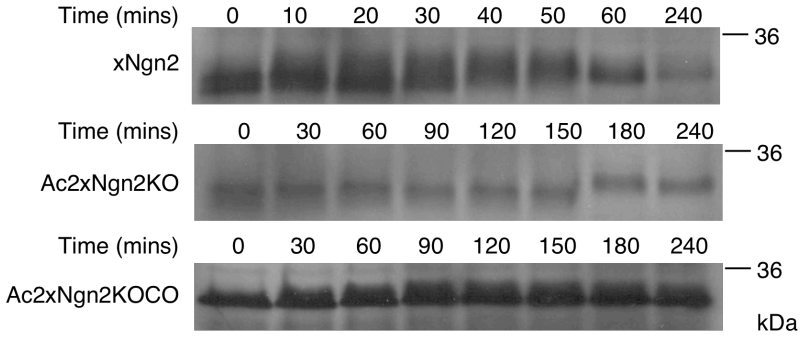

B

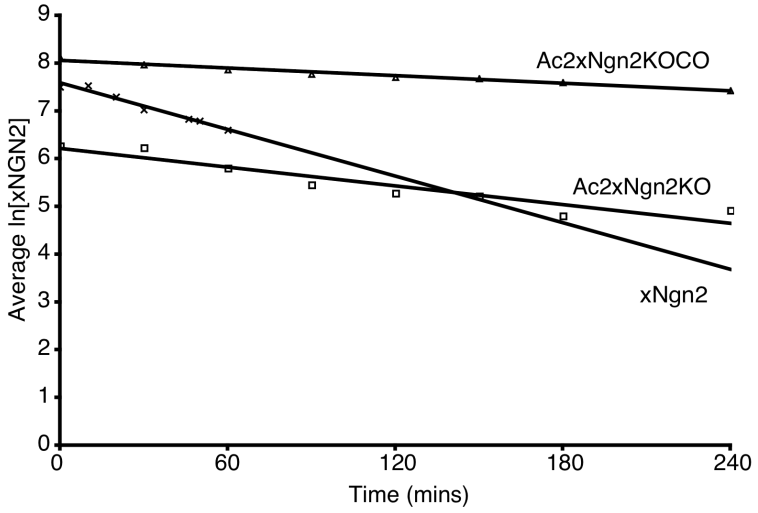

C

Sample	Half-life (mins)
xNgn2	42.8 +/- 2.4
Ac2xNgn2KO	112 +/- 7
Ac2xNgn2KOCO	> 240

Figure 4.14: Loss of non-canonical ubiquitylation sites further stabilises xNgn2 lacking canonical sites of ubiquitylation in *Xenopus* neurula extract.

Xenopus laevis neurula embryo extracts were supplemented with ^{35}S-labelled xNgn2, Ac2xNgn2KO or Ac2xNgn2KOCO IVT proteins and incubated at 21 °C. Samples were taken at the timepoints indicated and subjected to 15 % SDS-PAGE. Gels were analysed by autoradiography (A) and quantitative phosphorimaging analysis and average ratios of half-lives normalised to wild type stability in each experiment calculated (B). (C) Half-lives were calculated using first-order rate kinetics and errors calculated using the Standard Error of the Mean (SEM).

To observe whether xNgn2 is still modified by ubiquitylation after mutation of lysines, cysteines and the N-terminus, ubiquitylation assays were carried out. ^{35}S-radiolabelled IVT xNgn2, Ac2xNgn2KO, or Ac2xNgn2KOCO were added to *Xenopus laevis* neurula embryo extract supplemented with MG132 to prevent proteasomal degradation and His_6-Ub (Sigma). This reaction was incubated at 20 °C for 90 mins. Samples were then incubated with denaturing Vosper buffer (containing 8.5 M urea) and nickel-chelating agarose beads (Ni-NTA, Invitrogen) to purify his-tagged protein. Samples were eluted in a high pH reducing (R) SDS-LB, or in a non-reducing (N) SDS-LB and run out on 12 % SDS-PAGE (Figure 4.15).

xNgn2 is released from Ub in reducing conditions, demonstrating non-canonical ubiquitylation via thioester and ester linkages (Figure 4.15, marked by arrow, lane 1). This is due to ubiquitylated xNgn2 being pulled down by nickel beads, but under the high temperature, high pH and reducing conditions of the gel loading buffer, labile thioester and ester linkages are broken and xNgn2 is liberated. This band is not present under non-reducing conditions (Figure 4.15, lane 2). The effect is greater in Ac2xNgn2KO where higher molecular weight forms are lost in reducing conditions (Figure 4.15, lane 3) compared to non-reducing conditions (Figure 4.15, lane 4) to release unmodified protein. Ac2xNgn2KOCO is not only still ubiquitylated in non-reducing conditions (Figure 4.15, lane 6) but under reducing conditions (Figure 4.15, lane 5) unmodified xNgn2 is released. Therefore non-canonical sites are ubiquitylated not only in Ac2xNgn2KO, where no canonical sites are present, but also in Ac2xNgn2KOCO, where there are also no cysteines present. Therefore this means that further non-canonical ubiquitylation must be occurring, using the hydroxyl groups on residues such as serine and threonine to form ester linkages with Ub.

xNgn2 is degraded in P19 cells by the proteasome and using non-canonical sites of ubiquitylation

So far evidence from *Xenopus laevis* extract systems has been presented in discussion of serines and threonines as well as cysteines in ubiquitylation of xNgn2 (Vosper et al., 2007, Vosper et al., 2009). The *Xenopus laevis* extract system is a simple and robust means of assaying processes such as protein ubiquitylation. However it is

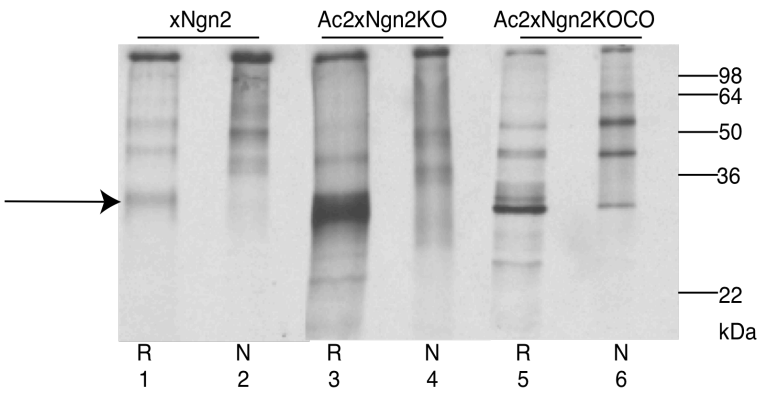

Figure 4.15: Ubiquitylation of non-canonical sites in xNgn2 in *Xenopus* neurula extract.
Xenopus laevis neurula embryo extracts were supplemented with ^{35}S-radiolabelled xNgn2, Ac2xNgn2KO or Ac2xNgn2KOCO with His_6-ubiquitin. Samples were isolated in either high pH 10 % β-mercaptoethanol reducing loading buffer (R) or non-reducing loading buffer (N). Sample of *in vitro* translated (IVT) radiolabelled protein were run out with samples on 12 % SDS-PAGE. Lanes are numbered 1-6 as described in text.

possible that ubiquitylation in a non-canonical fashion, despite showing cell cycle and developmental dependence, may be specific to this *in vitro* system. Therefore I decided to determine whether ubiquitylation occurs on non-canonical residues in cultured cells, using the *Mus musculus* P19 embryonal carcinoma cell line (McBurney and Rogers, 1982). The P19 cell line in particular was employed as these cells are capable of differentiating into neurons and so provide a physiologically relevant system with which to work (Jones-Villeneuve et al., 1982, McBurney et al., 1982).

To establish whether xNgn2 is degraded by the proteasome in P19 cells, and whether such degradation may be affected by loss of canonical sites of ubiquitylation, xNgn2 and Ac2xNgn2KO (both triply HA-tagged on the C-terminus) were transfected into P19 cells overnight. Cells were then treated with 20 μM cycloheximide to inhibit further protein translation and 20 μM MG132 as a proteasome inhibitor (or an equal volume of DMSO as a control). Then at certain timepoints cells were removed and lysed and proteins separated by 15 % SDS-PAGE, before Western blotting using α-HA-HRP antibody (Roche). The half-lives for xNgn2 proteasomal degradation were calculated by reading protein levels from autoradiography using ImageJ (Abramoff et al., 2004) software and using first-order kinetics (Figure 4.16).

xNgn2 has a half-life of 13.1 +/- 1.8 mins in P19 cells (Figure 4.16, C). However upon treatment with the proteasome inhibitor MG132 xNgn2 is stabilised (Figure 4.16, A and B) to a half-life of 200 +/- 118 mins (Figure 4.16, C). Ac2xNgn2KO has a half-life of 177 +/- 72 mins (Figure 4.16, C) and so is stabilised compared to xNgn2 in P19 cells. However on treatment with MG132, Ac2xNgn2KO is stabilised beyond the length of the 240 min timecourse (Figure 4.16). Therefore in P19 cells xNgn2 is proteasomally degraded, while loss of canonical ubiquitylation sites leads to partial stabilisation. However Ac2xNgn2KO is still degraded by the proteasome in P19 cells.

I have shown that mutation of xNgn2 to remove canonical sites of ubiquitylation can stabilise xNgn2 in *Xenopus laevis* interphase activated egg extract and neurula embryo degradation assays (Figures 4.7 and 4.13, respectively). Repeating this in the P19 cell line, xNgn2, xNgn2KO, Ac2xNgn2 and Ac2xNgn2KO (all triply HA-tagged on the C-terminus) were transfected into P19 cells overnight. Cells were then treated

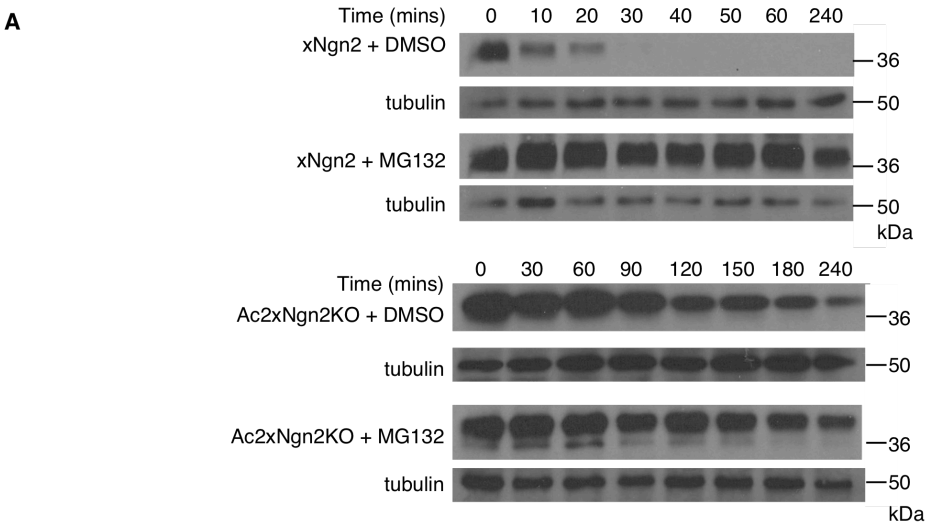

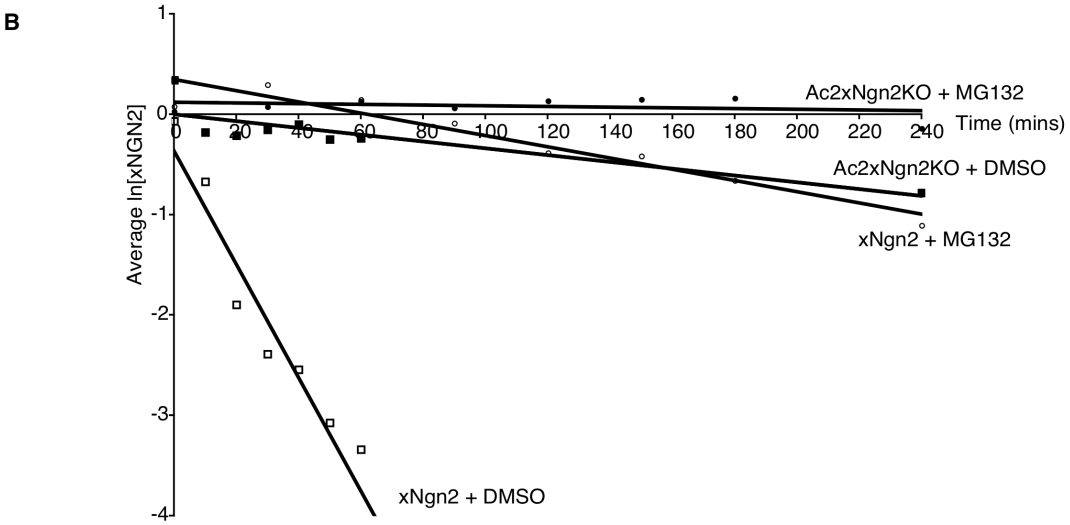

C

Sample	Half-life (mins)
xNgn2 + DMSO	13.1 +/- 1.8
xNgn2 + MG132	200 +/- 118
Ac2xNgn2KO + DMSO	177 +/- 72
Ac2xNgn2KO + MG132	>240

Figure 4.16: xNgn2 lacking canonical sites of ubiquitylation is still degraded in a proteasome-dependent manner.

P19 embryonal carcinoma cells were transfected with 5 μg xNgn2 or Ac2xNgn2KO DNA. 20 μM cycloheximide was added after either 20 μM MG132 or an equal volume of DMSO as a control and cells removed onto ice and lysed at the timepoints indicated in lysis buffer. Samples were separated by 15 % SDS-PAGE and Western blotting was undertaken using α-HA and α -tubulin antibodies. Half-lives were calculated by measuring exposures on film (A) using ImageJ software to determine protein quantity at each timepoint (B) and half-lives were calculated using first-order rate kinetics (C). Errors were calculated as the standard error of the mean (SEM). All xNgn2 proteins were triply HA tagged on the C-terminus.

with 20 μM cycloheximide to inhibit further protein translation. Then at certain timepoints cells were removed and lysed and proteins separated by 15 % SDS-PAGE, before Western blotting using α-HA-HRP antibody (Roche). xNgn2 half-lives were calculated by reading protein levels after densitometry using ImageJ (Abramoff et al., 2004) software and using first-order kinetics (Figure 4.17).

xNgn2 has a half-life of 9.93 +/- 2.74 mins (Figure 4.17, C). xNgn2KO and Ac2xNgn2 have half-lives of 25.6 +/- 7.5 mins and 38.3 +/- 26.0 mins respectively. However greatest stabilisation was achieved by mutating all canonical ubiquitylation sites in Ac2xNgn2KO, resulting in a half-life of 209 +/- 23 mins. Therefore mutation of canonical ubiquitylation sites stabilises xNgn2 against proteasomal degradation in P19 cells.

To investigate the role of non-canonical sites and in particular cysteine residues in regulating xNgn2 stability, xNgn2 and xNgn2CO (both triply HA-tagged on the C-terminus) were transfected into P19 cells overnight. Cells were then treated with 20 μM cycloheximide to inhibit further protein translation. Then at certain timepoints cells were removed and lysed and proteins separated by 15 % SDS-PAGE, before Western blotting using α-HA-HRP antibody (Roche). The half-lives of xNgn2 were calculated by reading protein levels after densitometry using ImageJ (Abramoff et al., 2004) software and using first-order kinetics (Figure 4.18).

In P19 cells, xNgn2 has a half-life of 9.93 +/- 2.74 mins, whereas xNgn2CO was more stable with a half-life of 39.2 +/- 19.4 mins (Figure 4.18, C). In *Xenopus laevis* mitotic activated egg extracts (Figure 4.12) and neurula embryo extracts (Figure 4.13), mutation of cysteines to alanines in xNgn2 can be sufficient to stabilise xNgn2. Therefore cysteines can also target xNgn2 for proteasomal degradation in this physiologically relevant setting in P19 cells.

Having investigated the half-life of various xNgn2 mutants in P19 cell degradation assays, I wished to investigate whether ubiquitylation of xNgn2 could be observed, and also whether ubiquitylation also occurred on serines and threonines in Ac2xNgn2KOCO.

A

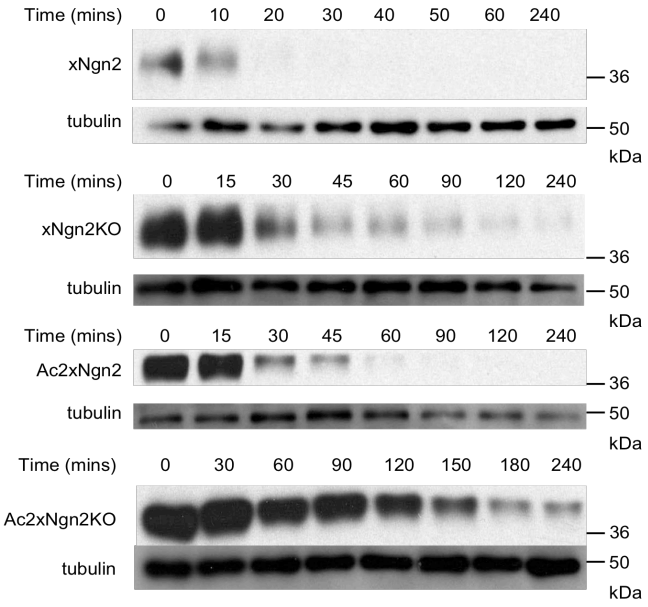

B

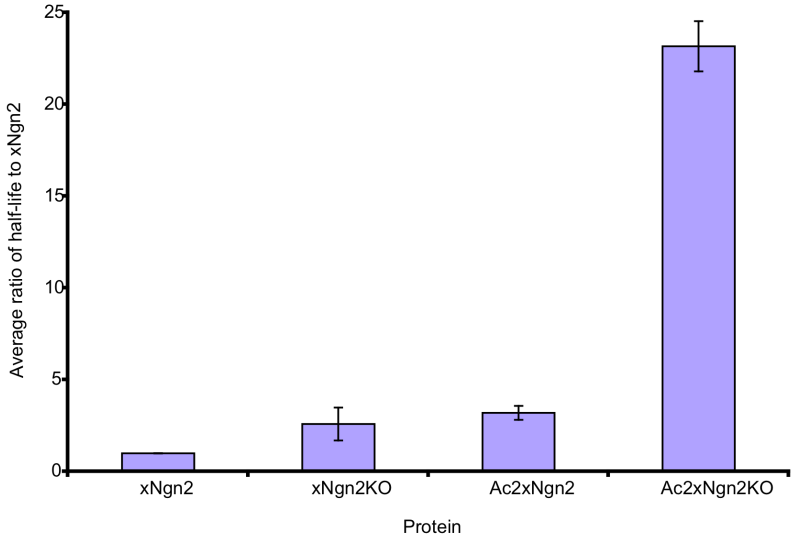

C

Sample	Half-life (mins)
xNgn2	9.93 +/- 2.74
xNgn2KO	25.6 +/- 7.5
Ac2xNgn2	39.3 +/- 26.0
Ac2xNgn2KO	209 +/- 23

Figure 4.17: Removing canonical sites stabilises xNgn2 in P19 cells.

P19 cells were transfected with 5 μg xNgn2, xNgn2KO, Ac2xNgn2 or Ac2xNgn2KO DNA. 20 μM cycloheximide was added and cells lysed at the timepoints indicated. Samples were separated by 15 % SDS-PAGE and Western blotting was undertaken using α-HA and α -tubulin antibodies. Half-lives were calculated by measuring exposures on film (A) and stability was plotted as the average of the stabilisation relative to wild type xNgn2 in each experiment (B). (C) Half-lives were calculated using first-order rate kinetics. Errors were calculated as SEM.

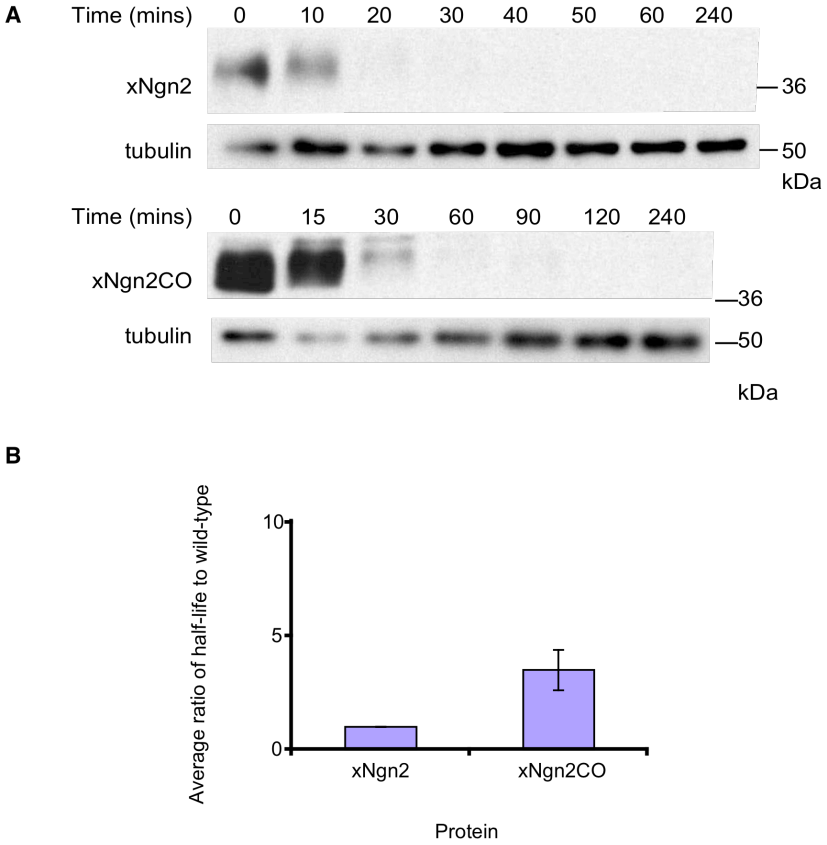

C

Sample	Half-life (mins)
xNgn2	9.93 +/- 2.74
xNgn2CO	39.2 +/- 19.4

Figure 4.18: Mutation of cysteines is sufficient to stabilise xNgn2 in P19 cells.

P19 embryonal carcinoma cells were transfected with 5 μg xNgn2 or xNgn2CO DNA. 20 μM cycloheximide was added and cells removed onto ice and lysed at the timepoints indicated in lysis buffer. Samples were separated by 15 % SDS-PAGE and Western blotting was undertaken using α-HA and α -tubulin antibodies. Half-lives were calculated by measuring exposures on film (A) and stability was plotted as the average of the stabilisation relative to wild type xNgn2 in each experiment (B). (C) Half-lives were calculated using first-order rate kinetics. Errors were calculated as the standard error of the mean (SEM). All xNgn2 proteins were triply HA tagged on the C-terminus.

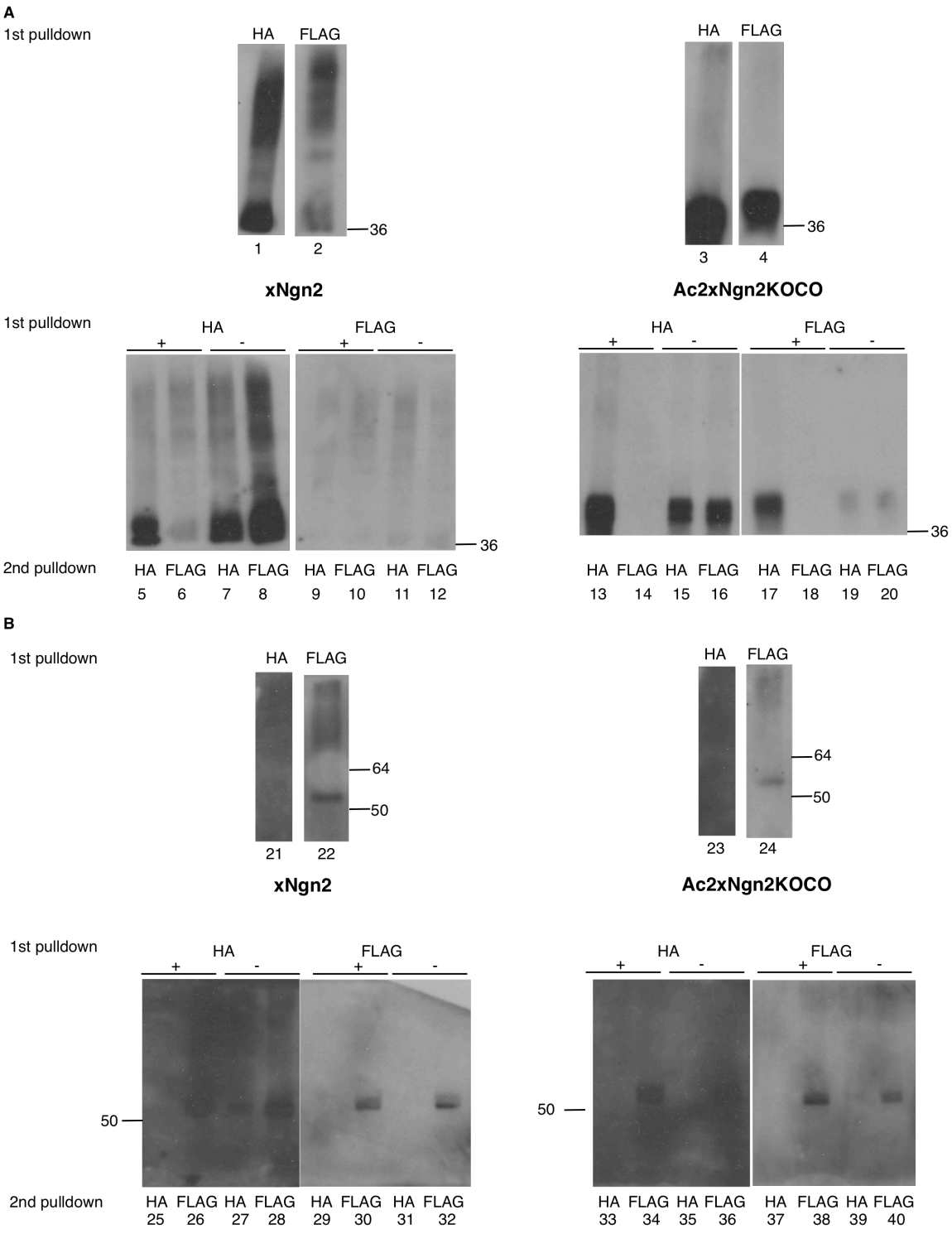

Figure 4.19: IP-re-IP of xNgn2 and Ub in P19 cells.

P19 cells were transfected with HA-tagged xNgn2 or Ac2xNgn2KOCO and FLAG-tagged ubiquitin. Cells were lysed and samples were pulled down using either α-HA antibody (1st pulldown HA) or α-FLAG antibody (1st pulldown FLAG). Samples were then pulled down again using either α-HA antibody (2nd pulldown HA) or α-FLAG antibody (2nd pulldown FLAG). Samples were treated either with reducing buffer (+) or non-reducing buffer (-) before being separated by 15 % SDS-PAGE. Western blotting was undertaken using α-HA (A) and α-FLAG (B) antibodies.

For this, an immunoprecipitation re-immunoprecipitation (IP-re-IP) was carried out. xNgn2 or Ac2xNgn2KOCO DNA (triply HA-tagged on the C-terminus) was transfected into P19 cells with FLAG-tagged Ub DNA and stored at 37 °C overnight. Cells were treated with MG132 for one hour before being collected onto ice and lysed. Samples were then either incubated with agarose beads coated with α-HA antibody to pull down xNgn2 proteins, or α-FLAG antibody to pull down ubiquitylated proteins.

These samples were eluted, divided into HA and FLAG samples, and the immunoprecipitation repeated again using either agarose beads coated with α-HA antibody to pull down xNgn2 proteins, or α-FLAG antibody to pull down ubiquitylated proteins.

After this second pulldown, samples were washed and eluted in either reducing or non-reducing buffer. All samples were heated before 12 % SDS-PAGE separation. Samples were subjected to Western Blotting using α-HA-HRP antibody (Figure 4.19, A) or α-FLAG antibody followed by α-rabbit-HRP secondary antibody (Figure 4.19, B).

First pulldown – blotting for HA (Figure 4.19, A, lanes 1-4):

At the first pulldown and blotting for HA-tagged protein, pulling down xNgn2 with α-HA beads produces an ubiquitylation ladder (Figure 4.19, A, lane 1) whereas pulling down Ac2xNgn2KOCO results in a single band with the mobility of the wild type protein (Figure 4.19, A, lane 3).

Likewise in FLAG pulldown, ubiquitylated HA-tagged proteins are present in the xNgn2 sample (Figure 4.19, A, lane 2) but only a single band appears for Ac2xNgn2KOCO (Figure 4.19, A, lane 4).

In these particular samples we should only be observing HA-tagged proteins so this suggests that we are able to pull down ubiquitylated xNgn2, but only unmodified Ac2xNgn2KOCO is observed as expected, as any linkages to Ac2xNgn2KOCO are labile and therefore linkages to Ub are broken under SDS-PAGE conditions and a band at

the level of unmodified xNgn2 is observed. This is as we would expect, for only labile non-canonical ubiquitylation linkages are available in Ac2xNgn2KOCO.

First pulldown – blotting for FLAG (Figure 4.19, B, lanes 21-24):

With the first pulldown with FLAG all that is observed is polyubiquitylated protein (Figure 4.19, B, lanes 22 and 24) whereas pulldown with HA does not seem to produce any visible bands even at high exposure of film to ECL-treated membrane (Figure 4.19, B, lanes 21 and 23).

Second pulldown – blotting for HA (lanes 5-20):

When a second pulldown is performed and blotted using α-HA, for xNgn2 pulldown 1st with FLAG and 2nd with HA or FLAG there are no visible bands (Figure 4.19, A, lanes 9-12). However as this occurs for all samples in this set this suggests that perhaps sample was lost between the 1st and 2nd pulldowns.

Pulling down xNgn2 protein with HA pulldown 1st and then HA again 2nd shows a clear band running at the level of unmodified protein in reducing conditions (+) (Figure 4.19, A, lane 5) and non-reducing conditions (-) (Figure 4.19, A, lane 7) suggesting a substantial amount of unmodified protein is present.

However when compared to Ac2xNgn2KOCO (Figure 4.19, A, lanes 6 and 8), there is greater evidence for a ladder of polyubiquitylated protein in xNgn2 in these lanes which does not appear to be present in Ac2xNgn2KOCO, with a more obvious ladder in the xNgn2 lane treated with non-reducing (-) conditions (Figure 4.19, A, lane 8). This suggests that polyubiquitylated protein is pulled down but that polyubiquitylation occurs at non-canonical sites, which are disrupted when heating xNgn2 samples but especially Ac2xNgn2KOCO.

There is also a strong reducing agent dependence on xNgn2 protein pulled down with HA beads 1st and then FLAG beads 2nd (Figure 4.19, A, lanes 6 and 8), which is repeated in Ac2xNgn2KOCO (Figure 4.19, A, lane 14 and 16). When reducing

conditions are used (+) no band appears (Figure 4.19, A, lanes 6 and 14), but when non-reducing conditions are used (-), there is a strong ladder in xNgn2 (Figure 4.19, A, lane 8), but a single band again in Ac2xNgn2KOCO (Figure 4.19, A, lane 16).

Under these conditions we expect to see xNgn2 protein that has been pulled down, then only polyubiquitylated xNgn2 should be selected in the second pulldown, and then using reducing or non-reducing conditions the samples are separated and blotted against α-HA-HRP to look for xNgn2. In Ac2xNgn2KOCO, this pattern is again observed when instead we pull down ubiquitylated protein with α-FLAG and then pull down with α-FLAG beads again and treat with either reducing (+) or non-reducing (-) conditions (Figure 4.19, A, lanes 18 and 20). Reducing conditions appear to result in loss of samples where ubiquitylated protein is pulled down in the second pulldown.

Second pulldown – blotting for FLAG (Figure 4.19, B, lanes 25-40):

Repeating these pulldowns but blotting for FLAG-tagged protein (Figure 4.19, B) seems to show that the 2nd pulldown using HA beads (Figure 4.19, B, lanes 25, 27, 29, 31, 33, 35, 37 and 39) results in either severe reduction or loss of signal. Conversely when the 2nd pulldown is carried out using α-FLAG (Figure 4.19, B, lanes 26, 28, 30, 32, 34, 36, 38 and 40) there is only a single clear band present. This band also migrates more slowly than xNgn2 protein and so this may represent a background band, as it is present whether the first pulldown is selecting for FLAG- or HA-tags, and it is present in both xNgn2 and Ac2xNgn2KOCO samples.

DISCUSSION

If a variety of different sites in a protein could target for UPS-mediated degradation, it could provide a highly dynamic system for swift ubiquitylation and deubiquitylation events. This may be required in maintaining short-lived proteins in a dynamic range that is rapidly altered in response to changing environmental and developmental cues.

The role of xNgn2 N-terminal ubiquitylation is clearly established and N-terminal ubiquitylation can be blocked through the mutually exclusive process of co-translational N-terminal acetylation in preference to using bulky tags (Vosper et al., 2009). Addition of citrate synthase and oxaloacetate depletes the reserve of acetyl CoA in extract systems and therefore co-translational acetylation cannot occur. Figure 4.3 clearly illustrates that upregulation of acetylation can be blocked to again free the N-terminus for ubiquitylation in Ac2xNgn2KO, whilst preventing N-terminal acetylation has no effect on wild type xNgn2. This demonstrates that the N-terminus acts as an important ubiquitylation site targeting xNgn2 for proteasomal degradation.

xNgn2 is degraded by the proteasome using canonical sites of ubiquitylation (Vosper et al., 2007). I wanted to confirm that non-canonical ubiquitylation can target for proteasome-mediated destruction.

Figure 4.4 shows clearly that xNgn2 degradation is ATP-dependent and that interestingly the mutant form of xNgn2 with no canonical sites of ubiquitylation available, Ac2xNgn2KO, also shows ATP-dependent degradation. This may suggest that ubiquitylation on non-canonical sites can target for proteasome-mediated destruction.

However this experiment does not clarify whether Ac2xNgn2KO may be targeted for degradation in an Ub-independent manner. It could be the case, for example, that xNgn2 can also be targeted for proteasomal degradation by unfolding properties alone (Prakash et al., 2004).

xNgn2 is ubiquitylated on non-canonical sites. This may be a more widespread phenomenon but we have not looked for it before. Reducing agents are usually used in running SDS-PAGE as part of a standard protocol. Bands at the level of native protein that would be released from polyUb chains anchored via thioester and possibly ester bonds may be mistaken for background non-specific binding in a ubiquitylation assay, if proper controls are not used. Assays in *Xenopus laevis* are also much more sensitive than those used so far in tissue culture.

MyoD is a basic helix-loop-helix protein involved in myogenesis, playing the same role as xNgn2 does in neurogenesis. MyoD is known to be ubiquitylated on lysines and the N-terminus in a similar manner to xNgn2 (Breitschopf et al., 1998) therefore I wanted to investigate if MyoD is also non-canonically ubiquitylated.

An ubiquitylation assay was performed for wild type MyoD and a mutant form with all lysines mutated to arginines. Ub is covalently attached to lysines and to the N-terminus. Therefore pulling out his-Ub-linked proteins should result in a ladder running at least 8 kDa higher than the unconjugated protein. However, if ubiquitylation occurs via labile linkages, chemical conditions that disrupt this linkage such as reducing agents and high pH will result in a release of unconjugated MyoD from the his-Ub chain. The results of the ubiquitylation assay in Figure 4.5 show that non-canonical ubiquitylation is also present in wild type MyoD, as well as the lysineless form. Polyubiquitylated forms of the proteins are clearly seen in the form of ladders spaced about 8kDa apart in both reducing and non-reducing conditions. Therefore other bHLH proteins are capable of being modified by Ub on non-canonical sites.

Having established that xNgn2 and MyoD are ubiquitylated on non-canonical sites I then wished to see if this ubiquitylation could target xNgn2 for proteasomal degradation. There are 7 cysteines to which Ub could potentially be attached via a thioester bond (see Figure 4.6). In an interphase degradation assay, mutation of cysteines to alanines has a slight stabilising effect on xNgn2 (Figure 4.7) and in interphase extract, non-canonical sites are clearly ubiquitylated (Figure 4.8) in xNgn2. This also occurs in Ac2xNgn2KO where only non-canonical sites are available and also in Ac2xNgn2KOCO, where only hydroxyl-bearing residues are present. The ubiquitylation assays in Figure 4.8, A do exhibit a large amount of background in the untagged Ub control samples, with bands running at the level of unconjugated protein, which is most likely due to insufficient washing. However I am confident of the results in the his-Ub samples particularly where non-modified protein appears, as in many assays no background is observed in the untagged Ub samples.

Samples of Mes1, a yeast protein implicated in cell cycle progression, were kindly donated by Hiro Yamano (Kimata et al., 2008, Yamano et al., 2004) for testing in the *Xenopus laevis* extract systems to see if a protein unrelated to bHLH transcription factors could be non-canonically ubiquitylated. Mes1 ubiquitylation is not altered by addition of reducing agents; however when all lysines are mutated to arginines, unmodified protein is released as demonstrated by the appearance of a band of protein of lower molecular weight. Therefore this protein exhibits a differing behaviour to xNgn2 and mMyoD illustrating that *Xenopus* extract systems do not force non-canonical ubiquitylation on all proteins.

Comparison between species identifies 2 conserved cysteine residues in Ngn2 from various species (Figure 4.9) and mutants of these cysteines were analysed in degradation assays in interphase activated egg extract (Figure 4.10). Cysteine mutation in this context does lead to subtle half-life changes but in these particular extracts, the half-life of xNgn2 and xNgn2KO were unusually long and so I cannot state with confidence that these cysteines truly have an effect. Also it may be more relevant to investigate these mutants in a different extract system such as mitotic activated egg extract, which in Figure 4.12 shows that cysteines alone can affect Ub-mediated destruction of xNgn2.

Blocking cysteine residues by alkylation with NEM was investigated in degradation assays to see if there was an effect on xNgn2 stability (Figure 4.11). The hypothesis was that xNgn2 and Ac2xNgn2KO stability may be affected as cysteines are present. Ac2xNgn2KOCO should show no difference compared with the control as there should be no groups available for alkylation of a soft electrophile such as NEM. This did not appear to be the case for xNgn2 and xNgn2CO although from Figure 4.11, B we see a greater difference between controls and NEM-treated samples where cysteine is available and all canonical sites of ubiquitylation are unavailable in Ac2xNgn2KO. It could be that cysteines only become important when canonical sites are unavailable for ubiquitylation. However NEM is a potent alkylating agent and whilst steps were taken to purify the IVT radiolabelled protein from the NEM before adding to extract, it is not certain whether NEM could have had effects on the ubiquitylation process in the extract other than those predicted. This seems to be the

case for the results for xNgn2CO, where NEM treatment stabilises the protein (albeit not significantly) but should not actually be alkylating it.

In mitosis, xNgn2 proteins had half-lives of 15.8 +/- 2.1 mins, 35.6 +/- 2.7 mins and 38.3 +/- 5.4 mins for xNgn2, xNgn2KO and xNgn2CO respectively (Figure 4.12). In interphase, xNgn2 proteins had half-lives of 30.5 +/- 2.5 mins, 36.3 +/- 2.9 mins and 33.0 +/- 2.0 mins for xNgn2, xNgn2KO and xNgn2CO respectively (Figure 4.10). xNgn2 is degraded more quickly in mitosis than in interphase and so the relative stabilisation of mutating cysteines or lysines is much greater in mitosis. As removal of cysteines is as stabilising as removal of lysines, it suggests a powerful role for non-canonical ubiquitylation in targeting xNgn2 for degradation in mitosis.

Similar results were observed in neurula extract (Figure 4.13) where conversely xNgn2 exhibits a slightly longer half-life than in interphase (Figure 4.13, C), therefore cysteines are as efficient at driving Ub-mediated proteolysis as lysines in neurulae. Furthermore whilst Ac2xNgn2KO, the form of xNgn2 lacking all canonical amine-based sites of ubiquitylation, exhibits a long half-life in degradation assays (Figure 4.14, C), further mutation to remove all cysteine residues and replace them with alanines stabilises the protein yet further (Figure 4.14). All this evidence suggests that cysteines have an important role to play in regulating stability and the ubiquitylation assay in Figure 4.15 illustrates that not only is Ac2xNgn2KO still ubiquitylated, but Ac2xNgn2KOCO is also. This implicates serines, threonines and possibly even tyrosines in the Ub-mediated proteolysis of xNgn2.

Having highlighted differences in various *Xenopus laevis* extracts in the cysteine dependence of xNgn2 stability I went on to compare the contribution of non-canonical ubiquitylation to degradation in mammalian P19 cells.

The results from Figure 4.16 show clearly that xNgn2 can be degraded by the Ub proteasome system in mammals but work has shown that xNgn2 cannot drive P19 neuronal differentiation, whereas mNgn2 can (Christelle Fiore-Heriche, unpublished data). However P19 cells are still adequate for investigation of mechanisms regulating xNgn2 ubiquitylation and degradation.

Due to the lack of a suitable xNgn2 antibody, HA-tagging is an undesirable yet necessary modification to the protein, which may affect its degradation. Such issues are minimised by placing the tag on the C-terminus – tagging the N-terminus, which provides a site of ubiquitylation, should be avoided – but there may still be effects on the C-terminus such as affecting folding properties. Also tissue culture information is arguably still an *in vitro* system. However it shows consistency with *Xenopus laevis,* which is very encouraging.

xNgn2 is proteasomally degraded in P19 cells, as is Ac2xNgn2KO. Therefore xNgn2 is degraded by Ub-mediated proteolysis, and despite mutating all amine-based ubiquitylation sites, Ac2xNgn2KO is stabilised on the addition of the proteasome inhibitor MG132 and so this suggests non-canonical ubiquitylation can target the protein for degradation. Figure 4.17 illustrates that xNgn2 stability is regulated by canonical ubiquitylation sites in P19 cells in an identical manner to *Xenopus laevis* extract systems and Figure 4.18 demonstrates that in an environment capable of neuronal differentiation that the P19 cell line provides, xNgn2CO is stabilised compared to xNgn2, demonstrating again that in a physiological setting cysteines alone are sufficient to target xNgn2 for proteasomal degradation.

The results of the IP-re-IP experiment in Figure 4.19 are inconclusive but do suggest that Ac2xNgn2KOCO can still be ubiquitylated. This experiment might be best repeated with no heating of the non-reducing agent samples as boiling will still liberate xNgn2 from labile bonds to polyubiquitin chains.

Having established that cysteine ubiquitylation can target for destruction, why should this be the case? As illustrated in Figure 4.20, thioester linkages to cysteine are actually the weakest bond a protein could form with Ub (Clayden et al., 2000). Ester linkages with hydroxyls have an intermediate stability and isopeptide or amide bonds with amine groups form the most stable linkages. Whilst an unstable link is perhaps useful in a highly dynamic signalling system, are cysteines not simply too weak to be relevant as a nucleophile for ubiquitylation?

In terms of thermodynamics, cysteines indeed would be a poor choice for stable ubiquitylation. However, the biochemical environment of the cell rarely ventures into the realm of stable thermodynamic equilibrium; rather, such biochemical reactions are governed by the kinetics of reactions and Figure 4.21 illustrates why cysteines may play a significant role particularly in modification for signalling. Ub is shuttled along the ubiquitylation cascade from an Ub-activating enzyme, or E1, to an Ub-conjugating enzyme, or E2, and in the case of HECT domains, onto an E3 ligase, and in all these cases, Ub is conjugated to a cysteine residue on the enzyme. Therefore a weak thioester linkage is always attacked by a nucleophilic group when ubiquitylating a substrate protein. As this thioester link consists of diffuse orbitals particularly from the large sulfur atom, and there is not a large polarisation of charge, this is classed as a soft electrophile (Clayden et al., 2000). Soft electrophiles react preferentially with nucleophiles which are also soft, that is with diffuse large orbitals and high energy highest occupied molecular orbitals (HOMOs) that overlap well with the lowest unoccupied molecular orbital (LUMOs) of the thioester linkage (which is the carbonyl π^* MO). In this respect, sulfur thiols will undergo the fastest reaction with a thioester carbonyl, followed by hydroxyls, followed by amines, which become harder, more charge-dominated nucleophiles. So whilst the link may be labile, it is formed more quickly than the more stable isopeptide bond and could potentially provide a greater range for dynamic signalling behaviour in ubiquitylation.

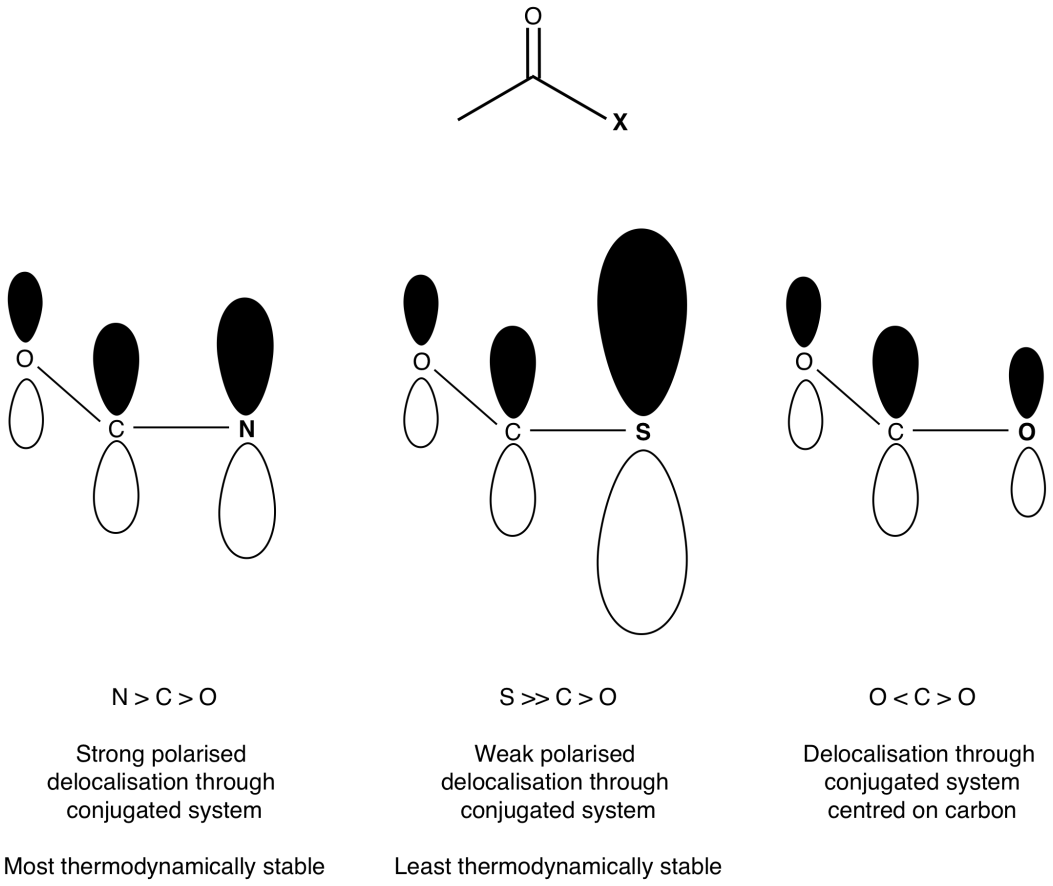

Figure 4.20: Extent of orbital overlap in linkages to ubiquitin.

In an ester-like linkage between the amino acid residue and the C-terminus of ubiquitin, the extent of orbital overlap relates to the size, symmetry and energy of the orbitals involved, how closely these properties match, and whether the bond is polarised. Hence amide bonds involving nitrogen are the strongest; and thioester linkages using sulfur are weakest.

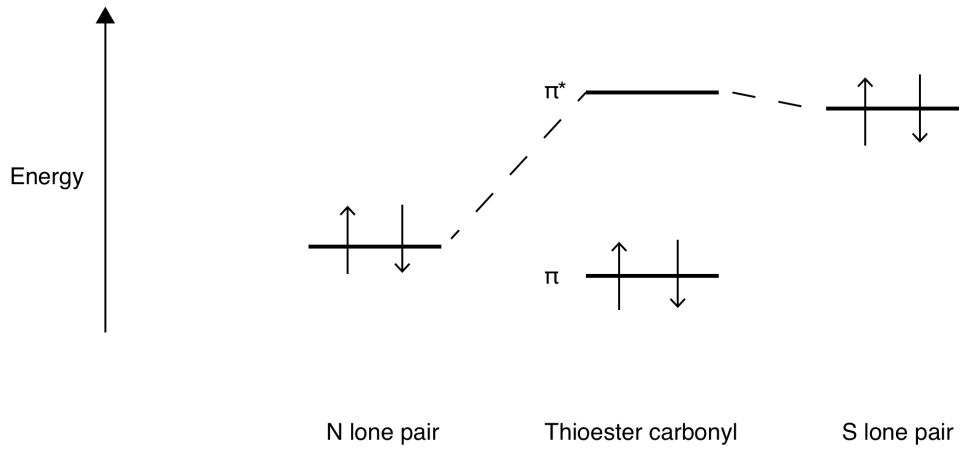

Figure 4.21: Kinetics of protein-ubiquitin covalent bond formation.
As a soft, high-energy nucleophile, the lone pair of electrons on sulfur actually form a better overlap with the lowest unoccupied molecular orbital (LUMO) of the E2-ubiquitin linkage, which is a soft electrophile, than the hard nucleophile presented by the nitrogen lone pair.

CHAPTER 5

Phosphorylation and Stability of xNgn2

INTRODUCTION

Transcription factor activity is tightly regulated and control can be achieved at the level of PTM, such as phosphorylation (Tootle and Rebay, 2005). Work on the cyclin dependent kinase inhibitor (cdki) Xic1, which stabilises xNgn2 (Vernon et al., 2003), has led to interest in the phosphorylation status of xNgn2 and the effect that this has on activity and stability. There is a clear link between the signalling roles of phosphorylation and ubiquitylation for proteasomal degradation (Hunter, 2007). The stability of many bHLH proteins such as MyoD is regulated by phosphorylation events (Tintignac et al., 2000, Kitzmann et al., 1999).

Phosphorylation may or may not have a role in proteasomal degradation. Targeting of substrates for degradation by the SCF complex (Skp-Cullin-F-box) requires phosphorylation of conditional 'phosphodegron' sites (Mayer, 2005, Willems et al., 2004). This phosphorylation is required for the production of substrate-E3 ligase interactions (Mayer, 2005). The stability of the related bHLH protein MyoD against degradation can be regulated by phosphorylation events on cdk consensus sites (Song et al., 1998) and cell cycle regulating proteins such as p27 are regulated by phosphorylation with respect to ubiquitylation (Montagnoli et al., 1999). xNgn2 contains a number of putative cdk consensus sites for phosphorylation as 'SP' or 'TP' sites (phosphorylation possibly occurring on the serine or threonine in each case), which may serve as interaction domains with WD40 domains present in many E3 ligases (Yaffe and Elia, 2001).

Jonathan Vosper identified a Casein Kinase II (CK2) consensus site at T118 in xNgn2 related to Mash1 (Vinals et al., 2004) and mutation at T118 to alanine in xNgn2 disrupts phosphorylation events shown to be linked to xE12-binding (Vosper et al., 2007). Therefore there may be a role for phosphorylation in stability with the

heterodimeric binding partner of xNgn2, namely xE12. Indeed E47 phosphorylation affects association with MyoD (Lluis et al., 2005) so phosphorylation has an important role to play in the activity of xNgn2 and a mechanism for the role of this modification is unknown.

xNgn2 is phosphorylated in a manner affecting its function (Hand et al., 2005) so I wanted to establish whether phosphorylation on cdk consensus sites had any effect on xNgn2 stability. This is an especially interesting question as removal of all putative SP consensus sites in xNgn2 results in a hyperactive form of xNgn2 in *Xenopus laevis* embryos (Ali et al., 2011). Therefore I wanted to see if this activity can be explained in terms of degradation of xNgn2.

RESULTS

Mutation of cyclin dependent kinase (cdk) consensus 'SP' sites in xNgn2 affects stability in a cell cycle dependent manner

xNgn2 contains a number of putative cyclin dependent kinase (cdk) consensus sites (Yaffe and Elia, 2001, Errico et al., 2010) which, taking the minimal consensus site as being a serine or threonine followed by a proline, are shown in Figure 5.1. There are 9 'SP' sites and one 'TP' site. All SP and TP sites lie in the disordered N- and C-termini and not within the bHLH domain.

Extensive work has been carried out showing that xNgn2 lacking all SP sites, where all serines are mutated to alanines to give 9S-AxNgn2, is hyperactive in neurogenic activity compared to wild type xNgn2 (Ali et al., 2011). However I am interested in whether this activity relating to xNgn2 phosphorylation state is related to the stability of xNgn2, or whether stability and activity are independently regulated.

To begin investigating xNgn2 stability I was able to use the mutant form of xNgn2 generated by gene synthesis (GeneCust) that mutates all serines followed by prolines

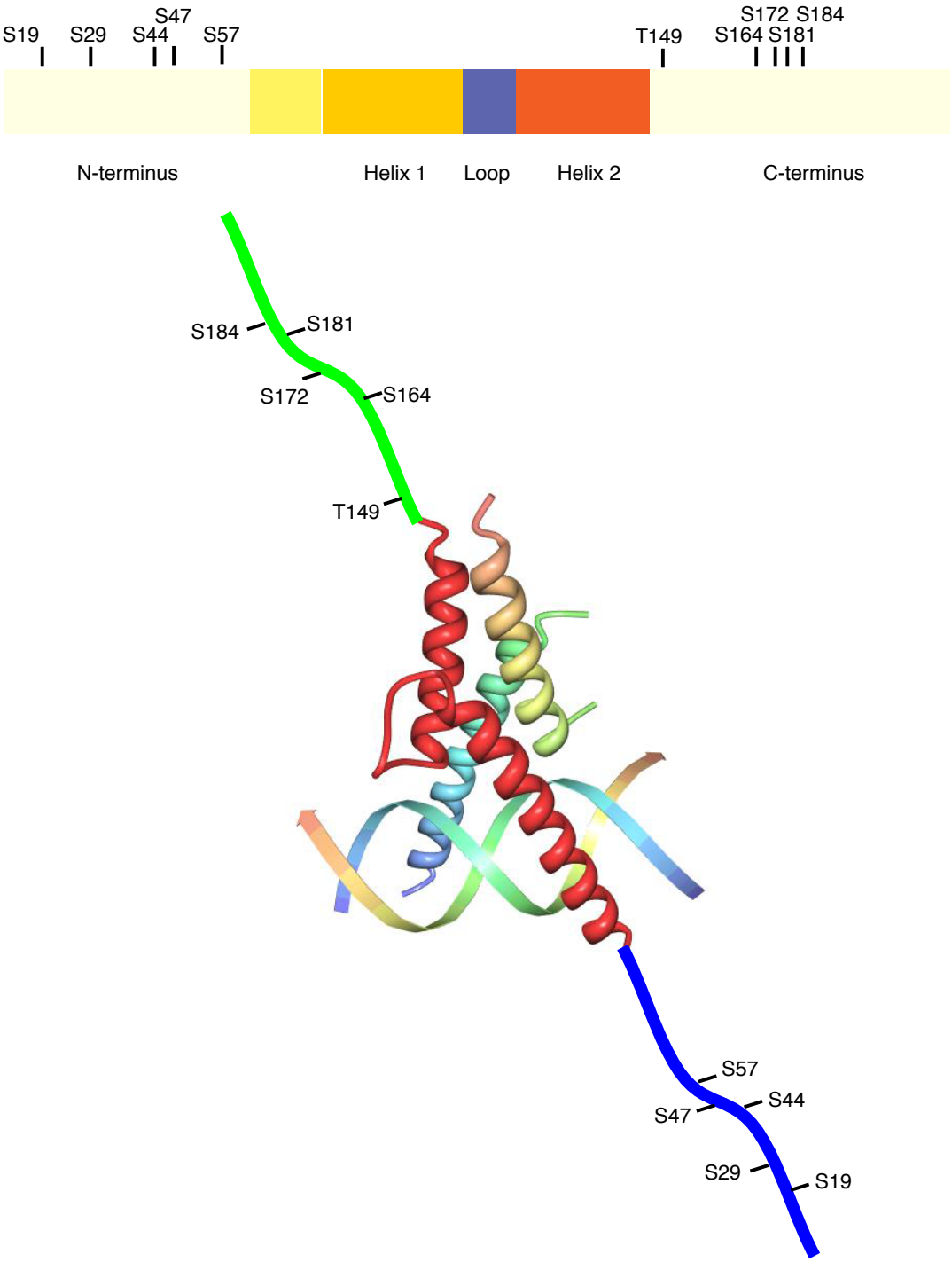

Figure 5.1: Cyclin dependent kinase (cdk) consensus serines and threonine in xNgn2.
Cyclin dependent kinases (cdks) are proline-directed kinases which phosphorylate serines or threonines followed by prolines , shown schematically. The sites are modelled onto a structure of a proneural bHLH heterodimer complexed to DNA. The disordered N-terminal domain is bordered in blue; the bHLH domain in red; and the disordered C-terminal domain in green.

to alanines, from SP to AP. Degradation assays were carried out in *Xenopus laevis* interphase activated egg extract by adding ^{35}S-radiolabelled IVT xNgn2 or the SP mutant, 9S-AxNgn2, and incubating samples at 21 °C. Aliquots of the reaction were removed at increasing timepoints, quenched in SDS-LB and samples were separated by 15 % SDS-PAGE to allow measurement of protein levels over time and calculation of the half-life for degradation using first-order rate kinetics (Figure 5.2).

The half-lives for degradation of xNgn2 and 9S-AxNgn2 are 22.0 +/- 2.2 mins and 19.3 +/- 2.0 mins in interphase egg extract respectively, and 39.5 +/- 5.1 mins and 34.2 +/- 7.4 mins correspondingly in neurula embryo extract (Figure 5.2, C). Therefore in interphase egg and neurula embryo settings, the potential for xNgn2 to be phosphorylated by cdks does not affect stability against degradation.

In mitotic egg extract the half-life for xNgn2 degradation is 18.5 +/- 3.2 mins whereas 9S-AxNgn2 has a half-life of 25.5 +/- 1.4 mins (Figure 5.2, C). This is accompanied by a contrasting appearance on SDS-PAGE; 9S-AxNgn2 runs as normal in comparison to the interphase and neurula xNgn2 and 9S-AxNgn2 samples; however from the 15 min timepoint onwards, xNgn2 migration is retarded on SDS-PAGE (Figure 5.2, A). Therefore the shift in xNgn2 migration in mitosis could be explained by phosphorylation altering the electrostatic charge of the protein. 9S-AxNgn2 is more stable than xNgn2 in mitotic egg extract.

To establish whether the shift in migration of xNgn2 on incubation in mitotic extract observed in Figure 5.2, A is due to phosphorylation, xNgn2 and 9S-AxNgn2 were incubated in interphase and mitotic egg and neurula embryo extracts, with either the cdk inhibitor roscovitine (Meijer et al., 1997, Luciani et al., 2004, Khoudoli et al., 2008) (DMSO was used as a control) or λ-phosphatase (with buffer alone as a control) (Figure 5.3). Roscovitine should prevent phosphorylation by cdks and was added to the IVT protein before incubation in extract; λ-phosphatase should dephosphorylate any phosphorylated protein and was added to the extracts.

There is no effect from any of the treatments on either xNgn2 or 9S-AxNgn2 in interphase extract. However in mitotic extract and, to a lesser extent, in neurula

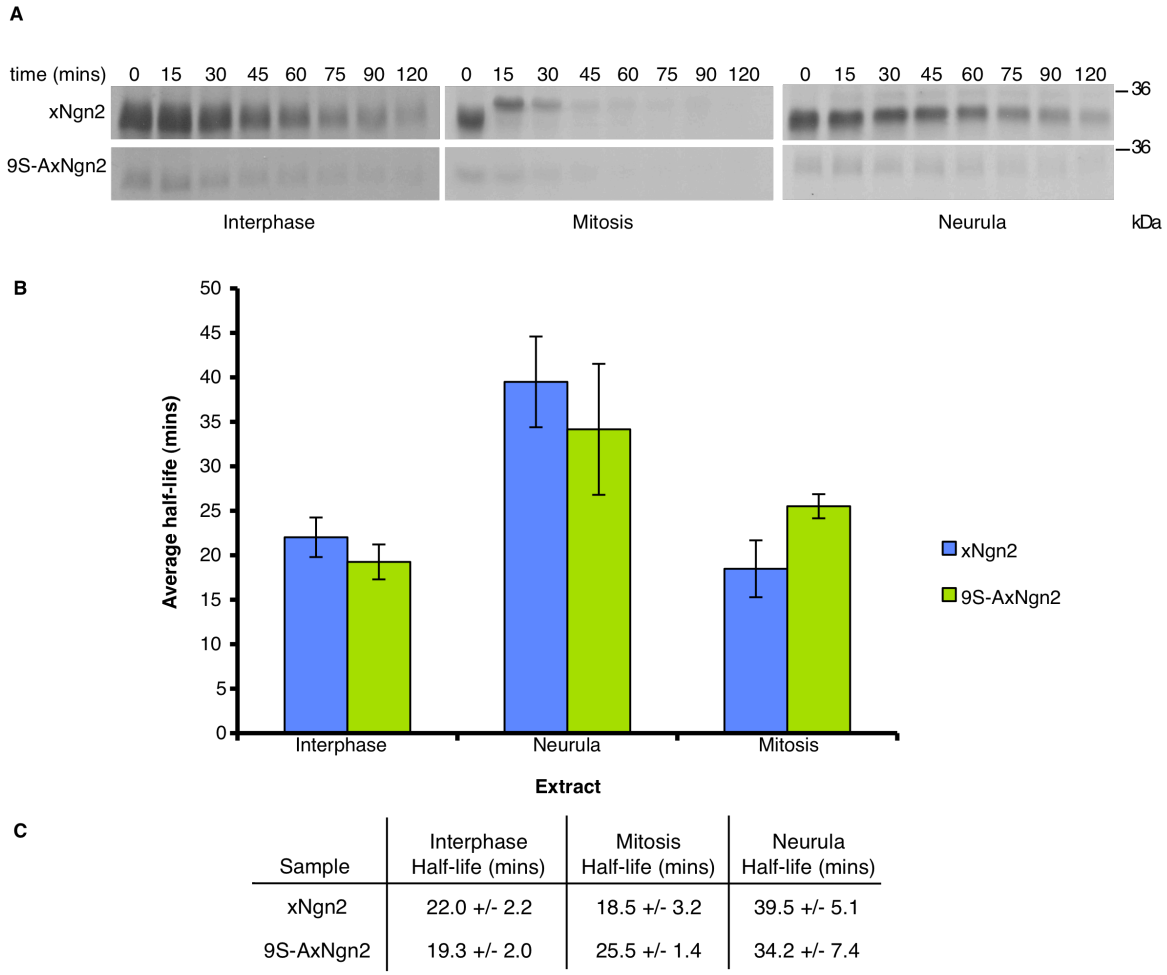

C

Sample	Interphase Half-life (mins)	Mitosis Half-life (mins)	Neurula Half-life (mins)
xNgn2	22.0 +/- 2.2	18.5 +/- 3.2	39.5 +/- 5.1
9S-AxNgn2	19.3 +/- 2.0	25.5 +/- 1.4	34.2 +/- 7.4

Figure 5.2: xNgn2 and 9S-AxNgn2 stability in *Xenopus laevis* extracts.

Xenopus laevis interphase activated egg extracts, mitotic activated egg extracts and neurula embryo extracts were supplemented with ^{35}S-labelled xNgn2 or 9S-AxNgn2 and incubated at 21 °C. Samples were taken at the timepoints indicated and subjected to 15 % SDS-PAGE. Gels were analysed by autoradiography (A) and quantitative phosphorimaging analysis, calculating the half-life for degradation in each extract (B). (C) Half-lives were calculated using first-order rate kinetics, and errors calculated using the Standard Error of the Mean (SEM).

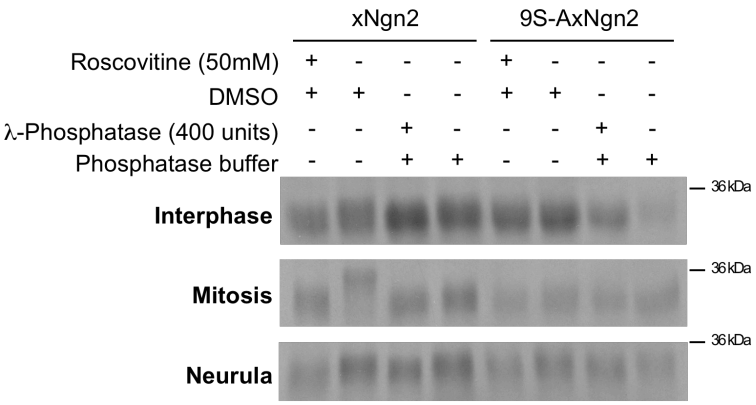

Figure 5.3: xNgn2 and 9S-AxNgn2 treated with the cdk inhibitor roscovitine and the dephosphorylating protein λ-phosphatase.

Xenopus laevis interphase activated egg extracts, mitotic activated egg extracts and neurula embryo extracts were supplemented with ^{35}S-labelled xNgn2 or 9S-AxNgn2 and incubated with either the blanket cdk inhibitor roscovitine or λ-phosphatase. Samples were subjected to 15 % SDS-PAGE. Gels were analysed by autoradiography.

extract, roscovitine treatment results in faster migration of xNgn2 than the DMSO-incubated control, but 9S-AxNgn2 gel migration is not affected (Figure 5.3). Likewise λ-phosphatase treated xNgn2 migrates more rapidly than the buffer-only sample in mitotic and neurula extracts. Again, 9S-AxNgn2 shows no alteration in its migration pattern. Therefore, the alteration in migration of xNgn2 but not 9S-AxNgn2 on λ-phosphatase treatment demonstrates that xNgn2 is phosphorylated in mitotic, and to a lesser extent neurula, extract in a manner that alters its migration in gel electrophoresis, whereas 9S-AxNgn2 is not. Phosphorylation cannot be observed by gel electrophoresis in interphase extract. Roscovitine treatment shows that this migration-altering phosphorylation of xNgn2 is due to cyclin dependent kinases.

Much of the work carried out on Ngn2 activity is divided between xNgn2 *in vivo* activity in *Xenopus laevis* embryos (Hindley, 2011) and mNgn2 activity in *Mus musculus* P19 embryonal carcinoma cells (Ali et al., 2011). Having investigated the degradation of xNgn2 in P19 cells (Figures 4.16-19) I decided to investigate whether the mouse protein, mNgn2 - which differs in distribution of SP sites from xNgn2 - and 9S-AmNgn2 would exhibit similar degradation properties to xNgn2 and 9S-AxNgn2 in *Xenopus laevis* extract systems. Therefore ^{35}S-radiolabelled IVT xNgn2 and mNgn2 and their 9S-A mutants were incubated in *Xenopus laevis* interphase and mitotic activated egg and neurula embryo extracts for degradation assays (Figure 5.4).

Whilst both xNgn2 and mNgn2 exhibit shifts in gel migration on incubation with mitotic extract (Figure 5.4, A), their behaviour in terms of degradation pattern is very different. mNgn2 is actually stabilised in mitotic and neurula extracts compared to interphase, with half-lives for degradation of 31.1 +/- 5.1 mins and 68.0 +/- 12.6 mins compared to just 21.3 +/- 4.8 mins in interphase. Also, 9S-AmNgn2 has a half-life in interphase of 28.3 +/- 0.7 mins which is significantly more than mNgn2 with a half-life of 21.3 +/- 4.8 mins, whereas xNgn2 and 9S-AxNgn2 exhibit similar stabilities in interphase extract with half-lives of 25.4 +/- 9.1 mins and 25.1 +/- 3.2 mins respectively. Therefore mNgn2 stability in relation to phosphorylation does not act as a good comparison with xNgn2 in *Xenopus laevis* extract systems.

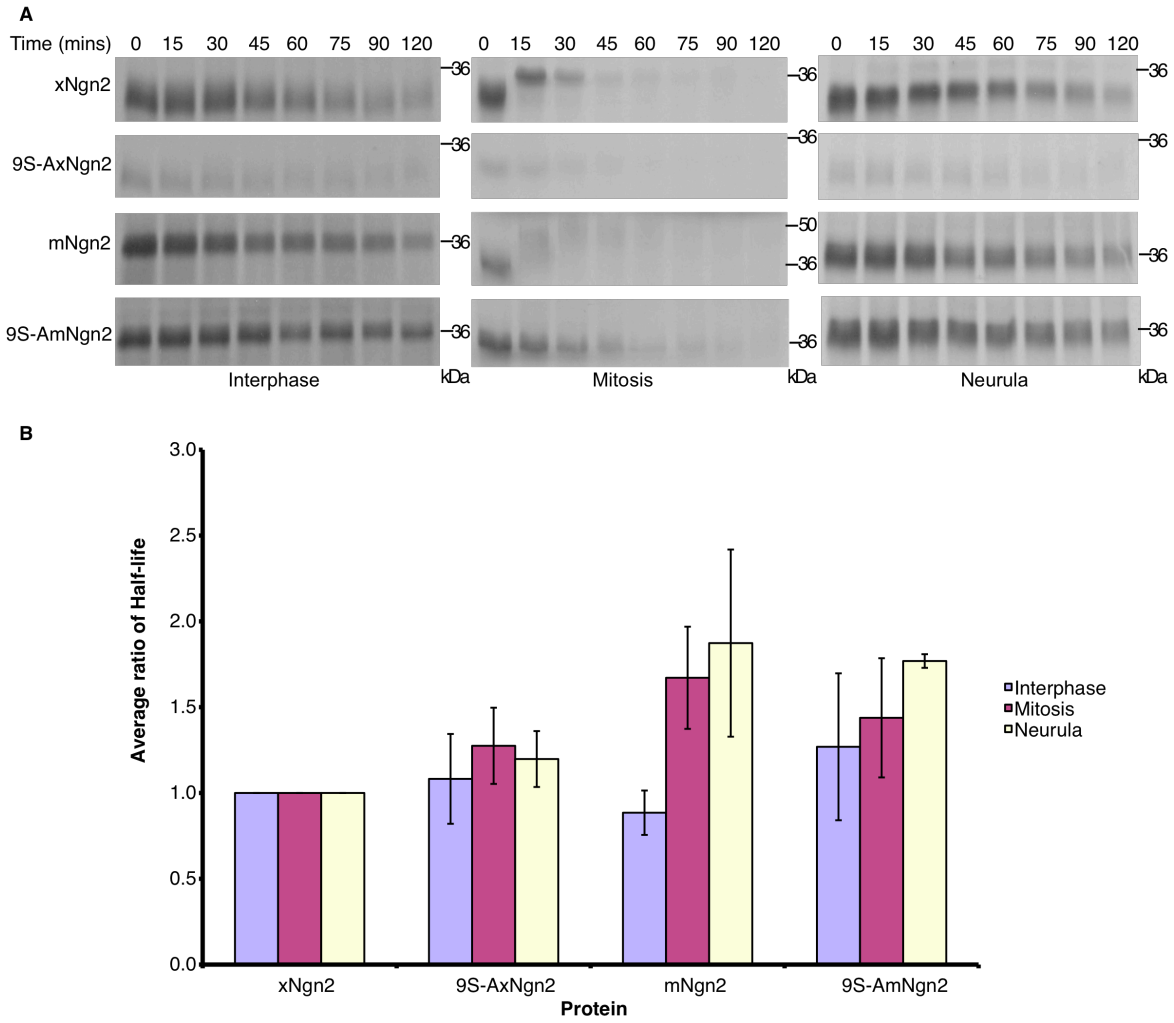

C

Sample	Interphase Half-life (mins)	Mitosis Half-life (mins)	Neurula Half-life (mins)
xNgn2	25.4 +/- 9.1	20.4 +/- 5.7	37.5 +/- 4.2
9S-AxNgn2	25.1 +/- 3.2	23.8 +/- 4.1	45.7 +/- 11.2
mNgn2	21.3 +/- 4.8	31.1 +/- 5.1	68.0 +/- 12.6
9S-AmNgn2	28.3 +/- 0.7	25.5 +/- 1.7	66.2 +/- 6.0

Figure 5.4: xNgn2 and mNgn2 and their 9S-A mutants are degraded in *Xenopus laevis* extracts.

Xenopus laevis interphase activated egg extracts, mitotic activated egg extracts and neurula embryo extracts were supplemented with ^{35}S-labelled xNgn2, 9S-AxNgn2, mNgn2 or 9S-AmNgn2 and incubated at 21 °C. Samples were taken at the timepoints indicated and subjected to 15 % SDS-PAGE. Gels were analysed by autoradiography (A) and quantitative phosphorimaging analysis, calculating the average stabilisation relative to wild-type xNgn2 within each extract (B). (C) Half-lives were calculated using first-order rate kinetics, and errors calculated using the Standard Error of the Mean (SEM). Experiments in interphase and neurula extracts were carried out in duplicate.

Mutation of 'TP' sites does not affect stability

As well as 9 'SP' sites, xNgn2 also has a 'TP' site at T149 in the C-terminal domain. Site-directed mutagenesis by Kate Wilson produced xNgn2 and 9S-AxNgn2 forms with this threonine mutated to alanine, namely T149AxNgn2 and 9S-AT149AxNgn2 (Figure 5.5). SP and TP mutants were also made in backgrounds of lysineless xNgn2KO and the N-terminal acetylation mutant Ac2xNgn2KO which also lacks lysines. Mutations of T118 (the casein kinase II site) to alanine were also made. To investigate any effect on stability of the TP site, degradation assays were carried out using ^{35}S-radiolabelled IVT proteins. Stability was assessed in *Xenopus laevis* interphase activated egg and neurula embryo extracts (Figure 5.6). A full list and description of all xNgn2 mutants can be found in the Abbreviations section.

xNgn2, 9S-AxNgn2, 9S-AT149AxNgn2 and 9S-AT(118,149)AxNgn2 have half-lives in interphase of 35.0 +/- 0.5 mins, 28.0 +/- 0.7 mins, 56.0 +/- 35 mins and 31.5 +/- 1.5 mins respectively. In neurula, they have half-lives of 39.5 +/- 5.1 mins, 34.2 +/- 7.4 mins, 30.0 +/- 2.6 and 34.3 +/- 6.0 mins respectively.

xNgn2KO, 9S-AxNgn2KO, 9S-AT149AxNgn2KO and 9S-AT(118,149)AxNgn2KO have half-lives in interphase of 63.8 +/- 9.8 mins, 76.3 +/- 12.3 mins, 44.8 +/- 22.3 mins and 59.8 +/- 17.3 mins respectively. In neurula, they have half-lives of 44.5 +/- 8.4 mins, 46.3 +/- 3.7 mins, 57.9 +/- 6.5 mins and 50.1 +/- 5.3 mins respectively.

Ac2xNgn2KO and 9S-AxNgn2KO have half-lives in interphase of 173 +/- 42 mins and 91.5 +/- 66.5 mins respectively. In neurula, they have half-lives of 79.2 +/- 13.1 and 82.2 +/- 7.9 mins respectively.

Therefore, the effect of mutating putative serine and threonine phosphorylation sites has very little effect on the stability of proteins which have all lysines and the N-terminus available for ubiquitylation; or just the N-terminus available; or no amino-based nucleophilic sites at all. The presence of ubiquitylation sites themselves is more important than the availability of phosphosites in regulating xNgn2 stability in interphase and neurula.

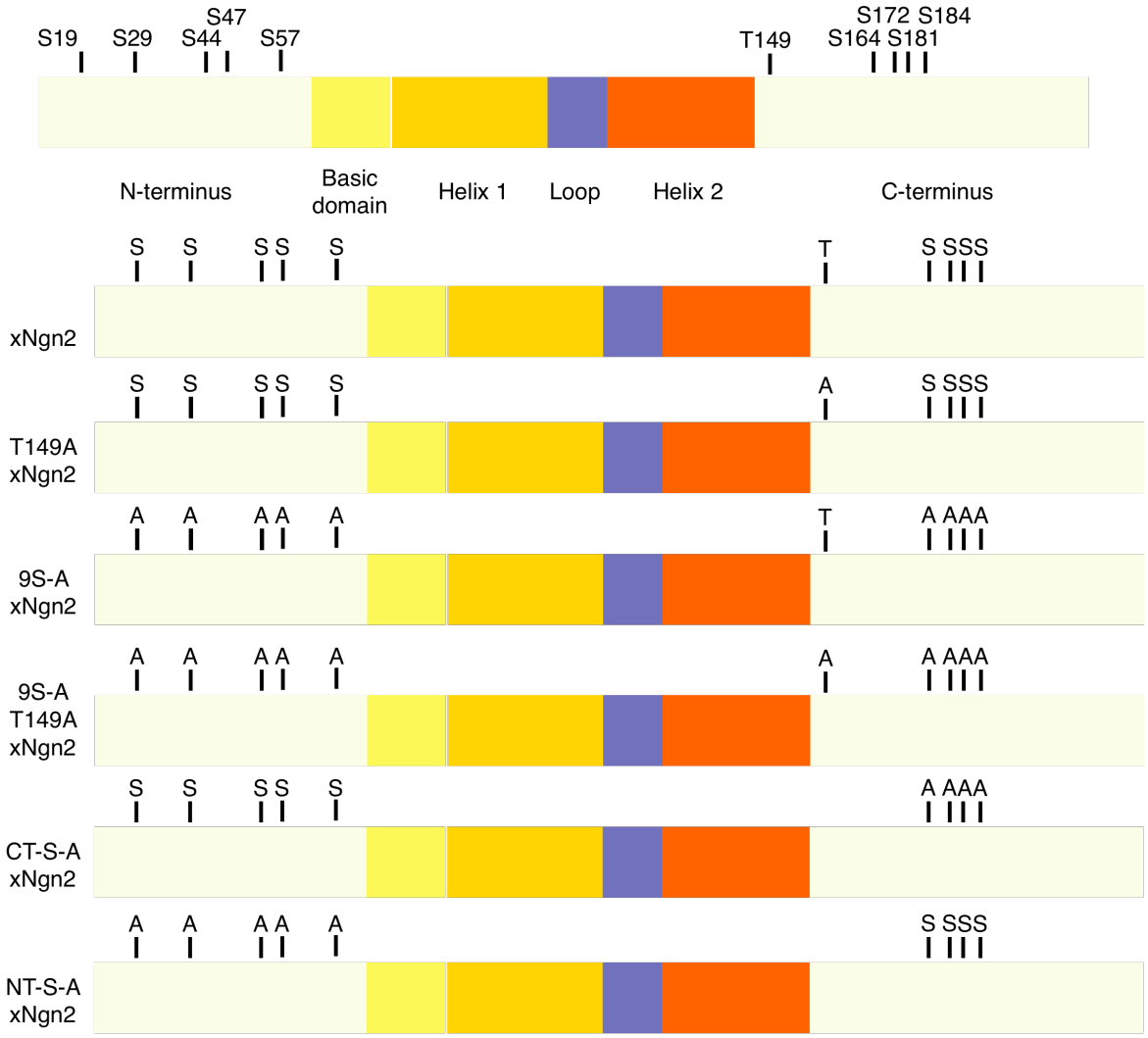

Figure 5.5: xNgn2 mutants lacking SP and TP sites.

Cyclin dependent kinases (cdks) are proline-directed kinases which phosphorylate serines or threonines followed by prolines. There are 9 such serines and one threonine in xNgn2 and various mutants described in the text were made which are shown schematically.

A

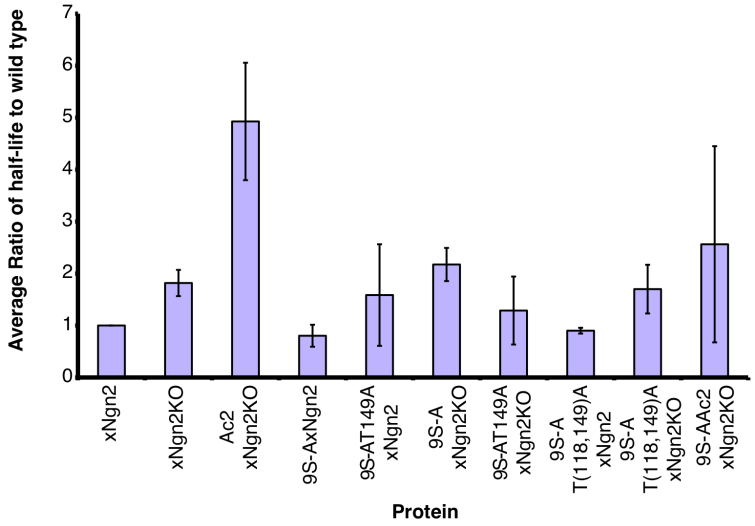

B

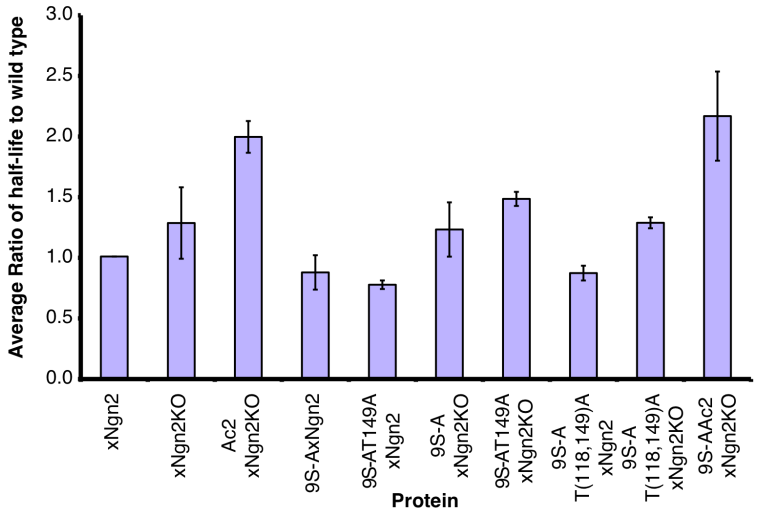

C

Sample	Interphase Half-life (mins)	Neurula Half-life (mins)
xNgn2	35.0 +/- 0.5	39.5 +/- 5.1
xNgn2KO	63.8 +/- 9.8	44.5 +/- 8.4
Ac2xNgn2KO	173 +/- 42	79.2 +/- 13.1
9S-AxNgn2	28.0 +/- 7.0	34.2 +/- 7.4
9S-AT149AxNgn2	56.0 +/- 35	30.0 +/- 2.6
9S-AxNgn2KO	76.3 +/- 12.3	46.3 +/- 3.7
9S-AT149AxNgn2KO	44.8 +/- 22.3	57.9 +/- 6.5
9S-AT(118,149)AxNgn2	31.5 +/- 1.5	34.3 +/- 6.0
9S-AT(118,149)AxNgn2KO	59.8 +/- 17.3	50.1 +/- 5.3
9S-AAc2xNgn2KO	91.5 +/- 66.5	82.2 +/- 7.9

Figure 5.6: Stability of xNgn2 SP/TP mutants in *Xenopus* interphase and neurula extracts.
Xenopus laevis interphase extracts and neurula extracts were supplemented with ^{35}S-labelled xNgn2 or xNgn2 phosphorylation mutants. Samples taken at 0, 15, 30, 45, 60, 90, 120 mins were subjected to 15 % SDS-PAGE. Gels were analysed by quantitative phosphorimaging analysis, calculating the average stabilisation relative to wild-type xNgn2 within interphase (A) and neurula extracts (B). (C) Half-lives calculated using first-order rate kinetics, and errors calculated SEM.

Incubation in *Xenopus laevis* mitotic activated egg extract is shown to result in extensive phosphorylation of xNgn2 (Figures 5.2 and 5.3) and so TP mutations were investigated by degradation assays in mitotic extract, as well as mutants of SP sites in xNgn2 mutating only the SP sites in the N-terminal domain (NT-S-AxNgn2) or C-terminal domain (CT-S-AxNgn2) (Figure 5.5). ^{35}S-radiolabelled IVT proteins were added to *Xenopus laevis* mitotic activated egg extract and incubated at 21 °C. Aliquots of the reaction were removed at increasing timepoints, quenched in SDS-LB and samples were separated by 15 % SDS-PAGE to allow measurement of protein levels over time and calculation of the half-life for degradation using first-order rate kinetics (Figure 5.7).

xNgn2 has a half-life of 33.0 +/- 2.1 mins whilst 9S-AxNgn2 is more stable with a half-life of 55.9 +/- 10.0 mins (Figure 5.7, B). Additional mutation of the TP site threonine to alanine to give AP gives a half-life of 44.1 +/ 3.4 mins and therefore does not affect the stability of xNgn2 any more than mutation of the SP sites.

The N-terminal SP mutants, NT-S-AxNgn2 and NT-S-AT149AxNgn2, have half-lives of 28.5 +/- 2.8 mins and 30.5 +/- 4.9 mins respectively that do not differ significantly from xNgn2. The C-terminal mutants, CT-S-AxNgn2 and CT-S-AT149AxNgn2, are degraded with half-lives of 74.4 +/- 20.3 mins and 42.2 +/- 11.9 mins respectively. Therefore the C-terminal SP sites, when mutated to alanines, confer a similar stability on xNgn2 as mutation of all the SP sites.

This data complements experiments showing that phosphorylation observed by retardation of xNgn2 on gel electrophoresis is lost when C-terminal SP sites are mutated to alanines (Ali et al., 2011). This would suggest that C-terminal phosphorylation is important in regulating xNgn2 stability in mitosis.

No individual SP site affects stability but combinations of sites in different domains of xNgn2 can affect stability

Figure 5.7 suggests that phosphorylation of xNgn2 differs in various regions of the protein. Mutants of xNgn2 were created using site-directed mutagenesis by Helen

A

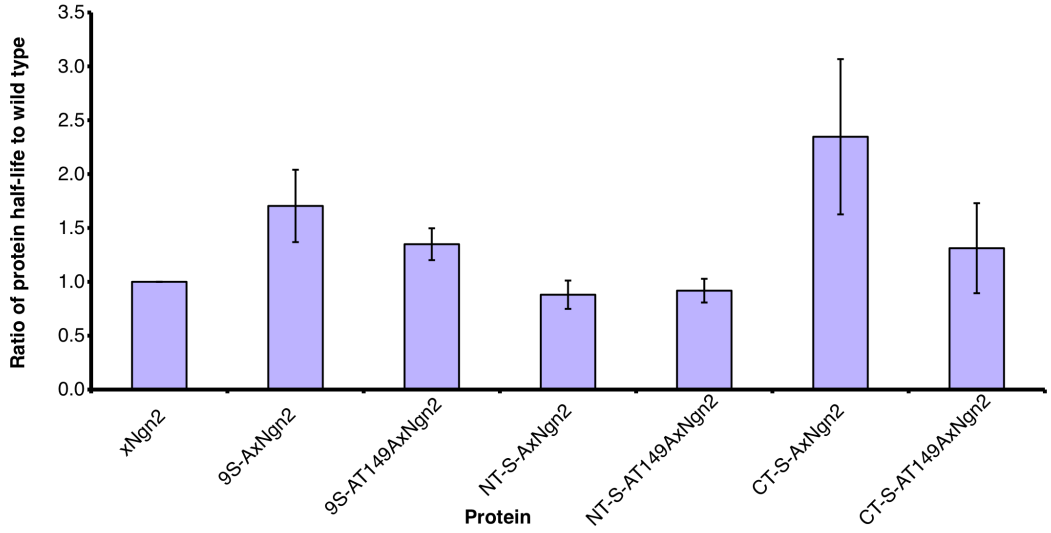

B

Sample	Half-life (mins)
xNgn2	33.0 +/- 2.1
9S-AxNgn2	55.9 +/- 10.0
9S-AT149AxNgn2	44.1 +/- 3.4
NT-S-AxNgn2	28.5 +/- 2.8
NT-S-AT149AxNgn2	30.5 +/- 4.9
CT-S-AxNgn2	74.4 +/- 20.3
CT-S-AT149AxNgn2	42.2 +/- 11.9

Figure 5.7: Stability of xNgn2 SP/TP mutants in *Xenopus* mitotic extract.

Xenopus laevis mitotic activated egg extracts were supplemented with ^{35}S-labelled xNgn2 or xNgn2 mutants lacking putative phosphorylation sites and incubated at 21 °C. Samples were taken at 0, 15, 30, 45, 60, 75, 90 and 120 mins and subjected to 15 % SDS-PAGE. Gels were analysed by quantitative phosphorimaging analysis, calculating the average stabilisation relative to wild-type xNgn2 within mitotic extract (A). (B) Half-lives were calculated using first-order rate kinetics, and errors calculated using the Standard Error of the Mean (SEM).

Wise to mutate each SP site to an alanine additively, beginning with the most C-terminal SP, S184, and mutating each SP serine in turn until all serines are mutated to 9S-AxNgn2 (Figure 5.8). To investigate the stability of these mutants I began with degradation assays in interphase and neurula extract. ^{35}S-radiolabelled IVT proteins were added to *Xenopus laevis* interphase activated egg and neurula embryo extract and incubated at 21 °C. Aliquots of the reaction were removed at increasing timepoints, quenched in SDS-LB and samples were separated by 15 % SDS-PAGE to allow measurement of protein levels over time and calculation of the half-life for degradation using first-order rate kinetics (Figure 5.9).

xNgn2 is degraded with a half-life of 22.0 +/- 2.2 mins in interphase extract and 49.1 +/- 12.8 mins in neurula extract (Figure 5.9, C). The serial SP mutants exhibit similar half-lives in interphase, and lower values in neurula which are however similar to one another. xNgn2 demonstrated a half-life longer than usually observed in neurula therefore these values were taken as not differing significantly from wild type stability. Therefore in interphase and neurula extracts, where protein phosphorylation (as observed by chanes in gel migration) is low, there does not appear to be a change in stability as SP sites are progressively removed.

As the most extensive phosphorylation of xNgn2 occurs in mitotic extract, the assays in Figure 5.9 were repeated in *Xenopus laevis* mitotic activated egg extract (Figure 5.10).

xNgn2 is degraded with a half-life of 18.5 +/- 0.9 mins. On mutation of the most C-terminal SP site, xS-A1 has a half-life for degradation of 37.5 +/- 8.7 mins. The half-life increases for additional mutation of SP sites to AP until xS-A4, with a half-life of 51.9 +/- 0.6 mins. The half-life then decreases upon additive mutation of SP sites towards the N-terminus, reaching 25.5 +/- 2.3 mins at 9S-AxNgn2 which is significantly but slightly more stable than xNgn2.

That the stability should increase to a maximum with successive SP mutations to AP from the C-terminus at xS-A4 is significant; at this point, all putative C-terminal serine phosphorylation sites are lost. This would suggest that phosphorylation at the C-

Figure 5.8: Serial SP mutants of xNgn2.

Cyclin dependent kinases (cdks) are proline-directed kinases which phosphorylate serines or threonines followed by prolines. There are 9 such serines in xNgn2 and mutants were constructed sequentially mutating serines to alanines beginning with the most C-terminal SP site, as shown.

A

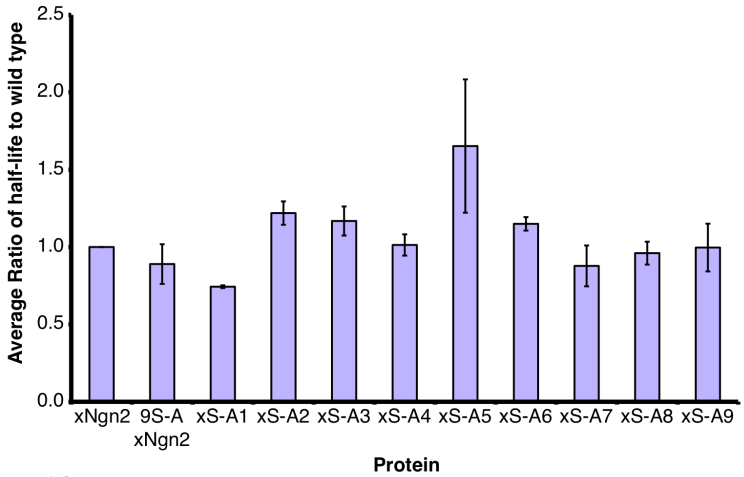

B

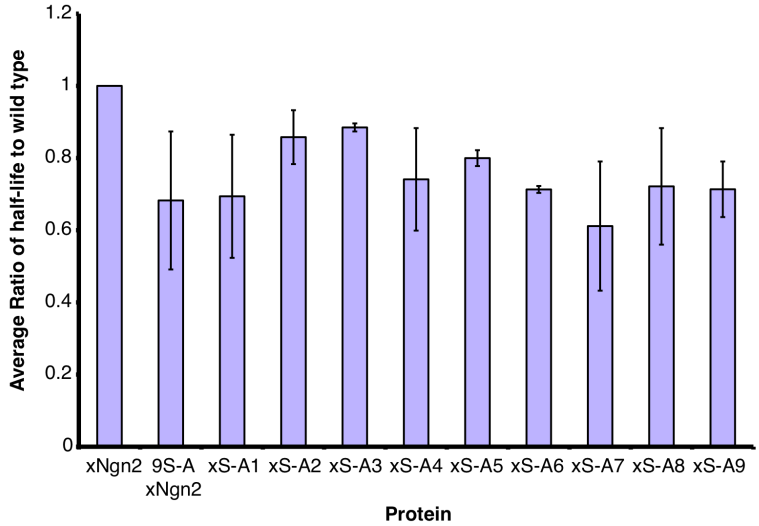

C

Sample	Interphase Half-life (mins)	Neurula Half-life (mins)
xNgn2	22.0 +/- 2.2	49.1 +/- 12.8
9S-AxNgn2	19.3 +/- 2.0	31.0 +/- 0.6
xS-A1	16.3 +/- 1.4	31.9 +/- 0.5
xS-A2	27.1 +/- 4.2	41.1 +/- 7.3
xS-A3	25.3 +/- 0,4	43.6 +/- 11.9
xS-A4	20.8 +/- 1.4	34.5 +/- 2.5
xS-A5	34.9 +/- 6.5	39.0 +/- 9.2
xS-A6	25.5 +/- 3.5	35.1 +/- 9.6
xS-A7	18.7 +/- 1.2	27.7 +/- 1.0
xS-A8	20.8 +/- 0.4	33.3 +/- 1.3
xS-A9	21.3 +/- 1.7	34.0 +/- 5.4

Figure 5.9: Stability of serial SP mutants of xNgn2 in interphase and neurula extracts.

Xenopus interphase extracts and duplicate neurula extracts were supplemented with ^{35}S-labelled xNgn2 or serial SP xNgn2 mutants. Samples taken at 0, 15, 30, 45, 60, 90 and 120 mins were subjected to 15 % SDS-PAGE and analysed by quantitative phosphorimaging analysis, calculating the average stabilisation relative to wild-type xNgn2 within interphase (A) and neurula extracts (B). (C) Half-lives were calculated using first-order rate kinetics, and errors calculated using SEM.

A

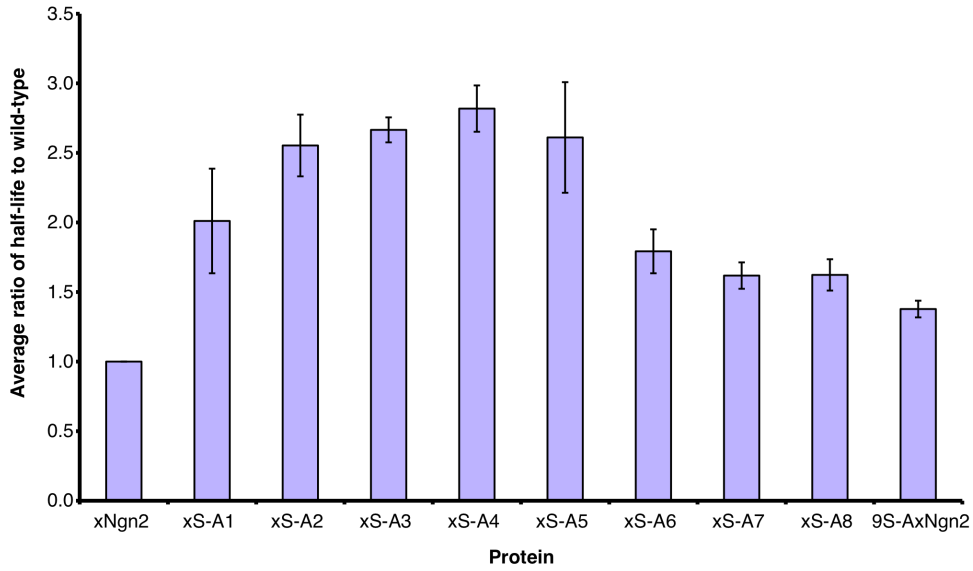

B

Sample	Half-life (mins)
xNgn2	18.5 +/- 0.9
xS-A1	37.5 +/- 8.7
xS-A2	47.4 +/- 6.4
xS-A3	49.2 +/- 0.7
xS-A4	51.9 +/- 0.6
xS-A5	48.6 +/- 9.7
xS-A6	33.0 +/- 1.3
xS-A7	29.8 +/- 0.3
xS-A8	29.9 +/- 0.6
9S-AxNgn2	25.5 +/- 2.3

Figure 5.10: Stability of serial SP mutants of xNgn2 in mitotic extract.

Xenopus laevis mitotic activated egg extracts were supplemented with ^{35}S-labelled xNgn2 or serial SP xNgn2 mutants and incubated at 21 °C. Samples were taken at 0, 15, 30, 45, 60, 75, 90 and 120 mins and subjected to 15 % SDS-PAGE. Gels were analysed by quantitative phosphorimaging analysis, calculating the average stabilisation relative to wild-type xNgn2 within mitotic extract (A). (B) Half-lives were calculated using first-order rate kinetics, and errors calculated using the Standard Error of the Mean (SEM). Results are from a duplicate set of experiments.

terminus is destabilising, but phosphorylation at the N-terminus then promotes stability. The activity of these mutants has been investigated *in vivo* in *Xenopus laevis* embryos by *in situ* hybridisation (Ali et al., 2011) and activity increases gradually along the series, suggesting that activity may not perfectly reflect protein stability.

To investigate whether individual serines are important in phosphorylation of xNgn2, Christopher Hindley and Ali Jones performed site-directed mutagenesis of 9S-AxNgn2 to reintroduce individual SP site serines, e.g. 8S-AxNgn2S19 denotes reintroduction of SP serine 19 (all mutants are listed in the Abbreviations). ^{35}S-radiolabelled IVT proteins of xNgn2, 9S-AxNgn2 and single SP sites reintroduced into 9S-AxNgn2 were added to *Xenopus laevis* mitotic activated egg extract and incubated at 21 °C. Aliquots of the reaction were removed at increasing timepoints, quenched in SDS-LB and samples were separated by 15 % SDS-PAGE to allow measurement of protein levels over time and calculation of the half-life for degradation using first-order rate kinetics (Figure 5.11).

xNgn2 has a half-life for degradation of 30.1 +/- 2.3 mins whereas 9S-AxNgn2 exhibits a half-life of 43.6 +/- 7.2 mins (Figure 5.11, B). All phosphomutants of xNgn2 with a single SP site reintroduced are degraded at the same rate as 9S-AxNgn2, with the exception of 8S-AxNgn2S181, which has a half-life of 37.0 +/- 5.6 mins and 8S-AxNgn2S184 with a half-life of 36.7 +/- 3.9 mins (Figure 5.11, B). 8S-AxNgn2S184 is also the only mutant not significantly stabilised when half-lives are normalised to xNgn2 within each experiment (Figure 5.11, A). The trend observed in Figure 5.11, A shows a decrease in stabilisation when mutating alanines back to serines in the C-terminus, for S172, S181 and significantly S184. This data hints again at the importance of the most C-terminal SP sites as demonstrated in Figure 5.10.

Serines 181 and 184 in fact constitute a GSK3-β consensus site (Kennelly and Krebs, 1991) and Christopher Hindley and Ali Jones constructed a SP site knock-out (7S-AxNgn2) and a SP site knock-in (2S-AxNgn2) of these sites (see Figure 5.12, A for a schematic). These mutants were also subjected to degradation assays in mitotic extract. ^{35}S-radiolabelled IVT proteins of xNgn2, 9S-AxNgn2, 7S-AxNgn2 and 2S-AxNgn2 were added to *Xenopus laevis* mitotic activated egg extract and incubated at

A

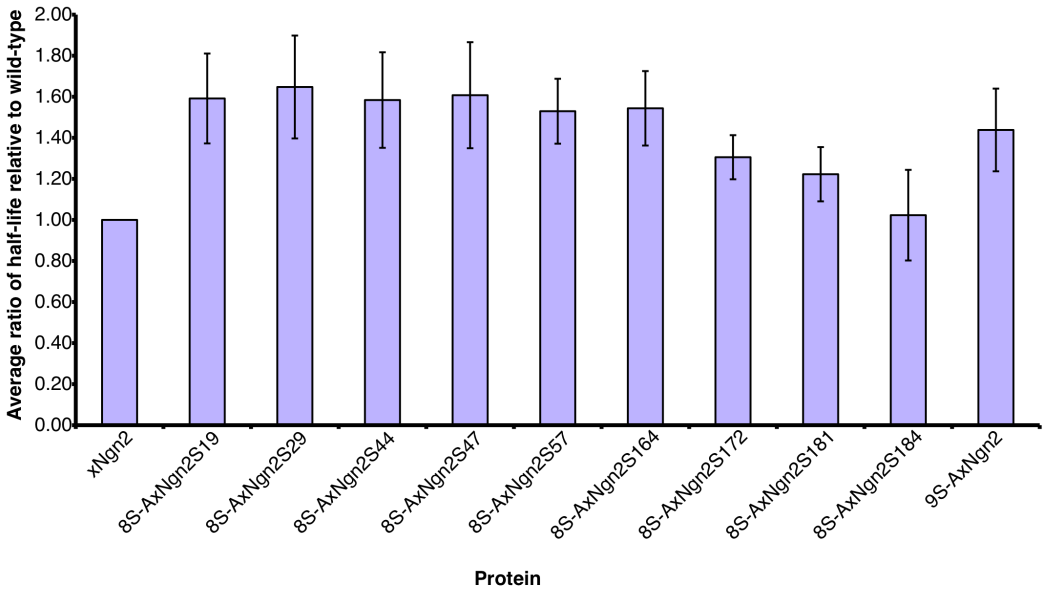

B

Sample	Half-life (mins)
xNgn2	30.1 +/- 2.3
8S-AxNgn2S19	48.4 +/- 7.8
8S-AxNgn2S29	50.4 +/- 8.7
8S-AxNgn2S44	47.4 +/- 7.5
8S-AxNgn2S47	45.8 +/- 3.5
8S-AxNgn2S57	45.1 +/- 4.4
8S-AxNgn2S164	47.7 +/- 7.9
8S-AxNgn2S172	40.3 +/- 5.6
8S-AxNgn2S181	37.0 +/- 5.6
8S-AxNgn2S184	36.7 +/- 3.9
9S-AxNgn2	43.6 +/- 7.2

Figure 5.11: Stability of single SP site knock-in mutants of xNgn2 in mitotic extract.

Xenopus laevis mitotic activated egg extracts were supplemented with ^{35}S-labelled xNgn2 or xNgn2 mutants containing single SP sites and incubated at 21 °C. Samples were taken at the timepoints indicated and subjected to 15 % SDS-PAGE. Gels were analysed by quantitative phosphorimaging analysis, calculating the average stabilisation relative to wild-type xNgn2 within mitotic extract (A). (B) Half-lives were calculated using first-order rate kinetics, and errors calculated using the Standard Error of the Mean (SEM). n= 6.

21 °C. Aliquots of the reaction were removed at increasing timepoints, quenched in SDS-LB and samples were separated by 15 % SDS-PAGE to allow measurement of protein levels over time and calculation of the half-life for degradation using first-order rate kinetics (Figure 5.12).

9S-AxNgn2 has a half-life of 26.9 +/- 2.9 mins compared to xNgn2 with a half-life of 23.2 +/- 2.8 mins (Figure 5.12, C).

7S-AxNgn2 exhibits a stability of 24.8 +/- 0.4 mins similar to wild type xNgn2. Therefore mutation of all SP serines except the GSK3-β consensus site has no effect on stability of xNgn2.

2S-AxNgn2 is in fact identical to xS-A2 (compare Figures 5.8 and 5.12, A), the half-life of which was found to be 47.4 +/- 6.4 mins (Figure 5.10, B) and 2S-AxNgn2 is degraded with a half-life of 43.5 +/- 5.8 mins (Figure 5.12, C). Therefore mutation of the GSK3-β consensus site stabilises xNgn2 significantly. This does not prove a role for GSK3-β phosphorylation of xNgn2 but highlights an important region of xNgn2 in the C-terminus with respect to phosphorylation potential.

Phosphomimetic xNgn2 is more stable than either xNgn2 or 9S-AxNgn2

Phosphorylation clearly affects xNgn2 stability and activity. Often to investigate constitutive phosphorylation effects, a 'phosphomimetic' can be made by site-directed mutagenesis of all phosphosites to aspartic or glutamic acid residues (Wang and Klemke, 2008). This approximates to the negative charge environment provided by a phosphate moiety and has been used to investigate phosphorylation of particular sites in proteins (Liang et al., 2007, Yang et al., 2007). A phosphomimetic of xNgn2 was made by Alison Jones using site-directed mutagenesis of all SP serines to glutamic acids to generate 9S-ExNgn2 (Figure 5.13, A). To assess the possible role of the phosphomimetic in stability, ^{35}S-radiolabelled IVT proteins of xNgn2, 9S-AxNgn2 and 9S-ExNgn2 were added to *Xenopus laevis* mitotic activated egg extract and incubated at 21 °C. Aliquots of the reaction were removed at increasing timepoints, quenched in SDS-LB and samples were separated by 15 % SDS-PAGE to

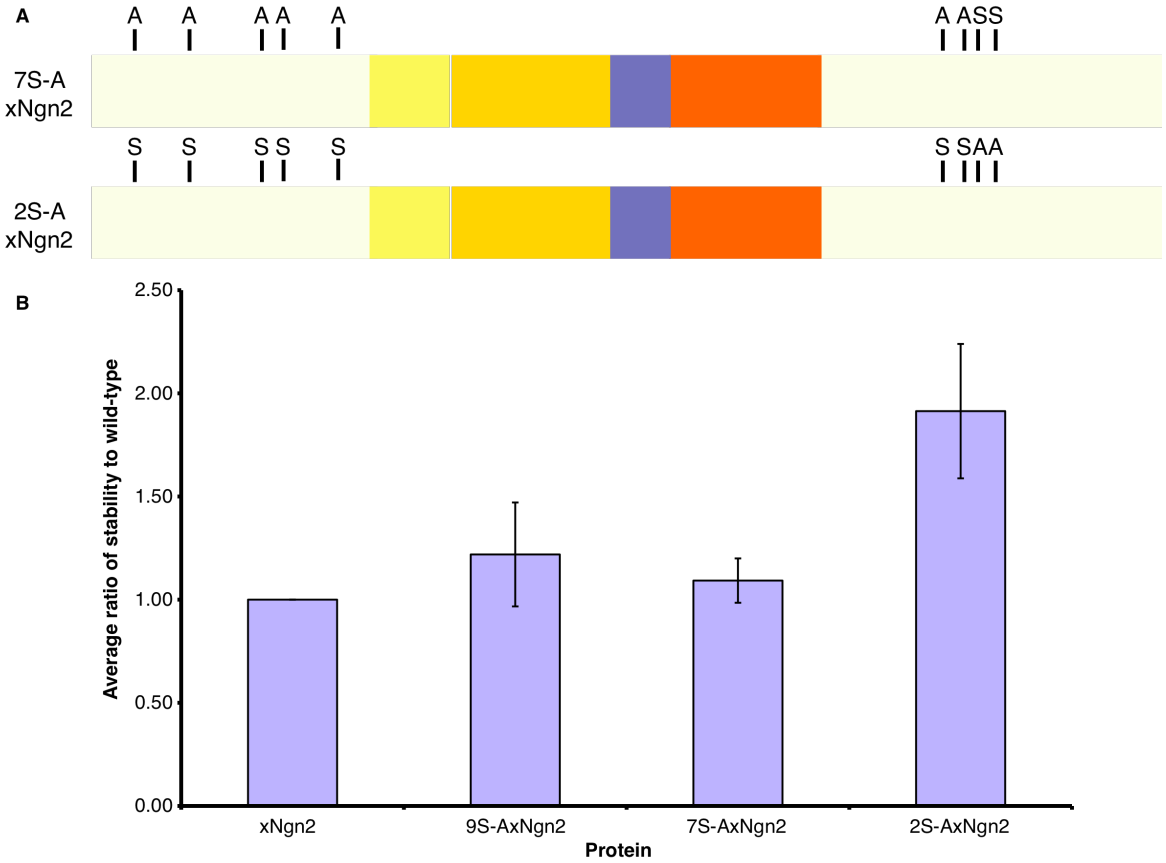

C

Sample	Half-life (mins)
xNgn2	23.2 +/- 2.8
9S-AxNgn2	26.9 +/- 2.9
7S-AxNgn2	24.8 +/- 0.4
2S-AxNgn2	43.5 +/- 5.8

Figure 5.12: GSK3-β consensus site mutant stability in *Xenopus* mitotic extract.

(A) xNgn2 mutants with only the GSK3-β consensus site present or with the GSK3-β consensus site absent were made as shown schematically. (B) *Xenopus laevis* mitotic activated egg extracts were supplemented with ^{35}S-labelled xNgn2 or xNgn2 GSK3-β site mutants and incubated at 21 °C. Samples were taken at the timepoints indicated and subjected to 15 % SDS-PAGE. Gels were analysed by quantitative phosphorimaging analysis, calculating the average stabilisation relative to wild-type xNgn2 within mitotic extract. (C) Half-lives were calculated using first-order rate kinetics, and errors calculated using the Standard Error of the Mean (SEM).

allow measurement of protein levels over time and calculation of the half-life for degradation using first-order rate kinetics (Figure 5.13).

Where xNgn2 is degraded with a half-life of 30.2 +/- 2.3 mins, and 9S-AxNgn2 with a half-life of 43.6 +/- 7.2 mins, 9S-ExNgn2 is degraded with a half-life of 53.0 +/- 4.9 mins in mitotic extract (Figure 5.13, C). Therefore the phosphomimetic is stabilised more than the wild type or phosphomutant proteins. This suggests that the phosphomimetic cannot accurately reflect the phosphorylation effects of xNgn2 as wild type xNgn2 is phosphorylated in mitotic extract and previous data (Figure 5.10) shows that blocking this phosphorylation in 9S-AxNgn2 is stabilising.

Phosphorylation affects stability in the presence of xE12

Phosphorylation of bHLH proteins, affecting their heterodimerisation with E2A gene products, has been identified in Mash1 (Vinals et al., 2004) and xE12 has been shown to stabilise xNgn2 (Vosper et al., 2007). Therefore I wished to investigate the effect of xE12 on stability of xNgn2 and 9S-AxNgn2. Using *Xenopus laevis* interphase and mitotic activated egg and neurula embryo extracts, ^{35}S-radiolabelled IVT xNgn2 or 9S-AxNgn2 were combined with an equal volume of non-radiolabelled IVT xE12 (or GFP as a control for addition of IVT protein) and incubated in extract at 21 °C. Aliquots of the reaction were removed at increasing timepoints, quenched in SDS-LB and samples were separated by 15 % SDS-PAGE to allow measurement of protein levels over time and calculation of the half-life for degradation using first-order rate kinetics (Figure 5.14).

xNgn2 is stabilised 2.5- to 3-fold by xE12 in all extracts (Figure 5.14, B). In interphase extract, xNgn2 is degraded with a half-life of 23.6 +/- 2.3 mins and in the presence of xE12, it has a half-life for degradation of 69.9 +/- 8.7 mins (Figure 5.14, C). Similarly, in interphase, 9S-AxNgn2 is degraded with a half-life of 25.4 +/- 1.0 mins and in the presence of xE12, the half-life for degradation of this protein is 70.1 +/- 23.0 mins. A similar pattern is observed in neurula extract (Figure 5.14, B and C).

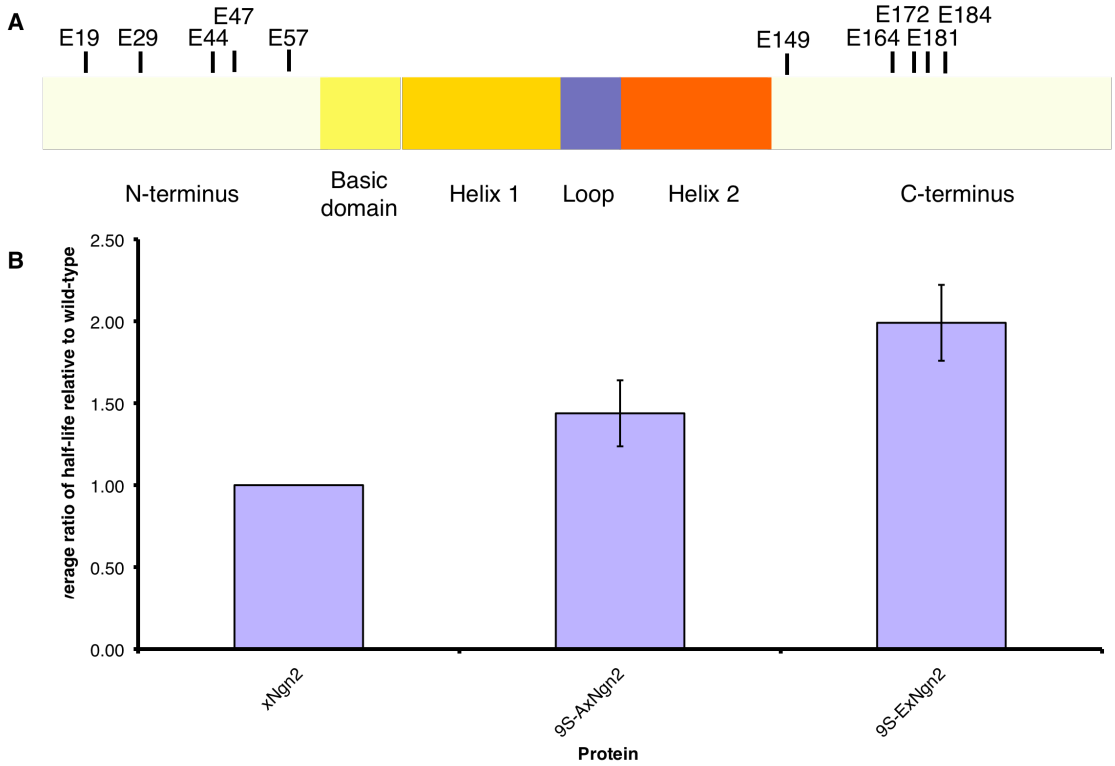

C

Sample	Half-life (mins)
xNgn2	30.2 +/- 2.3
9S-AxNgn2	43.6 +/- 7.2
9S-ExNgn2	53.0 +/- 4.9

Figure 5.13: Phosphomimetic xNgn2 stability in mitotic extract.

(A) A xNgn2 mutant with all SP serines mutated to aspartic acids was made as shown schematically. (B) *Xenopus laevis* mitotic activated egg extracts were supplemented with ^{35}S-labelled xNgn2, 9S-AxNgn2 or 9S-ExNgn2 and incubated at 21 °C. Samples were taken at the timepoints indicated and subjected to 15 % SDS-PAGE. Gels were analysed by quantitative phosphorimaging analysis, calculating the average stabilisation relative to wild-type xNgn2 within mitotic extract. (C) Half-lives were calculated using first-order rate kinetics, and errors calculated using the Standard Error of the Mean (SEM).

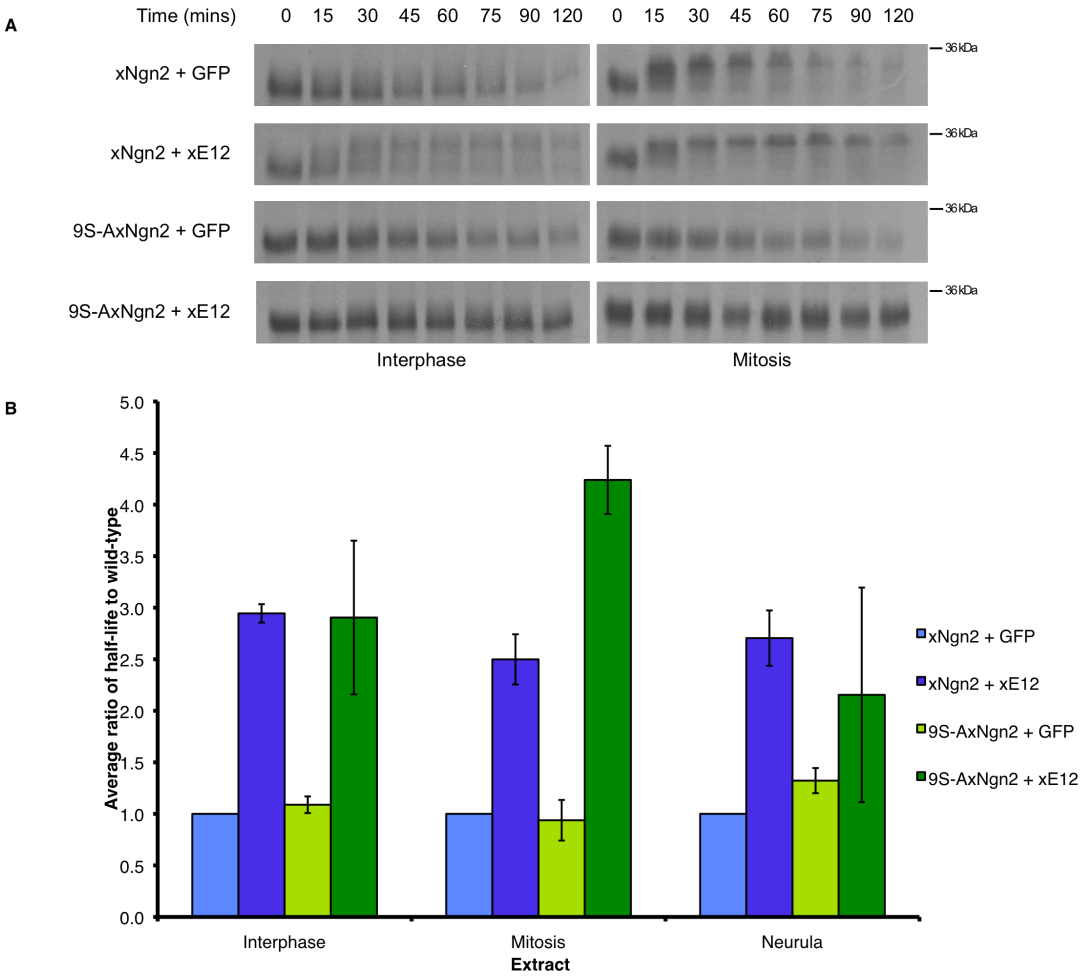

C

Sample	Interphase Half-life (mins)	Mitosis Half-life (mins)	Neurula Half-life (mins)
xNgn2 + GFP	23.6 +/- 2.3	25.1 +/- 4.3	26.5 +/- 3.3
xNgn2 + xE12	69.9 +/- 8.7	61.7 +/- 10.3	71.3 +/- 10.0
9S-AxNgn2 + GFP	25.4 +/- 1.0	22.5 +/- 1.7	34.0 +/- 2.7
9S-AxNgn2 + xE12	70.1 +/- 23.0	97.4 +/- 5.5	56.1 +/- 8.0

Figure 5.14: xNgn2 and 9S-AxNgn2 stability in *Xenopus* extracts with xE12.

Xenopus laevis interphase activated egg extracts, mitotic activated egg extracts and neurula embryo extracts were supplemented with ^{35}S-labelled xNgn2 or 9S-AxNgn2 each with either non-labelled IVT GFP or xE12 and incubated at 21 °C. Samples were taken at the timepoints indicated and subjected to 15 % SDS-PAGE. Gels were analysed by autoradiography (examples for interphase and mitotic extracts shown (A)) and quantitative phosphorimaging analysis, calculating the average stabilisation relative to wild-type xNgn2 within each extract (A). (B) Half-lives were calculated using first-order rate kinetics, and errors calculated using the Standard Error of the Mean (SEM).

However, in mitotic extract, whilst xNgn2 is stabilised 2.5-fold by xE12, 9S-AxNgn2 is stabilised 4-fold (Figure 5.14, B) and the half-life of xNgn2 in mitosis in the presence of xE12 is 61.7 +/- 10.3 mins whereas the corresponding value of 9S-AxNgn2 is 97.4 +/- 5.5 mins (Figure 5.14, C). Therefore xE12 stabilises the phosphomutant of xNgn2 more than wild type xNgn2 in mitosis. xE12 also promotes phosphorylation of xNgn2 in interphase where such phosphorylation is not usually observed, as seen by a retardation of gel-migration over time of xNgn2 in the presence of xE12, identical to the phosphorylation shift observed in mitotic extract (Figure 5.14, A).

Ubiquitylation of xNgn2 and 9S-AxNgn2 suggests a difference in xNgn2 behaviour dependent on phosphorylation

Phosphorylation would appear to be destabilising xNgn2. However it is unclear whether this destabilisation occurs at the point of ubiquitylation of xNgn2, or whether it is independent of the ubiquitylation process, for example perhaps instead assisting in unfolding xNgn2 at the proteasome. To fully assess the crosstalk between ubiquitylation and phosphorylation in xNgn2, *in vitro* and *in vivo* experiments in *Xenopus laevis* were carried out using xNgn2 mutants N-terminally fused to a single ubiquitin moiety, with a non-cleavable linker, as constructed by Alison Jones. Proteins so tagged are degraded by the ubiquitin fusion/degradation pathway (UFD) (Johnson et al., 1995). The stability of Ub-xNgn2 and Ub-9S-AxNgn2 was investigated by degradation assay in mitotic extract, where xNgn2 is maximally phosphorylated, in the presence or absence of xE12. ^{35}S-radiolabelled IVT xNgn2, 9S-AxNgn2, Ub-xNgn2 or Ub-9S-AxNgn2 were combined with an equal volume of non-radiolabelled IVT xE12, or GFP as a control for addition of IVT protein, and incubated in *Xenopus laevis* mitotic activated egg extract at 21 °C. Aliquots of the reaction were removed at increasing timepoints, quenched in SDS loading buffer and samples were separated by 15 % SDS-PAGE to allow measurement of protein levels over time and calculation of the half-life for degradation using first-order rate kinetics (Figure 5.15).

Fusion of xNgn2 to ubiquitin destabilises xNgn2 from 19.1 +/- 3.4 mins to 9.1 +/- 0.7 mins (Figure 5.15, C). Whilst 9S-AxNgn2 is stabilised by xE12 to a greater extent than xNgn2 as shown in Figure 5.14 (Figure 5.15, B), Ub-xNgn2 and Ub-9S-AxNgn2 are

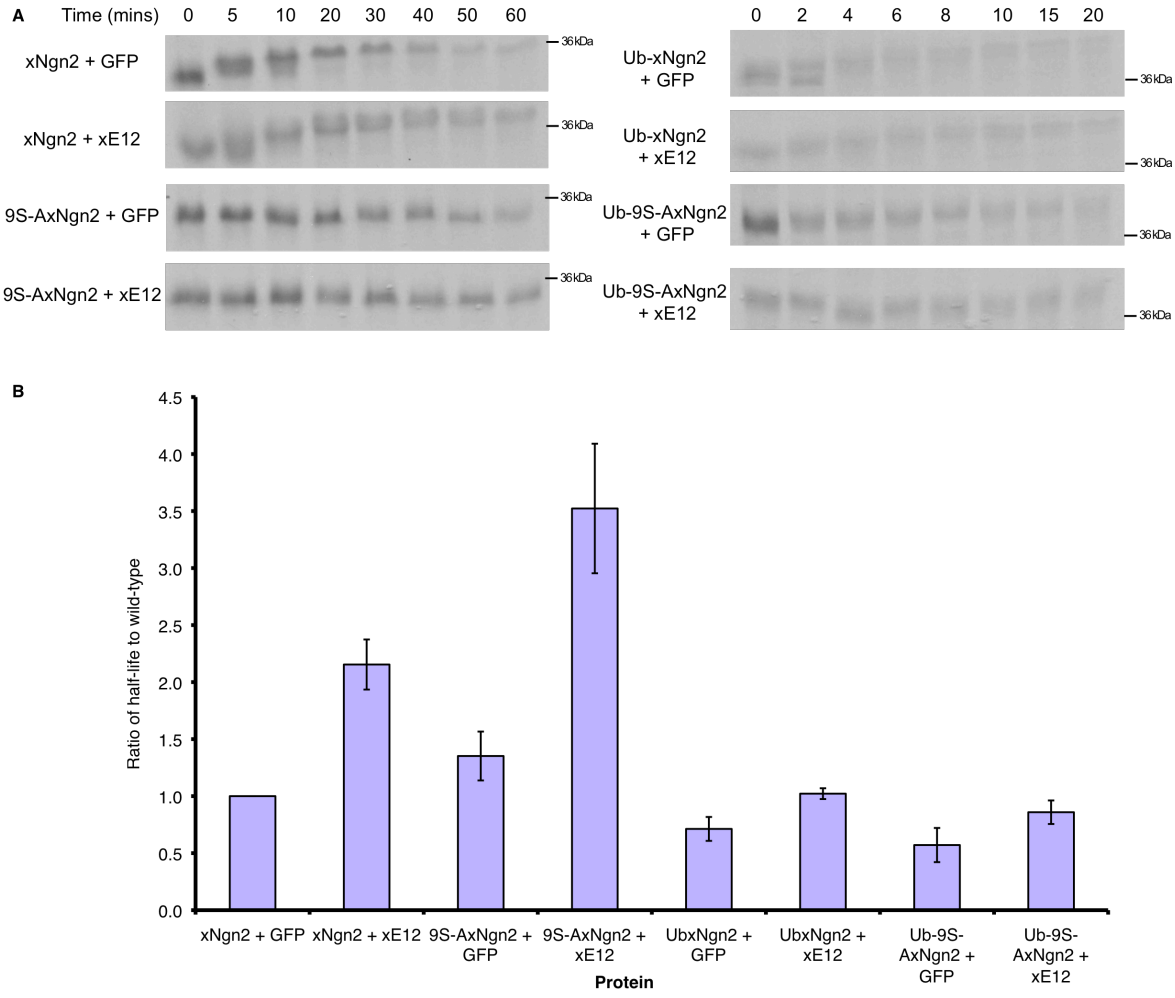

C

Sample	Half-life (mins)
xNgn2 + GFP	19.1 +/- 3.4
xNgn2 + xE12	42.6 +/- 9.8
9S-AxNgn2 + GFP	22.7 +/- 1.4
9S-AxNgn2 + xE12	67.1 +/- 13.9
Ub-xNgn2 + GFP	9.1 +/- 0.7
Ub-xNgn2 + xE12	13.3 +/- 1.2
Ub-9S-AxNgn2 + GFP	7.2 +/- 1.2
Ub-9S-AxNgn2 + xE12	11.6 +/- 2.5

Figure 5.15: Ubiquitylated xNgn2 and 9S-AxNgn2 stability in *Xenopus* mitotic extract with xE12.

Xenopus laevis mitotic activated egg extracts were supplemented with ^{35}S-labelled xNgn2, 9S-AxNgn2, Ub-xNgn2 or Ub-9S-AxNgn2 each with either non-labelled IVT GFP or xE12 and incubated at 21 °C. Samples were taken at the timepoints indicated and subjected to 15 % SDS-PAGE. Gels were analysed by autoradiography (A) and quantitative phosphorimaging analysis, calculating the average stabilisation relative to wild-type xNgn2 within each extract (B). (C) Half-lives were calculated using first-order rate kinetics, and errors calculated using the Standard Error of the Mean (SEM).

both stabilised by xE12 to a similar extent (Figure 5.15, B). The half-life of xNgn2 increases from 9.1 +/- 0.7 mins to 13.3 +/- 1.2 mins in the presence of xE12, and that of Ub-9S-AxNgn2 increases from 7.2 +/- 1.2 mins to 11.6 +/- 2.5 mins in xE12 (Figure 5.15, C). This would suggest that phosphorylation can assist with proteasomal degradation; when SP sites are absent, xE12 has a greater stabilising effect than with wild type xNgn2. However when xNgn2 is already tagged with ubiquitin, there is no difference in stabilisation whether or not SP sites are available.

There is a dramatic effect on stability *in vitro* in *Xenopus laevis* extract when xNgn2 proteins with varying phosphorylation potential are ubiquitin-tagged. I wished to investigate further *in vivo* how this stability might affect protein half-life and so 20 pg GFP, xNgn2, 9S-AxNgn2, Ub-xNgn2 and Ub-9S-AxNgn2 mRNA were injected into 1 cell of Stage 2 *Xenopus laevis* IVF embryos. mRNA was coinjected with β-galactosidase so that fixed embryos could be treated with X-gal to stain the injected side. Primary neurons were stained by *in situ* hybridisation (ISH) for neural β-tubulin and embryos scored for ectopic neurogenesis relative to the uninjected side of the embryo (Figure 5.16).

xNgn2 upregulates neurogenesis, whilst Ub-xNgn2 is completely inactive (Figure 5.16, A and B). 9S-AxNgn2 is hyperactive relative to wild type xNgn2 as has been seen previously (Hindley, 2011), however Ub-9S-AxNgn2, whilst promoting less ectopic neurogenesis than 9S-AxNgn2, is still active and to a similar extent as wild type xNgn2 (Figure 5.16, A and B). Therefore despite its instability, 9S-AxNgn2 is able to maintain a high level of activity.

xNgn2 is upstream of a cascade of bHLH transcription factors such as xNeuroD to promote neurogenesis; but it also activates Notch signalling by activating the transcription of the Delta ligand, to set up lateral inhibition, resulting in neurogenesis of primary neurons surrounded by undifferentiated neural precursors. To investigate whether phosphorylation and stability affect xNgn2 activity at the chromatin level, quantitative PCR (qPCR) analysis of these proteins was undertaken. 20 pg GFP, xNgn2, 9S-AxNgn2, Ub-xNgn2 and Ub-9S-AxNgn2 mRNA were injected into Stage 1 embryos which were lysed upon reaching stage 15. RNA was extracted and used for

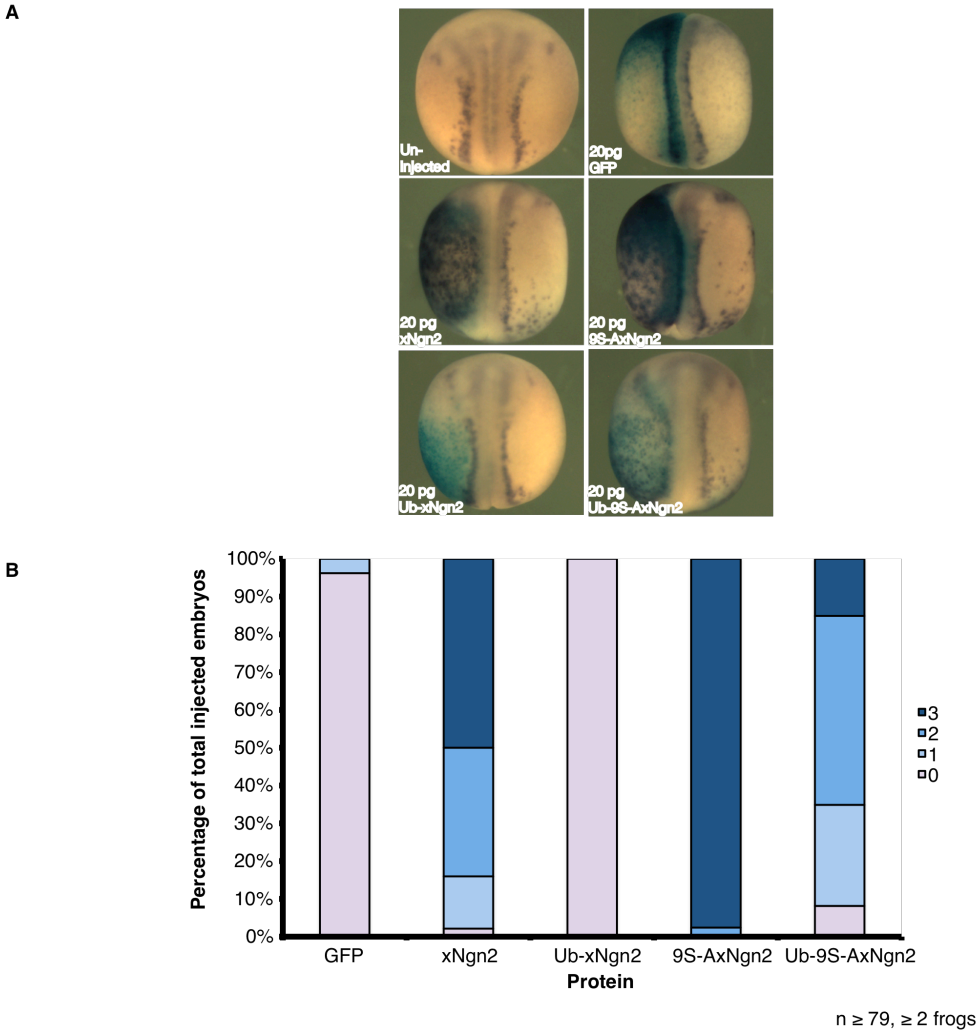

Figure 5.16: *In vivo* activity of ubiquitylated forms of xNgn2 and 9S-AxNgn2 by ISH.

(A) Xenopus embryos were injected in 1 of 2 cells with 20 pg of either xNgn2, UbxNgn2, 9S-A xNgn2 or Ub9S-AxNgn2 mRNA as well as 500 pg β-galactosidase mRNA, fixed at stage 15 and subject to in situ hybridization for neural β-tubulin expression with X-gal staining to show the injected side (n≥76) (injected side, left). (B) Embryos were scored for the extent of ectopic neurogenesis observed using the scale defined in Figure 2.3.

the synthesis of cDNA which was then used by Fahad Ali for qPCR of NeuroD and Delta transcripts using specific primers for each, as well as for a set of housekeeping genes as a control for transcript levels. The fold increase of transcript for NeuroD and Delta was then plotted (Figure 5.17, A and B respectively).

xNgn2 upregulates xNeuroD 7.4 +/- 2.8 fold but Ub-xNgn2 gives no detectable upregulation of xNeuroD (Figure 5.17, A). In contrast, 9S-AxNgn2 upregulates xNeuroD 29.3 +/- 3.5 whilst Ub-9S-AxNgn2 retains considerable activity with a NeuroD upregulation of 7.7 +/- 1.4 fold (Figure 5.17A).

Delta expression is upregulated by xNgn2 to 3.0 +/- 1.0 fold, and by 9S-AxNgn2 to 3.8 +/- 0.8 fold (Figure 5.17, B). They therefore exhibit similar activity at the Delta promoter. Ubiquitin-tagging reduces this activity for both proteins, to 1.7 +/- 0.3 fold for Ub-xNgn2 and 1.9 +/- 0.6 fold for Ub-9S-AxNgn2 (Figure 5.17, B). Therefore whilst both xNgn2 and 9S-AxNgn2 exert similar effects at the Delta promoter, activation of transcription of xNeuroD varies significantly between xNgn2 and 9S-AxNgn2, and ubiquitylation of xNgn2 can completely inactivate activation of transcription of xNeuroD whereas ubiquitylation of 9S-AxNgn2 merely reduces it. This implies differences in the ability of xNgn2 to initiate transcription at the promoters of Delta and xNeuroD.

DISCUSSION

xNgn2 contains a number of putative phosphorylation sites including serine proline motifs, which can be phosphorylated by proline-directed kinases such as cdks and GSK3-β. Mutation of all these serine proline sites to alanine prolines results in a hyperactive form of xNgn2 (Ali et al., 2011). Predicting which SP sites may be phosphorylated is not trivial (Errico et al., 2010) therefore mutating all SP sites is necessary to begin investigating proline-directed kinase phosphorylation of xNgn2. To investigate the role of these SP sites in xNgn2 stability, I began with degradation assays comparing xNgn2 and the phosphomutant 9S-AxNgn2 in *Xenopus laevis* extract systems (Figure 5.2). xNgn2 was minimally phosphorylated in interphase egg and neurula embryo extracts but maximally phosphorylated in mitotic extracts as

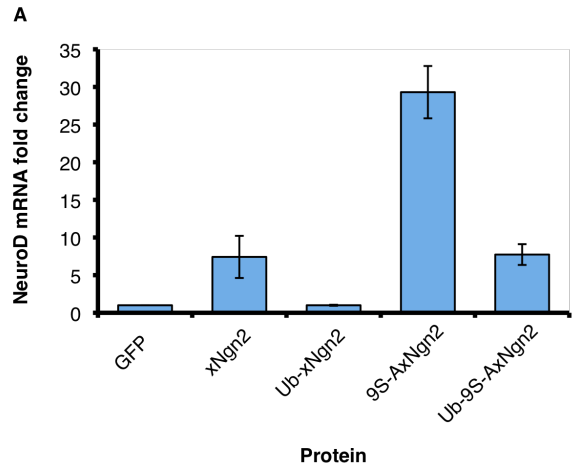

Sample	NeuroD mRNA fold change
xNgn2	7.4 +/- 2.8
Ub-xNgn2	1.0 +/- 0.1
9S-AxNgn2	29.3 +/- 3.5
Ub-9S-AxNgn2	7.7 +/- 1.4

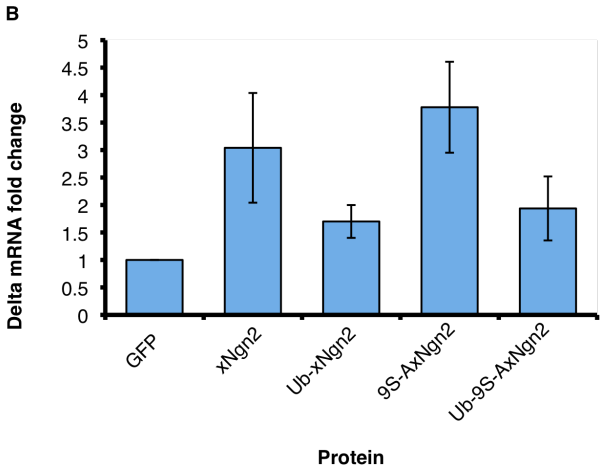

Sample	Delta mRNA fold change
xNgn2	3.0 +/- 1.0
Ub-xNgn2	1.7 +/- 0.3
9S-AxNgn2	3.8 +/- 0.8
Ub-9S-AxNgn2	1.9 +/- 0.6

Figure 5.17: *In vivo* activity of ubiquitylated forms of xNgn2 and 9S-AxNgn2 by qPCR.
qPCR analysis of NeuroD and Delta expression in Xenopus embryos. Embryos were injected at the 1 cell stage with 20 pg of either xNgn2, UbxNgn2, 9S-AxNgn2 or Ub9S-AxNgn2 mRNA and harvested at stage 15. Graphs show average fold increase in (A) NeuroD (B) Delta mRNA expression normalized to GFP.

assessed by gel migration (e.g. Figure 5.2). Loss of phosphorylation sites led to a small but significant increase in stability in mitotic extracts. There is also less 9S-AxNgn2 present to begin with in the extract due to differing translation efficiencies of xNgn2 and 9S-AxNgn2 *in vitro*.

Treatment with roscovitine (Figure 5.3) suggests that phosphorylation is indeed taking place and in a manner that can be blocked by using cyclin dependent kinase inhibitors. The major caveat in these experiments is that we are comparing the migration of bands under gel electrophoresis, which suggests a changing electrostatic environment consistent with phosphorylation, but which does not necessarily preclude either other post-translational modifications, nor the possibility that a band that is not shifted, such as 9S-AxNgn2 in Figure 5.3, is not still phosphorylated. However the roscovitine experiments in combination with the cell cycle dependence in such a shift suggests that phosphorylation is the modification that we are observing.

The differences in xNgn2 and mNgn2 stabilities observed in Figure 5.4 illustrate the caveats of comparing the two proteins, especially as the stability of a mouse protein is being assessed in a frog system. xNgn2 SP sites are distributed with 4 in the C-terminal domain and 5 in the N-terminal domain and whilst mNgn2 also has 9 SP sites, these are placed as 2 in the N-terminal domain and 7 in the C-terminal. Similar functional behaviour of mNgn2 in P19 cells has been observed (Fahad Ali, unpublished data) compared to xNgn2 in *Xenopus laevis* systems but comparison of both within the same system will yield no particularly useful information. Figure 5.4 does show that differences occur between extracts from different cell cycle and developmental phases in stability of mNgn2 protein and so suggest again cell cycle dependence of mNgn2 degradation.

The inclusion of the TP site in the analysis, such as in Figures 5.6 and 5.7, allows complete discussion of all serine and threonine sites forming a proline-directed kinase consensus site. No differences in activity have been found upon mutation of T149 to an alanine (Hindley, 2011) and this is also the case in terms of stability of xNgn2. That no visible shift in gel migration occurs in 9S-AxNgn2 corresponding to

possible phosphorylation may also suggest that TP site phosphorylation either does not occur or has no effect.

Figure 5.7 begins to highlight the importance of two obvious factors in relation to SP sites; the location of such sites, and which sites – and how many – are required to affect xNgn2 activity, and stability. Mutation of C-terminal SP sites to AP alone stabilises xNgn2 significantly (Figure 5.7) whereas mutation of the N-terminal sites does not seem to result in significant stabilisation. There is a strong C-terminal SP site dependence on the ability of xNgn2 and mNgn2 to induce neurogenesis also (Ali et al., 2011).

This point is further illustrated in degradation assays involving the mutants of xNgn2 sequentially removing SP sites starting from the C-terminus as depicted in Figure 5.8. There is no difference in stability on mutating these sites sequentially in interphase activated egg or neurula embryo extracts (Figure 5.9) but in mitotic activated egg extract (Figure 5.10) there is a very clear stabilisation of xNgn2 reaching a maximum at xS-A4, where all C-terminal SP sites are mutated to AP. This effect is presumably due to the loss of phosphorylation sites, suggesting that phosphorylation itself might destabilise xNgn2. However as the additive mutations continue, xNgn2 is destabilised again until all SP sites are lost in 9S-AxNgn2, which is only slightly more stable than xNgn2 in mitotic extract (Figure 5.10). As the two differing trends of stabilisation and destabilisation occur at opposite ends of the protein strand, this suggests that while phosphorylation on the C-terminus might destabilise xNgn2, phosphorylation on the N-terminus acts to stabilise xNgn2. Whether this is due to phosphorylation effect is uncertain. It could also be a structural effect and perhaps these serines form part of a binding region to a stabilising factor or form crucial hydrogen bonding contacts that prevent the protein from being unfolded. Under these conditions the cause cannot be determined but this striking effect perhaps hints at other factors in xNgn2 stabilisation.

Similarly reintroducing single serines at SP sites into 9S-AxNgn2 illustrates that the most C-terminal SP sites are destabilising (Figure 5.11) and that these sites also form a GSK3-β consensus site with a striking effect on xNgn2 stability as shown by

knocking in or knocking out both serines and investigating the effect on stability (Figure 5.12). Whether or not GSK3-β is the factor responsible is unclear and further work would be needed to identify if this was the case but the most C-terminal SP sites are certainly important in regulating xNgn2 stability.

The greater stability of the phosphomimetic 9S-ExNgn2, with all SP serines mutated to glutamic acids, compared to xNgn2 or 9S-AxNgn2 (Figure 5.13) is unexpected but perhaps not surprising. Whilst mutation of serines to aspartic or glutamic acid residues may appear to mimic phosphorylation in terms of the electrostatic environment produced, in reality a phosphate moiety and a carboxylate group are very different chemically. 9S-ExNgn2, if behaving as a true phosphomimetic, might be expected to have a stability similar to wild type xNgn2. However that it is more stable perhaps suggests that it may not be an appropriate phosphomimetic (discussed in (Tarrant and Cole, 2009, Dulhanty and Riordan, 1994, Germann et al., 1996, Gomez-del Arco et al., 2004, Huang and Erikson, 1994, Sun et al., 2007).

xE12 stabilises 9S-AxNgn2 more than xNgn2 only in mitosis (Figure 5.14) suggesting that SP sites and phosphorylation may regulate the structure of xNgn2 as an active heterodimer, which is interesting as it has been suggested that xE12 binding actually promotes phosphorylation of xNgn2 (Hand et al., 2005, Vosper et al., 2007). Indeed this appears to be the case as the presence of xE12 results in xNgn2 shifting in gel mobility in interphase extract (Figure 5.15, A). xE12 can no longer be observed stabilising 9S-AxNgn2 to a greater extent than it stabilises xNgn2 once Ub is fused to the N-terminus. This may suggest that ubiquitylation of xNgn2 is promoted by phosphorylation; in the absence of SP sites, xE12 can stabilise 9S-AxNgn2 to a greater extent in mitosis and 9S-AxNgn2 alone is more stable than xNgn2 in mitotic extract (Figure 5.2). However as Ub-9S-AxNgn2 is already fused to ubiquitin, presence or absence of putative phosphorylation sites no longer appears to affect stability. What is most important about the similar stabilities of Ub-xNgn2 and Ub-9S-AxNgn2 is that their *in vivo* activity as assessed by scoring of ectopic neurogenesis in ISH *Xenopus laevis* embryos injected with their mRNA is significantly different (Figure 5.16). The upregulation of neurogenesis caused by injection of xNgn2 mRNA is completely lost when Ub is fused to the N-terminus of xNgn2. When 9S-AxNgn2 is injected, this is

hyperactive and Ub-9S-AxNgn2 is less active than 9S-AxNgn2 but of a similar activity to xNgn2. Therefore stability does not apparently correlate with activity. Looking deeper into this activity by qPCR analysis of transcriptional targets of xNgn2 - xNeuroD promoting neurogenesis, and Delta setting up Notch signalling for lateral inhibition – highlights that the differing *in vivo* activity of these forms of xNgn2 lies in their ability to differentially activate transcription of different targets (Figure 5.17). xNgn2 upregulates xNeuroD and Delta expression; Ub-xNgn2 shows reduced Delta expression but no increase in xNeuroD expression compared to a GFP-injected control. 9S-AxNgn2 upregulates Delta to a similar extent as xNgn2, and Ub-9S-AxNgn2 shows a similar reduction in activating transcription of Delta as Ub-xNgn2. However, activation of transcription of xNeuroD mirrors exactly the results of the ISH experiment in Figure 5.16. 9S-AxNgn2 significantly upregulates activation of xNeuroD transcription, and whilst Ub-9S-AxNgn2 is reduced in this ability, it has a similar level of activity as wild type xNgn2 (Figure 5.17, A).

What therefore differs between the transcription of xNeuroD and Delta is the mode of interaction with the promoter region of these downstream targets of xNgn2. A schematic of a possible model is illustrated in Figure 5.18. In cycling cells where cdk levels are rising as the cell cycle progresses into mitosis, xNgn2 will be increasingly phosphorylated. This does not affect the interaction with the Delta promoter and Notch signalling, and therefore lateral inhibition, is maintained and the cell remains in a precursor state. However as the cell cycle lengthens and xNgn2 is less phosphorylated, its stability increases and occupancy of the xNeuroD promoter increases as xNgn2 is bound for longer periods of time and may be able to activate transcription at sites where assembly of transcription complexes is slower. Such differences in chromatin remodelling leading to transcriptional dynamics and varying "on/off" cycles of transcriptional complexes have been described (Hager et al., 2009) and the extent of chromatin remodelling required may affect the "speed" of the promoter, through to factors such as stalling of RNA polymerase II at the promoter during elongation (Nechaev and Adelman, 2008).

Such a mechanism ties together cell cycle dependence of xNgn2 and xNgn2 phosphomutant stability and differing *in vivo* activity. However there are still many

questions to answer regarding the phosphorylation of xNgn2; precisely which kinases are involved, which sites are modified and ultimately how phosphorylation may affect the structure of xNgn2, itself a highly disordered protein.

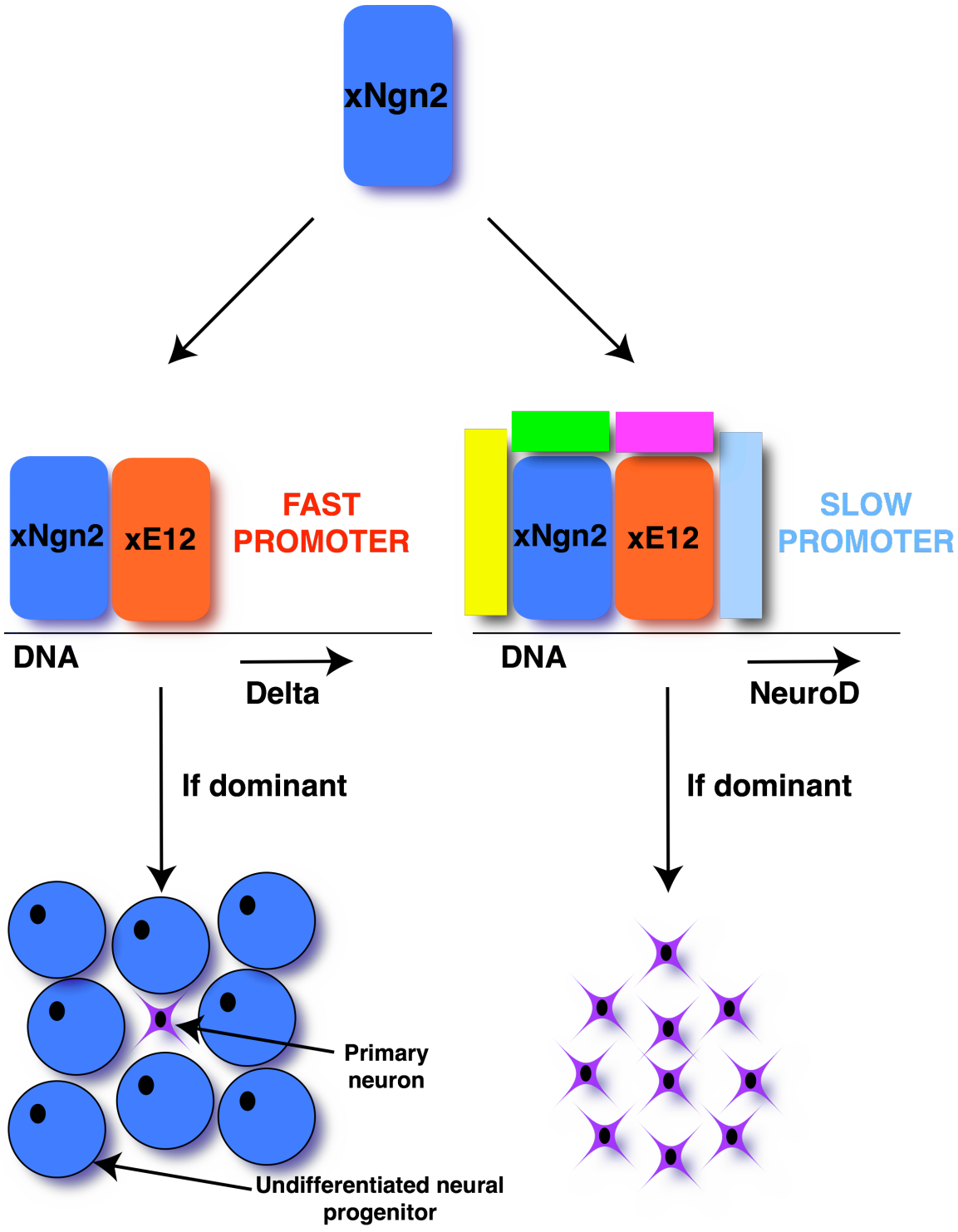

Figure 5.18: Suggested mechanism for xNgn2 using 'fast' or 'slow' promoters.
xNgn2 upregulates both Delta and xNeuroD transcription. If Delta is a 'faster' promoter – perhaps requiring a less complex assembly for activation of transcription – then Notch signalling can dominate and a primary neuron can maintain neighbouring cells in a precursor state. However, if xNeuroD at the 'slower' promoter is favoured by xNgn2 which is around longer, say by stabilisation, then xNeuroD is upregulated over Delta and lateral inhibition is lost.

CHAPTER 6

Protein Folding and xNgn2 Stability

INTRODUCTION

Protein stability can be controlled by PTMs, but the folding stability of xNgn2 itself may also be important. Proteins require unfolding to pass through the tight channel of the 26S proteasome (Prakash et al., 2004). An intrinsically disordered (ID, (Dyson and Wright, 2005b)) protein, which is highly disordered and possibly natively unfolded, can be targeted to the 26S proteasome by virtue of its unfolding alone if associated with a ubiquitylated protein (Prakash et al., 2009). Conversely, despite being ubiquitylated, if there is no unfolding initiation site close to the site of ubiquitylation, proteins cannot be degraded by the UPS (Prakash et al., 2004).

The neurogenins are disordered proteins with a highly dynamic structure even as an active complex (Aguado-Llera et al., 2010). They are rapidly ubiquitylated and degraded by the proteasome (Vosper et al., 2007) but their stability is also regulated by other factors, such as the *Xenopus* cyclin dependent kinase inhibitor (cdki) Xic1 (Vernon et al., 2003) and the heterodimeric binding partner of xNgn2, xE12 (Vosper et al., 2007).

This chapter looks at the role of structural components of xNgn2 stability, through potential binding of other factors and to DNA. The stability of xNgn2 is also compared to xNeuroD, a related protein downstream of xNgn2, which is highly ubiquitylated and yet stable (Vosper et al., 2007).

RESULTS

xNgn2 can be stabilised by tags

When originally trying to block the N-terminus of xNgn2 from ubiquitylation, bulky tags such as GFP were tested to see if they could stabilise xNgn2 in an analogous manner to other proteins (Trausch-Azar et al., 2010). Fusing GFP to the N-terminus does stabilise xNgn2 against degradation; however the control experiment fusing GFP to the C-terminus has the same effect (Vosper et al., 2009). The effect of this stabilisation cannot be due to blocking ubiquitylation form the N-terminal amino group. However, this does suggest that bulky tags can stabilise xNgn2. I have used C-terminally HA-tagged xNgn2 forms for experiments in P19 cell lines (Figures 4.16-19) and so I wished to investigate whether even a tag such as the short HA sequence (YPYDVPDYA) can have a stabilising effect on xNgn2 and mNgn2 in *Xenopus laevis* extract. ^{35}S-radiolabelled IVT xNgn2, xNgn2-HA, xNgn2-3HA, mNgn2 and mNgn2-HA were incubated in *Xenopus laevis* interphase activated egg extract at 21 °C. Aliquots of the reaction were removed at increasing timepoints, quenched in SDS-LB and samples were separated by 15 % SDS-PAGE to allow measurement of protein levels over time and calculation of the half-life for degradation using first-order rate kinetics (Figure 6.1).

xNgn2 exhibits a half-life of 25.0 +/- 0.8 mins in interphase extract (Figure 6.1, A) but addition of a single HA-tag increases that half-life for degradation to 34.5 +/- 1.9 mins. Addition of 3 tags has no greater effect than one tag as xNgn2-3HA is degraded with a half-life of 31.3 +/- 2.7 mins. mNgn2 shows no increase in stability on addition of an HA tag. mNgn2 is degraded with a half-life of 34.5 +/- 1.9 mins and mNgn2-HA is degraded with a similar half-life of 33.5 +/- 2.0 mins. Therefore xNgn2 can be stabilised slightly against degradation in interphase extract by the addition of a HA tag whereas mNgn2 cannot.

A

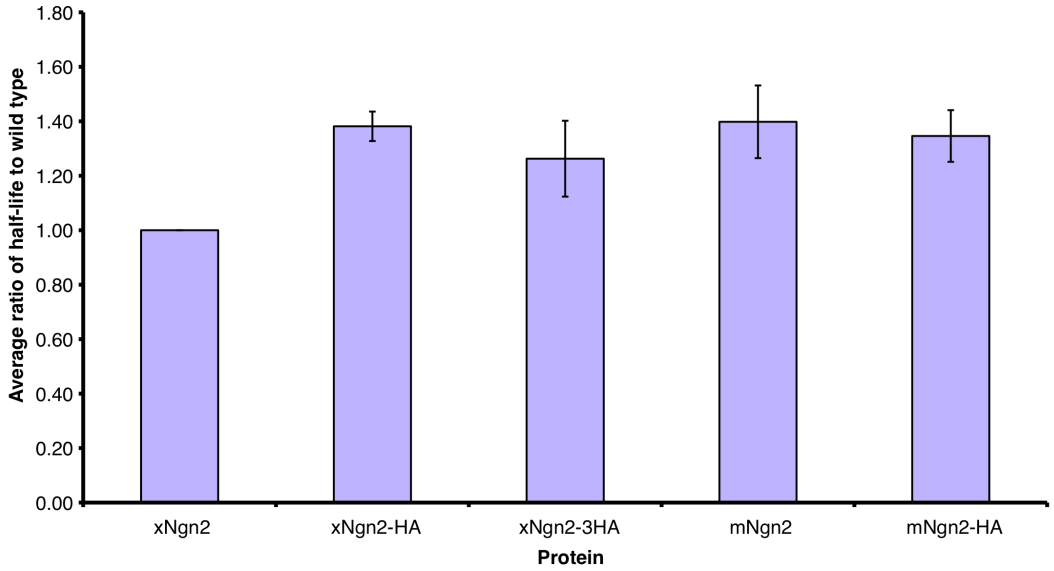

B

Sample	Half-life (mins)
xNgn2	25.0 +/- 0.8
xNgn2-HA	34.5 +/- 1.9
xNgn2-3HA	31.3 +/- 2.7
mNgn2	34.8 +/- 2.7
mNgn2-HA	33.5 +/- 2.0

Figure 6.1: C-terminal HA tags can stabilise xNgn2.

Xenopus laevis interphase activated egg extracts were supplemented with ^{35}S-labelled IVT xNgn2, mNgn2 or C-terminally HA-tagged or triply HA-tagged (3HA) forms and incubated at 21 °C. Samples were taken at 0, 15, 30, 45, 60, 75, 90 and 120 mins and subjected to 15 % SDS-PAGE. Gels were analysed by quantitative phosphorimaging analysis, calculating the average stabilisation relative to wild type xNgn2 (A). (B) Half-lives were calculated using first-order rate kinetics, and errors calculated using the Standard Error of the Mean (SEM).

p300 is unable to stabilise xNgn2

xNgn2 stability can be affected by binding of cofactors such as its heterodimeric binding partner xE12 (Figures 5.14 and 5.15). xNgn2 also associates with p300/CBP to form an active transcriptional complex (Bertrand et al., 2002). Therefore it is possible that binding to p300, like binding xE12, could affect xNgn2 stability. E1A12S protein binds to p300 (Fax et al., 2000) and inhibits its transcriptional activity (Oswald et al., 2001). Therefore I sought to investigate xNgn2 stability in extract with the functional N-terminal domain p300N, and the p300 inhibitor E1A12S. ^{35}S-radiolabelled IVT xNgn2 was incubated in *Xenopus laevis* interphase activated egg and neurula embryo extract with IVT non-radiolabelled p300N, E1A12S, or both (with GFP as a control) at 21 °C. Aliquots of the reaction were removed at increasing timepoints, quenched in SDS-LB and samples were separated by 15 % SDS-PAGE to allow measurement of protein levels over time and calculation of the half-life for degradation using first-order rate kinetics (Figure 6.2).

In interphase, xNgn2 is degraded with a half-life of 23.6 +/- 2.3 mins and addition of p300N and/or E1A12S has no effect on the stability of xNgn2 (Figure 6.2, A and C). In neurula extract, xNgn2 is degraded with a half-life of 27.4 +/- 4.5 mins. Addition of p300N has no effect on the stability as xNgn2 is degraded with a half-life of 31.4 +/- 4.5 mins on the addition of p300N. However E1A12S significantly stabilises xNgn2 to a half-life of 38.9 +/- 2.3 mins, but on addition of both p300N and E1A12S xNgn2 stability is returned to normal levels with a half-life of 25.7 +/- 0.3 mins (Figure 6.2, B and C).

Therefore any possible effect on xNgn2 stability of p300 is unclear. Preliminary results for xNeuroD in interphase (Figure 6.2C) further complicate the role of p300, as on addition of p300N, xNeuroD increases in stability from degrading with a half-life of 154 mins to 198 mins, which drops to 100 mins in E1A12S alone, and returns to near-wild type levels in the presence of both p300N and E1A12S to 138 mins. The role of p300 in bHLH protein stabilisation is therefore unclear.

A

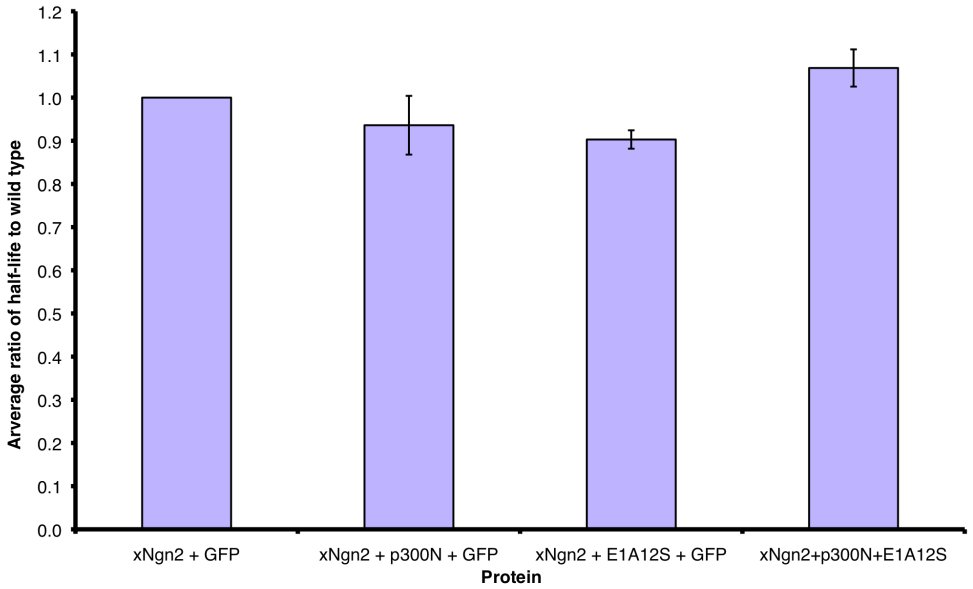

B

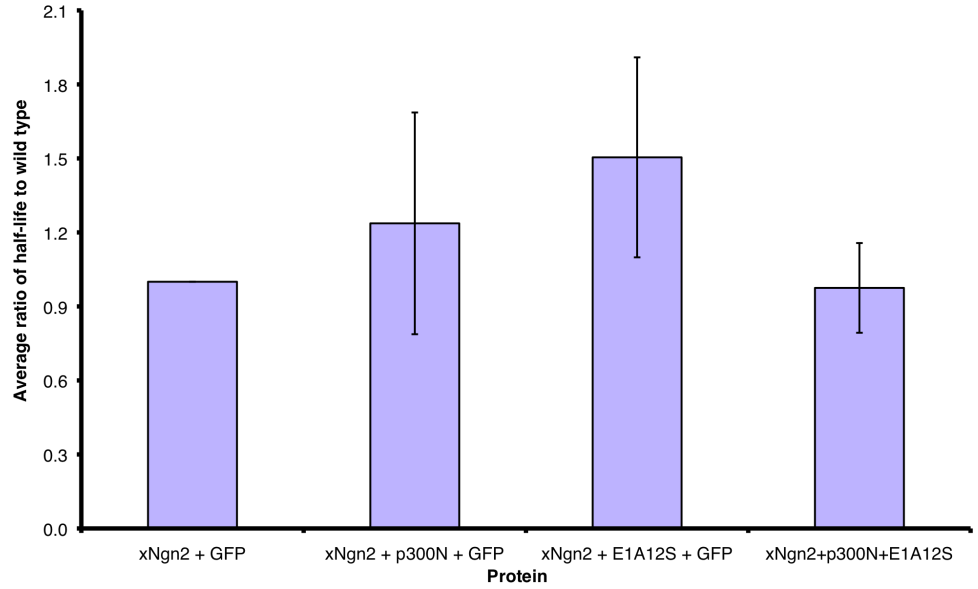

C

Sample	Interphase Half-life (mins)	Neurula Half-life (mins)
xNgn2 + GFP	23.6 +/- 2.3	27.4 +/- 4.5
xNgn2 + p300N + GFP	22.3 +/- 3.5	31.4 +/- 4.5
xNgn2 + E1A12S + GFP	21.4 +/- 2.4	38.9 +/- 2.3
xNgn2 + p300N + E1A12S	25.4 +/- 3.0	25.7 +/- 0.3

Sample	Interphase Half-life (mins)
xNeuroD + GFP	154
xNeuroD + p300N + GFP	198
xNeuroD + E1A12S + GFP	100
xNeuroD + p300N + E1A12S	138

Figure 6.2: xNgn2 stability in the presence of the transcriptional coactivator p300.

Xenopus laevis interphase activated egg extracts and neurula embryo extracts were supplemented with ^{35}S-labelled xNgn2 and non-radiolabelled IVT p300N and/or E1A12S and incubated at 21 °C. Samples were taken at 0, 15, 30, 45, 60, 90 and 120 mins and subjected to 15 % SDS-PAGE. Gels were analysed by quantitative phosphorimaging analysis, calculating the average stabilisation relative to wild type xNgn2 in interphase (A) and neurula (B) extracts. (C) Half-lives were calculated using first-order rate kinetics, and errors calculated using the Standard Error of the Mean (SEM). Experiments in neurula extract were carried out in duplicate. Preliminary experiments using xNeuroD carried out only once in interphase extract are also shown.

xNgn2 stabilisation with the cdki Xic1

The *Xenopus* cdki Xic1 has a stabilising effect on xNgn2 (Vernon et al., 2003, Roark, 2010). The mechanism of this stabilisation is thought to be through binding to xNgn2, rather than by its activity as an inhibitor of cdks (Roark, 2010). ^{35}S-radiolabelled IVT xNgn2 was incubated in *Xenopus laevis* interphase activated egg extracts with Xic1 (MBP-tagged, purified by Ryan Roark) or MBP alone as a control at 21 °C. Aliquots of the reaction were removed at increasing timepoints, quenched in SDS-LB and samples were separated by 15 % SDS-PAGE to allow measurement of protein levels over time and calculation of the half-life for degradation using first-order rate kinetics (Figure 6.3).

xNgn2 alone is degraded in interphase extract with a half-life of 20.1 +/- 2.1 mins. On addition of MBP this half-life increases to 27.5 +/- 2.0 mins – this is most likely due to dilution effects by adding MBP protein in solution, and is consistent with values found by Ryan Roark (Roark, 2010). On addition of Xic1, xNgn2 is degraded with a half-life of 42.6 +/- 1.8 mins (Figure 6.3, B). Therefore Xic1 does stabilise xNgn2 against proteasomal degradation.

This stabilising effect of Xic1 on xNgn2 has been investigated (Roark, 2010) but I wished to assess whether (like xE12) Xic1 was able to prevent ubiquitylated xNgn2, Ub-xNgn2, from being degraded. This form of xNgn2 with a single Ub fused linearly to the N-terminus acts as a pre-ubiquitylated priming site bypassing the first ubiquitylation event and allowing rapid degradation of xNgn2 (Figure 5.15). ^{35}S-radiolabelled IVT xNgn2 or Ub-xNgn2 were incubated in *Xenopus laevis* interphase activated egg extracts with Xic1 (MBP-tagged, purified by Ryan Roark) or MBP alone as a control at 21 °C. Aliquots of the reaction were removed at increasing timepoints, quenched in SDS-LB and samples were separated by 15 % SDS-PAGE to allow measurement of protein levels over time and calculation of the half-life for degradation using first-order rate kinetics (Figure 6.4).

xNgn2 in MBP is degraded with a half-life of 27.4 +/- 2.1 mins but after the addition of Xic1 the half-life increases to 37.9 +/- 5.8 mins (Figure 6.4, C). Therefore Xic1 is able

A

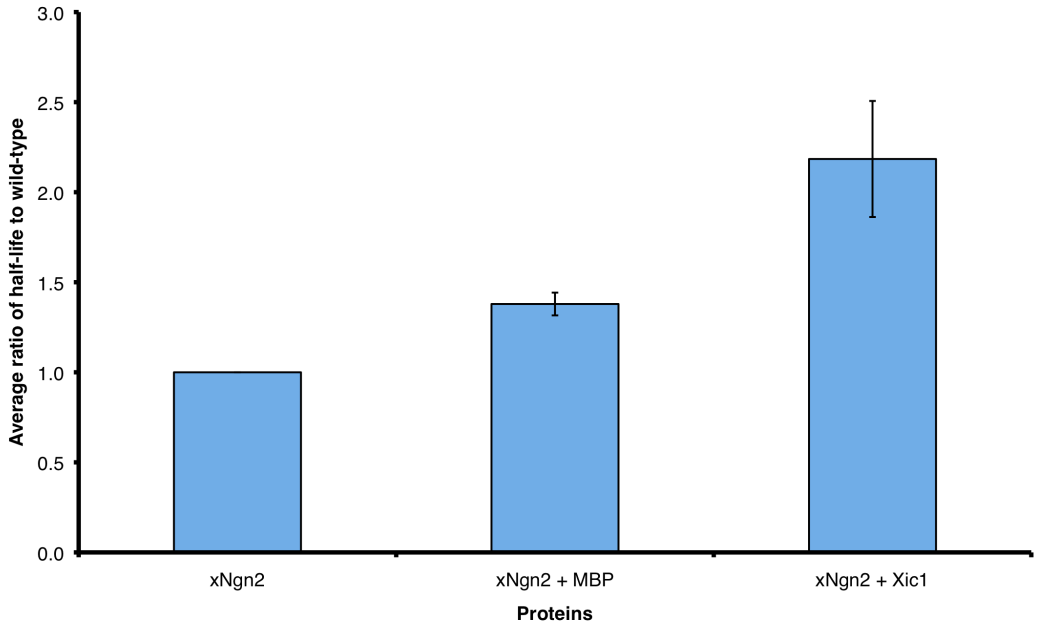

B

Sample	Half-life (mins)
xNgn2	20.1 +/- 2.1
xNgn2 + MBP	27.5 +/- 2.0
xNgn2 + Xic1	42.6 +/- 1.8

Figure 6.3: xNgn2 stability with the *Xenopus* cyclin dependent kinase inhibitor Xic1.
Xenopus laevis interphase activated egg extracts were supplemented with ^{35}S-labelled IVT xNgn2 and either maltose binding protein (MBP) or *Xenopus* cyclin dependent kinase inhibitor Xic1 protein and incubated at 21 °C. Samples were taken at 0, 5, 10, 20, 30, 40, 50 and 60 mins and subjected to 15 % SDS-PAGE. Gels were analysed by quantitative phosphorimaging analysis, calculating the average stabilisation relative to wild type xNgn2 (A). (B) Half-lives were calculated using first-order rate kinetics, and errors calculated using the Standard Error of the Mean (SEM).

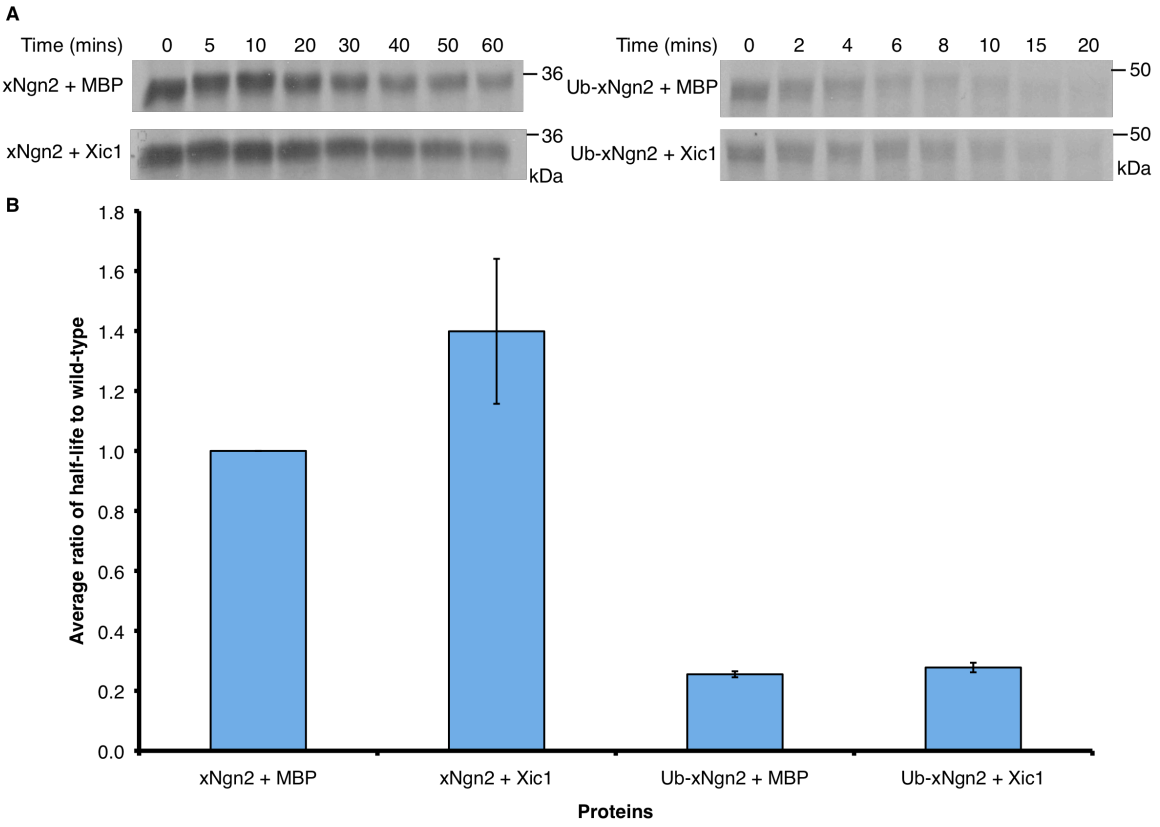

C

Sample	Half-life (mins)
xNgn2 + MBP	27.4 +/- 2.1
xNgn2 + Xic1	37.9 +/- 5.8
Ub-xNgn2 + MBP	7.0 +/- 0.4
Ub-xNgn2 + Xic1	7.6 +/- 0.8

Figure 6.4: Ubiquitylated xNgn2 stability with the *Xenopus* cyclin dependent kinase inhibitor Xic1 in interphase.

Xenopus laevis interphase activated egg extracts were supplemented with ^{35}S-labelled IVT xNgn2 or Ub-xNgn2 and either maltose binding protein (MBP) or *Xenopus* cyclin dependent kinase inhibitor Xic1 protein and incubated at 21 °C. Samples were taken at the timepoints indicated and subjected to 15 % SDS-PAGE. Gels were analysed by autoradiography (A) and quantitative phosphorimaging analysis, calculating the average stabilisation relative to wild type xNgn2 (B). (C) Half-lives were calculated using first-order rate kinetics, and errors calculated using the Standard Error of the Mean (SEM).

to stabilise xNgn2 in interphase extract. Ub-xNgn2 with MBP only is degraded with a half-life of 7.0 +/- 0.4 mins and similarly upon addition of Xic1 Ub-xNgn2 is degraded with a half-life of 7.6 +/- 0.8 mins (Figure 6.4, C). Therefore Xic1 is unable to stabilise ubiquitylated xNgn2 in interphase extract.

Phosphorylation affects xNgn2 stability, most notably in mitosis (see Chapter 5). Therefore to see if Xic1 regulates the stability of phosphorylated xNgn2, the experiments in Figure 6.4 were repeated in mitotic extract. ^{35}S-radiolabelled IVT xNgn2 or Ub-xNgn2 were incubated in *Xenopus laevis* mitotic activated egg extracts with Xic1 (MBP-tagged, purified by Ryan Roark) or MBP alone as a control at 21 °C. Aliquots of the reaction were removed at increasing timepoints, quenched in SDS-LB and samples were separated by 15 % SDS-PAGE to allow measurement of protein levels over time and calculation of the half-life for degradation using first-order rate kinetics (Figure 6.5).

Contrary to the results in Figure 6.4, xNgn2 is not stabilised by Xic1 in mitosis – with MBP alone it is degraded with a half-life of 15.0 +/- 0.9 mins and with Xic1 the half-life remains at 14.7 +/- 1.8 mins (Figure 6.5, C). Ub-xNgn2 is degraded with a half-life of 7.5 +/- 1.9 mins in MBP alone but with Xic1 the half-life is increased beyond wild type xNgn2 to 21.6 +/- 2.5 mins (Figure 6.5, C). Therefore Xic1 does not stabilise xNgn2 in mitosis but does stabilise ubiquitylated xNgn2.

xNgn2 stability in DNA-binding

xNgn2 binds xE12 as a heterodimer and binds to the E-box DNA consensus site of promoter regions of target genes (Bertrand et al., 2002). Therefore it is possible that DNA-binding itself may have a role in affecting xNgn2 stability. Ali Jones created a site-directed mutant of xNgn2 with arginine 82 mutated to alanine and arginine 83 mutated to glutamine – from RR to AQ - which should be unable to bind to DNA in analogy to similar mutants in Ngn1 (Gowan et al., 2001, Sun et al., 2001) and Mash1 (Nakada et al., 2004). I investigated the stability of this mutant in interphase, mitotic and neurula extracts. ^{35}S-radiolabelled IVT xNgn2 or xNgn2AQ were incubated in *Xenopus laevis* interphase and mitotic activated egg and neurula embryo extracts at

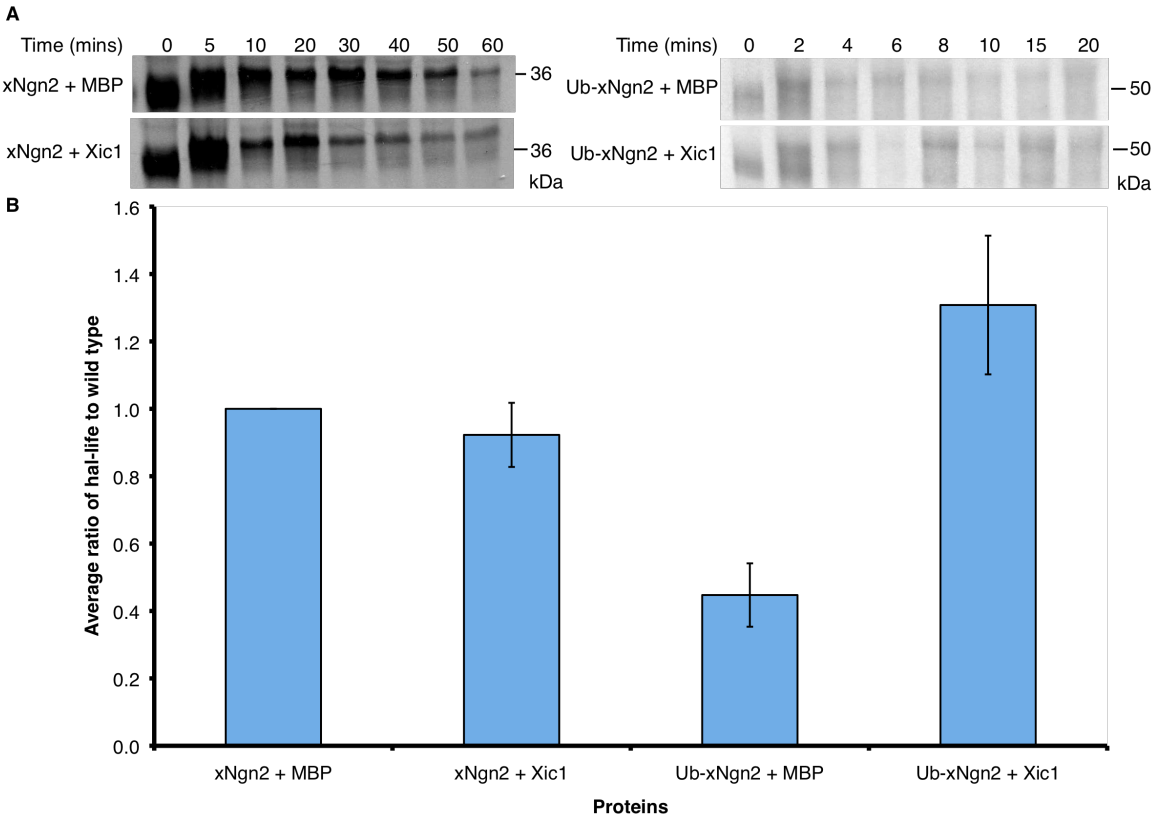

C

Sample	Half-life (mins)
xNgn2 + MBP	15.9 +/- 0.9
xNgn2 + Xic1	14.7 +/- 1.8
Ub-xNgn2 + MBP	7.5 +/- 1.9
Ub-xNgn2 + Xic1	21.6 +/- 2.5

Figure 6.5: Ubiquitylated xNgn2 stability with the *Xenopus* cyclin dependent kinase inhibitor Xic1 in mitosis.

Xenopus laevis mitotic activated egg extracts were supplemented with ^{35}S-labelled IVT xNgn2 or Ub-xNgn2 and either maltose binding protein (MBP) or *Xenopus* cyclin dependent kinase inhibitor Xic1 protein and incubated at 21 °C. Samples were taken at the timepoints indicated and subjected to 15 % SDS-PAGE. Gels were analysed by autoradiography (A) and quantitative phosphorimaging analysis, calculating the average stabilisation relative to wild type xNgn2 (B). (C) Half-lives were calculated using first-order rate kinetics, and errors calculated using the Standard Error of the Mean (SEM). Experiments were carried out in duplicate.

21 °C. Aliquots of the reaction were removed at increasing timepoints, quenched in SDS-LB and samples were separated by 15 % SDS-PAGE to allow measurement of protein levels over time and calculation of the half-life for degradation using first-order rate kinetics (Figure 6.6).

xNgn2 and xNgn2AQ exhibit identical half-lives for degradation in interphase (30.3 +/- 2.2 mins and 30.6 +/- 1.7 mins respectively) and mitotic (23.2 +/- 2.8 mins and 22.8 +/- 3.1 mins respectively) extracts (Figure 6.6, B). However in neurula extract xNgn2 is degraded with a half-life of 36.9 +/- 1.8 mins whilst xNgn2AQ is degraded with a half-life of 60.4 +/- 3.1 mins (Figure 6.6, B).

Therefore xNgn2AQ differs in stability from xNgn2 only in neurula extract where it is more stable. Interphase and mitotic extracts, being derived from single eggs, have a relatively low DNA content. However neurula embryo extracts contain many more cells within the same volume and so have a much higher DNA content. xNgn2AQ is more stable than the wild type protein in the presence of DNA.

mNgn2 and mNgn2AQ have also been investigated and it was observed that mNgn2AQ had a larger early shift in gel migration possibly corresponding to more extensive phosphorylation in P19 cells (Fahad Ali, unpublished data). Therefore to see if the same effect would be observed with xNgn2 and xNgn2AQ in *Xenopus* extract, ^{35}S-radiolabelled IVT xNgn2 or xNgn2AQ were incubated in *Xenopus laevis* mitotic activated egg extracts including the proteasome inhibitor MG132 at 21 °C. Aliquots of the reaction were removed at increasing timepoints, quenched in SDS-LB and samples were separated by 15 % SDS-PAGE to allow assessment of phosphorylation over time by autoradiography (Figure 6.6, C).

xNgn2 and xNgn2AQ both appear to undergo a shift in gel migration very quickly and to an identical extent in *Xenopus laevis* mitotic egg extract (Figure 6.6, C) and so the difference that appears in P19 cells with mNgn2 does not appear to be the case in xNgn2 in *Xenopus* extract.

A

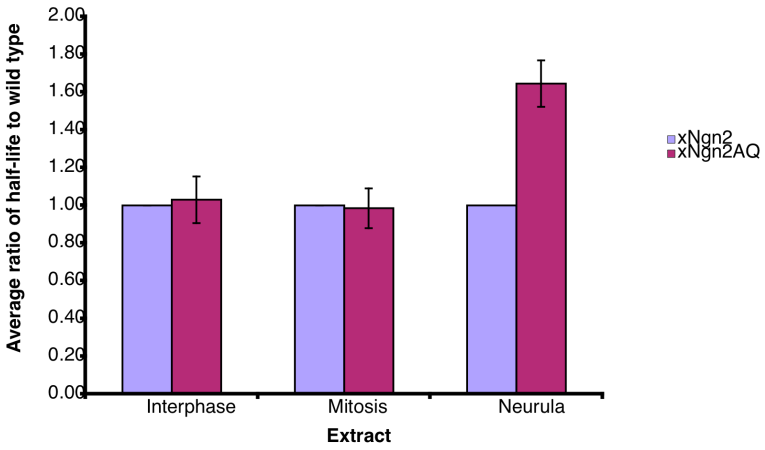

B

Extract	xNgn2 half-life (mins)	xNgn2AQ half-life (mins)
Interphase	30.3 +/- 2.2	30.6 +/- 1.7
Mitosis	23.2 +/- 2.8	22.8 +/- 3.1
Neurula	36.9 +/- 1.8	60.4 +/- 3.1

C

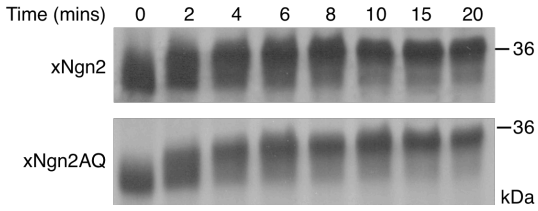

Figure 6.6: Stability and phosphorylation state of xNgn2 DNA-binding mutant, xNgn2AQ.
Xenopus laevis interphase and mitotic activated egg and neurula embryo extracts were supplemented with ^{35}S-labelled IVT xNgn2 or xNgn2AQ and incubated at 21 °C. Samples were taken at 0, 5, 10, 20, 30, 40, 50 and 60 mins and subjected to 15 % SDS-PAGE. Gels were analysed by quantitative phosphorimaging analysis, calculating the average stabilisation relative to wild-type xNgn2 within each extract (A). (B) Half-lives were calculated using first-order rate kinetics, and errors calculated using the Standard Error of the Mean (SEM). (C) ^{35}S-labelled IVT xNgn2 or xNgn2AQ were incubated in mitotic activated egg extract with MG132 at 21 °C. Samples were taken at the timepoints indicated and subjected to 15 % SDS-PAGE.

The difference in xNgn2 and xNgn2AQ stability in neurula embryo extract alone is not surprising, as this extract contains the same cytoplasmic volume per unit as egg extracts, but a much higher DNA content as cells are dividing but not yet growing in the early *Xenopus* embryo (Sive et al., 2000). To see if any further effect on stability occurs in the presence of a stabilising factor such as xE12, the heterodimeric binding partner in the DNA-bound xNgn2 complex, degradation assays were carried out in neurula extract. ^{35}S-radiolabelled IVT xNgn2 or xNgn2AQ were incubated in *Xenopus laevis* neurula embryo extracts with IVT non-radiolabelled xE12, or GFP as a protein control, at 21 °C. Aliquots of the reaction were removed at increasing timepoints, quenched in SDS-LB and samples were separated by 15 % SDS-PAGE to allow measurement of protein levels over time and calculation of the half-life for degradation using first-order rate kinetics (Figure 6.7).

In neurula extract there appears to be no difference in stability between xNgn2 and xNgn2AQ, xNgn2 being degraded with a half-life of 47.2 +/- 8.6 mins and xNgn2AQ being degraded with a half-life of 37.5 +/- 2.5 mins (Figure 6.7, C). However whilst xNgn2 is stabilised 2-fold by xE12 to 77.7 +/- 11.0 mins, xNgn2AQ is stabilised 3-fold to 118 +/- 39 mins in xE12 (Figure 6.7, B and C). Therefore xNgn2AQ can be stabilised by xE12 in neurula extract and to a greater extent than wild type xNgn2.

xNgn2 stability and unfolding

To investigate structural aspects of xNgn2 degradation it would be useful to dissect out the two components of degradation, protein ubiquitylation and protein unfolding. To this end I attempted to combine the form of xNgn2 with a single Ub linearly fused to the N-terminus, Ub-xNgn2, using extract increasingly diluted with XB for degradation assays. Diluting the extract would hopefully reduce molecular crowding, viscosity and proteasome concentration within the sample. This could limit the proteasome concentration and so reduce the stability of xNgn2 to a function of its rate of folding or unfolding, independent of ubiquitylation rates. ^{35}S-radiolabelled IVT xNgn2 or Ub-xNgn2 were incubated in *Xenopus laevis* interphase activated egg extracts diluted with XB buffer to give 90, 75, 50 and 25 % extracts by volume at 21 °C. Aliquots of the reaction were removed at increasing timepoints, quenched in SDS-

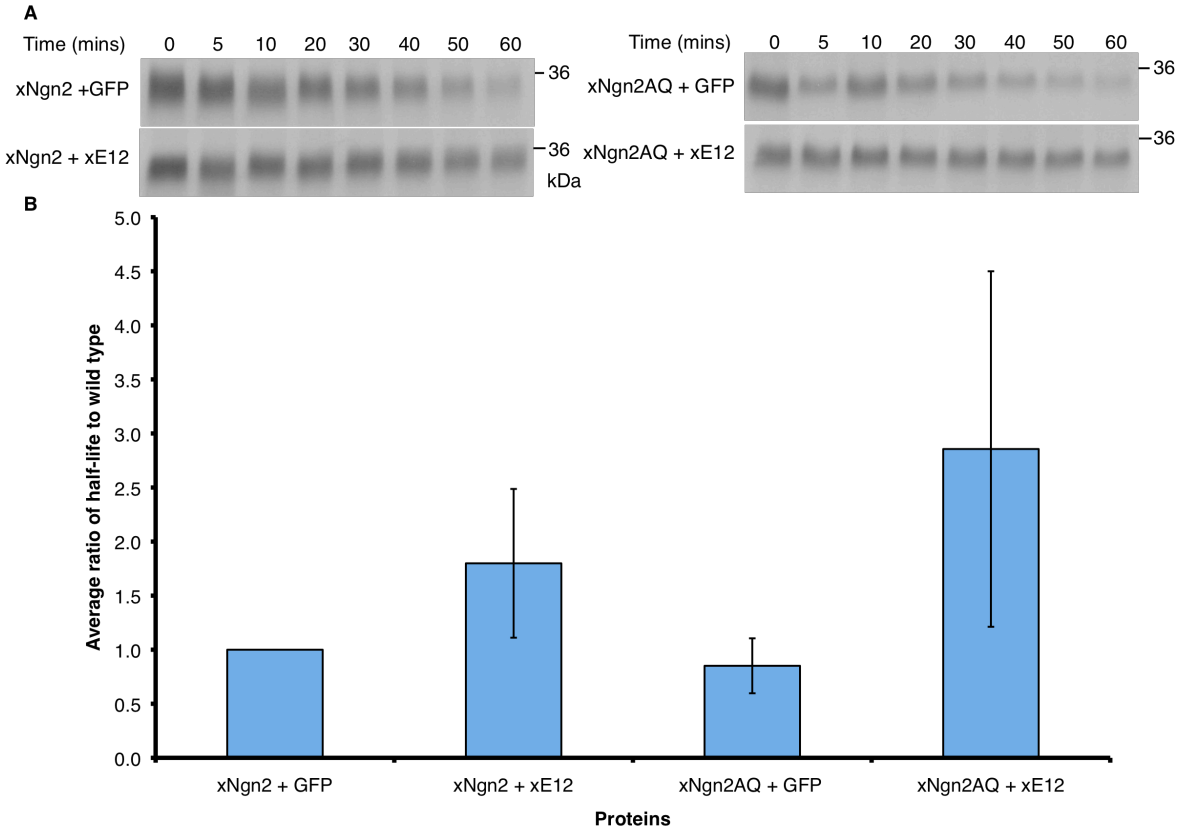

C

Sample	Half-life (mins)
xNgn2 + GFP	47.2 +/- 8.6
xNgn2 + xE12	77.7 +/- 11.0
xNgn2AQ + GFP	37.5 +/- 2.5
xNgn2AQ + xE12	118 +/- 39

Figure 6.7: Stability of xNgn2 DNA-binding mutant, xNgn2AQ, with xE12 in neurula extract. *Xenopus laevis* interphase and mitotic activated egg and neurula embryo extracts were supplemented with ^{35}S-labelled IVT xNgn2 or xNgn2AQ and incubated at 21 °C. Samples were taken at the timepoints indicated and subjected to 15 % SDS-PAGE. Gels were analysed by autoradiography (A) and quantitative phosphorimaging analysis, calculating the average stabilisation relative to wild-type xNgn2 (B). (C) Half-lives were calculated using first-order rate kinetics, and errors calculated using the Standard Error of the Mean (SEM). Experiments were carried out in duplicate.

LB and samples were separated by 15 % SDS-PAGE to allow measurement of protein levels over time and calculation of the half-life for degradation using first-order rate kinetics (Figure 6.8).

The results in Figure 6.8 show that dilution of extract to slow folding does not even appear to work for wild type xNgn2 as across 100, 90, 75, 50 and 25 % extracts by volume all half-lives are within error. 75 % and 25 % extracts demonstrate half-lives for degradation of Ub-xNgn2 of 16.0 +/- 5.5 mins and 12.4 +/- 1.8 mins respectively, but 50 % extract exhibits a half-life for Ub-xNgn2 degradation of 6.7 +/- 0.5 mins. Therefore unfolding of xNgn2 in stability cannot be experimentally investigated simply by using diluted *Xenopus* extract.

xNgn2 and xNeuroD domain swapping

xNgn2 and xNeuroD are both closely related bHLH proteins with a consensus bHLH motif providing the region of greatest homology (Bertrand et al., 2002). xNgn2 activates the transcription of xNeuroD (Ma et al., 1996, Seo et al., 2007) which itself activates the transcription of a cascade of bHLH transcription factors (Seo et al., 2007) resulting in cell cycle exit and differentiation of a neural precursor into a neuron. Despite their structural similarity xNeuroD is stable compared to xNgn2 whilst also being highly ubiquitylated in *Xenopus* interphase extract (Vosper, 2008, Vosper et al., 2007).

I decided to assay whether xNeuroD, like xNgn2, might be less stable in mitosis. ^{35}S-radiolabelled IVT xNgn2 or xNeuroD were incubated in *Xenopus laevis* interphase and mitotic activated egg extracts at 21 °C. Aliquots of the reaction were removed at increasing timepoints, quenched in SDS-LB and samples were separated by 15 % SDS-PAGE to allow measurement of protein levels over time and calculation of the half-life for degradation using first-order rate kinetics (Figure 6.9).

A

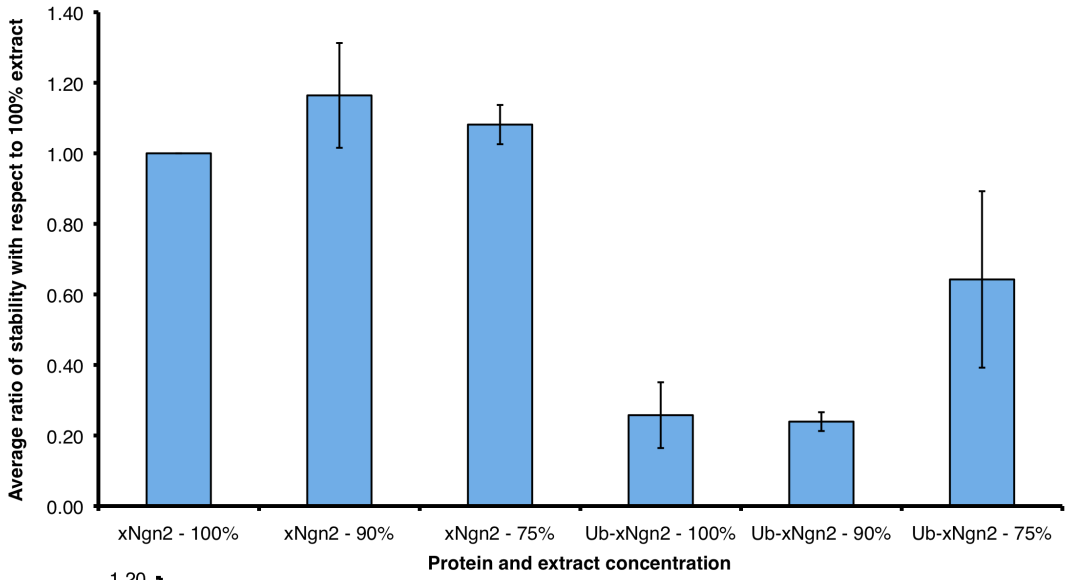

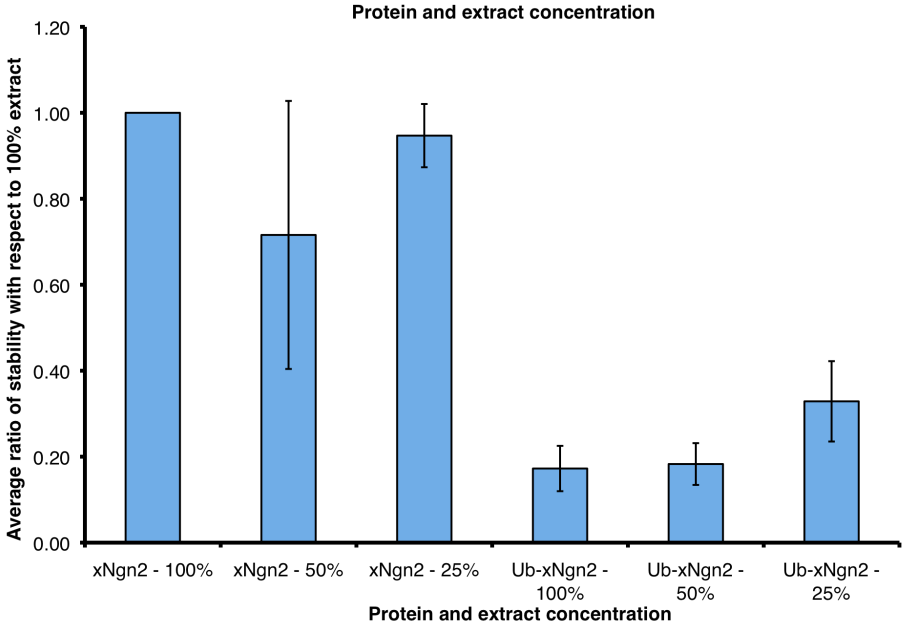

B

Experiment	% extract	xNgn2 Half-life (mins)	Ub-xNgn2 Half-life (mins)
1	100	26.2 +/- 2.5	6.9 +/- 2.7
1	90	30.4 +/- 4.8	6.2 +/- 0.8
1	75	28.2 +/- 2.1	16.0 +/- 5.5
2	100	47.2 +/- 19.7	6.2 +/- 0.6
2	50	24.3 +/- 5.6	6.7 +/- 0.5
2	25	41.8 +/- 13.8	12.4 +/- 1.8

Figure 6.8: xNgn2 stability in diluted *Xenopus* extract.

Xenopus laevis interphase activated egg extracts were diluted with XB buffer and supplemented with ^{35}S-labelled xNgn2 or Ub-xNgn2 and incubated at 21 °C. Samples were taken at 0, 5, 10, 20, 30, 40, 50 and 60 mins for xNgn2, and 0, 2, 4, 6, 8, 10, 15 and 20 mins for Ub-xNgn2 and subjected to 15 % SDS-PAGE. Gels were analysed by quantitative phosphorimaging analysis, calculating the average stabilisation relative to wild-type xNgn2 (A). (B) Half-lives were calculated using first-order rate kinetics, and errors calculated using the Standard Error of the Mean (SEM).

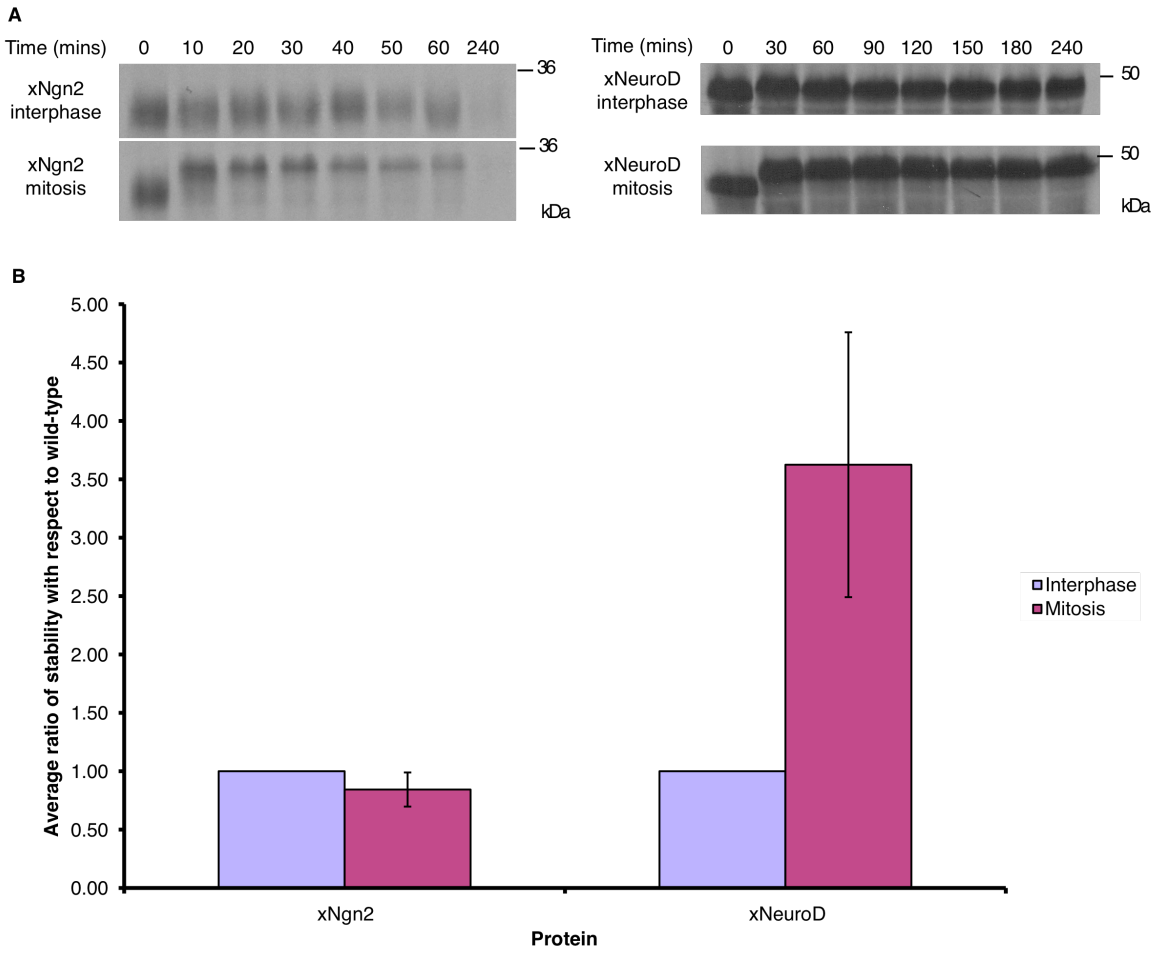

C

Extract	xNgn2 Half-life (mins)	xNeuroD Half-life (mins)
Interphase	37.4 +/- 10.0	> 240
Mitosis	29.0 +/- 3.9	> 240

Figure 6.9: Stability of xNeuroD in interphase and mitosis.

Xenopus laevis interphase and mitotic activated egg extracts were supplemented with ^{35}S-labelled IVT xNgn2 or xNeuroD and incubated at 21 °C. Samples were taken at 0, 15, 30, 45, 60, 75, 90 and 120 mins and subjected to 15 % SDS-PAGE. Gels were analysed by autoradiography (A) and quantitative phosphorimaging analysis, calculating the average stabilisation of each protein relative to interphase (B). (C) Half-lives were calculated using first-order rate kinetics, and errors calculated using the Standard Error of the Mean (SEM). Results are from a duplicate set of experiments.

xNgn2 is degraded with a half-life of 37.4 +/- 10.0 mins in interphase, which decreases to 29.0 +/- 3.9 mins in mitosis (Figure 6.9, C). The half-lives for xNeuroD in interphase and mitosis are both longer than the length of the 240 min timecourse and so cannot be stated with accuracy but xNeuroD is clearly more stable in mitosis than in interphase by an order of 3.5-fold (Figure 6.9, B). Therefore xNeuroD is indeed a highly stable protein compared to xNgn2 and, unlike xNgn2, is more stable in mitosis than in interphase.

As xNeuroD contains more lysines and therefore more canonical sites of ubiquitylation than xNgn2 (see Figure 6.10, A for a ClustalW2 analysis (Chenna et al., 2003)) I decided to compare ubiquitylation of xNgn2 and xNeuroD by ubiquitylation assay. ^{35}S-radiolabelled IVT xNgn2 and xNeuroD were added to *Xenopus laevis* interphase activated egg extract supplemented with MG132 to prevent proteasomal degradation, and either His_6-Ub (Sigma) or untagged Ub (Sigma). This reaction was incubated at 20 °C for 90 mins. Samples were then incubated with denaturing Vosper buffer (containing 8.5 M urea) and nickel-chelating agarose beads (Ni-NTA, Invitrogen) to purify his-tagged protein. These samples were eluted in either high pH, reducing SDS-LB or non-reducing SDS-LB and separated by 12 % SDS-PAGE (Figure 6.10, B).

xNgn2 (Figure 6.10, B, lanes 1, 3, 5, 7) and xNeuroD (Figure 6.10, B, lanes 2, 4, 6, 8) are ubiquitylated in *Xenopus* extract producing polyubiquitylation ladders on incubation with his-tagged Ub followed by pulldown on nickel beads (Figure 6.10, B, lanes 1-4).

The polyubiquitylation ladder of xNgn2 in reducing conditions (lane 1) differs from the ladder produced in non-reducing conditions (lane 3) in the presence of a faster-migrating band running at the level of the xNgn2 IVT run out in reducing conditions (adjacent to lane 1). As discussed previously, this band running at the level of unmodified protein represents xNgn2 conjugated to his-tagged Ub through labile linkages that are broken under reducing conditions, liberating unmodified xNgn2. The band does not appear in lane 3 as the labile linkages are maintained in non-reducing conditions.

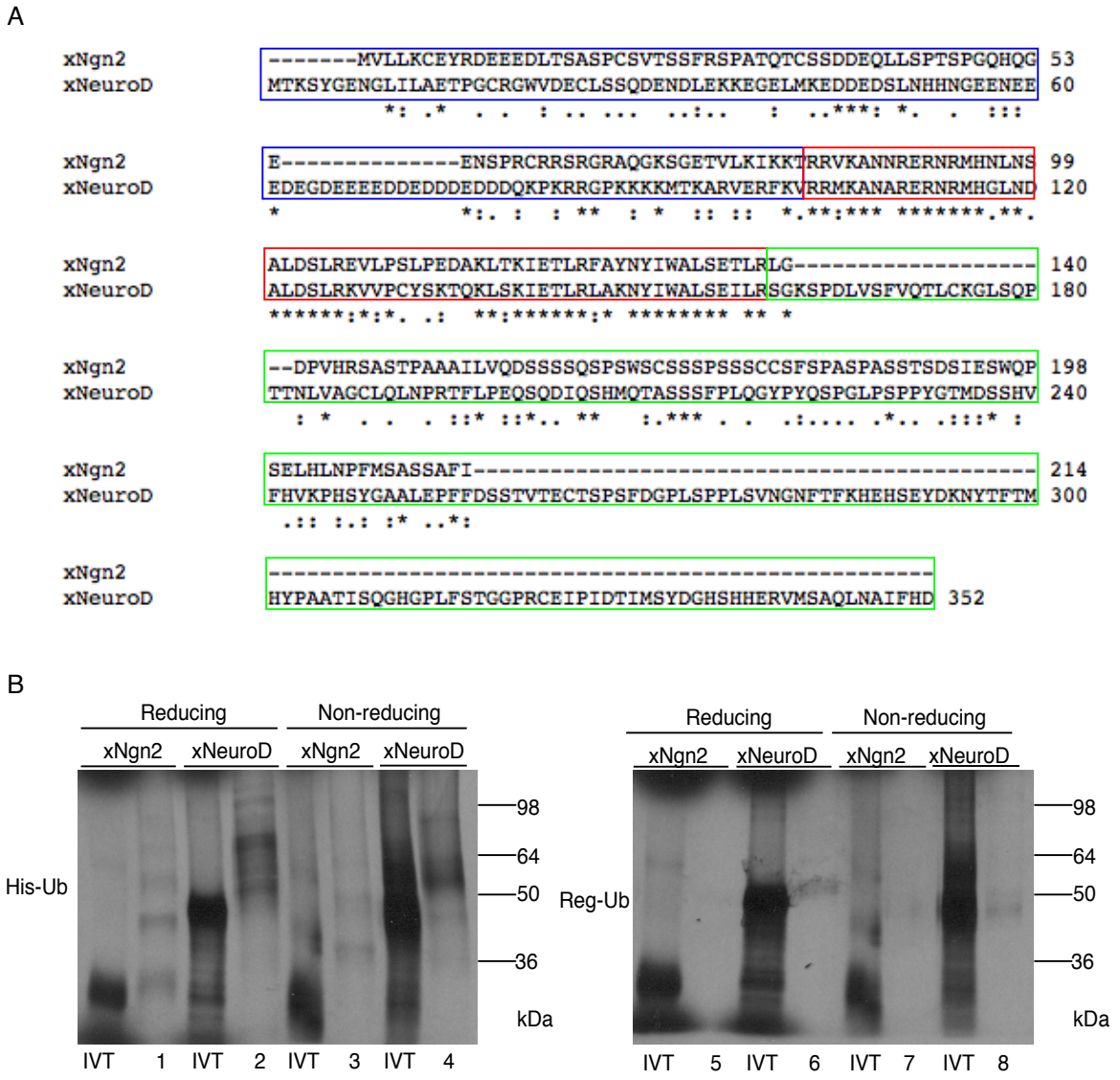

Figure 6.10: Ubiquitylation of xNeuroD.

A) ClustalW2 analysis of sequences from xNgn2 and xNeuroD. The disordered N-terminal domain is bordered in blue; the bHLH domain in red; and the disordered C-terminal domain in green.

B) *Xenopus laevis* interphase activated egg extracts were supplemented with ^{35}S-labelled IVT xNgn2 or xNeuroD in the presence of MG132 and either His_6-ubiquitin (His-Ub) or untagged ubiquitin (Reg-Ub) and incubated at 20 °C for 90 mins. Samples were bound to Ni-NTA Agarose beads for 75 mins and subjected to 15 % SDS-PAGE in either reducing or non-reducing conditions. Gels were analysed by autoradiography. Experiments were carried out in duplicate. Lanes are numbered 1-8 as described in the text.

However the xNeuroD polyubiquitylation ladder in reducing conditions (Figure 6.10, B, lane 2) does not contain a band representing unmodified xNeuroD running at the level of IVT. xNeuroD is polyubiquitylated in both reducing (lane 2) and non-reducing (lane 4) conditions.

Therefore whilst wild type xNgn2 and xNeuroD are both polyubiquitylated in *Xenopus* egg extract, xNgn2 demonstrates reducing agent, high pH-dependent ubiquitylation whilst xNeuroD does not.

xNgn2 and xNeuroD are similar proteins but with differing degradation properties. There may be particular regions of xNgn2 that are destabilising or conversely regions of xNeuroD which stabilise the protein against proteasomal degradation, perhaps by affecting the availability of unfolding initiation sites which are required for degradation (Prakash et al., 2004). To compare and contrast these regions of xNgn2 and xNeuroD fusion proteins were made to create "domain swaps" of xNgn2 and xNeuroD. These were constructed to place the N-terminus of one protein onto the bHLH and C-terminal domains of another protein, and *vice-versa*; likewise to place the N-terminal and bHLH domains onto the C-terminal domain of the other. For these the definition of where the N- and C-termini begin and end, and where the bHLH domain resides, was taken from a review of bHLH proteins (Bertrand et al., 2002). These 'domain swap' chimeric proteins were made as outlined in Figure 6.11, but their most important feature is at the junction of the two fusion proteins. The simpler strategy practically speaking would be to produce polymerase chain reaction (PCR) products that represent the two parts of the protein to be fused, and fuse them together by ligating them with a restriction site between them. However, in order to do so, 2 extra amino acids would need to be introduced to the protein sequence. Not wishing to introduce non-native residues to an already non-native fusion protein, the protein fusions were instead made entirely by PCR, using primers complementary to sequence in both proteins, so that one when the required domains of one protein had been produced by PCR, they would have one part at the point of fusion that could act as a primer for the other protein (a schematic of the chimeric proteins is given in Figure 6.12, E).

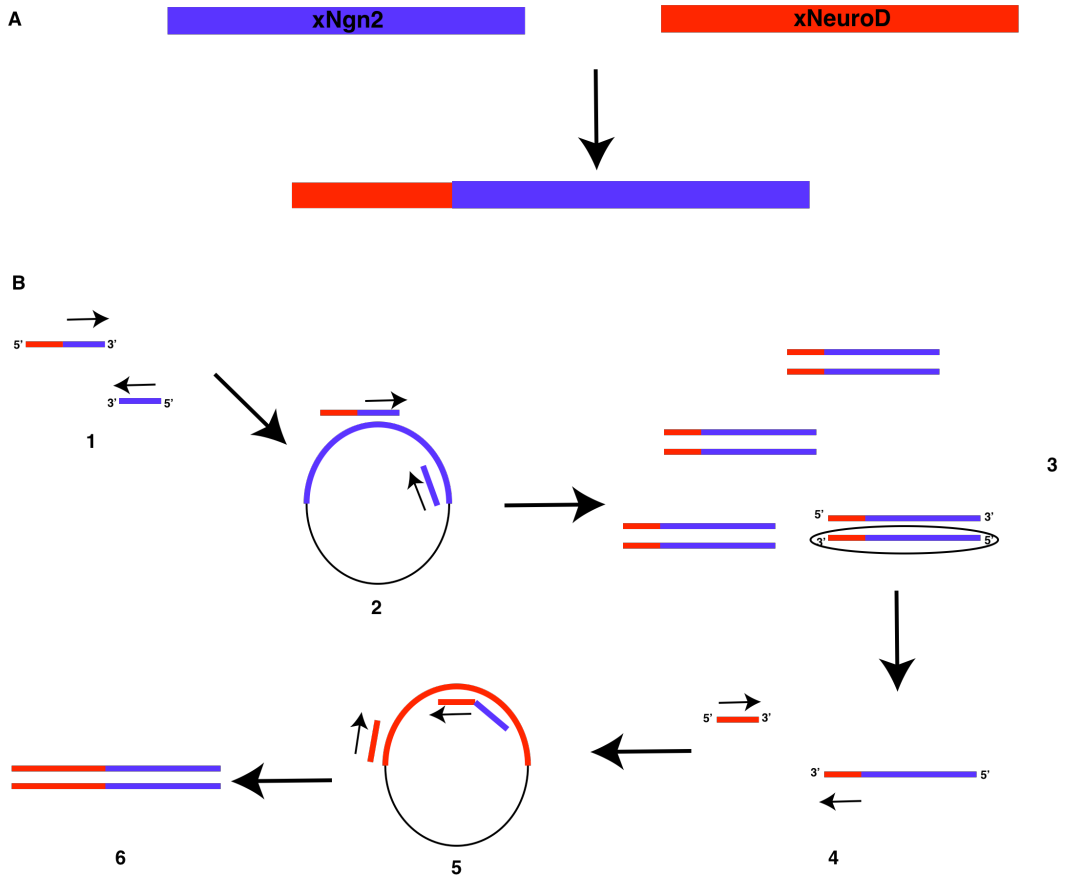

Figure 6.11: Strategy for xNgn2/xNeuroD domain swapping.

(A) The ultimate goal of the domain swap cloning is to fuse different regions of xNgn2 and xNeuroD together, e.g. the N-terminal domain of xNeuroD to the bHLH and C-terminus of xNgn2 to create N-Ngn/BC-NeuroD, but without introducing extra amino acid residues between the domains as would occur if linking domains together using restriction sites. (B) 1) A reverse primer is made for the C-terminus of xNgn2, with a XhoI restriction site at the 5' end, and a forward primer begins from the basic domain of xNgn2, but with the end of the xNeuroD N-terminal domain sequence preceding it. 2) These primers are used in PCR using xNgn2 as a vector. 3) PCR products are generated of the bHLH and C-terminal domains of xNgn2, with a small region complementary to the end of the xNeuroD N-terminal domain at the start. 4) The PCR product can then be used as a primer itself as it has a short complementary sequence to xNeuroD. This can be used with a forward primer from the start of the N-terminus of xNeuroD, with a BamHI site at the 5' end, in a PCR reaction 5) using xNeuroD as the template. When the PCR product is denatured, it can reanneal to the vector through the complementary sequence and act as a reverse primer. 6) The final product has the N-terminal domain of xNeuroD fused to the bHLH and C-terminal domains of xNgn2. The PCR product is flanked by BamHI and XhoI sites, which can be used to digest and ligate into pCS2+ vector.

I produced ^{35}S-radiolabelled IVT chimeric proteins in the presence or absence of the proteasome inhibitor MG132 and separated the proteins by 15 % SDS-PAGE before assessing by autoradiography (Figure 6.12, A). The proteins are named according to which domains they contain: N for N-terminal; B for bHLH; C for C-terminal. Therefore N-Ngn/BC-NeuroD has the N-terminal domain of xNgn2 fused to the bHLH and C-terminal domains of xNeuroD (see Figure 6.12, E).

Figure 6.12, A shows that there is a difference in the size of the proteins. This is due to the C-terminal domain, which in xNeuroD is far larger than xNgn2. Bands with the N-terminal domain of xNeuroD run as a cleaner band than the smeared band of proteins with the N-terminal domain of xNgn2.

To assess the stability of the domain swap proteins against proteasomal degradation, ^{35}S-radiolabelled IVT domain swap proteins, xNgn2 or xNeuroD were incubated in *Xenopus laevis* interphase activated egg extracts at 21 °C. Aliquots of the reaction were removed at increasing timepoints, quenched in SDS-LB and samples were separated by 15 % SDS-PAGE to allow measurement of protein levels over time and calculation of the half-life for degradation using first-order rate kinetics (Figure 6.12, B, C and D).

xNgn2 is degraded with a half-life of 22.2 +/- 3.1 mins whilst xNeuroD is stable with a half-life of degradation greater than the length of the 240 min timecourse and so not accurately determinable (Figure 6.12, D).

N-Ngn/BC-NeuroD is stabilised relative to xNgn2, with a half-life of 128 +/- 7 mins. However swapping the bHLH domains to give NB-Ngn/C-NeuroD decreases the half-life of degradation to 69.2 +/- 11.1 mins. This means that the bHLH and C-terminal domains of xNeuroD are stabilising on the N-terminal domain of xNgn2, but when the bHLH domain of xNeuroD is swapped with that of xNgn2, the protein is destabilised. Therefore the bHLH domain of xNgn2 is less stable than that of xNeuroD in this setting, despite being 73 % identical. N-NeuroD/BC-Ngn and NB-NeuroD/C-Ngn have similar half-lives for degradation of 112 +/- 20 mins and 126 +/- 21 mins respectively.

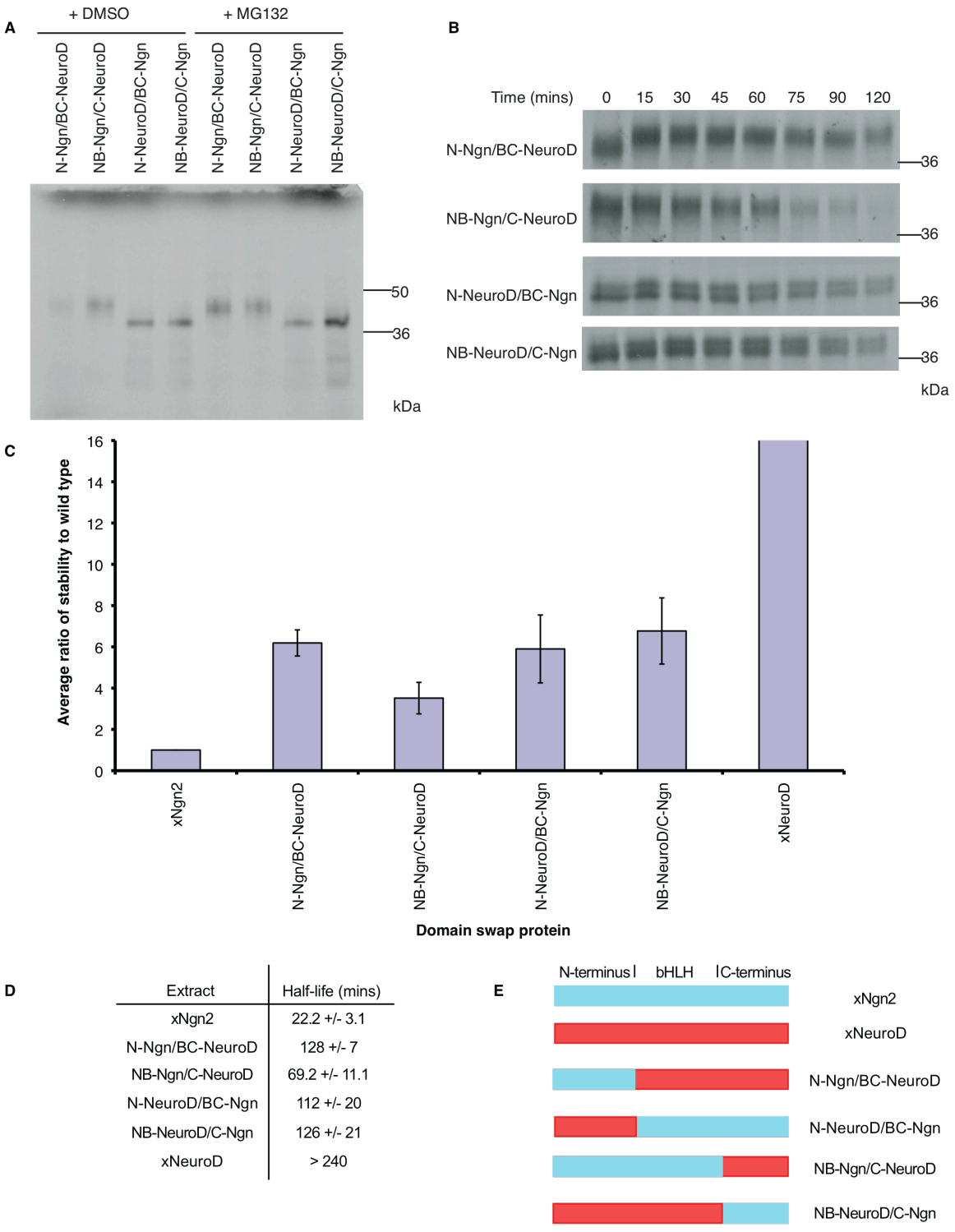

Figure 6.12: xNgn2/xNeuroD domain swap stability in interphase.

MG132-treated ^{35}S-radiolabelled IVT chimeric proteins analysed by autoradiography (A). *Xenopus* interphase extracts were supplemented with ^{35}S-labelled IVT xNgn2, xNeuroD or chimeric protein. Samples were taken at indicated timepoints, subjected to 15 % SDS-PAGE and analysed by autoradiography (B). The average stabilisation relative to wild-type xNgn2 within interphase extract was calculated (C). (D) Half-lives were calculated using first-order rate kinetics, and errors calculated using SEM. $n \geq 3$. (E) Schematic of chimeric proteins.

Therefore, with respect to xNgn2, replacing any domain with one from xNeuroD can be stabilising; however the least stable combination is the N-terminal and bHLH domain of xNgn2.

As xNeuroD is even more stable in mitosis, these degradation assays were repeated in a mitotic setting to see if any further difference was observed. ^{35}S-radiolabelled IVT domain swap proteins, xNgn2 or xNeuroD were incubated in *Xenopus laevis* mitotic egg extracts at 21 °C. Aliquots of the reaction were removed at increasing timepoints, quenched in SDS-LB and samples were separated by 15 % SDS-PAGE to allow measurement of protein levels over time and calculation of the half-life for degradation using first-order rate kinetics (Figure 6.13).

xNgn2 has a half-life for degradation of 23.2 +/- 5.0 mins whilst xNeuroD is stable with a half-life of degradation greater than the length of the 240 min timecourse and so not accurately determinable (Figure 6.13, C).

N-Ngn/BC-NeuroD is also stable with a half-life of degradation greater than the length of the 240 min timecourse and so not accurately determinable. Therefore the N-terminal domain of xNgn2 is not destabilising in mitosis. However changing the bHLH domain of xNeuroD for that of xNgn2 in NB-Ngn/C-NeuroD reduces the half-life for degradation down to 75.5 +/- 10.8 mins. Therefore the bHLH domain of xNgn2 is destabilising in mitosis as well as in interphase in this domain swap. N-NeuroD/BC-Ngn and NB-NeuroD/C-Ngn exhibit half-lives for degradation of 110 +/- 57 mins and 146 +/- 61 mins respectively which do not differ significantly from NB-Ngn/C-NeuroD. Therefore the C-terminal domain of xNgn2 appears destabilising, which was not the case in interphase extract (Figure 6.12, C).

To look at the ubiquitylation of the domain swap proteins, I subjected xNgn2, xNeuroD and the domain swap proteins to ubiquitylation assays. ^{35}S-radiolabelled IVT proteins were added to *Xenopus laevis* interphase activated egg extract supplemented with MG132 to prevent proteasomal degradation, and either His_6-Ub (Sigma) or untagged Ub (Sigma). This reaction was incubated at 20 °C for 90 mins. Samples were then incubated with denaturing Vosper buffer (containing 8.5 M urea)

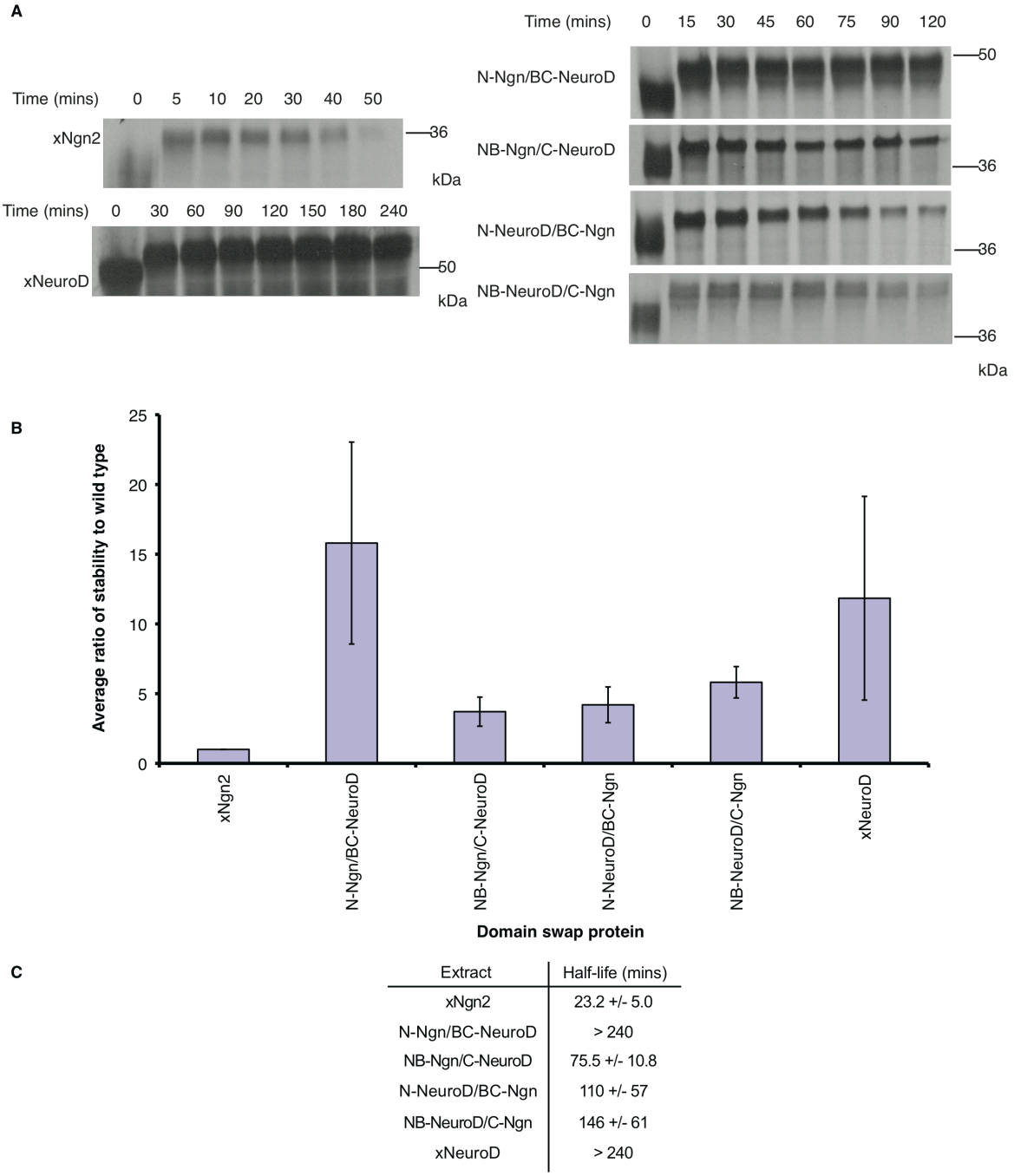

C

Extract	Half-life (mins)
xNgn2	23.2 +/- 5.0
N-Ngn/BC-NeuroD	> 240
NB-Ngn/C-NeuroD	75.5 +/- 10.8
N-NeuroD/BC-Ngn	110 +/- 57
NB-NeuroD/C-Ngn	146 +/- 61
xNeuroD	> 240

Figure 6.13: xNgn2/xNeuroD domain swap stability in mitosis.

Xenopus laevis mitotic egg extracts were supplemented with ^{35}S-labelled IVT xNgn2, xNeuroD or domain swapped protein and incubated at 21 °C. Samples were taken at the timepoints indicated and subjected to 15 % SDS-PAGE. Gels were analysed by autoradiography (A) and quantitative phosphorimaging analysis, calculating the average stabilisation relative to wild-type xNgn2 within mitotic extract (B). (C) Half-lives were calculated using first-order rate kinetics, and errors calculated using the Standard Error of the Mean (SEM). $n \geq 2$.

and nickel-chelating agarose beads (Ni-NTA, Invitrogen) to purify his-tagged protein. These samples were eluted in reducing or non-reducing loading buffer and separated by 12 % SDS-PAGE (Figure 6.14).

Polyubiquitylation ladders are present in all xNgn2 and xNeuroD chimeric proteins, illustrated in Figure 6.14, B, where all chimeric proteins treated with His-Ub and reducing conditions are run out on a single SDS-PAGE gel.

Pulling down his-tagged proteins results in a polyubiquitylation ladder of radiolabelled xNgn2 in both reducing and non-reducing treatments (Figure 6.14, A, lanes 1 and 2). The band in lane 1 running at the same mass as the IVT radiolabelled protein sample is not present in lane 2. Therefore under reducing conditions, unmodified xNgn2 is liberated from polyubiquitin chains after pulldown on nickel beads. This has been discussed previously and is due to linkage of ubiquitin to xNgn2 through labile covalent bonds, which are broken in reducing conditions.

For chimeric proteins containing the C-terminal domain of xNeuroD (N-Ngn/BC-NeuroD and NB-Ngn/C-NeuroD) the polyubiquitylation ladders in His-Ub treated samples (Figure 6.14, A, lanes 5 and 6, 9 and 10) show no obvious difference between reducing and non-reducing treatments (comparing lane 5 with 6, and lane 9 with 10). Although bands at the mass of the major band in the IVT protein of NB-Ngn/C-NeuroD are present, this is most likely due to the large amount of protein in the IVT sample affecting the level at which the band appears on SDS-PAGE. The polyubiquitylation ladders are smeared, like xNeuroD (lanes 21 and 22), compared to the clean defined polyubiquitylation ladder of xNgn2 (lanes 1 and 2). Therefore whilst chimeric proteins containing the C-terminal domain of xNeuroD are highly ubiquitylated, no reducing agent dependence is exhibited in this ubiquitylation suggesting non-canonical ubiquitylation may not occur on the N-terminal domain or bHLH domain of xNgn2.

In contrast, the chimeric proteins containing the C-terminal domain of xNgn2 (N-NeuroD/BC-Ngn and NB-NeuroD/C-Ngn) exhibit a band at the level of the IVT sample in the reducing buffer-treated lanes only (Figure 6.14, lanes 13 and 17). This is less

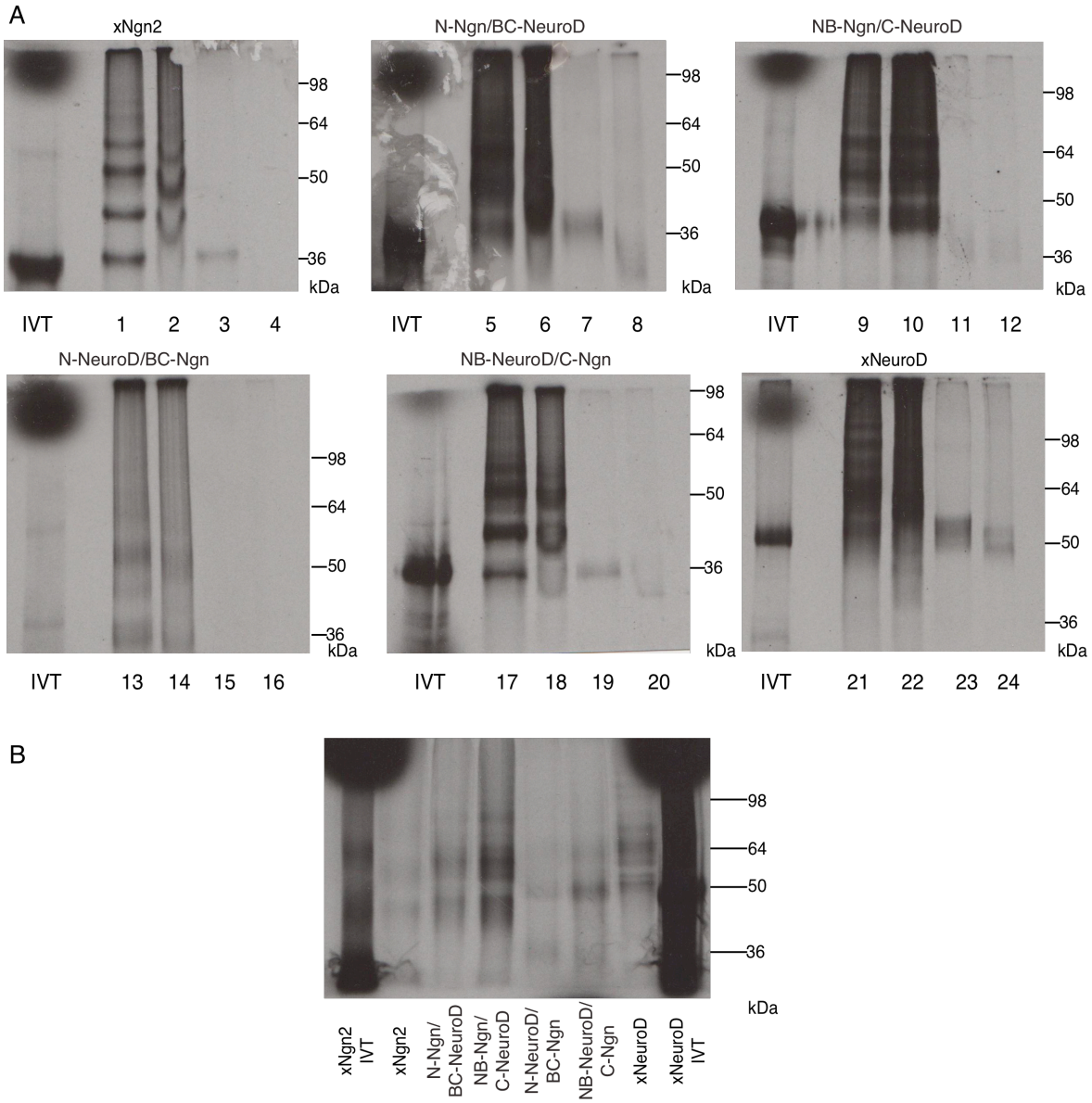

Figure 6.14: Ubiquitylation of xNgn2/xNeuroD domain swap proteins.

(A) *Xenopus laevis* interphase activated egg extracts were supplemented with ^{35}S-labelled IVT xNgn2, xNeuroD or chimeric domain swap proteins (marked IVT) in the presence of MG132 and either His-Ub (lanes 1, 2, 5, 6, 9, 10, 13, 14, 17, 18, 21 and 22) or untagged Ub (lanes 3, 4, 7, 8, 11, 12, 15, 16, 19, 20, 23 and 24) and incubated at 20 °C for 90 mins. Samples were bound to Ni-NTA Agarose beads for 75 mins and subjected to 12 % SDS-PAGE in either reducing (odd-numbered lanes) or non-reducing conditions (even-numbered lanes). Gels were analysed by autoradiography. Experiments were carried out in duplicate. Lanes are numbered as described in the text. (B) All proteins from (A) treated with His-Ub and reducing conditions were run out on 12 % SDS-PAGE and analysed by autoradiography.

clear for N-NeuroD/BC-Ngn where there is a low level of IVT but in reducing conditions (lane 13), a low band is clearly seen at 36 kDa that is not present in non-reducing conditions (lane 14). The polyubiquitylation ladders also resemble the clean ladders of xNgn2 (lanes 1 and 2) compared to the smeared ladder of xNeuroD (lanes 21 and 22). The C-terminal domain of xNgn2 is therefore non-canonically ubiquitylated. As the C-terminus of xNgn2 does not contain any lysines, this is the only possible mode of ubiquitylation in this region.

Whilst ubiquitylation occurs in both xNgn2 and xNeuroD, the nature of this ubiquitylation is different for these two structurally related but quite distinct proteins.

DISCUSSION

xNgn2 is a highly unstable protein and its degradation by the proteasome in a Ub-dependent manner is discussed in detail in Chapter 3 and 4. The effects of cdk phosphorylation on ubiquitylation and stability are then covered in Chapter 5. This chapter however has looked at the role of protein structure in controlling degradation. The stabilising effect of bulky tags such as GFP on the N- and C-terminus has been described (Vosper et al., 2009) but a much smaller HA tag is also stabilising when fused to the C-terminus (Figure 6.1). As a practical concern, no experiments have been carried out in *Xenopus laevis* extract using HA-tagged xNgn2. xNgn2-3HA – the triply C-terminally HA-tagged form of xNgn2 – has been used only in P19 cell experiments such as described in Chapter 4. There being no suitable xNgn2 antibody, HA-tagging is necessary to assess protein degradation by Western blot. In this case all proteins are compared with other HA-tagged proteins and so the HA tag is assumed to have an equal effect on all proteins. This seems to be the case from the experiments carried out in cell lines in Chapter 4. mNgn2 does not appear to be affected by HA-tagging, which is encouraging evidence for work in P19 cells using mNgn2. Again this hints at significant differences between xNgn2 and mNgn2 stability as suggested in Chapter 5.

xNgn2 associates with many factors that confer a stabilising effect on the protein, such as xE12 and Xic1 (Vernon et al., 2003, Vosper et al., 2007). p300 also binds the transcriptional complex of xNgn2 and xE12 and therefore may also affect xNgn2 stability. Figure 6.2 suggests that there is no effect on xNgn2 stability with p300N, the functional N-terminal domain of p300, in these interactions. There is some suggestion that E1A12S may stabilise xNgn2 somehow in neurula extract. Indeed neurula extract may be the more relevant setting for this experiment given its higher DNA content, perhaps providing the more relevant setting for assembly of the active complex. However, without xE12 added to the mix, assessment of stability in these experiments would not be worthwhile. There may also be a limit to the number of IVT proteins combined in this fashion, where the concentration of protein involved is poorly quantified. The preliminary experiment with xNeuroD has only been undertaken once no meaningful conclusions can be drawn from it. Xic1 stabilises xNgn2 (Roark, 2010, Vernon et al., 2003). Results in Figure 6.3 correspond to values for stability obtained by Ryan Roark (Roark, 2010). Addition of MBP or MBP-tagged Xic1 adds a substantial volume of solution to the reaction mixture, and dilution may lead to the increased half-life of xNgn2 with MBP alone. If MBP alone is exerting an effect on stability, then using this control to compare the effect of Xic1-MBP on stability is essential.

N-terminally ubiquitylated xNgn2 is not stabilised by Xic1 in interphase (Figure 6.4) therefore if Xic1 stabilises xNgn2 by binding as suspected (Roark, 2010), it could stabilise xNgn2 by binding to some ubiquitylation site and so preventing modification. If a priming ubiquitylation event has already occurred, as in Ub-xNgn2, then blocking any other site becomes redundant.

Figure 6.5 also shows that xNgn2 is not stabilised by Xic1 in mitosis whereas Ub-xNgn2 is. xNgn2 is phosphorylated in mitotic extract as discussed in Chapter 5 but Xic1 stabilisation of xNgn2 is not thought to be through its role as a cdki (Vernon et al., 2003). Action as a cdki seems the least likely means of stabilisation as both Ub-xNgn2 and Ub-9S-AxNgn2 demonstrated similar stability in Chapter 5 and so preventing phosphorylation does not provide stability to N-terminally ubiquitylated xNgn2. Ubiquitylation of xNgn2 perhaps differs in interphase and mitosis, or how

Xic1 interacts with xNgn2 may change, leading to a difference in the ability of Xic1 to stabilise xNgn2. Ubiquitylation assays of xNgn2 in interphase and mitosis with Xic1 may be able to shed more light on this problem.

To investigate whether DNA binding affects stability, we tested the xNgn2AQ mutant, which is no longer able to bind to the E-box site in DNA (Nakada et al., 2004). xNgn2AQ is identical in stability to xNgn2 in interphase and mitotic extracts, but is more stable in neurula extract (Figure 6.6). Neurula extract is perhaps the most relevant extract to work with for DNA-binding as it contains a higher DNA concentration than egg extracts. Fertilised eggs have only a diploid genome whilst neurula embryos contain thousands of cells each with a tetraploid genome and so have much more DNA. The result from Figure 6.6 suggests that when xNgn2 is unable to bind DNA, it is more stable than xNgn2 bound to DNA. It could be that binding to DNA reveals a ubiquitylation site not exposed in the xNgn2/xE12 heterodimer; perhaps there is a structural distortion of the heterodimer on DNA binding that affects the folding stability of xNgn2; or recruitment of another factor at the transcription site could affect stability. It has been suggested that the Ngn1/E47 heterodimer bound to DNA is a "fuzzy" complex (Aguado-Llera et al., 2010) where Ngn1 lacks the disordered N- and C-terminal domains. Figure 6.7 shows that xNgn2AQ is more stabilised by xE12 than xNgn2, but the xNgn2AQ mutant shows similar stability to xNgn2 in this experiment. Figure 6.7 was produced using neurula extract that had been snap-frozen and stored at -80 °C before being defrosted and used in this experiment. The long half-life for degradation of xNgn2 alone (47.2 +/- 8.6 mins, Figure 6.7, C) suggests a difference between fresh and previously frozen extracts. To date no controlled comparison of fresh and frozen *Xenopus* extracts has been carried out and so to compare results between the two is inadvisable. This experiment would be best carried out again in fresh neurula extract to compare with Figure 6.6. It does suggest that xNgn2AQ may be more stabilised by xE12 than xNgn2.

Figure 6.8 shows that diluted extracts do not seem to be suitable for investigating unfolding of xNgn2 independent of ubiquitylation. The simplest method will probably be fusion of xNgn2 to tetra-Ub, the minimal signal required for targeting to

the proteasome without a requirement for further ubiquitylation (Thrower et al., 2000). Therefore no further ubiquitylation will be required and attempts to maintain xNgn2 folding such as by addition of cofactors could then be attempted in extract systems.

Comparison of xNgn2 and xNeuroD is useful as whilst the two proteins are generally similar, particularly with 73 % homology in their bHLH domains, there are some key differences between the 2 proteins. Certain amino acids within the bHLH domain (particularly in the loop region), and parts of the N- and C-terminal domains differ. For example, xNeuroD has a large acidic region in its N-terminus; and perhaps surprisingly xNeuroD has more lysine residues than xNgn2, and whilst being ubiquitylated is not degraded efficiently by the proteasome (Vosper, 2008, Vosper et al., 2007). Figure 6.9 again shows that xNeuroD is more stable than xNgn2 in interphase, but that it is stabilised even further in mitotic extract where xNgn2 is actually destabilised. Figure 6.10 shows that xNeuroD is still ubiquitylated but that the reducing agent-dependence of ubiquitylation exhibited in xNgn2 (highlighting non-canonical ubiquitylation) is not demonstrated for xNeuroD. xNeuroD is much more stable than xNgn2 and it may be that non-canonical ubiquitylation is necessary in xNgn2 to ensure rapid degradation, whilst this is not required in xNeuroD.

Swapping the domains of xNgn2 and xNeuroD directly using overlapping PCR primers rather than using restriction sites at the points of fusion is a more difficult technique, but ultimately prevents the introduction of non-native amino acids into the xNgn2/xNeuroD fusion protein sequence. In Figure 6.12 all fusion proteins show intermediate stability between xNgn2 and xNeuroD. The most intriguing result is that N-Ngn/BC-NeuroD and NB-Ngn/C-NeuroD, which differ only in their bHLH domains and so might be expected to be almost identical, have significantly different stabilities suggesting that the bHLH domain of xNgn2 can confer more instability than that of xNeuroD. However this is not repeated in the comparison between N-NeuroD/BC-Ngn and NB-NeuroD/C-Ngn, suggesting that the N-terminal domain of xNgn2 is required as a destabilising accomplice to the bHLH domain. In fact, one possible explanation is that the N-terminal and bHLH domains of xNeuroD are less easily unfolded than the corresponding domains in xNgn2. Therefore the N-terminus

of xNgn2 could act as an unfolding initiation site and induce unfolding in the weakly folded xNgn2 bHLH domain. However the bHLH domain of xNeuroD, perhaps being more stably folded, could resist this; likewise, though the xNgn2 bHLH domain is less stably folded than the xNeuroD counterpart, if the N-terminal domain of xNeuroD does not act as an unfolding initiation site, then unfolding of the xNgn2 bHLH domain may not occur. It could also be that the N-terminal and bHLH domains differ in likely ubiquitylation sites compared to xNeuroD – crucially, all lysines in xNgn2 occur in the N-terminus and bHLH domains; there are none in the C-terminal domain. Of course, it could be that both work in concert, and that the unfolding initiation site is required next to a ubiquitylation site as is required for proteasomal degradation (Prakash et al., 2004); if xNeuroD is more stable against unfolding, then this could explain why it is not degraded despite being ubiquitylated, there being no suitable unfolding initiation site present.

Comparing the domain swap proteins in mitotic extract could hint at the importance of unfolding, ubiquitylation and phosphorylation all coming together to tightly regulate xNgn2 stability. Like interphase extract, N-Ngn/BC-NeuroD and NB-Ngn/C-NeuroD differ only in their bHLH domains but the protein with the xNgn2 bHLH domain is less stable than that with the xNeuroD bHLH domain. In fact, in mitosis, the xNeuroD bHLH domain-containing protein is stable, like xNeuroD. Therefore in mitosis it would appear that replacing its N-terminal domain with the N-terminal domain of xNgn2 is insufficient to destabilise xNeuroD. However in comparison with interphase, N-NeuroD/BC-Ngn and NB-NeuroD/C-Ngn are as unstable as NB-Ngn/C-NeuroD and what seems to be destabilising here is the C-terminal domain of xNgn2. This is the very region that appears most important for phosphorylation and controlling stability in a phosphorylation dependent manner in mitotic extract (Chapter 5 and (Hindley, 2011)). Therefore the arguments in interphase for unfolding and ubiquitylation still hold true in the mitotic case but in conjunction with phosphorylation. Ubiquitylation can only occur on lysines in the N-terminal and bHLH domains and, in the wild type protein in interphase, canonical sites of ubiquitylation appear important, whereas non-canonical residues, such as cysteines, serines and threonines (all of which are present in the C-terminus) are not as important in targeting xNgn2 for degradation in interphase – but they are in mitosis

(Chapters 3 and 4). Phosphorylation is shown to be most important on the C-terminus. Therefore in mitosis xNgn2 would appear to have many destabilising features.

Ubiquitylation in the chimeric proteins shows variation (Figure 6.14). Chimeric proteins containing the C-terminal domain of xNeuroD show smeared polyubiquitylation ladders with no reducing agent-dependent ubiquitylation, like xNeuroD. Proteins containing the xNgn2 C-terminal domain are ubiquitylated in a reducing agent-dependent manner with a clear polyubiquitylation ladder displayed in ubiquitylation assays. The assays in Figure 6.14 could be repeated with less loading of IVT protein on SDS-PAGE. The extent to which xNeuroD is ubiquitylated, and the smeary nature of the polyubiquitylation ladders to xNeuroD, make detailed analysis of the ubiquitylation assays of xNeuroD proteins difficult. Also, non-reducing SDS-LB often results in distorted bands on a gel and proteins running at different masses than in reducing SDS-LB (e.g., Figure 6.14, A, lane 18 compared to lane 17). However enough information can be obtained from these assays to show that there is a difference in the ubiquitylation of xNgn2 and xNeuroD and apparently relating to the C-terminal domains of these proteins.

Therefore overall, alterations in the structure of xNgn2, by affecting folding or interaction with other factors, have an important role in affecting xNgn2 degradation.

CHAPTER 7

Nuclear Magnetic Resonance Spectroscopy of mNgn2

INTRODUCTION

There is no direct structural information available for Ngn2 but based on homology with other bHLH proteins it is supposed to consist of a structured bHLH domain flanked by disordered N- and C-termini (Bertrand et al., 2002). The closest structural data to Ngn2 within the literature relate to the crystal structure of NeuroD in complex with E47 bound to the consensus E-box DNA sequence (Longo et al., 2008) and to the NMR structure of Ngn1 bound to E47 and the E-box (Aguado-Llera et al., 2010).

Ngn2 shares many similarities with intrinsically disordered (ID) proteins with regard to amino acid composition (Dunker et al., 2001), function (Ward et al., 2004) and stabilisation upon binding other cofactors (Wright and Dyson, 2009) (Vosper et al., 2007). In addition the bHLH proteins show significant sequence homology in the bHLH domain only (Bertrand et al., 2002) and large sequence variability in the disordered regions as suggested in the evolutionary comparison of related ID proteins (Brown et al., 2002). It is a highly unstable protein (Vosper et al., 2007, Vosper et al., 2009, McDowell et al., 2010), which appears to be highly phosphorylated by cell cycle-related kinases (Hindley, 2011, Gsponer et al., 2008). The related protein Ngn1 even forms a "fuzzy complex" (Tompa and Fuxreiter, 2008) in NMR studies (Aguado-Llera et al., 2010). It is possible that Ngn2 carries out many of the functions of ID proteins (Dunker et al., 2002) especially in displaying sites for binding other factors such as LMO4 (Asprer et al., 2011) xE12, p300/CBP, and DNA (Bertrand et al., 2002), which are associated with its stability (Vosper et al., 2009).

Protein NMR gives information about protein structure at the atomic detail and in particular ID proteins or disordered regions can be studied (Verdegem, 2009). Therefore I wished, in collaboration with the lab of Guy Lippens at Université de Sciences et Technologies Lille, to investigate the behaviour of Ngn2 in NMR using

mouse Ngn2, or mNgn2. 2D ^{1}H-^{15}N heteronuclear single quantum coherence (HSQC) and 3D ^{1}H-^{15}N-^{13}C HSQC techniques allow identification of amino acid residues in proteins in regions that are disordered. Ordered regions are not seen due to technical effects connecting the rate of nuclear relaxation in structured regions with the peak width in the NMR spectrum.

Phosphorylation of proteins can also be studied by HSQC as the amide proton chemical shift is affected by its electronic environment. Therefore there is a large change in shift upon phosphorylation as demonstrated in the Tau protein, related to Alzheimer's disease (Landrieu et al., 2006). I also wished to investigate whether such an effect could be seen in mNgn2 upon *in vitro* kinase treatment.

RESULTS

mNgn2 and xNgn2 are predicted to be intrinsically disordered (ID) proteins

xNgn2 exhibits some of the features identified with ID proteins. There are a large number of charged residues leading to a low level of hydrophobicity (Dunker et al., 2001) and the protein runs at a higher molecular mass (around 36 kDa) than its calculated molecular mass (23.4 kDa) (Weinreb et al., 1996). ID proteins show an increased rate of evolution in disordered regions and this appears to be the case in the N- and C-termini of bHLH proteins (Figure 3.6 and see comparison of xNgn2 and mNgn2 by ClustalW2 analysis (Chenna et al., 2003), Figure 7.1A). bHLH protein crystal structures are often carried out excluding the N- and C-termini outside the bHLH domain (Longo et al., 2008) as these regions are predicted to be disordered, but evidence exists that the bHLH domain tends towards disorder even when bound to DNA with its heterodimeric binding partner (Aguado-Llera et al., 2010).

There are a number of computational predictors of protein disorder available through the database of disordered proteins, DisProt (www.DisProt.org, (Sickmeier et al., 2007)). The peptide sequences of xNgn2 and mNgn2 were submitted to PONDR-FIT (available from www.DisProt.org/pondr-fit.php, (Xue et al., 2010)), which combines various predictor programme outputs to produce a disorder

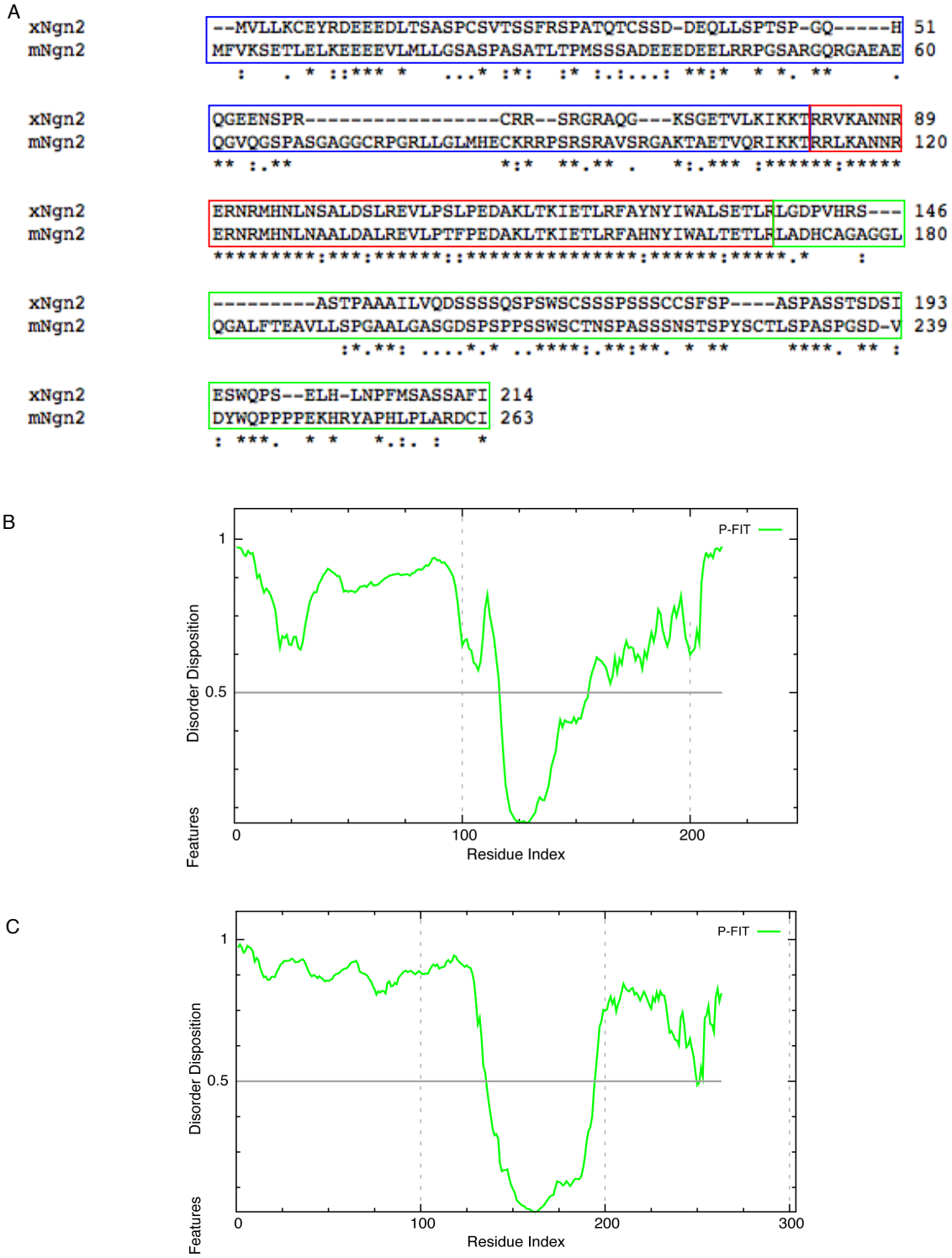

Figure 7.1: xNgn2 and mNgn2 are predicted to be disordered proteins

(A) ClustalW2 sequence alignment of xNgn2 and mNgn2. The disordered N-terminal domain is bordered in blue; the bHLH domain in red; and the disordered C-terminal domain in green. PONDR-FIT disorder predictions of (B) xNgn2 and (C) mNgn2.

prediction. Disposition towards disorder was plotted for each residue. There is a high degree of disorder in the N- and C-terminal regions of xNgn2 (Figure 7.1, B) and mNgn2 (Figure 7.1, C) with a highly ordered segment in the middle of the sequence. The ordered region corresponds with the bHLH domain.

Both xNgn2 and mNgn2 exhibit low sequence conservation in the N- and C-terminal domains (Figure 7.1, A) but these regions are both highly disordered to a similar extent (Figure 7.1, B and C). Further disorder predictions were carried out with mNgn2 to compare the results from various disorder predictors. DISOPRED2 (http://bioinf.cs.ucl.ac.uk/disopred/, (Ward et al., 2004)) is a predictor that has been developed using standards for prediction identified in earlier experiments. The disorder prediction using DISOPRED2 is plotted in Figure 7.2, A. This plot shows highly disordered N- and C-termini flanking a folded region in agreement with the PONDR-FIT prediction in Figure 7.1, C. FoldIndex (http://bip.weizmann.ac.il/fldbin/findex, (Prilusky et al., 2005)) uses the hydrophobicity and charge of the amino acid sequence to make a prediction and for mNgn2 this is plotted in Figure 7.2, B. Here again we see disordered regions at the N- and C-termini and a folded region in-between. However, compared to the previous predictions (Figure 7.1, C and Figure 7.2, A), the folded region is shifted towards the N-terminus and is much larger. This correlates with the distribution of hydrophobic and charged residues in mNgn2 (Figure 7.1, A).

Therefore whilst Ngn2, and other bHLH proteins, may not be entirely disordered, the difficulties in protein purification and the disorder predictions for mNgn2 described above suggest that intrinsically disordered regions are present.

mNgn2 solubility is improved upon fusion to a GST-tag

I wished to begin structural studies of Ngn2 and for this I decided to use mouse Ngn2 (mNgn2) for NMR studies in collaboration with Isabelle Landrieu in the laboratory of Guy Lippens at Université de Sciences et Technologies Lille. The mouse protein was used as this was also studied in the Philpott lab particularly in relation to

A

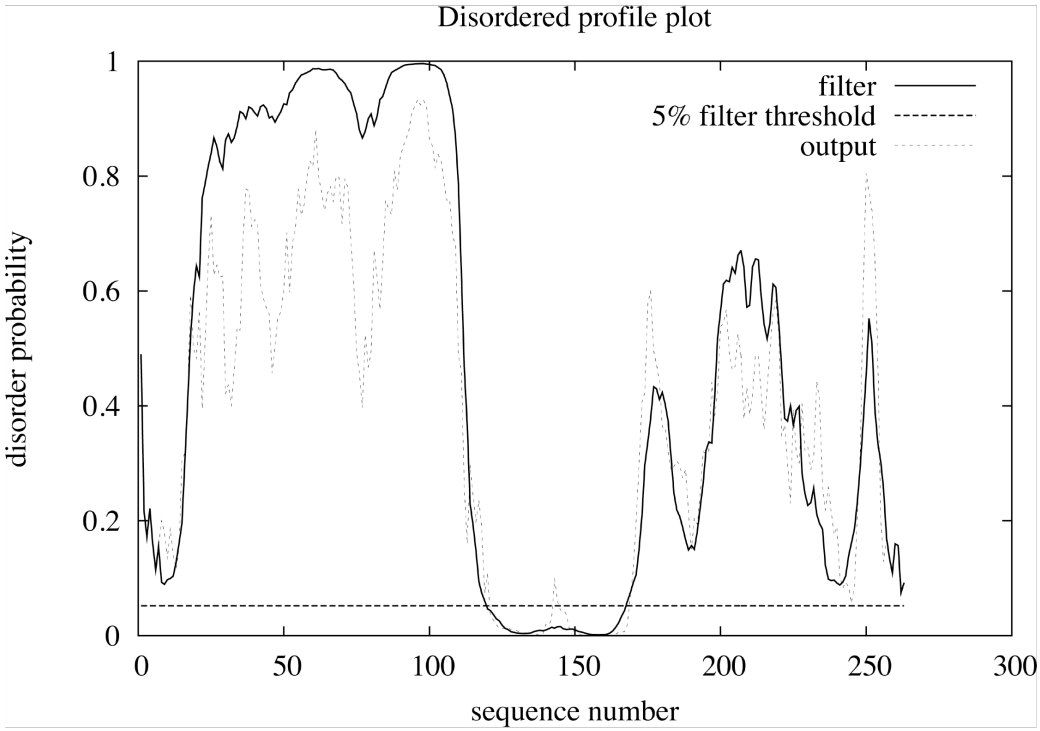

B

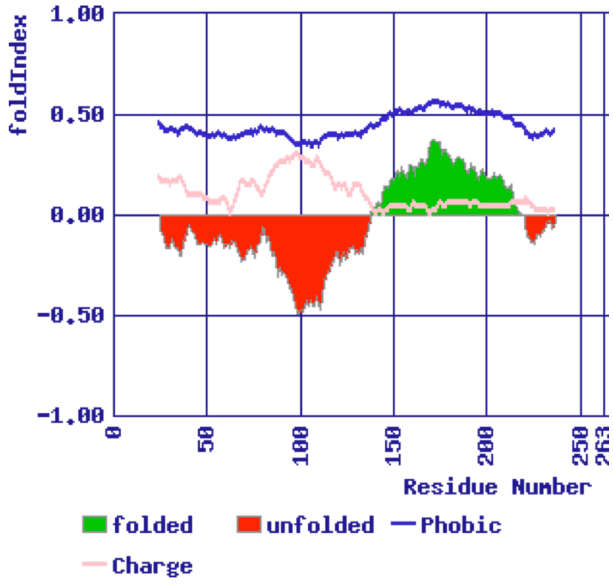

Figure 7.2: mNgn2 protein disorder predictions.

mNgn2 disorder predictions using (A) DISOPRED2 and (B) FoldIndex.

phosphorylation and activity (Ali et al., 2011) and allows use of mammalian cdks for *in vitro* phosphorylation experiments.

Purification of bHLH proteins is difficult and often results in production of insoluble products (Longo et al., 2008). In fact, purification of these proteins has proved so difficult that in one case, purification was abandoned and the bHLH domain of Ngn1 was chemically synthesised (Aguado-Llera et al., 2010). Purification of bHLH proteins directly has been achieved by cotransformation of the heterodimeric binding partners, such as MyoD with E47 (Cottle et al., 2007).

DNA constructs of mNgn2, codon optimised for bacterial expression, were produced by Genecust (Luxembourg) in pUC vectors. These were subcloned into pGEX (N-terminal GST-tagging vector, (Kaelin et al., 1992)) and pET (N-terminal His-tagging vector, Novagen, (Studier et al., 1990)) vectors. GST-tagged and His-tagged mNgn2 proteins were bacterially expressed, with clear production of protein in bacteria after overnight induction (Figure 7.3, A: lane 2 for His-mNgn2 and lane 4 for GST-mNgn2).

Upon cell lysis, however, there was a clear difference in the solubility of the proteins, for although GST-mNgn2 was present in both soluble (S) and insoluble (I) fractions (Fig 7.3, A, lanes 6 and 7 respectively), His-mNgn2 was entirely insoluble (Fig 7.3, A, lane 10). Recovery of insoluble proteins using urea is undesirable for NMR but is possible using particular detergents (Tao et al., 2010). Whilst preliminary experiments trying to extract His-mNgn2 from the insoluble phase were promising, I decided to continue the NMR experiments with the GST-tagged protein.

Upon cleavage of the GST-tag from mNgn2, mNgn2 was liberated (Figure 7.3, B, lane 11, arrow) but there also appeared a higher band (Figure 7.3, B, lane 11, asterisk), which ran at a higher molecular mass than GST-mNgn2 (such as in Figure 7.3, A, lane 4). Upon *in vitro* kinase treatment with cyclinA/cdk2 at 30 °C, the lower band disappeared and the higher band had shifted to a slightly higher molecular mass (Figure 7.3, B, lane 12). This band appears to be a dimeric form of mNgn2 that is somehow resistant to the conditions of SDS-PAGE.

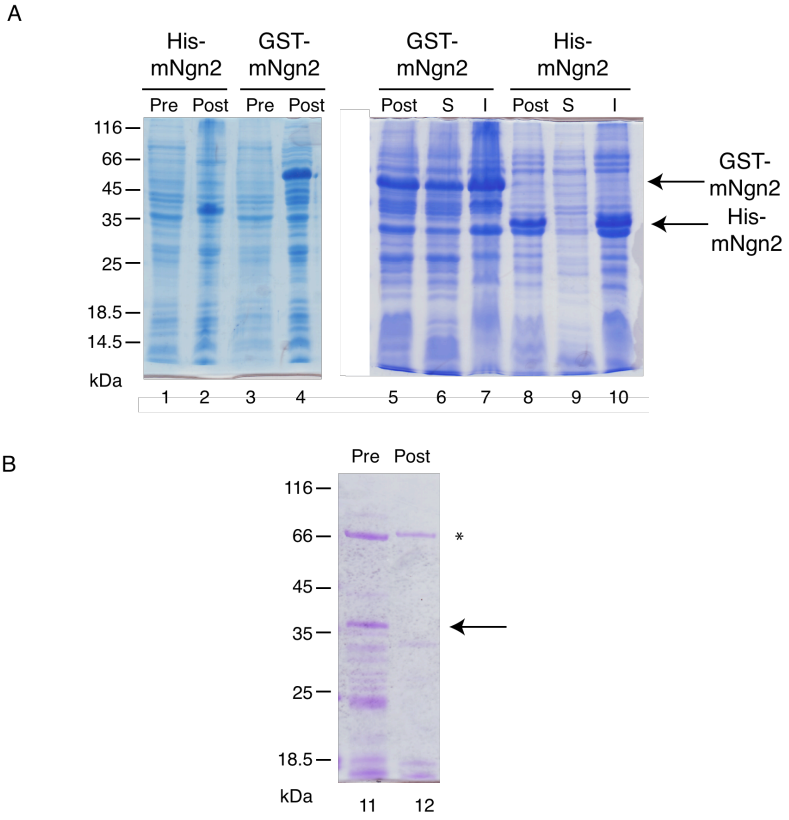

Figure 7.3: Protein purification of mNgn2.

(A) Overexpression of His-mNgn2 and GST-mNgn2 demonstrated on SDS-PAGE. Pre: pre-induction; Post: post-induction; S: soluble cell lysis fraction; I: insoluble cell lysis fraction. (B) mNgn2 protein (after GST-tag cleavage) Pre and Post *in vitro* kinase treatment with cyclinA/cdk2 on SDS-PAGE.

CyclinA/cdk2 phosphorylates mNgn2 *in vitro*

To investigate the structure of mNgn2, ^{1}H-^{15}N HSQC was performed using bacterially expressed, ^{1}H and ^{15}N-labelled mNgn2 at 600 MHz. The spectrum is shown in Figure 7.4A (spectra prepared by Isabelle Landrieu). Each peak identifies an amino acid residue by virtue of the contact between the amide proton and its corresponding isotopically-labelled nitrogen. However this means that prolines are not identified as they lack the amide backbone proton. In 2D HSQC experiments such as this, whilst estimates of the type of amino acid residue at particular chemical shifts can be made, the amino acids cannot be assigned precisely and further experiments are required. The number of peaks present correspond to regions of intrinsic disorder, as ordered residues in structural regions are not seen under the conditions of this experiment. Only residues where the labelled nuclei are in dynamic regions are observed, as nuclei in structured regions relax too quickly for a signal to be observed.

To investigate the effect of phosphorylation on this structure, I purified mNgn2 and phosphorylated the protein *in vitro* with cyclinA/cdk2, which phosphorylates Ngn2 *in vitro* (Ali et al., 2011). This treatment affects the appearance of mNgn2 on SDS-PAGE (Figure 7.3, B, lanes 11 and 12). ^{1}H-^{15}N HSQC was performed at 600 MHz by Guy Lippens, to give the spectrum in red overlaid onto the spectrum of unphosphorylated mNgn2 (Figure 7.4, B and zoomed-in, C, spectra prepared by Isabelle Landrieu). The spectrum overlays very neatly onto the unphosphorylated mNgn2 spectrum and so phosphorylation does not result in major structural changes. However there is a shift of 3 peaks, highlighted by arrows in Figure 7.4, B and C. This shift corresponds to a phosphorylation event on threonine or serine residues (Bienkiewicz and Lumb, 1999). Therefore mNgn2 is phosphorylated *in vitro* by cyclinA/cdk2 on 3 sites but without resulting in major structural rearrangements.

3D ^{1}H-^{15}N-^{13}C HSQC adds an extra dimension onto the NMR spectrum and allows more direct identification of residues using ^{13}C chemical shifts for Cα and Cβ in the amino acid residue peak given by the 2D HSQC experiment. 3D ^{1}H-^{15}N-^{13}C HSQC was carried out on phosphorylated mNgn2 by Isabelle Landrieu to produce the spectrum in Figure 7.5. The phosphorylated serine/threonine residues have been highlighted

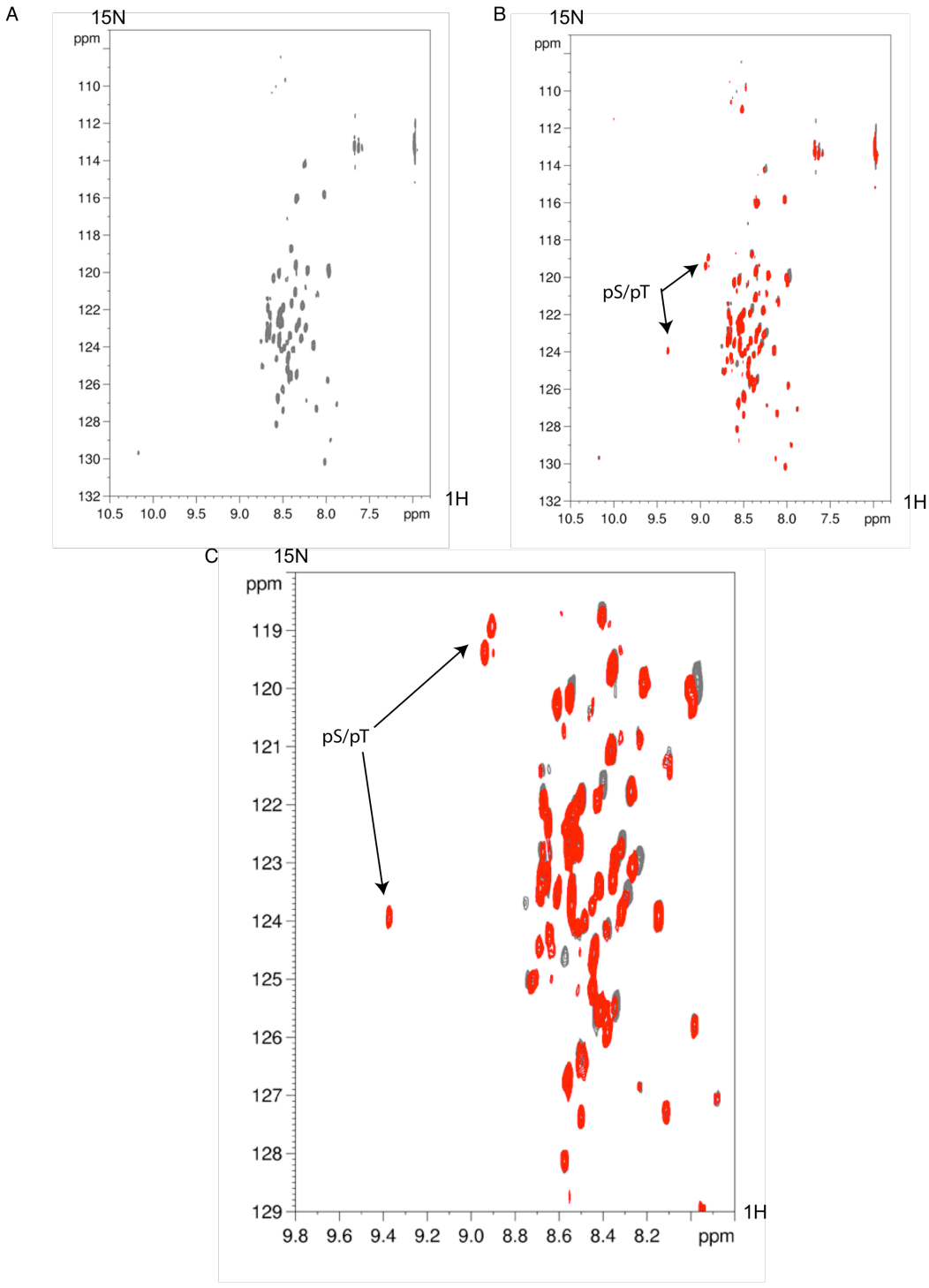

Figure 7.4: ^{1}H-^{15}N HSQC spectrum of mNgn2 and cyclinA/cdk2-treated mNgn2.

^{1}H-^{15}N HSQC experiments were carried out at 600 MHz on (A) mNgn2 (grey) and (B), (C) cyclinA/cdk2-treated mNgn2 (red) superimposed over the unphosphorylated mNgn2 spectrum. Spectra produced by Isabelle Landrieu and phosphorylated mNgn2 experiment run by Guy Lippens.

and were identified by Isabelle Landrieu using the ^{13}C chemical shifts as illustrated in Figure 7.6. The Cα and Cβ of the amino acid residue in question can be identified by their chemical shift (Bienkiewicz and Lumb, 1999, Wishart and Sykes, 1994). With good resolution, the Cα and Cβ of the amino acid residue immediately N-terminal to the residue under consideration (i.e., residue i-1 compared to residue i) can also be seen. Therefore a sequence can be assembled from a 3D NMR spectrum.

Some particular details also assist in assignment. Phosphorylation has a particular effect on the shift of serines and threonines (Bienkiewicz and Lumb, 1999). Glycines do not have a Cβ (as illustrated in Figure 7.6, C). Individual peaks for prolines are not seen as mentioned above; however, when a proline is immediately C-terminal to a residue (i.e. i+1), the normal ^{13}C chemical shift for a residue's Cα is shifted by -2 ppm, and for Cβ by -1 ppm. This is illustrated for all residues in Figure 7.6 and the phosphorylated residues with their preceding and succeeding residues are highlighted in Figure 7.5.

Therefore mNgn2 is phosphorylated on the two SP sites and one TP site. From the sequence information given by NMR we can identify these sites as the three cdk consensus sites (Errico et al., 2010) in the N-terminus of mNgn2. Therefore we can infer that cyclinA/cdk2 can phosphorylate all available N-terminal SP sites and therefore, that the N-terminal domain of mNgn2 is disordered, as this is the region visible in NMR experiments used for observing ID proteins.

DISCUSSION

Disorder-predicting programmes are based upon protein sequence information alone and the *in vitro* environment is not yet accurately reproducible *in silico*. The predictions in Figures 7.1 and 7.2 do correlate well for mNgn2 and so this suggests a high degree of disorder is likely, particularly in the N- and C-terminal domains. The FoldIndex prediction (Figure 7.2, B) does not correlate as well with the other predictions. However, there is a greater bias placed upon the hydrophobicity and charge of the residues in the peptide sequence (Prilusky et al., 2005) and whilst this is a good predictor of intrinsic disorder (Dunker et al., 2001) it may be insufficient. The

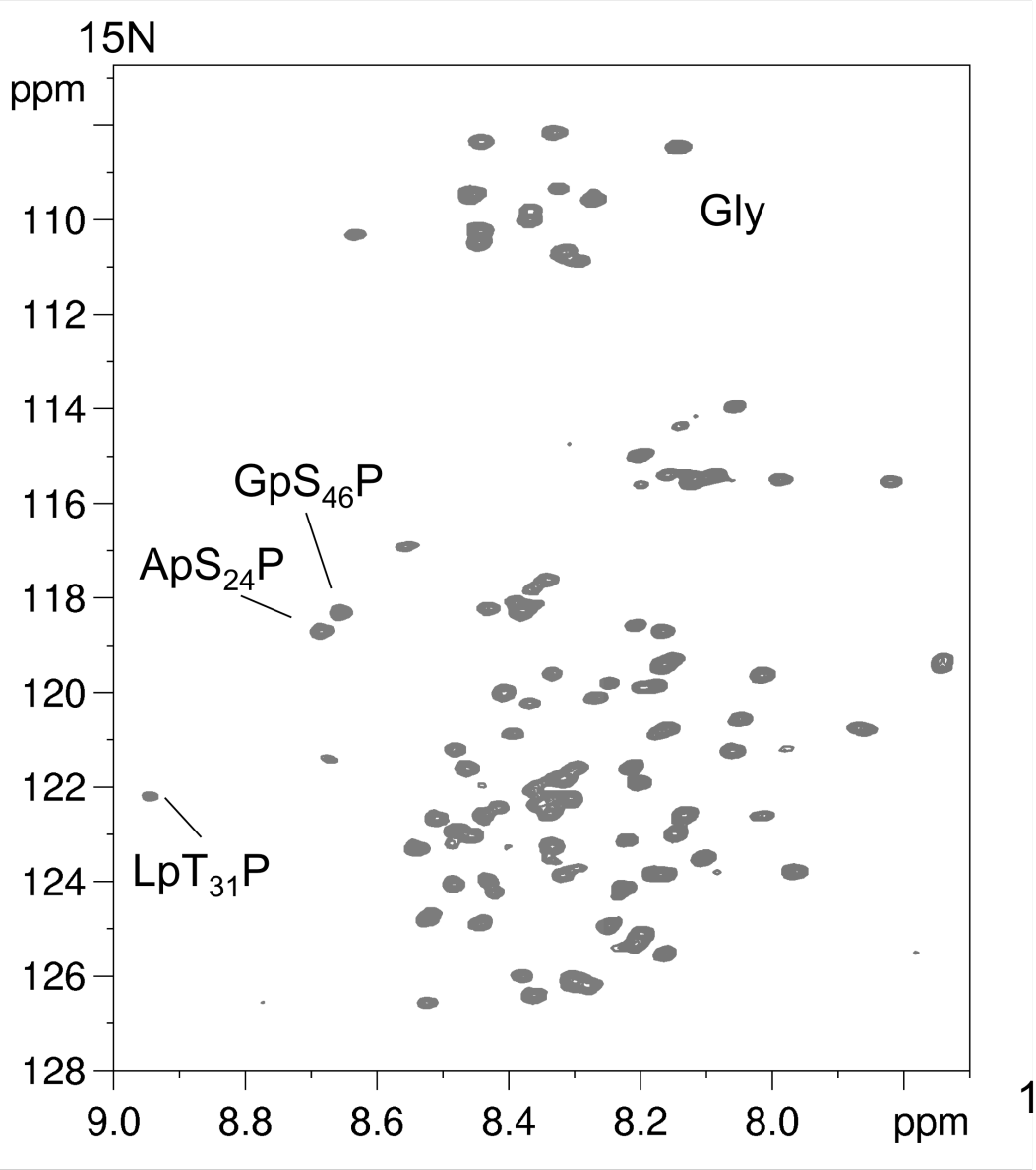

Figure 7.5: ^{1}H-^{15}N-^{13}C HSQC spectrum of phosphorylated mNgn2.

^{1}H-^{15}N-^{13}C HSQC experiment with cyclinA/cdk2-treated mNgn2. Phosphorylated SP and TP sites are labelled. Experiment carried out and spectrum prepared by Isabelle Landrieu.

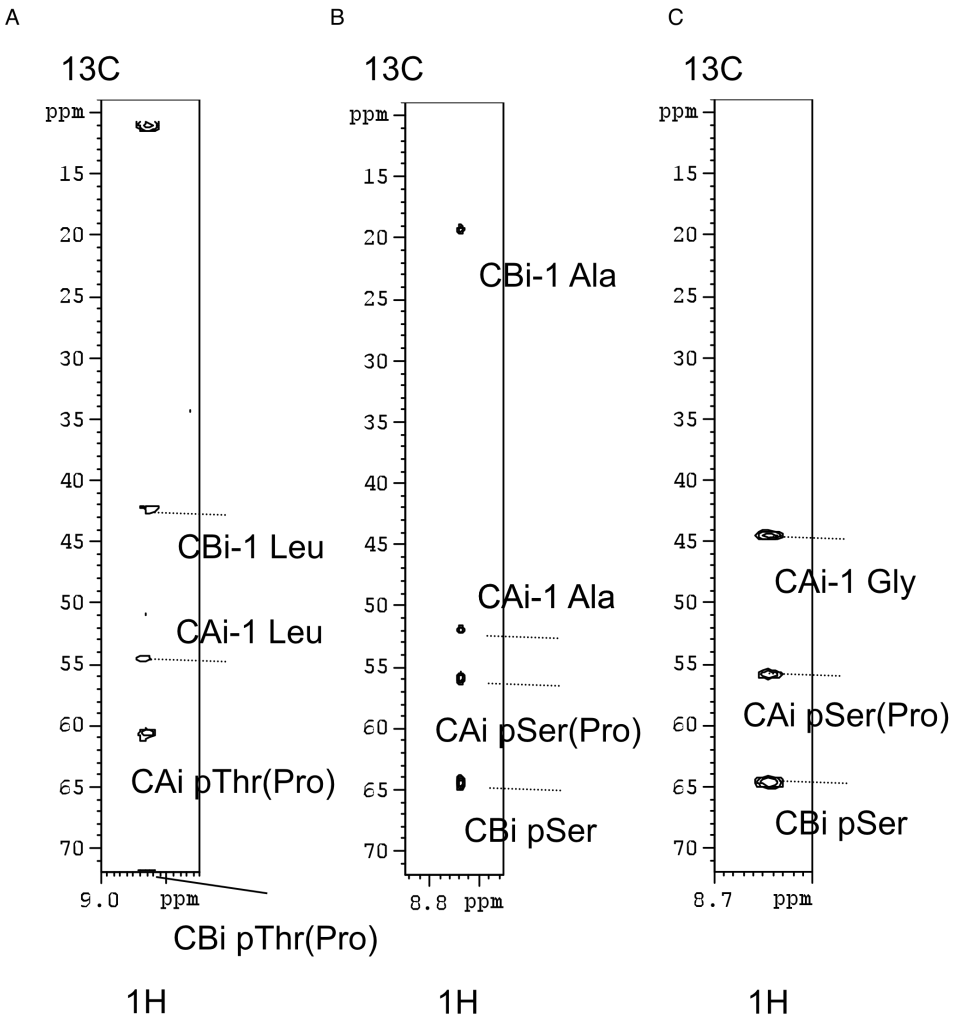

Figure 7.6: Assignment of phosphorylated residues in mNgn2.

^{13}C chemical shifts for Cα (CA) and Cβ (CB) nuclei of phosphorylated amino acid residues were assigned by Isabelle Landrieu. i: residue corresponding to 2D HSQC peak; i-1: preceding residue (N-terminal to residue i).

FoldIndex output is one prediction included in the assessment performed by the PONDR-FIT predictor (Xue et al., 2010) and so as these have two differing outputs clearly other predictors incorporating other factors may be required to produce an accurate assessment of disorder.

The purification of bHLH proteins is difficult as illustrated in (Aguado-Llera et al., 2010). The authors attempted to purify the bHLH domain of Ngn1 using His-tagged, GST-tagged, maltose binding protein-tagged, biotin-tagged and thioredoxin-tagged protein constructs in BL21, Rosetta, C41 and BL21pLys cells with induction at several different temperatures and with varying concentrations of IPTG; only one combination appeared to work at all but it turned out to be partially degraded. The authors turned to chemical synthesis of the bHLH domain of Ngn1 instead. That the purification of mNgn2 proved to be difficult was not surprising as I have made previous attempts to purify xNgn2, both using bacterial expression (with some success) and baculovirus (with none). Solubility was greatly improved using a GST-tag, and Sarkosyl-based treatment (Tao et al., 2010) can result in liberating some His-mNgn2 from the insoluble fraction of cell lysis. The strange behaviour even of the GST-tagged protein – which appears to dimerise and/or be partially degraded upon liberation from the GST tag – did not appear to affect the results of the NMR experiments. Whilst *in vitro* kinase treatment resulted in an apparent disappearance of any monomeric protein by Coomassie staining, the NMR results suggest that in fact protein is still present and effects on the structure are minimal. Dimerisation of the protein upon phosphorylation is not surprising as heterodimerisation with E12 and phosphorylation have been linked in xNgn2 before (Vosper et al., 2007).

That the NMR results have given spectra allowing identification of phosphorylated SP and TP sites in the N-terminus illustrates not only quite specific phosphorylation of consensus cdk sites *in vitro* but also that the N-terminus is disordered. It is not possible to speculate on the phosphorylation of the C-terminus because this region is not observed as a disordered region in the NMR experiment, but work by Christopher Hindley and Fahad Ali has highlighted the important role of C-terminal SP sites in particular in xNgn2 and mNgn2 (Ali et al., 2011). Therefore it is interesting to observe phosphorylation occurring on the N-terminus also. That the N-terminus if

Ngn2 is disordered also supports results in Chapter 6, where degradation of chimeric xNgn2/xNeuroD proteins showed a destabilising role for the N-terminus and bHLH of xNgn2. Therefore the N-terminus of xNgn2 may provide the unfolding initiation site required for degradation by the 26S proteasome (Prakash et al., 2004). I would like to have used different kinase concentrations, and varying time periods for incubating the protein with the kinase for *in vitro* phosphorylation, to see if one site is phosphorylated before others. Concentration dependence of cyclins on xNgn2 phosphorylation has been demonstrated (Ali et al., 2011).

In-cell NMR is even possible in *Xenopus* oocytes, an example of which again looks at Tau (Bodart et al., 2008). Structural analysis of Ngn2 could be carried out in this system to provide further information on the degree of disorder *in vivo*.

CHAPTER 8

Conclusions

xNgn2 is a transcription factor that regulates cell division and differentiation in the developing brain. The regulation of xNgn2 activity through its stability is the focus of this thesis. I have investigated the roles of ubiquitylation and phosphorylation, as well as protein folding and structural stability of xNgn2. This work has been carried out using *Xenopus laevis* extract systems and *Mus musculus* P19 embryonal carcinoma cell lines, with structural studies carried out by NMR using mNgn2.

Firstly, I demonstrated that xNgn2 is ubiquitylated on multiple lysine residues. No specific lysine is essential for ubiquitylation, including lysines conserved in the neurogenin sequence between species. Whilst mutation of all lysines to arginines renders xNgn2 more stable *in vitro*, xNgn2KO is less able to bind DNA *in vitro* (as demonstrated by EMSA) and promote ectopic neurogenesis *in vivo* (as demonstrated by embryo microinjection). Furthermore, lysineless xNgn2 is still degraded by the UPS.

Other sites are present in proteins that can act as nucleophiles and pick up Ub from the E2 enzymes. The N-terminal amino group is amino-based, identically to lysine residues, and is ubiquitylated to target xNgn2 for proteasomal degradation as demonstrated by blocking the N-terminus with cotranslational acetylation. Acetylated, lysineless xNgn2 (Ac2xNgn2KO) is still proteasomally degraded. Through ubiquitylation assays manipulating the reducing environment of gel loading buffers, non-canonical ubiquitylation through labile linkages is observed on cysteines, serines and threonines. Mutation of cysteines to alanines in xNgn2 has a stabilising effect in mitotic and neurula extracts. Non-canonical ubiquitylation is evident in wild type xNgn2. Work carried out in *Xenopus* extracts was replicated in P19 cells, yielding the same results.

xNgn2 is also modified by phosphorylation . Investigation of cdk consensus SP sites shows that mutation of all SP serines to alanines affects xNgn2 phosphorylation in mitosis. C-terminal phosphorylation sites in particular affect stability of xNgn2. The stability of xNgn2 in association with xE12 is enhanced when all SP serines are mutated to alanines although stability of xNgn2 and 9S-AxNgn2 is similar in extract. When Ub is fused to the N-terminus of xNgn2 or 9S-AxNgn2, xE12 confers the same stabilisation upon both proteins. However, 9S-AxNgn2 is hyperactive *in vivo* at promoting ectopic neurogenesis compared to xNgn2 and fusion of Ub to the N-terminus reduces but does not abolish this activity, in particular at the xNeuroD promoter. Complete inactivity of both proteins at the Delta promoter upon ubiquitylation highlights the role of phosphorylation in regulating cell differentiation, for as the cell cycle lengthens, phosphorylation of xNgn2 will reduce and xNeuroD transcription will be favoured over Delta, inducing neurogenesis and cell cycle exit.

Numerous factors such as bulky tags, xE12, Xic1 and DNA-binding affect xNgn2 stability. xNgn2 is an unstructured protein and associated factors appear to regulate stability by binding to xNgn2 and affecting structural properties to regulate proteasomal degradation. The downstream target of xNgn2, xNeuroD, whilst ubiquitylated is not degraded and domain swapping experiments between xNgn2 and xNeuroD suggest that the N-terminal domain of xNgn2 is destabilising and that the C-terminal domains of both proteins exhibit different ubiquitylation patterns, with non-canonical ubiquitylation observed on xNgn2 only. Therefore xNgn2 can be ubiquitylated on many more possible sites to allow maintenance of a short half life and rapid degradation, whilst the N-terminus may provide the unfolding initiation site required to feed into the 26S proteasome and allow proteasomal degradation.

The role of the N-terminal domain in unfolding is shown in the NMR experiments proving that the N-terminal domain of the mouse homologue, mNgn2, is disordered. This domain is also phosphorylated on cdk consensus SP and TP sites but phosphorylation does not affect the structure observed by NMR spectroscopy.

xNgn2 stability is therefore tightly regulated by many factors, regulating its activity and allowing precise control of cell fate.

BIBLIOGRAPHY

ABRAMOFF, M. D., MAGALHAES, P. J. & RAM, S. J. 2004. Image Processing with ImageJ. *Biophotonics International,* 11**,** 36-42.

ABU HATOUM, O., GROSS-MESILATY, S., BREITSCHOPF, K., HOFFMAN, A., GONEN, H., CIECHANOVER, A. & BENGAL, E. 1998. Degradation of myogenic transcription factor MyoD by the ubiquitin pathway in vivo and in vitro: regulation by specific DNA binding. *Mol Cell Biol,* 18**,** 5670-7.

AGUADO-LLERA, D., GOORMAGHTIGH, E., DE GEEST, N., QUAN, X. J., PRIETO, A., HASSAN, B. A., GOMEZ, J. & NEIRA, J. L. 2010. The basic helix-loop-helix region of human neurogenin 1 is a monomeric natively unfolded protein which forms a "fuzzy" complex upon DNA binding. *Biochemistry,* 49**,** 1577-89.

ALI, F., HINDLEY, C. J., MCDOWELL, G. S., DEIBLER, R., JONES, A., KIRSCHNER, M. W., GUILLEMOT, F. & PHILPOTT, A. 2011. Cell cycle-regulated multi-site phosphorylation of Neurogenin2 coordinates cell cycling with differentiation during neurogenesis. *Development,* 138, 4267-77.

ASPRER, J. S., LEE, B., WU, C. S., VADAKKAN, T., DICKINSON, M. E., LU, H. C. & LEE, S. K. 2011. LMO4 functions as a co-activator of neurogenin 2 in the developing cortex. *Development,* 138**,** 2823-32.

AVILES, F. J., CHAPMAN, G. E., KNEALE, G. G., CRANE-ROBINSON, C. & BRADBURY, E. M. 1978. The conformation of histone H5. Isolation and characterisation of the globular segment. *European journal of biochemistry / FEBS,* 88**,** 363-71.

BACHMAIR, A., FINLEY, D. & VARSHAVSKY, A. 1986. In vivo half-life of a protein is a function of its amino-terminal residue. *Science,* 234**,** 179-86.

BAE, Y., CHOI, D., RHIM, H. & KANG, S. 2010. Hip2 interacts with cyclin B1 and promotes its degradation through the ubiquitin proteasome pathway. *FEBS letters,* 584**,** 4505-10.

BALDI, L., BROWN, K., FRANZOSO, G. & SIEBENLIST, U. 1996. Critical role for lysines 21 and 22 in signal-induced, ubiquitin-mediated proteolysis of I kappa B-alpha. *J Biol Chem,* 271**,** 376-9.

BARNABE-HEIDER, F., WASYLNKA, J. A., FERNANDES, K. J., PORSCHE, C., SENDTNER, M., KAPLAN, D. R. & MILLER, F. D. 2005. Evidence that embryonic neurons regulate the onset of cortical gliogenesis via cardiotrophin-1. *Neuron,* 48**,** 253-65.

BASHIR, T., DORRELLO, N. V., AMADOR, V., GUARDAVACCARO, D. & PAGANO, M. 2004. Control of the SCF(Skp2-Cks1) ubiquitin ligase by the APC/C(Cdh1) ubiquitin ligase. *Nature,* 428**,** 190-3.

BASSERMANN, F., FRESCAS, D., GUARDAVACCARO, D., BUSINO, L., PESCHIAROLI, A. & PAGANO, M. 2008. The Cdc14B-Cdh1-Plk1 axis controls the G2 DNA-damage-response checkpoint. *Cell,* 134**,** 256-67.

BATONNET, S., LEIBOVITCH, M. P., TINTIGNAC, L. & LEIBOVITCH, S. A. 2004. Critical role for lysine 133 in the nuclear ubiquitin-mediated degradation of MyoD. *The Journal of biological chemistry,* 279**,** 5413-20.

BECK, C. W. & SLACK, J. M. 2001. An amphibian with ambition: a new role for Xenopus in the 21st century. *Genome Biol,* 2**,** REVIEWS1029.

BELLEFROID, E. J., BOURGUIGNON, C., HOLLEMANN, T., MA, Q., ANDERSON, D. J., KINTNER, C. & PIELER, T. 1996. X-MyT1, a Xenopus C2HC-type zinc finger protein with a regulatory function in neuronal differentiation. *Cell,* 87**,** 1191-202.

BEN-SAADON, R., FAJERMAN, I., ZIV, T., HELLMAN, U., SCHWARTZ, A. L. & CIECHANOVER, A. 2004. The tumor suppressor protein p16(INK4a) and the human papillomavirus oncoprotein-58 E7 are naturally occurring lysine-less proteins that are degraded by the ubiquitin system. Direct evidence for ubiquitination at the N-terminal residue. *The Journal of biological chemistry,* 279**,** 41414-21.

BENEZRA, R. 1994. An intermolecular disulfide bond stabilizes E2A homodimers and is required for DNA binding at physiological temperatures. *Cell,* 79**,** 1057-67.

BENEZRA, R., DAVIS, R. L., LOCKSHON, D., TURNER, D. L. & WEINTRAUB, H. 1990. The protein Id: a negative regulator of helix-loop-helix DNA binding proteins. *Cell,* 61**,** 49-59.

BERSE, M., BOUNPHENG, M., HUANG, X., CHRISTY, B., POLLMANN, C. & DUBIEL, W. 2004. Ubiquitin-dependent degradation of Id1 and Id3 is mediated by the COP9 signalosome. *J Mol Biol,* 343**,** 361-70.

BERTRAND, N., CASTRO, D. S. & GUILLEMOT, F. 2002. Proneural genes and the specification of neural cell types. *Nat Rev Neurosci,* 3**,** 517-30.

BHANDARI, R. K., SADLER-RIGGLEMAN, I., CLEMENT, T. M. & SKINNER, M. K. 2011. Basic Helix-Loop-Helix Transcription Factor TCF21 Is a Downstream Target of the Male Sex Determining Gene SRY. *PloS one,* 6**,** e19935.

BHAVESH, N. S., PANCHAL, S. C. & HOSUR, R. V. 2001. An efficient high-throughput resonance assignment procedure for structural genomics and protein folding research by NMR. *Biochemistry,* 40**,** 14727-35.

BIENKIEWICZ, E. A. & LUMB, K. J. 1999. Random-coil chemical shifts of phosphorylated amino acids. *Journal of biomolecular NMR,* 15**,** 203-6.

BLOOMER, A. C., CHAMPNESS, J. N., BRICOGNE, G., STADEN, R. & KLUG, A. 1978. Protein disk of tobacco mosaic virus at 2.8 A resolution showing the interactions within and between subunits. *Nature,* 276**,** 362-8.

BODART, J. F., WIERUSZESKI, J. M., AMNIAI, L., LEROY, A., LANDRIEU, I., ROUSSEAU-LESCUYER, A., VILAIN, J. P. & LIPPENS, G. 2008. NMR observation of Tau in Xenopus oocytes. *Journal of magnetic resonance,* 192**,** 252-7.

BONNI, A., SUN, Y., NADAL-VICENS, M., BHATT, A., FRANK, D. A., ROZOVSKY, I., STAHL, N., YANCOPOULOS, G. D. & GREENBERG, M. E. 1997. Regulation of gliogenesis in the central nervous system by the JAK-STAT signaling pathway. *Science,* 278**,** 477-83.

BORNSTEIN, G., BLOOM, J., SITRY-SHEVAH, D., NAKAYAMA, K., PAGANO, M. & HERSHKO, A. 2003. Role of the SCFSkp2 ubiquitin ligase in the degradation of p21Cip1 in S phase. *The Journal of biological chemistry,* 278**,** 25752-7.

BOUNPHENG, M. A., DIMAS, J. J., DODDS, S. G. & CHRISTY, B. A. 1999. Degradation of Id proteins by the ubiquitin-proteasome pathway. *The FASEB journal : official publication of the Federation of American Societies for Experimental Biology,* 13**,** 2257-64.

BRADSHAW, R. A., BRICKEY, W. W. & WALKER, K. W. 1998. N-terminal processing: the methionine aminopeptidase and N alpha-acetyl transferase families. *Trends Biochem Sci,* 23**,** 263-7.

BRAUN, B. C., GLICKMAN, M., KRAFT, R., DAHLMANN, B., KLOETZEL, P. M., FINLEY, D. & SCHMIDT, M. 1999. The base of the proteasome regulatory particle exhibits chaperone-like activity. *Nature cell biology,* 1**,** 221-6.

BREITSCHOPF, K., BENGAL, E., ZIV, T., ADMON, A. & CIECHANOVER, A. 1998. A novel site for ubiquitination: the N-terminal residue, and not internal lysines of MyoD, is essential for conjugation and degradation of the protein. *Embo J,* 17**,** 5964-73.

BROWN, C. J., TAKAYAMA, S., CAMPEN, A. M., VISE, P., MARSHALL, T. W., OLDFIELD, C. J., WILLIAMS, C. J. & DUNKER, A. K. 2002. Evolutionary rate heterogeneity in proteins with long disordered regions. *Journal of molecular evolution,* 55**,** 104-10.

CADWELL, K. & COSCOY, L. 2005. Ubiquitination on nonlysine residues by a viral E3 ubiquitin ligase. *Science,* 309**,** 127-30.

CADWELL, K. & COSCOY, L. 2008. The specificities of Kaposi's sarcoma-associated herpesvirus-encoded E3 ubiquitin ligases are determined by the positions of lysine or cysteine residues within the intracytoplasmic domains of their targets. *J Virol,* 82**,** 4184-9.

CAI, Y., HUANG, T., HU, L., SHI, X., XIE, L. & LI, Y. 2011. Prediction of lysine ubiquitination with mRMR feature selection and analysis. *Amino acids*.

CALLERY, E. M. 2006. There's more than one frog in the pond: a survey of the Amphibia and their contributions to developmental biology. *Semin Cell Dev Biol,* 17**,** 80-92.

CANE, D. E. & WALSH, C. T. 1999. The parallel and convergent universes of polyketide synthases and nonribosomal peptide synthetases. *Chemistry & biology,* 6**,** R319-25.

CARVALHO, A. F., PINTO, M. P., GROU, C. P., ALENCASTRE, I. S., FRANSEN, M., SA-MIRANDA, C. & AZEVEDO, J. E. 2007. Ubiquitination of mammalian Pex5p, the peroxisomal import receptor. *J Biol Chem,* 282**,** 31267-72.

CAU, E., GRADWOHL, G., FODE, C. & GUILLEMOT, F. 1997. Mash1 activates a cascade of bHLH regulators in olfactory neuron progenitors. *Development,* 124**,** 1611-21.

CAVANAGH, J., FAIRBROTHER, W. J., PALMER, A. G., SKELTON, N. J. & RANCE, M. 2006. *Protein NMR Spectroscopy, Second Edition: Principles and Practice*, Academic Press.

CHEN, X., CHI, Y., BLOECHER, A., AEBERSOLD, R., CLURMAN, B. E. & ROBERTS, J. M. 2004. N-acetylation and ubiquitin-independent proteasomal degradation of p21(Cip1). *Mol Cell,* 16**,** 839-47.

CHENNA, R., SUGAWARA, H., KOIKE, T., LOPEZ, R., GIBSON, T. J., HIGGINS, D. G. & THOMPSON, J. D. 2003. Multiple sequence alignment with the Clustal series of programs. *Nucleic acids research,* 31**,** 3497-500.

CHITNIS, A. & KINTNER, C. 1996. Sensitivity of proneural genes to lateral inhibition affects the pattern of primary neurons in Xenopus embryos. *Development,* 122**,** 2295-301.

CHITNIS, A. B. 1999. Control of neurogenesis--lessons from frogs, fish and flies. *Curr Opin Neurobiol,* 9**,** 18-25.

CHU, I., SUN, J., ARNAOUT, A., KAHN, H., HANNA, W., NAROD, S., SUN, P., TAN, C. K., HENGST, L. & SLINGERLAND, J. 2007. p27 phosphorylation by Src regulates inhibition of cyclin E-Cdk2. *Cell,* 128**,** 281-94.

CIECHANOVER, A. 1994. The ubiquitin-proteasome proteolytic pathway. *Cell,* 79**,** 13-21.

CIECHANOVER, A. & BEN-SAADON, R. 2004. N-terminal ubiquitination: more protein substrates join in. *Trends Cell Biol,* 14**,** 103-6.

CIECHANOVER, A., HELLER, H., KATZ-ETZION, R. & HERSHKO, A. 1981. Activation of the heat-stable polypeptide of the ATP-dependent proteolytic system. *Proc Natl Acad Sci U S A,* 78**,** 761-5.

CIECHANOVER, A., HOD, Y. & HERSHKO, A. 1978. A heat-stable polypeptide component of an ATP-dependent proteolytic system from reticulocytes. *Biochemical and biophysical research communications,* 81**,** 1100-5.

CLAYDEN, J., GREEVES, N., WARREN, S. & WOTHERS, P. 2000. *Organic Chemistry,* Oxford, Oxford University Press.

CLURMAN, B. E., SHEAFF, R. J., THRESS, K., GROUDINE, M. & ROBERTS, J. M. 1996. Turnover of cyclin E by the ubiquitin-proteasome pathway is regulated by cdk2 binding and cyclin phosphorylation. *Genes & development,* 10**,** 1979-90.

COSTER, G., HAYOUKA, Z., ARGAMAN, L., STRAUSS, C., FRIEDLER, A., BRANDEIS, M. & GOLDBERG, M. 2007. The DNA damage response mediator MDC1 directly interacts with the anaphase-promoting complex/cyclosome. *The Journal of biological chemistry,* 282**,** 32053-64.

COTTLE, D. L., MCGRATH, M. J., COWLING, B. S., COGHILL, I. D., BROWN, S. & MITCHELL, C. A. 2007. FHL3 binds MyoD and negatively regulates myotube formation. *Journal of cell science,* 120**,** 1423-35.

COUX, O., TANAKA, K. & GOLDBERG, A. L. 1996. Structure and functions of the 20S and 26S proteasomes. *Annual review of biochemistry,* 65**,** 801-47.

CUTRESS, M. L., WHITAKER, H. C., MILLS, I. G., STEWART, M. & NEAL, D. E. 2008. Structural basis for the nuclear import of the human androgen receptor. *Journal of cell science,* 121**,** 957-68.

DAVID, Y., ZIV, T., ADMON, A. & NAVON, A. 2010. The E2 ubiquitin-conjugating enzymes direct polyubiquitination to preferred lysines. *The Journal of biological chemistry,* 285**,** 8595-604.

DENG, L., WANG, C., SPENCER, E., YANG, L., BRAUN, A., YOU, J., SLAUGHTER, C., PICKART, C. & CHEN, Z. J. 2000. Activation of the IkappaB kinase complex by TRAF6 requires a dimeric ubiquitin-conjugating enzyme complex and a unique polyubiquitin chain. *Cell,* 103**,** 351-61.

DIEHL, J. A., ZINDY, F. & SHERR, C. J. 1997. Inhibition of cyclin D1 phosphorylation on threonine-286 prevents its rapid degradation via the ubiquitin-proteasome pathway. *Genes & development,* 11**,** 957-72.

DILL, K. A., OZKAN, S. B., SHELL, M. S. & WEIKL, T. R. 2008. The protein folding problem. *Annual review of biophysics,* 37**,** 289-316.

DINGWALL, C. & LASKEY, R. A. 1991. Nuclear targeting sequences--a consensus? *Trends in biochemical sciences,* 16**,** 478-81.

DULHANTY, A. M. & RIORDAN, J. R. 1994. Phosphorylation by cAMP-dependent protein kinase causes a conformational change in the R domain of the cystic fibrosis transmembrane conductance regulator. *Biochemistry,* 33**,** 4072-9.

DUNKER, A. K., BROWN, C. J., LAWSON, J. D., IAKOUCHEVA, L. M. & OBRADOVIC, Z. 2002. Intrinsic disorder and protein function. *Biochemistry,* 41**,** 6573-82.

DUNKER, A. K., LAWSON, J. D., BROWN, C. J., WILLIAMS, R. M., ROMERO, P., OH, J. S., OLDFIELD, C. J., CAMPEN, A. M., RATLIFF, C. M., HIPPS, K. W., AUSIO, J., NISSEN, M. S., REEVES, R., KANG, C., KISSINGER, C. R., BAILEY, R. W., GRISWOLD, M. D., CHIU, W., GARNER, E. C. & OBRADOVIC, Z. 2001. Intrinsically disordered protein. *Journal of molecular graphics & modelling,* 19**,** 26-59.

DUNKER, A. K., OLDFIELD, C. J., MENG, J., ROMERO, P., YANG, J. Y., CHEN, J. W., VACIC, V., OBRADOVIC, Z. & UVERSKY, V. N. 2008a. The unfoldomics decade: an update on intrinsically disordered proteins. *BMC genomics,* 9 Suppl 2**,** S1.

DUNKER, A. K., SILMAN, I., UVERSKY, V. N. & SUSSMAN, J. L. 2008b. Function and structure of inherently disordered proteins. *Current opinion in structural biology,* 18**,** 756-64.

DYSON, H. J. & WRIGHT, P. E. 2004. Unfolded proteins and protein folding studied by NMR. *Chemical reviews,* 104**,** 3607-22.

DYSON, H. J. & WRIGHT, P. E. 2005a. Elucidation of the protein folding landscape by NMR. *Methods in enzymology,* 394**,** 299-321.

DYSON, H. J. & WRIGHT, P. E. 2005b. Intrinsically unstructured proteins and their functions. *Nature reviews. Molecular cell biology,* 6**,** 197-208.

DYSON, H. J. & WRIGHT, P. E. 2006. According to current textbooks, a well-defined three-dimensional structure is a prerequisite for the function of a protein. Is this correct? *IUBMB life,* 58**,** 107-9.

DYSON, H. J., WRIGHT, P. E. & SCHERAGA, H. A. 2006. The role of hydrophobic interactions in initiation and propagation of protein folding. *Proceedings of the National Academy of Sciences of the United States of America,* 103**,** 13057-61.

ELLENBERGER, T., FASS, D., ARNAUD, M. & HARRISON, S. C. 1994. Crystal structure of transcription factor E47: E-box recognition by a basic region helix-loop-helix dimer. *Genes & development,* 8**,** 970-80.

ERRICO, A., DESHMUKH, K., TANAKA, Y., POZNIAKOVSKY, A. & HUNT, T. 2010. Identification of substrates for cyclin dependent kinases. *Advances in enzyme regulation,* 50**,** 375-99.

EVANS, T., ROSENTHAL, E. T., YOUNGBLOM, J., DISTEL, D. & HUNT, T. 1983. Cyclin: a protein specified by maternal mRNA in sea urchin eggs that is destroyed at each cleavage division. *Cell,* 33**,** 389-96.

FALK, A., HOLMSTROM, N., CARLEN, M., CASSIDY, R., LUNDBERG, C. & FRISEN, J. 2002. Gene delivery to adult neural stem cells. *Experimental cell research,* 279**,** 34-9.

FARAH, M. H., OLSON, J. M., SUCIC, H. B., HUME, R. I., TAPSCOTT, S. J. & TURNER, D. L. 2000. Generation of neurons by transient expression of neural bHLH proteins in mammalian cells. *Development,* 127**,** 693-702.

FAX, P., LEHMKUHLER, O., KUHN, C., ESCHE, H. & BROCKMANN, D. 2000. E1A12S-mediated activation of the adenovirus type 12 E2 promoter depends on the histone acetyltransferase activity of p300/CBP. *The Journal of biological chemistry,* 275**,** 40554-60.

FERBER, S. & CIECHANOVER, A. 1987. Role of arginine-tRNA in protein degradation by the ubiquitin pathway. *Nature,* 326**,** 808-11.

FODE, C., GRADWOHL, G., MORIN, X., DIERICH, A., LEMEUR, M., GORIDIS, C. & GUILLEMOT, F. 1998. The bHLH protein NEUROGENIN 2 is a determination factor for epibranchial placode-derived sensory neurons. *Neuron,* 20**,** 483-94.

FODE, C., MA, Q., CASAROSA, S., ANG, S. L., ANDERSON, D. J. & GUILLEMOT, F. 2000. A role for neural determination genes in specifying the dorsoventral identity of telencephalic neurons. *Genes & development,* 14**,** 67-80.

FOLIN, O. 1905. A theory of protein metabolism. *J. Am. Physiol.,* 13**,** 117-138.

FREIMAN, R. N. & TJIAN, R. 2003. Regulating the regulators: lysine modifications make their mark. *Cell,* 112**,** 11-7.

GALEA, C. A., WANG, Y., SIVAKOLUNDU, S. G. & KRIWACKI, R. W. 2008. Regulation of cell division by intrinsically unstructured proteins: intrinsic flexibility, modularity, and signaling conduits. *Biochemistry,* 47**,** 7598-609.

GARCIA-HIGUERA, I., MANCHADO, E., DUBUS, P., CANAMERO, M., MENDEZ, J., MORENO, S. & MALUMBRES, M. 2008. Genomic stability and tumour suppression by the APC/C cofactor Cdh1. *Nature cell biology,* 10**,** 802-11.

GARRELL, J. & MODOLELL, J. 1990. The Drosophila extramacrochaetae locus, an antagonist of proneural genes that, like these genes, encodes a helix-loop-helix protein. *Cell,* 61**,** 39-48.

GAST, K., DAMASCHUN, H., ECKERT, K., SCHULZE-FORSTER, K., MAURER, H. R., MULLER-FROHNE, M., ZIRWER, D., CZARNECKI, J. & DAMASCHUN, G. 1995. Prothymosin alpha: a biologically active protein with random coil conformation. *Biochemistry,* 34**,** 13211-8.

GERMANN, U. A., CHAMBERS, T. C., AMBUDKAR, S. V., LICHT, T., CARDARELLI, C. O., PASTAN, I. & GOTTESMAN, M. M. 1996. Characterization of phosphorylation-defective mutants of human P-glycoprotein expressed in mammalian cells. *The Journal of biological chemistry,* 271**,** 1708-16.

GLICKMAN, M. H. & CIECHANOVER, A. 2002. The ubiquitin-proteasome proteolytic pathway: destruction for the sake of construction. *Physiological Reviews,* 82**,** 373-428.

GLICKMAN, M. H., RUBIN, D. M., COUX, O., WEFES, I., PFEIFER, G., CJEKA, Z., BAUMEISTER, W., FRIED, V. A. & FINLEY, D. 1998. A subcomplex of the proteasome regulatory particle required for ubiquitin-conjugate degradation and related to the COP9-signalosome and eIF3. *Cell,* 94**,** 615-23.

GLOTZER, M., MURRAY, A. W. & KIRSCHNER, M. W. 1991. Cyclin is degraded by the ubiquitin pathway. *Nature,* 349**,** 132-8.

GOMEZ-DEL ARCO, P., MAKI, K. & GEORGOPOULOS, K. 2004. Phosphorylation controls Ikaros's ability to negatively regulate the G(1)-S transition. *Molecular and cellular biology,* 24**,** 2797-807.

GOTZ, M. & BARDE, Y. A. 2005. Radial glial cells defined and major intermediates between embryonic stem cells and CNS neurons. *Neuron,* 46**,** 369-72.

GOWAN, K., HELMS, A. W., HUNSAKER, T. L., COLLISSON, T., EBERT, P. J., ODOM, R. & JOHNSON, J. E. 2001. Crossinhibitory activities of Ngn1 and Math1 allow specification of distinct dorsal interneurons. *Neuron,* 31**,** 219-32.

GRABBE, C., HUSNJAK, K. & DIKIC, I. 2011. The spatial and temporal organization of ubiquitin networks. *Nature reviews. Molecular cell biology,* 12**,** 295-307.

GRADWOHL, G., DIERICH, A., LEMEUR, M. & GUILLEMOT, F. 2000. neurogenin3 is required for the development of the four endocrine cell lineages of the pancreas. *Proceedings of the National Academy of Sciences of the United States of America,* 97**,** 1607-11.

GRIMMLER, M., WANG, Y., MUND, T., CILENSEK, Z., KEIDEL, E. M., WADDELL, M. B., JAKEL, H., KULLMANN, M., KRIWACKI, R. W. & HENGST, L. 2007. Cdk-inhibitory activity and stability of p27Kip1 are directly regulated by oncogenic tyrosine kinases. *Cell,* 128**,** 269-80.

GROSS, C. G. 2000. Neurogenesis in the adult brain: death of a dogma. *Nat Rev Neurosci,* 1**,** 67-73.

GROSSMAN, S. R., DEATO, M. E., BRIGNONE, C., CHAN, H. M., KUNG, A. L., TAGAMI, H., NAKATANI, Y. & LIVINGSTON, D. M. 2003. Polyubiquitination of p53 by a ubiquitin ligase activity of p300. *Science,* 300**,** 342-4.

GROU, C. P., CARVALHO, A. F., PINTO, M. P., WIESE, S., PIECHURA, H., MEYER, H. E., WARSCHEID, B., SA-MIRANDA, C. & AZEVEDO, J. E. 2008. Members of the E2D (UbcH5) family mediate the ubiquitination of the conserved cysteine of Pex5p, the peroxisomal import receptor. *J Biol Chem,* 283**,** 14190-7.

GSPONER, J., FUTSCHIK, M. E., TEICHMANN, S. A. & BABU, M. M. 2008. Tight regulation of unstructured proteins: from transcript synthesis to protein degradation. *Science,* 322**,** 1365-8.

HAGAI, T. & LEVY, Y. 2010. Ubiquitin not only serves as a tag but also assists degradation by inducing protein unfolding. *Proceedings of the National Academy of Sciences of the United States of America,* 107**,** 2001-6.

HAGER, G. L., MCNALLY, J. G. & MISTELI, T. 2009. Transcription dynamics. *Molecular cell,* 35**,** 741-53.

HAGLUND, K. & DIKIC, I. 2005. Ubiquitylation and cell signaling. *Embo J,* 24**,** 3353-9.

HAND, R., BORTONE, D., MATTAR, P., NGUYEN, L., HENG, J. I., GUERRIER, S., BOUTT, E., PETERS, E., BARNES, A. P., PARRAS, C., SCHUURMANS, C., GUILLEMOT, F. & POLLEUX, F. 2005. Phosphorylation of Neurogenin2 specifies the migration properties and the dendritic morphology of pyramidal neurons in the neocortex. *Neuron,* 48**,** 45-62.

HANOULLE, X., VERDEGEM, D., BADILLO, A., WIERUSZESKI, J. M., PENIN, F. & LIPPENS, G. 2009. Domain 3 of non-structural protein 5A from hepatitis C virus is natively unfolded. *Biochemical and biophysical research communications,* 381**,** 634-8.

HASSAN, B. A. & BELLEN, H. J. 2000. Doing the MATH: is the mouse a good model for fly development? *Genes Dev,* 14**,** 1852-65.

HEEMERS, H. V. & TINDALL, D. J. 2007. Androgen receptor (AR) coregulators: a diversity of functions converging on and regulating the AR transcriptional complex. *Endocrine reviews,* 28**,** 778-808.

HELMS, A. W., BATTISTE, J., HENKE, R. M., NAKADA, Y., SIMPLICIO, N., GUILLEMOT, F. & JOHNSON, J. E. 2005. Sequential roles for Mash1 and Ngn2 in the generation of dorsal spinal cord interneurons. *Development,* 132**,** 2709-19.

HENG, J. I., NGUYEN, L., CASTRO, D. S., ZIMMER, C., WILDNER, H., ARMANT, O., SKOWRONSKA-KRAWCZYK, D., BEDOGNI, F., MATTER, J. M., HEVNER, R. &

GUILLEMOT, F. 2008. Neurogenin 2 controls cortical neuron migration through regulation of Rnd2. *Nature,* 455**,** 114-8.

HERSHKO, A. 1988. Ubiquitin-mediated protein degradation. *The Journal of biological chemistry,* 263**,** 15237-40.

HERSHKO, A. & CIECHANOVER, A. 1998. THE UBIQUITIN SYSTEM. *Annual review of biochemistry,* 67**,** 425-479.

HERSHKO, A., CIECHANOVER, A., HELLER, H., HAAS, A. L. & ROSE, I. A. 1980. Proposed role of ATP in protein breakdown: conjugation of protein with multiple chains of the polypeptide of ATP-dependent proteolysis. *Proc Natl Acad Sci U S A,* 77**,** 1783-6.

HERSHKO, A., CIECHANOVER, A. & ROSE, I. A. 1981. Identification of the active amino acid residue of the polypeptide of ATP-dependent protein breakdown. *J Biol Chem,* 256**,** 1525-8.

HERSHKO, A., GANOTH, D., PEHRSON, J., PALAZZO, R. E. & COHEN, L. H. 1991. Methylated ubiquitin inhibits cyclin degradation in clam embryo extracts. *The Journal of biological chemistry,* 266**,** 16376-9.

HERSHKO, A., GANOTH, D., SUDAKIN, V., DAHAN, A., COHEN, L. H., LUCA, F. C., RUDERMAN, J. V. & EYTAN, E. 1994. Components of a system that ligates cyclin to ubiquitin and their regulation by the protein kinase cdc2. *The Journal of biological chemistry,* 269**,** 4940-6.

HERSHKO, A., HELLER, H., ELIAS, S. & CIECHANOVER, A. 1983. Components of ubiquitin-protein ligase system. Resolution, affinity purification, and role in protein breakdown. *J Biol Chem,* 258**,** 8206-14.

HERSHKO, A., HELLER, H., EYTAN, E. & REISS, Y. 1986. The protein substrate binding site of the ubiquitin-protein ligase system. *The Journal of biological chemistry,* 261**,** 11992-9.

HERSHKO, A., LESHINSKY, E., GANOTH, D. & HELLER, H. 1984. ATP-dependent degradation of ubiquitin-protein conjugates. *Proceedings of the National Academy of Sciences of the United States of America,* 81**,** 1619-23.

HERSHKO, A. & TOMKINS, G. M. 1971. Studies on the degradation of tyrosine aminotransferase in hepatoma cells in culture. Influence of the composition of the medium and adenosine triphosphate dependence. *The Journal of biological chemistry,* 246**,** 710-4.

HICKE, L. & DUNN, R. 2003. Regulation of membrane protein transport by ubiquitin and ubiquitin-binding proteins. *Annual review of cell and developmental biology,* 19**,** 141-72.

HINDLEY, C. J. 2011. *Regulation of the proneural protein xNgn2 by cell cycle-mediated phosphorylation.* PhD, University of Cambridge.

HINDLEY, C. J., MCDOWELL, G. S., WISE, H. & PHILPOTT, A. 2011. Regulation of cell fate determination by Skp1-Cullin1-F-box (SCF) E3 ubiquitin ligases. *The International journal of developmental biology,* 55**,** 249-60.

HOFSTETTER, C. P., HOLMSTROM, N. A., LILJA, J. A., SCHWEINHARDT, P., HAO, J., SPENGER, C., WIESENFELD-HALLIN, Z., KURPAD, S. N., FRISEN, J. & OLSON, L. 2005. Allodynia limits the usefulness of intraspinal neural stem cell grafts; directed differentiation improves outcome. *Nature neuroscience,* 8**,** 346-53.

HOGNESS, D. S., COHN, M. & MONOD, J. 1955. Studies on the induced synthesis of beta-galactosidase in Escherichia coli: the kinetics and mechanism of sulfur incorporation. *Biochimica et biophysica acta,* 16**,** 99-116.

HOLLAND, L. Z., SCHUBERT, M., HOLLAND, N. D. & NEUMAN, T. 2000. Evolutionary conservation of the presumptive neural plate markers AmphiSox1/2/3 and AmphiNeurogenin in the invertebrate chordate amphioxus. *Dev Biol,* 226**,** 18-33.

HONG, J., ZHOU, J., FU, J., HE, T., QIN, J., WANG, L., LIAO, L. & XU, J. 2011. Phosphorylation of Serine 68 of Twist1 by MAPKs Stabilizes Twist1 Protein and Promotes Breast Cancer Cell Invasiveness. *Cancer research,* 71**,** 3980-90.

HU, Y., WANG, T., STORMO, G. D. & GORDON, J. I. 2004. RNA interference of achaete-scute homolog 1 in mouse prostate neuroendocrine cells reveals its gene targets and DNA binding sites. *Proc Natl Acad Sci U S A,* 101**,** 5559-64.

HUANG, W. & ERIKSON, R. L. 1994. Constitutive activation of Mek1 by mutation of serine phosphorylation sites. *Proceedings of the National Academy of Sciences of the United States of America,* 91**,** 8960-3.

HUBER, A. H., STEWART, D. B., LAURENTS, D. V., NELSON, W. J. & WEIS, W. I. 2001. The cadherin cytoplasmic domain is unstructured in the absence of beta-catenin. A possible mechanism for regulating cadherin turnover. *The Journal of biological chemistry,* 276**,** 12301-9.

HUIBREGTSE, J. M., SCHEFFNER, M., BEAUDENON, S. & HOWLEY, P. M. 1995. A family of proteins structurally and functionally related to the E6-AP ubiquitin-protein ligase. *Proc Natl Acad Sci U S A,* 92**,** 2563-7.

HUNTER, T. 2007. The age of crosstalk: phosphorylation, ubiquitination, and beyond. *Mol Cell,* 28**,** 730-8.

HWANG, J., WINKLER, L. & KALEJTA, R. F. 2011. Ubiquitin-independent proteasomal degradation during oncogenic viral infections. *Biochimica et biophysica acta,* 1816**,** 147-157.

IAKOUCHEVA, L. M., RADIVOJAC, P., BROWN, C. J., O'CONNOR, T. R., SIKES, J. G., OBRADOVIC, Z. & DUNKER, A. K. 2004. The importance of intrinsic disorder for protein phosphorylation. *Nucleic acids research,* 32**,** 1037-49.

IK TSEN HENG, J. & TAN, S. S. 2003. The role of class I HLH genes in neural development--have they been overlooked? *Bioessays,* 25**,** 709-16.

IMAYOSHI, I. & KAGEYAMA, R. 2011. The role of notch signaling in adult neurogenesis. *Molecular neurobiology,* 44**,** 7-12.

ISHIKURA, S., WEISSMAN, A. M. & BONIFACINO, J. S. 2010. Serine residues in the cytosolic tail of the T-cell antigen receptor alpha-chain mediate ubiquitination and endoplasmic reticulum-associated degradation of the unassembled protein. *The Journal of biological chemistry,* 285**,** 23916-24.

JACKSON, P. K., ELDRIDGE, A. G., FREED, E., FURSTENTHAL, L., HSU, J. Y., KAISER, B. K. & REIMANN, J. D. 2000. The lore of the RINGs: substrate recognition and catalysis by ubiquitin ligases. *Trends in cell biology,* 10**,** 429-39.

JARIEL-ENCONTRE, I., BOSSIS, G. & PIECHACZYK, M. 2008. Ubiquitin-independent degradation of proteins by the proteasome. *Biochimica et biophysica acta,* 1786**,** 153-77.

JENNY, M., UHL, C., ROCHE, C., DULUC, I., GUILLERMIN, V., GUILLEMOT, F., JENSEN, J., KEDINGER, M. & GRADWOHL, G. 2002. Neurogenin3 is differentially required for endocrine cell fate specification in the intestinal and gastric epithelium. *The EMBO journal,* 21**,** 6338-47.

JESSELL, T. M. 2000. Neuronal specification in the spinal cord: inductive signals and transcriptional codes. *Nature reviews. Genetics,* 1**,** 20-9.

JIMENEZ, G. S., KHAN, S. H., STOMMEL, J. M. & WAHL, G. M. 1999. p53 regulation by post-translational modification and nuclear retention in response to diverse stresses. *Oncogene,* 18**,** 7656-65.

JOHNSON, E. S. 2004. PROTEIN MODIFICATION BY SUMO. *Annual review of biochemistry,* 73**,** 355-382.

JOHNSON, E. S., BARTEL, B., SEUFERT, W. & VARSHAVSKY, A. 1992. Ubiquitin as a degradation signal. *The EMBO journal,* 11**,** 497-505.

JOHNSON, E. S., MA, P. C., OTA, I. M. & VARSHAVSKY, A. 1995. A proteolytic pathway that recognizes ubiquitin as a degradation signal. *The Journal of biological chemistry,* 270**,** 17442-56.

JONES, S. 2004. An overview of the basic helix-loop-helix proteins. *Genome biology,* 5**,** 226.

JONES-VILLENEUVE, E. M., MCBURNEY, M. W., ROGERS, K. A. & KALNINS, V. I. 1982. Retinoic acid induces embryonal carcinoma cells to differentiate into neurons and glial cells. *The Journal of cell biology,* 94**,** 253-62.

JUSTICE, N. J. & JAN, Y. N. 2002. Variations on the Notch pathway in neural development. *Curr Opin Neurobiol,* 12**,** 64-70.

KAELIN, W. G., JR., KREK, W., SELLERS, W. R., DECAPRIO, J. A., AJCHENBAUM, F., FUCHS, C. S., CHITTENDEN, T., LI, Y., FARNHAM, P. J., BLANAR, M. A. & ET AL. 1992. Expression cloning of a cDNA encoding a retinoblastoma-binding protein with E2F-like properties. *Cell,* 70**,** 351-64.

KAGEYAMA, R. & NAKANISHI, S. 1997. Helix-loop-helix factors in growth and differentiation of the vertebrate nervous system. *Curr Opin Genet Dev,* 7**,** 659-65.

KATZMANN, D. J., ODORIZZI, G. & EMR, S. D. 2002. Receptor downregulation and multivesicular-body sorting. *Nature reviews. Molecular cell biology,* 3**,** 893-905.

KELE, J., SIMPLICIO, N., FERRI, A. L., MIRA, H., GUILLEMOT, F., ARENAS, E. & ANG, S. L. 2006. Neurogenin 2 is required for the development of ventral midbrain dopaminergic neurons. *Development,* 133**,** 495-505.

KENNELLY, P. J. & KREBS, E. G. 1991. Consensus sequences as substrate specificity determinants for protein kinases and protein phosphatases. *The Journal of biological chemistry,* 266**,** 15555-8.

KERSCHER, O., FELBERBAUM, R. & HOCHSTRASSER, M. 2006. Modification of proteins by ubiquitin and ubiquitin-like proteins. *Annu Rev Cell Dev Biol,* 22**,** 159-80.

KHO, C. J., HUGGINS, G. S., ENDEGE, W. O., HSIEH, C. M., LEE, M. E. & HABER, E. 1997. Degradation of E2A proteins through a ubiquitin-conjugating enzyme, UbcE2A. *J Biol Chem,* 272**,** 3845-51.

KHOUDOLI, G. A., GILLESPIE, P. J., STEWART, G., ANDERSEN, J. S., SWEDLOW, J. R. & BLOW, J. J. 2008. Temporal profiling of the chromatin proteome reveals system-wide responses to replication inhibition. *Current biology : CB,* 18**,** 838-43.

KIM, H. J., SUGIMORI, M., NAKAFUKU, M. & SVENDSEN, C. N. 2007. Control of neurogenesis and tyrosine hydroxylase expression in neural progenitor cells through bHLH proteins and Nurr1. *Experimental neurology,* 203**,** 394-405.

KIMATA, Y., TRICKEY, M., IZAWA, D., GANNON, J., YAMAMOTO, M. & YAMANO, H. 2008. A mutual inhibition between APC/C and its substrate Mes1 required for meiotic progression in fission yeast. *Dev Cell,* 14**,** 446-54.

KING, R. W., GLOTZER, M. & KIRSCHNER, M. W. 1996. Mutagenic analysis of the destruction signal of mitotic cyclins and structural characterization of ubiquitinated intermediates. *Mol Biol Cell,* 7**,** 1343-57.

KING, R. W., PETERS, J. M., TUGENDREICH, S., ROLFE, M., HIETER, P. & KIRSCHNER, M. W. 1995. A 20S complex containing CDC27 and CDC16 catalyzes the mitosis-specific conjugation of ubiquitin to cyclin B. *Cell,* 81**,** 279-88.

KITZMANN, M., VANDROMME, M., SCHAEFFER, V., CARNAC, G., LABBE, J. C., LAMB, N. & FERNANDEZ, A. 1999. cdk1- and cdk2-mediated phosphorylation of MyoD Ser200 in growing C2 myoblasts: role in modulating MyoD half-life and myogenic activity. *Mol Cell Biol,* 19**,** 3167-76.

KOEGL, M., HOPPE, T., SCHLENKER, S., ULRICH, H. D., MAYER, T. U. & JENTSCH, S. 1999. A novel ubiquitination factor, E4, is involved in multiubiquitin chain assembly. *Cell,* 96**,** 635-44.

KORZH, V., SLEPTSOVA, I., LIAO, J., HE, J. & GONG, Z. 1998. Expression of zebrafish bHLH genes ngn1 and nrd defines distinct stages of neural differentiation. *Dev Dyn,* 213**,** 92-104.

KORZH, V. & STRAHLE, U. 2002. Proneural, prosensory, antiglial: the many faces of neurogenins. *Trends Neurosci,* 25**,** 603-5.

KOYANO-NAKAGAWA, N., WETTSTEIN, D. & KINTNER, C. 1999. Activation of Xenopus genes required for lateral inhibition and neuronal differentiation during primary neurogenesis. *Mol Cell Neurosci,* 14**,** 327-39.

KRAGT, A., VOORN-BROUWER, T., VAN DEN BERG, M. & DISTEL, B. 2005. The Saccharomyces cerevisiae peroxisomal import receptor Pex5p is monoubiquitinated in wild type cells. *J Biol Chem,* 280**,** 7867-74.

KRIWACKI, R. W., HENGST, L., TENNANT, L., REED, S. I. & WRIGHT, P. E. 1996. Structural studies of p21Waf1/Cip1/Sdi1 in the free and Cdk2-bound state: conformational disorder mediates binding diversity. *Proceedings of the National Academy of Sciences of the United States of America,* 93**,** 11504-9.

KUO, M. L., DEN BESTEN, W., BERTWISTLE, D., ROUSSEL, M. F. & SHERR, C. J. 2004. N-terminal polyubiquitination and degradation of the Arf tumor suppressor. *Genes Dev,* 18**,** 1862-74.

LAHAV-BARATZ, S., SUDAKIN, V., RUDERMAN, J. V. & HERSHKO, A. 1995. Reversible phosphorylation controls the activity of cyclosome-associated cyclin-ubiquitin ligase. *Proceedings of the National Academy of Sciences of the United States of America,* 92**,** 9303-7.

LAI, Z., FERRY, K. V., DIAMOND, M. A., WEE, K. E., KIM, Y. B., MA, J., YANG, T., BENFIELD, P. A., COPELAND, R. A. & AUGER, K. R. 2001. Human mdm2 mediates multiple mono-ubiquitination of p53 by a mechanism requiring enzyme isomerization. *The Journal of biological chemistry,* 276**,** 31357-67.

LANDRIEU, I., LACOSSE, L., LEROY, A., WIERUSZESKI, J. M., TRIVELLI, X., SILLEN, A., SIBILLE, N., SCHWALBE, H., SAXENA, K., LANGER, T. & LIPPENS, G. 2006. NMR analysis of a Tau phosphorylation pattern. *Journal of the American Chemical Society,* 128**,** 3575-83.

LEON, S. & SUBRAMANI, S. 2007. A conserved cysteine residue of Pichia pastoris Pex20p is essential for its recycling from the peroxisome to the cytosol. *J Biol Chem,* 282**,** 7424-30.

LEVINTHAL, C. How to Fold Graciously. *In:* DEBRUNNER, J. T. P. & MUNCK, E., eds. Mossbauer Spectroscopy in Biological Systems: Proceedings of a meeting held

at Allerton House, Monticello, Illinois., 1969 Allerton House, Monticello, Illinois.: University of Illinois Press, 22-24.

LI, H., OKAMOTO, K., PEART, M. J. & PRIVES, C. 2009. Lysine-independent turnover of cyclin G1 can be stabilized by B'alpha subunits of protein phosphatase 2A. *Molecular and cellular biology,* 29**,** 919-28.

LI, M. & ZHANG, P. 2009. The function of APC/CCdh1 in cell cycle and beyond. *Cell division,* 4**,** 2.

LIANG, J., SHAO, S. H., XU, Z. X., HENNESSY, B., DING, Z., LARREA, M., KONDO, S., DUMONT, D. J., GUTTERMAN, J. U., WALKER, C. L., SLINGERLAND, J. M. & MILLS, G. B. 2007. The energy sensing LKB1-AMPK pathway regulates p27(kip1) phosphorylation mediating the decision to enter autophagy or apoptosis. *Nature cell biology,* 9**,** 218-24.

LINDON, C., ALBAGLI, O., DOMEYNE, P., MONTARRAS, D. & PINSET, C. 2000. Constitutive instability of muscle regulatory factor Myf5 is distinct from its mitosis-specific disappearance, which requires a D-box-like motif overlapping the basic domain. *Molecular and cellular biology,* 20**,** 8923-32.

LLUIS, F., BALLESTAR, E., SUELVES, M., ESTELLER, M. & MUNOZ-CANOVES, P. 2005. E47 phosphorylation by p38 MAPK promotes MyoD/E47 association and muscle-specific gene transcription. *Embo J,* 24**,** 974-84.

LO, L., DORMAND, E., GREENWOOD, A. & ANDERSON, D. J. 2002. Comparison of the generic neuronal differentiation and neuron subtype specification functions of mammalian achaete-scute and atonal homologs in cultured neural progenitor cells. *Development,* 129**,** 1553-67.

LONGO, A., GUANGA, G. P. & ROSE, R. B. 2008. Crystal structure of E47-NeuroD1/beta2 bHLH domain-DNA complex: heterodimer selectivity and DNA recognition. *Biochemistry,* 47**,** 218-29.

LU, S. M., YU, L., TIAN, J. J., MA, J. K., LI, J. F., XU, W. & WANG, H. B. 2011. Twist modulates lymphangiogenesis and correlates with lymph node metastasis in supraglottic carcinoma. *Chinese medical journal,* 124**,** 1483-7.

LUCIANI, M. G., OEHLMANN, M. & BLOW, J. J. 2004. Characterization of a novel ATR-dependent, Chk1-independent, intra-S-phase checkpoint that suppresses initiation of replication in Xenopus. *Journal of cell science,* 117**,** 6019-30.

MA, P. C., ROULD, M. A., WEINTRAUB, H. & PABO, C. O. 1994. Crystal structure of MyoD bHLH domain-DNA complex: perspectives on DNA recognition and implications for transcriptional activation. *Cell,* 77**,** 451-9.

MA, Q., FODE, C., GUILLEMOT, F. & ANDERSON, D. J. 1999. Neurogenin1 and neurogenin2 control two distinct waves of neurogenesis in developing dorsal root ganglia. *Genes Dev,* 13**,** 1717-28.

MA, Q., KINTNER, C. & ANDERSON, D. J. 1996. Identification of neurogenin, a vertebrate neuronal determination gene. *Cell,* 87**,** 43-52.

MA, Y. C., SONG, M. R., PARK, J. P., HENRY HO, H. Y., HU, L., KURTEV, M. V., ZIEG, J., MA, Q., PFAFF, S. L. & GREENBERG, M. E. 2008. Regulation of motor neuron specification by phosphorylation of neurogenin 2. *Neuron,* 58**,** 65-77.

MACHIYA, Y., HARA, S., ARAWAKA, S., FUKUSHIMA, S., SATO, H., SAKAMOTO, M., KOYAMA, S. & KATO, T. 2010. Phosphorylated alpha-synuclein at Ser-129 is targeted to the proteasome pathway in a ubiquitin-independent manner. *The Journal of biological chemistry,* 285**,** 40732-44.

MANCHADO, E., EGUREN, M. & MALUMBRES, M. 2010. The anaphase-promoting complex/cyclosome (APC/C): cell-cycle-dependent and -independent functions. *Biochemical Society transactions,* 38**,** 65-71.

MARSH, J. A., DANCHECK, B., RAGUSA, M. J., ALLAIRE, M., FORMAN-KAY, J. D. & PETI, W. 2010. Structural diversity in free and bound states of intrinsically disordered protein phosphatase 1 regulators. *Structure,* 18**,** 1094-103.

MASSARI, M. E. & MURRE, C. 2000. Helix-loop-helix proteins: regulators of transcription in eucaryotic organisms. *Mol Cell Biol,* 20**,** 429-40.

MATHIAS, N., JOHNSON, S. L., WINEY, M., ADAMS, A. E., GOETSCH, L., PRINGLE, J. R., BYERS, B. & GOEBL, M. G. 1996. Cdc53p acts in concert with Cdc4p and Cdc34p to control the G1-to-S-phase transition and identifies a conserved family of proteins. *Molecular and cellular biology,* 16**,** 6634-43.

MATTAR, P., BRITZ, O., JOHANNES, C., NIETO, M., MA, L., REBEYKA, A., KLENIN, N., POLLEUX, F., GUILLEMOT, F. & SCHUURMANS, C. 2004. A screen for downstream effectors of Neurogenin2 in the embryonic neocortex. *Dev Biol,* 273**,** 373-89.

MAYER, R. C., A & RECHSTEINER, M (ed.) 2005. *Protein Degradation: Ubiquitin and the Chemistry of Life*: Wiley.

MCBURNEY, M. W., JONES-VILLENEUVE, E. M., EDWARDS, M. K. & ANDERSON, P. J. 1982. Control of muscle and neuronal differentiation in a cultured embryonal carcinoma cell line. *Nature,* 299**,** 165-7.

MCBURNEY, M. W. & ROGERS, B. J. 1982. Isolation of male embryonal carcinoma cells and their chromosome replication patterns. *Developmental biology,* 89**,** 503-8.

MCDOWELL, G. S., KUCEROVA, R. & PHILPOTT, A. 2010. Non-canonical ubiquitylation of the proneural protein Ngn2 occurs in both Xenopus embryos and mammalian cells. *Biochemical and biophysical research communications,* 400**,** 655-60.

MCEWAN, I. J., DAHLMAN-WRIGHT, K., FORD, J. & WRIGHT, A. P. 1996. Functional interaction of the c-Myc transactivation domain with the TATA binding protein: evidence for an induced fit model of transactivation domain folding. *Biochemistry,* 35**,** 9584-93.

MEIJER, L., BORGNE, A., MULNER, O., CHONG, J. P., BLOW, J. J., INAGAKI, N., INAGAKI, M., DELCROS, J. G. & MOULINOUX, J. P. 1997. Biochemical and cellular effects of roscovitine, a potent and selective inhibitor of the cyclin-dependent kinases cdc2, cdk2 and cdk5. *European journal of biochemistry / FEBS,* 243**,** 527-36.

MEINNEL, T., PEYNOT, P. & GIGLIONE, C. 2005. Processed N-termini of mature proteins in higher eukaryotes and their major contribution to dynamic proteomics. *Biochimie,* 87**,** 701-12.

MEINNEL, T., SERERO, A. & GIGLIONE, C. 2006. Impact of the N-terminal amino acid on targeted protein degradation. *Biol Chem,* 387**,** 839-51.

MICHEL, D. 2009. Fine tuning gene expression through short DNA-protein binding cycles. *Biochimie,* 91**,** 933-41.

MONTAGNOLI, A., FIORE, F., EYTAN, E., CARRANO, A. C., DRAETTA, G. F., HERSHKO, A. & PAGANO, M. 1999. Ubiquitination of p27 is regulated by Cdk-dependent phosphorylation and trimeric complex formation. *Genes Dev,* 13**,** 1181-9.

MORRISON, S. J., PEREZ, S. E., QIAO, Z., VERDI, J. M., HICKS, C., WEINMASTER, G. & ANDERSON, D. J. 2000. Transient Notch activation initiates an irreversible switch from neurogenesis to gliogenesis by neural crest stem cells. *Cell,* 101**,** 499-510.

MURRAY, A. W. 1989. Cyclin synthesis and degradation and the embryonic cell cycle. *Journal of cell science. Supplement,* 12**,** 65-76.

MURRAY, A. W. 1991. Chapter 30 Cell Cycle Extracts. *In:* BRIAN, K. K. & PENG, H. B. (eds.) *Methods in Cell Biology.* Academic Press.

MURRE, C., BAIN, G., VAN DIJK, M. A., ENGEL, I., FURNARI, B. A., MASSARI, M. E., MATTHEWS, J. R., QUONG, M. W., RIVERA, R. R. & STUIVER, M. H. 1994. Structure and function of helix-loop-helix proteins. *Biochim Biophys Acta,* 1218**,** 129-35.

MURTAUGH, L. C. & MELTON, D. A. 2003. Genes, signals, and lineages in pancreas development. *Annual review of cell and developmental biology,* 19**,** 71-89.

NAKADA, Y., HUNSAKER, T. L., HENKE, R. M. & JOHNSON, J. E. 2004. Distinct domains within Mash1 and Math1 are required for function in neuronal differentiation versus neuronal cell-type specification. *Development,* 131**,** 1319-30.

NASH, P., TANG, X., ORLICKY, S., CHEN, Q., GERTLER, F. B., MENDENHALL, M. D., SICHERI, F., PAWSON, T. & TYERS, M. 2001. Multisite phosphorylation of a CDK inhibitor sets a threshold for the onset of DNA replication. *Nature,* 414**,** 514-21.

NAUJOKAT, C. & SARIC, T. 2007. Concise review: role and function of the ubiquitin-proteasome system in mammalian stem and progenitor cells. *Stem Cells,* 25**,** 2408-18.

NECHAEV, S. & ADELMAN, K. 2008. Promoter-proximal Pol II: when stalling speeds things up. *Cell cycle,* 7**,** 1539-44.

NGUYEN, L., BESSON, A., HENG, J. I., SCHUURMANS, C., TEBOUL, L., PARRAS, C., PHILPOTT, A., ROBERTS, J. M. & GUILLEMOT, F. 2006. p27kip1 independently promotes neuronal differentiation and migration in the cerebral cortex. *Genes Dev,* 20**,** 1511-24.

NGUYEN, V., CHOKAS, A. L., STECCA, B. & RUIZ I ALTABA, A. 2005. Cooperative requirement of the Gli proteins in neurogenesis. *Development,* 132**,** 3267-79.

NIE, L., XU, M., VLADIMIROVA, A. & SUN, X. H. 2003. Notch-induced E2A ubiquitination and degradation are controlled by MAP kinase activities. *Embo J,* 22**,** 5780-92.

NIEBER, F., PIELER, T. & HENNINGFELD, K. A. 2009. Comparative expression analysis of the neurogenins in Xenopus tropicalis and Xenopus laevis. *Developmental dynamics : an official publication of the American Association of Anatomists,* 238**,** 451-8.

NIETO, M., SCHUURMANS, C., BRITZ, O. & GUILLEMOT, F. 2001. Neural bHLH genes control the neuronal versus glial fate decision in cortical progenitors. *Neuron,* 29**,** 401-13.

NIEUWKOOP, P. D. & FABER, J. 1994. Normal table of *Xenopus laevis*. *New York: Garland Publishing*.

NOVITCH, B. G., CHEN, A. I. & JESSELL, T. M. 2001. Coordinate regulation of motor neuron subtype identity and pan-neuronal properties by the bHLH repressor Olig2. *Neuron,* 31**,** 773-89.

OHNUMA, S. & HARRIS, W. A. 2003. Neurogenesis and the cell cycle. *Neuron,* 40**,** 199-208.

OHNUMA, S., PHILPOTT, A., WANG, K., HOLT, C. E. & HARRIS, W. A. 1999. p27Xic1, a Cdk inhibitor, promotes the determination of glial cells in Xenopus retina. *Cell,* 99**,** 499-510.

OLDFIELD, C. J., CHENG, Y., CORTESE, M. S., ROMERO, P., UVERSKY, V. N. & DUNKER, A. K. 2005. Coupled folding and binding with alpha-helix-forming molecular recognition elements. *Biochemistry,* 44**,** 12454-70.

OSWALD, F., TAUBER, B., DOBNER, T., BOURTEELE, S., KOSTEZKA, U., ADLER, G., LIPTAY, S. & SCHMID, R. M. 2001. p300 acts as a transcriptional coactivator for mammalian Notch-1. *Molecular and cellular biology,* 21**,** 7761-74.

PALMITER, R. D. 1977. Prevention of NH2-terminal acetylation of proteins synthesized in cell-free systems. *J Biol Chem,* 252**,** 8781-3.

PANCHISION, D. M. & MCKAY, R. D. 2002. The control of neural stem cells by morphogenic signals. *Current opinion in genetics & development,* 12**,** 478-87.

PAPALEO, E., RANZANI, V., TRIPODI, F., VITRIOLO, A., CIRULLI, C., FANTUCCI, P., ALBERGHINA, L., VANONI, M., DE GIOIA, L. & COCCETTI, P. 2011. An acidic loop and cognate phosphorylation sites define a molecular switch that modulates ubiquitin charging activity in cdc34-like enzymes. *PLoS computational biology,* 7**,** e1002056.

PARRAS, C. M., SCHUURMANS, C., SCARDIGLI, R., KIM, J., ANDERSON, D. J. & GUILLEMOT, F. 2002. Divergent functions of the proneural genes Mash1 and Ngn2 in the specification of neuronal subtype identity. *Genes Dev,* 16**,** 324-38.

PENG, J., SCHWARTZ, D., ELIAS, J. E., THOREEN, C. C., CHENG, D., MARSISCHKY, G., ROELOFS, J., FINLEY, D. & GYGI, S. P. 2003. A proteomics approach to understanding protein ubiquitination. *Nat Biotechnol,* 21**,** 921-6.

PENG, K., VUCETIC, S., RADIVOJAC, P., BROWN, C. J., DUNKER, A. K. & OBRADOVIC, Z. 2005. Optimizing long intrinsic disorder predictors with protein evolutionary information. *Journal of bioinformatics and computational biology,* 3**,** 35-60.

PETERS, J. M. 2006. The anaphase promoting complex/cyclosome: a machine designed to destroy. *Nature reviews. Molecular cell biology,* 7**,** 644-56.

PETROSKI, M. D. & DESHAIES, R. J. 2005. Function and regulation of cullin-RING ubiquitin ligases. *Nat Rev Mol Cell Biol,* 6**,** 9-20.

PHILPOTT, A. 2010. Neural Development: bHLH Genes. *eLS.* John Wiley & Sons, Ltd.

PICKART, C. M. 2001a. Mechanisms underlying ubiquitination. *Annual review of biochemistry,* 70**,** 503-33.

PICKART, C. M. 2001b. Ubiquitin enters the new millennium. *Molecular cell,* 8**,** 499-504.

PICKART, C. M. 2002. DNA repair: right on target with ubiquitin. *Nature,* 419**,** 120-1.

PICKART, C. M. & COHEN, R. E. 2004. Proteasomes and their kin: proteases in the machine age. *Nat Rev Mol Cell Biol,* 5**,** 177-87.

PICKART, C. M. & FUSHMAN, D. 2004. Polyubiquitin chains: polymeric protein signals. *Curr Opin Chem Biol,* 8**,** 610-6.

POLEVODA, B. & SHERMAN, F. 2000. Nalpha -terminal acetylation of eukaryotic proteins. *J Biol Chem,* 275**,** 36479-82.

POLEVODA, B. & SHERMAN, F. 2002. The diversity of acetylated proteins. *Genome Biol,* 3**,** reviews0006.

POLEVODA, B. & SHERMAN, F. 2003a. Composition and function of the eukaryotic N-terminal acetyltransferase subunits. *Biochem Biophys Res Commun,* 308**,** 1-11.

POLEVODA, B. & SHERMAN, F. 2003b. N-terminal acetyltransferases and sequence requirements for N-terminal acetylation of eukaryotic proteins. *J Mol Biol,* 325**,** 595-622.

PORNILLOS, O., GARRUS, J. E. & SUNDQUIST, W. I. 2002. Mechanisms of enveloped RNA virus budding. *Trends in cell biology,* 12**,** 569-79.

PRAKASH, S., INOBE, T., HATCH, A. J. & MATOUSCHEK, A. 2009. Substrate selection by the proteasome during degradation of protein complexes. *Nature chemical biology,* 5**,** 29-36.

PRAKASH, S., TIAN, L., RATLIFF, K. S., LEHOTZKY, R. E. & MATOUSCHEK, A. 2004. An unstructured initiation site is required for efficient proteasome-mediated degradation. *Nat Struct Mol Biol,* 11**,** 830-7.

PRILUSKY, J., FELDER, C. E., ZEEV-BEN-MORDEHAI, T., RYDBERG, E. H., MAN, O., BECKMANN, J. S., SILMAN, I. & SUSSMAN, J. L. 2005. FoldIndex: a simple tool to predict whether a given protein sequence is intrinsically unfolded. *Bioinformatics,* 21**,** 3435-8.

QIAN, X., SHEN, Q., GODERIE, S. K., HE, W., CAPELA, A., DAVIS, A. A. & TEMPLE, S. 2000. Timing of CNS cell generation: a programmed sequence of neuron and glial cell production from isolated murine cortical stem cells. *Neuron,* 28**,** 69-80.

QUAN, X. J., DENAYER, T., YAN, J., JAFAR-NEJAD, H., PHILIPPI, A., LICHTARGE, O., VLEMINCKX, K. & HASSAN, B. A. 2004. Evolution of neural precursor selection: functional divergence of proneural proteins. *Development,* 131**,** 1679-89.

RAJAN, P. & MCKAY, R. D. 1998. Multiple routes to astrocytic differentiation in the CNS. *The Journal of neuroscience : the official journal of the Society for Neuroscience,* 18**,** 3620-9.

RAWLINGS, N. D. & BARRETT, A. J. 1994. Families of serine peptidases. *Methods in enzymology,* 244**,** 19-61.

REBEIZ, M., STONE, T. & POSAKONY, J. W. 2005. An ancient transcriptional regulatory linkage. *Dev Biol,* 281**,** 299-308.

ROARK, R. 2010. *Regulation of ubiquitin-mediated proteolysis in Xenopus laevis and mammalian cells.* PhD, University of Cambridge.

ROMANI, S., CAMPUZANO, S., MACAGNO, E. R. & MODOLELL, J. 1989. Expression of achaete and scute genes in Drosophila imaginal discs and their function in sensory organ development. *Genes Dev,* 3**,** 997-1007.

ROSS, S. E., GREENBERG, M. E. & STILES, C. D. 2003. Basic helix-loop-helix factors in cortical development. *Neuron,* 39**,** 13-25.

RUDNICKI, M. A. & MCBURNEY, M. W. 1987. Cell culture methods and induction of differentiation of embryonal carcinoma cell lines. From Teratocarcinomas and embryonic stem cells: A Practical Approach (Edited by Rpbertson, E.J.). 19-49.

SADEH, R., BREITSCHOPF, K., BERCOVICH, B., ZOABI, M., KRAVTSOVA-IVANTSIV, Y., KORNITZER, D., SCHWARTZ, A. & CIECHANOVER, A. 2008. The N-terminal domain of MyoD is necessary and sufficient for its nuclear localization-dependent degradation by the ubiquitin system. *Proc Natl Acad Sci U S A,* 105**,** 15690-5.

SALAMA-COHEN, P., AREVALO, M. A., GRANTYN, R. & RODRIGUEZ-TEBAR, A. 2006. Notch and NGF/p75NTR control dendrite morphology and the balance of excitatory/inhibitory synaptic input to hippocampal neurones through Neurogenin 3. *Journal of neurochemistry,* 97**,** 1269-78.

SALIC, A., LEE, E., MAYER, L. & KIRSCHNER, M. W. 2000. Control of beta-catenin stability: reconstitution of the cytoplasmic steps of the wnt pathway in Xenopus egg extracts. *Mol Cell,* 5**,** 523-32.

SAMBROOK, J., FRITSCH, E. F. & MANIATIS, T. 1989. *Molecular Cloning: A Laboratory Manual*, Cold Spring Harbor Laboratory Press.

SCHAFER, K. A. 1998. The cell cycle: a review. *Veterinary pathology,* 35**,** 461-78.

SCHEFFNER, M., HUIBREGTSE, J. M., VIERSTRA, R. D. & HOWLEY, P. M. 1993. The HPV-16 E6 and E6-AP complex functions as a ubiquitin-protein ligase in the ubiquitination of p53. *Cell,* 75**,** 495-505.

SCHIMKE, R. T. & DOYLE, D. 1970. Control of enzyme levels in animal tissues. *Annual review of biochemistry,* 39**,** 929-76.

SCHOENHEIMER, R. 1942. *The Dynamic State of Body Constituents.,* Cambridge, Massachusetts, Harvard University Press.

SCHOENHEIMER, R., RATNER, S. & RITTENBERG, D. 1939. The Process of Continuous Deamination and Reamination of Amino Acids in the Proteins of Normal Animals. *Science,* 89**,** 272-3.

SCHRADER, E. K., HARSTAD, K. G. & MATOUSCHEK, A. 2009. Targeting proteins for degradation. *Nature chemical biology,* 5**,** 815-22.

SELENKO, P., FRUEH, D. P., ELSAESSER, S. J., HAAS, W., GYGI, S. P. & WAGNER, G. 2008. In situ observation of protein phosphorylation by high-resolution NMR spectroscopy. *Nature structural & molecular biology,* 15**,** 321-9.

SEMPLE, C. A. 2003. The comparative proteomics of ubiquitination in mouse. *Genome Res,* 13**,** 1389-94.

SEO, S., LIM, J. W., YELLAJOSHYULA, D., CHANG, L. W. & KROLL, K. L. 2007. Neurogenin and NeuroD direct transcriptional targets and their regulatory enhancers. *Embo J,* 26**,** 5093-108.

SERRANO, J., HIGGINS, L., WITTHUHN, B. A., ANDERSON, L. B., MARKOWSKI, T., HOLCOMBE, G. W., KOSIAN, P. A., KORTE, J. J., TIETGE, J. E. & DEGITZ, S. J. 2010. In vivo assessment and potential diagnosis of xenobiotics that perturb the thyroid pathway: Proteomic analysis of Xenopus laevis brain tissue following exposure to model T4 inhibitors. *Comparative biochemistry and physiology. Part D, Genomics & proteomics,* 5**,** 138-50.

SHIRASAKI, R. & PFAFF, S. L. 2002. Transcriptional codes and the control of neuronal identity. *Annual review of neuroscience,* 25**,** 251-81.

SHOU, J., RIM, P. C. & CALOF, A. L. 1999. BMPs inhibit neurogenesis by a mechanism involving degradation of a transcription factor. *Nature neuroscience,* 2**,** 339-45.

SICKMEIER, M., HAMILTON, J. A., LEGALL, T., VACIC, V., CORTESE, M. S., TANTOS, A., SZABO, B., TOMPA, P., CHEN, J., UVERSKY, V. N., OBRADOVIC, Z. & DUNKER, A. K. 2007. DisProt: the Database of Disordered Proteins. *Nucleic acids research,* 35**,** D786-93.

SIMIONATO, E., KERNER, P., DRAY, N., LE GOUAR, M., LEDENT, V., ARENDT, D. & VERVOORT, M. 2008. atonal- and achaete-scute-related genes in the annelid Platynereis dumerilii: insights into the evolution of neural basic-Helix-Loop-Helix genes. *BMC Evol Biol,* 8**,** 170.

SIVE, H. L., GRAINGER, R. L. & HARLAND, R. M. 2000. *Early Development of Xenopus laevis. A Laboratory Manual*, Cold Spring Harbour Laboratory Press.

SOMMER, L., MA, Q. & ANDERSON, D. J. 1996. neurogenins, a novel family of atonal-related bHLH transcription factors, are putative mammalian neuronal determination genes that reveal progenitor cell heterogeneity in the developing CNS and PNS. *Mol Cell Neurosci,* 8**,** 221-41.

SONG, A., WANG, Q., GOEBL, M. G. & HARRINGTON, M. A. 1998. Phosphorylation of nuclear MyoD is required for its rapid degradation. *Mol Cell Biol,* 18**,** 4994-9.

SONG, J., WANG, J., JOZWIAK, A. A., HU, W., SWIDERSKI, P. M. & CHEN, Y. 2009. Stability of thioester intermediates in ubiquitin-like modifications. *Protein science : a publication of the Protein Society,* 18**,** 2492-9.

SONG, L. & RAPE, M. 2011. Substrate-specific regulation of ubiquitination by the anaphase-promoting complex. *Cell cycle,* 10**,** 52-6.

SOUOPGUI, J., SOLTER, M. & PIELER, T. 2002. XPak3 promotes cell cycle withdrawal during primary neurogenesis in Xenopus laevis. *Embo J,* 21**,** 6429-39.

SRIURANPONG, V., BORGES, M. W., STROCK, C. L., NAKAKURA, E. K., WATKINS, D. N., BLAUMUELLER, C. M., NELKIN, B. D. & BALL, D. W. 2002. Notch signaling induces rapid degradation of achaete-scute homolog 1. *Mol Cell Biol,* 22**,** 3129-39.

STUDIER, F. W., ROSENBERG, A. H., DUNN, J. J. & DUBENDORFF, J. W. 1990. Use of T7 RNA polymerase to direct expression of cloned genes. *Methods in enzymology,* 185**,** 60-89.

SU, J. Y., REMPEL, R. E., ERIKSON, E. & MALLER, J. L. 1995. Cloning and characterization of the Xenopus cyclin-dependent kinase inhibitor p27XIC1. *Proc Natl Acad Sci U S A,* 92**,** 10187-91.

SUDAKIN, V., GANOTH, D., DAHAN, A., HELLER, H., HERSHKO, J., LUCA, F. C., RUDERMAN, J. V. & HERSHKO, A. 1995. The cyclosome, a large complex containing cyclin-selective ubiquitin ligase activity, targets cyclins for destruction at the end of mitosis. *Molecular biology of the cell,* 6**,** 185-97.

SUGASE, K., DYSON, H. J. & WRIGHT, P. E. 2007. Mechanism of coupled folding and binding of an intrinsically disordered protein. *Nature,* 447**,** 1021-5.

SUGIMORI, M., NAGAO, M., BERTRAND, N., PARRAS, C. M., GUILLEMOT, F. & NAKAFUKU, M. 2007. Combinatorial actions of patterning and HLH transcription factors in the spatiotemporal control of neurogenesis and gliogenesis in the developing spinal cord. *Development,* 134**,** 1617-29.

SUN, K., MONTANA, V., CHELLAPPA, K., BRELIVET, Y., MORAS, D., MAEDA, Y., PARPURA, V., PASCHAL, B. M. & SLADEK, F. M. 2007. Phosphorylation of a conserved serine in the deoxyribonucleic acid binding domain of nuclear receptors alters intracellular localization. *Molecular endocrinology,* 21**,** 1297-311.

SUN, X. H. & BALTIMORE, D. 1991. An inhibitory domain of E12 transcription factor prevents DNA binding in E12 homodimers but not in E12 heterodimers. *Cell,* 64**,** 459-70.

SUN, Y., MEIJER, D. H., ALBERTA, J. A., MEHTA, S., KANE, M. F., TIEN, A. C., FU, H., PETRYNIAK, M. A., POTTER, G. B., LIU, Z., POWERS, J. F., RUNQUIST, I. S., ROWITCH, D. H. & STILES, C. D. 2011. Phosphorylation state of Olig2 regulates proliferation of neural progenitors. *Neuron,* 69**,** 906-17.

SUN, Y., NADAL-VICENS, M., MISONO, S., LIN, M. Z., ZUBIAGA, A., HUA, X., FAN, G. & GREENBERG, M. E. 2001. Neurogenin promotes neurogenesis and inhibits glial differentiation by independent mechanisms. *Cell,* 104**,** 365-76.

TAIT, S. W., DE VRIES, E., MAAS, C., KELLER, A. M., D'SANTOS, C. S. & BORST, J. 2007. Apoptosis induction by Bid requires unconventional ubiquitination and degradation of its N-terminal fragment. *J Cell Biol,* 179**,** 1453-66.

TALIKKA, M., PEREZ, S. E. & ZIMMERMAN, K. 2002. Distinct patterns of downstream target activation are specified by the helix-loop-helix domain of proneural basic helix-loop-helix transcription factors. *Developmental biology,* 247**,** 137-48.

TAO, H., LIU, W., SIMMONS, B. N., HARRIS, H. K., COX, T. C. & MASSIAH, M. A. 2010. Purifying natively folded proteins from inclusion bodies using sarkosyl, Triton X-100, and CHAPS. *BioTechniques,* 48**,** 61-4.

TARRANT, M. K. & COLE, P. A. 2009. The chemical biology of protein phosphorylation. *Annual review of biochemistry,* 78**,** 797-825.

TERAMOTO, S., KIHARA-NEGISHI, F., SAKURAI, T., YAMADA, T., HASHIMOTO-TAMAOKI, T., TAMURA, S., KOHNO, S. & OIKAWA, T. 2005. Classification of neural differentiation-associated genes in P19 embryonal carcinoma cells by their expression patterns induced after cell aggregation and/or retinoic acid treatment. *Oncology reports,* 14**,** 1231-8.

THAYER, M. J., TAPSCOTT, S. J., DAVIS, R. L., WRIGHT, W. E., LASSAR, A. B. & WEINTRAUB, H. 1989. Positive autoregulation of the myogenic determination gene MyoD1. *Cell,* 58**,** 241-8.

THIEN, C. B. & LANGDON, W. Y. 2001. Cbl: many adaptations to regulate protein tyrosine kinases. *Nature reviews. Molecular cell biology,* 2**,** 294-307.

THOMPSON, L. H., ANDERSSON, E., JENSEN, J. B., BARRAUD, P., GUILLEMOT, F., PARMAR, M. & BJORKLUND, A. 2006. Neurogenin2 identifies a transplantable dopamine neuron precursor in the developing ventral mesencephalon. *Exp Neurol,* 198**,** 183-98.

THROWER, J. S., HOFFMAN, L., RECHSTEINER, M. & PICKART, C. M. 2000. Recognition of the polyubiquitin proteolytic signal. *Embo J,* 19**,** 94-102.

TINTIGNAC, L. A., LEIBOVITCH, M. P., KITZMANN, M., FERNANDEZ, A., DUCOMMUN, B., MEIJER, L. & LEIBOVITCH, S. A. 2000. Cyclin E-cdk2 phosphorylation promotes late G1-phase degradation of MyoD in muscle cells. *Exp Cell Res,* 259**,** 300-7.

TOMITA, K., MORIYOSHI, K., NAKANISHI, S., GUILLEMOT, F. & KAGEYAMA, R. 2000. Mammalian achaete-scute and atonal homologs regulate neuronal versus glial fate determination in the central nervous system. *The EMBO journal,* 19**,** 5460-72.

TOMPA, P. & FUXREITER, M. 2008. Fuzzy complexes: polymorphism and structural disorder in protein-protein interactions. *Trends in biochemical sciences,* 33**,** 2-8.

TOOTLE, T. L. & REBAY, I. 2005. Post-translational modifications influence transcription factor activity: a view from the ETS superfamily. *Bioessays,* 27**,** 285-98.

TOWNSEND, K., MASON, H., BLACKFORD, A. N., MILLER, E. S., CHAPMAN, J. R., SEDGWICK, G. G., BARONE, G., TURNELL, A. S. & STEWART, G. S. 2009. Mediator of DNA damage checkpoint 1 (MDC1) regulates mitotic progression. *The Journal of biological chemistry,* 284**,** 33939-48.

TRAUSCH-AZAR, J., LEONE, T. C., KELLY, D. P. & SCHWARTZ, A. L. 2010. Ubiquitin proteasome-dependent degradation of the transcriptional coactivator PGC-1{alpha} via the N-terminal pathway. *The Journal of biological chemistry,* 285**,** 40192-200.

TREIER, M., STASZEWSKI, L. M. & BOHMANN, D. 1994. Ubiquitin-dependent c-Jun degradation in vivo is mediated by the delta domain. *Cell,* 78**,** 787-98.

TRUONG, K., SU, Y., SONG, J. & CHEN, Y. 2011. Entropy-driven mechanism of an e3 ligase. *Biochemistry,* 50**,** 5757-66.

UTSUMI, T., SATO, M., NAKANO, K., TAKEMURA, D., IWATA, H. & ISHISAKA, R. 2001. Amino acid residue penultimate to the amino-terminal gly residue strongly affects two cotranslational protein modifications, N-myristoylation and N-acetylation. *J Biol Chem,* 276**,** 10505-13.

UVERSKY, V. N., GILLESPIE, J. R. & FINK, A. L. 2000. Why are "natively unfolded" proteins unstructured under physiologic conditions? *Proteins-Structure Function and Genetics,* 41**,** 415-27.

VAN LEUKEN, R., CLIJSTERS, L. & WOLTHUIS, R. 2008. To cell cycle, swing the APC/C. *Biochimica et biophysica acta,* 1786**,** 49-59.

VARSHAVSKY, A. 1997. The N-end rule pathway of protein degradation. *Genes to cells : devoted to molecular & cellular mechanisms,* 2**,** 13-28.

VARSHAVSKY, A. 2011. The N-end rule pathway and regulation by proteolysis. *Protein science : a publication of the Protein Society*.

VERDEGEM, D. 2009. *Probing the edge of protein (non)-structuration with NMR. A case study of the intrinsically disordered proteins human Tau and HCV NS5A.* PhD, Universite de Sciences et Technologies Lille – Lille 1.

VERMA, R., ARAVIND, L., OANIA, R., MCDONALD, W. H., YATES, J. R., 3RD, KOONIN, E. V. & DESHAIES, R. J. 2002. Role of Rpn11 metalloprotease in deubiquitination and degradation by the 26S proteasome. *Science,* 298**,** 611-5.

VERNON, A. E., DEVINE, C. & PHILPOTT, A. 2003. The cdk inhibitor p27Xic1 is required for differentiation of primary neurones in Xenopus. *Development,* 130**,** 85-92.

VERNON, A. E., MOVASSAGH, M., HORAN, I., WISE, H., OHNUMA, S. & PHILPOTT, A. 2006. Notch targets the Cdk inhibitor Xic1 to regulate differentiation but not the cell cycle in neurons. *EMBO Rep,* 7**,** 643-8.

VERNON, A. E. & PHILPOTT, A. 2003a. The developmental expression of cell cycle regulators in Xenopus laevis. *Gene Expr Patterns,* 3**,** 179-92.

VERNON, A. E. & PHILPOTT, A. 2003b. A single cdk inhibitor, p27Xic1, functions beyond cell cycle regulation to promote muscle differentiation in Xenopus. *Development,* 130**,** 71-83.

VINALS, F., REIRIZ, J., AMBROSIO, S., BARTRONS, R., ROSA, J. L. & VENTURA, F. 2004. BMP-2 decreases Mash1 stability by increasing Id1 expression. *Embo J,* 23**,** 3527-37.

VISINTIN, R., PRINZ, S. & AMON, A. 1997. CDC20 and CDH1: a family of substrate-specific activators of APC-dependent proteolysis. *Science,* 278**,** 460-3.

VOSPER, J. M. 2008. *Regulation of Neurogenin stability by the ubiquitin proteasome system during the early development of Xenopus laevis.* PhD, University of Cambridge.

VOSPER, J. M., FIORE-HERICHE, C. S., HORAN, I., WILSON, K., WISE, H. & PHILPOTT, A. 2007. Regulation of neurogenin stability by ubiquitin-mediated proteolysis. *Biochem J,* 407**,** 277-84.

VOSPER, J. M., MCDOWELL, G. S., HINDLEY, C. J., FIORE-HERICHE, C. S., KUCEROVA, R., HORAN, I. & PHILPOTT, A. 2009. Ubiquitylation on canonical and non-canonical sites targets the transcription factor neurogenin for ubiquitin-mediated proteolysis. *J Biol Chem,* 284**,** 15458-68.

WALSH, K. & PERLMAN, H. 1997. Cell cycle exit upon myogenic differentiation. *Current opinion in genetics & development,* 7**,** 597-602.

WANG, K. H., ROMAN-HERNANDEZ, G., GRANT, R. A., SAUER, R. T. & BAKER, T. A. 2008. The molecular basis of N-end rule recognition. *Molecular cell,* 32**,** 406-14.

WANG, X., HERR, R. A., CHUA, W. J., LYBARGER, L., WIERTZ, E. J. & HANSEN, T. H. 2007. Ubiquitination of serine, threonine, or lysine residues on the cytoplasmic tail can induce ERAD of MHC-I by viral E3 ligase mK3. *J Cell Biol,* 177**,** 613-24.

WANG, Y. & KLEMKE, R. L. 2008. PhosphoBlast, a computational tool for comparing phosphoprotein signatures among large datasets. *Molecular & cellular proteomics : MCP,* 7**,** 145-62.

WARD, J. J., SODHI, J. S., MCGUFFIN, L. J., BUXTON, B. F. & JONES, D. T. 2004. Prediction and functional analysis of native disorder in proteins from the three kingdoms of life. *Journal of molecular biology,* 337**,** 635-45.

WEINREB, P. H., ZHEN, W., POON, A. W., CONWAY, K. A. & LANSBURY, P. T., JR. 1996. NACP, a protein implicated in Alzheimer's disease and learning, is natively unfolded. *Biochemistry,* 35**,** 13709-15.

WEISSMAN, A. M. 2001. Themes and variations on ubiquitylation. *Nature reviews. Molecular cell biology,* 2**,** 169-78.

WENDT, H., THOMAS, R. M. & ELLENBERGER, T. 1998. DNA-mediated folding and assembly of MyoD-E47 heterodimers. *J Biol Chem,* 273**,** 5735-43.

WILKINSON, K. D. 1997. Regulation of ubiquitin-dependent processes by deubiquitinating enzymes. *The FASEB journal : official publication of the Federation of American Societies for Experimental Biology,* 11**,** 1245-56.

WILKINSON, K. D., URBAN, M. K. & HAAS, A. L. 1980. Ubiquitin is the ATP-dependent proteolysis factor I of rabbit reticulocytes. *The Journal of biological chemistry,* 255**,** 7529-32.

WILLEMS, A. R., SCHWAB, M. & TYERS, M. 2004. A hitchhiker's guide to the cullin ubiquitin ligases: SCF and its kin. *Biochim Biophys Acta,* 1695**,** 133-70.

WILLIAMS, C., VAN DEN BERG, M., SPRENGER, R. R. & DISTEL, B. 2007. A conserved cysteine is essential for Pex4p-dependent ubiquitination of the peroxisomal import receptor Pex5p. *J Biol Chem,* 282**,** 22534-43.

WINSTON, J. T., STRACK, P., BEER-ROMERO, P., CHU, C. Y., ELLEDGE, S. J. & HARPER, J. W. 1999. The SCFbeta-TRCP-ubiquitin ligase complex associates specifically with phosphorylated destruction motifs in IkappaBalpha and beta-catenin and stimulates IkappaBalpha ubiquitination in vitro. *Genes Dev,* 13**,** 270-83.

WISHART, D. S. & SYKES, B. D. 1994. The 13C chemical-shift index: a simple method for the identification of protein secondary structure using 13C chemical-shift data. *Journal of biomolecular NMR,* 4**,** 171-80.

WON, K. A. & REED, S. I. 1996. Activation of cyclin E/CDK2 is coupled to site-specific autophosphorylation and ubiquitin-dependent degradation of cyclin E. *The EMBO journal,* 15**,** 4182-93.

WRIGHT, P. E. & DYSON, H. J. 2009. Linking folding and binding. *Current opinion in structural biology,* 19**,** 31-8.

WU, J. T., LIN, H. C., HU, Y. C. & CHIEN, C. T. 2005. Neddylation and deneddylation regulate Cul1 and Cul3 protein accumulation. *Nature cell biology,* 7**,** 1014-20.

WU, P. Y., HANLON, M., EDDINS, M., TSUI, C., ROGERS, R. S., JENSEN, J. P., MATUNIS, M. J., WEISSMAN, A. M., WOLBERGER, C. & PICKART, C. M. 2003. A conserved catalytic residue in the ubiquitin-conjugating enzyme family. *The EMBO journal,* 22**,** 5241-50.

WU, R. C., FENG, Q., LONARD, D. M. & O'MALLEY, B. W. 2007. SRC-3 coactivator functional lifetime is regulated by a phospho-dependent ubiquitin time clock. *Cell,* 129**,** 1125-40.

XUE, B., DUNBRACK, R. L., WILLIAMS, R. W., DUNKER, A. K. & UVERSKY, V. N. 2010. PONDR-FIT: a meta-predictor of intrinsically disordered amino acids. *Biochimica et biophysica acta,* 1804**,** 996-1010.

YAFFE, M. B. & ELIA, A. E. 2001. Phosphoserine/threonine-binding domains. *Curr Opin Cell Biol,* 13**,** 131-8.

YAMANO, H., GANNON, J., MAHBUBANI, H. & HUNT, T. 2004. Cell cycle-regulated recognition of the destruction box of cyclin B by the APC/C in Xenopus egg extracts. *Mol Cell,* 13**,** 137-47.

YANG, Y., CRAIG, T. J., CHEN, X., CIUFO, L. F., TAKAHASHI, M., MORGAN, A. & GILLIS, K. D. 2007. Phosphomimetic mutation of Ser-187 of SNAP-25 increases both syntaxin binding and highly Ca2+-sensitive exocytosis. *The Journal of general physiology,* 129**,** 233-44.

YEO, W. & GAUTIER, J. 2005. XNGNR1-dependent neurogenesis mediates early neural cell death. *Mech Dev,* 122**,** 635-44.

YOKOYAMA, S. & ASAHARA, H. 2011. The myogenic transcriptional network. *Cellular and molecular life sciences : CMLS,* 68**,** 1843-9.

YU, H., KING, R. W., PETERS, J. M. & KIRSCHNER, M. W. 1996. Identification of a novel ubiquitin-conjugating enzyme involved in mitotic cyclin degradation. *Current biology : CB,* 6**,** 455-66.

ZHANG, N. Y., JACOBSON, A. D., MACFADDEN, A. & LIU, C. W. 2011. Ubiquitin chain trimming recycles the substrate binding sites of the 26 S proteasome and promotes degradation of lysine 48-linked polyubiquitin conjugates. *The Journal of biological chemistry*.

ZHONG, S., MULLER, S., RONCHETTI, S., FREEMONT, P. S., DEJEAN, A. & PANDOLFI, P. P. 2000. Role of SUMO-1-modified PML in nuclear body formation. *Blood,* 95**,** 2748-52.

ZOU, H., MCGARRY, T. J., BERNAL, T. & KIRSCHNER, M. W. 1999. Identification of a vertebrate sister-chromatid separation inhibitor involved in transformation and tumorigenesis. *Science,* 285**,** 418-22.

APPENDIX 1

Schematic of bHLH conserved region and heterodimer taken from (Bertrand et al., 2002)

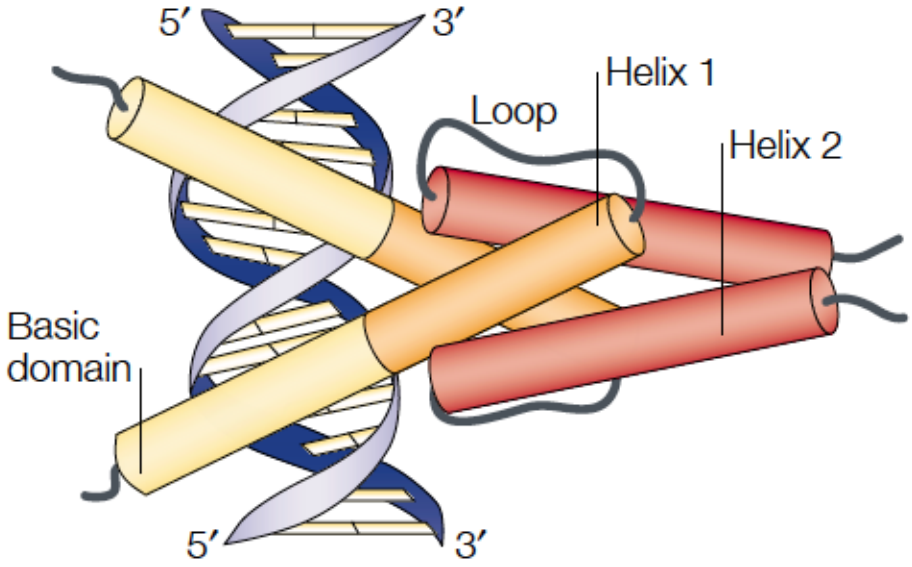

From (Bertrand et al., 2002): Schematic representation of the structure of a bHLH dimer that is complexed to DNA. The basic region fits in the main groove of the DNA, and many residues in this region make direct contact with the E-box sequence. The two α-helices of both partners together form a four-helix bundle.

Structure of proneural bHLH/E2A/DNA complex, adapted from (Longo et al., 2008), PDB file 2QL2

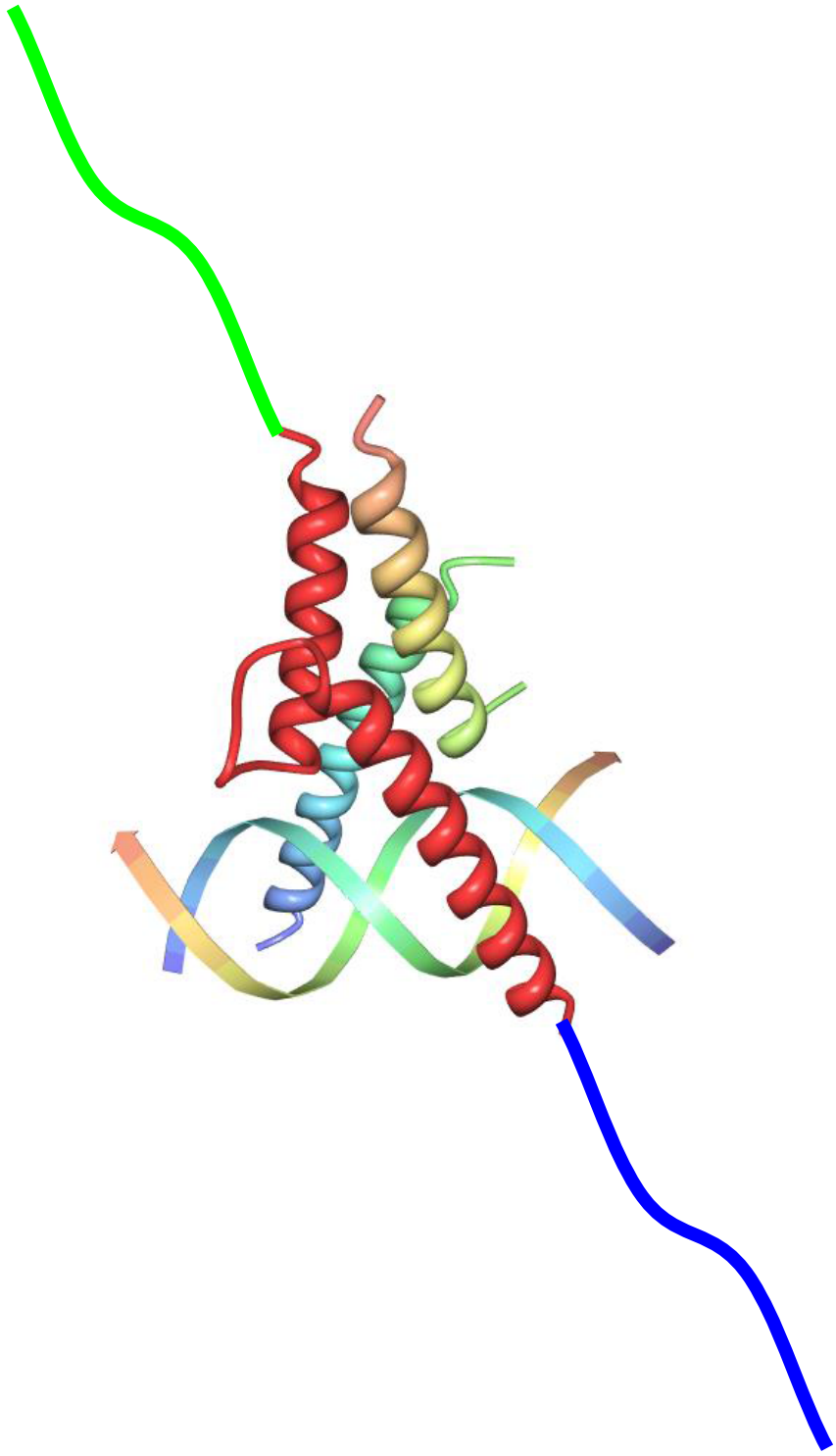

Structure of a proneural bHLH heterodimer complexed to DNA. There is no structural information for the intrinsically disordered N- and C-terminal domains and so representative strands have been added to illustrate the full xNgn2 protein. The disordered N-terminal domain is bordered in blue; the bHLH domain in red; and the disordered C-terminal domain in green.

Supplemental Material can be found at:
http://www.jbc.org/content/suppl/2009/04/01/M809366200.DC1.html

THE JOURNAL OF BIOLOGICAL CHEMISTRY VOL. 284, NO. 23, pp. 15458–15468, June 5, 2009
© 2009 by The American Society for Biochemistry and Molecular Biology, Inc. Printed in the U.S.A.

Ubiquitylation on Canonical and Non-canonical Sites Targets the Transcription Factor Neurogenin for Ubiquitin-mediated Proteolysis*[S]

Received for publication, December 12, 2008, and in revised form, March 19, 2009 Published, JBC Papers in Press, March 31, 2009, DOI 10.1074/jbc.M809366200

Jonathan M. D. Vosper[1], Gary S. McDowell, Christopher J. Hindley[2], Christelle S. Fiore-Heriche, Romana Kucerova, Ian Horan, and Anna Philpott[3]

From the Department of Oncology, University of Cambridge, Hutchison/Medical Research Council (MRC) Research Centre, Addenbrooke's Hospital, Cambridge CB2 0XZ, United Kingdom

Polyubiquitylation targets multiple proteins for degradation by the proteasome. Typically, the first ubiquitin is linked to lysine residues in the substrate for degradation via an isopeptide bond, although rarely ubiquitin linkage to the N-terminal residue has also been observed. We have recently shown that Neurogenin (NGN), a basic helix-loop-helix transcription factor that plays a central role in regulating neuronal differentiation, is degraded by ubiquitin-mediated proteolysis. We have taken a biochemical and mutagenesis approach to investigate sites of ubiquitylation of NGN, initially using extracts of eggs from the frog *Xenopus laevis* as a source of ubiquitylation and degradation components. NGN can be targeted for destruction by ubiquitylation via lysines or the N terminus. However, we see that a modified NGN, where canonical lysine ubiquitylation and N-terminally linked ubiquitylation are prevented, is nevertheless ubiquitylated and degraded by the proteasome. We show that polyubiquitin chains covalently attach to non-canonical cysteine residues in NGN, and these non-canonical linkages alone are capable of targeting NGN protein for destruction. Importantly, canonical and non-canonical ubiquitylation occurs simultaneously in the native protein and may differ in importance for driving degradation in interphase and mitosis. We conclude that native NGN is ubiquitylated on multiple canonical and non-canonical sites by cellular ubiquitin ligases, and all types of linkage can contribute to protein turnover.

The selective degradation of proteins by ubiquitin-mediated proteolysis is a crucial regulator of diverse cellular processes in eukaryotes. Ub[4] is classically conjugated to the ϵ-amino group of a substrate lysine by an isopeptide bond (1). This serves as an anchor point to build a polyubiquitin chain that results in subsequent targeting to the proteasome for destruction. In a small number of proteins, Ub has been shown to be conjugated to the N-terminal α-amino group of a protein via a peptide linkage used as an anchor site for assembly of a lysine-linked polyubiquitin chain (2).

The conjugation of ubiquitin to substrate proceeds when a nucleophilic substrate amino group attacks the labile E2-ubiquitin thioester bond. This mechanism does not exclude the possibility that ubiquitylation can occur on other substrate nucleophilic groups on amino acid side chains, such as the thiol groups present on cysteines. The resultant thioester-anchored ubiquitin chains would, however, be predicted to be less stable than the isopeptide/peptide bonds formed between ubiquitin and lysine/N-terminal amino groups (3, 4). Based on this, cysteine residues have generally been considered to be unlikely targets for ubiquitin modification (4).

However, there is recent evidence that ubiquitylation can occur on substrate cysteine residues, albeit in a very limited number of cases, largely regulating intracellular protein movements and usually driven by viral E3 ligases (3, 5–7). Only one substrate, the N-terminal fragment of the Bcl2-related protein Bid, has been described thus far to undergo both non-canonical ubiquitylation and proteasomal degradation by cellular E3 ligases (8), but mutational analyses failed to demonstrate a link between removing the non-canonical ubiquitylated residues and increased stability. In addition, the E2 UBC7 undergoes auto-polyubiquitylation via cysteine and proteasomal degradation (7).

We have been studying the degradation of the proneural transcription factor Neurogenin (NGN), which plays a pivotal role in the neural *versus* glial decision during embryonic central nervous system formation (9). To this end, we have exploited the highly versatile *Xenopus* egg extract system. Centrifugal extracts of *Xenopus* egg cytoplasm contain a large stockpile of enzymes required for early stages of embryogenesis including multiple components of the ubiquitin-proteasome system (UPS) and have been used extensively to explore the biochemistry of ubiquitylation (10). Using *Xenopus* eggs and embryos and mammalian cultured cells, we have demonstrated that NGN is a very short-lived protein whose rapid turnover is controlled by the UPS (11).

In this study, we demonstrate that NGN is one of the small number of proteins that can be targeted for destruction by

* This work was supported by training awards from the MRC (to J. V. and G. M.), MRC Grants GO500101 (to C. F.-H.) and G0700758 (R. K.), and Biotechnology and Biological Sciences Research Council Grant BB/C 004 108/1.

[S] The on-line version of this article (available at http://www.jbc.org) contains three supplemental figures.

[1] Present address: Division of Medical Biochemistry, Biocenter, Innsbruck Medical University, Fritz Pregl Strasse 3, A-6020 Innsbruck, Austria.

[2] Recipient of a Cancer Research UK studentship.

[3] To whom correspondence should be addressed. Tel.: 44-1223-762675; Fax 44-1223-336902; E-mail: ap113@cam.ac.uk.

[4] The abbreviations used are: Ub, ubiquitin; UPS, ubiquitin-proteasome system; E2, ubiquitin carrier protein; E3, ubiquitin-protein isopeptide ligase; NGN, Neurogenin; IVT, *in vitro* translated; DMSO, dimethyl sulfoxide; NeuroD neurogenic differentiation protein.

Downloaded from www.jbc.org at Cambridge University Library, on September 29, 2010

Supplemental Material can be found at:
http://www.jbc.org/content/suppl/2009/04/01/M809366200.DC1.html

ubiquitylation on both the N terminus and the internal lysines, and both contribute to its rapid degradation. Strikingly, we also found that a mutant NGN protein, where Ub conjugation to either lysines or the N terminus had been prevented, was still degraded by the UPS. Under these circumstances, ubiquitylation of NGN can occur on non-canonical cysteine sites. We show that polyubiquitylation on both canonical and non-canonical residues also simultaneously occurs in the wild-type native protein, and the relative contribution of these Ub linkages to speed of protein degradation may vary according to cell cycle stage. Moreover, in the absence of other potential sites for ubiquitylation, Ubs can also be added to serines and/or threonines, demonstrating the remarkable flexibility of the ubiquitylation machinery.

EXPERIMENTAL PROCEDURES

Plasmids and Constructs—NGN (also known as X-NGNR1a) and NeuroD constructs were described previously (11). NGNKO, NGNCO, and NGNKOCO mutants were generated using the QuikChange® multisite-directed mutagenesis kit (Stratagene). AC1, AC2, AC3 NGN, and NGN mutant constructs were generated by PCR and cloned into the pCS2 vector. Ub and UbKO were amplified by PCR without the last two glycine codons to prevent cleavage of the fusion by cytoplasmic deubiquitinating enzymes (12) and fused in-frame to NGNKO by a polar tetrapeptide linker (13).

In Vitro Translation—TnT® SP6 quick coupled transcription/translation system (Promega), in the presence of [^{35}S] methionine (Amersham Biosciences), was carried out according to the manufacturer's instructions.

Mitotic Extracts—Activated interphase egg extracts were prepared as described previously (11) and were then supplemented with 5 μg of recombinant non-degradable cyclin B delta 90 per 100 μl of extract. Extracts were incubated at room temperature for 20 min to enable extracts to enter mitosis. The effectiveness of this treatment in driving extracts into mitosis was determined initially by examining the morphology of sperm nuclei added to the extract.

Degradation Assays—Activated interphase and mitotic egg extracts were prepared as described previously (11). Extracts were supplemented with ubiquitin (from bovine erythrocytes, Sigma) at a final concentration of 1.25 mg/ml. ^{35}S-IVT protein (protein generated by *in vitro* translation in the presence of [^{35}S]methionine) was added to the extract (8 μl of ^{35}S-IVT protein per 36 μl of extract) and incubated at 21 °C. Aliquots were taken at various time points and mixed with 2× Laemmli sample buffer containing 100 mM β-mercaptoethanol. Samples were denatured for 3–5 min at 95 °C and separated by SDS-PAGE (15% Tris-glycine). The half-life of the protein was calculated by plotting the concentration of protein against time and finding the first order rate constant for degradation.

Where appropriate, proteasome inhibitors were added to extracts at the concentrations indicated, 5 min prior to the addition of ^{35}S-IVT protein. Mg132 and epoxomicin were obtained commercially (BIOMOL) and used at the concentrations indicated (200 and 100 μM, respectively, or adding DMSO (1% (v/v)) in place of proteasome inhibitors in controls. Where appropriate, extracts supplemented with a final concentration of 10 mg/ml methylated ubiquitin (BIOMOL) were used in degradation assays where indicated with ubiquitin from bovine erythrocytes at a final concentration of 10 mg/ml as a control.

Ubiquitylation Assays—Ubiquitylation assays were performed in accordance with the protocol described by Salic *et al.* (10), with minor alterations. 5 μl of ^{35}S-IVT protein (or IVT reaction with pCS2+ vector as control) was added as indicated to 23 μl of activated interphase or mitotic egg extracts, supplemented with 200 μM MG132 and either 2.5 mg/ml His-ubiquitin (N-terminally hexahistidine tagged ubiquitin, Sigma) or 1.25 mg/ml ubiquitin. Extract reactions were incubated at 20 °C for 1 h. Following incubation, the reactions were diluted 10-fold in His buffer (100 mM Tris/HCl (pH 7.4), 1% (v/v) Nonidet P-40, 8 M urea, 20 mM imidazole, 600 mM NaCl and 10% (v/v) ethanol) and supplemented with 15 μl (~5% (v/v)) of Ni^{2+}-nitrilotriacetate-agarose beads (Qiagen). Reactions were incubated for 90 min at room temperature, rotating at 12 rpm, and then washed five times with His buffer prior to elution with 2× Laemmli sample buffer supplemented with 100 mM β-mercaptoethanol. Samples were heat-treated for 5 min at 95 °C prior to separation on 15% Tris-glycine SDS-PAGE gels.

Reducing Treatments—Reducing ubiquitylation assays were performed as described above except that at the elution step, samples were eluted with either reducing 2× Laemmli sample buffer (2× Laemmli sample buffer (pH 10.5) + 10% (v/v) β-mercaptoethanol) or non-reducing 2× Laemmli sample buffer (2× Laemmli sample buffer (pH 6.8) + 10% (v/v) water), see Fig. 4, *B* and *C*). Sample buffers also included 100 mM imidazole in the case of Fig. 6*A* and were rocked at room temperature for 20 min after sample buffer addition but before SDS-PAGE.

Blocking N-terminal Acetylation—The blocking of N-terminal acetylation in reticulocyte lysates was based on procedures described previously (14, 15). Briefly, 120 μl of quick coupled *in vitro* transcription/translation system (Promega) was supplemented with 1 mM oxaloacetic acid (Sigma) and 50 units/ml of citrate synthase (from porcine heart, Sigma), incubated at 25 °C for 7 min, and then supplemented with desulfo CoA lithium salt (Sigma) to give a final concentration of 1 mM after the addition of plasmid DNA and [^{35}S]methionine. Reactions were incubated for 2 h at 30 °C. Oxaloacetate and desulfo CoA were removed using Zeba microspin columns (Pierce). A control reaction was included to which citrate synthase only was added.

ATP Depletion—8 μl of *in vitro* translated ^{35}S-methione-labeled protein was combined with 40 μl of high speed interphase-activated egg extract, cleared of ribosomes by spinning at 107,400 × *g* for 40 min, supplemented with 200 μg/ml cycloheximide, 10 μg/ml leupeptin, pepstatin, and chymostatin, 1.5 mg/ml ubiquitin, and 2 μl of Energy Regeneration mix (20 μl of 100 mM EGTA; 20 μl of 1 M $MgCl_2$; 150 μl of 1 M phosphocreatine (Sigma); 200 μl of 100 mM adenosine 5′-triphosphate (GE Healthcare)) or 0.8 μl of 1600 units/ml hexokinase with 0.8 μl of 1 M glucose. Samples were used as in a normal degradation assay, described above.

RESULTS

NGN Can Be Ubiquitylated on Both Lysines and the N Terminus—We have previously demonstrated that NGN is turned over extremely rapidly in *Xenopus* eggs and embryos via

Downloaded from www.jbc.org at Cambridge University Library, on September 29, 2010

Supplemental Material can be found at:
http://www.jbc.org/content/suppl/2009/04/01/M809366200.DC1.html

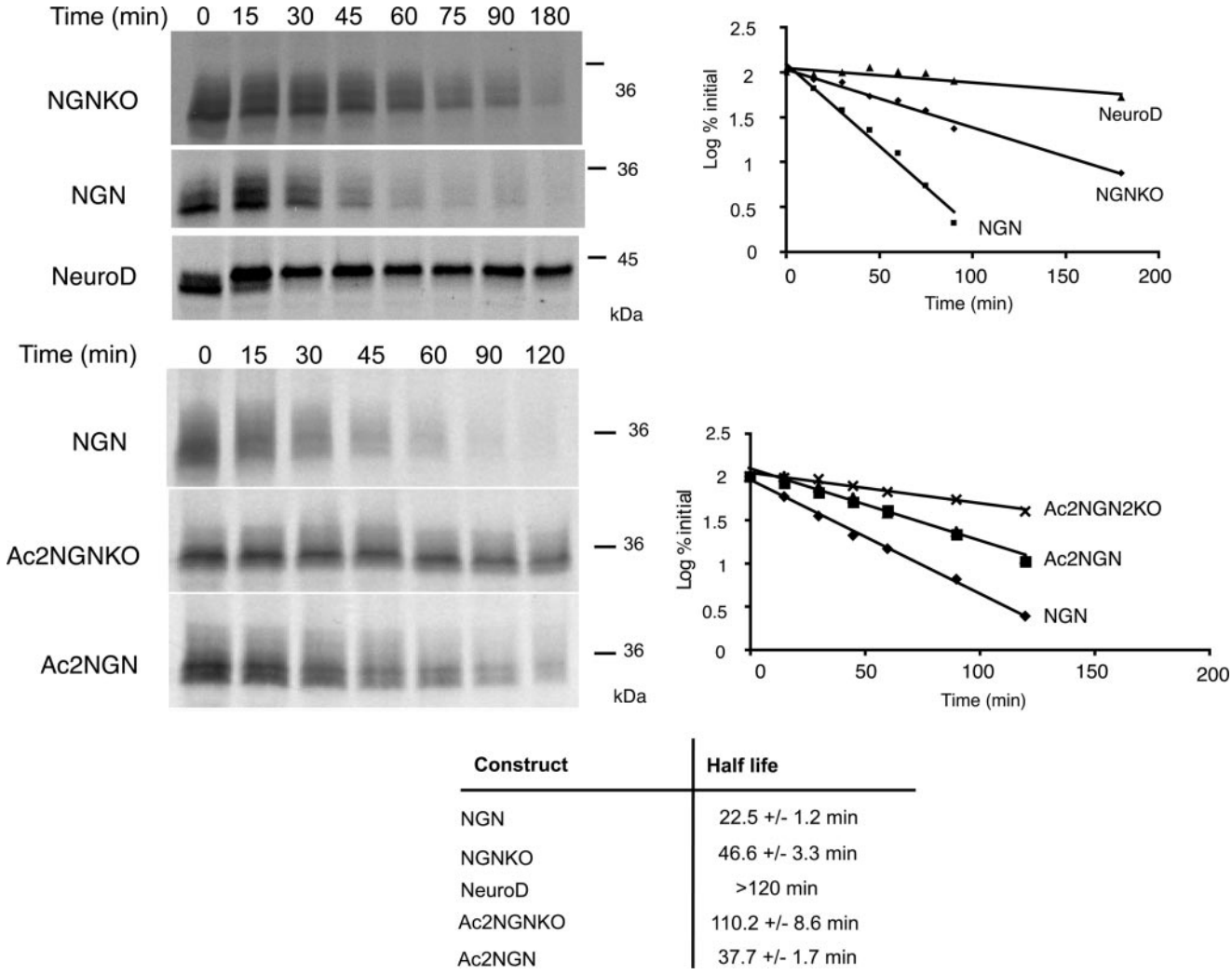

Construct	Half life
NGN	22.5 +/- 1.2 min
NGNKO	46.6 +/- 3.3 min
NeuroD	>120 min
Ac2NGNKO	110.2 +/- 8.6 min
Ac2NGN	37.7 +/- 1.7 min

FIGURE 1. **Neurogenin is degraded by both a lysine-dependent pathway and an N-terminal-dependent pathway.** Degradation assays in interphase egg extract were performed using [^{35}S]methionine-radiolabeled NGN, NGNKO, Ac2NGNKO, Ac2NGN, and NeuroD, as indicated, and analyzed by autoradiography (*left panels*) and quantitative phosphorimaging analysis (*right graphs*). Half-lives for degradation were calculated using first order kinetics (*bottom table*).

the UPS, whereas a related proneural protein NeuroD is stable (11). In an attempt to generate a stabilized form of NGN, its 8 lysine residues were mutated to arginines to produce a lysine-less protein (NGNKO). Arginine cannot be ubiquitylated but preserves the basic character of the lysine residues they replace (16). Both NGNKO and wild-type protein (NGN) were *in vitro* translated (IVT) in rabbit reticulocyte lysates in the presence of [^{35}S]methionine and added to *Xenopus* egg extracts, and the half-life was determined after SDS-PAGE analysis at increasing time points in a standard degradation assay. NGNKO had approximately double the half-life of the wild-type protein (46.6 ± 3.3 min *versus* 22.5 ± 1.2 min, Fig. 1) but was still degraded. We investigated whether NGN could join the small number of proteins thus far identified as being ubiquitylated on the N terminus.

Bulky N-terminal tags, such as six consecutive Myc tags, are thought to impede the accessibility of the α-amino group to the ubiquitylation machinery and so prevent N-terminal ubiquitylation (17). However, adding bulky tags (Myc tags or green fluorescent protein) to both the N termini and the C termini of NGN resulted in its stabilization (supplemental Fig. 1*A* and data not shown). Although this observation may have important implications for the use of tags on short-lived transcription factors, it led us to seek other ways to prevent N-terminal ubiquitylation.

Blocking the N Terminus by Promoting N-terminal Acetylation—A free, unmodified α-amino group of the substrate protein is required for N-terminal ubiquitylation. N-terminal cotranslational acetylation of the α-amino group is a common protein modification in eukaryotes, occurring in up to 80% of cytosolic proteins (18). The presence of an acetyl group at the N terminus prevents the attachment of ubiquitin (19), and this modification is thought to be irreversible (18). Primary sequence requirements for N-terminal acetylation in eukaryotes have been identified (18) and can be used to predict whether a protein with a given N-terminal sequence will be cotranslationally acetylated (20). We used an online prediction tool (Termi*N*ator, available from the CNRS) to determine the likelihood that NGN is cotranslationally acetylated. This analysis revealed that NGN is highly likely to be expressed with a free, unmodified N terminus (supplemental Fig. 1*B*). We then devised two alterations to the N terminus of NGN (MVLLK to

Downloaded from www.jbc.org at Cambridge University Library, on September 29, 2010

Supplemental Material can be found at:
http://www.jbc.org/content/suppl/2009/04/01/M809366200.DC1.html

MSESK and to MAESK, forming Ac1NGN and Ac2NGN, respectively) to promote its cotranslational acetylation (18). Additionally, a mutant was made in which the penultimate residue of NGN was replaced with proline (MVLLK to MPLLK, forming Ac3NGN), which completely blocks its N-terminal acetylation and therefore represents an appropriate control for our experiments (18).

Using our degradation assay, we compared the stability of Ac1NGN, Ac2NGN, and Ac3NGN with the wild-type protein. As we would predict whether N-terminal ubiquitylation contributes to NGN destruction, Ac1NGN and Ac2NGN had enhanced stability when compared with wild-type NGN (33.7 ± 1.7 min and 37.7 ± 1.7 min *versus* 22.5 ± 1.2 min). Ac3NGN had a half-life similar to the wild-type NGN protein (26.1 ± 0.6 min *versus* 22.5 ± 1.2 min).

To see whether ubiquitylation on lysines and the N terminus target for destruction additively or redundantly, we constructed NGNKO mutants where the N terminus was additionally modified to block ubiquitylation to produce Ac1NGNKO and Ac2NGNKO. The half-life of Ac1NGNKO and Ac2NGNKO was substantially increased (103.4 ± 3.9 min and 110.2 ± 8.6 min, respectively) when compared with NGN (22.5 ± 1.2 min), NGNKO (46.6 ± 3.3 min), and Ac2NGN (37.7 ± 1.7 min) (Fig. 1). Thus, ubiquitylation on internal lysines and the N terminus both contribute to the rapid degradation of NGN protein.

To confirm that these sequence alterations block degradation by promoting cotranslational acetylation, we examined the degradation of NGN, Ac3NGNKO, and Ac2NGNKO where cotranslational acetylation had been enzymatically inhibited. Methods for inhibiting translational acetylation in reticulocyte lysates have been previously described (14, 15). These involve enzymatic depletion of free acetyl CoA in reticulocyte lysates using citrate synthase and oxaloacetate followed by *in vitro* translation in the presence of a dead end analogue of acetyl CoA to competitively inhibit acetyl CoA-dependent N-terminal acetyltransferases. When Ac2NGNKO is *in vitro* translated under these conditions (Fig. 2), a marked destabilization in egg extract is observed (half-life of 42.5 ± 5.9 min after blocking acetylation when compared with 91.4 ± 10.1 min in the control). In contrast, NGNKO and Ac3NGNKO were found to be refractory to this treatment (Fig. 2), consistent with the non-acetylated status of the N termini of these proteins under normal *in vitro* translation conditions.

NGN Is Stabilized by Truncation at the N Terminus—It has been shown that several of the substrates of N-terminal ubiquitylation can be stabilized by the deletion of 5–30 amino acids from the N terminus. We took this approach with NGN as a further line of evidence for N-terminal ubiquitylation. We observed that an N-terminally truncated form of NGNKO where the first 20 amino acids had been removed (NGNKO Δ1–20) was also degraded more slowly than NGNKO (63.4 ± 4.4 min *versus* 45.3 ± 4 min, (supplemental Fig. 2*A*), again indicative of N-terminal ubiquitylation.

To mimic N-terminal ubiquitylation, we generated non-cleavable fusions of Ub and UbKO to NGNKO and examined the degradation kinetics. Consistent with N-terminal ubiquitylation contributing to NGN turnover, UbNGNKO was degraded faster than wild-type NGN (half-life of 10.5 ± 1 min *versus* 22.5 ± 1.2 min, respectively). In contrast, when we blocked N-terminal polyubiquitylation using an N-terminal fusion of ubiquitin where lysines had been mutated to arginines, this UbKONGNKO form of NGN was considerably stabilized when compared with both wild-type NGN and NGNKO (half-lives of 110.8 ± 10.7 min *versus* 22.5 ± 1.2 min and 46.6 ± 3.3 min, respectively, and see supplemental Fig. 2*B*). This further indicates that N-terminal ubiquitylation contributes to NGN instability. However, we were intrigued to see that, like Ac2NGNKO, slow degradation of UbKONGNKO was still observed.

In summary, the evidence presented above shows that NGN is ubiquitylated on the N terminus and on internal lysines, and both contribute to the instability of the protein. However, it is clear that, even when these two canonical modes of ubiquitylation are prevented, NGN is still subject to slow proteolysis. We have explored this further.

NGN Is Ubiquitylated on Cysteines—Despite the apparent absence of canonical ubiquitylation sites, Ac2NGNKO is still degraded in *Xenopus* egg extracts. Mg132 addition to the extract resulted in stabilization of Ac2NGNKO, as did the addition of a different proteasomal inhibitor epoxomicin (Fig. 3*A*; at 180 min on average, 32% of the Ac2NGNKO protein remained after the addition of DMSO when compared with 74 and 84% after the addition of MG132 and epoxomicin, respectively), indicating degradation by the proteasome. Furthermore, depletion of ATP by the addition of glucose and hexokinase, which would inactivate ATP-dependent proteasomal-mediated degradation, also resulted in stabilization of both wild-type NGN and Ac2NGNKO (Fig. 3*B*).

To determine whether degradation of Ac2NGNKO requires polyubiquitylation, we added methyl-Ub, a form of Ub that cannot support chain formation (21), to the extract. As expected, methylated Ub competes with an endogenous pool of free Ub in the extract resulting in stabilization of Ac2NGNKO (Fig. 3*C*); at 180 min, an average of 34% of the Ac2NGNKO protein still remained after the addition of Ub when compared with 76% after the addition of methylated Ub. To confirm that ubiquitylation was occurring even in the absence of canonical ubiquitylation sites, we performed an assay to detect ubiquitylated forms of NGN directly.

IVT [^{35}S]methionine-labeled NGN and mutants thereof were incubated in egg extract in the presence of Mg132 to prevent protein degradation by the 26 S proteasome and allow ubiquitylation to be observed. Proteins covalently bound to His-Ub (with untagged Ub as a control) were then pulled down using Ni^{2+}-nitrilotriacetate-agarose, in the presence of 8 M urea. Proteins covalently attached to His-Ub were separated by SDS-PAGE and subjected to autoradiography (Fig. 4*A*). After His-Ub pull down, as expected, multiple slower migrating forms of NGN and Ac2NGN were visible as a ladder specifically in the presence of His-Ub, consistent with multiply ubiquitylated forms of the protein (Fig. 4*A*), presumably linked to lysines. A similar ladder was seen using NGNKO, where ubiquitylation on the N terminus is possible. However, Ac2NGNKO (Fig. 4*A*), which does not have canonical Ub sites, was also precipitated using His-Ub, although the ladder at higher molecular

Downloaded from www.jbc.org at Cambridge University Library, on September 29, 2010

Supplemental Material can be found at:
http://www.jbc.org/content/suppl/2009/04/01/M809366200.DC1.html

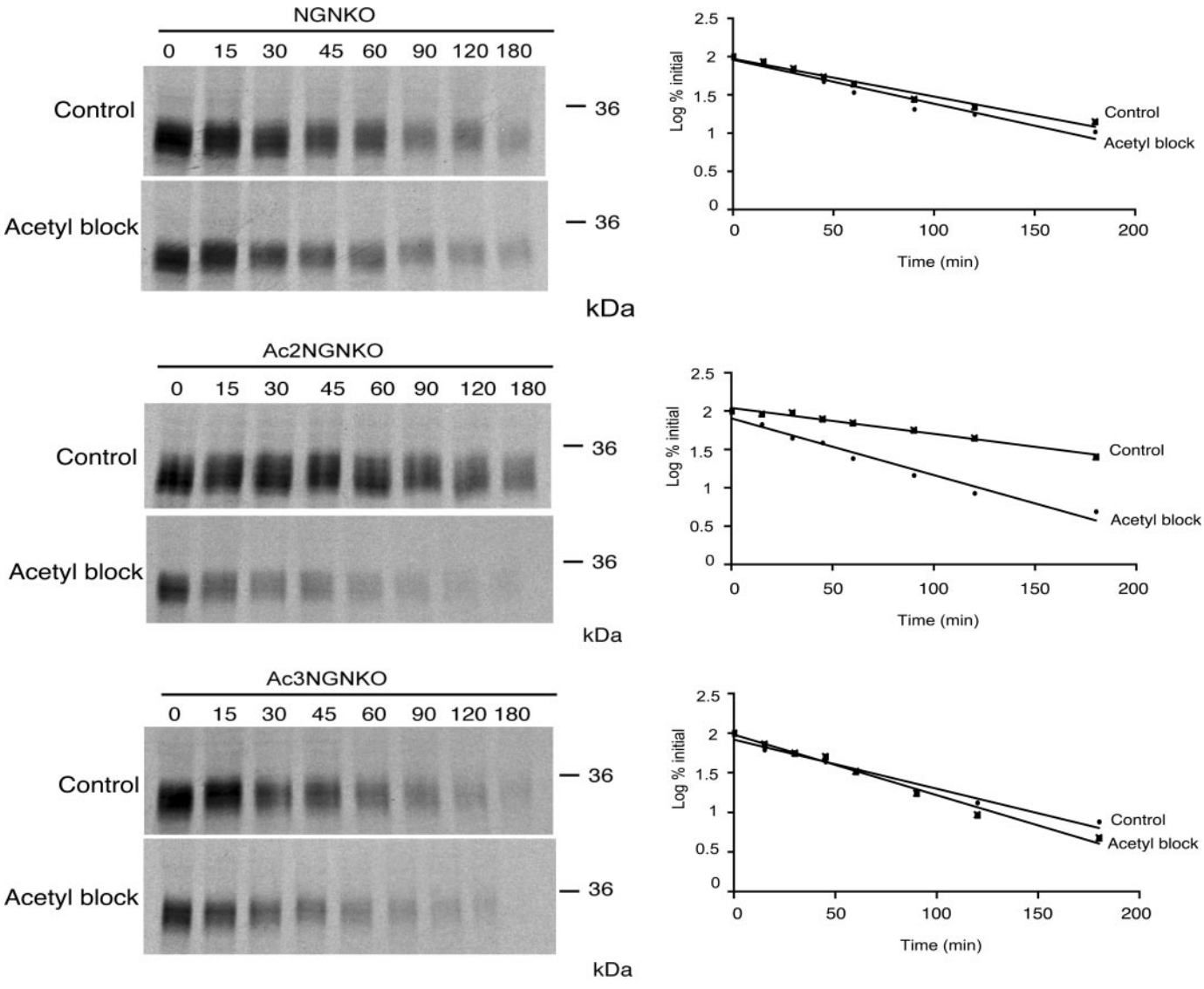

Construct	Half life (acetyl block)	Half life (control)
NGNKO	60.9 +/- 15.7 min	67.8 +/- 19.2 min
Ac2NGNKO	42.5 +/- 5.9 min	91.4 +/- 10.1 min
Ac3NGNKO	53.7 +/- 11.4 min	41.2 +/- 6.6 min

FIGURE 2. **Stability of acetylation mutants of NGN is affected by acetylation-blocking.** Degradation assays in interphase egg extract were performed on NGN constructs, as indicated, *in vitro* translated either in the absence (*Control*) or in the presence of citrate synthase, oxaloacetate, and desulfo CoA (*Acetyl block*). Assays were analyzed by autoradiography (*left panels*) and quantitative phosphorimaging analysis (*right graphs*).

weights tended to be somewhat reduced. Significantly, in addition to this faint ladder of polyubiquitylated forms, a band was observed running below 36 kDa, the size at which unmodified NGN protein migrates on SDS-PAGE. Moreover, this band appears more prominent in NGNKO mutants, although it is clearly detectable even in the wild-type NGN sample. We reasoned that unconjugated NGN protein would be released from Ub chains if attachment were via linkages labile to the conditions used in SDS-PAGE, which involve sample preparation at high temperature and include reducing agents, conditions that would break thioester bonds.

To test whether NGN can be conjugated to Ub via such labile linkages, we performed a standard ubiquitylation assay but separated bound proteins by SDS-PAGE either without reducing agents (non-reducing (Fig. 4*B* (*Non red*)) or with reducing agents at high pH (reducing (*red*) conditions), based upon conditions that have previously been used to disrupt labile Ub thioester linkages to cysteines (3) (Fig. 4*B*). NGN showed a ladder of

Downloaded from www.jbc.org at Cambridge University Library, on September 29, 2010

Supplemental Material can be found at:
http://www.jbc.org/content/suppl/2009/04/01/M809366200.DC1.html

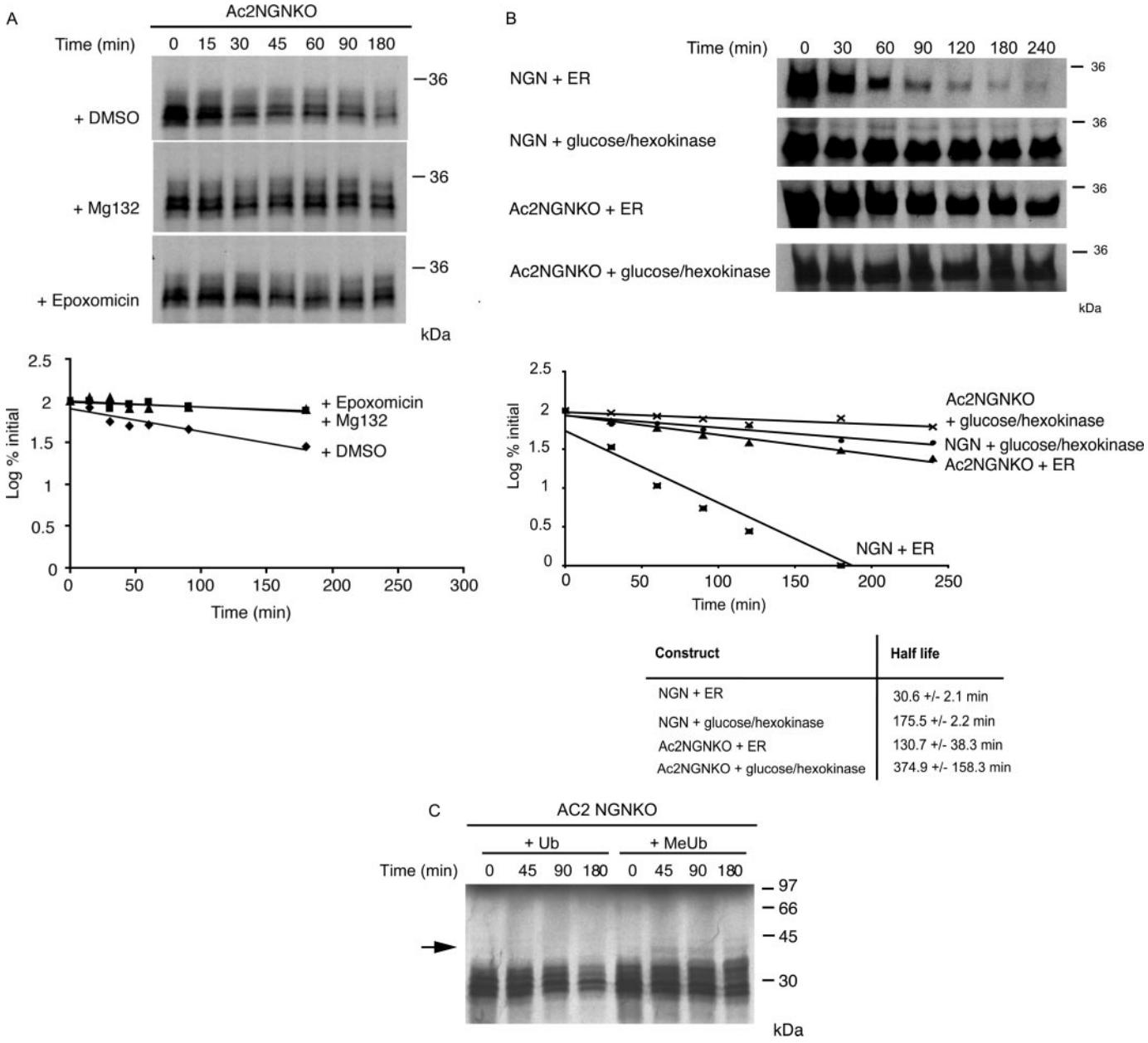

FIGURE 3. **N-terminally blocked NGN lacking lysines is still degraded in a ubiquitin-dependent manner in egg extracts.** *A*, degradation assays in interphase egg extract of [^{35}S]methionine-radiolabeled Ac2NGNKO were performed in the presence of the proteasome inhibitor Mg132 (200 μM), epoxomicin (100 μM) or DMSO alone and analyzed by autoradiography and quantitative phosphorimaging analysis. *B*, degradation assays in interphase egg extract of [^{35}S]methionine-radiolabeled NGN or Ac2NGNKO were performed in the presence (+*ER*) or absence (+*glucose/hexokinase*) of ATP, where ER represents Energy Regeneration mix. *C*, degradation assays of Ac2NGNKO was performed in the presence of ubiquitin or methylated ubiquitin (*MeUb*).

polyubiquitylated species in both reducing and non-reducing conditions (Fig. 4*B*), indicating that most Ubs are indeed conjugated to lysine, an isopeptide linkage insensitive to these conditions. However, in reducing conditions, we saw a prominent band at the size corresponding to unmodified NGN that is barely present with non-reducing sample preparation (Fig. 4*B*, marked with *), indicating that a proportion of ubiquitylated wild-type NGN is conjugated through labile linkages.

In contrast to wild-type NGN, forms of NGN lacking lysines and precipitated by His-Ub (NGNKO, Ac2NGNKO, Ac3NGNKO) appeared strikingly different when separated by SDS-PAGE in non-reducing and reducing conditions (Fig. 4*C*). In non-reducing conditions, a ladder of polyubiquitylated species is present, but this is substantially diminished under reducing conditions, and this coincides with the appearance of a strong band of unconjugated NGN. This is consistent with substantial ubiquitylation of NGNKO via linkages that are labile to reducing conditions, which would include thioester linkages between Ub and cysteine.

To investigate this further, we generated an NGN mutant where all 7 cysteines had been mutated to alanine (NGNCO). Importantly, this mutant version of NGN, NGNCO, as well as the other mutant forms of NGN assayed above, are all able to bind to DNA and to activate an NGN reporter construct after expression in *Xenopus* embryos (Fig. 5). Functionality indicates largely intact structures of the mutant forms. We did note that

Downloaded from www.jbc.org at Cambridge University Library, on September 29, 2010

Supplemental Material can be found at:
http://www.jbc.org/content/suppl/2009/04/01/M809366200.DC1.html

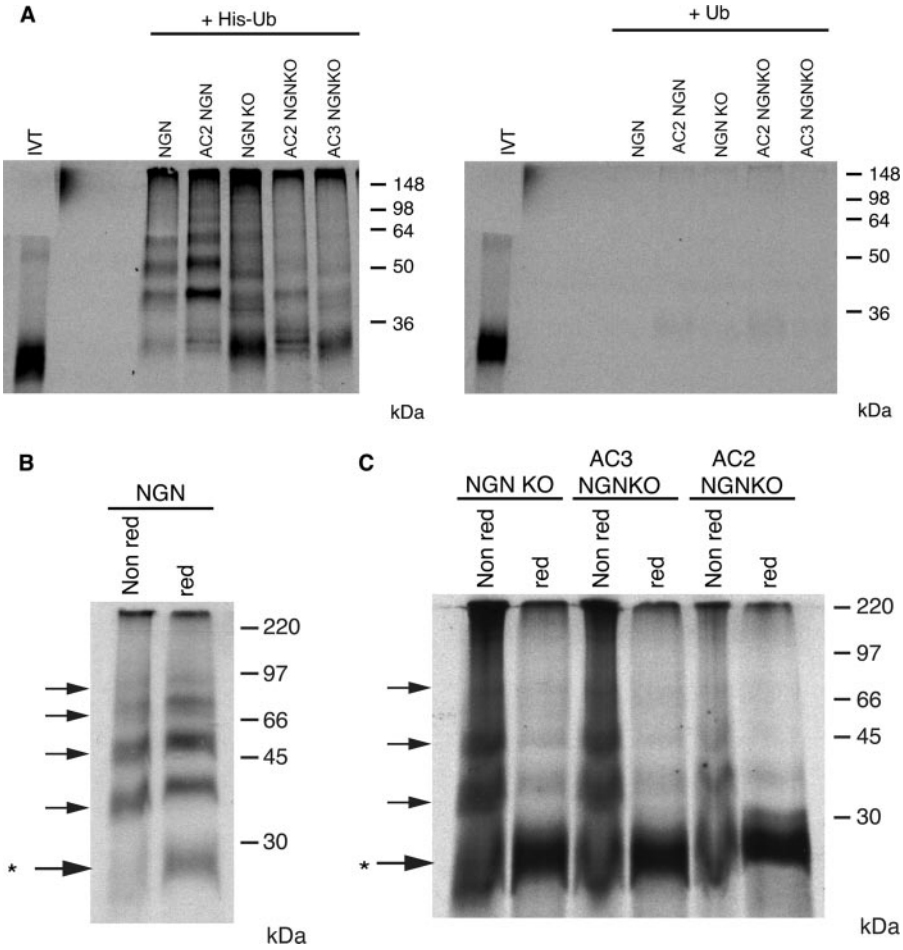

FIGURE 4. **N-terminally blocked NGN lacking lysines is still ubiquitylated in egg extracts.** *A*, ubiquitylation assays were performed using NGN, Ac2NGN, NGNKO, Ac2NGNKO, and Ac3NGNKO in the presence of His-ubiquitin or ubiquitin. *B*, ubiquitylation assays were performed with NGN. Reactions were eluted either under non-reducing (*Non red*) or under reducing/pH 10 conditions (*red*). *C*, ubiquitylation assays were performed using NGNKO, Ac2NGNKO, and Ac3NGNKO. Reactions were eluted either under non-reducing or under reducing/pH 10 conditions. Note that NGN and NGN mutant samples were from the same experiment with identical conditions and exposures. Non-modified NGN is marked by *.

NGNCO mutants do run as a tighter band than NGN on SDS-PAGE (Fig. 6). To determine whether the presence of cysteine residues contributes to NGN instability, we tested the half-life of NGNCO in interphase, which was similar to that of wild-type NGN (24.2 ± 1.9 min *versus* 22.5 ± 1.2 min). We constructed forms of NGN with other potential ubiquitylation sites mutated (see above) in a background where cysteines were also mutated (Ac2NGNCO, NGNKOCO, and Ac2NGNKOCO). Half-life analyses (Fig. 6, *A* and *B*) show that mutation of cysteines results in slower degradation of all these modified forms of NGN. In particular, in interphase, when the N-terminal ubiquitylation pathway is blocked, ubiquitylation on lysines cannot fully compensate for the loss of cysteines; Ac2NGNCO is degraded more slowly than Ac2NGN, although lysines are intact in both (Fig. 6*B*). However, although ubiquitylation on canonical residues and on cysteines can both target for degradation in interphase, redundancy between ubiquitylation pathways exists under these conditions as cysteines are not absolutely required for rapid degradation (Fig. 6*A*).

NGN protein has a short half-life in interphase extracts, but the control of degradation of proteins can often vary between interphase and mitosis (22). Hence, we investigated the half-life of NGN in egg extracts that had been rendered mitotic by the addition of a non-degradable form of cyclin B (23) (Fig. 6*C*). Strikingly, in mitosis, NGN is degraded even more rapidly than in interphase, with a half-life of 15.8 ± 2.1 min. We then compared the contribution of lysines and cysteines with the degradation of NGN in mitosis. NGNKO had an increased half-life of 35.6 ± 2.7 min in mitotic extracts. Importantly and in contrast to interphase, NGNCO was also significantly stabilized when compared with wild-type NGN, with a half-life, 38.3 ± 5.4 min, almost three times that of the wild-type protein. These results indicate that ubiquitylation on cysteine and lysine both contribute to the very rapid rate of degradation seen in mitosis. N-terminal ubiquitylation can also contribute to degradation in mitosis; Ac2NGNKO had a half-life of 82.0 ± 47.8 min when compared with 35.6 ± 2.7 min for NGNKO.

We then determined whether NGN lacking both canonical and cysteine ubiquitylation sites was fully stable, investigating the degradation of Ac2NGNKOCO, where the N terminus was blocked by acetylation and both lysines and cysteines were mutated to arginines and alanines, respectively. When compared with NGNKO, we observed that Ac2NGNKOCO was dramatically stabilized, with a half-life of greater than 180 min, and appeared more stable than Ac2NGNKO, yet we still observed very slow degradation (Fig. 7). Moreover, the stability of Ac2NGNKOCO was further enhanced by the presence of Mg132 (Fig. 7*B*) and epoxomicin (Fig. 7*B*). Under these condition, ubiquitins may still form ester linkages to serines and/or threonines, which have been predicted to be broken by high pH alone (4, 24). To investigate these potential linkages further, we performed ubiquitylation assays using wild-type NGN, NGNCO, and Ac2NGNKOCO either in the absence or in the presence of reducing agents or at high pH (Fig. 7*C*).

NGN Can Be Ubiquitylated on Serines and/or Threonines—To determine whether Ub was linked to Ac2NGNKOCO via ester bonds, we performed ubiquitylation assays and separated samples by SDS-PAGE either in the presence of reducing agents (with sample heating) or at high pH (Fig. 7*C*). In the absence of reducing agents, His-Ub precipitation of polyubiquitylated NGN, as expected, showed a multitude of higher molecular weight forms, corresponding to polyubiquitylated

Downloaded from www.jbc.org at Cambridge University Library, on September 29, 2010

Supplemental Material can be found at:
http://www.jbc.org/content/suppl/2009/04/01/M809366200.DC1.html

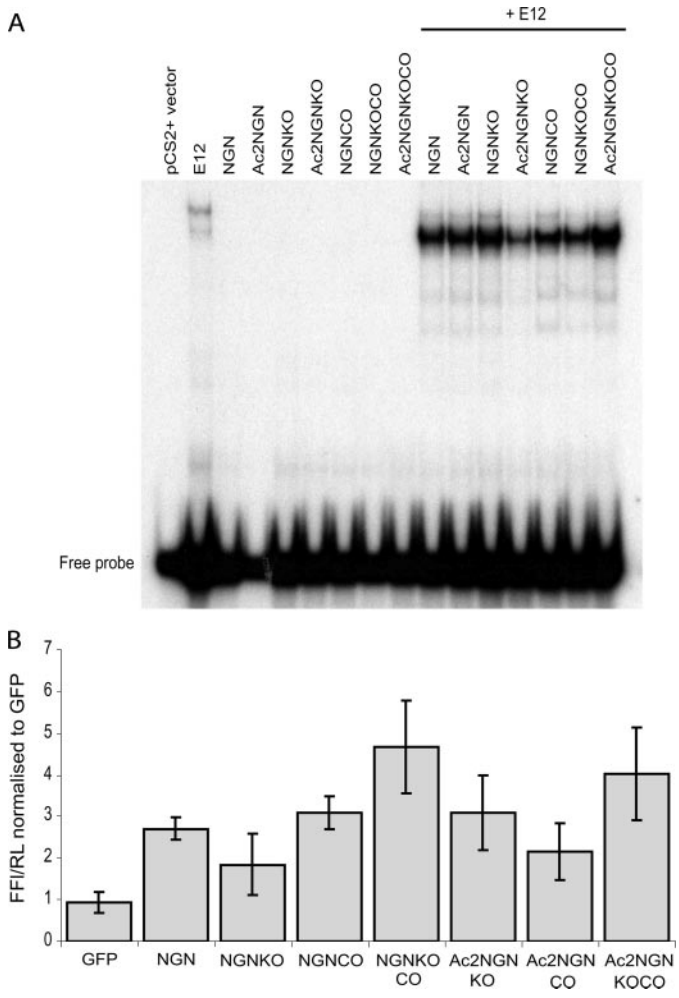

FIGURE 5. **Mutant NGN protein shows wild-type DNA binding.** *A*, NGN constructs, as indicated, were translated *in vitro* and incubated with ^{32}P-labeled E-box DNA probe in the presence or absence of the heterodimeric binding partner, E12. In the absence of E12, neither wild-type nor mutant NGN proteins are able to bind the probe. In the presence of E12, all NGN derivatives show wild-type binding to the probe. The experiment has been performed in triplicate; slight variations in binding efficiency seen here were not consistently observed. *B*, mutant NGN constructs activate a reporter gene at wild-type levels *in vivo*. *Xenopus laevis* embryos were injected with 50 pg of NGN mRNA as indicated, together with 200 pg of Beta2 reporter Firefly luciferase construct (*FFL*), as a direct downstream target of NGN, and 6 pg of constitutively expressed *Renilla* luciferase (*RL*), as an internal control. There is no significant difference between activation of the reporter gene by wild-type NGN or by mutant NGN constructs. Values obtained are from independent duplicate experiments (each sample in triplicate) and show mean ± S.E. *GFP*, green fluorescent protein.

NGN protein. Unconjugated NGN was visible particularly after the addition of dithiothreitol, indicating that a population of wild-type NGN is linked to Ub via thioester linkages, as described above. A polyubiquitylated ladder of NGNCO was also visible, where presumably most Ubs are linked to lysines via isopeptide bonds. Interestingly, when ubiquitylated NGNCO was run after sample treatment at high temperature and pH, conditions that would break ester bonds, free NGNCO is released, indicating that in the absence of cysteines, ubiquitylation can occur on serines and/or threonines instead. We did note that when NGNCO samples were run in the presence of reducing agents, we still observed higher forms of NGNCO, although some release of free NGNCO did occur. This is most likely due to breaking of highly labile ester linkages on sample heating as cysteine residues are not available for thioester bond formation.

In contrast to NGN and NGNCO, His-Ub pull down of Ac2NGNKOCO showed reduced very high molecular mass forms of the proteins, but instead, we saw a prominent short ladder of NGN conjugates between 30 and 60 kDa. When samples were run in the presence of reducing agents, we still observed higher forms of wild-type NGN, although again some release of free Ac2NGNKOCO did occur, most likely due to breaking of labile ester linkages on sample heating. However, raising the sample pH as well as heating, which results in efficient alkaline hydrolysis of ester bonds, led to substantial collapse of slower migrating forms of NGN, releasing almost entirely unconjugated Ac2NGNKOCO. Thus, in the absence of a free N terminus, lysines, and cysteines, Ubs can still conjugate via ester linkages to serines and/or threonines (Fig. 7*C*), and these linkages alone can result in very slow turnover of the protein (Fig. 7). We would note that high pH treatment alone of ubiquitylated wild-type NGN did not release substantial free NGN protein, indicating that Ser/Thr ubiquitylation of NGN does not usually occur to a great extent.

DISCUSSION

For the first time, we demonstrate here that ubiquitylation of an intact and active cellular protein occurs at three distinct types of site: Ub conjugation to the N terminus, Ub conjugation to lysines, and Ub conjugation via non-canonical linkages to cysteines. In addition, in the absence of other available sites, ubiquitylation can be redirected to serines and/or threonine residues. Ubiquitylation on cysteine residues has been theoretically postulated for many years, yet it has only been very recently shown to occur in a cellular setting, almost exclusively to regulate intracellular movement. We show here that it can occur and act in parallel with canonical ubiquitylation to target a protein for destruction. Moreover, non-canonical ubiquitylation via cysteines may play a greater role in NGN turnover in mitosis, where degradation rate is faster than in interphase, indicating that different Ub acceptors may change in prominence under different cellular conditions. Although different modes of ubiquitylation may individually contribute to small differences in protein stability, nevertheless, this may lead to a significant difference in the steady state level of the protein (25).

Several studies (3, 5, 6, 8) have reported very unusual non-canonical ubiquitylation including on cysteines, but none have demonstrated this modification directly by mass spectroscopy. It has been proposed that one explanation is the small amount of ubiquitylated molecules available for purification (3). In addition, thioester and ester bonds are very labile and may not withstand sample preparation. We have also encountered technical problems purifying sufficient NGN monomeric protein for mass spectroscopy analysis. Hence, for these reasons, we have instead used biochemical methods to demonstrate non-canonical ubiquitylation.

Non-canonical ubiquitylation does occur on the wild-type NGN protein, but we did observe that these non-canonical linkages assumed more experimental prominence in the absence of lysines; we would note that very few proteins have had ubiqui-

Downloaded from www.jbc.org at Cambridge University Library, on September 29, 2010

Supplemental Material can be found at:
http://www.jbc.org/content/suppl/2009/04/01/M809366200.DC1.html

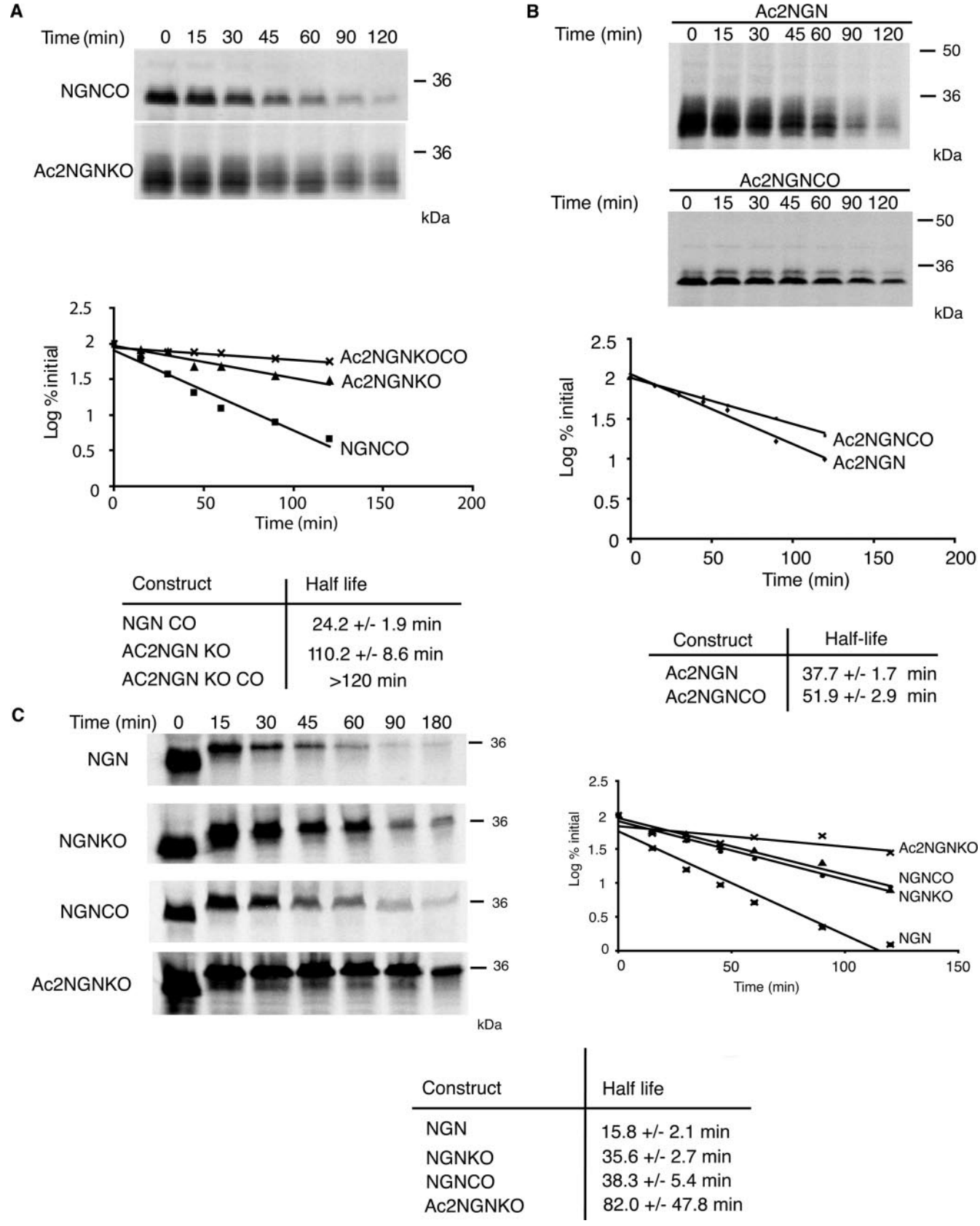

Construct	Half life
NGN CO	24.2 +/- 1.9 min
AC2NGN KO	110.2 +/- 8.6 min
AC2NGN KO CO	>120 min

Construct	Half-life
Ac2NGN	37.7 +/- 1.7 min
Ac2NGNCO	51.9 +/- 2.9 min

Construct	Half life
NGN	15.8 +/- 2.1 min
NGNKO	35.6 +/- 2.7 min
NGNCO	38.3 +/- 5.4 min
Ac2NGNKO	82.0 +/- 47.8 min

FIGURE 6. **NGN lacking canonical ubiquitylation sites is still ubiquitylated and degraded in a proteasomal-dependent manner.** Degradation assays in interphase egg extract of [^{35}S]methionine-radiolabeled constructs of NGN were performed using NGNCO, Ac2NGNKO, and Ac2NGNKOCO (*A*) or Ac2NGN and Ac2NGNCO (*B*). Assays were analyzed by autoradiography and quantitative phosphorimaging analysis. *C*, degradation assays in mitotic egg extract were performed using NGN, NGNKO, NGNCO, and Ac2NGNKO and analyzed by autoradiography and quantitative phosphorimaging analysis.

Downloaded from www.jbc.org at Cambridge University Library, on September 29, 2010

Supplemental Material can be found at:
http://www.jbc.org/content/suppl/2009/04/01/M809366200.DC1.html

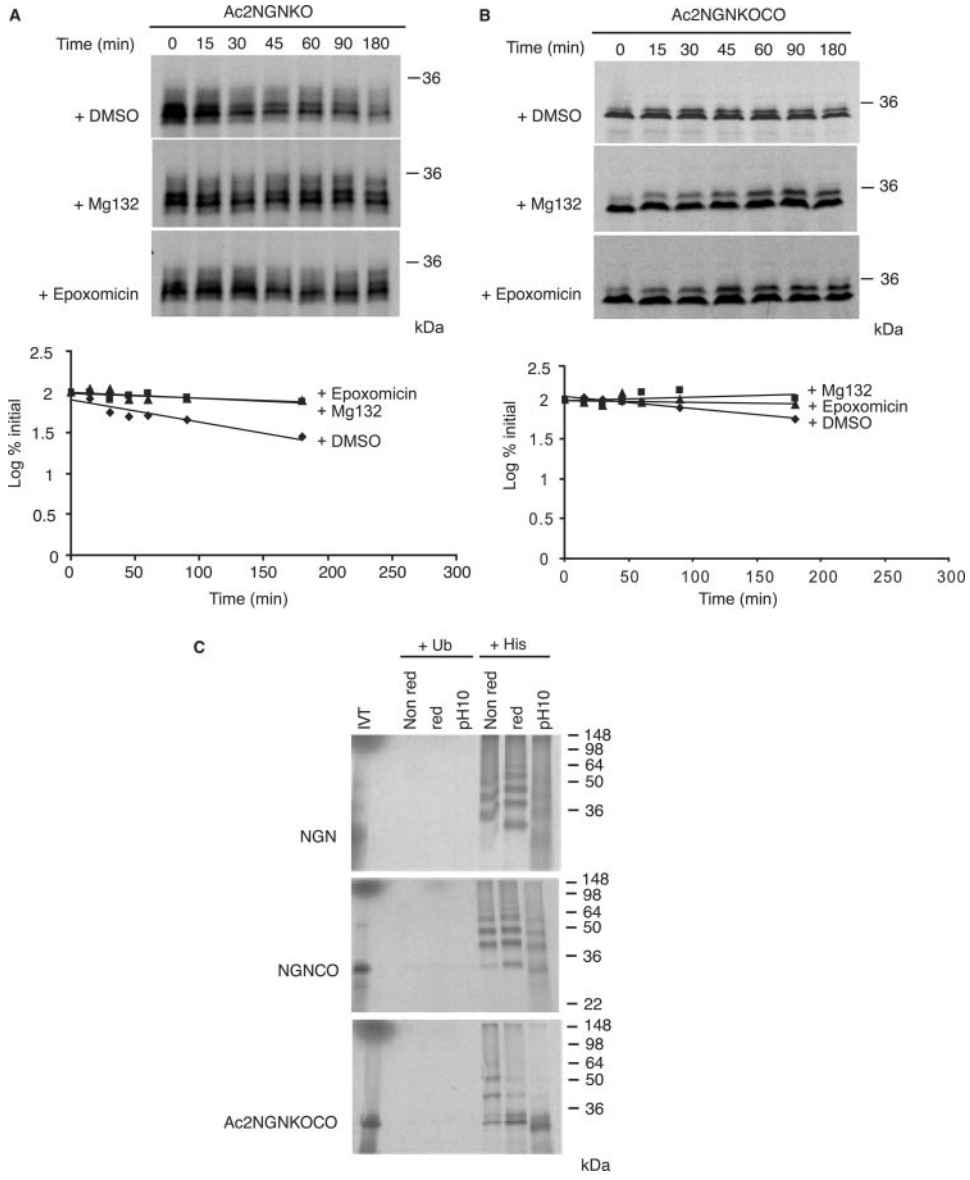

FIGURE 7. **NGN lacking canonical ubiquitylation sites and non-canonical cysteines is still ubiquitylated and degraded by the proteasome.** Degradation assays in interphase egg extract of [^{35}S]methionine-radiolabeled constructs of NGN were performed using Ac2NGNKO (*A*) and Ac2NGNKOCO (*B*) in the presence or absence of proteasome inhibitors Mg132 and epoxomicin. Assays were analyzed by autoradiography and quantitative phosphorimaging analysis. *C*, ubiquitylation assays were performed in interphase extract using NGN, NGNCO, and Ac2NGNKOCO in the presence of His-Ub or Ub, and samples prepared for SDS-PAGE under non-reducing conditions (*Non red*), reducing conditions (*red*), or high pH (*pH10*) conditions (with samples heated to 95 °C for 5 min prior to loading in all cases).

tylation analyzed after all lysine residues have been mutated. Cysteine ubiquitylation may be more important under these circumstances or where native lysines are not available for ubiquitylation due to other modifications such as acetylation. However, it is quite possible that non-canonical ubiquitylation may occur more widely than has previously been supposed, but these modifications could have been overlooked by current experimental approaches, particularly as assay and analysis conditions very commonly including sample preparation involving high temperature and reducing agents, conditions that will break these non-canonical linkages.

If simultaneous canonical and non-canonical ubiquitylation occurs on other proteins and site prominence varies at different cell cycle phases, this would substantially increase the complexity of the UPS system and require reanalysis of, for instance, some proteins thought to be targeted to the proteasome in the absence of ubiquitylation (for a review, see Ref.26). Possible candidates for non-canonical ubiquitylation include other basic helix-loop-helix proteins such as MyoD, which shows different modes of canonical ubiquitylation to NGN (27, 28). In addition, naturally lysineless proteins such as $p14^{ARF}$ (29, 30) may also undergo ubiquitylation on non-canonical sites such as cysteine to target for proteasomal degradation.

Non-canonical ubiquitylation of NGN does lead to Ub chains of sufficient length and with the correct linkage to target for destruction. The ability to ubiquitylate on multiple canonical and non-canonical sites demonstrates remarkable flexibility of the ubiquitylation apparatus. Ubiquitin ligases for NGN have yet to be identified and, at present, it is not clear whether the same enzymes that catalyze ubiquitylation of lysines can also target the N terminus and/or cysteine residues and indeed also serines and threonines in the absence of other available ubiquitylation sites. There clearly is much flexibility in the machinery that ubiquitylates NGN; we have seen that no single lysine in NGN is indispensable for canonical ubiquitylation (supplemental Fig. 3). Thus, how specificity of these ubiquitylation reactions is controlled remains to be established.

Another important point to note is that, in our system, ubiquitylation on canonical and non-canonical sites can be brought about entirely by cellular ubiquitin ligases found in the *Xenopus* egg extract. We have preliminary data that ubiquitylation on non-canonical residues may also occur in mammalian cells (data not shown), indicating that non-canonical ubiquitylation is a more widespread phenomenon. In summary, our analyses demonstrate that both canonical and non-canonical ubiquitylation brought about by the cellular ubiquitylation machinery occur simultaneously, and both can drive proteasomal degradation. We postulate that such regulation of a single protein by multiple canonical and non-canonical ubiquitylation events may be found to be more widespread on closer study of other proteins and systems and that the importance of these two modes of

Downloaded from www.jbc.org at Cambridge University Library, on September 29, 2010

Supplemental Material can be found at:
http://www.jbc.org/content/suppl/2009/04/01/M809366200.DC1.html

ubiquitylation may differ for the same protein under differing cellular conditions.

Acknowledgments—We thank Helen Wise for preliminary findings on activity of NGN mutants, Catherine Wilson for technical support, and Francois Guillemot, Laura Itzhaki, Shin-ichi Ohnuma, Ashok Venkitaraman, and Ron Laskey for helpful discussions. Ubiquitin constructs were a kind gift of C. Holt.

REFERENCES

1. Glickman, M. H., and Ciechanover, A. (2002) *Physiol. Rev.* **82,** 373–428
2. Ciechanover, A., and Ben-Saadon, R. (2004) *Trends Cell Biol.* **14,** 103–106
3. Cadwell, K., and Coscoy, L. (2005) *Science* **309,** 127–130
4. Breitschopf, K., Bengal, E., Ziv, T., Admon, A., and Ciechanover, A. (1998) *EMBO J.* **17,** 5964–5973
5. Carvalho, A. F., Pinto, M. P., Grou, C. P., Alencastre, I. S., Fransen, M., Sá-Miranda, C., and Azevedo, J. E. (2007) *J. Biol. Chem.* **282,** 31267–31272
6. Williams, C., van den Berg, M., Sprenger, R. R., and Distel, B. (2007) *J. Biol. Chem.* **282,** 22534–22543
7. Ravid, T., and Hochstrasser, M. (2007) *Nat. Cell Biol.* **9,** 422–427
8. Tait, S. W., de Vries, E., Maas, C., Keller, A. M., D'Santos, C. S., and Borst, J. (2007) *J. Cell Biol.* **179,** 1453–1466
9. Sun, Y., Nadal-Vicens, M., Misono, S., Lin, M. Z., Zubiaga, A., Hua, X., Fan, G., and Greenberg, M. E. (2001) *Cell* **104,** 365–376
10. Salic, A., Lee, E., Mayer, L., and Kirschner, M. W. (2000) *Mol. Cell* **5,** 523–532
11. Vosper, J. M., Fiore-Heriche, C. S., Horan, I., Wilson, K., Wise, H., and Philpott, A. (2007) *Biochem. J.* **407,** 277–284
12. Butt, T. R., Khan, M. I., Marsh, J., Ecker, D. J., and Crooke, S. T. (1988) *J. Biol. Chem.* **263,** 16364–16371
13. Raiborg, C., Bache, K. G., Gillooly, D. J., Madshus, I. H., Stang, E., and Stenmark, H. (2002) *Nat. Cell Biol.* **4,** 394–398
14. Rubenstein, P., Smith, P., Deuchler, J., and Redman, K. (1981) *J. Biol. Chem.* **256,** 8149–8155
15. Palmiter, R. D. (1977) *J. Biol. Chem.* **252,** 8781–8783
16. Chau, V., Tobias, J. W., Bachmair, A., Marriott, D., Ecker, D. J., Gonda, D. K., and Varshavsky, A. (1989) *Science* **243,** 1576–1583
17. Ciechanover, A. (2005) in *Ubiquitin-Proteasome Protocols* (Patterson, C., and Cyr, D. M., eds) pp. 255–270, Humana Press, New York
18. Polevoda, B., and Sherman, F. (2003) *J. Mol. Biol.* **325,** 595–622
19. Kuo, M. L., den Besten, W., Bertwistle, D., Roussel, M. F., and Sherr, C. J. (2004) *Genes Dev.* **18,** 1862–1874
20. Meinnel, T., Peynot, P., and Giglione, C. (2005) *Biochimie* **87,** 701–712
21. Hershko, A., Ganoth, D., Pehrson, J., Palazzo, R. E., and Cohen, L. H. (1991) *J. Biol. Chem.* **266,** 16376–16379
22. Lindon, C., Albagli, O., Domeyne, P., Montarras, D., and Pinset, C. (2000) *Mol. Cell. Biol.* **20,** 8923–8932
23. Murray, A. W., and Kirschner, M. W. (1989) *Nature* **339,** 275–280
24. Passmore, L. A., and Barford, D. (2004) *Biochem. J.* **379,** 513–525
25. Lingbeck, J. M., Trausch-Azar, J. S., Ciechanover, A., and Schwartz, A. L. (2003) *J. Biol. Chem.* **278,** 1817–1823
26. Hoyt, M. A., and Coffino, P. (2004) *Cell Mol Life Sci.* **61,** 1596–1600
27. Sadeh, R., Breitschopf, K., Bercovich, B., Zoabi, M., Kravtsova-Ivantsiv, Y., Kornitzer, D., Schwartz, A., and Ciechanover, A. (2008) *Proc. Natl. Acad. Sci. U. S. A.* **105,** 15690–15695
28. Tintignac, L. A., Lagirand, J., Batonnet, S., Sirri, V., Leibovitch, M. P., and Leibovitch, S. A. (2005) *J. Biol. Chem.* **280,** 2847–2856
29. Rodway, H., Llanos, S., Rowe, J., and Peters, G. (2004) *Oncogene* **23,** 6186–6192
30. Pollice, A., Vivo, M., and La Mantia, G. (2008) *FEBS Lett.* **582,** 3257–3262

Downloaded from www.jbc.org at Cambridge University Library, on September 29, 2010

Biochemical and Biophysical Research Communications xxx (2010) xxx–xxx

Contents lists available at ScienceDirect

Biochemical and Biophysical Research Communications

journal homepage: www.elsevier.com/locate/ybbrc

Non-canonical ubiquitylation of the proneural protein Ngn2 occurs in both *Xenopus* embryos and mammalian cells

Gary S. McDowell [a], Romana Kucerova [a,b], Anna Philpott [a,*]

[a] Department of Oncology, University of Cambridge, Hutchison/Medical Research Council (MRC) Research Centre, Addenbrooke's Hospital, Cambridge CB2 0XZ, UK
[b] Department of Transcriptional Regulation, Institute of Molecular Genetics, Videnska 1083, Prague, 142 20, Czech Republic

ARTICLE INFO

Article history:
Received 23 August 2010
Available online xxxx

Keywords:
Xenopus
Ubiquitylation
bHLH
Ngn2
Neurogenesis
Cysteine

ABSTRACT

Poly-ubiquitin chains targeting proteins for 26S proteasomal degradation are classically anchored on internal lysines of substrates via iso-peptide linkages. However recently, linkage of ubiquitin moieties to non-canonical nucleophilic residues, such as cysteines, serines and threonines, has been demonstrated in a small number of cases.

Non-canonical ubiquitylation of the proneural protein Ngn2 has previously been seen in *Xenopus* egg extract, but it was not clear whether such highly unusual modes of ubiquitylation were restricted to the environment of egg cytoplasm. Here we show that Ngn2 is, indeed, ubiquitylated on non-canonical sites in extracts from neurula stage *Xenopus* embryos, when Ngn2 is usually active. Moreover, in the P19 mammalian embryonal carcinoma cell line capable of differentiating into neurons, xNgn2 is ubiquitylated on both canonical and non-canonical sites. We see that mutation of cysteines alone results stabilisation of the protein in P19 cells, indicating that non-canonical ubiquitylation on these residues normally contributes to the fast turnover of xNgn2 in mammalian cells.

© 2010 Elsevier Inc. All rights reserved.

Introduction

The levels of individual proteins must be tightly controlled to generate a highly dynamic cellular environment adapted to respond to changing environmental and developmental cues. Large numbers of proteins are targeted by the ubiquitin–proteasome system, resulting in their rapid and responsive regulation [1,2]. The small protein ubiquitin (Ub), when covalently fused to its substrate, plays a context dependent role in signalling the destination of a protein, for instance localising the protein to the nucleus, or dispatching the protein to cellular compartments such as the lysozome [3]. Poly-ubiquitin chains are built up on a substrate protein via covalent linkages, typically to lysine48 of the first Ub moiety, and this is sufficient to deliver the substrate to the 26S proteasome where unfolding and cleavage into peptides, and subsequent degradation, occurs [4].

The sites on the substrate protein to which the first Ub is attached, providing an anchor point for subsequent Ub chain elongation, have been well-studied in many proteins, and typically occurs on substrate lysines via an iso-peptide linkage. In a small number of proteins, often those lacking lysines, ubiquitylation has been shown to occur on the N-terminal alpha-amino group via a peptide linkage [5,6]. It is chemically possible for other nucleophilic amino acid side chains to covalently link to Ub. While formerly considered unlikely as these bonds would be considerably weaker than the canonical iso-peptide and peptide bonds described above, such ubiquitylation events via cysteine (and even serines and threonines) have recently been shown to occur on both viral and cellular proteins, although such examples remain very rare [7–12].

Amongst classes of proteins that may be targeted for proteasomal destruction, transcription factors in particular have short half-lives and their ubiquitin-mediated degradation has been proposed to play a key role in their function at the promoter [13]. For instance *Xenopus* Neurogenin 2 (xNgn2) [14], a basic helix–loop–helix (bHLH) proneural protein that plays a key role in neuronal differentiation in the developing central nervous system [15], is very rapidly degraded by the UPS. We have previously shown that xNgn2 is targeted for destruction by ubiquitylation on both lysines and the N-terminus [16]. Moreover, in *Xenopus* eggs, xNgn2 is ubiquitylated on cysteines and this can be sufficient to drive protein degradation [17]. However, these studies were performed in extracts of unfertilised *Xenopus* eggs where xNgn2 would not normally be expressed. We have shown that xNgn2 is ubiquitylated in mammalian cells, but have not investigated whether non-canonical ubiquitylation of xNgn2 is occurring [17].

Here we show that xNgn2 is, indeed, ubiquitylated on cysteines in *Xenopus* embryos at neurula stage where it would be transcriptionally active. Moreover, using P19 embryonal carcinoma cells that can respond to bHLH overexpression by undergoing neuronal differentiation [18], we see that xNgn2 is ubiquitylated on the

* Corresponding author. Fax: +44 1223763241.
E-mail addresses: gsm26@cam.ac.uk (G.S. McDowell), kucerova@img.cas.cz (R. Kucerova), ap113@cam.ac.uk (A. Philpott).

0006-291X/$ - see front matter © 2010 Elsevier Inc. All rights reserved.
doi:10.1016/j.bbrc.2010.08.122

Please cite this article in press as: G.S. McDowell et al., Non-canonical ubiquitylation of the proneural protein Ngn2 occurs in both *Xenopus* embryos and mammalian cells, Biochem. Biophys. Res. Commun. (2010), doi:10.1016/j.bbrc.2010.08.122

N-terminus, lysine residues and cysteine residues. Multiple sites of ubiquitylation result in the very rapid degradation that we observe for xNgn2, which is likely important for its role as a regulator of the transition between stem/progenitor and neuronal identity during development of the nervous system.

Materials and methods

Plasmid constructs

Constructs were made by site-directed mutagenesis (Stratagene) and cloned into pCS2+ as described previously [16,17]. Tagged constructs were made by sub-cloning into pCS2+ containing a triple HA tag.

Xenopus laevis neurula embryo extract

Female wild-type *Xenopus laevis* were primed using Pregnant Mare Serum Gonadotropin and ovulation induced using Human Chorionic Gonadotropin. Eggs were fertilised *in vitro*. Neurula stage embryos [19] were lysed in XB (extract buffer: 100 mM KCl; 1 mM $MgCl_2$; 0.1 mM $CaCl_2$; 50 mM sucrose; 10 mM HEPES pH 7.7) with 10 μg ml^{-1} Cytochalasin B in a microcentrifuge at 4 °C to isolate cytoplasmic extract.

Ubiquitylation assays

Extract was supplemented with 10 μg ml^{-1} LPC (10 μg ml^{-1} leupeptin, 10 μg ml^{-1} pepstatin, 10 μg ml^{-1} chymostatin; Sigma); 20 μg ml^{-1} cycloheximide (Sigma); ER (energy regeneration mix: 20 μl 100 mM EGTA; 20 μl 1 M $MgCl_2$; 150 μl 1 M phosphocreatine (Sigma); 200 μl 100 mM adenosine 5′triphosphate (GE Healthcare); 1 μM Mg132 (Biomol); 3.75 mg ml^{-1} His-tagged ubiquitin (Sigma). For each condition 5 μl *in-vitro* translated ^{35}S-methionine-radiolabelled protein (SP6 TNT® Master Mix (Promega), ^{35}S-methionine (Perkin Elmer)) was added. Samples were incubated at 20 °C for 90 min then supplemented with VOSPER buffer (8 M urea, 0.1 M Tris pH 7.4, 20 mM imidazole, 6 mM NaCl, 1% Nonidet P40 (Sigma), 10 μg ml^{-1} LPC) and Ni–NTA™ agarose beads (Qiagen) and rotated for 75 min at room temperature. Samples were washed in VOSPER buffer and eluted in either reducing buffer (Laemmli buffer pH 10; 100 μl β-mercaptoethanol; 100 mM imidazole) or non-reducing buffer (Laemmli buffer; 100 μl H_2O; 100 mM imidazole). Samples were rocked at room temperature for 20 min and separated using SDS–PAGE.

Xenopus laevis degradation assays

Degradation assays were performed as described previously [17] using neurula embryo extract.

P19 cell degradation assays

P19 cells were grown as described previously [20]. Prior to transfection cells on plates were incubated in antibiotic-free α-MEM for 2 h at 37 °C. DNA (5 μg) (encoding triply-HA-tagged protein) was transfected with lipofectamine (Invitrogen) and OPTI-MEM (Invitrogen) overnight at 37 °C. Protein synthesis was blocked using 100 μg ml^{-1} cycloheximide (with 50 μM Mg132 (BioMol) or an equivalent volume of DMSO if investigating proteasome inhibition). Cells were lysed in lysis buffer (50 mM Tris/HCl pH 7.5; 150 mM NaCl; 1% IgePal (Sigma); protease inhibitors (Sigma); 1 μM pepstatin) and subjected to Western blot analysis using 20 μg total protein. Proteins were detected using an HRP-coupled anti-HA antibody (Roche) or anti-tubulin antibody (Sigma) followed by anti-mouse secondary antibody (GE Healthcare). Immunodetection was performed using ECL Plus™ Western Blotting Reagent (GE Healthcare). Protein levels were quantified using ImageJ software (http://rsb.info.nih.gov/ij/) [21] and half-lives calculated using first-order kinetics. The half-life for each mutant was normalised to the wild-type in each experiment. The average ratio compared to wild-type stability from the triplicate data set was then calculated.

P19 immunoprecipitation assays

HA-tagged or untagged xNgn2 constructs were cotransfected with FLAG-Ubiquitin in P19 cells overnight using Lipofectamine2000™ (Invitrogen). Cells were incubated in 50 μM MG132 for 1 h and lysed in lysis buffer (50 mM Tris/HCl pH 7.5; 150 mM NaCl; 1% (v/v) IgePal (Sigma); complete proteasome inhibitor cocktail (Roche); 1 μM pepstatin). xNgn2 was immunoprecipitated in IP buffer (50 mM Tris/HCl pH 7.5; 150 mM NaCl, 0.1% (v/v) NP40, complete proteasome inhibitor cocktail (Roche), 1 μM pepstatin) using an anti-HA antibody (Roche) and HA-matrix. Ubiquitylated proteins were immunoprecipitated using an anti-FLAG antibody (M2 clone, Sigma) and Protein-A Sepharose (GE Healthcare). For IP pull down 400 μg of protein was diluted in 1 ml of IP buffer for each condition and further incubated with primary antibody overnight. The next day samples were subjected to Western blot analysis and proteins were detected using an HRP-coupled anti-HA antibody (Roche) or anti-FLAG antibody (Sigma) followed by α-mouse secondary antibody (GE Healthcare).

Results

Xenopus Ngn2 (xNgn2) is degraded very rapidly in *Xenopus* egg extracts [16], which contain all components of the UPS system. Moreover, this ubiquitylation can occur on multiple sites including the N-terminus, lysines and cysteine residues and all can target the protein for destruction [17]. However, xNgn2 is normally first expressed post-gastrulation [14], raising the question as to whether degradation in egg extracts is via physiologically relevant mechanisms. To address this, we wanted to determine whether xNgn2 was also ubiquitylated on canonical and non-canonical sites in embryos at neural plate stage 15 [19], when the endogenous protein is most active. We investigated ubiquitylation of wild-type xNgn2, of Ac2xNGNKO where N-terminal sequence of xNgn2 had been mutated to one that will direct co-translational acetylation, preventing N-terminal ubiquitylation, and where all lysines have been mutated to arginines [17], and of Ac2xNgn2KOCO where additionally cysteine residues, potential sites of non-canonical ubiquitylation, were also mutated to alanine.

Several hundred *Xenopus* eggs were fertilised *in vitro* then allowed to develop until neurula stage 15 [19]. Cytoplasmic extracts were prepared and incubated with *in-vitro* translated ^{35}S-methionine-radiolabelled xNgn2 protein (either xNgn2, Ac2xNgn2KO, or Ac2xNgn2KOCO), proteasome inhibitor MG132, and His-tagged ubiquitin. Ubiquitylation was allowed to occur for 90 min then ubiquitylated proteins were isolated on Ni–NTA beads. After 8 M urea washes to remove non-covalently bound proteins, proteins were eluted into SDS–PAGE loading buffer either under hydrolysing, reducing conditions (Red/pH10: 1.3 mM β-ME, pH10), or non-reducing, non-hydrolysing conditions (Non-red: no β-ME, pH7.5). After SDS–PAGE separation, ubiquitylated conjugates of the different xNgn2 mutants were compared by autoradiography (Fig. 1A).

xNgn2 normally runs on SDS–PAGE at around 36 kDa. However, each additional 7 kDa Ub moiety should result in slowed migration on SDS–PAGE; multiple ubiquitylation events will produce a ladder

Please cite this article in press as: G.S. McDowell et al., Non-canonical ubiquitylation of the proneural protein Ngn2 occurs in both *Xenopus* embryos and mammalian cells, Biochem. Biophys. Res. Commun. (2010), doi:10.1016/j.bbrc.2010.08.122

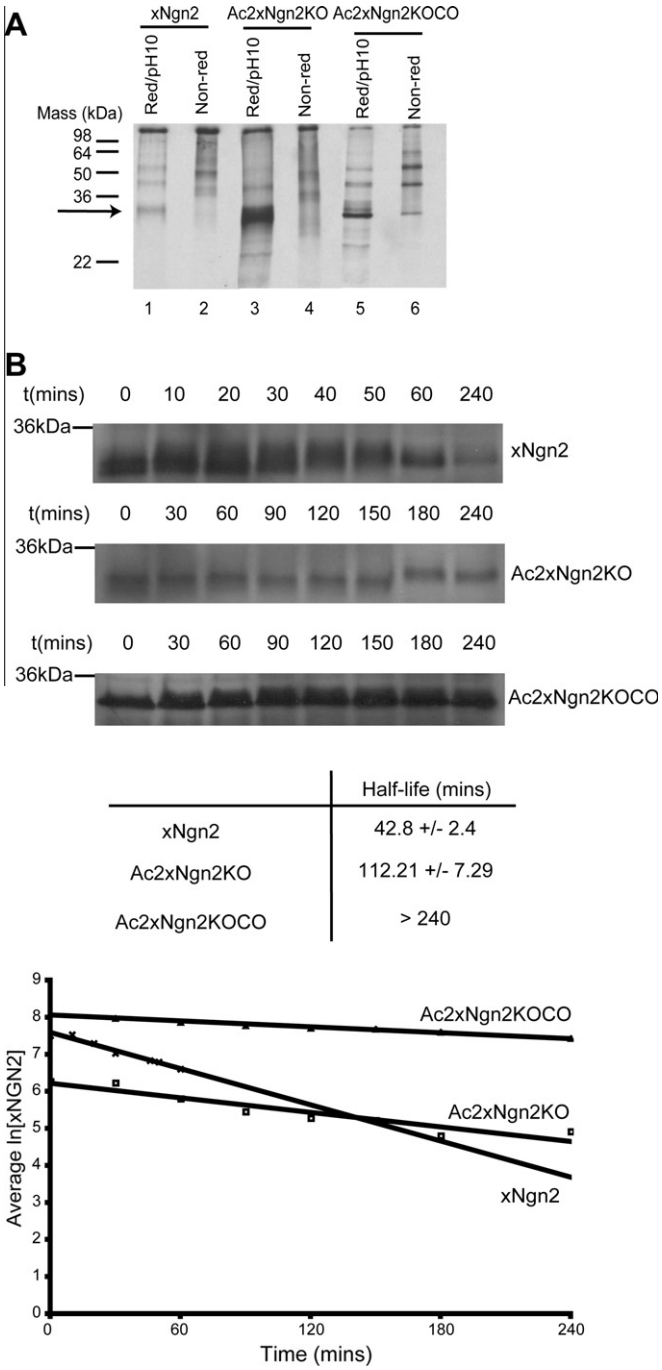

	Half-life (mins)
xNgn2	42.8 +/- 2.4
Ac2xNgn2KO	112.21 +/- 7.29
Ac2xNgn2KOCO	> 240

Fig. 1. Non-canonical ubiquitylation targets xNgn2 for degradation. (A) IVT ^{35}S xNgn2, Ac2xNgn2KO, and Ac2xNgn2KOCO were incubated in neurula *Xenopus* embryo extracts in the presence of His-ubiquitin (His-Ub) and MG132. Proteins covalently linked to His-ubiquitin were purified by affinity chromatography with Ni–NTA agarose under denaturing conditions. Reactions were either eluted using pH 6.8 SDS–PAGE buffer, which should not promote the hydrolysis of thioester and ester bonds (Non-red) or with pH 10 SDS–PAGE buffer containing 1.3 mM β-mercaptoethanol to promote hydrolysis of thioester bonds (Red). Experiments were then subjected to SDS–PAGE and quantitative phosphorimaging analysis. (B) IVT samples were incubated in neurula *Xenopus* embryo extracts at 21 °C. Aliquots of the reaction were added to SDS–PAGE loading buffer and separated by SDS–PAGE. Protein levels at each timepoint were quantified by autoradiography and the half-life of the protein calculated using first-order rate kinetics.

of gel-retarded forms (e.g., Fig. 1A, lane 1). Wild-type xNgn2 shows a prominent ladder of ubiquitylated forms running above the position of unconjugated xNgn2 under Non-red conditions (Fig. 1A, lane 2). Under reducing conditions, this ladder is still visible, indicating that much ubiquitylation is occurring via stable peptide and iso-peptide linkages. However, we now see the appearance of an unconjugated xNgn2 band, indicating that some Ubs are bound to xNgn2 via bonds that can be broken under these conditions (Fig. 1A, lane 1; unconjugated xNgn2 marked with an arrow). Such bonds would include thioester linkages between xNgn2 and Ub, as has been observed in *Xenopus* egg extracts [17]. To confirm that, in the absence of canonical ubiquitylation sites, ubiquitylation occurs via labile linkages, we looked at ubiquitylation of Ac2xNgn2KO in embryo extracts. Similar to our observations in eggs [17], despite lacking canonical Ub sites, Ac2xNgn2KO is extensively ubiquitylated in Non-red conditions (Fig. 1A, lane 4). However, after incubation in Red/pH10 conditions, poly-ubiquitylated forms largely collapse and the majority of the protein runs as the unconjugated form (Fig. 1A, lane 3), indicating that, in the absence of canonical ubiquitylation sites, extensive Ub conjugation can still occur via labile linkages potentially to cysteine, serine or threonine residues.

To determine whether non-canonical ubiquitylation could still occur in the absence of cysteines (as observed in egg cytoplasm [17]), we investigated the behaviour of ubiquitylated Ac2xNgn2-KOCO under Red/Ph10 and Non-red conditions. This form of xNgn2 can still be ubiquitylated, although we saw release of free Ac2xNgn2KOCO protein from these weak linkages even in Non-red conditions, possibly due to sample heating (Fig. 1A, lane 6). However, considerably more free protein was liberated after Red/Ph10 treatment (Fig. 1A, lane 5), further indicating ubiquitylation via ester linkages to serines and/or threonines.

To examine whether non-canonical ubiquitylation could affect the stability of xNgn2, we carried out degradation assays in cytoplasmic extract from neurula stage *X. laevis* embryos. *In-vitro* translated protein was incubated with extract at 21 °C and aliquots were removed at increasing times into SDS–PAGE loading buffer. After SDS–PAGE separation the level of xNgn2 protein at each timepoint was quantified by autoradiography (Fig. 1B). xNgn2 exhibits a half-life of 42.8 ± 2.4 min whereas Ac2xNgn2KO is stabilised, half-life 112.21 ± 7.29 min. Ac2xNgn2KOCO has a half-life greater than the range of the timecourse. Therefore loss of non-canonical sites of ubiquitylation can further stabilise xNgn2 in the absence of canonical ubiquitylation sites.

Thus, xNgn2 protein can be extensively and multiply ubiquitylated on both canonical and non-canonical sites in *Xenopus* embryos to target xNgn2 for degradation. This was similar to observations in *Xenopus* eggs, indicating that non-canonical ubiquitylation is not restricted to egg cytoplasm. Nevertheless, it is possible that this highly unusual non-canonical ubiquitylation of xNgn2 is a consequence of specialised mechanisms present in *Xenopus* not found in mammalian cells. As manipulating Ngn2 activity in mammalian stem and progenitor cells has become a focus for groups keen to potentiate generation of neurons for transplantation, it is important to fully characterise mechanisms of post-translational control of xNgn2 protein. We wished to determine whether xNgn2 is also subject to non-canonical ubiquitylation in mammalian cells and whether this contributes to its rapid rate of destruction.

We have chosen to investigate ubiquitylation and degradation of xNgn2, and mutants thereof, in mammalian P19 embryonal carcinoma cells, which are capable of differentiating into neurons in response to retinoic acid or proneural protein expression [18]. These cells offer a cellular environment resembling many aspects of differentiating neurons during development.

We have previously demonstrated that xNgn2 can be rapidly degraded in P19 cells by the UPS system [16]. To determine whether destruction was solely due to ubiquitylation on canonical sites, i.e., lysines and the N-terminus, we conducted degradation assays for xNgn2, xNgn2KO, Ac2xNgn2 and Ac2xNgn2KO. P19 cells, transfected with plasmids encoding HA-tagged xNgn2 or derivatives thereof, were incubated for approx. 24 h before cyclohexi-

Please cite this article in press as: G.S. McDowell et al., Non-canonical ubiquitylation of the proneural protein Ngn2 occurs in both *Xenopus* embryos and mammalian cells, Biochem. Biophys. Res. Commun. (2010), doi:10.1016/j.bbrc.2010.08.122

mide addition preventing further protein synthesis. Samples were then removed at intervals. Cell lysates were separated by SDS–PAGE and subjected to Western blotting to detect HA-tagged proteins (using tubulin as a loading control). The half-life of each sample was normalised to wild-type xNgn2 (Fig 2A).

xNgn2KO was stabilised by 2.6-fold ±0.4 and Ac2xNgn2 was stabilised by 3.2-fold ±1.4 compared to the wild-type protein, respectively. The mutant lacking all sites of canonical ubiquitylation, Ac2xNgn2KO, showed considerably greater stability, 23.2-fold ±4.6 more stable that xNgn2. Degradation of xNgn2 in mammalian cells is driven by ubiquitylation on both lysines and the N-terminus, as in *Xenopus* egg extracts, indicating mechanistic conservation between the systems. However, we also saw that, even when all canonical ubiquitylation sites were mutated, xNgn2 still underwent slow proteolysis, raising the possibility that ubiquitylation on non-canonical sites was also occurring. To investigate further, we looked to see whether degradation of Ac2xNgn2KO could be further slowed by proteasome inhibition.

P19 cells were transfected with plasmids encoding HA-tagged xNgn2 or Ac2xNgn2KO, incubated for approx. 24 h then cycloheximide added with or without MG132 and samples removed for Western blot analysis. As expected, addition of MG132 led to considerable stabilisation of xNgn2 (Fig. 2B). We also saw that MG132 enhanced the stability of Ac2xNgn2KO, indicating that, in the absence of canonical ubiquitylation sites, xNgn2 is subject to non-canonical ubiquitylation. To confirm this, we undertook immunoprecipitation experiments to demonstrate that Ac2xNgn2-KO is still ubiquitylated.

Ac2xNgn2KO is still degraded by the proteasome, but proteins have been identified which do not require prior ubiquitylation for this to occur [22]. To demonstrate that Ac2xNgn2KO is, indeed, ubiquitylated, we transfected P19 cells with HA-tagged xNgn2 or Ac2xNgn2KO with or without FLAG-tagged Ub. After 24 h, we lysed the cells and undertook immunoprecipitation of either FLAG-Ub or HA-xNgn2 or Ac2xNgn2KO, as labelled (Fig. 3). After SDS–PAGE separation, we probed the FLAG-Ub immunoprecipitates by Western blotting to detect the HA epitope on xNgn2/Ac2xNgn2KO, and probed the HA-xNgn2/Ac2xNgn2KO immunoprecipitates to detect FLAG-Ub. All samples were expressing similar levels of xNgn2/Ac2xNgn2KO (see loading control).

When HA-tagged xNgn2 or Ac2xNgn2KO were immunoprecipitated and probed for presence of FLAG-Ub, high molecular weight forms corresponding to poly-Ub xNgn2 were observed. When FLAG-tagged Ub was immunoprecipitated, then subsequently blotted for HA-xNgn2, we saw a prominent ladder of poly-ubiquitylated forms of xNgn2 stretching up the gel. In contrast, Ub

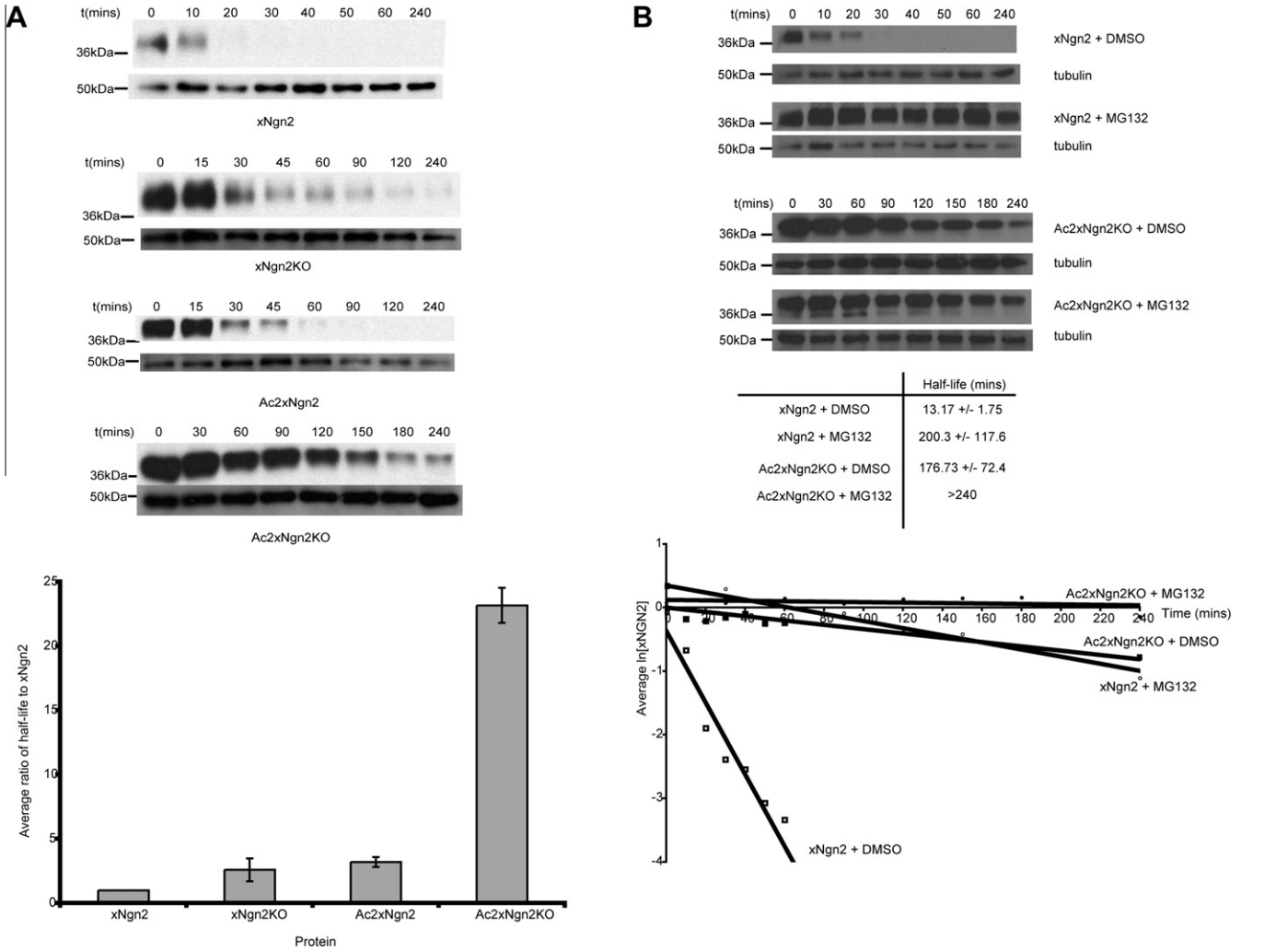

Fig. 2. xNgn2 is stabilised by mutation of canonical sites of ubiquitylation in a proteasome-dependent manner in P19 cells. (A) P19 cells were transfected with triply C-terminally HA-tagged xNgn2, xNgn2KO, Ac2xNgn2 or Ac2xNgn2KO. Cells were lysed at the timepoints indicated after cycloheximide addition to inhibit protein translation and proteins detected by Western blot analysis using anti-HA antibody. Proteins were detected by chemiluminescence and quantified using ImageJ software. (B) Degradation assays were carried out with xNgn2 or Ac2xNgn2KO in the presence or absence of the proteasome inhibitor MG132.

Please cite this article in press as: G.S. McDowell et al., Non-canonical ubiquitylation of the proneural protein Ngn2 occurs in both *Xenopus* embryos and mammalian cells, Biochem. Biophys. Res. Commun. (2010), doi:10.1016/j.bbrc.2010.08.122

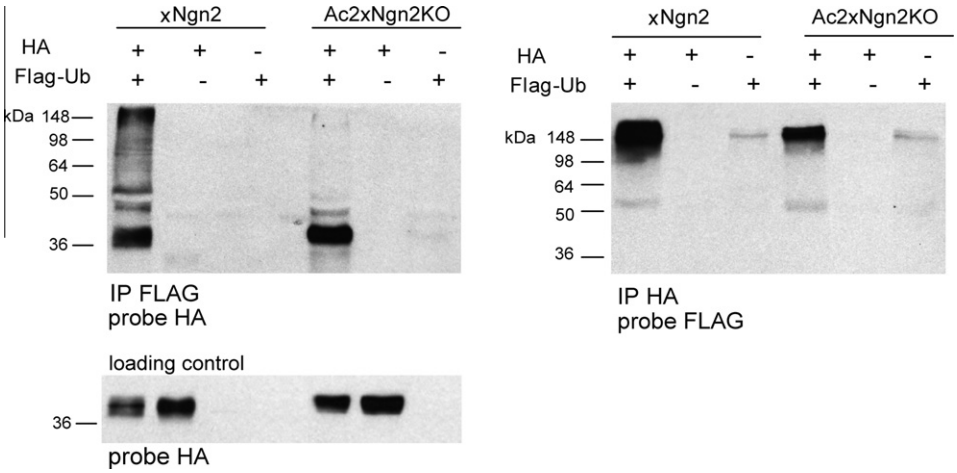

Fig. 3. Immunoprecipitation indicates Ac2xNgn2KO is still ubiquitylated. HA-tagged xNgn2 or HA-tagged Ac2xNgn2KO were transfected alone, or with FLAG-tagged ubiquitin, into P19 cells. Cells were lysed and immunoprecipitation carried out to pull down either FLAG-associated proteins, using Protein-A Sepharose beads, or HA-associated proteins using Protein-G Sepharose beads. Samples were subjected to Western blotting using α-HA or α-FLAG antibody.

immunoprecipitates containing Ac2xNgn2KO did not result in high molecular weight Ub-Ac2xNgn2KO conjugates, a result that would be expected if Ub chains had been released under reducing gel conditions. Consistent with this, a prominent band of unconjugated Ac2xNgn2KO was present. We noted that there was also a clear band of unconjugated xNgn2 under these conditions, which would suggest that a subset of xNgn2 is also conjugated to poly-Ub chains via labile linkages. Thus, our evidence indicates that xNgn2 is ubiquitylated on both canonical and non-canonical residues in both *Xenopus* and mammalian cells. We then wished to determine whether ubiquitylation on cysteines contributed to the rapid degradation of xNgn2.

To determine the effect of cysteine ubiquitylation on the half-life of xNgn2, we used a mutant form of xNgn2 where all 7 cysteine residues were mutated to alanines (xNgn2CO). xNgn2CO is still largely structurally intact as it is still able to site-specifically bind to DNA with its heterodimeric E protein partner [17]. xNgn2 and xNgn2CO were transfected into P19 cells, and after approx. 24 h, cycloheximide was added and cell samples removed at increasing times. Extracted proteins were separated by SDS–PAGE and Western blotted to detect xNgn2/xNgn2CO protein (Fig. 4).

We noted that even at the time of cycloheximide addition, $t = 0$, xNgn2CO had accumulated to a higher level than the wild-type protein, indicating that mutation of cysteines did stabilise xNgn2 in mammalian cells. This was confirmed when we quantitatively analysed the amount of protein present at increasing times; we saw that xNgn2CO was 3.5 ± 0.9 times more stable than xNgn2. Taken together our results demonstrate that xNgn2 lacking canonical ubiquitylation sites can still be degraded by the UPS system and that ubiquitylation occurs on cysteine residues. Moreover, in the absence of cysteines, ubiquitylation on canonical sites is not sufficient to drive the very rapid degradation of the wild-type protein, demonstrating that non-canonical ubiquitylation contributes to rapid destruction in mammalian cells as well as in *Xenopus*.

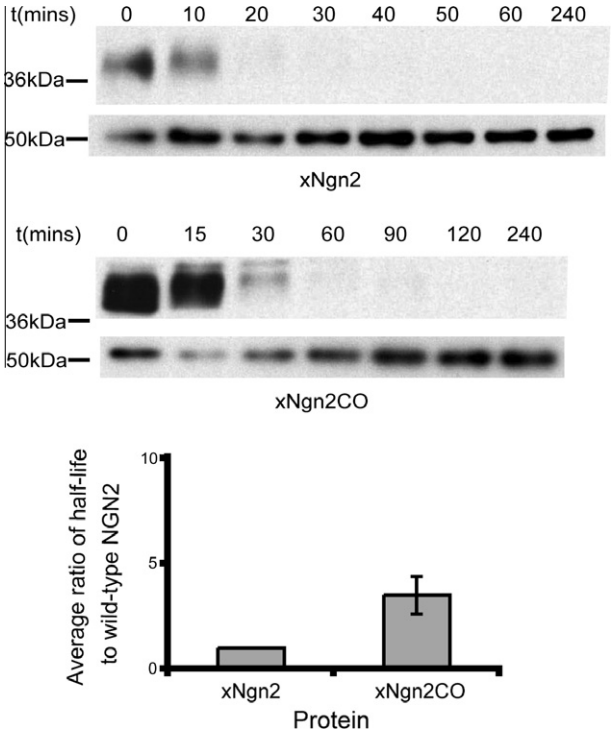

Fig. 4. Mutation of cysteines alone stabilises xNgn2. P19 cells were transfected with HA-tagged xNgn2 or xNgn2CO and treated with or without MG132. Cells were lysed at the timepoints indicated after cycloheximide addition and analysed by Western blot using α-HA antibody. Proteins were detected by chemiluminescence and quantified using ImageJ software.

Discussion

Modification of proteins by ubiquitylation controls a multitude of molecular systems, yet we are still learning new information about the basic biochemistry of the process. Originally, ubiquitylation was thought to occur exclusively on lysines, before ubiquitylation on the N-terminus of selected proteins was identified [6]. More recently, ubiquitylation on non-canonical sites has been demonstrated in a handful of proteins [9,11,12].

Our recent work showed that cellular E3 ligases could target the proneural transcription factor xNgn2 for degradation by ubiquitylation on the N-terminus, lysines or cysteines, resulting in a very short protein half-life [17]. However, these biochemical studies were conducted using extracts from *Xenopus* frog eggs at a developmental stage when xNgn2 would not normally be expressed. Here, we set out to investigate whether xNgn2 undergoes this highly unusual non-canonical ubiquitylation in both neurula *Xenopus* embryos, when the protein would be active, and in mammalian P19 cells which are capable of differentiating into neurons.

We see that both N-terminal and lysine ubiquitylation contribute to degradation of xNgn2 in *Xenopus* embryos and P19 cells;

Please cite this article in press as: G.S. McDowell et al., Non-canonical ubiquitylation of the proneural protein Ngn2 occurs in both *Xenopus* embryos and mammalian cells, Biochem. Biophys. Res. Commun. (2010), doi:10.1016/j.bbrc.2010.08.122

mutation of these acceptor sites alone leads to a more than 10-fold increase in half-life of the protein. However, these mutant xNgn2 constructs are still ubiquitylated and degraded by the proteasome in both these systems, strengthening the possibility of ubiquitylation on non-canonical sites targeting the protein for destruction. Indeed, we see that mutation of cysteine residues alone in xNgn2 results in a 2-fold increase in xNgn2 half-life in P19 cells, strongly indicating that ubiquitylation on cysteines contributes to rapid degradation in mammalian cells. Moreover, when proteins are ubiquitylated with His-Ub and pulled down with Nickel affinity resin, free xNgn2 protein is released on treatment with reducing agents in both P19 cells and neurula stage embryos, demonstrating ubiquitylation via labile linkages.

Why would xNgn2 be ubiquitylated on so many sites? xNgn2 is a highly unstable transcription factor whose activity is required to oscillate to maintain "stem-ness" in neural progenitor cells of the developing brain [13]. Such dynamic behaviour may require the multiple sites of ubiquitylation that we observe. Most of the lysine residues are found around and within the bHLH domain of xNgn2 required for binding to the heterodimeric partner protein xE12 and to its cognate DNA sequence. Binding of xE12 to xNgn2 increases protein half-life [16], and which could potentially occur through slowing unfolding of the ubiquitylated protein by the proteasome. Recent work has demonstrated that ubiquitylation must occur near a region of structural instability to allow proteasomal unfolding [23]. Cysteine residues, in contrast to lysines, are found fairly evenly distributed in the N- and C-terminae of xNgn2, and so may aid in ubiquitylation-mediated unfolding of the transcription factor when it is bound to E proteins and DNA.

Non-canonical ubiquitylation is gradually being observed in more and more proteins [12,24] and offers an alternative or complimentary method for targeting proteins for ubiquitin-mediated processes. The labile nature of the covalent attachment of ubiquitin chains, and the reducing conditions often used routinely for biochemical analysis, makes non-canonical ubiquitylation more difficult to identify. However, it is becoming increasing probable that these modifications will play a widespread role in dynamic protein control.

Acknowledgments

We thank Ian Horan for help with construction of plasmids; Jon Vosper for help with ubiquitylation assays and Christelle Fiore-Heriche for help in tissue culture and all three for preliminary observations that led up to this study. This work was supported by MRC Research Grant G0700758. G.M. was funded by a Medical Research Council Studentship.

References

[1] A. Hershko, H. Heller, S. Elias, A. Ciechanover, Components of ubiquitin-protein ligase system. Resolution, affinity purification, and role in protein breakdown, J. Biol. Chem. 258 (1983) 8206–8214.
[2] C. Naujokat, T. Saric, Concise review: role and function of the ubiquitin–proteasome system in mammalian stem and progenitor cells, Stem Cells 25 (2007) 2408–2418.
[3] O. Kerscher, R. Felberbaum, M. Hochstrasser, Modification of proteins by ubiquitin and ubiquitin-like proteins, Annu. Rev. Cell Dev. Biol. 22 (2006) 159–180.
[4] M.H. Glickman, A. Ciechanover, The ubiquitin–proteasome proteolytic pathway: destruction for the sake of construction, Physiol. Rev. 82 (2002) 373–428.
[5] K. Breitschopf, E. Bengal, T. Ziv, A. Admon, A. Ciechanover, A novel site for ubiquitination: the N-terminal residue, and not internal lysines of MyoD, is essential for conjugation and degradation of the protein, EMBO J. 17 (1998) 5964–5973.
[6] A. Ciechanover, R. Ben-Saadon, N-terminal ubiquitination: more protein substrates join in, Trends Cell Biol. 14 (2004) 103–106.
[7] A.F. Carvalho, M.P. Pinto, C.P. Grou, I.S. Alencastre, M. Fransen, C. Sa-Miranda, J.E. Azevedo, Ubiquitination of mammalian Pex5p, the peroxisomal import receptor, J. Biol. Chem. 282 (2007) 31267–31272.
[8] C. Williams, M. van den Berg, R.R. Sprenger, B. Distel, A conserved cysteine is essential for Pex4p-dependent ubiquitination of the peroxisomal import receptor Pex5p, J. Biol. Chem. 282 (2007) 22534–22543.
[9] K. Cadwell, L. Coscoy, Ubiquitination on nonlysine residues by a viral E3 ubiquitin ligase, Science 309 (2005) 127–130.
[10] K. Cadwell, L. Coscoy, The specificities of Kaposi's sarcoma-associated herpesvirus-encoded E3 ubiquitin ligases are determined by the positions of lysine or cysteine residues within the intracytoplasmic domains of their targets, J. Virol. 82 (2008) 4184–4189.
[11] S.W. Tait, E. de Vries, C. Maas, A.M. Keller, C.S. D'Santos, J. Borst, Apoptosis induction by Bid requires unconventional ubiquitination and degradation of its N-terminal fragment, J. Cell. Biol. 179 (2007) 1453–1466.
[12] S. Ishikura, A.M. Weissman, J.S. Bonifacino, Serine residues in the cytosolic tail of the T-cell antigen receptor α-chain mediate ubiquitination and ER-associated degradation of the unassembled protein, J. Biol. Chem. 285 (2010) 23916–23924.
[13] R. Kageyama, T. Ohtsuka, H. Shimojo, I. Imayoshi, Dynamic Notch signaling in neural progenitor cells and a revised view of lateral inhibition, Nat. Neurosci. 11 (2008) 1247–1251.
[14] Q. Ma, C. Kintner, D.J. Anderson, Identification of neurogenin, a vertebrate neuronal determination gene, Cell 87 (1996) 43–52.
[15] Y. Sun, M. Nadal-Vicens, S. Misono, M.Z. Lin, A. Zubiaga, X. Hua, G. Fan, M.E. Greenberg, Neurogenin promotes neurogenesis and inhibits glial differentiation by independent mechanisms, Cell 104 (2001) 365–376.
[16] J.M. Vosper, C.S. Fiore-Heriche, I. Horan, K. Wilson, H. Wise, A. Philpott, Regulation of neurogenin stability by ubiquitin-mediated proteolysis, Biochem. J. 407 (2007) 277–284.
[17] J.M. Vosper, G.S. McDowell, C.J. Hindley, C.S. Fiore-Heriche, R. Kucerova, I. Horan, A. Philpott, Ubiquitylation on canonical and non-canonical sites targets the transcription factor neurogenin for ubiquitin-mediated proteolysis, J. Biol. Chem. 284 (2009) 15458–15468.
[18] M.H. Farah, J.M. Olson, H.B. Sucic, R.I. Hume, S.J. Tapscott, D.L. Turner, Generation of neurons by transient expression of neural bHLH proteins in mammalian cells, Development 127 (2000) 693–702.
[19] P.D. Nieuwkoop, J. Faber, Normal Table of *Xenopus laevis*, Garland Publishing, New York, 1994.
[20] M.A. Rudnicki, M.W. McBurney, Cell culture methods and induction of differentiation of embryonal carcinoma cell lines, in: E.J. Robertson (Ed.), Teratocarcinomas and Embryonic Stem Cells: A Practical Approach, IRL Press, 1987, pp. 19–49.
[21] M.D. Abramoff, P.J. Magelhaes, S.J. Ram, Image processing with image, J. Biophoton. Int. 11 (2004) 36–42.
[22] D.P. Stewart, B. Koss, M. Bathina, R.M. Perciavalle, K. Bisanz, J.T. Opferman, Ubiquitin-independent degradation of antiapoptotic MCL-1, Mol. Cell Biol. 30 (2010) 3099–3110.
[23] S. Prakash, L. Tian, K.S. Ratliff, R.E. Lehotzky, A. Matouschek, An unstructured initiation site is required for efficient proteasome-mediated degradation, Nat. Struct. Mol. Biol. 11 (2004) 830–837.
[24] N. Shabek, A. Ciechanover, Degradation of ubiquitin: the fate of the cellular reaper, Cell Cycle 9 (2010) 523–530.

Please cite this article in press as: G.S. McDowell et al., Non-canonical ubiquitylation of the proneural protein Ngn2 occurs in both *Xenopus* embryos and mammalian cells, Biochem. Biophys. Res. Commun. (2010), doi:10.1016/j.bbrc.2010.08.122

Int. J. Dev. Biol. 55: 249-260 (2011)
doi: 10.1387/ijdb.103171ch

THE INTERNATIONAL JOURNAL OF DEVELOPMENTAL BIOLOGY
www.intjdevbiol.com

Regulation of cell fate determination by Skp1-Cullin1-F-box (SCF) E3 ubiquitin ligases

CHRISTOPHER J. HINDLEY[1], GARY S. MCDOWELL[1], HELEN WISE[1,2] and ANNA PHILPOTT*

Department of Oncology, University of Cambridge, Hutchison/Medical Research Council (MRC) Research Centre, Addenbrooke's Hospital, Cambridge, U.K.

ABSTRACT The developing embryo is patterned by a complex set of signals and interactions resulting in changes in cell division, cell fate determination and differentiation. An increasing body of evidence points to the role of the ubiquitin proteasome system (UPS) and ubiquitin-mediated protein degradation as a major mechanism of protein regulation, crucial for control of developmental processes. The specific and irreversible signal generated by protein degradation can function as an integrator of cell signaling events, coupled with other post-translational protein modifications, but also as a master switch for differentiation in its own right. The UPS also displays more subtle mechanisms of regulating signaling than decreasing protein levels, such as proteolytic processing and altering subcellular localization. In particular, the SCF E3 ligase family plays pivotal roles in regulating diverse developmental events in varied species. This review will focus on the role played by SCF E3 ligases in cell fate determination and differentiation.

KEY WORDS: *differentiation, SCF, signaling, ubiquitylation, UPS*

Introduction

During embryogenesis, individual cells must respond to signaling within the developing embryo and elicit the appropriate response. Such responses involve changes in the level and/or activity of proteins and must be dynamic. Within the field of developmental biology, most emphasis has traditionally been placed on regulation of protein levels by control of transcription. However, it is becoming clear that many proteins are subject to regulated degradation and that this plays a critical regulatory role during embryogenesis. Regulated protein degradation has three key features: irreversibility, responsiveness and selectivity.

Regulated proteolysis of up to 90% of short-lived proteins is achieved by the ubiquitin proteasome system (UPS) (Ciechanover *et al*., 1984). Ubiquitin-mediated degradation is initiated by the covalent attachment of ubiquitin (Ub), a 76-amino acid protein, onto a substrate (Ciechanover *et al*., 1980a; Ciechanover *et al*., 1980b; Hershko *et al*., 1980; Wilkinson *et al*., 1980). Subsequent rounds of ubiquitylation attach additional Ubs to the first to build up a chain; chains of at least 4 Ubs then facilitate the recognition and destruction of the substrate by the 26S proteasome (reviewed in Pickart and Cohen, 2004; Wolf and Hilt, 2004).

The addition of Ub onto substrate proteins is catalysed by a multi-enzyme cascade (Fig. 1). Firstly, Ub is activated using energy from ATP hydrolysis, resulting in the fusion of AMP to the C-terminal carboxyl group. The active site cysteine of an E1 (Ub activating) enzyme can then form a thioester bond with activated Ub. Ub is then passed to the active site cysteine of an E2 (Ub conjugating) enzyme. The last enzyme in the cascade, an E3 (Ub ligase), facilitates the attachment of Ub onto the substrate protein from the E2 enzyme (Hershko *et al*., 1983; Pickart and Rose, 1985). Successive Ub moieties can be added to the first by a

Abbreviations used in this paper: APC/C, anaphase promoting complex/cyclosome; Arm, armadillo; bHLH, basic helix-loop-helix; β-TRCP, β-transducin repeat containing protein; Ci, Cubitus interruptus; CKI, cyclin dependent kinase inhibitor; Dlg, discs large; dpp, decapentaplegic; Fbw, F-box protein containing WD40 repeats; Fbx, F-box protein; GCM, glial cells missing; GSK3, glycogen synthase kinase 3; HECT, homologous to E6-associated protein C-terminus; Hh, hedgehog; IKK, IκB kinase; MAFbx, muscle atrophy F-box; NβT, neural β-tubulin; NC, neural crest; NF-κB, nuclear factor-κB; PKA, protein kinase A; Ppa, partner of paired; Ptc, patched; REST, RE1-silencing transcription factor; RING, really interesting new gene; SCF, Skp1-cullin1-F-box complex; Smo, smoothened; Ub, ubiquitin; UPS, ubiquitin proteasome system.

***Address correspondence to:** Anna Philpott. Department of Oncology, University of Cambridge, Hutchison/Medical Research Council (MRC) Research Centre, Addenbrooke's Hospital, Cambridge. CB2 0XZ, UK. Fax: +44-1223-763-241. e-mail:ap113@cam.ac.uk
web: http://www.hutchison-mrc.cam.ac.uk/Research/Anna_Philpott/index.html
Note 1: All these authors have contributed equally to this work.
Note 2: Current Address is Department of Pathology, University of Cambridge, Tennis Court Road, Cambridge. CB2 1QP, UK.

Accepted: 19 August 2010. *Final author corrected PDF published online:* 15 June 2011.

ISSN: Online 1696-3547, Print 0214-6282
© 2011 UBC Press
Printed in Spain

sequential enzyme cascade. Alternatively, entire polyUb chains may be attached to the substrate protein by the action of an E4 enzyme, such as p300, which has been demonstrated to add chains of polyUb to p53 at sites previously monoubiquitylated by Mdm2 (Grossman *et al.*, 2003; reviewed in Hoppe, 2005). In humans, only 2 E1 enzymes and approximately 100 E2 enzymes have been characterised. By contrast, it is estimated that there may be as many as 1000 E3 ligases (reviewed in Hicke *et al.*, 2005) further divided into 3 classes: Homologous to E6-Associated Protein C-Terminus (HECT), Really Interesting New Gene (RING) and U-box.

Probably the most diverse family is that of the RING E3 ligases; there are almost 400 proteins with RING domains in the human genome, compared to around 38 with HECT domains (Semple, 2003). RING E3 ligases are characterised by the presence of a RING motif (consensus $CX_2CX_{9-39}CX_{1-3}HX_{2-3}[C/H]X_2CX_{4-48}CX_2C$). Based on bioinformatic data, RING E3 ligases can be further divided into single subunit and modular classes. Single subunit RING E3 ligases bind to both E2 enzymes and substrates. In the case of modular RING E3 ligases, the RING protein functions as part of a multi protein complex and substrates are recruited by a separate subunit (reviewed in Deshaies and Joazeiro, 2009). Examples include the Anaphase Promoting Complex/Cyclosome (APC/C) and Cullin-based RING E3 ligases. Cullin-based E3 ligases (reviewed in Petroski and Deshaies, 2005) use the RING protein Roc1 (also known as Rbx1 and Hrt1) to recruit E2 enzymes (Chen *et al.*, 2000; Furukawa *et al.*, 2002; Ohta *et al.*, 1999).

This review will concentrate on the role in development of the most well characterised sub-group of Cullin-based RING E3 ligases, the Skp1-Cullin1-F-box (SCF) E3 ligase complexes. Within the SCF complex, Cullin1 binds to Roc1, Skp1 and a variable F-box protein (Lyapina *et al.*, 1998; Wu *et al.*, 2000), and it is this latter component that confers the SCF complex designation, e.g. SCF^{Skp2}, where Skp2 is the F-box component. The SMART database (http://smart.embl-heidelberg.de/) gives an estimated 56 F-box proteins in humans, 77 in mice and 30-50 in *Xenopus laevis*, compared to the 600-700 found in the large gene networks of *Arabidopsis* and rice (Gagne *et al.*, 2002; Jain *et al.*, 2007; Kuroda *et al.*, 2002). In the crystal structure of SCF^{Skp2} (Schulman *et al.*, 2000; Zheng *et al.*, 2002), which is, to date, the only structure of a complete SCF complex described, Cullin1 forms a rigid, bi-lobed structure which acts as a 'molecular scaffold' on which to assemble the SCF complex. The C-terminal globular domain recruits Roc1, which in turn recruits the E2 enzyme. The Cullin1 N-terminal domain recruits Skp1, which then binds to the F-box protein substrate recognition subunit via interactions between the C-terminus of Skp1 and the F-box domain.

Structural studies are also providing insight into further mechanisms of SCF activity. Many F-box proteins interact with their cognate substrates only after the substrates have been post-translationally modified, adding an extra level of regulation. Although the most widely reported prior modification is phosphorylation, substrates have also been reported to require acetylation, glycosylation or nitration (Guinez *et al.*, 2008; Hwang *et al.*, 2010). For instance, it is known that degradation of cyclin E by SCF^{Fbw7}

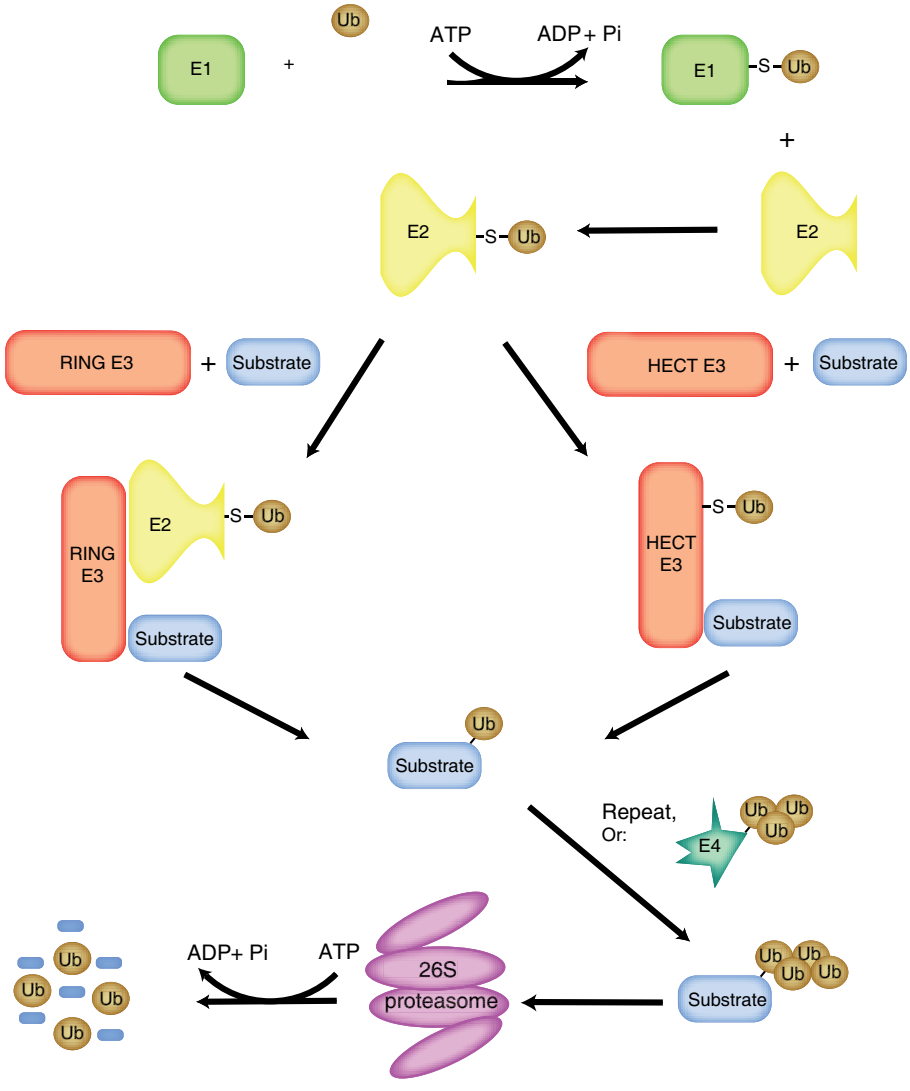

Fig. 1. Schematic of Ub mediated protein degradation. *Ub is first covalently linked to an E1 (Ub-activating) enzyme using energy from ATP hydrolysis before being shuttled to an E2 (Ub-conjugating) enzyme. Ub is then either conjugated directly to a HECT E3 ligase before transfer to the substrate or the E2-Ub is recruited via a RING E3 ligase into a complex containing the substrate. Note that all Ub conjugation from E1 to E3 is via thioester linkage to a cysteine sidechain sulfur. Further attachment of Ub to internal lysines on the original substrate Ub is achieved either by repetition of the above scheme or the action of an E4 enzyme, which transfers polyUb chains to monoubiquitylated substrate ubiquitin. A chain of four or more K48-linked polyUb targets the substrate to the 26S proteasome where it is unfolded and degraded in an ATP-dependent manner into small peptides with concurrent deubiquitylation to recycle Ub.*

is triggered only following phosphorylation at multiple sites (Ye *et al.*, 2004). Binding partners increase or inhibit the activity of SCF complexes and in particular binding or covalent modification of the C-terminal winged helix bundle domain of the Cullin subunit plays an important role in regulating SCF activity (Duda *et al.*, 2008; Liu *et al.*, 2002). Versatility in substrate specificity for the SCF E3 ligases is provided by the recognition subunit F-box proteins, which bind distinct substrates. Structural analysis of SCF complexes and their cognate substrates is beginning to reveal a wide range of mechanisms for substrate recognition. For example, the atypical F-box protein Fbx4 contains a GTPase domain which is crucial for the binding of a globular domain of its TRF1 substrate (Zeng *et al.*, 2010). By contrast, the *Arabidopsis* F-box protein TIR1 requires only the presence of the plant hormone auxin in order to bind to its cognate substrates, the Aux/IAA proteins (Kepinski and Leyser, 2004). Structural studies have revealed that TIR1 is itself the sensor of auxin and that the binding of auxin to TIR1 is necessary to complete the docking site for Aux/IAA proteins (Tan *et al.*, 2007). Thus, although the F-box motif provides a consistent recognition motif for binding to the SCF scaffold, the mechanism of substrate recognition by the F-box protein varies.

A number of F-box proteins have exhibited roles in development through regulation of substrate levels (see Table 1). This review will focus on the role that F-box proteins play in cell fate determination and signaling during embryogenesis and organogenesis. Although many F-box proteins are also involved in the degradation of cell cycle components (Skaar *et al.*, 2009a; Skaar *et al.*, 2009b), this aspect of F-box protein activity has been previously described in detail (reviewed in Ang and Harper, 2004; Skaar and Pagano, 2009) and this role in development will not be considered here.

F-box proteins and signaling: patterning in the early embryo

Several F-box proteins have key roles in major signaling pathways involved in patterning of the embryo, for instance *β-Transducin Repeat Containing Protein* (*β-TRCP*), which plays pleiotropic roles in regulation of cell signaling. Indeed, *β-TRCP* is one of the best studied of this class of E3 ubiquitin ligases because of its multiple important substrates. *Xenopus* has 2 F-box *β-TRCP* genes, *β-TRCP1* and *β-TRCP2* (also known as *FBXW1 and FBXW11* respectively). 4 transcripts of *β-TRCP* are expressed in *Xenopus*, which differ in the presence or absence of amino acid sequences at the N- or C-termini (Ballarino *et al.*, 2004; Ballarino *et al.*, 2002). Similarly, 2 distinct genes exist in humans with multiple isoforms expressed (Fuchs *et al.*, 1999; Suzuki *et al.*, 1999). Recent evidence suggests that different isoforms of *β-TRCP* play different roles in development, with differing tissue-specific expression in mouse, while assays in *Xenopus* demonstrate differential isoform activity (Seo *et al.*, 2009).

β-TRCP recognises substrates via binding to seven WD40 repeats present in its C-terminus and phosphorylation of substrates is a prerequisite for binding (for example, Winston *et al.*, 1999). Most β-TRCP substrates identified to date have a specific phosphodegron (DpSGϕXpS, where ϕ is a hydrophobic amino acid, and p denotes phosphorylation), a motif which, when phosphorylated, allows targeting of the substrate for degradation (reviewed in Ang and Wade Harper, 2005; Jin *et al.*, 2003; Winston *et al.*, 1999). In addition, lysines that are 9-13 amino acids N-terminal to this phosphodegron are preferentially ubiquitylated. This is due to structural constraints associated with optimal presentation of the substrate to the E2 enzyme (Wu *et al.*,

TABLE 1

SUMMARY OF F BOX PROTEINS INVOLVED IN CELL FATE DETERMINATION

Tissue/cell type	F-box component	Substrate	Function	Ref
Extraembryonic	Fbw2	GCM1	GCM1 required for development of extraembryonic tissue in mammals	Schreiber *et al.*, 2000
Early embryo	β-TRCP	β-Catenin	Regulation of β-Catenin stability and transcriptional activity	Latres *et al.*, 1999; Kitagawa *et al.*, 1999; Hart *et al.*, 1999
		Cactus	Regulation of Dorsal transcriptional activity and dorsal-ventral patterning in *Drosophila*	Belvin *et al.*, 1995; Maniatis, 1999
		Ci	Regulation of Ci transcriptional activity	Jia *et al.*, 2005; Wang and Li, 2006
	Fbw7	Notch	Phosphorylation-dependent degradation of Notch-ICD and regulation of transcription	Gupta-Rossi *et al.*, 2001; Wu *et al.*, 2001
Epithelia	β-TRCP	hDLG	Dlg inhibits epithelial differentiation in *Drosophila*, interaction with β-TRCP seen only with hDLG so far	Mantovani and Banks, 2003; Woods *et al.*, 1996
		IκB	NF-κB signalling implicated in proliferation and differentiation of basal layer of epidermis	Hu *et al.*, 1999, Takeda *et al.*, 1999
		TAp63γ	Possible role in epidermal differentiation via regulation of transcriptional activity	Gallegos *et al.*, 2008
Haematopoietic	Fbw7	c-Myc	Abnormal thymocyte development due to aberrant c-myc regulation; regulates haematopoietic stem cell gene expression signature	Onoyama *et al.*, 2007, Reavie *et al.*, 2010
		Notch	Negative regulation of Notch signalling in haematopoietic, vascular and cardiac development in mice	Tetzlaff *et al.*, 2004
Muscle	MAFbx	MyoD	Promotes MyoD polyubiquitylation and degradation *in vitro* and *in vivo*	Lagirand-Cantaloube *et al.*, 2009, Tintignac *et al.*, 2005
		myogenin	Promotes myogenin polyubiquitylation and degradation	Jogo *et al.*, 2009
Neural	β-TRCP	REST	Degradation of transcriptional repressor, promoting neuronal differentiation	Chong *et al.*, 1995, Westbrook *et al.*, 2008
	Fbw2	gcm	Degradation of gcm allows cell cycle exit and differentiation of glial progenitors in *Drosophila*	Ho *et al.*, 2009, Hosoya *et al.*, 1995
	Skp2	Xic1	Regulation of primary neuronal differentiation in *Xenopus*	Boix-Perales *et al.*, 2007
Neural crest	Ppa	Slug	Regulation of Slug stability during neural crest development	Vernon *et al.*, 2006
	Fbw7	Unknown	Fbw7 necessary for development of neural crest	Almeida *et al.*, 2010

Known SCF substrates per tissue and cell type for each F-box protein are summarized along with their roles.

2003). The phosphodegron is a highly efficient binding motif that can act as a transferable destruction signal (Wulczyn *et al.*, 1998).

A role for *β-TRCP* was first identified from studies with the *Drosophila* orthologue, *Slimb* (Jiang and Struhl, 1998). Loss of function of *Slimb* resulted in the accumulation of the transcription factors *Armadillo/β-catenin* (*Arm*) and *Cubitus interruptus* (*Ci*), components of the *Wnt* and *Hedgehog* (*Hh*) signaling pathways, respectively. It was proposed that *Slimb* negatively regulates these pathways through proteolysis of Arm and Ci. Since then, SCF$^{\beta\text{-TRCP}}$ complexes have been demonstrated to degrade a large number of substrates, many of which have roles during development (reviewed in Fuchs *et al.*, 2004).

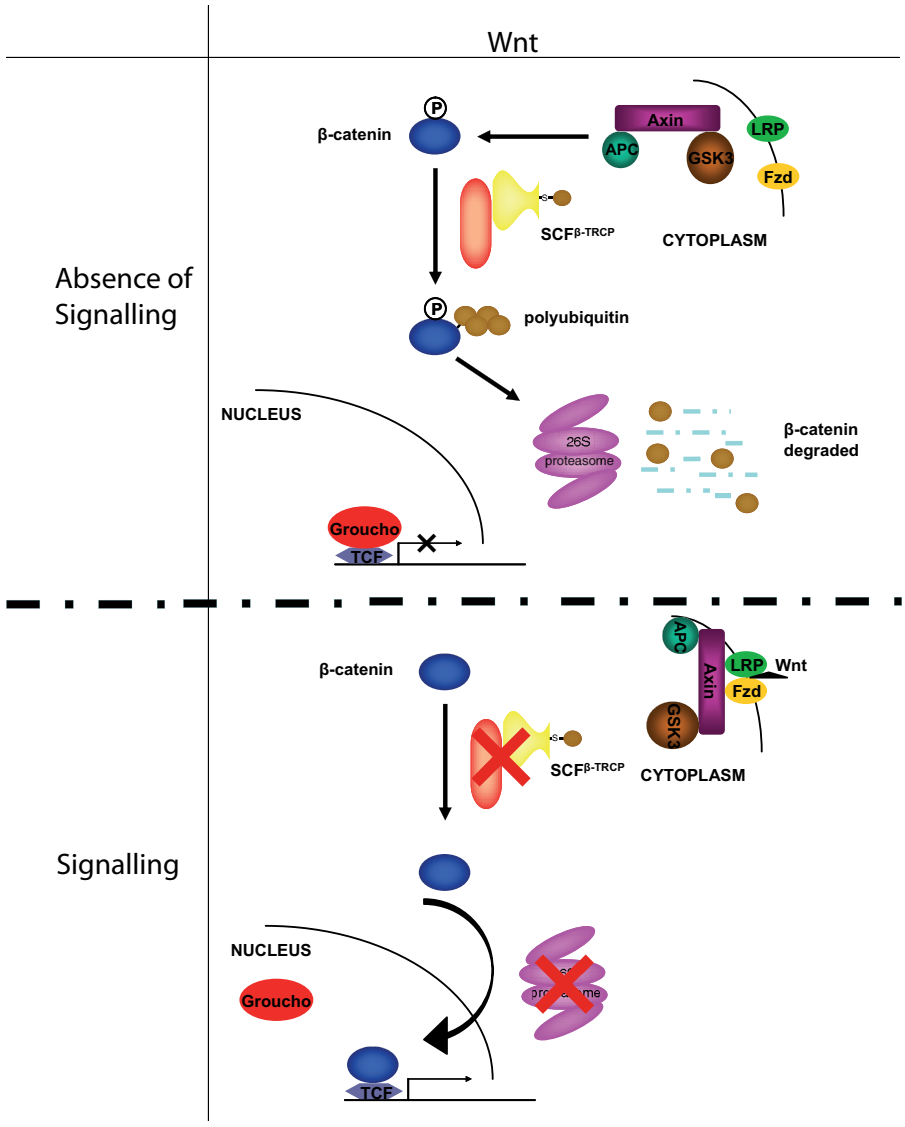

Fig. 2. Regulation of Wnt signaling by Ub mediated protein degradation. *The Wnt pathway is shown in the presence and absence of Wnt, leading to activation and inhibition, respectively, of β-catenin transcriptional activity. In the absence of Wnt, β-catenin is phosphorylated by GSK3 and targeted for degradation by SCF$^{\beta\text{-TRCP}}$. When Wnt is present, binding by the Fzd receptor leads to the complex containing GSK3 being bound at the membrane and unavailable to phosphorylate β-catenin. β-catenin is therefore not degraded and enters the nucleus to form a transcriptionally active complex with TCF, displacing the repressor, Groucho. APC, adenomatous polyposis coli; Fzd, frizzled; GSK3, glycogen synthase kinase 3; LRP, low density lipoprotein receptor related protein; TCF, T cell factor. P is used to denote phosphorylation.*

Wnt signaling

The transcription factor *β-catenin* mediates signaling via the canonical *Wnt* pathway, which regulates multiple developmental processes, for instance dorsal-ventral axis formation in *Xenopus*. β-catenin has an asymmetric localisation in the early *Xenopus* embryo, concentrated on the future dorsal side of the embryo, allowing the expression of dorsal-specific genes. Elevations in dorsal β-catenin levels are attributed to activation of *Wnt* signaling (Larabell *et al.*, 1997); β-catenin is degraded by Ub-mediated proteolysis, and removal of glycogen synthase kinase 3β (GSK3β) phosphorylation sites or activation of *Wnt* signaling stabilises the protein (Aberle *et al.*, 1997). This has led to a model whereby, in the absence of *Wnt* signaling, β-catenin is degraded in a manner dependent upon phosphorylation at GSK3β sites (Fig. 2), but in response to *Wnt* signaling, β-catenin is stabilised and can promote gene expression. *β-TRCP* has been characterised as a negative regulator of *Wnt* signaling; overexpression of *β-TRCP* reduces formation of *Wnt8*-induced secondary axes in *Xenopus*, and inhibition of SCF$^{\beta\text{-TRCP}}$ using a dominant negative F-box deleted (ΔF-box) mutant results in formation of secondary axes (Lagna *et al.*, 1999; Marikawa and Elinson, 1998). The latter effect is inhibited by co-overexpression of mediators of the *Wnt* pathway (Marikawa and Elinson, 1998). Subsequently, SCF$^{\beta\text{-TRCP}}$ was demonstrated to be the E3 ligase for β-catenin (Fuchs *et al.*, 1999; Hart *et al.*, 1999; Latres *et al.*, 1999).

A distinct role has been identified for SCF $^{\beta\text{-TRCP}}$ in neural crest formation. Neural crest (NC) development depends on the activity of the *Snail* family of transcription factors, which trigger the epithelial to mesenchymal transition, via repression of *E-cadherin* that results in the migration of NC cells from the neural tube throughout the embryo. Work in several cell lines has demonstrated that *Wnt* signaling leads to stabilisation of Snail through inhibition of SCF$^{\beta\text{-TRCP}}$ mediated degradation. GSK3β targets human Snail for phosphorylation at serines between amino acids 92-120 and this is required for nuclear export, β-TRCP binding and proteasomal degradation (Yook *et al.*, 2005; Zhou *et al.*, 2004).

Hh signaling

The *Hh* signaling pathway is involved in a range of patterning processes during development, many of which have been identified using *Drosophila* as a model system (reviewed in Ingham and McMahon, 2001; Ingham and Placzek, 2006). In the absence of signaling, a G-protein coupled receptor, *Smoothened* (*Smo*), is

inhibited by a multipass transmembrane receptor for Hh, *Patched* (*Ptc*). Binding of secreted Hh proteins to Ptc alleviates inhibition of Smo and results in the activation of signaling within the cell. The transcription factor *Ci* (the *Gli* family in mammals) is the major mediator of *Hh* signaling in cells. In the absence of *Hh* signaling, *Ci* is a transcriptional repressor for genes such as *Decapentaplegic* (*dpp*). However, when *Hh* signaling is activated, *dpp* expression is de-repressed. The duality of *Ci* activity is achieved by proteolytic processing; full length Ci (Ci155) is a transcriptional activator and a C-terminally truncated form (Ci75) is a repressor. It appears that processing of Ci to repressor forms is mediated by the SCF^{Slimb} complex, the *Drosophila* homologue of $SCF^{\beta\text{-}TRCP}$. Recruitment of SCF^{Slimb} to Ci requires phosphorylation of Ci protein at multiple residues in the C-terminus by Protein Kinase A (PKA) and GSK3. This facilitates further phosphorylation by Casein Kinase I A and E, followed by SCF^{Slimb} recruitment (Jia *et al.*, 2005; Smelkinson *et al.*, 2007). SCF^{Slimb}-mediated processing of Ci is unusual, as ubiquitylation triggers partial proteolysis rather than full destruction (Fig. 3). SCF^{Slimb} activity must be inhibited following *Hh* pathway activation; this allows accumulation of the Ci activator form (Ci155) rather than its repressor form (Ci75). The situation in mammals is more complex. There are 3 Gli proteins, homologues of Ci, Gli1, Gli2 and Gli3. Mouse Gli3 is efficiently processed to a repressive form (Pan *et al.*, 2006), most likely by $SCF^{\beta\text{-}TRCP}$ (Wang and Li, 2006), whilst *Gli2* is important for transcriptional activation. In mouse, Gli2 is inefficiently processed to the repressive form and instead can be degraded fully by the $SCF^{\beta\text{-}TRCP}$ complex (Bhatia *et al.*, 2006; Pan *et al.*, 2006).

NF-κB signaling

Nuclear factor-κB (*NF-κB*) was first identified as a transcription factor involved in expression of the *immunoglobulin κ light chain* gene in B cells (Sen and Baltimore, 1986). It is a member of the *Rel* family of transcription factors, of which there are three genes in *Drosophila*: *Dorsal*, *Dif* and *Relish* (Dushay *et al.*, 1996; Ip *et al.*, 1993; Steward, 1987). Also important in mounting an effective immune response, the developmental role played by *NF-κB* was elucidated through genetic analysis of signaling by its *Drosophila* homologue, *Dorsal* (reviewed in Karin and Ben-Neriah, 2000). Ablation of *Dorsal* activity resulted in embryos lacking ventral structures, which require nuclear localisation of *Dorsal* at the ventral side of the embryo. *Dorsal* is usually bound in the cytoplasm by its inhibitor, *Cactus*, a homologue of mammalian *IκB* (Geisler *et al.*, 1992), such that its nuclear localisation signal is obscured and entry to the nucleus does not occur (Henkel *et al.*, 1992; Wu and Anderson, 1998). Ventral activation of the *IL-1 receptor* homologue, *Toll* (Hashimoto *et al.*, 1988), leads to phosphorylation and degradation of *Cactus*, allowing *Dorsal* to dimerise and enter the nucleus as an active complex (Belvin *et al.*, 1995).

The SCF complex responsible for targeting *IκB* for degradation is, once again, $SCF^{\beta\text{-}TRCP}$, which ubiquitylates *IκB* at lysines 21 and 22 (Maniatis, 1999) after modification of *IκB* by phosphoryla-

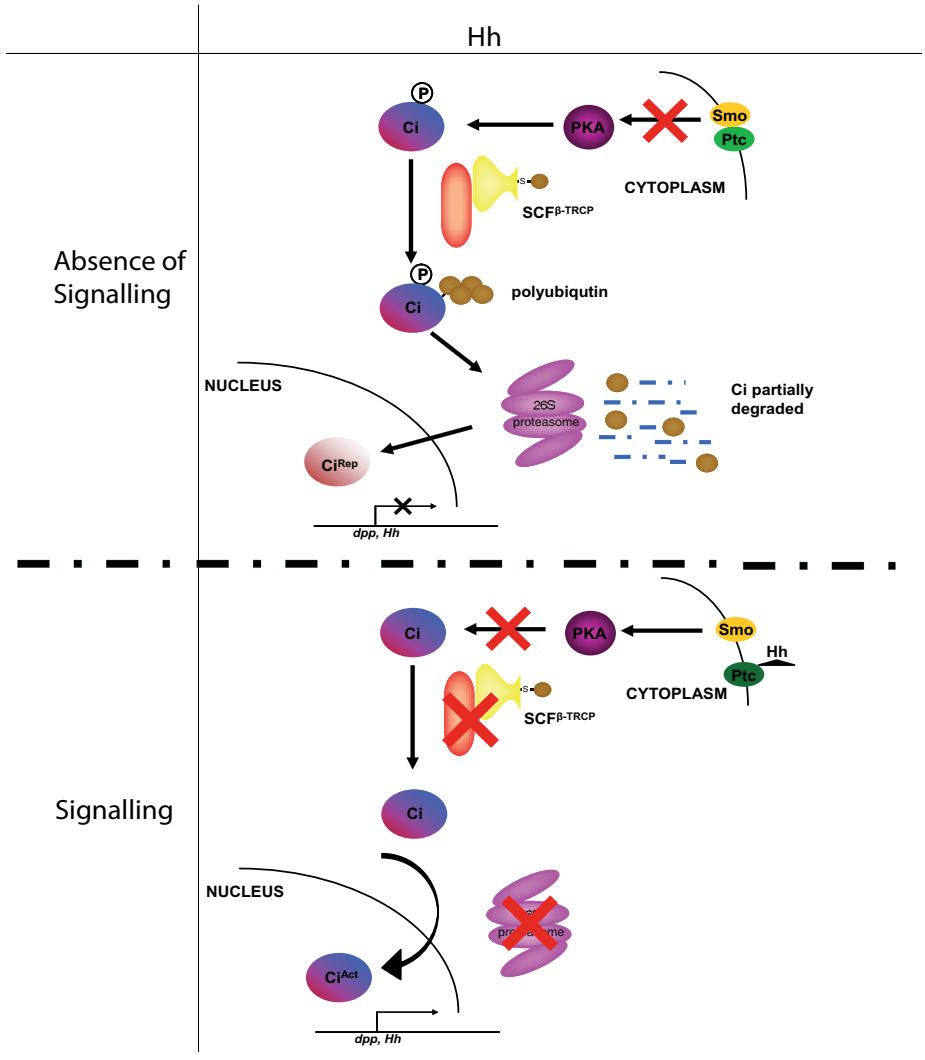

Fig. 3. Regulation of Hh signaling by Ub mediated protein processing. *The Hh pathway is shown in the presence and absence of Hh, leading to activation and inhibition, respectively, of Ci transcriptional activity. In the absence of Hh, Ci is phosphorylated by PKA, active in the presence of inhibited Smo, and polyubiquitylated by $SCF^{\beta\text{-}TRCP}$. This targets Ci for partial proteolysis by the 26S proteasome, leading to the formation of a transcriptional repressor form. When Hh is present, the binding of Hh to Ptc alleviates repression of Smo and inhibits activation of PKA and phosphorylation of Ci. Ci therefore enters the nucleus in a transcriptionally active form that has not been proteolysed. Note the similarities between the Wnt and Hh pathways: signaling at the external surface of the membrane inhibits intracellular signaling and phosphorylation of a transcription factor, which in turn inhibits targeting by $SCF^{\beta\text{-}TRCP}$ to the 26S proteasome. Ci, Cubitus interruptus (Act and Rep are used to denote activator and repressor forms, respectively); dpp, decapentaplegic; Hh, Hedgehog; PKA, protein kinase A; Ptc, Patched; Smo, Smoothened. P is used to denote phosphorylation.*

tion (Alkalay *et al.*, 1995). Inhibition of the 26S proteasome also inhibits *NF-κB* signaling, suggesting that the post-translational modifications that occur to *IκB* are insufficient to cause dissociation from *NF-κB* (Lin *et al.*, 1995). Intriguingly, a role for *NF-κB* signaling in dorsal-ventral patterning in vertebrates has not been established and *NF-κB1*-null mice do not display any gross developmental abnormalities (reviewed in Attar *et al.*, 1997). However, *NF-κB* signaling does seem to play a role in the formation of the epidermis, as knockout of a kinase responsible for phosphorylation of *IκB*, *IκB kinase α (IKKα)*, leads to severe deformity and death of neonates 4 hours post-partum due to thickening of the epidermis (see below).

The examples given above highlight several common features of signaling regulated by $SCF^{\beta\text{-}TRCP}$. Most notably, they illustrate how the UPS can produce a rapid response to signaling events. For instance, in the absence of *Wnt* signaling, β-catenin is degraded by $SCF^{\beta\text{-}TRCP}$, while activation of *Wnt* signaling rapidly stabilises the protein through inhibition of GSK3β. This allows a much faster response than if β-catenin needed to be synthesised *de novo*. Similarly, the response allowed by the switching of Ci from a repressor to an activator form, following inhibition of SCF^{Slimb} by *Hh* signaling, is more rapid than that allowed by changes in expression of repressor and activator genes. It is also noteworthy that, in all these cases, signaling begins with kinases and, for instance, targeting of the substrate to $SCF^{\beta\text{-}TRCP}$ is mediated by phosphorylation of a phosphodegron motif. Integration of the UPS and phosphorylation cascades allows a fine-tuning of the system by combining reversible and irreversible aspects of regulation.

β-TRCP and epidermal development

The epidermis consists of a stratified epithelium that is made up of keratinocytes. Mitotically active keratinocytes reside in the inner basal layer and continuously renew the surface of the epidermis by detaching from the basement membrane and migrating to the outer, terminally differentiated, layer. The transcription factor *p63*, a member of the *p53* family, is crucial for the differentiation of keratinocytes and *p63*-null mice lack epidermis, epidermal structures and squamous epithelia (Mills *et al.*, 1999; Yang *et al.*, 1999). The gross manifestation of the lack of epidermis is the truncation of the limbs and severe craniofacial abnormalities.

There are 6 isoforms of *p63* resulting from differential promoter usage, producing the full N-terminal TAp63 and the N-terminally truncated ΔNp63, and alternative splicing at the 3' end of the transcripts, to produce the α, β and γ isoforms of both TAp63 and ΔNp63. Both TAp63 and ΔNp63 are transcriptionally active, although only TAp63 contains the transactivation domain (reviewed in Candi *et al.*, 2008). In mature epidermis, ΔNp63α appears to be the major isoform expressed in proliferating keratinocytes in the basal layer, but not present in suprabasal layers, although several isoforms are claimed to be required for normal stratification in the embryo (Gu *et al.*, 2006; Koster and Roop, 2004). It has been reported that there is an interaction between endogenous $SCF^{\beta\text{-}TRCP}$ and TAp63γ in a human keratinocyte cell line, HaCaT (Gallegos *et al.*, 2008). Unexpectedly, the interaction with $SCF^{\beta\text{-}TRCP}$ increases the half life of p63 and ubiquitylation of TAp63γ appears to increase its transcriptional activity by around 50%, as assessed by RT-PCR. Although it is likely that $SCF^{\beta\text{-}TRCP}$ has a role in epidermal development *in vivo* there are, as yet, no data to confirm this.

In contrast to its role in promoting the stability and activity of *p63*, $SCF^{\beta\text{-}TRCP}$ also interacts with *hDLG*, the human homologue of *Drosophila discs large* (*Dlg*). Mutations in *Dlg* result in invasive growth of epithelial cells in *Drosophila* (Woods *et al.*, 1996) and *hDLG* is recruited to the plasma membrane by E-cadherin cell-cell adhesion, where it organises junction structures and the actin cytoskeleton (Ide *et al.*, 1999; Reuver and Garner, 1998). Interaction with $SCF^{\beta\text{-}TRCP}$ promotes the ubiquitylation and degradation of hDLG (Mantovani and Banks, 2003). The interaction appears to be promoted by phosphorylation of the SH3 domain of hDLG (Mantovani *et al.*, 2001), although the physiological relevance of this interaction remains unclear.

As well as the central role played by *p63* in epidermal formation and stratification, it appears that *NF-κB* signaling may also play a role in the differentiation of epidermal cells. The inhibitory binding partner of *NF-κB*, *IκB*, is targeted for degradation following phosphorylation by *IKK*, (reviewed in Karin and Ben-Neriah, 2000). The *IKKα*-null mouse appears to phenocopy the *p63*-null mouse, as at a superficial level the neonates lack limbs and show aberrant craniofacial development (Hu *et al.*, 1999; Takeda *et al.*, 1999). Closer inspection of the *IKKα* mutants shows that skeletal organisation is approximately wild type, but the epidermis is 5- to 10-fold thicker and so limbs cannot emerge out of the thickened skin. The epidermis is composed of a single layer and it would appear that the loss of *NF-κB* signaling leads to gross overproliferation of the basal layer.

Intriguingly, in *Drosophila* one of the target genes of *Dorsal* is *twist*, ablation of which is associated with craniofacial abnormalities (Howard *et al.*, 1997). Further, *IKKα* is a direct and indirect target of TAp63, both by direct binding to a *p53*-like consensus sequence on the *IKKα* promoter and by upregulation of the transactivators *Ets-1* and *GATA-3* (Candi *et al.*, 2006; Gu *et al.*, 2004; Sil *et al.*, 2004). IKK interacts with ΔNp63α and promotes its Ub mediated degradation (Chatterjee *et al.*, 2010), suggesting that *NF-κB* and *p63* share multiple components which regulate their activities, the most prominent being the $SCF^{\beta\text{-}TRCP}$ E3 ligase. However, the exact level of crosstalk between these two transcription factors remains to be firmly established.

Other developmental signaling pathways

$SCF^{\beta\text{-}TRCP}$ is not the only SCF complex to play a role in major signaling pathways. Mammalian *FBW7* was initially identified as an F-box protein in a yeast screen for effectors of the cell cycle and termed *cdc4* (Nurse *et al.*, 1976). The *Caenorhabditis elegans* homologue, *SEL-10*, was found through mutational analysis to be responsible for the degradation of the *Notch* intracellular domain, the effector of *Notch* signaling, and thus termination of the *Notch* signal (Gupta-Rossi *et al.*, 2001; Wu *et al.*, 2001). In *C. elegans*, mutation of *SEL-10* resulted in aberrant vulval development, a process dependent upon *Notch* signaling (Hubbard *et al.*, 1997). In mice, knockout of *FBW7* results in embryonic lethality at E10.5 through a combination of aberrant haematopoietic and vascular development and heart maturation defects (Tetzlaff *et al.*, 2004). Defects in neural tube closure and development of all brain regions were also observed at E9.5. Intriguingly $FBW7^{+/-}$ mice appear grossly phenotypically normal up to 1 year of age and, despite reports of mutation of *FBW7* in T-ALL cell lines and

patient samples (O'Neil *et al.*, 2007), did not display an increased incidence of tumorigenesis (Tetzlaff *et al.*, 2004).

However, a role for *FBW7* as a tumour suppressor has been observed in the absence of *p53* activity (Mao *et al.*, 2004). Most recently, conditional inactivation of *FBW7* in murine T cells was found to increase the number of double-positive thymocytes but not single-positive thymocytes, due to increased apoptosis of double-positive thymocytes (Onoyama *et al.*, 2007). This is suggestive of a developmental block in thymocyte maturation and is supported by an increased incidence of thymic lymphoma in Lck-Cre/*FBW7*$^{F/F}$ mice resulting from clonal expansion of progenitors bearing an immature, double-positive phenotype. These abnormalities in thymocyte development were also observed in CD4-Cre/*FBW7* $^{F/F}$/*RBP-J*$^{F/F}$ mice but not in CD4-Cre/*FBW7*$^{F/F}$/*c-Myc*$^{F/F}$ mice, leading the authors to conclude that abnormal thymocyte development arises due to disregulation of *c-Myc* and not *Notch* signaling (Onoyama *et al.*, 2007). More recently, *FBW7* has been found to play a more general role in haematopoiesis, as regulation of the level of c-Myc was found to be sufficient to direct the gene expression signature of haematopoietic stem cells. Intriguingly, adult and embryonic haematopoietic stem cells displayed different responses to c-Myc levels at the level of gene expression (Reavie *et al.*, 2010).

Skp2, β-TRCP, FBW2 and neural differentiation

SCF^{Skp2} is an SCF complex containing the leucine rich repeat F-box protein *Skp2* (also known as *FBXL1*). SCF^{Skp2} has been shown to ubiquitinate a number of cell cycle substrates, including c-Myc (Kim *et al.*, 2003; von der Lehr *et al.*, 2003), Cyclin E (Nakayama *et al.*, 2000), the cyclin dependent kinase inhibitors (CKI) p27^{Kip1} (Carrano *et al.*, 1999), p57^{Kip2} (Kamura *et al.*, 2003) and the *Xenopus* CKI Xic1 (Lin *et al.*, 2006), and has been implicated in development of many cancers (Bashir *et al.*, 2004; Kitagawa *et al.*, 2008; Signoretti *et al.*, 2002). However, in addition to a central role in proteolysis of cell cycle regulators, SCF^{Skp2} may have additional functions in differentiation and development.

Recent work has highlighted a role for *Skp2* during neural development in *Xenopus.* Primary neurogenesis in this species results in differentiation of neurons that mediate the early movements of the embryo. This process is driven by a cascade of proneural basic Helix-Loop-Helix (bHLH) transcription factors, resulting in the expression of markers of terminal neuronal differentiation, such as *neural β-tubulin* (*NβT*) (reviewed in Lee, 1997). Depletion of Skp2 protein using translation-blocking anti-sense morpholinos promotes primary neurogenesis, as assessed by expression of *NβT*, by a mechanism independent of changes in the cell cycle. Conversely, overexpression of *Skp2* inhibits formation of primary neurons and this inhibition occurs at an early point in the bHLH cascade (Boix-Perales *et al.*, 2007). *Skp2*-mediated inhibition of this process is likely to occur via ubiquitylation of substrates by the SCF^{Skp2} complex, as overexpression of a ΔF-box form of *Skp2*, which can no longer bind to Skp1 and therefore the rest of the SCF complex, has no effect on formation of primary neurons (Boix-Perales *et al.*, 2007). As the CKI *Xic1* is required for differentiation of primary neurons in *Xenopus* (Vernon *et al.*, 2003), degradation of Xic1 in neural precursors may be the major mechanism by which SCF^{Skp2} regulates this process. It is interesting to note in this regard that the CKI p57^{Kip2} has been reported to associate with several proteins involved in differentiation, such as MyoD (reviewed in Besson *et al.*, 2008; Reynaud *et al.*, 2000). However, unlike the degradation of the CKI p27^{Kip1} by SCF^{Skp2} in mammals, Xic1 degradation in *Xenopus* by SCF^{Skp2} does not require prior phosphorylation of its CKI target (Lin *et al.*, 2006).

The stability of Skp2 itself is regulated by the UPS in mammals, and the E3 ligase responsible is the APC/C coupled to the substrate recognition subunit, Cdh1 (Bashir *et al.*, 2004; Wei *et al.*, 2004). Degradation of Skp2 by APC/C^{Cdh1} is also important for myogenesis, as depletion of Cdh1 by siRNA in the mouse skeletal muscle cell line, C2C12, reduces cellular elongation and myogenic fusion (Li *et al.*, 2007). It was found that the attachment of Ub to and degradation of Skp2 was greatly reduced in Cdh1-depleted cells when compared to control C2C12 cells. The authors speculated that the increase in Skp2 levels in Cdh1-depleted cells would lead to reduced levels of p21 and p27, cell cycle regulators which are crucial for muscle differentiation (Vernon and Philpott, 2003; Zhang *et al.*, 1999). However, it was also suggested that the myogenic transcription factor myf5 is a target for APC/C^{Cdh1} (Li *et al.*, 2007).

Although a key determinant in neural differentiation, SCF^{Skp2} is not the only E3 ligase to have been implicated in this process. Recently it has been shown that the master repressor of neuronal gene expression, *RE1 silencing transcription factor* (*REST*), is a substrate for SCF$^{β\text{-}TRCP}$-mediated degradation (Chong *et al.*, 1995; Schoenherr and Anderson, 1995; Westbrook *et al.*, 2008). However, the functional relevance of this interaction to neural development is not clear, as the *in vivo* data presented are mostly obtained from epithelial cells or cell lines of non-neural origin. Nevertheless, data from neural stem and progenitor cells seem to suggest that endogenous REST stability is regulated by SCF$^{β\text{-}TRCP}$ during early neural differentiation (Westbrook *et al.*, 2008).

FBW2, another F-box protein, currently has only one known substrate, *glial cells missing homologue 1* (*GCM1*), an interaction observed in a placental cell line (Chiang *et al.*, 2008). In *Drosophila*, *glial cells missing* (*gcm*) was first identified as a glial fate switch gene which, when overexpressed, caused an increase in the number of glial cells but not total number of cells in the nervous system (Hosoya *et al.*, 1995; Jones *et al.*, 1995). More recent work suggests that *gcm* degradation allows cell cycle exit and differentiation of glial progenitors in *Drosophila* (Ho *et al.*, 2009). Rapid degradation of gcm allows the daughter cells of the thoracic neuroglioblast, NB6-4T, which expresses *gcm* at low levels, to adopt differing cell fates following asymmetric segregation of *gcm* transcript. Recently, a role for *gcm* in the differentiation of the *Drosophila* haemocyte lineage has also been reported (Jacques *et al.*, 2009). Intriguingly, although the mammalian homologues *GCM1* and *GCM2* share high sequence homology in the DNA binding domain and conservation of domain structure (Akiyama *et al.*, 1996; Altshuller *et al.*, 1996; Kim *et al.*, 1998), there appears to be no functional conservation between *Drosophila* and mammals (Basyuk *et al.*, 1999; Kanemura *et al.*, 1999).

GCM1 is mainly expressed in the placenta, with lower levels of expression in the thymus, whilst *GCM2* is expressed in the developing mouse parathyroid gland (Basyuk *et al.*, 1999; Kim *et al.*, 1998). In the placenta, *GCM1* is absolutely required for expression of the fusogenic protein syncytin and knockout leads to embryonic lethality at E9.5-10 due to aberrant labyrinth forma-

tion (Anson-Cartwright *et al.*, 2000; Schreiber *et al.*, 2000). In contrast to the extraembryonic tissue, there appear to be no embryonic abnormalities associated with *GCM1* knockout. Although little is known about the role of degradation in the regulation of *GCM1*, it is noteworthy that both *Drosophila* and mammalian homologues have a conserved role for the UPS despite a complete lack of conservation of developmental function.

Ppa, Fbw7 and neural crest development

The transcription factor *Slug* is required for NC development in *Xenopus* (for example, LaBonne and Bronner-Fraser, 2000), and the degradation of Slug by the F-box protein Partner of Paired (Ppa, also known as FBXL14 in vertebrates) has been reported in *Xenopus* (Vernon and LaBonne, 2006). Using overexpression and knock-down techniques, it was demonstrated that SCF^{Ppa}-mediated degradation of Slug was important for patterning the neural plate border; overexpression of *Ppa* expanded the neural plate, at the expense of the NC, whereas by contrast, overexpression of a *Ppa*-refractory *Slug* mutant expanded the NC and led to premature migration of NC cells in the spinal cord. It is interesting to note that two key regulators of NC development, *Slug* and *Snail*, are degraded by SCF E3 ligases (SCF^{Ppa} and $SCF^{\beta\text{-}TRCP}$ respectively, see above).

A further role for F-box proteins in the development of the NC has been recently described in *Xenopus*, where the function of *Fbw7* was perturbed by expression of an *Fbw7ΔF-box* mutant (Almeida *et al.*, 2010). Loss of Fbw7 activity led to reduced expression of both *Slug* and *Snail*, as well as *c-Myc*, and the loss of NC-derived tissues, such as melanocytes. The activity of Fbw7 appeared to be required specifically for development of NC, as expression of early markers in other tissues was unperturbed when Fbw7 activity was inhibited. Thus it appears that several stages of NC development are regulated by SCF complexes.

MAFbx and myogenesis

Muscle Atrophy F-box (*MAFbx*), also known as *Atrogin-1* and *FBXO32*, was first identified as an E3 ligase that could target MyoD, the master regulator of myogenesis, for Ub-mediated proteolysis (Davis *et al.*, 1987; Lassar *et al.*, 1991) and is a muscle-specific gene upregulated during muscle atrophy (Bodine *et al.*, 2001; Gomes *et al.*, 2001). In C2C12 cells, *MAFbx* expression increased during *ex vivo* differentiation (Tintignac *et al.*, 2005).

MAFbx was first characterised following a yeast two-hybrid screen using Skp1 binding proteins as prey and MyoD as bait (Tintignac *et al.*, 2005), establishing that the two proteins interacted via an LXXLL motif on MyoD. This suggests that, unusually for an F-box protein, MAFbx recognises MyoD independently of MyoD phosphorylation state. Overexpression of *MAFbx* reduced the half-life of MyoD and also increased the ubiquitylation of MyoD. Conversely, inhibition of *MAFbx* using a dominant negative ΔF-box construct (*MAFbxΔF*) increased the half-life of MyoD. As well as the considerable evidence for MyoD degradation by MAFbx *in vitro*, a recent report has also demonstrated increased polyubiquitylation of MyoD following transfection of *MAFbx*, but not *MAFbxΔF*, into C2C12 cells (Lagirand-Cantaloube *et al.*, 2009). A direct interaction between SCF^{MAFbx} and myogenin, a bHLH transcription factor downstream of MyoD, has been demonstrated and SCF^{MAFbx} was seen to promote polyubiquitylation and degradation of myogenin *in vivo* (Jogo *et al.*, 2009).

Conclusions

The UPS is well known for its housekeeping role in protein turnover but it is becoming increasingly clear that it also plays a crucial role in dynamic processes involved in development, where ubiquitylation can result in either protein destruction, proteolytic processing or change in sub-cellular localization. Single SCF E3 ligase complexes may have multiple targets, exemplified by $SCF^{\beta\text{-}TRCP}$, which potentially results in co-ordination of developmental signaling pathways, while single targets can be ubiquitylated by more than one E3 ligase complex. The selectivity, irreversibility and responsiveness of SCF complexes make them excellent candidates for developmental regulation, while substrate ubiquitylation is also often regulated by further post-translational substrate modification such as phosphorylation, which can fine-tune cellular responses.

Such complexity, illustrated well by the multiple roles of $SCF^{\beta\text{-}TRCP}$, often makes it difficult to define the role of individual E3 ligases in distinct developmental events. However, the use of multiple model systems and analysis of individual substrates can both facilitate this reductionist approach to identifying the role of distinct SCF complexes, and allow us to explore the role of multiple ubiquitylation pathways in regulating complex developmental events. There is clearly a lot to learn.

Acknowledgements

GSM was funded by a Medical Research Council studentship, CJH by a Cancer Research UK studentship and HW was funded by a Wellcome Trust studentship. Work in AP's lab is funded by MRC Research Grant G0700758

References

ABERLE, H., BAUER, A., STAPPERT, J., KISPERT, A. and KEMLER, R. (1997). beta-catenin is a target for the ubiquitin-proteasome pathway. *EMBO J* 16: 3797-3804.

AKIYAMA, Y., HOSOYA, T., POOLE, A.M. and HOTTA, Y. (1996). The gcm-motif: a novel DNA-binding motif conserved in *Drosophila* and mammals. *Proc Natl Acad Sci USA* 93: 14912-14916.

ALKALAY, I., YARON, A., HATZUBAI, A., ORIAN, A., CIECHANOVER, A. and BEN-NERIAH, Y. (1995). Stimulation-dependent I kappa B alpha phosphorylation marks the NF-kappa B inhibitor for degradation via the ubiquitin-proteasome pathway. *Proc Natl Acad Sci USA* 92: 10599-10603.

ALMEIDA, A., WISE, H., HINDLEY, C., SLEVIN, M., HARTLEY, R. and PHILPOTT, A. (2010). The F-box protein Cdc4/Fbxw7 is a novel regulator of neural crest development in *Xenopus laevis*. *Neural Dev* 5: 1.

ALTSHULLER, Y., COPELAND, N.G., GILBERT, D.J., JENKINS, N.A. and FROHMAN, M.A. (1996). Gcm1, a mammalian homolog of *Drosophila* glial cells missing. *FEBS Lett* 393: 201-204.

ANG, X.L. and HARPER, J.W. (2004). Interwoven Ubiquitination Oscillators and Control of Cell Cycle Transitions. *Sci STKE* 2004: pe31.

ANG, X.L. and WADE HARPER, J. (2005). SCF-mediated protein degradation and cell cycle control. *Oncogene* 24: 2860-2870.

ANSON-CARTWRIGHT, L., DAWSON, K., HOLMYARD, D., FISHER, S.J., LAZZARINI, R.A. and CROSS, J.C. (2000). The glial cells missing-1 protein is essential for branching morphogenesis in the chorioallantoic placenta. *Nat Genet* 25: 311-314.

ATTAR, R.M., CAAMANO, J., CARRASCO, D., IOTSOVA, V., ISHIKAWA, H., RYSECK, R.P., WEIH, F. and BRAVO, R. (1997). Genetic approaches to study Rel/NF-kappa B/I kappa B function in mice. *Semin Cancer Biol* 8: 93-101.

BALLARINO, M., FRUSCALZO, A., MARCHIONI, M. and CARNEVALI, F. (2004). Identification of positive and negative regulatory regions controlling expression of the *Xenopus laevis* betaTrCP gene. *Gene* 336: 275-285.

BALLARINO, M., MARCHIONI, M. and CARNEVALI, F. (2002). The *Xenopus laevis* beta TrCP gene: genomic organization, alternative splicing, 5' and 3' region characterization and comparison of its structure with that of human beta TrCP genes. *Biochim Biophys Acta* 1577: 81-92.

BASHIR, T., DORRELLO, N.V., AMADOR, V., GUARDAVACCARO, D. and PAGANO, M. (2004). Control of the SCF(Skp2-Cks1) ubiquitin ligase by the APC/C(Cdh1) ubiquitin ligase. *Nature* 428: 190-193.

BASYUK, E., CROSS, J.C., CORBIN, J., NAKAYAMA, H., HUNTER, P., NAIT-OUMESMAR, B. and LAZZARINI, R.A. (1999). Murine Gcm1 gene is expressed in a subset of placental trophoblast cells. *Dev Dyn* 214: 303-311.

BELVIN, M.P., JIN, Y. and ANDERSON, K.V. (1995). Cactus protein degradation mediates *Drosophila* dorsal-ventral signaling. *Genes Dev* 9: 783-793.

BESSON, A., DOWDY, S.F. and ROBERTS, J.M. (2008). CDK Inhibitors: Cell Cycle Regulators and Beyond. *Dev Cell* 14: 159-169.

BHATIA, N., THIYAGARAJAN, S., ELCHEVA, I., SALEEM, M., DLUGOSZ, A., MUKHTAR, H. and SPIEGELMAN, V.S. (2006). Gli2 is targeted for ubiquitination and degradation by beta-TrCP ubiquitin ligase. *J Biol Chem* 281: 19320-19326.

BODINE, S.C., LATRES, E., BAUMHUETER, S., LAI, V.K., NUNEZ, L., CLARKE, B.A., POUEYMIROU, W.T., PANARO, F.J., NA, E., DHARMARAJAN, K. *et al.* (2001). Identification of ubiquitin ligases required for skeletal muscle atrophy. *Science* 294: 1704-1708.

BOIX-PERALES, H., HORAN, I., WISE, H., LIN, H.R., CHUANG, L.C., YEW, P.R. and PHILPOTT, A. (2007). The E3 ubiquitin ligase skp2 regulates neural differentiation independent from the cell cycle. *Neural Dev* 2: 27.

CANDI, E., CIPOLLONE, R., RIVETTI DI VAL CERVO, P., GONFLONI, S., MELINO, G. and KNIGHT, R. (2008). p63 in epithelial development. *Cell Mol Life Sci* 65: 3126-3133.

CANDI, E., TERRINONI, A., RUFINI, A., CHIKH, A., LENA, A.M., SUZUKI, Y., SAYAN, B.S., KNIGHT, R.A. and MELINO, G. (2006). p63 is upstream of IKK alpha in epidermal development. *J Cell Sci* 119: 4617-4622.

CARRANO, A.C., EYTAN, E., HERSHKO, A. and PAGANO, M. (1999). SKP2 is required for ubiquitin-mediated degradation of the CDK inhibitor p27. *Nat Cell Biol* 1: 193-199.

CHATTERJEE, A., CHANG, X., SEN, T., RAVI, R., BEDI, A. and SIDRANSKY, D. (2010). Regulation of p53 family member isoform DeltaNp63alpha by the nuclear factor-kappaB targeting kinase IkappaB kinase beta. *Cancer Res* 70: 10.

CHEN, A., WU, K., FUCHS, S.Y., TAN, P., GOMEZ, C. and PAN, Z.Q. (2000). The conserved RING-H2 finger of ROC1 is required for ubiquitin ligation. *J Biol Chem* 275: 15432-15439.

CHIANG, M.H., CHEN, L.F. and CHEN, H. (2008). Ubiquitin-conjugating enzyme UBE2D2 is responsible for FBXW2 (F-box and WD repeat domain containing 2)-mediated human GCM1 (glial cell missing homolog 1) ubiquitination and degradation. *Biol Reprod* 79: 914-920.

CHONG, J.A., TAPIA-RAMIREZ, J., KIM, S., TOLEDO-ARAL, J.J., ZHENG, Y., BOUTROS, M.C., ALTSHULLER, Y.M., FROHMAN, M.A., KRANER, S.D. and MANDEL, G. (1995). REST: a mammalian silencer protein that restricts sodium channel gene expression to neurons. *Cell* 80: 949-957.

CIECHANOVER, A., ELIAS, S., HELLER, H., FERBER, S. and HERSHKO, A. (1980a). Characterization of the heat-stable polypeptide of the ATP-dependent proteolytic system from reticulocytes. *J Biol Chem* 255: 7525-7528.

CIECHANOVER, A., FINLEY, D. and VARSHAVSKY, A. (1984). Ubiquitin dependence of selective protein degradation demonstrated in the mammalian cell cycle mutant ts85. *Cell* 37: 57-66.

CIECHANOVER, A., HELLER, H., ELIAS, S., HAAS, A.L. and HERSHKO, A. (1980b). ATP-dependent conjugation of reticulocyte proteins with the polypeptide required for protein degradation. *Proc Natl Acad Sci USA* 77: 1365-1368.

DAVIS, R.L., WEINTRAUB, H. and LASSAR, A.B. (1987). Expression of a single transfected cDNA converts fibroblasts to myoblasts. *Cell* 51: 987-1000.

DESHAIES, R.J. and JOAZEIRO, C.A. (2009). RING domain E3 ubiquitin ligases. *Annu Rev Biochem* 78: 399-434.

DUDA, D.M., BORG, L.A., SCOTT, D.C., HUNT, H.W., HAMMEL, M. and SCHULMAN, B.A. (2008). Structural Insights into NEDD8 Activation of Cullin-RING Ligases: Conformational Control of Conjugation. *Cell* 134: 995-1006.

DUSHAY, M.S., ASLING, B. and HULTMARK, D. (1996). Origins of immunity: Relish, a compound Rel-like gene in the antibacterial defense of *Drosophila*. *Proc Natl Acad Sci USA* 93: 10343-10347.

FUCHS, S.Y., CHEN, A., XIONG, Y., PAN, Z.Q. and RONAI, Z. (1999). HOS, a human homolog of Slimb, forms an SCF complex with Skp1 and Cullin1 and targets the phosphorylation-dependent degradation of IkappaB and beta-catenin. *Oncogene* 18: 2039-2046.

FUCHS, S.Y., SPIEGELMAN, V.S. and KUMAR, K.G. (2004). The many faces of beta-TrCP E3 ubiquitin ligases: reflections in the magic mirror of cancer. *Oncogene* 23: 2028-2036.

FURUKAWA, M., OHTA, T. and XIONG, Y. (2002). Activation of UBC5 ubiquitin-conjugating enzyme by the RING finger of ROC1 and assembly of active ubiquitin ligases by all cullins. *J Biol Chem* 277: 15758-15765.

GAGNE, J.M., DOWNES, B.P., SHIU, S.H., DURSKI, A.M. and VIERSTRA, R.D. (2002). The F-box subunit of the SCF E3 complex is encoded by a diverse superfamily of genes in *Arabidopsis*. *Proc Natl Acad Sci USA* 99: 11519-11524.

GALLEGOS, J.R., LITERSKY, J., LEE, H., SUN, Y., NAKAYAMA, K., NAKAYAMA, K. and LU, H. (2008). SCF TrCP1 activates and ubiquitylates TAp63gamma. *J Biol Chem* 283: 66-75.

GEISLER, R., BERGMANN, A., HIROMI, Y. and NUSSLEIN-VOLHARD, C. (1992). cactus, a gene involved in dorsoventral pattern formation of *Drosophila*, is related to the I kappa B gene family of vertebrates. *Cell* 71: 613-621.

GOMES, M.D., LECKER, S.H., JAGOE, R.T., NAVON, A. and GOLDBERG, A.L. (2001). Atrogin-1, a muscle-specific F-box protein highly expressed during muscle atrophy. *Proc Natl Acad Sci USA* 98: 14440-14445.

GROSSMAN, S.R., DEATO, M.E., BRIGNONE, C., CHAN, H.M., KUNG, A.L., TAGAMI, H., NAKATANI, Y. and LIVINGSTON, D.M. (2003). Polyubiquitination of p53 by a ubiquitin ligase activity of p300. *Science* 300: 342-344.

GU, L., ZHU, N., FINDLEY, H.W., WOODS, W.G. and ZHOU, M. (2004). Identification and characterization of the IKKalpha promoter: positive and negative regulation by ETS-1 and p53, respectively. *J Biol Chem* 279: 52141-52149.

GU, X., LUNDQVIST, E.N., COATES, P.J., THURFJELL, N., WETTERSAND, E. and NYLANDER, K. (2006). Dysregulation of TAp63 mRNA and protein levels in psoriasis. *J Invest Dermatol* 126: 137-141.

GUINEZ, C., MIR, A.-M., DEHENNAUT, V., CACAN, R., HARDUIN-LEPERS, A., MICHALSKI, J.-C. and LEFEBVRE, T. (2008). Protein ubiquitination is modulated by O-GlcNAc glycosylation. *FASEB* 22: 2901-2911.

GUPTA-ROSSI, N., LE BAIL, O., GONEN, H., BROU, C., LOGEAT, F., SIX, E., CIECHANOVER, A. and ISRAEL, A. (2001). Functional interaction between SEL-10, an F-box protein, and the nuclear form of activated Notch1 receptor. *J Biol Chem* 276: 34371-34378.

HART, M., CONCORDET, J.P., LASSOT, I., ALBERT, I., DEL LOS SANTOS, R., DURAND, H., PERRET, C., RUBINFELD, B., MARGOTTIN, F., BENAROUS, R. *et al.* (1999). The F-box protein beta-TrCP associates with phosphorylated beta-catenin and regulates its activity in the cell. *Curr Biol* 9: 207-210.

HASHIMOTO, C., HUDSON, K.L. and ANDERSON, K.V. (1988). The Toll gene of *Drosophila*, required for dorsal-ventral embryonic polarity, appears to encode a transmembrane protein. *Cell* 52: 269-279.

HENKEL, T., ZABEL, U., VAN ZEE, K., MULLER, J.M., FANNING, E. and BAEUERLE, P.A. (1992). Intramolecular masking of the nuclear location signal and dimerization domain in the precursor for the p50 NF-kappa B subunit. *Cell* 68: 1121-1133.

HERSHKO, A., CIECHANOVER, A., HELLER, H., HAAS, A.L. and ROSE, I.A. (1980). Proposed role of ATP in protein breakdown: conjugation of protein with multiple chains of the polypeptide of ATP-dependent proteolysis. *Proc Natl Acad Sci USA* 77: 1783-1786.

HERSHKO, A., HELLER, H., ELIAS, S. and CIECHANOVER, A. (1983). Components of ubiquitin-protein ligase system. Resolution, affinity purification, and role in protein breakdown. *J Biol Chem* 258: 8206-8214.

HICKE, L., SCHUBERT, H.L. and HILL, C.P. (2005). Ubiquitin-binding domains. *Nat Rev Mol Cell Biol* 6: 610-621.

HO, M.S.-C., CHEN, H., CHEN, M., JACQUES, C.C., GIANGRANDE, A. and CHIEN, C.-T. (2009). Gcm protein degradation suppresses proliferation of glial progenitors. *Proc Natl Acad Sci U S A* 106: 6778-6783.

HOPPE, T. (2005). Multiubiquitylation by E4 enzymes: [']one size' doesn't fit all. *Trends Biochem Sci* 30: 183-187.

HOSOYA, T., TAKIZAWA, K., NITTA, K. and HOTTA, Y. (1995). glial cells missing: a binary switch between neuronal and glial determination in *Drosophila*. *Cell* 82: 1025-1036.

HOWARD, T.D., PAZNEKAS, W.A., GREEN, E.D., CHIANG, L.C., MA, N., ORTIZ DE LUNA, R.I., GARCIA DELGADO, C., GONZALEZ-RAMOS, M., KLINE, A.D. and JABS, E.W. (1997). Mutations in TWIST, a basic helix-loop-helix transcription factor, in Saethre-Chotzen syndrome. *Nat Genet* 15: 36-41.

HU, Y., BAUD, V., DELHASE, M., ZHANG, P., DEERINCK, T., ELLISMAN, M., JOHNSON, R. and KARIN, M. (1999). Abnormal morphogenesis but intact IKK activation in mice lacking the IKKalpha subunit of IkappaB kinase. *Science* 284: 316-320.

HUBBARD, E.J., WU, G., KITAJEWSKI, J. and GREENWALD, I. (1997). sel-10, a negative regulator of lin-12 activity in Caenorhabditis elegans, encodes a member of the CDC4 family of proteins. *Genes Dev* 11: 3182-3193.

HWANG, C.-S., SHEMORRY, A. and VARSHAVSKY, A. (2010). N-Terminal Acetylation of Cellular Proteins Creates Specific Degradation Signals. *Science* 327: 973-977.

IDE, N., HATA, Y., NISHIOKA, H., HIRAO, K., YAO, I., DEGUCHI, M., MIZOGUCHI, A., NISHIMORI, H., TOKINO, T., NAKAMURA, Y. *et al.* (1999). Localization of membrane-associated guanylate kinase (MAGI)-1/BAI-associated protein (BAP) 1 at tight junctions of epithelial cells. *Oncogene* 18: 7810-7815.

INGHAM, P.W. and MCMAHON, A.P. (2001). Hedgehog signaling in animal development: paradigms and principles. *Genes Dev* 15: 3059-3087.

INGHAM, P.W. and PLACZEK, M. (2006). Orchestrating ontogenesis: variations on a theme by sonic hedgehog. *Nat Rev Genet* 7: 841-850.

IP, Y.T., REACH, M., ENGSTROM, Y., KADALAYIL, L., CAI, H., GONZÁLEZ-CRESPO, S., TATEI, K. and LEVINE, M. (1993). Dif, a dorsal-related gene that mediates an immune response in *Drosophila*. *Cell* 75: 753-763.

JACQUES, C., SOUSTELLE, L., NAGY, I., DIEBOLD, C. and GIANGRANDE, A. (2009). A novel role of the glial fate determinant glial cells missing in hematopoiesis. *Int J Dev Biol* 53: 1013-1022.

JAIN, M., NIJHAWAN, A., ARORA, R., AGARWAL, P., RAY, S., SHARMA, P., KAPOOR, S., TYAGI, A.K. and KHURANA, J.P. (2007). F-box proteins in rice. Genome-wide analysis, classification, temporal and spatial gene expression during panicle and seed development, and regulation by light and abiotic stress. *Plant Physiol* 143: 1467-1483.

JIA, J., ZHANG, L., ZHANG, Q., TONG, C., WANG, B., HOU, F., AMANAI, K. and JIANG, J. (2005). Phosphorylation by double-time/CKIepsilon and CKIalpha targets cubitus interruptus for Slimb/beta-TRCP-mediated proteolytic processing. *Dev Cell* 9: 819-830.

JIANG, J. and STRUHL, G. (1998). Regulation of the Hedgehog and Wingless signalling pathways by the F-box/WD40-repeat protein Slimb. *Nature* 391: 493-496.

JIN, J., SHIROGANE, T., XU, L., NALEPA, G., QIN, J., ELLEDGE, S.J. and HARPER, J.W. (2003). SCFbeta-TRCP links Chk1 signaling to degradation of the Cdc25A protein phosphatase. *Genes Dev* 17: 3062-3074.

JOGO, M., SHIRAISHI, S. and TAMURA, T.-A. (2009). Identification of MAFbx as a myogenin-engaged F-box protein in SCF ubiquitin ligase. *FEBS Lett* 583: 2715-2719.

JONES, B.W., FETTER, R.D., TEAR, G. and GOODMAN, C.S. (1995). glial cells missing: a genetic switch that controls glial versus neuronal fate. *Cell* 82: 1013-1023.

KAMURA, T., HARA, T., KOTOSHIBA, S., YADA, M., ISHIDA, N., IMAKI, H., HATAKEYAMA, S., NAKAYAMA, K. and NAKAYAMA, K.I. (2003). Degradation of p57Kip2 mediated by SCFSkp2-dependent ubiquitylation. *Proc Natl Acad Sci USA* 100: 10231-10236.

KANEMURA, Y., HIRAGA, S., ARITA, N., OHNISHI, T., IZUMOTO, S., MORI, K., MATSUMURA, H., YAMASAKI, M., FUSHIKI, S. and YOSHIMINE, T. (1999). Isolation and expression analysis of a novel human homologue of the *Drosophila* glial cells missing (gcm) gene. *FEBS Lett* 442: 151-156.

KARIN, M. and BEN-NERIAH, Y. (2000). Phosphorylation meets ubiquitination: the control of NF-[kappa]B activity. *Annu Rev Immunol* 18: 621-663.

KEPINSKI, S. and LEYSER, O. (2004). Auxin-induced SCFTIR1-Aux/IAA interaction involves stable modification of the SCFTIR1 complex. *Proc Natl Acad Sci USA* 101: 12381-12386.

KIM, J., JONES, B.W., ZOCK, C., CHEN, Z., WANG, H., GOODMAN, C.S. and ANDERSON, D.J. (1998). Isolation and characterization of mammalian homologs of the *Drosophila* gene glial cells missing. *Proc Natl Acad Sci USA* 95: 12364-12369.

KIM, S.Y., HERBST, A., TWORKOWSKI, K.A., SALGHETTI, S.E. and TANSEY, W.P. (2003). Skp2 regulates Myc protein stability and activity. *Mol Cell* 11: 1177-1188.

KITAGAWA, M., LEE, S.H. and MCCORMICK, F. (2008). Skp2 suppresses p53-dependent apoptosis by inhibiting p300. *Mol Cell* 29: 217-231.

KOSTER, M.I. and ROOP, D.R. (2004). p63 and epithelial appendage development. *Differentiation* 72: 364-370.

KURODA, H., TAKAHASHI, N., SHIMADA, H., SEKI, M., SHINOZAKI, K. and MATSUI, M. (2002). Classification and expression analysis of *Arabidopsis* F-box-containing protein genes. *Plant Cell Physiol* 43: 1073-1085.

LABONNE, C. and BRONNER-FRASER, M. (2000). Snail-related transcriptional repressors are required in *Xenopus* for both the induction of the neural crest and its subsequent migration. *Dev Biol* 221: 195-205.

LAGIRAND-CANTALOUBE, J., CORNILLE, K., CSIBI, A., BATONNET-PICHON, S., LEIBOVITCH, M.P. and LEIBOVITCH, S.A. (2009). Inhibition of atrogin-1/MAFbx mediated MyoD proteolysis prevents skeletal muscle atrophy *in vivo*. *PLoS One* 4: e4973.

LAGNA, G., CARNEVALI, F., MARCHIONI, M. and HEMMATI-BRIVANLOU, A. (1999). Negative regulation of axis formation and Wnt signaling in *Xenopus* embryos by the F-box/WD40 protein beta TrCP. *Mech Dev* 80: 101-106.

LARABELL, C.A., TORRES, M., ROWNING, B.A., YOST, C., MILLER, J.R., WU, M., KIMELMAN, D. and MOON, R.T. (1997). Establishment of the dorso-ventral axis in *Xenopus* embryos is presaged by early asymmetries in beta-catenin that are modulated by the Wnt signaling pathway. *J Cell Biol* 136: 1123-1136.

LASSAR, A.B., DAVIS, R.L., WRIGHT, W.E., KADESCH, T., MURRE, C., VORONOVA, A., BALTIMORE, D. and WEINTRAUB, H. (1991). Functional activity of myogenic HLH proteins requires hetero-oligomerization with E12/E47-like proteins *in vivo*. *Cell* 66: 305-315.

LATRES, E., CHIAUR, D.S. and PAGANO, M. (1999). The human F box protein beta-Trcp associates with the Cul1/Skp1 complex and regulates the stability of beta-catenin. *Oncogene* 18: 849-854.

LEE, J.E. (1997). Basic helix-loop-helix genes in neural development. *Curr Opin Neurobiol* 7: 13-20.

LI, W., WU, G. and WAN, Y. (2007). The dual effects of Cdh1/APC in myogenesis. *FASEB J* 21: 3606-3617.

LIN, H.R., CHUANG, L.C., BOIX-PERALES, H., PHILPOTT, A. and YEW, P.R. (2006). Ubiquitination of cyclin-dependent kinase inhibitor, Xic1, is mediated by the *Xenopus* F-box protein xSkp2. *Cell Cycle* 5: 304-314.

LIN, Y.C., BROWN, K. and SIEBENLIST, U. (1995). Activation of NF-kappa B requires proteolysis of the inhibitor I kappa B-alpha: signal-induced phosphorylation of I kappa B-alpha alone does not release active NF-kappa B. *Proc Natl Acad Sci USA* 92: 552-556.

LIU, J., FURUKAWA, M., MATSUMOTO, T. and XIONG, Y. (2002). NEDD8 Modification of CUL1 Dissociates p120CAND1, an Inhibitor of CUL1-SKP1 Binding and SCF Ligases. *Mol Cell* 10: 1511-1518.

LYAPINA, S.A., CORRELL, C.C., KIPREOS, E.T. and DESHAIES, R.J. (1998). Human CUL1 forms an evolutionarily conserved ubiquitin ligase complex (SCF) with SKP1 and an F-box protein. *Proc Natl Acad Sci USA* 95: 7451-7456.

MANIATIS, T. (1999). A ubiquitin ligase complex essential for the NF-kappaB, Wnt/Wingless, and Hedgehog signaling pathways. *Genes Dev* 13: 505-510.

MANTOVANI, F. and BANKS, L. (2003). Regulation of the discs large tumor suppressor by a phosphorylation-dependent interaction with the beta-TrCP ubiquitin ligase receptor. *J Biol Chem* 278: 42477-42486.

MANTOVANI, F., MASSIMI, P. and BANKS, L. (2001). Proteasome-mediated regulation of the hDlg tumour suppressor protein. *J Cell Sci* 114: 4285-4292.

MAO, J.H., PEREZ-LOSADA, J., WU, D., DELROSARIO, R., TSUNEMATSU, R., NAKAYAMA, K.I., BROWN, K., BRYSON, S. and BALMAIN, A. (2004). Fbxw7/

Cdc4 is a p53-dependent, haploinsufficient tumour suppressor gene. *Nature* 432: 775-779.

MARIKAWA, Y. and ELINSON, R.P. (1998). beta-TrCP is a negative regulator of Wnt/beta-catenin signaling pathway and dorsal axis formation in *Xenopus* embryos. *Mech Dev* 77: 75-80.

MILLS, A.A., ZHENG, B., WANG, X.J., VOGEL, H., ROOP, D.R. and BRADLEY, A. (1999). p63 is a p53 homologue required for limb and epidermal morphogenesis. *Nature* 398: 708-713.

NAKAYAMA, K., NAGAHAMA, H., MINAMISHIMA, Y.A., MATSUMOTO, M., NAKAMICHI, I., KITAGAWA, K., SHIRANE, M., TSUNEMATSU, R., TSUKIYAMA, T., ISHIDA, N. *et al.* (2000). Targeted disruption of Skp2 results in accumulation of cyclin E and p27(Kip1), polyploidy and centrosome overduplication. *EMBO J* 19: 2069-2081.

NURSE, P., THURIAUX, P. and NASMYTH, K. (1976). Genetic control of the cell division cycle in the fission yeast Schizosaccharomyces pombe. *Mol Gen Genet* 146: 167-178.

O'NEIL, J., GRIM, J., STRACK, P., RAO, S., TIBBITTS, D., WINTER, C., HARDWICK, J., WELCKER, M., MEIJERINK, J.P., PIETERS, R. *et al.* (2007). FBW7 mutations in leukemic cells mediate NOTCH pathway activation and resistance to gamma-secretase inhibitors. *J Exp Med* 204: 1813-1824.

OHTA, T., MICHEL, J.J., SCHOTTELIUS, A.J. and XIONG, Y. (1999). ROC1, a homolog of APC11, represents a family of cullin partners with an associated ubiquitin ligase activity. *Mol Cell* 3: 535-541.

ONOYAMA, I., TSUNEMATSU, R., MATSUMOTO, A., KIMURA, T., DE ALBORAN, I.M., NAKAYAMA, K. and NAKAYAMA, K.I. (2007). Conditional inactivation of Fbxw7 impairs cell-cycle exit during T cell differentiation and results in lymphomatogenesis. *J Exp Med* 204: 2875-2888.

PAN, Y., BAI, C.B., JOYNER, A.L. and WANG, B. (2006). Sonic hedgehog signaling regulates Gli2 transcriptional activity by suppressing its processing and degradation. *Mol Cell Biol* 26: 3365-3377.

PETROSKI, M.D. and DESHAIES, R.J. (2005). Mechanism of lysine 48-linked ubiquitin-chain synthesis by the cullin-RING ubiquitin-ligase complex SCF-Cdc34. *Cell* 123: 1107-1120.

PICKART, C.M. and COHEN, R.E. (2004). Proteasomes and their kin: proteases in the machine age. *Nat Rev Mol Cell Biol* 5: 177-187.

PICKART, C.M. and ROSE, I.A. (1985). Functional heterogeneity of ubiquitin carrier proteins. *J Biol Chem* 260: 1573-1581.

REAVIE, L., GATTA, G.D., CRUSIO, K., ARANDA-ORGILLES, B., BUCKLEY, S.M., THOMPSON, B., LEE, E., GAO, J., BREDEMEYER, A.L., HELMINK, B.A. *et al.* (2010). Regulation of hematopoietic stem cell differentiation by a single ubiquitin ligase-substrate complex. *Nat Immunol* 11: 207-215.

REUVER, S.M. and GARNER, C.C. (1998). E-cadherin mediated cell adhesion recruits SAP97 into the cortical cytoskeleton. *J Cell Sci* 111: 1071-1080.

REYNAUD, E.G., LEIBOVITCH, M.P., TINTIGNAC, L.A.J., PELPEL, K., GUILLIER, M. and LEIBOVITCH, S.A. (2000). Stabilization of MyoD by Direct Binding to p57Kip2. *J Biol Chem* 275: 18767-18776.

SCHOENHERR, C.J. and ANDERSON, D.J. (1995). The neuron-restrictive silencer factor (NRSF): a coordinate repressor of multiple neuron-specific genes. *Science* 267: 1360-1363.

SCHREIBER, J., RIETHMACHER-SONNENBERG, E., RIETHMACHER, D., TUERK, E.E., ENDERICH, J., BOSL, M.R. and WEGNER, M. (2000). Placental failure in mice lacking the mammalian homolog of glial cells missing, GCMa. *Mol Cell Biol* 20: 2466-2474.

SCHULMAN, B.A., CARRANO, A.C., JEFFREY, P.D., BOWEN, Z., KINNUCAN, E.R., FINNIN, M.S., ELLEDGE, S.J., HARPER, J.W., PAGANO, M. and PAVLETICH, N.P. (2000). Insights into SCF ubiquitin ligases from the structure of the Skp1-Skp2 complex. *Nature* 408: 381-386.

SEMPLE, C.A. (2003). The comparative proteomics of ubiquitination in mouse. *Genome Res* 13: 1389-1394.

SEN, R. and BALTIMORE, D. (1986). Inducibility of [kappa] immunoglobulin enhancer-binding protein NF-[kappa]B by a posttranslational mechanism. *Cell* 47: 921-928.

SEO, E., KIM, H., KIM, R., YUN, S., KIM, M., HAN, J.-K., COSTANTINI, F. and JHO, E.-H. (2009). Multiple isoforms of [beta]-TrCP display differential activities in the regulation of Wnt signaling. *Cellular Signalling* 21: 43-51.

SIGNORETTI, S., DI MARCOTULLIO, L., RICHARDSON, A., RAMASWAMY, S., ISAAC, B., RUE, M., MONTI, F., LODA, M. and PAGANO, M. (2002). Oncogenic role of the ubiquitin ligase subunit Skp2 in human breast cancer. *J Clin Invest* 110: 633-641.

SIL, A.K., MAEDA, S., SANO, Y., ROOP, D.R. and KARIN, M. (2004). IkappaB kinase-alpha acts in the epidermis to control skeletal and craniofacial morphogenesis. *Nature* 428: 660-664.

SKAAR, J.R., D'ANGIOLELLA, V., PAGAN, J.K. and PAGANO, M. (2009a). SnapShot: F Box Proteins II. *Cell* 137: 1358.e1351-1358.e1352.

SKAAR, J.R., PAGAN, J.K. and PAGANO, M. (2009b). SnapShot: F Box Proteins I. *Cell* 137: 1160-1160.e1161.

SKAAR, J.R. and PAGANO, M. (2009). Control of cell growth by the SCF and APC/C ubiquitin ligases. *Current Opinion in Cell Biology* 21: 816-824.

SMELKINSON, M.G., ZHOU, Q. and KALDERON, D. (2007). Regulation of Ci-SCFSlimb binding, Ci proteolysis, and hedgehog pathway activity by Ci phosphorylation. *Dev Cell* 13: 481-495.

STEWARD, R. (1987). Dorsal, an embryonic polarity gene in *Drosophila*, is homologous to the vertebrate proto-oncogene, c-rel. *Science* 238: 692-694.

SUZUKI, H., CHIBA, T., KOBAYASHI, M., TAKEUCHI, M., SUZUKI, T., ICHIYAMA, A., IKENOUE, T., OMATA, M., FURUICHI, K. and TANAKA, K. (1999). IkappaBalpha ubiquitination is catalyzed by an SCF-like complex containing Skp1, cullin-1, and two F-box/WD40-repeat proteins, betaTrCP1 and betaTrCP2. *Biochem Biophys Res Commun* 256: 127-132.

TAKEDA, K., TAKEUCHI, O., TSUJIMURA, T., ITAMI, S., ADACHI, O., KAWAI, T., SANJO, H., YOSHIKAWA, K., TERADA, N. and AKIRA, S. (1999). Limb and skin abnormalities in mice lacking IKKalpha. *Science* 284: 313-316.

TAN, X., CALDERON-VILLALOBOS, L.I., SHARON, M., ZHENG, C., ROBINSON, C.V., ESTELLE, M. and ZHENG, N. (2007). Mechanism of auxin perception by the TIR1 ubiquitin ligase. *Nature* 446: 640-645.

TETZLAFF, M.T., YU, W., LI, M., ZHANG, P., FINEGOLD, M., MAHON, K., HARPER, J.W., SCHWARTZ, R.J. and ELLEDGE, S.J. (2004). Defective cardiovascular development and elevated cyclin E and Notch proteins in mice lacking the Fbw7 F-box protein. *Proc Natl Acad Sci USA* 101: 3338-3345.

TINTIGNAC, L.A., LAGIRAND, J., BATONNET, S., SIRRI, V., LEIBOVITCH, M.P. and LEIBOVITCH, S.A. (2005). Degradation of MyoD mediated by the SCF (MAFbx) ubiquitin ligase. *J Biol Chem* 280: 2847-2856.

VERNON, A.E., DEVINE, C. and PHILPOTT, A. (2003). The cdk inhibitor p27Xic1 is required for differentiation of primary neurones in *Xenopus*. *Development* 130: 85-92.

VERNON, A.E. and LABONNE, C. (2006). Slug stability is dynamically regulated during neural crest development by the F-box protein Ppa. *Development* 133: 3359-3370.

VERNON, A.E. and PHILPOTT, A. (2003). A single cdk inhibitor, p27Xic1, functions beyond cell cycle regulation to promote muscle differentiation in *Xenopus*. *Development* 130: 71-83.

VON DER LEHR, N., JOHANSSON, S., WU, S., BAHRAM, F., CASTELL, A., CETINKAYA, C., HYDBRING, P., WEIDUNG, I., NAKAYAMA, K., NAKAYAMA, K.I. *et al.* (2003). The F-box protein Skp2 participates in c-Myc proteosomal degradation and acts as a cofactor for c-Myc-regulated transcription. *Mol Cell* 11: 1189-1200.

WANG, B. and LI, Y. (2006). Evidence for the direct involvement of {beta}TrCP in Gli3 protein processing. *Proc Natl Acad Sci USA* 103: 33-38.

WEI, W., AYAD, N.G., WAN, Y., ZHANG, G.J., KIRSCHNER, M.W. and KAELIN, W.G., JR. (2004). Degradation of the SCF component Skp2 in cell-cycle phase G1 by the anaphase-promoting complex. *Nature* 428: 194-198.

WESTBROOK, T.F., HU, G., ANG, X.L., MULLIGAN, P., PAVLOVA, N.N., LIANG, A., LENG, Y., MAEHR, R., SHI, Y., HARPER, J.W. *et al.* (2008). SCFbeta-TRCP controls oncogenic transformation and neural differentiation through REST degradation. *Nature* 452: 370-374.

WILKINSON, K.D., URBAN, M.K. and HAAS, A.L. (1980). Ubiquitin is the ATP-dependent proteolysis factor I of rabbit reticulocytes. *J Biol Chem* 255: 7529-7532.

WINSTON, J.T., STRACK, P., BEER-ROMERO, P., CHU, C.Y., ELLEDGE, S.J. and HARPER, J.W. (1999). The SCFbeta-TRCP-ubiquitin ligase complex associates specifically with phosphorylated destruction motifs in IkappaBalpha and beta-catenin and stimulates IkappaBalpha ubiquitination *in vitro*. *Genes*

Dev 13: 270-283.

WOLF, D.H. and HILT, W. (2004). The proteasome: a proteolytic nanomachine of cell regulation and waste disposal. *Biochim Biophys Acta* 1695: 19-31.

WOODS, D.F., HOUGH, C., PEEL, D., CALLAINI, G. and BRYANT, P.J. (1996). Dlg protein is required for junction structure, cell polarity, and proliferation control in *Drosophila* epithelia. *J Cell Biol* 134: 1469-1482.

WU, G., LYAPINA, S., DAS, I., LI, J., GURNEY, M., PAULEY, A., CHUI, I., DESHAIES, R.J. and KITAJEWSKI, J. (2001). SEL-10 is an inhibitor of notch signaling that targets notch for ubiquitin-mediated protein degradation. *Mol Cell Biol* 21: 7403-7415.

WU, G., XU, G., SCHULMAN, B.A., JEFFREY, P.D., HARPER, J.W. and PAVLETICH, N.P. (2003). Structure of a beta-TrCP1-Skp1-beta-catenin complex: destruction motif binding and lysine specificity of the SCF(beta-TrCP1) ubiquitin ligase. *Mol Cell* 11: 1445-1456.

WU, K., FUCHS, S.Y., CHEN, A., TAN, P., GOMEZ, C., RONAI, Z. and PAN, Z.Q. (2000). The SCF(HOS/beta-TRCP)-ROC1 E3 ubiquitin ligase utilizes two distinct domains within CUL1 for substrate targeting and ubiquitin ligation. *Mol Cell Biol* 20: 1382-1393.

WU, L.P. and ANDERSON, K.V. (1998). Regulated nuclear import of Rel proteins in the *Drosophila* immune response. *Nature* 392: 93-97.

WULCZYN, F.G., KRAPPMANN, D. and SCHEIDEREIT, C. (1998). Signal-dependent degradation of IkappaBalpha is mediated by an inducible destruction box that can be transferred to NF-kappaB, bcl-3 or p53. *Nucleic Acids Res* 26: 1724-1730.

YANG, A., SCHWEITZER, R., SUN, D., KAGHAD, M., WALKER, N., BRONSON, R.T., TABIN, C., SHARPE, A., CAPUT, D., CRUM, C. *et al.* (1999). p63 is essential for regenerative proliferation in limb, craniofacial and epithelial development. *Nature* 398: 714-718.

YE, X., NALEPA, G., WELCKER, M., KESSLER, B.M., SPOONER, E., QIN, J., ELLEDGE, S.J., CLURMAN, B.E. and HARPER, J.W. (2004). Recognition of Phosphodegron Motifs in Human Cyclin E by the SCFFbw7 Ubiquitin Ligase. *J Biol Chem* 279: 50110-50119.

YOOK, J.I., LI, X.Y., OTA, I., FEARON, E.R. and WEISS, S.J. (2005). Wnt-dependent regulation of the E-cadherin repressor snail. *J Biol Chem* 280: 11740-11748.

ZENG, Z., WANG, W., YANG, Y., CHEN, Y., YANG, X., DIEHL, J.A., LIU, X. and LEI, M. (2010). Structural Basis of Selective Ubiquitination of TRF1 by SCFFbx4. *Dev Cell* 18: 214-225.

ZHANG, P., WONG, C., LIU, D., FINEGOLD, M., HARPER, J.W. and ELLEDGE, S.J. (1999). p21(CIP1) and p57(KIP2) control muscle differentiation at the myogenin step. *Genes Dev* 13: 213-224.

ZHENG, N., SCHULMAN, B.A., SONG, L., MILLER, J.J., JEFFREY, P.D., WANG, P., CHU, C., KOEPP, D.M., ELLEDGE, S.J., PAGANO, M. *et al.* (2002). Structure of the Cul1-Rbx1-Skp1-F boxSkp2 SCF ubiquitin ligase complex. *Nature* 416: 703-709.

ZHOU, B.P., DENG, J., XIA, W., XU, J., LI, Y.M., GUNDUZ, M. and HUNG, M.C. (2004). Dual regulation of Snail by GSK-3beta-mediated phosphorylation in control of epithelial-mesenchymal transition. *Nat Cell Biol* 6: 931-940.

Further Related Reading, published previously in the *Int. J. Dev. Biol.*

Patterning and cell fate in ear development
Berta Alsina, Fernando Giraldez and Cristina Pujades
Int. J. Dev. Biol. (2009) 53: 1503-1513

A novel role of the glial fate determinant glial cells missing in hematopoiesis
Cécile Jacques, Laurent Soustelle, István Nagy, Céline Diebold and Angela Giangrande
Int. J. Dev. Biol. (2009) 53: 1013-1022

Fate of cranial neural crest cells during craniofacial development in endothelin-A receptor-deficient mice
Makoto Abe, Louis-Bruno Ruest and David E. Clouthier
Int. J. Dev. Biol. (2007) 51: 97-105

The fate of larval flagellated cells during metamorphosis of the sponge Halisarca dujardini
Yulia I. Mukhina, Vadim V. Kumeiko, Olga I. Podgornaya and Sofia M. Efremova
Int. J. Dev. Biol. (2006) 50: 533-541

Heparan sulfates isolated from adult neural progenitor cells can direct phenotypic maturation
Hiram Chipperfield, Kuldip S Bedi, Simon M Cool and Victor Nurcombe
Int. J. Dev. Biol. (2002) 46: 661-670

The CNS midline cells control the spitz class and Egfr signaling genes to establish the proper cell fate of the Drosophila ventral neuroectoderm
J Chang, I O Kim, J S Ahn and S H Kim
Int. J. Dev. Biol. (2001) 45: 715-724

The role of stem cell factor and of alternative c-kit gene products in the establishment, maintenance and function of germ cells
C Sette, S Dolci, R Geremia and P Rossi
Int. J. Dev. Biol. (2000) 44: 599-608

Regulation of primordial germ cell development in the mouse
M De Felici
Int. J. Dev. Biol. (2000) 44: 575-580

Nerve growth factor induced neurite outgrowth from amphibian neuroepithelial precursor cells is prevented by dipeptides inhibiting ubiquitin-mediated proteolysis
J P Maufroid, R A Bradshaw, B Boilly and H Hondermarck
Int. J. Dev. Biol. (1996) 40: 609-611

5 yr ISI Impact Factor (2009) = 3.253

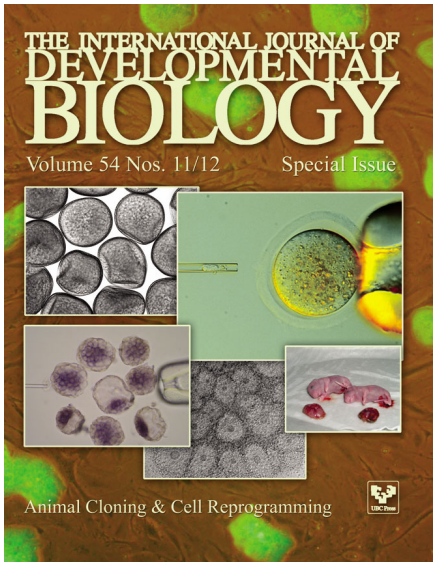

Development ePress online publication date 18 August 2011

Development 138, 4267-4277 (2011) doi:10.1242/dev.067900
© 2011. Published by The Company of Biologists Ltd

Cell cycle-regulated multi-site phosphorylation of Neurogenin 2 coordinates cell cycling with differentiation during neurogenesis

Fahad Ali[1,*], Chris Hindley[1,*], Gary McDowell[1], Richard Deibler[2], Alison Jones[1], Marc Kirschner[2], Francois Guillemot[3] and Anna Philpott[1,†]

SUMMARY

During development of the central nervous system, the transition from progenitor maintenance to differentiation is directly triggered by a lengthening of the cell cycle that occurs as development progresses. However, the mechanistic basis of this regulation is unknown. The proneural transcription factor Neurogenin 2 (Ngn2) acts as a master regulator of neuronal differentiation. Here, we demonstrate that Ngn2 is phosphorylated on multiple serine-proline sites in response to rising cyclin-dependent kinase (cdk) levels. This multi-site phosphorylation results in quantitative inhibition of the ability of Ngn2 to induce neurogenesis in vivo and in vitro. Mechanistically, multi-site phosphorylation inhibits binding of Ngn2 to E box DNA, and inhibition of DNA binding depends on the number of phosphorylation sites available, quantitatively controlling promoter occupancy in a rheostat-like manner. Neuronal differentiation driven by a mutant of Ngn2 that cannot be phosphorylated by cdks is no longer inhibited by elevated cdk kinase levels. Additionally, phosphomutant Ngn2-driven neuronal differentiation shows a reduced requirement for the presence of cdk inhibitors. From these results, we propose a model whereby multi-site cdk-dependent phosphorylation of Ngn2 interprets cdk levels to control neuronal differentiation in response to cell cycle lengthening during development.

KEY WORDS: Cell cycle, Neuronal differentiation, Ngn2, Phosphorylation, *Xenopus*

INTRODUCTION

During development of the central nervous system, cell cycle lengthening accompanies the transition from stem cell-like to neurogenic divisions, and this is subsequently followed by differentiation (Lange and Calegari, 2010; Miyata et al., 2010). However, recent experiments show that lengthening (but not necessarily arresting) the cell cycle alone by perturbation of the core cell cycle machinery is sufficient to trigger neuronal differentiation, whereas shortening the cell cycle inhibits neurogenesis (Lange et al., 2009). These findings indicate that cell cycle length is itself a regulator of the balance between progenitor maintenance and differentiation, although the mechanism for this regulation is unknown.

The proneural basic helix-loop-helix (bHLH) transcription factor Neurogenin 2 (Ngn2, or Neurog2) is required for development of cranial and spinal sensory ganglia, as well as for the ventral spinal cord (Bertrand et al., 2002). Moreover, in the embryonic cortex, Ngn2 is required for neuronal commitment and inhibition of the astrocytic fate of progenitors, as well as for the specification of glutamatergic neurotransmitter identity and the migration of cortical neurons (Bertrand et al., 2002). Ngn2 has been shown to transcriptionally upregulate multiple direct targets. Among these, one crucial Ngn2 target is the bHLH transcription factor NeuroD, which plays a central role in driving neuronal differentiation.

Although transcriptional regulation of *Ngn2* itself is complex, evidence has emerged of additional Ngn2 control by post-translational modification. A limited exploration of the role of phosphorylation in Ngn2 activity has been undertaken (Hand et al., 2005; Vosper et al., 2007; Ma et al., 2008). For example, phosphorylation of tyrosine 241 in Ngn2 is important for the migration and dendritic morphology of cortical neurons (Hand et al., 2005) and phosphorylation on two specific C-terminal serines, which are GSK3β consensus sites, appears to have no effect on neurogenesis per se in the spinal cord but does regulate motoneuron specification in this tissue (Ma et al., 2008).

Ngn2 protein level is regulated by ubiquitin-mediated proteolysis, and the rate of proteolysis is sensitive to cell cycle stage; *Xenopus* Ngn2 [xNgn2, also known as XNgnR1 (Nieber et al., 2009)], the frog homologue of mammalian Ngn2 (Ma et al., 1996; Nieber et al., 2009), has a shorter half-life in mitosis than in interphase (Vosper et al., 2009). Accumulation of cyclin-dependent kinase inhibitors (cdkis), which occurs upon cell cycle lengthening and exit, promotes neurogenesis mediated by Ngn2 (Vernon et al., 2003). Surprisingly, this particular effect of cdkis is independent of their ability to inhibit cdk kinase activity, but instead results from an independent role for cdkis in stabilising the Ngn2 protein (Vernon et al., 2003; Nguyen et al., 2006). In addition, it is also possible that Ngn2 protein undergoes other post-translational modifications, including phosphorylation, that might be used to coordinate its activity with cell cycle progression.

Cyclin A/*cdk2* overexpression inhibits primary neurogenesis in *Xenopus* embryos. Moreover, ectopic neurogenesis in embryos driven by *Ngn2* mRNA injection is still inhibited by cdk activation

[1]Department of Oncology, University of Cambridge, Hutchison/Medical Research Council (MRC) Research Centre, Cambridge CB2 0XZ, UK. [2]Department of Systems Biology, Harvard Medical School, 200 Longwood Avenue, Boston, MA 02115, USA. [3]Division of Molecular Neurobiology, National Institute for Medical Research, Mill Hill, London NW7 1AA, UK.

*These authors contributed equally to this work
†Author for correspondence (ap113@cam.ac.uk)

Accepted 18 July 2011

(Richard-Parpaillon et al., 2004), indicating that cell cycle control does not occur at the level of *Ngn2* transcription. Instead, cell cycle-dependent post-translational regulation of Ngn2 protein has the potential to directly regulate the ability of Ngn2 to drive neuronal differentiation. Here, we demonstrate how multi-site post-translational modification of Ngn2 is used as a sensor of cdk kinase levels to balance progenitor maintenance and differentiation, in coordination with cell cycle length.

MATERIALS AND METHODS

Xenopus laevis extracts and embryos

Acquisition of *Xenopus laevis* eggs and embryos, preparation and injection of synthetic mRNA and DNA morpholinos, staging of embryos, in situ hybridisation and egg extract preparation have been described previously (Vernon et al., 2003; Vosper et al., 2007; Vosper et al., 2009).

In vitro translated (IVT) protein synthesis and assay

Degradation assays were performed as described previously (Vosper et al., 2007; Vosper et al., 2009). Phosphorylation assays in *Xenopus* extract were performed as for degradation assays, except that extract was supplemented with 0.2 mM MG132 (Biomol) and samples were incubated for 45 minutes unless otherwise indicated. Where indicated, extracts were supplemented with the GSK3 inhibitor (2′Z,3′E)-6-bromoindirubin-3′-oxime (BIO) (Sigma) at 100 nM or with roscovitine (VWR) at 50 mM. Where indicated, following the 45 minute incubation in extract, 400 units λ-phosphatase (NEB) were incubated with the sample at 30°C for 30 minutes.

Cell culture, transfection, immunocytochemistry and western blotting

Mouse P19 cells were cultured in α-MEM (Gibco) with 7.5% newborn calf serum and 2.5% fetal bovine serum (HyClone), 1% Glutamax (Gibco), and 100 units/ml penicillin/100 μg/ml streptomycin (Sigma). Cells were transfected with Lipofectamine 2000 (Invitrogen), and extracts western blotted with anti-HA-peroxidase (3F10; Roche) or anti-c-Myc (9E10; Santa-Cruz). Where indicated, cells were treated with either 5-25 μm roscovitine or 400 units λ-phosphatase. P19 cells plated on poly-D-lysine and laminin (Sigma) and fixed in 4% formaldehyde for 15 minutes were stained with anti-TuJ1 (neuronal class III β-Tubulin; 1:200; Covance) and chicken anti-green fluorescent protein (GFP; 1:500; Invitrogen).

Somatic cell extract preparation for Ngn2 phosphorylation assay

Somatic cell extracts were prepared as described previously (Deibler and Kirschner, 2010).

Quantitative real-time PCR (qPCR)

cDNA was generated from either P19 cells or stage 15 *Xenopus* embryos and 50 ng used per qPCR reaction in a Light-Cycler 480 PCR system with SYBR Green mix (Roche). β-actin, *Gapdh* and *EF1α* were used as housekeeping genes. Thermal cycling conditions: 95°C for 5 minutes, then 45 cycles of 95°C for 10 seconds, 60°C for 10 seconds and 72°C for 10 seconds. For primer sequences, see Table S1 in the supplementary material.

Electrophoretic mobility shift assay (EMSA)

Non-radiolabelled IVT protein was prepared and incubated in XB buffer or *Xenopus* egg extract as for phosphorylation assays before EMSA analysis as previously described (Vosper et al., 2009), using the annealed, end-labelled oligonucleotide pair (5′-TCTAACTGGCGACAGATGGG-CCACTTTCTT-3′ and complement).

Chromatin Immunoprecipitation assay (ChIP)

DNA-protein complexes from P19 cells transfected with either HA-tagged wild-type mNgn2 or 9S-A mNgn2 for 24 hours and normalised for mNgn2/9S-A mNgn2 expression (see Results) were cross-linked with 1% formaldehyde. Five micrograms of rat monoclonal anti-HA antibody (Roche) or anti-IgG (Abcam) (as a control) were used per ChIP reaction and quantified using SYBR Green mix. The signal over background normalisation method was used to quantify immunoprecipitated DNA. For primer sequences, see Table S1 in the supplementary material.

Statistical analysis

Data were subjected to statistical analysis using a two-tailed Student's *t*-test ($P \leq 0.05$). The standard error of the mean (s.e.m.) was calculated from at least three independent experiments. Immunostaining, western blotting and in situ hybridisation experiments were performed in three independent experiments and representative results are shown.

RESULTS

Neurogenin 2 phosphorylation is regulated during the cell cycle

Ngn2 phosphorylation has previously been demonstrated on tyrosine and GSK3β consensus sites (Hand et al., 2005; Vosper et al., 2007; Ma et al., 2008), but cell cycle-dependent phosphorylation has not been investigated. We have previously observed that Ngn2 protein can be phosphorylated in *Xenopus* egg extract, which provides a complex biochemical environment that contains stockpiles of many of the kinases and phosphatases required for cell cycle transitions and early embryonic

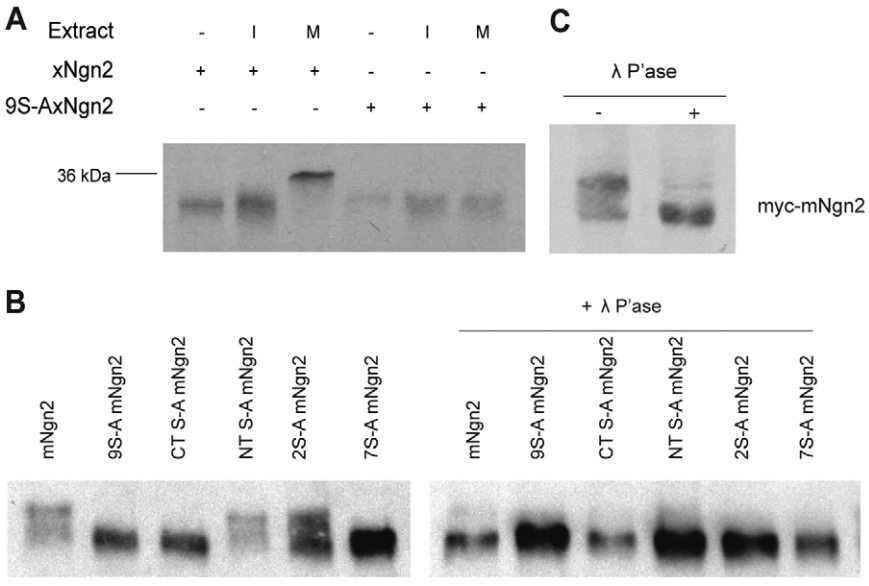

Fig. 1. Ngn2 undergoes cell cycle-regulated phosphorylation. (**A**) In vitro translated (IVT) [^{35}S]methionine-labelled xNgn2 and 9S-A xNgn2 were incubated in interphase (I) and mitotic (M) *Xenopus* egg extracts before SDS-PAGE and autoradiography. In M extracts, phosphorylated xNgn2 runs at the level of the 36 kDa molecular weight marker (indicated). (**B**) Western blot analysis of HA-tagged mNgn2 and mutants thereof, transfected into mouse P19 cells with and without λ-phosphatase treatment. (**C**) Western blot analysis of myc-mNgn2 from E16.5 mouse cortex, with and without λ-phosphatase treatment.

development, and results in slowed migration of Ngn2 in SDS-PAGE (Vosper et al., 2007). We hypothesised that this phosphorylation might be regulated by the cell cycle.

We compared SDS-PAGE migration of in vitro translated (IVT) [^{35}S]methionine-labelled *Xenopus* Ngn2 (xNgn2) in interphase egg extract (I) or in extract driven into mitosis (M) by addition of non-degradable cyclin B Δ90 (King et al., 1996). IVT xNgn2 runs at ~28 kDa by SDS-PAGE, and its migration is slowed slightly after incubation in I extract (Fig. 1A), and more dramatically after incubation in M extract, resulting in the appearance of one or more forms of Ngn2 running up to 8 kDa 'larger' (Fig. 1A, see Fig. S2 in the supplementary material). Retardation was reversed by incubation with λ-phosphatase (data not shown).

Although predictions of consensus sequences that contribute to kinase recognition are imprecise (Errico et al., 2010), several prominent kinases potentially present in the egg extract, such as cdks, MAP kinases and GSK3β, preferentially phosphorylate on serine or threonine residues followed by a proline (SP or TP sites) (Ubersax and Ferrell, 2007). xNgn2 contains nine SP and one TP site. To prevent phosphorylation on SP sites, a mutant form of xNgn2, 9S-A xNgn2, in which all SP sites are mutated to alanine-proline (S-A mutant) was generated. 9S-A xNgn2 ran similarly to the IVT protein after incubation in I or M extracts (Fig. 1A), indicating that the phosphorylation seen for the wild-type protein does not occur on 9S-A xNgn2. We did not detect significant phosphorylation of the TP site by SDS-PAGE migration (data not shown), and did not consider modification of this site further.

Mouse Ngn2 (mNgn2) can drive neuronal differentiation of mouse embryonal carcinoma P19 cells when overexpressed (Farah et al., 2000), and also contains nine SP sites. However, only the position of the two most C-terminal GSK3β consensus sites, which have previously been shown to be phosphorylated in spinal cord (Ma et al., 2008), is conserved with xNgn2. After transfection into P19 cells, at least two phosphoforms of mNgn2 were seen, as evidenced by migration in SDS-PAGE and phosphatase treatment, whereas 9S-A mNgn2 ran as a single, faster migrating band (Fig. 1B). Further analysis of Ngn2 mutants in which SP sites in the N- and C-termini have been separately mutated shows that xNgn2 and mNgn2 are both phosphorylated on multiple sites in both the N- and C-terminal domains (Fig. 1B, see Fig. S2 in the supplementary material). Analysis of phosphorylation of 2S-A Ngn2 (which lacks the potential GSK3β sites) and 7S-A Ngn2 (in which only the two potential GSK3β SP sites are present in an otherwise S-A background) indicates that phosphorylation does not predominantly occur on these GSK3β SP sites (Fig. 1B).

To determine the phosphorylation status of Ngn2 expressed from its endogenous locus, we investigated the migration of a myc-tagged form of mNgn2 in embryonic brain from a mouse line in which *myc-mNgn2* is inserted in the place of endogenous *mNgn2* (Hand et al., 2005). Western blotting demonstrated that mNgn2 is phosphorylated in the developing mouse brain (Fig. 1C).

Ngn2 is phosphorylated on multiple sites by cyclin-dependent kinases

Cdks drive cell cycle progression and are known to target SP (and TP) sites (Errico et al., 2010). We postulated that Ngn2 might be a direct cdk substrate. Addition of roscovitine, a chemical cdk inhibitor with marked specificity for cdks alone (Bain et al., 2007), results in a dose-dependent reduction of the slower migrating form of mNgn2 expressed in P19 cells (Fig. 2A). Roscovitine also reversed the reduction in mobility seen when xNgn2 was incubated in neurula stage *Xenopus* embryo extracts (see Fig. S3 in the supplementary material).

To quantitatively analyse the sensitivity of Ngn2 to increasing cdk activity, we turned to an in vitro human HeLa cell extract system that exhibits quantitative cyclin dose-dependent effects on substrate phosphorylation (Deibler and Kirschner, 2010), as evidenced by slowed migration in SDS-PAGE, and recapitulates cell cycle-relevant transitions. From entry into S phase through prometaphase, cyclin A concentration increases in the cell, and this can be reproduced by increasing the dose of cyclin in the cell extract (Deibler and Kirschner, 2010). mNgn2 is highly sensitive to cyclin A-dependent kinase, and phosphorylation is evident when only 12.5 nM cyclin A is added (Fig. 2B). As the cyclin A

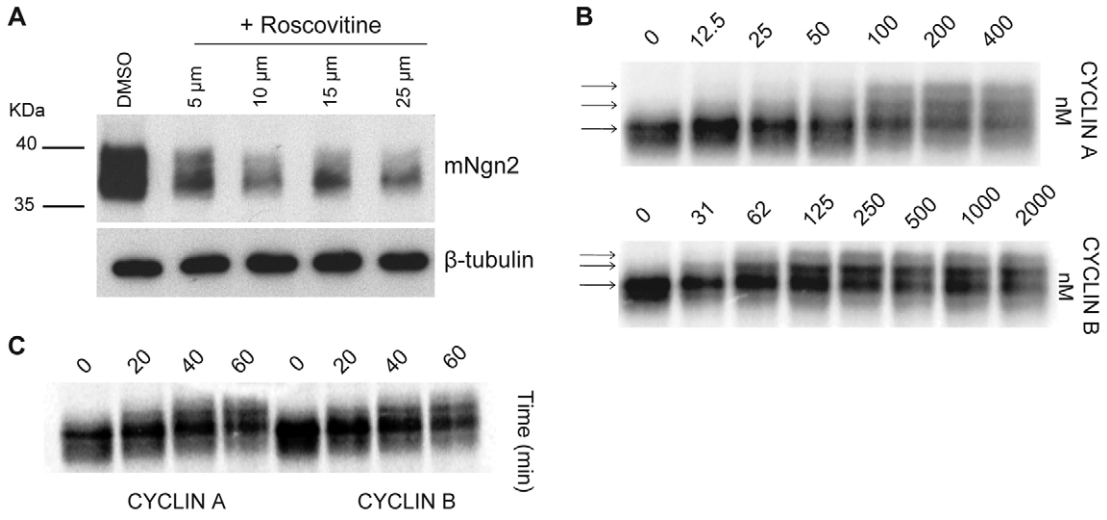

Fig. 2. Ngn2 is phosphorylated by cyclin-dependent kinases. (**A**) Western blot analysis of HA-tagged mNgn2 and 9S-A mNgn2 24 hours after transfection into mouse P19 cells with and without treatment with the cdk inhibitor roscovitine. β-Tubulin provides a loading control. (**B**) SDS-PAGE analysis of IVT mNgn2 in human HeLa cell extract in response to increasing doses of recombinant cyclin A (top) or cyclin B (bottom). Arrows indicate different phosphoforms of mNgn2. (**C**) SDS-PAGE analysis of the kinetics of phosphorylation of IVT mNgn2 when added to HeLa extracts containing recombinant cyclin A or cyclin B proteins.

concentration rises, at least two or three increasingly retarded mNgn2 forms appear (Fig. 2B), indicating that mNgn2 is phosphorylated on multiple sites. That slower migrating phosphoforms require higher cyclin A concentrations demonstrates that there is no single threshold at which multiple sites are phosphorylated, but rather that the extent of phosphorylation is sensitive to the level of kinase activity. Above 100 nM cyclin A, when cyclin A-dependent kinase levels are saturating, the fastest migrating mNgn2 band is lost, indicating that all Ngn2 is essentially phosphorylated. These results demonstrate that mNgn2, together with Wee1, is one of the most sensitive substrates of cyclin A-dependent kinase currently known (Deibler and Kirschner, 2010), although in contrast to Wee1, as cyclin A levels rise mNgn2 becomes further phosphorylated on additional sites.

The addition of cyclin B to these G2 phase HeLa extracts leads to triphasic cdk kinase activation: a first phase in which cdk kinase activity increases in proportion to cyclin B up to ~100 nM, followed by a plateau of kinase activity between 125-400 nM, and finally a further increase to saturation above 400 nM (Deibler and Kirschner, 2010). mNgn2 is also highly sensitive to cyclin B-dependent kinase (Fig. 2B), showing phosphorylation at the lowest concentration of cyclin B assayed, 31 nM, with maximal phosphorylation at additional sites achieved around the plateau stage from 125 nM cyclin B upwards, indicating dose-dependent sensitivity to cdk kinase levels.

Ngn2 phosphorylation is rapid. After addition of cyclins A or B, histone H1 kinase levels become maximal after a 16-minute lag required for cdk kinase activation. When mNgn2 was added to these extracts, initial phosphorylation at some sites occurred within 20 minutes (Fig. 2C), but additional phosphorylations took longer, indicating that some sites are phosphorylated before others and that phosphorylation continues over a considerable period. We see greater phosphorylation in these mitosis-like extracts than in P19 lysates from asynchronous P19 cells representing all cell cycle stages, where interphase will predominate (Fig. 1). Immunodepletion of specific cdks from HeLa extracts indicates that Ngn2 is a substrate of both cdk1 and cdk2 (see Fig. S4 in the supplementary material).

Phosphorylation of Ngn2 reduces its ability to induce neuronal differentiation

Ngn2 can be phosphorylated on multiple sites by cdks. What is the effect of phosphorylation on Ngn2 activity in the developing embryo? To distinguish effects of post-translational modification from fluctuating levels of *Ngn2* transcripts, which vary from cell to cell and as development progresses (Ma et al., 1996; Bertrand et al., 2002; Shimojo et al., 2008), we chose to express xNgn2 from microinjected mRNA in order to allow us to control the level of xNgn2 expression in vivo in *Xenopus* embryos that are at the correct developmental stage to provide the physiological response of primary neuron differentiation (Ma et al., 1996).

Injection of 5 pg *xNgn2* mRNA results in a small increase in neurogenesis within the neural plate in individual embryos, but little ectopic neurogenesis outside the neural plate, indicating a similar level of expression to endogenous *xNgn2* mRNA. Injection of 5 pg *9S-A xNgn2* mRNA, by contrast, induces both a significant increase in neurogenesis in the neural plate and is sufficient to change the fate of epidermis to differentiated neurons (Fig. 3A) (Ma et al., 1996). At 20 pg mRNA, *xNgn2* was still only able to induce a modest increase in neurogenesis, although now neurons were present outside the neural plate, whereas the same amount of *9S-A xNgn2* mRNA induced very extensive neurogenesis (Fig. 3A). Quantitation of *neural* β*-tubulin* levels in these neural plate stage embryos by qPCR demonstrates that *9S-A xNgn2* is ~7-fold more active than wild-type *xNgn2* when expressed at near physiological levels in *Xenopus* embryos (Fig. 3B).

Testing of seven mutants, in which individual SP sites had been reintroduced into a phosphomutant xNgn2 background, demonstrated a similar level of activity of each to 9S-A xNgn2 (see Fig. S5 in the supplementary material), indicating that no individual SP site is responsible for substantially limiting Ngn2 activity, but instead that phosphorylation at a combination of sites might be required to limit the ability of Ngn2 to induce neurogenesis.

Mutation of SP sites also promotes Ngn2-driven neurogenesis in P19 cells. Significantly more extensive neurogenesis was seen in P19 cells expressing 9S-A mNgn2 than in cells expressing wild-type mNgn2, as measured by TuJ1 staining (Fig. 3C) and confirmed by qPCR analysis (Fig. 3D). Analysis of mutants indicated that potential phosphorylation on the GSK3β sites might contribute to phosphoregulation of Ngn2 activity to a small extent, but that phosphorylation of other sites accounts for the majority of the inhibition of Ngn2-dependent neuronal differentiation (see Fig. S6 in the supplementary material).

Mechanism of regulation of Ngn2 activity by phosphorylation

The transcriptional activation of promoters of genes promoting differentiation may require many cycles of productive transcription factor binding and greater promoter occupancy to bring about progressive chromatin modification, ultimately resulting in an active transcribable state (Koyano-Nakagawa et al., 1999; Hager et al., 2009; Michel, 2009). Ngn2 must bind and activate the promoters of key target genes, such as *NeuroD*, to drive neuronal differentiation. Hence, we reasoned that phosphorylation might affect Ngn2 half-life or its ability to stably bind to promoter DNA, either of which could affect the duration and/or productivity of the interaction between Ngn2 and target promoters driving differentiation.

We first investigated whether phosphorylation status affects Ngn2 protein stability. Ngn2 has a short half-life of ~20 minutes in *Xenopus* and P19 cells, which is enhanced by binding to its heterodimeric E protein partner (Vosper et al., 2007). We determined whether phosphorylation directly affects Ngn2 half-life by incubating IVT xNgn2 or 9S-A xNgn2 in I and M extract. The half-life of 9S-A xNgn2 was similar to that of xNgn2 in both I and M (Fig. 4A) and in neurula stage *Xenopus* embryo extracts (data not shown). Addition of E12 protein stabilised xNgn2 and 9S-A xNgn2 in both I and M extracts (Fig. 4A). However, in M extract, where cdk-dependent phosphorylation is maximal, E12 stabilised 9S-A xNgn2 to a greater extent than it stabilised the wild-type protein. Hence, the phosphorylation status of Ngn2 affects its ability to be stabilised by E protein binding; un(der)phosphorylated, and therefore more stable, Ngn2-E protein complexes might be expected to show greater promoter occupancy than the phosphorylated form of the protein.

To test this we investigated whether phosphorylation affects Ngn2 binding to the *NeuroD* (*Neurod1*) and *Delta* (*Dll1*) promoters, which are direct downstream targets of Ngn2, by chromatin immunoprecipitation (ChIP) in P19 cells, 24 hours post-transfection. As described above, phosphorylation status affects the stabilisation of Ngn2 by E proteins (Fig. 4A). To distinguish differences in chromatin affinity from potential differences in mNgn2 and 9S-A mNgn2 protein levels, we quantitated the

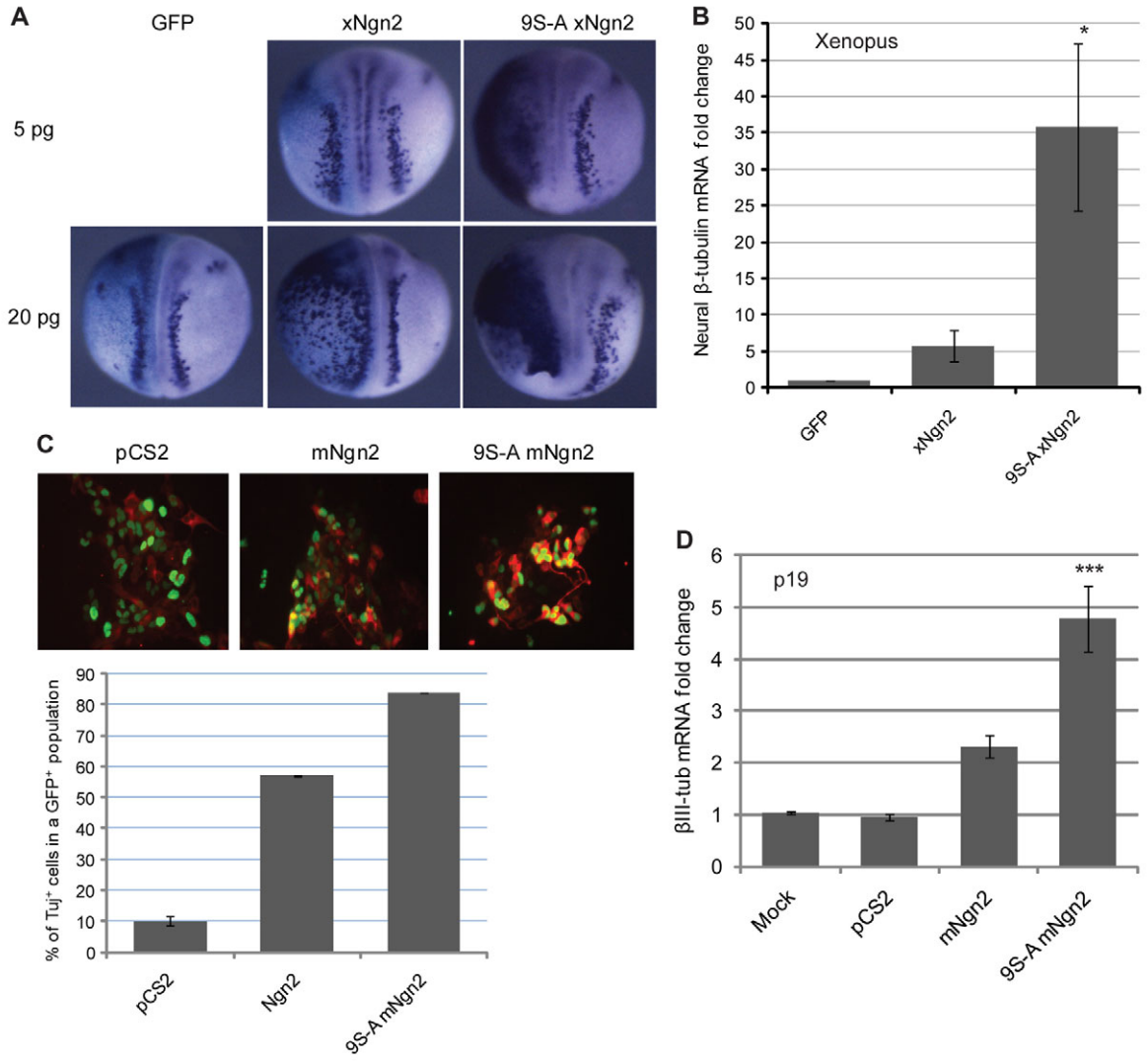

Fig. 3. Mutation of phosphorylation sites promotes Ngn2 activity. (**A**) *Xenopus* embryos were injected (left side) in one of two cells with either 5 or 20 pg mRNA as indicated, fixed at stage 15 and subject to in situ hybridisation for *neural* β-*tubulin*. The number of embryos scored was 39-90 per condition. (**B**) qPCR analysis of *neural* β-*tubulin* in stage 15 *Xenopus* embryos injected at the one-cell stage with 20 pg *xNgn2* or *9S-A xNgn2* mRNA. Average fold increase in *neural* β-*tubulin* mRNA expression is shown normalised to *GFP*-injected control (mean ± s.e.m.; *, $P \leq 0.05$). (**C**) Mouse P19 cells transfected with *mNgn2* or *9S-A mNgn2* with GFP were fixed 24 hours after transfection and stained for expression of neuron-specific *βIII-tubulin* (TuJ1) (red), quantitating TuJ1$^+$ among GFP$^+$ cells (mean ± s.e.m.). (**D**) qPCR analysis of *βIII-tubulin* in P19 cells 24 hours following transfection with *mNgn2* and *9S-A mNgn2*. Average fold increase in mRNA expression is shown normalised to housekeeping gene expression (mean ± s.e.m.; ***, $P \leq 0.005$).

expression of wild-type mNgn2 versus 9S-A mNgn2 by western blot, allowing normalisation of the amount of Ngn2 protein prior to chromatin immunoprecipitation. After normalisation, 9S-A mNgn2 was more than 2-fold enriched compared with wild-type mNgn2 on each promoter, but promoter-specific differences in mNgn2 versus 9S-A mNgn2 binding were not observed (Fig. 4B).

To test directly whether phosphorylation of Ngn2 affects its ability to associate with DNA, we investigated the binding of xNgn2-E12 complexes to their cognate E box-binding motif in an electrophoretic mobility shift assay (EMSA) in I and M extracts. Wild-type xNgn2 and 9S-A xNgn2 had similar DNA-binding activity in I extract, where xNgn2 phosphorylation is low, but 9S-A xNgn2-E12 bound DNA with considerably greater affinity than the wild-type protein in M extracts, where Ngn2 phosphorylation is maximal (Fig. 4C).

Multi-site phosphorylation of Ngn2 acts quantitatively to control DNA binding

Promoter activation requires productive transcription factor binding cycles, which in turn depend on the strength and/or duration of promoter occupancy by that transcription factor. Phosphorylation of Ngn2 occurs on multiple sites, which together can regulate DNA and promoter binding. We investigated whether specific SP sites are responsible for Ngn2 phosphoregulation or whether regulation is attained by the additive effect of individual phosphorylation events, each one quantitatively having a small effect on promoter occupancy by Ngn2, the number of sites phosphorylated being quantitatively dependent on the cdk kinase level (Fig. 2). We tested whether the mutation of an increasing number of phosphorylation sites had an additive effect on Ngn2 DNA binding and its ability to induce neuronal differentiation.

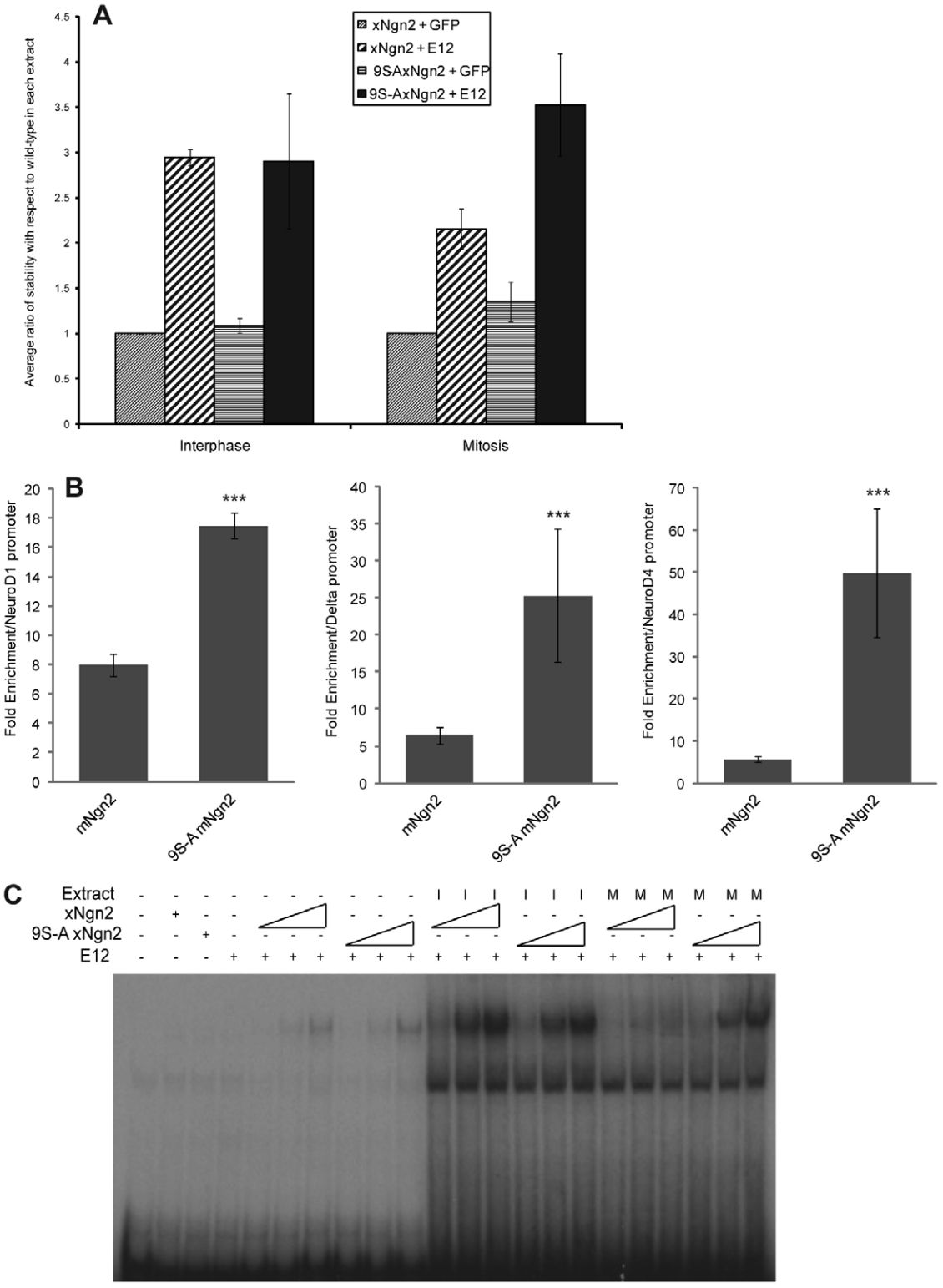

Fig. 4. Phosphomutant Ngn2 binds more efficiently than wild-type Ngn2 protein to DNA and is stabilised more by E12. (**A**) IVT [^{35}S]methionine-labelled xNgn2 or 9S-A xNgn2 were incubated in I or M *Xenopus* egg extracts in the presence of unlabelled IVT GFP or E12. Samples were removed every 10 minutes, separated by SDS-PAGE and the amount of Ngn2 protein determined by phosphorimaging, calculating the half-life of Ngn2 protein degradation using first-order rate kinetics. Half-lives were normalised to that of xNgn2 with GFP in each experiment and the average ratios of stability relative to xNgn2 with GFP for three experiments were plotted (mean ± s.e.m.). (**B**) Chromatin immunoprecipitation (ChIP) analysis of cell extracts containing normalised amounts of HA-tagged mNgn2 and 9S-A mNgn2, assessing binding to the promoters of *Neurod1*, delta-like 1 (*Dll1*) and *Neurod4* in mouse P19 cells, 24 hours following transfection (IgG control for non-specific background binding). ***, $P \leq 0.005$. (**C**) Electrophoretic mobility shift assay (EMSA) showing E box binding of normalised IVT xNgn2 or 9S-A xNgn2 in I and M extracts with and without E12.

A panel of S-A mutant versions of mNgn2 was constructed in which the mutation of SP sites was undertaken additively from the N-terminus (i.e. mS-A1 has the most N-terminal SP site mutated to AP, mS-A2 has the first two N-terminal sites mutated, and so on; see Fig. S1 in the supplementary material), and their DNA binding tested by EMSA. As previously seen with xNgn2 and 9S-A xNgn2 (Fig. 4C), there was little difference in the DNA binding of any of our additive mNgn2 phosphomutants in I extract (see Fig. S7 in the supplementary material). However, in M extract, the E box binding increases progressively as phosphorylation sites are lost (Fig. 5A).

To determine whether the number of SP sites available for phosphorylation is more important than the location of those sites, we investigated a series of xNgn2 phosphomutants in which SP sites were additively mutated, but this time from the C-terminus (see Fig. S1 in the supplementary material). Again, we saw that the availability of SP sites quantitatively regulates DNA binding in M; as each SP site was additionally mutated, DNA-binding activity progressively increased (Fig. 5A). Thus, phosphorylation of multiple SP sites can act quantitatively, in a rheostat-like manner, to control E box binding by mNgn2 and

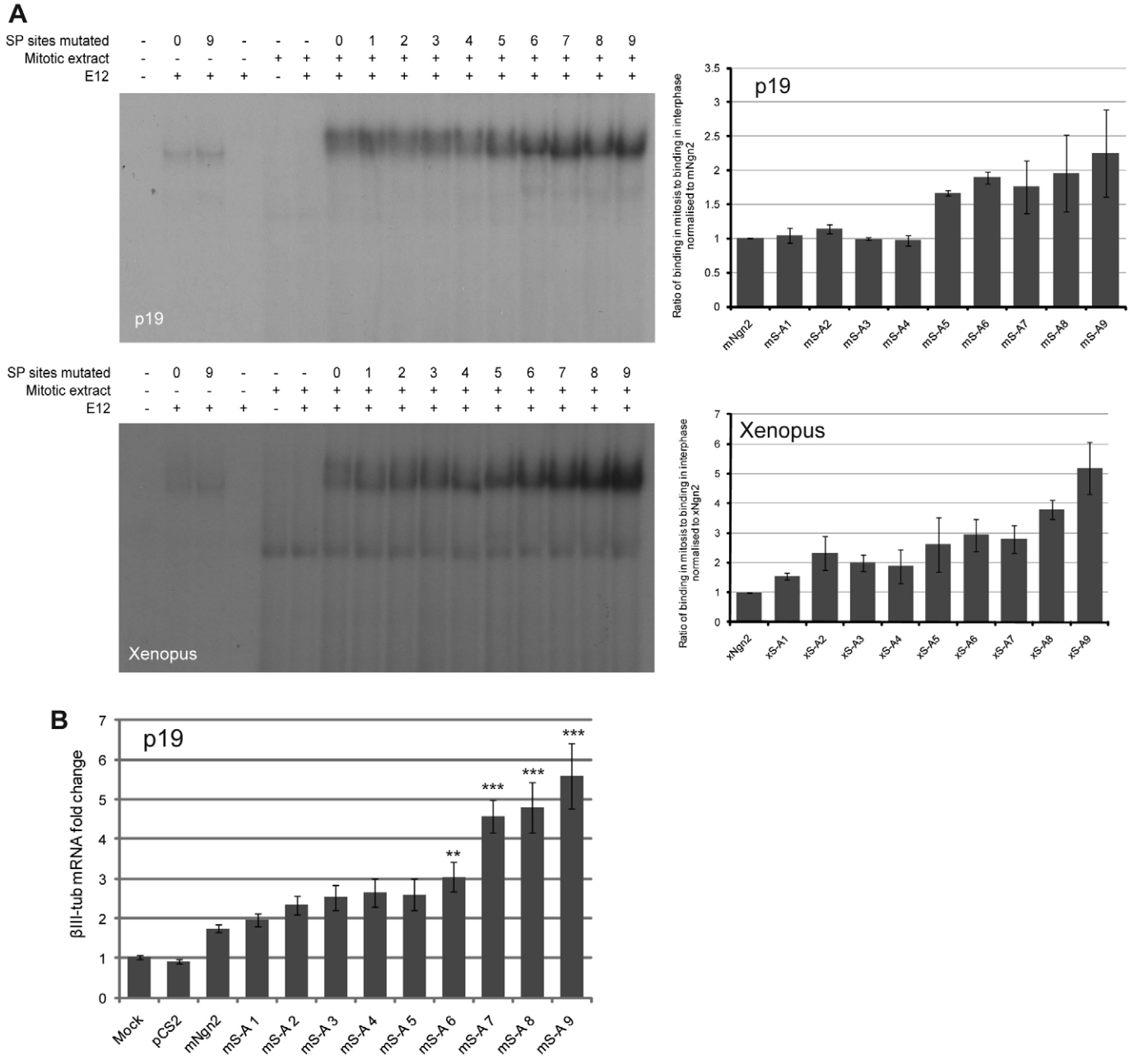

Fig. 5. Phosphorylation on multiple serine-proline (SP) sites has an additive effect on Ngn2 DNA binding. (**A**) EMSA analyses in *Xenopus* M extracts showing E box binding of normalised IVTs of xNgn2 or mNgn2 and additive phosphorylation site mutants of *xNgn2* or *mNgn2* as labelled. Graphs show quantitation of E box binding of phosphorylation site mutants by phosphorimaging, normalised to DNA binding of xNgn2 or mNgn2 as appropriate (see Fig. S1 in the supplementary material). (**B**) qPCR analysis of neural *βIII-tubulin* in P19 cells. P19 cells were transiently transfected with *mNgn2* and additive phosphorylation site mutants thereof for 24 hours. Average fold increase (± s.e.m.) in *βIII-tubulin* mRNA expression normalised to housekeeping genes [β-actin (*Actb*) and *Gapdh*]. **, $P \leq 0.05$; ***, $P \leq 0.005$.

xNgn2, even though the context and location of only the two most C-terminal SP sites are conserved between these two species.

We next investigated whether the ability of Ngn2 to induce neuronal differentiation of P19 cells is quantitatively dependent on the number of phosphorylation sites available. Using our mNgn2 phosphomutant series (see Fig. S1 in the supplementary material), we saw a fairly gradual increase in βIII-tubulin expression as additional SP sites were mutated (Fig. 5B), demonstrating that the propensity of Ngn2 to drive neuronal differentiation depends, at least semi-quantitatively, on the number of phosphorylation sites available. However, mutation of the final three (most C-terminal) SP sites had the biggest effect.

Cell cycle regulators control neuronal differentiation by post-translational regulation of Ngn2 protein

Enhancing cdk activity inhibits neurogenesis in vivo (Richard-Parpaillon et al., 2004; Lange et al., 2009). The results presented above led us to hypothesise that its inhibitory activity is via post-translational modification of the Ngn2 protein, and so phosphomutant Ngn2 would not be susceptible to inhibition by *cyclin A*/*cdk2* overexpression. To test this, we chose to inject levels of *xNgn2* mRNA that induce limited ectopic neurogenesis, largely within the neural plate, to mimic in vivo expression levels.

As previously reported, injection of *cyclin A*/*cdk2* mRNA promotes cell cycling within the ectoderm and inhibits endogenous neurogenesis (Richard-Parpaillon et al., 2004). *Cyclin A*/*cdk2* overexpression also inhibited neurogenesis in the presence of ectopic *xNgn2* mRNA, indicating that inhibition occurs at the level of post-translational modification of xNgn2 or, potentially, of a downstream target (Fig. 6A,B). 9S-A xNgn2 induced substantially greater ectopic neurogenesis in both the neural plate and epidermis than the wild-type protein, as expected. Strikingly, this extensive ectopic neurogenesis induced by *9S-A xNgn2* overexpression was unaffected by *cyclin A*/*cdk2* overexpression (Fig. 6A,B). This demonstrates that enhanced cyclin/cdk kinase activity, which promotes more rapid cell cycling (Richard-Parpaillon et al., 2004), also directly inhibits the neurogenesis-inducing ability of xNgn2 protein in vivo by post-translational modification.

Cdk inhibitors (cdkis) accumulate as the cell cycle lengthens and their expression is associated with both a drop in cdk kinase levels and neuronal differentiation (e.g. Cremisi et al., 2003; Vernon et al., 2003; Nguyen et al., 2006). We have previously shown that cdkis have an additional role in neurogenesis independent of, but complementary to, their role in inhibiting cyclin/cdk kinase activity: the *Xenopus* Cip/Kip family cdk inhibitor, Xic1, is required for neuronal differentiation in the developing embryo, where it functions to stabilise xNgn2 protein independently of its ability to inhibit overall cdk kinase activity. Similarly, $p27^{Kip1}$ stabilises Ngn2 in the mouse cortex (Nguyen et al., 2006).

Because of their more stable association with promoter DNA, we hypothesised that 9S-A xNgn2-E protein complexes might be less dependent on the presence of Xic1 to enhance Ngn2 protein stability and hence drive neuronal differentiation in vivo than the wild-type protein. To test this, we investigated the ability of *xNgn2* and *9S-A xNgn2* to induce neurogenesis in the presence of a Xic1 morpholino (Xic1 Mo), which has previously been shown to abolish Xic1 protein expression and inhibit Ngn2-dependent neuronal differentiation (Vernon et al., 2003). As expected, Xic1 Mo injection significantly reduced endogenous neurogenesis, as assayed by in situ hybridisation, whereas the control morpholino (Con Mo) had little effect (Fig. 7A,B) (Vernon et al., 2003). The low doses of *xNgn2* mRNA chosen to achieve near-physiological levels of expression induced modest but clear ectopic neurogenesis both within and outside the neural plate in the presence of Con Mo. Both the ectopic and endogenous neurogenesis seen in *xNgn2*-injected embryos were largely abolished by co-injection of Xic1 Mo, confirming that wild-type xNgn2 requires Xic1 for full activity (Fig. 7A,B) (Vernon et al., 2003).

As expected, extensive neurogenesis was induced by *9S-A xNgn2* mRNA plus Con Mo both within and outside the neural plate. However, in contrast to *xNgn2*, *9S-A xNgn2* could induce

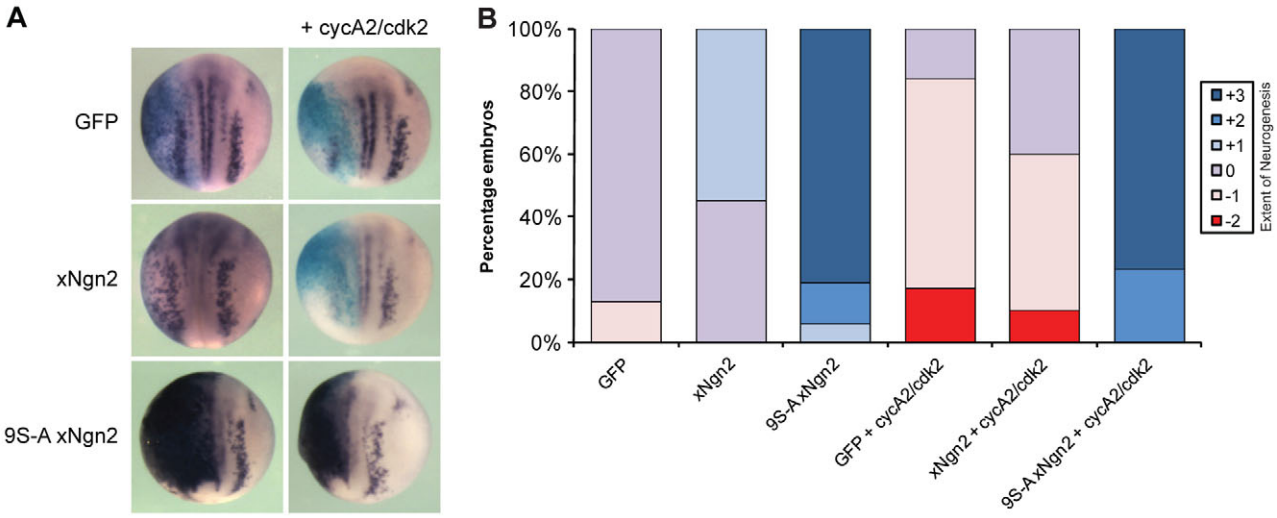

Fig. 6. 9S-A xNgn2 is resistant to cyclin A2/cdk2-mediated suppression of neurogenesis in vivo. (**A**) *Xenopus* embryos were injected (left side) in one of two cells with 20 pg *xNgn2* or *9S-A xNgn2* mRNA, together with 500 pg *cyclin A2* and *cdk2* mRNA, assaying for expression of neural *β-tubulin* at stage 15 by in situ hybridisation. (**B**) Semi-quantitative analysis of in situ hybridisation data. The number of embryos scored was 48-86 per condition. Neurogenesis was enhanced (+3, +2, +1), the same as (0) or reduced (–1, –2, –3) compared with the uninjected side (see Fig. S8 in the supplementary material).

DEVELOPMENT

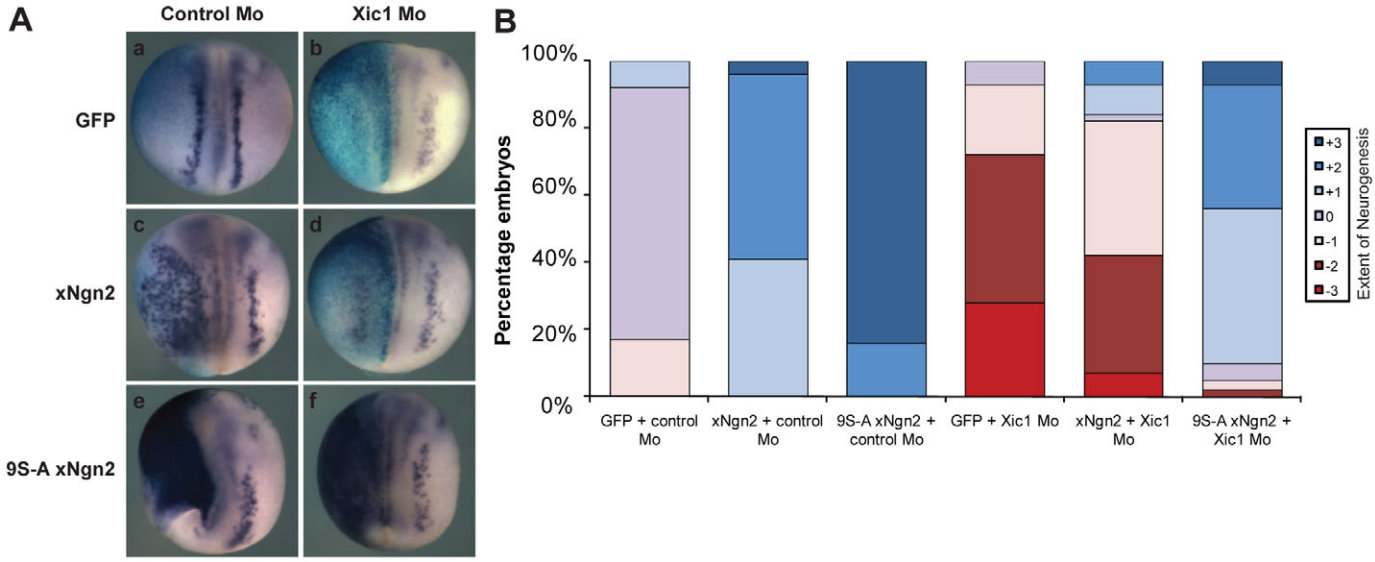

Fig. 7. 9S-A xNgn2 does not require the cdk inhibitor Xic1 for activity. (**A**) *Xenopus* embryos were injected (left side) in one of four cells (dorsally targeted) with 20 pg mRNA as indicated, together with 20 ng of either control (**a**,**c**,**e**) or Xic1 (**b**,**d**,**f**) morpholino, fixed at stage 15 and subject to in situ hybridisation for *neural* β-*tubulin* expression. (**B**) Semi-quantitative analysis of in situ hybridisation data. The number of embryos scored was 43-59 per condition. Neurogenesis was enhanced (+3, +2, +1), the same as (0) or reduced (–1, –2, –3) compared with the uninjected side (see Fig. S8 in the supplementary material for examples of the scoring method).

substantial neurogenesis even in the presence of Xic1 Mo (Fig. 7A,B). Thus, 9S-A xNgn2 has a reduced requirement for Xic1 compared with the wild-type protein, consistent with the enhanced stability of un(der)phosphorylated Ngn2.

DISCUSSION

Ngn2 acts as a master regulatory transcription factor that controls the balance between progenitor maintenance and differentiation in response to increasing cell cycle length as development progresses. We show that this is achieved by multi-site phosphorylation of Ngn2, which is quantitatively sensitive to cdk levels and quantitatively regulates the stability of Ngn2 binding to promoters of key downstream transcriptional targets, resulting in the regulation of neuronal differentiation.

Transcription factors undergo dynamic binding cycles on promoters. Increased dwell time on promoters is associated with more active transcription; for example, a slower exchange rate of the glucocorticoid receptor at promoters would promote the assembly of additional components required for chromatin remodelling and transcriptional activation (Stavreva et al., 2004; Hager et al., 2009). The requirement for stable association of Ngn2 with the target promoter to drive differentiation leads directly to a mechanism whereby post-translational modification of Ngn2 in response to the cellular environment, and the cdk kinase level in particular, can influence the propensity to differentiate.

Cdk-dependent inhibitory phosphorylation of Ngn2 complements another level of cell cycle-dependent post-translational regulation of Ngn2. We have previously shown that the cdkis $p27^{Xic1}$ in *Xenopus* and $p27^{Kip1}$ (Cdkn1b) in mouse are required for transcriptional activity of Ngn2 (Nguyen et al., 2006; Vernon et al., 2003). Acting independently of (but complementary to) their ability to inhibit cyclins and cdks, these cdkis inhibit ubiquitin-mediated proteolysis of Ngn2 protein, thus facilitating neuronal differentiation. In addition to this stabilising effect, accumulation of cdkis in neural precursors with lengthening cell cycles will also directly inhibit cdk activity, reducing the inhibitory phosphorylation of Ngn2 and so enhancing its transcriptional activity on differentiation targets. However, it should be noted that these cdkis themselves have not been shown to be direct transcriptional targets of Ngn2 (Seo et al., 2007).

From our biochemical in vitro assays, coupled with overexpression experiments in both cultured P19 cells and *Xenopus* embryos, we propose the following model (Fig. 8). In cycling cells, cdk levels rise rapidly on transition through late G1 and S phase into G2 and mitosis, promoting increasing phosphorylation of Ngn2 by cdk2 and cdk1, and resulting in reduced promoter occupancy, which is insufficient to activate the Ngn2-responsive promoters of genes required for neuronal differentiation, such as *NeuroD*. By contrast, cell cycle lengthening results in a longer time spent in G1, where cdk levels are low and cdk inhibitors accumulate. This favours un(der)phosphorylated, more stable Ngn2, which binds E box DNA more tightly. This greater promoter occupancy would be permissive for transcription of Ngn2 targets driving neuronal differentiation. Moreover, the graded response of neural β-tubulin to Ngn2 phosphorylation on additive sites allows cdk levels to be interpreted in a rheostat-like manner (Deshaies and Ferrell, 2001; Pufall et al., 2005). Here, we have concentrated on cdk-dependent phosphorylation of Ngn2. However, multi-site phosphorylation could be used as a mechanism to integrate a range of signals that culminate in proline-directed kinase activity.

The promoter of the *NeuroD* gene is known to respond slowly to Ngn2 expression and to require extensive chromatin modification for activation (Koyano-Nakagawa et al., 1999), which fits with our model in which stable promoter association is required to drive neuronal differentiation. Ngn2 has many direct downstream targets with potentially differing requirements for epigenetic modification, and hence for recruitment of chromatin modifiers, before activation (Koyano-Nakagawa et al., 1999; Seo et al., 2007). Different promoters might therefore respond

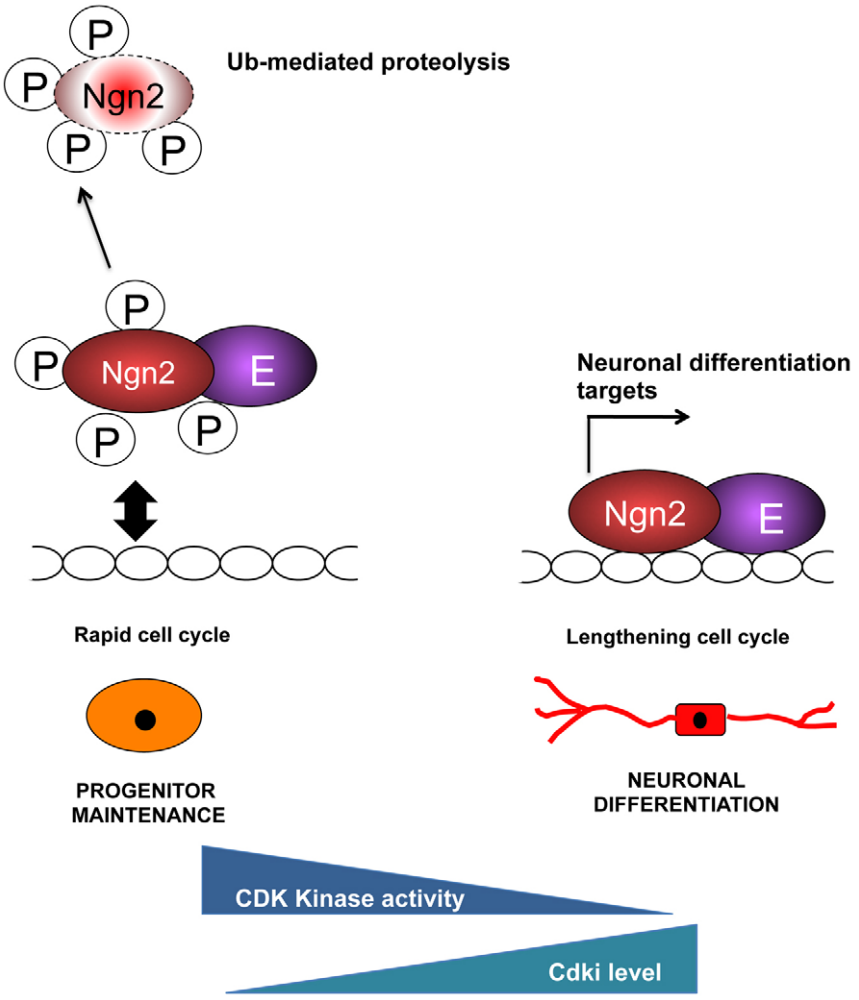

Fig. 8. Model of control of neuronal differentiation via cell cycle length and Ngn2 phosphorylation. Phosphorylation of Ngn2 protein occurs in rapid progenitor cell cycles. Cell cycle lengthening results in an accumulation of un(der)phosphorylated Ngn2, enhancing promoter binding and resulting in the activation of downstream target genes that drive differentiation. E, E protein; Ub, ubiquitin; P, phosphorylation.

differently to changes in Ngn2 phosphorylation status, affecting the frequency/duration of promoter occupancy, and we are currently exploring this possibility.

Our analyses indicate the importance of the number of SP sites modified, rather than their precise location, for regulation of protein function (Fig. 5). Native Ngn2 might be largely unstructured, like the related protein Ngn1 (Aguado-Llera et al., 2010), and hence might have limited structural constraints for phosphorylation on SP sites. Several classes of transcription factors have been identified in which unstructured N- and C-terminal extensions from the known DNA-binding domains contribute to DNA-binding affinity (Crane-Robinson et al., 2006), which would in turn affect the frequency and duration of DNA-protein binding cycles (Michel, 2009). Our data demonstrate that phosphorylation of residues in both the N- and C-termini quantitatively reduce Ngn2 DNA-binding activity.

In summary, we have shown here that Ngn2 is directly phosphorylated at multiple sites by cdk kinases and that this directly controls its ability to drive neuronal differentiation. Hence, we have uncovered a molecular mechanism whereby cell cycle lengthening can directly trigger neuronal differentiation.

Acknowledgements
We thank Helen Wise, Christelle Fiore-Heriche, Romana Kucerova and Jon Vosper for important initial observations leading up to this study; Ian Horan, Kate Wilson, Chris Hurley and Venkat Pisupati for technical assistance; and Jeremy Gunewardena, Hanno Steen and Bill Harris for helpful discussions.

Funding
This work was supported by MRC Research Grant G0700758, an MRC DTA studentship (G.M.) and a Cancer Research UK Studentship (C.H.). F.G. is supported by a Grant-in-Aid from the Medical Research Council (U117570528). M.K. and R.D. acknowledge a grant from the National Institute of General Medical Sciences (GM26875). Deposited in PMC for release after 6 months.

Competing interests statement
The authors declare no competing financial interests.

Supplementary material
Supplementary material for this article is available at
http://dev.biologists.org/lookup/suppl/doi:10.1242/dev.067900/-/DC1

References

Aguado-Llera, D., Goormaghtigh, E., de Geest, N., Quan, X. J., Prieto, A., Hassan, B. A., Gomez, J. and Neira, J. L. (2010). The basic helix-loop-helix region of human neurogenin 1 is a monomeric natively unfolded protein which forms a "fuzzy" complex upon DNA binding. *Biochemistry* **49**, 1577-1589.
Bain, J., Plater, L., Elliott, M., Shpiro, N., Hastie, C. J., McLauchlan, H., Klevernic, I., Arthur, J. S., Alessi, D. R. and Cohen, P. (2007). The selectivity of protein kinase inhibitors: a further update. *Biochem. J.* **408**, 297-315.
Bertrand, N., Castro, D. S. and Guillemot, F. (2002). Proneural genes and the specification of neural cell types. *Nat. Rev. Neurosci.* **3**, 517-530.
Crane-Robinson, C., Dragan, A. I. and Privalov, P. L. (2006). The extended arms of DNA-binding domains: a tale of tails. *Trends Biochem. Sci.* **31**, 547-552.
Cremisi, F., Philpott, A. and Ohnuma, S. (2003). Cell cycle and cell fate interactions in neural development. *Curr. Opin. Neurobiol.* **13**, 26-33.
Deibler, R. W. and Kirschner, M. W. (2010). Quantitative reconstitution of mitotic CDK1 activation in somatic cell extracts. *Mol. Cell* **37**, 753-767.

Deshaies, R. J. and Ferrell, J. E., Jr (2001). Multisite phosphorylation and the countdown to S phase. *Cell* **107**, 819-822.
Errico, A., Deshmukh, K., Tanaka, Y., Pozniakovsky, A. and Hunt, T. (2010). Identification of substrates for cyclin dependent kinases. *Adv. Enzyme Regul.* **50**, 375-399.
Farah, M. H., Olson, J. M., Sucic, H. B., Hume, R. I., Tapscott, S. J. and Turner, D. L. (2000). Generation of neurons by transient expression of neural bHLH proteins in mammalian cells. *Development* **127**, 693-702.
Hager, G. L., McNally, J. G. and Misteli, T. (2009). Transcription dynamics. *Mol. Cell* **35**, 741-753.
Hand, R., Bortone, D., Mattar, P., Nguyen, L., Heng, J. I., Guerrier, S., Boutt, E., Peters, E., Barnes, A. P., Parras, C. et al. (2005). Phosphorylation of Neurogenin2 specifies the migration properties and the dendritic morphology of pyramidal neurons in the neocortex. *Neuron* **48**, 45-62.
King, R. W., Glotzer, M. and Kirschner, M. W. (1996). Mutagenic analysis of the destruction signal of mitotic cyclins and structural characterization of ubiquitinated intermediates. *Mol. Biol. Cell* **7**, 1343-1357.
Koyano-Nakagawa, N., Wettstein, D. and Kintner, C. (1999). Activation of Xenopus genes required for lateral inhibition and neuronal differentiation during primary neurogenesis. *Mol. Cell. Neurosci.* **14**, 327-339.
Lange, C. and Calegari, F. (2010). Cdks and cyclins link G(1) length and differentiation of embryonic, neural and hematopoietic stem cells. *Cell Cycle* **9**, 1893-1900.
Lange, C., Huttner, W. B. and Calegari, F. (2009). Cdk4/cyclinD1 overexpression in neural stem cells shortens G1, delays neurogenesis, and promotes the generation and expansion of basal progenitors. *Cell Stem Cell* **5**, 320-331.
Ma, Q., Kintner, C. and Anderson, D. J. (1996). Identification of neurogenin, a vertebrate neuronal determination gene. *Cell* **87**, 43-52.
Ma, Y. C., Song, M. R., Park, J. P., Ho, H.-Y. H., Hu, L., Kurtev, M. V., Zieg, J., Ma, Q., Pfaff, S. L. and Greenberg, M. E. (2008). Regulation of motor neuron specification by phosphorylation of neurogenin 2. *Neuron* **58**, 65-77.
Michel, D. (2009). Fine tuning gene expression through short DNA-protein binding cycles. *Biochimie* **91**, 933-941.
Miyata, T., Kawaguchi, D., Kawaguchi, A. and Gotoh, Y. (2010). Mechanisms that regulate the number of neurons during mouse neocortical development. *Curr. Opin. Neurobiol.* **20**, 22-28.
Nguyen, L., Besson, A., Heng, J. I., Schuurmans, C., Teboul, L., Parras, C., Philpott, A., Roberts, J. M. and Guillemot, F. (2006). p27kip1 independently promotes neuronal differentiation and migration in the cerebral cortex. *Genes Dev.* **20**, 1511-1524.
Nieber, F., Pieler, T. and Henningfeld, K. A. (2009). Comparative expression analysis of the neurogenins in Xenopus tropicalis and Xenopus laevis. *Dev. Dyn.* **238**, 451-458.
Pufall, M. A., Lee, G. M., Nelson, M. L., Kang, H. S., Velyvis, A., Kay, L. E., McIntosh, L. P. and Graves, B. J. (2005). Variable control of Ets-1 DNA binding by multiple phosphates in an unstructured region. *Science* **309**, 142-145.
Richard-Parpaillon, L., Cosgrove, R. A., Devine, C., Vernon, A. E. and Philpott, A. (2004). G1/S phase cyclin-dependent kinase overexpression perturbs early development and delays tissue-specific differentiation in Xenopus *Development* **131**, 2577-2586.
Seo, S., Lim, J. W., Yellajoshyula, D., Chang, L. W. and Kroll, K. L. (2007). Neurogenin and NeuroD direct transcriptional targets and their regulatory enhancers. *EMBO J.* **26**, 5093-5108.
Shimojo, H., Ohtsuka, T. and Kageyama, R. (2008). Oscillations in notch signaling regulate maintenance of neural progenitors. *Neuron* **58**, 52-64.
Stavreva, D. A., Muller, W. G., Hager, G. L., Smith, C. L. and McNally, J. G. (2004). Rapid glucocorticoid receptor exchange at a promoter is coupled to transcription and regulated by chaperones and proteasomes. *Mol. Cell. Biol.* **24**, 2682-2697.
Ubersax, J. A. and Ferrell, J. E., Jr (2007). Mechanisms of specificity in protein phosphorylation. *Nat. Rev. Mol. Cell Biol.* **8**, 530-541.
Vernon, A. E., Devine, C. and Philpott, A. (2003). The cdk inhibitor p27Xic1 is required for differentiation of primary neurones in Xenopus. *Development* **130**, 85-92.
Vosper, J. M., Fiore-Heriche, C. S., Horan, I., Wilson, K., Wise, H. and Philpott, A. (2007). Regulation of neurogenin stability by ubiquitin-mediated proteolysis. *Biochem. J.* **407**, 277-284.
Vosper, J. M., McDowell, G. S., Hindley, C. J., Fiore-Heriche, C. S., Kucerova, R., Horan, I. and Philpott, A. (2009). Ubiquitylation on canonical and non-canonical sites targets the transcription factor neurogenin for ubiquitin-mediated proteolysis. *J. Biol. Chem.* **284**, 15458-15468.

APPENDIX 6

UbxNgn2: Ubiquitin fused to N-terminus of xNgn2

N-Ngn/BC-NeuroD: N-terminal domain of xNgn2 fused to bHLH and C-terminal domains of xNeuroD
N-NeuroD/BC-Ngn: N-terminal domain of xNeuroD fused to bHLH and C-terminal domains of xNgn2
NB-Ngn/C-NeuroD: N-terminal and bHLH domains of xNgn2 fused to C-terminal domain of xNeuroD
NB-NeuroD/C-Ngn: N-terminal and bHLH domains of xNeuroD fused to C-terminal domain of xNgn2

NgnNDNgn: N- and C-terminal domains of xNgn2 fused to bHLH domain of xNeuroD
NDNgnND: N- and C-terminal domains of xNeuroD fused to bHLH domain of xNgn2

NTNeuroD: N-terminal domain of xNeuroD
ΔNTNeuroD: bHLH and C-terminal domains of xNeuroD
ΔbHLHNeuroD: N-terminal domain of xNeuroD fused directly to C-terminal domain
CTNeuroD: C-terminal domain of xNeuroD
ΔCTNeuroD: N-terminal and bHLH domains of xNeuroD
UD-NeuroD/NeuroD-UD: Unfolded residues 1–95 of cytochrome b2 fused to N- or C-terminus of xNeuroD, respectively

NTSPxNgn2: xNgn2 with all N-terminal SP site serines mutated to alanines
NTSPTPxNgn2: xNgn2 with all N-terminal SP/TP sites mutated to alanines
CTSPxNgn2: xNgn2 with all C-terminal SP site serines mutated to alanines
N-SP/BC-NeuroD: N-terminal domain of 9S-AxNgn2 fused to bHLH and C-terminal domains of xNeuroD
NB-SP/C-NeuroD: N-terminal and bHLH domains of 9S-AxNgn2 fused to C-terminal domain of xNeuroD
NB-NeuroD/C-SP: N-terminal and bHLH domains of xNeuroD fused to C-terminal domain of 9S-AxNgn2

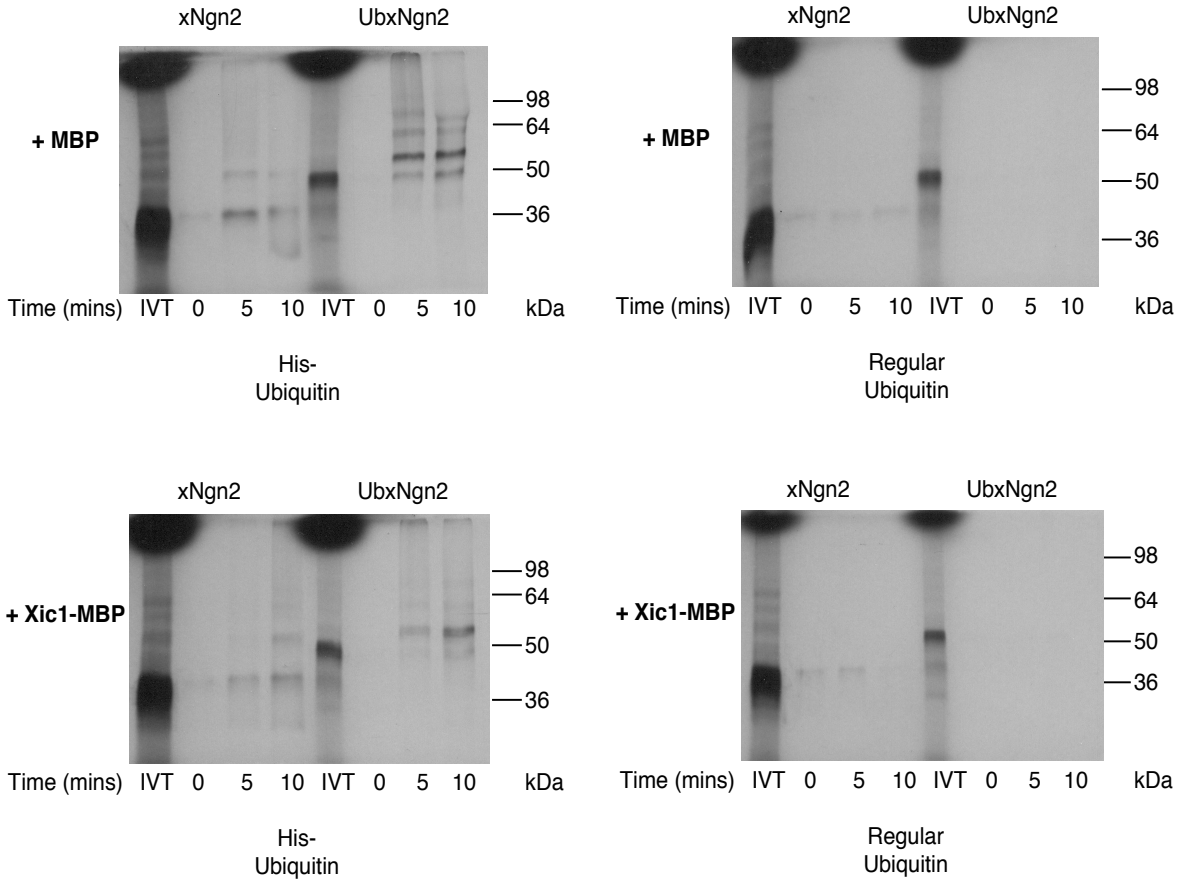

Figure A1: Ubiquitylation timecourse for xNgn2 and UbxNgn2 in the presence or absence of Xic1.

35S-radiolabelled in vitro translated (IVT) xNgn2 or UbxNgn2 were incubated in previously frozen Xenopus laevis interphase activated egg extract, supplemented with the proteasome inhibitor MG132. Samples were treated with His6-ubiquitin (His-Ubiquitin) or untagged ubiquitin (Regular Ubiquitin). Samples were further treated with maltose binding protein (MBP)-fused Xic1 (+ Xic1-MBP) or MBP alone (+ MBP). The reactions were incubated at 20ºC for 0, 5 or 10 minutes, before dilution in Vosper buffer and incubation with Ni-NTA (Qiagen) beads at room temperature for 75 minutes. SDS-LB was added and samples boiled before running on SDS-PAGE with untreated in vitro translated radiolabelled protein (IVT).

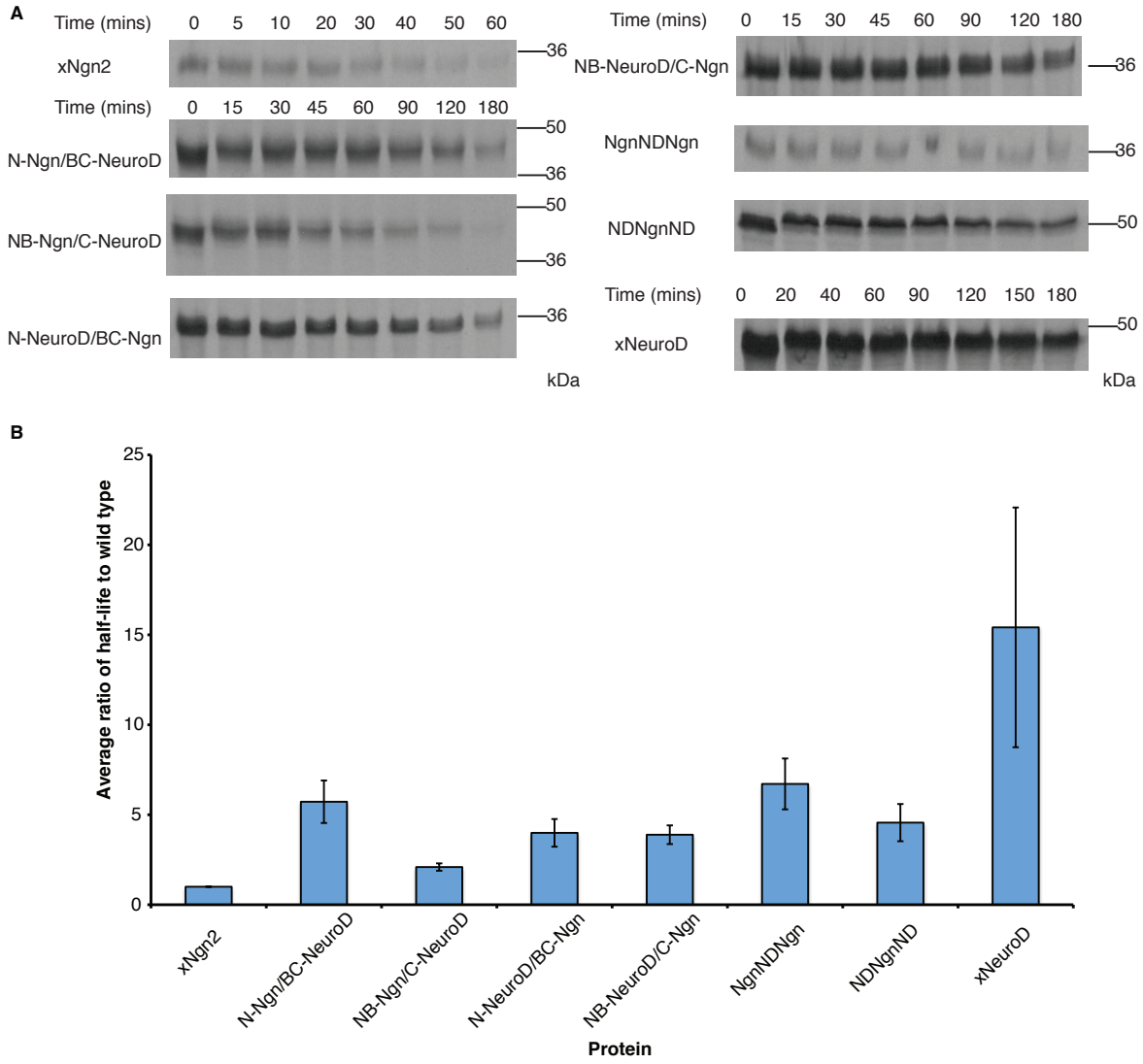

C

Extract	Half-life (mins)
xNgn2	30.4 +/- 5.4
N-Ngn/BC-NeuroD	183 +/- 63
NB-Ngn/C-NeuroD	60.9 +/- 7.8
N-NeuroD/BC-Ngn	111 +/- 17
NB-NeuroD/C-Ngn	110 +/- 8
NgnNDNgn	185 +/- 25
NDNgnND	124 +/- 6
xNeuroD	> 180

Figure A2: xNgn2/xNeuroD domain swap stability in interphase.

Xenopus interphase extracts were supplemented with ^{35}S-labelled IVT xNgn2, xNeuroD or chimeric protein. Samples were taken at indicated timepoints, subjected to 15 % SDS-PAGE and analysed by autoradiography (A). The average stabilisation relative to wild-type xNgn2 within interphase extract was calculated (B). (C) Half-lives were calculated using first-order rate kinetics, and errors calculated using SEM. $n \geq 4$.

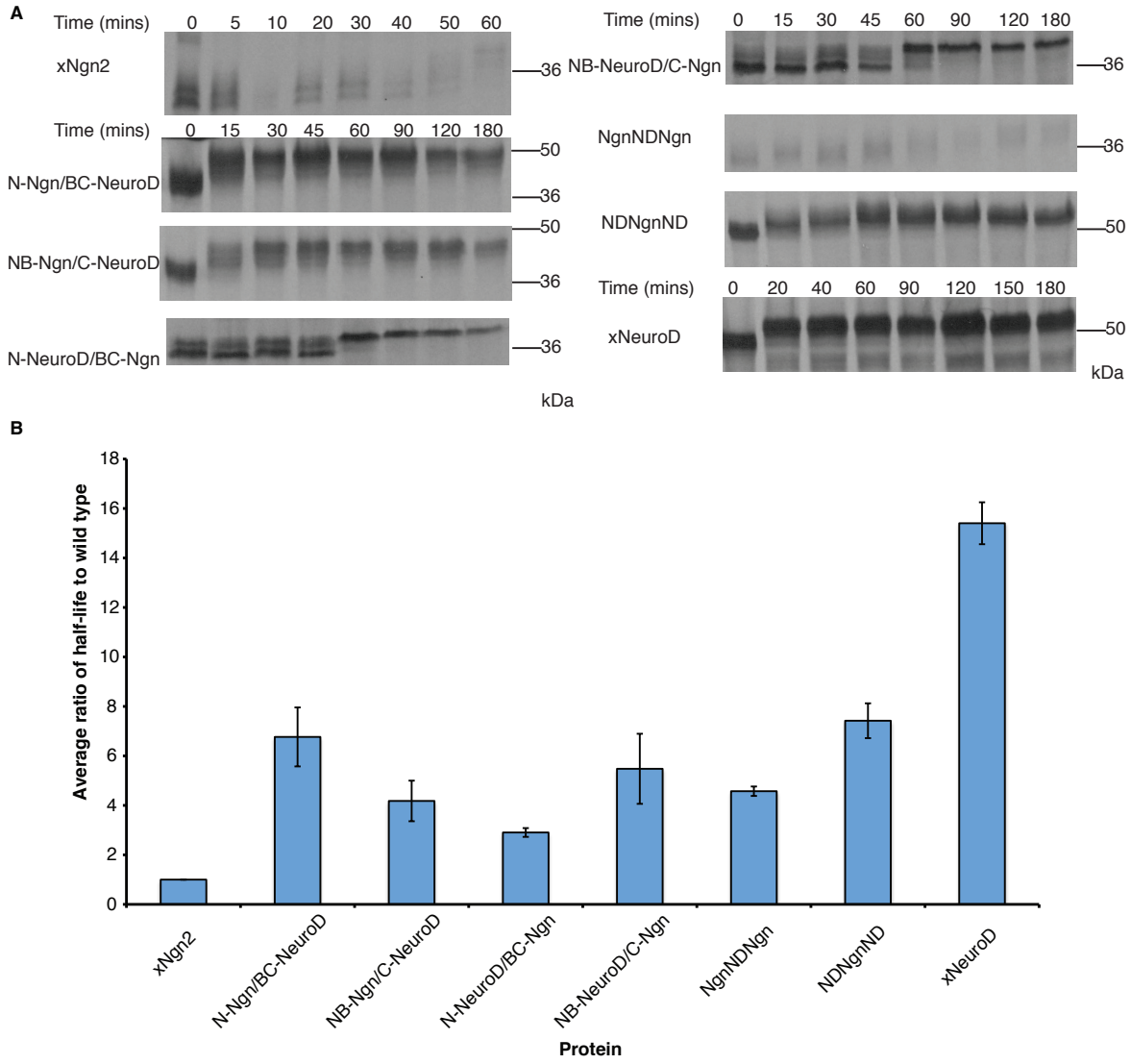

C

Extract	Half-life (mins)
xNgn2	22.1 +/- 4.3
N-Ngn/BC-NeuroD	145 +/- 3
NB-Ngn/C-NeuroD	88.9 +/- 0
N-NeuroD/BC-Ngn	65.0 +/- 16.6
NB-NeuroD/C-Ngn	127 +/- 55
NgnNDNgn	102 +/- 24
NDNgnND	161 +/- 17
xNeuroD	> 180

Figure A3: xNgn2/xNeuroD domain swap stability in mitosis.

Xenopus laevis mitotic egg extracts were supplemented with ^{35}S-labelled IVT xNgn2, xNeuroD or domain swapped protein and incubated at 21 °C. Samples were taken at the timepoints indicated and subjected to 15 % SDS-PAGE. Gels were analysed by autoradiography (A) and quantitative phosphorimaging analysis, calculating the average stabilisation relative to wild-type xNgn2 within mitotic extract (B). (C) Half-lives were calculated using first-order rate kinetics, and errors calculated using the Standard Error of the Mean (SEM). $n \geq 2$.

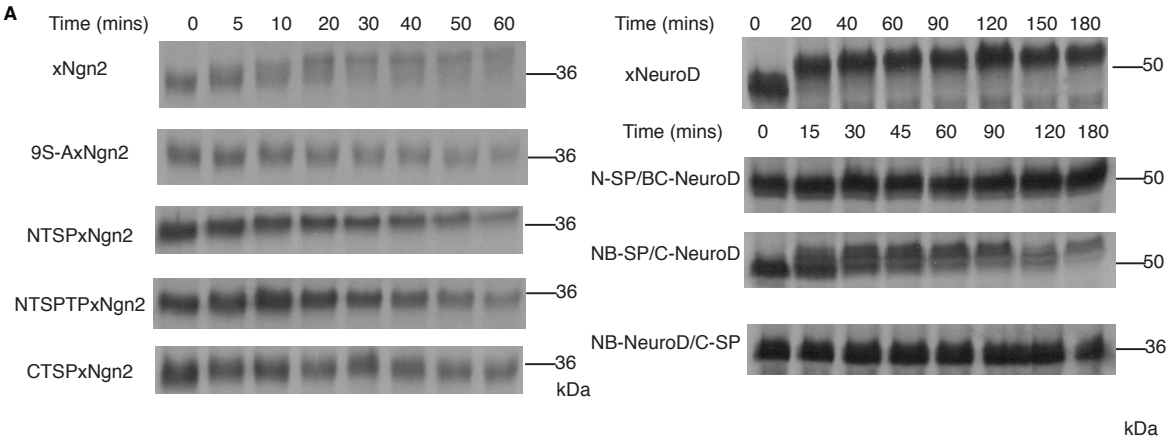

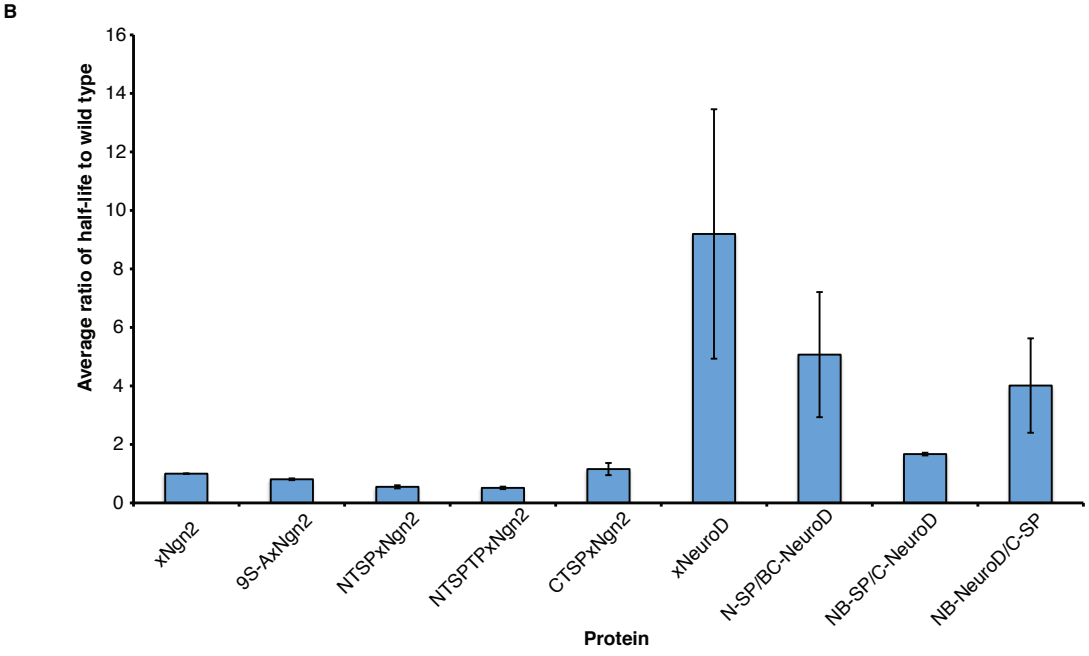

C

Extract	Half-life (mins)
xNgn2	45.8 +/- 2.3
9S-AxNgn2	36.9 +/- 1.0
NTSPxNgn2	25.5 +/- 3.7
NTSPTPxNgn2	23.7 +/- 3.1
CTSPxNgn2	53.0 +/- 9.8
xNeuroD	> 180
N-SP/BC-NeuroD	>180
NB-SP/C-NeuroD	76.4 +/- 2.8
NB-NeuroD/C-SP	177 +/- 4.0

Figure A4: xNgn2/xNeuroD SP domain swap stability in mitosis.

Xenopus laevis mitotic egg extracts were supplemented with ^{35}S-labelled IVT xNgn2, xNeuroD or SP domain swapped protein and incubated at 21 °C. Samples were taken at the timepoints indicated and subjected to 15 % SDS-PAGE. Gels were analysed by autoradiography (A) and quantitative phosphorimaging analysis, calculating the average stabilisation relative to wild-type xNgn2 within mitotic extract (B). (C) Half-lives were calculated using first-order rate kinetics, and errors calculated using the Standard Error of the Mean (SEM). n ≥ 3.

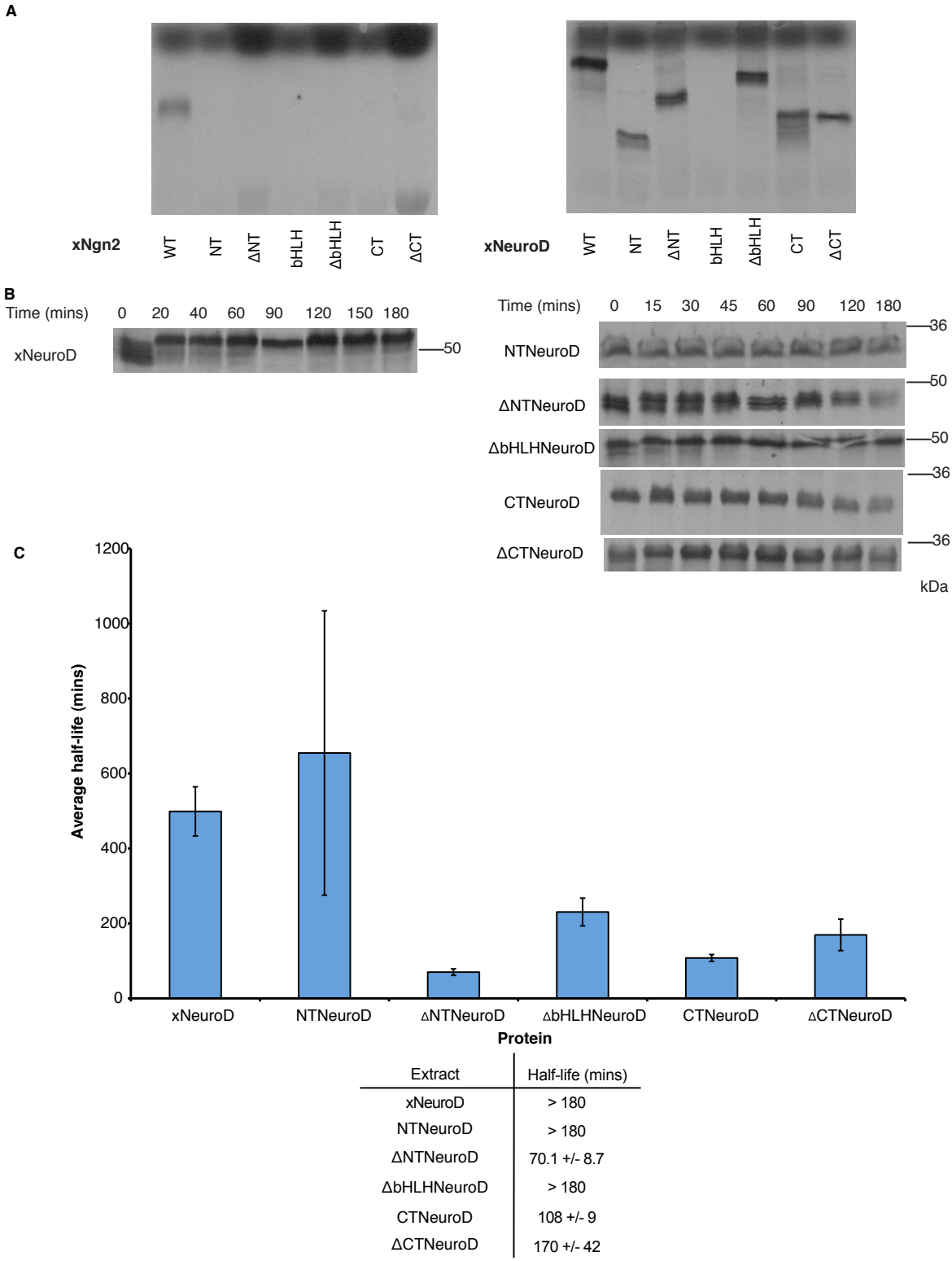

Extract	Half-life (mins)
xNeuroD	> 180
NTNeuroD	> 180
ΔNTNeuroD	70.1 +/- 8.7
ΔbHLHNeuroD	> 180
CTNeuroD	108 +/- 9
ΔCTNeuroD	170 +/- 42

Figure A5: xNeuroD domain deletions affect protein stability in interphase.

(A) IVT radiolabelled proteins for domain deletions of xNgn2 and xNeuroD. *Xenopus laevis* interphase egg extracts were supplemented with ^{35}S-labelled IVT xNeuroD domain deleted proteins and incubated at 21 °C. Samples were taken at timepoints indicated and subjected to 15 % SDS-PAGE. Gels were analysed by autoradiography (B) and quantitative phosphorimaging analysis, calculating the half-life (C) using the standard error of the mean (SEM). n = 3

A

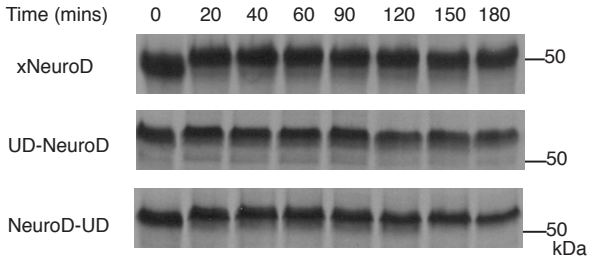

B

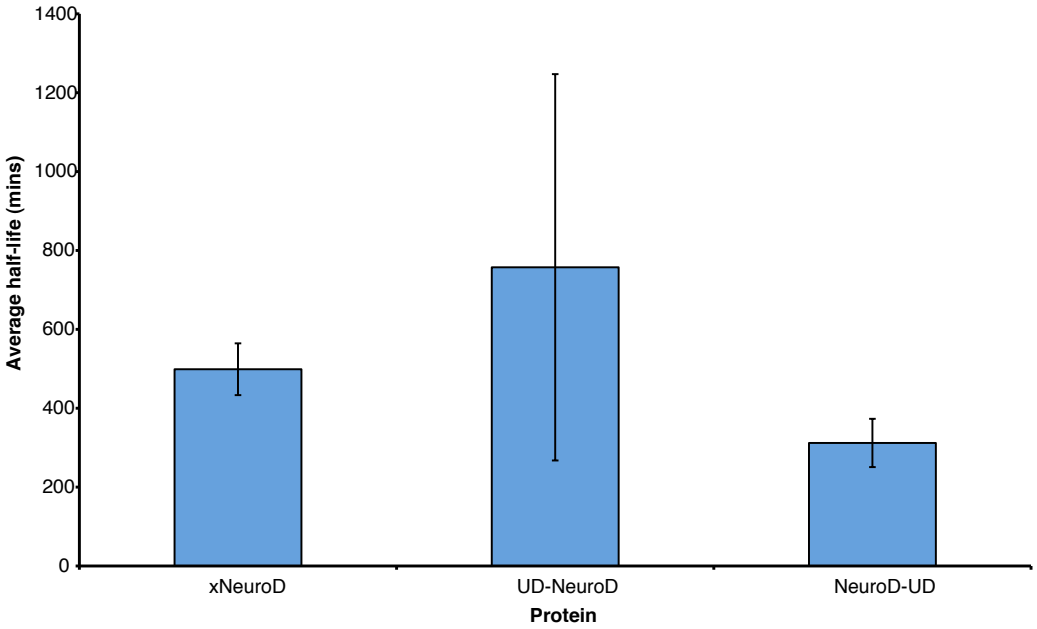

C

Extract	Half-life (mins)
xNeuroD	> 180
UD-NeuroD	> 180
NeuroD-UD	> 180

Figure A6: Unstructured domains do not affect xNeuroD stability in interphase.

Xenopus laevis interphase egg extracts were supplemented with ^{35}S-labelled IVT xNeuroD proteins fused to unstructured regions and incubated at 21 °C. Samples were taken at timepoints indicated and subjected to 15 % SDS-PAGE. Gels were analysed by autoradiography (A) and quantitative phosphorimaging analysis, calculating the half-life (B, C) using the standard error of the mean (SEM). n = 3